UNIVERSITY OF HULL

The Language of Abiotic Stress in Aquatic Animals:

Molecular Characterisation of

Stress Metabolite-Mediated Stress Communication

This thesis is submitted for the degree of Doctor of Philosophy,

Department of Biological and Marine Sciences

University of Hull, United Kingdom

by

Lauric Feugère

BSc., MSc. (Hons), University of Western Brittany

Supervised by:

Katharina C. Wollenberg Valero

Pedro Beltran-Alvarez

December 2022

This page is intentionally left blank.

Significance statement

Living organisms exposed to predation threat release chemicals eliciting antipredatory responses in neighbours, which can be interpreted as a biotic stress-induced stress propagation. However, whether abiotic factors such as pH and heat stress likewise induce stress propagation has received little focus. This Ph.D. thesis uncovers a novel dimension of chemical communication: animals exposed to abiotic stressors propagate stress to naive receivers. I propose a mechanism wherein abiotic stress elicits cellular and physiological responses, triggering the release of cues, dubbed "stress metabolites", into the environment. These stress metabolites induce fine-tuned molecular responses in receivers, resulting in fitness-relevant changes such as hypoactivity or reduced chances to seek food or shelter. Combining stress metabolites with abiotic stressors can modify stress responses. Stress, experienced directly or through stress metabolites, may alter fitness responses to novel stressors. This research extends the principles of stress propagation to abiotic stress, which warrants consideration to predict the fate of populations in a changing climate.

Graphical Abstract

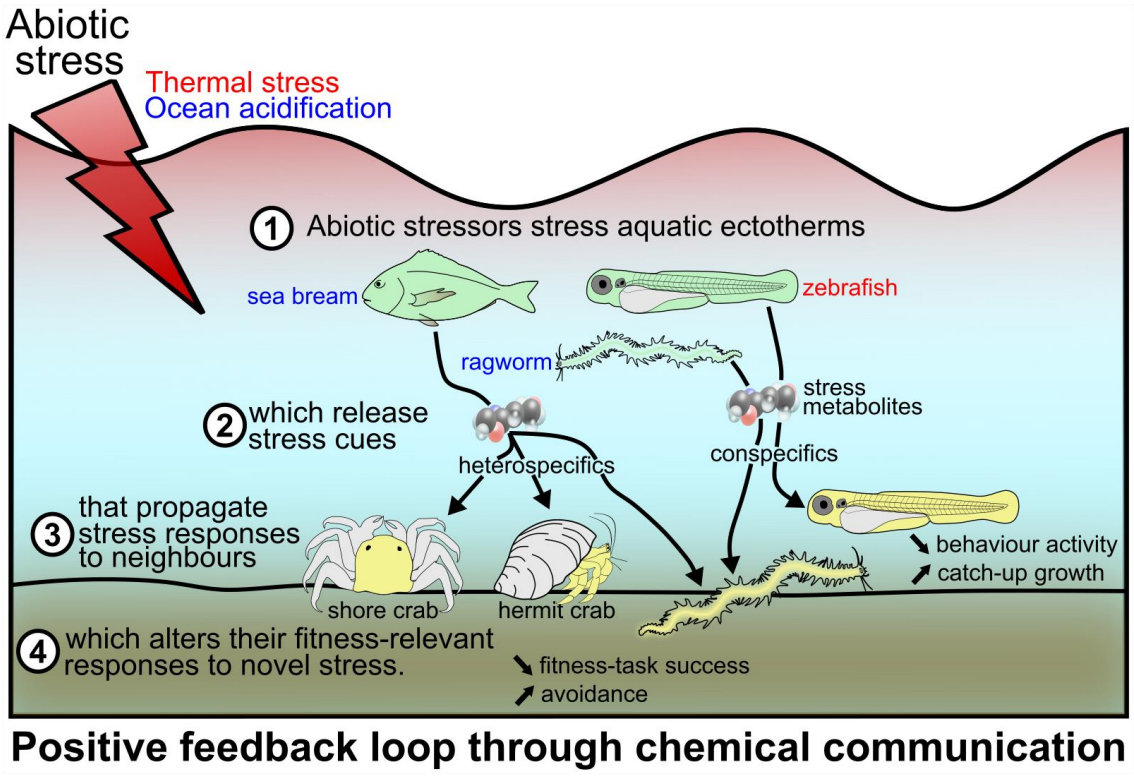

Highlights

- Both repeated heat stress and short-term pH drop induced stress responses in aquatic animals.

- Stress-induced shifts in cellular and molecular pathways altered the excreted metabolome of aquatic animals, leading to the release of stress metabolites into their environment.

- Stress metabolite receivers showed fine-tuned transcriptome changes involved in lipid transport, keratan, immune, antioxidant, cholinergic, and signalling pathways.

- Stress metabolite chemicals are the language of abiotic stress, that receivers may use to adjust their stress- and risk-coping strategies.

- I extend known concepts of predation-induced disturbance and alarm cues, shock-induced mammalian stress odours, and abiotic stress-induced plant stress chemicals, to abiotic stress-induced chemical communication in aquatic animals. This suggests that stress chemical communication is widespread in living organisms.

- Stress, whether direct or indirectly experienced (through stress cues), alters fitness-relevant responses to novel stressors such as predation risk and mutagenic environments.

Abstract

It is well established that aquatic animals inform their neighbours of predation risk through chemical cues. In this thesis, I tested the hypothesis that stress propagation is a widespread mechanism also activated by abiotic stressors – such as those arising from climate change. Inter-individual stress propagation was explored at different organisational levels (molecular to phenotypic), using different abiotic stressors (heat and pH), aquatic species (crustaceans, worms, fishes), ontogenic stages (embryos and adults), and types of interactions (intra- vs. interspecific). The molecular and phenotypic responses were measured in individuals directly stressed by abiotic stressors and in receivers exposed to stress metabolites released by abiotically-stressed individuals. As expected, abiotic stressors induced stress responses in donors. Heat-stressed zebrafish (*Danio rerio*) increased their cortisol levels and showed cellular stress responses, resulting in developmental and behavioural impairments. Fitness-relevant behaviours were impaired in pH-stressed ragworms (*Hediste diversicolor*) and hermit crabs (*Diogenes pugilator*), whilst shore crabs (*Carcinus maenas*) were resilient to pH stress. All tested species showed stress propagation, as donors and/or receivers of stress metabolites. Intraspecific stress propagation was observed in pH-stressed marine ragworms (but not crustaceans) and heat-stressed zebrafish embryos, through the release of stress metabolites that impaired the behaviour of their conspecifics. Conditioned water from pH-stressed sea bream (*Sparus aurata*) altered the behaviour of marine ragworm, shore crabs, and hermit crabs, suggesting interspecific stress propagation. Chemicals released by stressed animals differed to that from control individuals. The effects of stress metabolites were disrupted by acidic pH and amplified by high temperatures. Multi-omics showed that abiotic stressors shifted the metabolism of zebrafish embryo donors, which released stress metabolites (such as lipids and sulphur-containing compounds), that altered lipid transport, keratan sulfate, immune, antioxidant, cholinergic, and signalling pathways in receivers. Altogether, the findings from this thesis support the hypothesis that stress propagation is a widespread phenomenon existing in marine and freshwater species from embryos to adult stages, and that can be induced by abiotic stressors. Such stress propagation may have far-reaching consequences for populations under climate change-induced abiotic stress.

Acknowledgments

First, I wish to sincerely thank both my supervisors, Katharina Wollenberg Valero and Pedro Beltran-Alvarez, for being so supportive and patient with me during my Ph.D., and for guiding me through all aspects of science from experiments to writing to publishing. I am very grateful to the internal examiner, Domino Joyce, and the external examiner, Shaun Killen, for accepting to review my Ph.D. thesis, their very insightful comments about my projects, and the stimulating discussion we had during my *viva voce* examination. I also thank Jörg Hardege for taking the role of the academic jury during the *viva voce* examination. I would like to thank all members of the MolStressH2O, Odysyslab, ChemEcoHull, and EvoHull research groups, and more generally from the biology department at the University of Hull, for providing me with a safe environment to learn and become a better scientist. For their immense assistance in the laboratory, I would like to thank Emma Chapman and Robert Donnelly. I am very thankful to Alan Smith and Sonia Jennings for taking care of the fish in the aquarium facility. I would like to thank Chris Collins and Darren Bird from the VIPER Supercomputing Team for their many efforts in implementing bioinformatic pipelines. I thank all members of the MolStressH2O and ChemEcolHull research clusters, as well as Jacky L., for valuable peer-review. I would like to thank Quentin Rodriguez-Barucg, Linsey Malcom, Kathleen Bulmer, and Pedro Beltran-Alvarez for conducting analyses of heat shock proteins.

For their help in Chapter 2, I wish to acknowledge João Pena dos Reis, Peter Hubbard, Zélia Velez, and all staff members of the CCMAR-Ramalhete Marine Station. I would like to thank the graduate students from the University of Hull for their help in collecting behavioural data: Lauren Angell, James Fagents, Rebecca Nightingale, Kirsty Rowland, and Saffiyah Skinner. I acknowledge funding by the Natural Environment Research Council (NERC grant #NE/T001577/1), and funding from the University of Hull towards the MolStressH2O research cluster. I thank Andrea Murcia for the animal drawings of *Diogenes pugilator, Sparus aurata, and Hediste diversicolor* in Chapter 2.

For their support in experiments for Chapter 3, I acknowledge Emma Chapman, Robert Donnelly, Adam Bates, and Paulo Saldanha (University of Hull, UK) for laboratory advice. For help with initial zebrafish method development for Chapter 3, I thank Antoinette DeStefano, Amber Pinnock, Tiana Weeks, and Tia Rusciano (Bethune-Cookman University, USA); and Tyrese Taylor (Indiana University, USA). I

am very thankful to Victoria Scott for introducing me to zebrafish embryo procedures. Experiments from Chapter 3 were funded by the University of Hull and the Royal Society (RGS\R2\180033).

For their help in Chapter 4, I acknowledge Paul Green (for shipping samples), and the animal facility staff of the University of Sheffield (for providing me with AB strain zebrafish). I thank Tony Larson, Swen Langer, Adam Dowle, and all members of the Metabolomics & Proteomics Facility of the University of York for conducting LC-MS/MS analyses. I acknowledge Matthew Arno and other members of the Edinburgh Genomics Facility for performing the RNA-sequencing. I thank Emma Chapman and Timothy Emagbetere for the acquisition of LAMP-PCR data. I wish to thank Adam Bates for his help in optimising RNA extraction methods and RNA-seq analysis pipelines.

Regarding Chapter 5, I would like to thank the technical staff from the Biology and Marine Sciences department at the University of Hull for providing me with PCR handheld stations for experimental ultraviolet exposure. I acknowledge Kenneth Storey (Carleton University, Canada) for peer-review of Chapter 5.

I thank Jörg Hardege and Helga Bartels-Hardege for their valuable comments about my research and for introducing me to the field of chemical ecology. I felt very welcomed in the ChemEcoHull laboratory, and I thoroughly enjoyed all the writing retreats and lab days out. During my time at the University of Hull, I have met many great lab mates and friends: I cannot thank you enough for your help and recommendations in the lab, our discussions, and for making our office and laboratory a great place to work in and return to every day. I would like to thank Adam, Luana, Paulo, Paula, Angus, Amber, Quentin, Dai, Jess, and Vicky, for good times inside and outside the lab. I am also thankful to all my football, squash, and tennis friends for all the great games we had and for giving me a place to free my mind. I also would like to thank all my former supervisors and professors at the University of Western Brittany for guiding me through my studies. Finally, I would like to thank my family and friends in France, for their continuous support: *je vous remercie de votre soutien constant durant toutes mes années d'études.*

Authorship, Publications, and Conferences

I declare that the work herein is my own. All raw data is my own unless stated otherwise. All data and statistical analyses are my own. I wrote chapter drafts, which received revision and contribution from my supervisors, Katharina Wollenberg Valero and Pedro Beltran-Alvarez as well as collaborators (see below for each chapter).

Chapter 2. Behavioural stress propagation in benthic invertebrates caused by acute pH drop-induced metabolites

Publication: Feugere, L., Angell, L., Fagents, J., Nightingale, R., Rowland, K., Skinner, S., Hardege, J., Bartels-Hardege, H. & Wollenberg Valero, K.C. (2021). Behavioural stress propagation in benthic invertebrates caused by acute pH drop-induced metabolites. *Front. Mar. Sci*. 8. doi: 10.3389/fmars.2021.773870.

Conference talk: Feugere, L., Angell, L., Fagents, J., Nightingale, R., Rowland, K., Skinner, S., Hardege, J., Bartels-Hardege, H. & Wollenberg Valero, K.C. (January 29th, 2021). Behavioural Stress Feedback Loops in benthic invertebrates caused by low pH-induced metabolites. Post-Graduate Day at the University of Hull.

Data availability statement: Data from Chapter 2 can be found online from the publisher.

Author statement: Katharina Wollenberg Valero designed the study. Experiments were performed by me, Lauren Angell, James Fagents, Rebecca Nightingale, Kirsty Rowland, Saffiyah Skinner, and Katharina Wollenberg Valero. I analysed the data and wrote the first manuscript draft with Katharina Wollenberg Valero, Jörg D. Hardege and Helga Bartels-Hardege. All authors contributed to the final manuscript.

Chapter 3. Thermal stress induces a positive phenotypic and molecular feedback loop in zebrafish

Publication: Feugere, L., Scott, V. F., Rodriguez-Barucg, Q., Beltran-Alvarez, P., and Wollenberg Valero, K. C. (2021). Thermal stress induces a positive phenotypic and molecular feedback loop in zebrafish embryos. *J. Therm. Biol.* 102, 103114. doi: 10.1016/j.jtherbio.2021.103114.

Data availability statement: Data from Chapter 3 can be found online from the publisher.

Author statement: Katharina Wollenberg Valero designed the study. Preliminary experiments were performed by Victoria Scott. I conducted experiments, analysed the data, and wrote the first manuscript draft with Katharina Wollenberg Valero. All authors contributed to the final manuscript.

Chapter 4. Heat induces multi-omic and phenotypic stress propagation in zebrafish embryos

Publication: Feugere, L., Bates, A., Emagbetere, T., Chapman, E., Malcolm, L., Bulmer, K., Hardege, J., Beltran-Alvarez, P., Wollenberg Valero, K.C., Heat induces multiomic and phenotypic stress propagation in zebrafish embryos (2023). Accepted in PNAS Nexus on April 11, 2023 (https://doi.org/10.1093/pnasnexus/pgad137). Preprint available on bioRxiv 2022.09.15.508176; doi: https://doi.org/10.1101/2022.09.15.508176.

Data availability statement: Processed datasets are available in the Supplementary Material along with the published manuscript at https://doi.org/10.1093/pnasnexus/pgad137.

Raw data are available: Feugere L, et al. 2023. Data for: Heat induces multiomic and phenotypic stress propagation in zebrafish embryos (Version v1) [Dataset]. https:/doi.org/10.5281/zenodo.7308630.

Sequencing data are available under the GEO accession number GSE220546 (https://www.ncbi.nlm.nih.gov/geo/query/acc.cgi?acc=GSE220546).

Conference talk: Feugere, L., Bates, A., Emagbetere, T., Hardege, J., Beltran-Alvarez, P., Wollenberg Valero, K.C., (June 30th, 2022, 20-minute presentation). Stress Your Neighbour! Molecular And Phenotypic Evidence That Zebrafish Embryos Chemically Propagate Heat Stress To Each Other. 14th International Congress on the Biology of Fish (ICBF2022), Montpellier, France. Session: Sensing the Environment: Molecules to Populations (Sensing the Anthropocene).

Author statement: Katharina Wollenberg Valero and Pedro Beltran-Alvarez designed the study. Adam Bates and I optimised RNA extraction and sequencing analysis protocols. I conducted laboratory experiments and analysed behavioural and multi-omic data. Emma Chapman and Timothy Emagbetere obtained LAMP data. Katharina Wollenberg Valero performed cross-comparison analysis with hair cell data (Elkon et

al., 2015). Adam Bates designed LAMP experiments and calculations. Linsey Malcolm, Kath Bulmer, and Pedro Beltran-Alvarez conducted HSP70 measurements. Jörg D. Hardege guided metabolomic experiments. I wrote the chapter draft and Pedro Beltran-Alvarez and Katharina Wollenberg Valero contributed to revisions. All authors agreed on the final draft.

Chapter 5. Consequences of directly- and indirectly-experienced heat stress in a mutagenic environment

Publication: Feugere, L., Silva, C., Bates, A., Storey, K., Beltran-Alvarez, P., Wollenberg Valero, K. Consequences of directly- and indirectly-experienced heat stress in a mutagenic environment. (*Manuscript under review*)

Data availability statement: Data from Chapter 5 will be made publicly available upon publication of the manuscript version. Processed data will be available with the published article on the publisher's website. Raw data will be available on Zenodo (DOI: 10.5281/zenodo.7566285). Sequencing data will be available under the accession number GSE223685.

Author statement: Katharina Wollenberg Valero designed the study. I performed laboratory experiments, software analyses, and statistical analyses. I wrote the chapter draft and Kenneth Storey, Pedro Beltran-Alvarez, and Katharina Wollenberg Valero contributed to revisions. Adam Bates and I optimised RNA extraction and sequencing data analysis protocols. All authors agreed on the final draft.

Table of Content

List of Figures

List of Tables

List of Acronyms

Treatments:

C: control (unstressed individuals) in fresh E3 medium

TS: repeated thermal stress

pH drop: drop of pH from 8.1 to 7.6

SM: stress metabolites/medium

CM: control metabolites/medium

Other acronyms:

AB: inbred laboratory zebrafish strain and **PET:** outcrossing, non-laboratory strain

ANOVA: analysis of variance

ATP: adenosine triphosphate

CNS: Central Nervous System

CSR: Cellular Stress Response

DEGs: Differentially Expressed Gene

FC: Fold-Change and **LFC**: log Fold-Change

GSTs: Glutathione-S-Transferases

GO: Gene Ontology

hpf: hours post fertilisation and **dpf**: days post fertilisation

HSP: Heat Shock Proteins and **HSR**: Heat Shock Response

HPI: Hypothalamus-pituitary-interrenal

IL-1β: interleukin-1β

LAMP: Loop-Mediated Isothermal Amplification

LEL: longest embryo length and **SEL**: shortest embryo length

NMD: nonsense mediated decay

PCA: principal component analysis

PERMANOVA: permutational multivariate ANOVA

RIN: RNA integrity number

SCCs: Solitary Chemosensory Cells

SOD: superoxide dismutase

SQOR: sulfide:quinone oxidoreductase

VOCs: volatile organic compounds

Glossary

"Language of abiotic stress": ensemble of chemical cues and genes that are used to propagate information about risks of abiotic stress between aquatic animals.

Stress communication: mechanism of chemical communication between two individuals wherein at least one individual is directly exposed to an abiotic stressor.

Stress metabolites (SM): infochemicals released into the environment specifically upon abiotic stress. Analogous to **stress odours** (in mammals) and **phytohormones** (in plants, e.g., **volatile organic compounds**, VOCs). **Stress Medium** contains putative stress metabolites.

Control metabolites (CM): chemicals, such as metabolic wastes, released by unstressed animals, as part of their basal metabolism. **Control Medium** contains putative control metabolites.

Donor: animal directly exposed to abiotic stressors, and that releases stress metabolites.

Naïve receiver: animal that is naïve to the abiotic stress but is exposed to stress metabolites released by a donor, which is equivalent to an indirect abiotic stress exposure.

Conditioned medium/water: water containing putative metabolites released by a donor exposed to an experimental condition.

Stress propagation: characterises the presence of a stress response in both the donor and the receiver of stress metabolites.

Positive feedback loop: positive directionality of stress propagation, where the stress responses of stress metabolite receivers are similar to the stress responses of donors directly stressed by an abiotic stressor.

Infochemical: chemical cue that conveys information between organisms.

Semiochemical: infochemicals released by one animal to alter the behaviour or physiology of its receiver.

Pheromone: semiochemical acting between organisms of the same species (conspecifics).

Allelochemical: semiochemical acting between organisms of different species (heterospecifics).

Alarm cues: infochemicals released by animals injured upon biotic stress (predation) that induce anti-predatory behaviours in receivers.

Disturbance cues: infochemicals released by animals startled by biotic stress (e.g., predation) that increase alertness in receivers.

Hormesis (or hormetic effect): low dose stimulating effect of stress, which improves resistance to subsequent stress at levels higher than in unstressed individuals.

Chapter 1. General Introduction

In aquatic environments, organisms face environmental stressors, particularly in a changing climate. Aquatic animals must cope with these stressors through a range of responses from subcellular levels to phenotypes to populations and ecosystems. Prior studies evidenced that animals utilise chemical cues to propagate predation risk information to neighbouring individuals. Such communication upon biotic stress paved the way to a novel question, which I address in this Ph.D. thesis: can stress propagation can be extended to abiotic stressors? If this is the case, then it may have dramatic effects in aquatic species because stress responses would be amplified beyond the individual level. However, one needs to understand the direct effects of abiotic stressors and the mode of chemoperception in aquatic animals before exploring the mechanistic basis of stress propagation. For this purpose, the following paragraphs will introduce the concepts of stress responses and chemical communication in aquatic species before outlining the aims of this Ph.D. thesis.

1.1. Stress in aquatic animals

1.1.1. Stressors in a changing climate: rising temperatures and ocean acidification

All living organisms must maintain an optimal and stable physiological state, referred to as homeostasis (McEwen and Wingfield, 2003). Extrinsic and intrinsic factors challenging this homeostasis are called stressors. When perceiving stressors, aquatic animals activate stress responses to restore their homeostasis (Moberg, 2000; Chrousos, 2009; Clark et al., 2011; Schreck and Tort, 2016). Aquatic animals face environmental and anthropogenic stressors of biotic and abiotic nature, both in the natural environment and in aquaculture settings (Iwama et al., 2004; Schulte, 2007). Biotic stress represents interactions between living organisms (invasive species, pathogens and predators) (Gutha et al., 2018). Abiotic stressors include chemical and physical alterations in water parameters, such as dissolved oxygen, temperature, pollutants, and pH (Iwama et al., 2004; Storey and Storey, 2011; Gutha et al., 2018). Two stressors of major interest with respect to climate change are temperature, since ectotherms cannot regulate their internal temperature (Scott and Johnston, 2012); and pH levels, which alter the water carbonate chemistry (Zeebe, 2012). The warming of the climate is unequivocal and caused by anthropogenic activities releasing greenhouse gases such as carbon dioxide (CO_2) into the atmosphere (Doney et al., 2009; IPCC, 2014). The ocean absorbed thirty percent of this atmospheric CO_2, lowering its average

surface water pH by 0.1 unit (from 8.2 to 8.1) since the industrial revolution. This is known as "ocean acidification" (Feely et al., 2004; Doney et al., 2009; Zeebe, 2012; IPCC, 2014). Ocean acidification is expected to lower pH levels by another 0.3 pH unit by the end of the century (Caldeira and Wickett, 2003; Sabine et al., 2004; Pörtner et al., 2019). The Earth's mean global temperature has increased by 0.68°C since the industrial era, and will rise by another 1.6°C to 4.3°C by the end of the century, depending on scenarios (Pörtner et al., 2019). Superimposed to the increase in mean temperatures, the warming of the climate will be characterised by fluctuating and extreme thermal conditions (IPCC, 2014; Colinet et al., 2015), which will become more frequent, intense, and last longer (Vasseur et al., 2014; Pörtner et al., 2019).

It is therefore of the utmost importance to understand the biological responses of aquatic animals to abiotic stressors to better predict their fate in an increasingly stressful aquatic environment. In fish, temperature drives all physiological, biochemical, and life-history processes (Beitinger et al., 2000), including behaviour (Almeida et al., 2015), development (Schröter et al., 2008), metabolism (Simčič et al., 2015), morphology (Georgakopoulou et al., 2007), mortality (Jungwirth and Winkler, 1984), and reproduction (Abozaid et al., 2011). Fish early developmental stages are most vulnerable to heat stress due to their "bottleneck effect" controlling fish population dynamics (Kamler et al., 1998; Madeira et al., 2016a; Dahlke et al., 2020a, 2020b). Tropical fish species may be more vulnerable to heat stress than temperate species as they live closer to their thermal limits and have a less plastic thermal tolerance (Nati et al., 2021). Likewise, ocean acidification threatens aquatic animals, from marine invertebrate behaviour (Clements and Hunt, 2015; Clements and Darrow, 2018) to fish physiology (Heuer and Grosell, 2014). Furthermore, aquatic animals may face multiple stressors in the environment, which may have interactive effects on their health (Brown et al., 2015). For instance, ultraviolet radiation combined with other stressors can have synergistic negative effects on the biology of fish (Alves and Agustí, 2020). To survive such stressors, all organisms use stress-coping strategies (Cockram, 2002; Romero et al., 2009). These stress responses are integrated across several organisational levels: molecular, cellular, tissues, whole-body, populations and ecosystems (Skomal and Mandelman, 2012) (**Figure 1.1**).

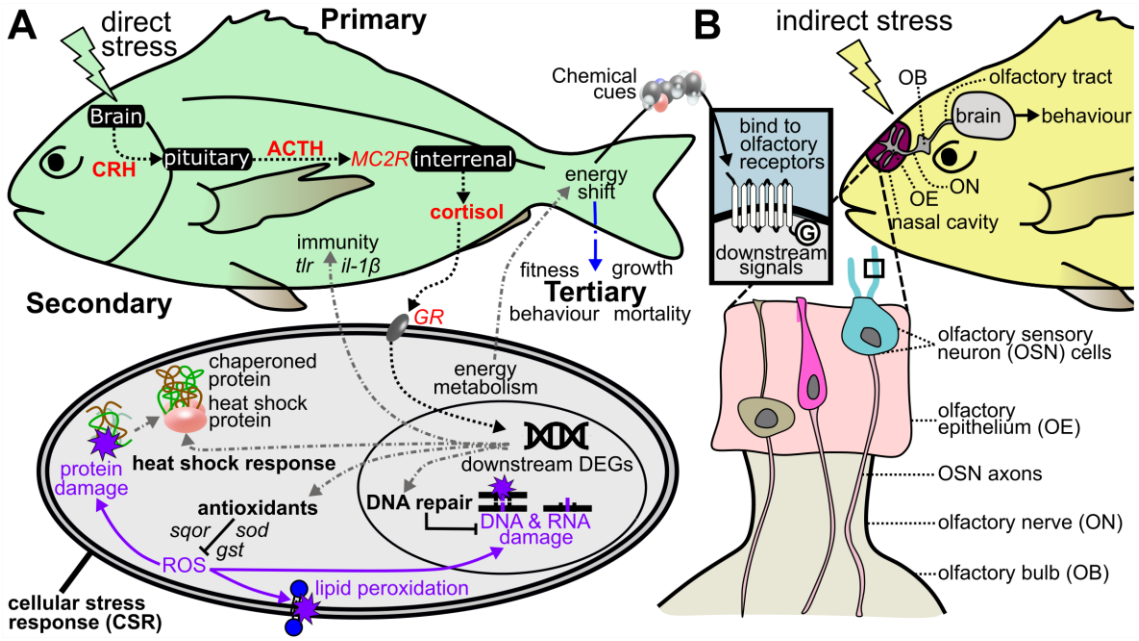

Figure 1.1. Stress response and chemical communication in fish. A) Stress response in fish (see section 1.1.2 for details). CRH: corticotropin releasing hormone, ACTH: adrenocorticotropic hormone, GR: glucocorticoid receptors, DEGs: differential gene expression MC2R: melanocortin 2 receptor, ROS: reactive oxygen species. Five genes of interest are represented, including interleukin-1β (*il-1β*), toll-like receptors (*tlr*), heat shock proteins, glutathione-s-transferase (*gst*), superoxide dismutase (*sod*), and sulfide:quinone oxidoreductase (*sqor*). Adapted from Schreck and Tort (2016). B) Stress-induced chemical cues may activate olfactory receptors in olfactory cells, transmitting signals towards the brain and eliciting behavioural responses (see section 1.2.3 for details). Adapted from Ferrando and Gallus (2013), Kermen et al. (2013), and Shinohara and Kobayashi (2020).

1.1.2. Stress response: from cortisol to transcriptomes to phenotypes

To explore the mechanism of stress propagation, it is firstly necessary to confirm that donors are stressed by the abiotic stressor, as a baseline for comparison with indirectly-stressed receivers. One species in which the stress axis is best described is zebrafish (*Danio rerio*), including at early stages (Alsop and Vijayan, 2009a; Eachus et al., 2021). The stress response can be subdivided into primary, secondary and tertiary responses (Iwama, 1998; Iwama et al., 2004; Schreck and Tort, 2016) (**Figure 1.1A**).

1.1.2.1 Primary response

The primary response involves neuroendocrine reactions to threats (Gamperl et al., 1994a; Skomal and Mandelman, 2012; Schreck and Tort, 2016). In fish, the stress response is mainly directed by the hypothalamus-pituitary-interrenal (HPI) axis (Denver, 2009; Steenbergen *et al.*, 2012). Parallel to the HPI axis, the adrenergic stress response of teleosts involves the hypothalamus-sympathetic system-chromaffin tissue (HSC) axis for the immediate release of catecholamines (e.g. noradrenaline and adrenaline) that readjust heart rates for oxygen and substrate mobilisation (Conde-Sieira et al., 2018;

Kalamarz-Kubiak, 2018; Souza et al., 2019). Upon stress recognition in the central nervous system (CNS), the hypothalamus secretes the corticotropic releasing factor (CRF), which mediates the release of adrenocorticotropic hormone (ACTH) by corticotrophic cells (Alsop and Vijayan, 2009b). ACTH binds to its receptor melanocortin 2 receptor (MC2R) in interrenal cells to activate cortisol secretion into the circulation (Alsop and Vijayan, 2009b) (**Figure 1.1A**). Cortisol levels increase in responses to most stressors, such as handling, UV, and temperature stress in zebrafish (Ramsay et al., 2009; Bai et al., 2016; Sua-Cespedes et al., 2021). Zebrafish embryos first use maternal cortisol deposits, before *de novo* synthesis begins around 2-4 days post fertilisation (dpf) (Alderman and Bernier, 2009; Alsop and Vijayan, 2009b; Eto et al., 2014). The binding of corticosteroids to glucocorticoid receptors (GRs) transfers downstream signals towards target genes, causing stress-induced transcriptomic changes (Schulte, 2007; Aluru and Vijayan, 2009). Cortisol therefore plays central roles in immunity, osmotic regulation, and the metabolism of glucose, proteins, and lipids (Gamperl et al., 1994b; Schulte, 2007; Alsop and Vijayan, 2008). Importantly, alterations in the HPI axis during early development may have "programming" effects on later life stages (Auperin and Geslin, 2008; Best et al., 2017), highlighting the importance of studying the stress response of early fish stages.

1.1.2.2 Secondary response

Downstream to the primary response, a range of physiological and cellular changes take place during the secondary response (Gamperl et al., 1994a; Iwama et al., 2004; Schreck and Tort, 2016). These involve cardiovascular, respiratory, and metabolic adjustments to mobilise energy substrates towards energetically demanding cellular stress responses (Rodnick and Planas, 2016; Schreck and Tort, 2016). The Cellular Stress Response (CSR) is a conserved mechanism involving the upregulation of molecular chaperone heat shock proteins (HSPs) during the heat shock response (HSR) (Pirkkala et al., 2001; Iwama et al., 2004; Logan and Buckley, 2015). HSPs repair stress-induced misfolded and damaged proteins that threaten the integrity of cells (Morimoto, 1998; Feder and Hofmann, 1999; Bowler, 2005). HSPs are evolutionary conserved proteins synthesised in all organisms exposed to abiotic (e.g. temperature, hypoxia) and biotic stressors (e.g. predators, pathogens) of sufficient intensity (Krone et al., 1997; Feder and Hofmann, 1999; Basu et al., 2002). Interestingly, HSPs activated by one stressor may enhance the resistance to subsequent stress exposure at levels exceeding the response of untreated individuals. This phenomenon is termed hormesis

(Basu et al., 2002; Calabrese et al., 2007; Berry and López-Martínez, 2020). Stressors lead to the accumulation of reactive oxygen species (ROS) altering the cellular redox status and causing "oxidative stress" (Kassahn et al., 2009; Madeira et al., 2016c; de Barros and Paula-Lopes, 2018). Oxidative species degrade cellular components from lipids to proteins to nucleic acids, leading to apoptosis (Kassahn et al., 2009; Lushchak, 2011; Dutta et al., 2018). The antioxidant system alleviates oxidative stress by capturing reactive species to limit cellular damage (Martínez-Álvarez et al., 2005; Madeira et al., 2016b). Antioxidants may include the glutathione (GSH) pathway involving glutathione-s-transferases (*gst*) (Hayes and McLellan, 1999; Timme-Laragy et al., 2013), superoxide dismutase (*sod*) and catalase (*cat*) (Fridovich, 1995; Atli et al., 2016; Madeira et al., 2016c; Shi et al., 2022), but also sulfide:quinone oxidoreductase (*sqor*) (Wollenberg Valero et al., 2021). Ocean acidification forces aquatic animals to maintain CO_2 excretion by increasing extracellular H^+, chloride (Cl^-), and bicarbonate (HCO_3^-) concentrations, which lowers extracellular pH levels and causes internal acidosis. This altered acid-base impairs calcification, protein synthesis, and ventilation rate processes (Pörtner, 2008; Esbaugh, 2018). In turn, ocean acidification may alter behaviour by impairing brain functions through the reversal of the cellular transport of gamma-aminobutyric acid (GABA) neurotransmitters (Tresguerres and Hamilton, 2017) and by modifying the pH-dependant conformation of odorant receptors and downstream signalling (Porteus et al., 2021). In response to these stress-induced cellular and physiological changes, aquatic animals may show alterations in gene transcription (Long et al., 2012) and genetic pathways involved in cell cycle (Kassahn et al., 2007), DNA repair (Kim et al., 2021), immunity (Mariana and Badr, 2019), metabolism (Beemelmanns et al., 2021), and growth (Jesus et al., 2016) (**Figure 1.1A**). However, repeated exposure to acute stress can desensitise the stress axis and impair physiological pathways, lowering the threshold for pathological effects (Barton, 2002; Alfonso et al., 2020; Brandl et al., 2022). For instance, repeated heat stress attenuates the heat shock response of lake whitefish embryos *Coregonus clupeaformis* (Whitehouse et al., 2017).

1.1.2.3 Tertiary response

In turn, physiological and metabolism shifts mediate changes at whole-body and population levels, as part of the tertiary response (Iwama, 1998; Donaldson et al., 2008; Schreck and Tort, 2016). Stress may alter fish behaviour, including locomotion, sociality, anxiety, boldness, and escape responses (Alfonso et al., 2020; Angiulli et al., 2020; Killen, 2020; Nonnis et al., 2021; Otsuka et al., 2022). Thermal stress can alter

development, which is delayed at low temperatures and accelerates at high temperatures (Kamler et al., 1998; Schröter et al., 2008). This heat-induced faster growth can produce smaller fish and advance the onset of hatching resulting in premature embryos (Kamler et al., 1998; López-Olmeda and Sánchez-Vázquez, 2011). Temperature stress can also impair fish external morphology (Georgakopoulou et al., 2007), the number and shape of vertebrae (Wargelius et al., 2005; Schmidt and Starck, 2010), heart shape (Dimitriadi et al., 2018), and body composition (Long et al., 2012). Ocean acidification may alter fish and invertebrate behaviours from feeding to predator escape to anxiety. Nevertheless, contrasting negative, null, or positive effects were reported depending on phyla, stages, and exposure duration (Clements and Hunt, 2015; Clements and Darrow, 2018). Arthropods may be more resilient to acidified conditions through efficient feeding strategies and acid-base regulation (Appelhans et al., 2012; Clements and Darrow, 2018). The effects of ocean acidification on fish behaviour exist (Jutfelt et al., 2013) but may have been overestimated in prior research (Clements et al., 2022). Extreme stressors and/or mutagens such as heat and UV radiation may cause severe malformations leading to mortality (Pype et al., 2015; Icoglu Aksakal and Ciltas, 2018; Genin et al., 2020) (**Figure 1.1A**). Since population dynamics are governed by the reproduction, growth, and mortality of its individuals, cumulating such behavioural and physiological alterations can put populations at risk in both aquaculture and natural environments (Barton and Iwama, 1991; Power, 1997). However, stress responses are energetically costly. Therefore, natural selection may have favoured animals that recognise chemical cues released by stressed animals as risk information, and respond to it (e.g. by moving away) to improve their fitness (Crane et al., 2022). As a result, the effects of abiotic stressors can scale up to the group level through chemical communication (Brandl et al., 2022).

1.2. Stress and communication

1.2.1. Chemical communication: concepts and definitions

Chemical communication requires an emitter (donor), a receiver, and an environment to transmit information (Venuleo et al., 2017). Infochemicals are chemical cues that convey such information between organisms (Dicke and Sabelis, 1988; Sbarbati and Osculati, 2006). Semiochemicals are infochemicals released by one animal to alter the behaviour or physiology of its receiver (Regnier, 1971; Dicke and Sabelis, 1988; Sbarbati and Osculati, 2006). Semiochemicals are categorised as pheromones for within-species communication (Karlson and Lüscher, 1959a, 1959b) and

allelochemicals for cross-species interactions (Nielsen et al., 2015). Pheromones evoke specific developmental processes and behaviours in their receivers (Karlson and Lüscher, 1959a, 1959b). Allelochemicals are odours released by one species that alter the growth, health, and behaviour in another species (Whittaker and Feeny, 1971; Dicke and Sabelis, 1988; Sbarbati and Osculati, 2006).

1.2.2. Stress signalling in nature: alarm, disturbance, and stress cues

1.2.2.1 Stress propagation

This Ph.D. thesis focuses on the propagation of stress between abiotically-stressed aquatic animals. Similar concepts of chemical communication exist in different fields of biology, under many names: xenohormesis (Howitz and Sinclair, 2008; Hooper et al., 2010), danger communication (Brechbühl et al., 2013), chemical empathy or stress information transfer (Bombail, 2019), social contagion or stress transmission (Brandl et al., 2022), and bystander effect (Choi et al., 2010, 2013; Mothersill et al., 2018; Fernandes et al., 2020). Here, the transmission of stress responses from an individual directly exposed to abiotic stress to a naïve animal will be termed "**stress propagation**". If phenotypes are similar in donors and receivers; and if group stress responses are amplified (Brandl et al., 2022), this then warrants designation as "**positive feedback loops".** Likewise, many names exist for the chemicals involved in stress propagation, including distress signals (Bombail, 2019), alarm cues (Ferrari et al., 2010), disturbance cues (Crane et al., 2022), or stress odours (Bombail et al., 2018). Alarm cues are released when animals are injured upon predation (Ferrari et al., 2010) and disturbance cues when they are "startled but not injured" (Ferrari et al., 2010; Crane et al., 2022). However, "startled" means "surprised and slightly frightened" (Cambridge Dictionary). This term seems suitable for predation-induced chemical communication, which has received the most focus (Crane et al., 2022). However, abiotic stress can (i) be introduced gradually and persist over longer periods of time than instantaneous predation events, (ii) induce chronic stress responses in animals and (ii) result in the non-intentional release of metabolic by-products into the environment. Therefore, I propose the term "**stress metabolites"** for chemicals released, intentionally or not, by an animal in response to abiotic stressors; and that propagate stress responses to others. Scarantino (2010) proposes that animal signals are simply informative of an event – for instance "a predator is here!". By analogy, stress metabolites may be honest information that means "this environment is stressful!". However, compounds involved in predation (alarm cues), biotic stress (disturbance cues), and abiotic stress (stress metabolites) and

any other type of chemical communication may overlap, since these cues are rarely chemically identified.

1.2.2.2 Alarm signalling

Amongst the most studied cases of stress propagation are antipredatory responses induced by damage-released alarm cues (Ferrari et al., 2010; Crane et al., 2022). Karl von Frisch (1938; 1942) first discovered that European minnow *Phoxinus phoxinus* were frightened and swam away (*Schreckreaktion*) from "frightening substances" (*Schreckstoff*) released by one injured fish. In this example, alarm cues are released from mechanically-damaged epidermal club cells of predated and injured fish, and induce antipredatory responses in receivers to reduce predation risk to the group (Ferrari et al., 2010; Mathuru, 2016; Wisenden, 2019). Therefore, alarm cues are viewed as "public information" in the form of involuntarily-released injury by-products that inform receivers of predation threat (Ferrari et al., 2010). Smith (1992) conceptualised this phenomenon as "alarm signalling", which exists across taxa from insects to fish (Regnier, 1971; Smith, 1992; Ferrari et al., 2010). Marine invertebrates also use alarm signalling. For instance, marine polychaetes *Nereis virens* showed alarm reactions to conspecific alarm cues (Watson et al., 2005) and *Hediste diversicolor* detected chemical cues from predator fish (Schaum et al., 2013).

1.2.2.3 Disturbance cues

Disturbance cues are another class of stress information chemicals, released by startled or disturbed preys (Ferrari et al., 2010; Crane et al., 2022). These chemical cues may inform members of group-living animals about predation danger (Bairos-Novak et al., 2017). However, disturbance cues may be less potent than alarm cues and simply increase their receivers' vigilance (Jordão, 2004; Ferrari et al., 2010; Gonzalo et al., 2010). Disturbance cues thus function as "early warning" signals (Wisenden et al., 1995; Kiesecker et al., 1999; Vavrek et al., 2008; Brown et al., 2012; Crane et al., 2022). Disturbance cues exist in arthropods – including insects (Siepielski et al., 2016; Yost et al., 2021) and decapods (Hazlett, 1990b, 1990a); echinoderms (Nishizaki and Ackerman, 2005), amphibians (Bairos-Novak et al., 2017), and fishes (Wisenden et al., 1995; Jordão, 2004) including zebrafish (Oliveira et al., 2013; Barcellos et al., 2014; Abreu et al., 2016). For instance, intertidal hermit crabs *Calcinus laevimanus* increased their locomotion when detecting disturbance cues from conspecifics stressed by shell removal (Hazlett, 1990a). Vertebrates and invertebrates coexist in ecosystems,

suggesting that they chemically communicate to each other (Sbarbati and Osculati, 2006), including by cross-species and cross-taxa reactions to disturbance cues. Supporting this, disturbance cues from perch-like fishes *Ambloplites rupestris* and iowa darter *Etheostoma exile* as well as annelid leeches *Macrobdella decora* elicited stress propagation towards the crayfish *Orconectes virilis* (Hazlett, 1990b).

1.2.2.4 Abiotic stress-induced stress cues

Additionally to alarm (successful predation) and disturbance (predation risk) cues, organisms may use stress cues to signal general stress information. Such stress-induced chemicals are well studied in plants, which emit volatile organic compounds (VOCs or phytohormones) for within- (adjacent branches and leaves) and between-plant stress propagation that protect receivers against future stressors (Frost et al., 2007; Holopainen and Gershenzon, 2010; Allwood et al., 2021). These volatiles are termed herbivore-induced plant volatiles (HIPVs) when induced by grazing (Dicke and Baldwin, 2010), a concept resembling predation-induced alarm cues. Most studies focused on biotic stress and less on abiotic stress-induced interplant signalling (Landi, 2020) – just like in animal communication. Yet, many abiotic stressors, including temperature, may trigger the release of plant volatiles (Loreto et al., 2006; Meents and Mithöfer, 2020). For instance, stomatal closure was observed in plants directly exposed to drought or osmotic stress, but also in their neighbours connected by root-root communication, which the authors interpreted as an anticipatory response to the upcoming stress (Falik et al., 2012). Likewise, salt-stressed plants emitted phytohormones that increased receiver tolerance to saline stress, in basil *Ocimum basilicum* (Landi et al., 2020), broad bean *Vicia faba* (Caparrotta et al., 2018), and thale cress *Arabidopsis thaliana* (Lee and Seo, 2014). Microorganisms also use volatile compounds to transfer abiotic stress information from stressed or dying cells to prepare naive cells to stress (Pozzer et al., 2022). Interestingly, phytohormones from mite-infested Lima bean *Phaseolus lunatus* (Arimura et al., 2000) and virus-infected tobacco plants *Nicotiana tabacum* (Shulaev et al., 1997) activated the transcription of defence genes in naïve receivers; and receivers of UVC-induced volatiles showed genomic instability in *A. thaliana* and *N. tabacum* (Yao et al., 2011). This evidences that stress signals can induce changes at the transcriptomic and genetic level in receivers.

It is now well-established (i) that biotic stress induces interindividual alarm signalling both in plants (phytohormones upon herbivore stress) and animals (alarm cues upon predation), and (ii) that plants and microorganisms release bioactive stress

cues upon abiotic stress. However, there is little knowledge about the existence of abiotic stress-induced chemical communication in aquatic animals. In fact, it has been proposed that disturbance cues are released not only upon predation, but more generally when animals are stressed (Jordão, 2004). For instance, electric shock-induced "*Drosophila* stress odorants" (dSO) cause aversion in conspecifics (Yost et al., 2021). Stress signalling also exists in mammals experiencing social and physical stressors and is mediated by "stress odours" released in excreta (urine and faeces) and directly as airborne chemicals (Bombail et al., 2018; Bombail, 2019). Stress information may be transmitted through chemical cues that receivers interpret as the activation of the stress axis in donors (Brandl et al., 2022). For instance, cattles *Bos taurus* were less bold and increased cortisol levels in presence of electric-shocked conspecifics (Boissy et al., 1998). Similar stress propagation was shown in rodents exposed to physical stress and electric shocks (Moynihan et al., 2000; Kikusui et al., 2001; Sakuma et al., 2013; Inagaki et al., 2014; Bombail et al., 2018). Humans, too, react to stress odours and can detect whether mice were stressed (by shaking, fasting, or physical restraining) by recognising an impleasant sulfurous smell from their faeces containing stress-induced odours (Sakuma et al., 2013). Likewise, humans can transmit fear, stress, and anxiety information through their body odours (de Groot and Smeets, 2017). Another study revealed that the emotion-controlling brain zone, the amygdala, is activated when human subjects smelled skydiving stress-induced sweat – but not exercice-associated sweat – which the authors attributed to an alarm substance released by skydiving-stressed individuals (Mujica-Parodi et al., 2009). The evolutionary conserved stress system suggest that stress propagation is widespread across vertebrates (Brandl et al., 2022). Only very few examples of abiotically-induced stress propagation exist in aquatic species. For instance, chemicals released by heat-stressed crayfish *Orconectes virilis* increased alertness in receivers (Hazlett, 1985); and zebrafish avoided water conditioned by low pH-stressed conspecifics (Abreu et al., 2016) – although these effects have been ascribed to disturbance cues. However, Abreu and collaborators (2016) do not specify whether the conditioned water from pH-stressed zebrafish donors was buffered back to normal pH levels before being given to receivers, which would introduce the original pH drop stressor as a confounding variable in the receivers' avoidance to stress-conditioned water. Another type of abiotic stress propagation is the "bystander effect" where animals exposed to genotoxic stress (e.g., cadmium or irradiation) release chemical cues that propagate genotoxic effects to naïve fish and oligochaete (Choi et al., 2010, 2013; Mothersill et al., 2018; Fernandes et al., 2020).

1.2.3. Chemical communication: from signals to olfaction to behaviours

Chemical communication requires a biological machinery involving genes, RNA, proteins, and chemical messengers for the production, the release, and detection of chemical cues (Venuleo et al., 2017). Although waterborne cues are poorly characterised (Poulin et al., 2018), several compounds have been proposed as key mediators of chemical communication. Living organisms synthesise low-molecular weight molecules (< 900 Daltons), which can be non-volatile or become volatile if carrying polar groups (Hadacek, 2015) and can travel far from their source through water (Pozzer et al., 2022). Volatile organic compounds exist in aquatic animals (Fink, 2007), including sex pheromones in marine polychaetes *Arenicola marina* (Hardege et al., 1996) and *Platynereis dumerilii* (Zeeck et al., 1988), or parasite-attracting semiochemicals in fish *Salmo salar* (Ingvarsdóttir et al., 2002). Alarm signals should be highly volatile so that their short life spans limit their action once their function is served (Alberts, 1992). Peptides are another well-suited class of signalling chemicals in aquatic environment: animals have all the components to code, synthesise, and terminate such signals, which can be water soluble (Decho et al., 1998). Proteins, particularly small proteins, may function as pheromones in mammals (Singer, 1991). Likewise, both serotonin (Desban et al., 2022) and trypsin (Kim et al., 2009; Alsrhani et al., 2021) may act as alarm pheromone in fish as they are released upon stress and cause antipredatory behaviours in receivers. Whilst the chemistry of disturbance cues remains largely uncharacterised (Crane et al., 2022), they may involve cortisol (Vavrek et al., 2008), urea (Brown et al., 2012), ammonium (Kiesecker et al., 1999) or generalised metabolic by-products (Vavrek et al., 2008) – all of which may result from the primary and secondary stress responses. Disturbance cues may be excreted from the gills or the antennulae green glands in crustaceans (Hazlett, 1990b) and through the gills and urine in fish (Vavrek et al., 2008).

For chemoreception, fish utilise the olfactory, the diffuse chemosensory, and the gustatory (or taste) systems (Aurangzeb et al., 2021). Fish olfaction functions as follows: chemicals are detected by olfactory receptors expressed by different types of olfactory sensory neurons (OSNs) located in the olfatory epithelia (OE) in nostrils. OSNs project their axons via the olfactory nerve (ON) into the olfactory bulb (OB) and the olfactory tract to transmit downstream signals to the brain, which elicits behavioural responses (Hamdani and Døving, 2007; Hussain, 2011; Kermen et al., 2013; Calvo-Ochoa and Byrd-Jacobs, 2019) (**Figure 1.1B**). In contrast, marine annelid worms mainly use their

antennae to detect chemicals (Chartier et al., 2018), whilst crustaceans utilise long-range olfactory sensillae (or aesthetascs) on their antennulae as well as short-range chemosensory sensillae distributed over their entire body and concentrated on the antennae, mouthparts, and legs (Hallberg and Skog, 2010). Fish possess four types of olfactory receptors, each specialised in detecting distinct classes of chemicals. Olfactory receptors include odorant receptor (ORs), trace amine-associated receptors (TAARs), as well as vomeronasal receptors such as V1R (*ora* family) and V2R (*olfC* family) – the latter inducing fright reactions in fish (Korsching, 2008; Cong et al., 2019; Yang et al., 2019; Kowatschew et al., 2022). Upon binding, an odorant alters the conformation of its transmembrane receptor, which activates an intracellular secondary messenger that binds to its channel to influx calcium ions, resulting in the depolarisation of the olfactory sensory neuron (Aurangzeb et al., 2021) – a discovery for which Linda Buck and Richard Axel won the Nobel Prize in 2004 (Buck and Axel, 1991; Buck, 2005). In turn, the olfactory system allows fish to feed, migrate, reproduce, and recognise their kins (Aurangzeb et al., 2021). Fish also possess a diffuse (i.e. not structured as organs) chemosensory system composed of solitary chemosensory cells (SCCs), in the epithelia of their gills, head and body skin, and oropharynx (Whitear, 1971; Sbarbati and Osculati, 2003). SCCs may recognise a wide variety of chemical cues (Aurangzeb et al., 2021) and may act as a "bulk-water sampling system" to detect other fish nearby (Kotrschal, 1996). Furthermore, specialised sensory hair cells organised in neuromasts distributed along the lateral line system, a mechanosensory structure that detects water movement (Bleckmann and Zelick, 2009; Mogdans, 2019). However, recent research uncovered an unexpected chemosensory function to the lateral line system (Mojib et al., 2017; Desban et al., 2022).

Most studies on biotic stress signalling focused on adult and juvenile life stages (Crane et al., 2022). Early developing stages of aquatic animals are also capable of chemical communication as they respond to alarm cues (Oulton et al., 2013; Atherton and McCormick, 2015, 2017; Poisson et al., 2017) and disturbance cues (Siepielski et al., 2016; Bairos-Novak et al., 2017), even within their eggs (Mezrai et al., 2020). This suggests that aquatic animals innately react to semiochemicals (Magellan et al., 2020). Zebrafish embryos also showed reaction to alarm cues as early as 12 hours post fertilisation (Lucon-Xiccato et al., 2020). In zebrafish embryos, the olfactory system develops within the first 24 hours (Handsen and Zeiske 1993), whilst solitary chemosensory cells appear at 3 days (around hatching), and taste buds appear with the

onset of exogenous feeding at 5 days (Kotrschal et al., 1997). However, little is known about the capacity of fish embryos and larvae to use abiotic stress-induced cues. If they do, the presence of specialised chemoreceptor cells in zebrafish embryos makes olfactory receptors good candidate structures to detect such stress cues.

1.2.4. Alteration of chemical communication in a changing environment

In an era of fast-changing environments, there is an urgent need to understand stress propagation between organisms (Landi, 2020) to predict population dynamics in response to climate change. The impairment of chemical communication by anthropogenic disturbance is termed "infodisruption" (Lürling and Scheffer, 2007) and makes animals "nose-blind" (Roggatz et al., 2022). Environmental stressors can alter (i) the production of the signal, (ii) the release and transport of chemical cues, (iii) their interaction with receptors, and (iv) downstream signal transduction and translation leading to (v) changes of the receivers' responses (Schirrmacher et al., 2021; Roggatz et al., 2022). For instance, at higher temperatures, poorly-fed marine tropical fish *Pomacentrus moluccensis* lost efficiency in producing alarm cues (Lienart et al., 2016) and Qinling lenok fish (*Brachymystax lenok tsinlingensis*) failed to react to alarm substances (Xia et al., 2021). This suggests that warming may alter stress propagation. Likewise, a lower pH deactivates certain chemical alarm cues in fish (Ferrari et al., 2010). Several experiments by Leduc and colleagues (2003, 2004, 2006, 2007) evidenced that acidic pH disrupts alarm signalling in perciforms (pumpkinseed *Lepomis gibbosus* and green sunfish *L. cyanellus*) and salmonids (Atlantic salmon *Salmo salar* and rainbow trout *Oncorhynchus mykiss*). Chivers et al (2013) correlated peaks in temperatures, UV radiations, pH, and oxygen levels with faster degradation times of alarm cues. Similar to predator or food odours, both warming and ocean acidification may impair the detection of stress cues. Moreover, animals in the natural environment may encounter stress cues simultaneously with abiotic stressors, which led me to explore the effects of stress metabolites combined with heat and pH stressors in this thesis.

1.3. Objectives, hypotheses, and rationale of the thesis

Alarm cues and disturbance cues released upon biotic stress received the most attention in prior work about stress communication. In contrast, since Hazlett's first report (1985) of heat stress propagation in crayfish, abiotic stress-induced communication has been largely overlooked in aquatic animals – despite the far-

reaching implications that stress propagation would have in species living in increasingly stressful aquatic environments. Therefore, the main knowledge gap addressed in this Ph.D. thesis was to explore the "language of abiotic stress" by determining whether abiotic stressors can trigger stress communication. The three main hypotheses of this Ph.D. thesis are that **(i)** donors are stressed by abiotic stressors which shift their molecular and physiological status, **(ii)** triggering the release of stress-specific cues into their environment, **(iii)** that transmit stress information to receivers, in turn also showing stress responses (**Figure 1.2**).

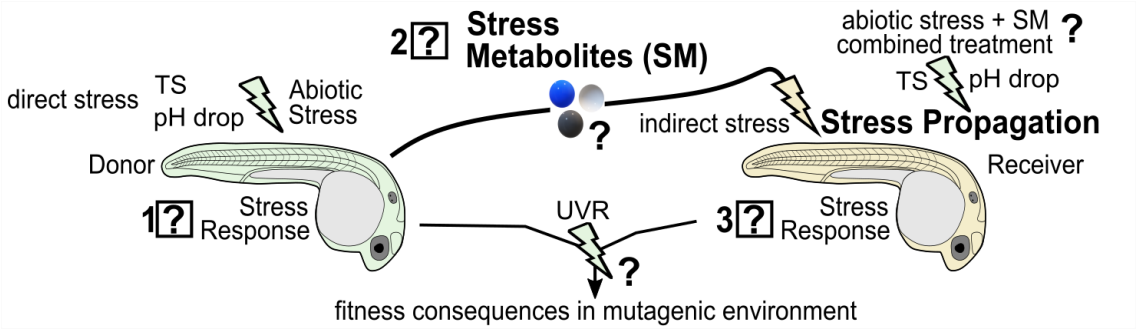

Figure 1.2. Main hypotheses of metabolite-mediated stress propagation. Schematic of the three main hypotheses to test (squared ? symbols): abiotic stressors initiate stress responses (1) in directly-stressed donors which release stress metabolites (SM, 2) that trigger a similar stress response in receivers (3).

To test these hypotheses, I combined multi-omic and phenotypic approaches to unravel the molecular and phenotypic responses of directly abiotically-stressed donors and naïve receivers of stress metabolites. The main objectives of this Ph.D. thesis were fivefold:

(i) To explore the stress response of individuals directly exposed to abiotic stressors, to identify pathways that lead to the synthesis of stress metabolites.

(ii) To characterise the chemical nature of stress metabolites released specifically by abiotically-stressed donors and not by control individuals.

(iii) To identify the molecular pathways activated by stress metabolites in receivers.

(iv) To evaluate the significance of stress communication by exploring the fitness outcomes of stress metabolite receivers.

(v) To evaluate the significance of abiotic stress and stress propagation by combining abiotic stressors and stress metabolites when faced with a mutagenic environment.

In addition to exploring the mechanistic basis of abiotic stress communication, I aimed to evaluate the extent of this phenomenon by investigating different species,

developmental stages, and two stressors: pH drop associated with ocean acidification and repeated thermal stress linked to increased heat events (**Figure 1.3)**.

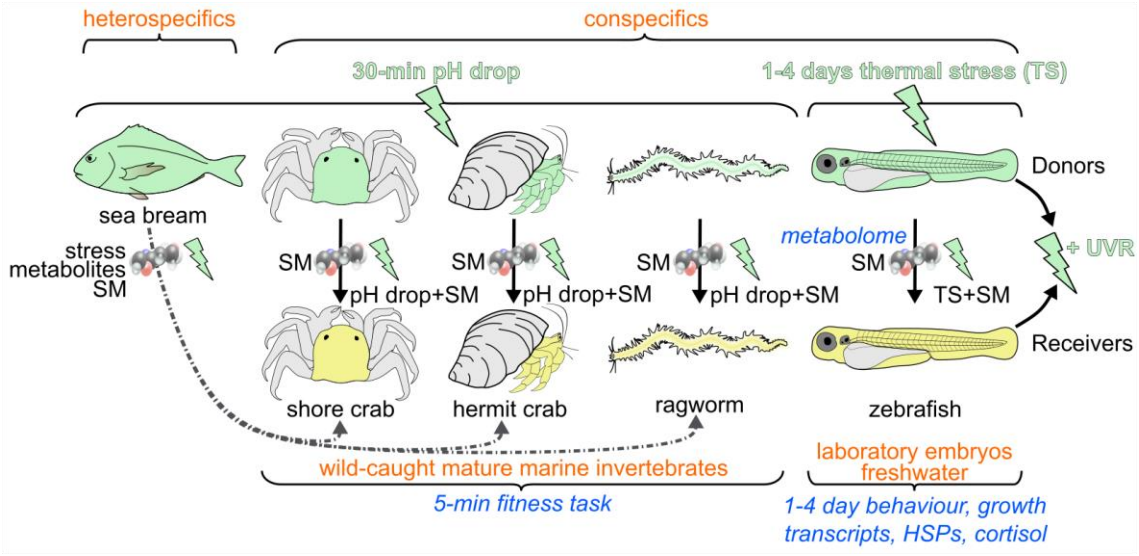

Figure 1.3. Experimental testing of stress metabolite-mediated stress propagation, using several endpoints (blue italic font) in different models (orange font, left to right: sea bream *Sparus aurata*, shore crab *Carcinus maenas*, hermit crab *Diogenes pugilator*, ragworm *Hediste diversicolor*, and zebrafish *Danio rerio*). This project tested the hypothesis that two abiotic stressors (heat and pH drop, in green) can cause stress propagation between directly-stressed donors (green, top row) towards receivers (yellow, bottom row) exposed to stress metabolites released by conspecifics (black solid arrows) or heterospecifics (grey dot-dash arrows). Combined conditions (pH drop+SM and TS+SM) were also tested. The effects of abiotic stress and stress metabolites were tested in a mutagenic environment (ultraviolet radiations, UVR) in zebrafish.

Chapter 2 is a proof-of-concept experiment showing that water conditioned by conspecifics and heterospecifics stressed by abiotic stress, here ocean acidification-related pH drop, can alter the response of receivers. In this experiment, individuals of three wild-caught benthic invertebrate marine species were used to measure fitness-relevant outcomes during short-time (5 min) behavioural assays.

Chapter 3 brought findings from **Chapter 2** into the laboratory by exposing another species and life stages, zebrafish embryos and larvae, to another stressor: repeated heat stress. This chapter confirmed that heat-induced stress metabolites influenced embryonic growth and behaviour. The involvement in stress propagation of three candidate genes was evaluated using quantitative PCR.

Chapter 4 explored "the language of abiotic stress" by unravelling the molecular mechanisms of stress propagation both in donors and receivers of stress metabolites, using RNA-sequencing and metabolomics. Zebrafish were observed at 1- and 4-days

post fertilisation (dpf) to measure the phenotypic effects of abiotic stress and stress propagation from early embryos to larval stages.

Chapter 5 evaluated the ecological significance of abiotic stress and stress propagation during early embryogenesis by observing the fitness outcome in mutagenic environment. This experiment specifically asked whether early stress impairs the capacity to cope with subsequent stressors.

Finally, the discussion chapter (**Chapter 6**) gathers evidence from each experiment showing that (i) water conditioned by pH-stressed marine worms induced avoidance and disrupted burrowing behaviour in conspecifics; (ii) water conditioned by a pH-stressed marine fish induced avoidance behaviours in three invertebrates species; and (iii) heat-stressed zebrafish embryos and larvae released stress metabolites that propagated stress responses to conspecifics. Using this experimental evidence, the final chapter extends the concept of alarm cues and disturbance cues released upon biotic stress to stress metabolites-mediated stress propagation induced by abiotic stressors. In conclusions, I emphasise on the ecological relevance of such findings, before proposing directions for future studies.

Chapter 2. Behavioural stress propagation in benthic invertebrates caused by acute pH drop-induced metabolites

2.1. Significance statement

This chapter provides experimental evidence for the concept of abiotic stress propagation by showing that three species of wild-caught marine benthic invertebrates reacted to acidity-induced stress cues from conspecifics and/or a predator. This chapter shows that stress from ocean acidification is not limited to the individual level and can alter stress within groups and interspecies interactions.

2.2. Graphical Abstract

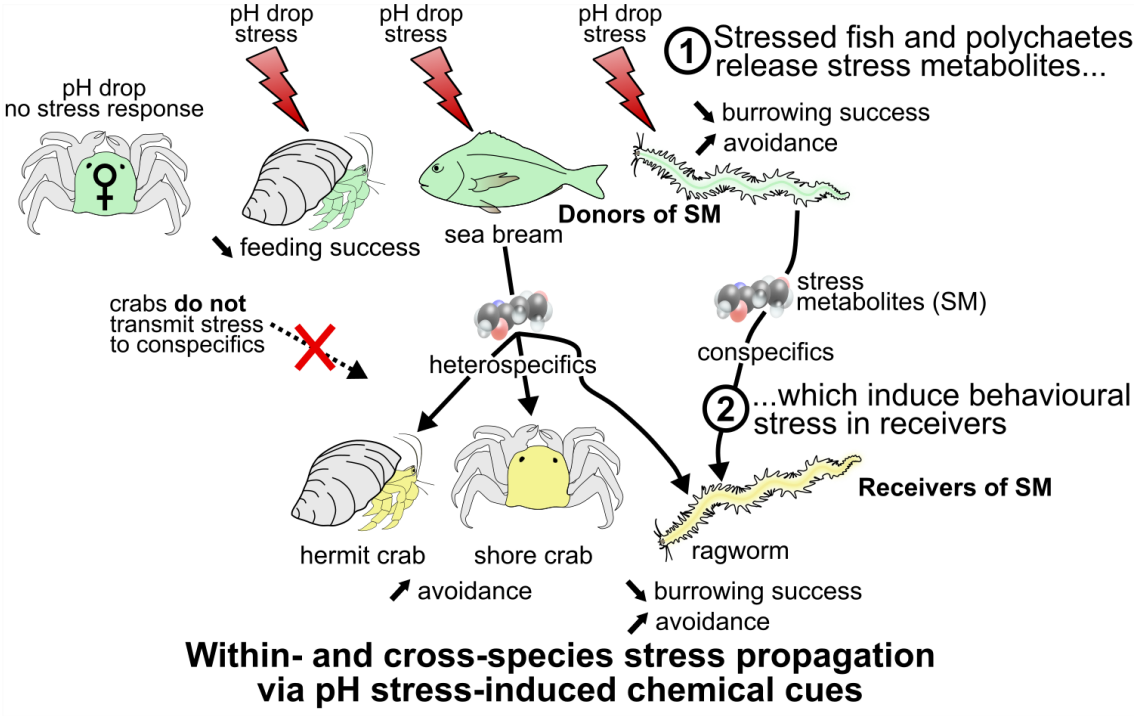

2.3. Highlights

- Low pH stress delayed success in seeking food in hermit crabs and burrowing in ragworm but did not alter feeding time and success in shore crabs.
- pH stress-conditioned water from conspecifics delayed burrowing in ragworm suggesting that ragworms produced stress cues at pH 7.6, whilst crabs did not.
- pH-stressed sea breams released stress metabolites that induced avoidance in crabs and ragworms, and delayed burrowing in ragworms.
- Beyond individual stress, pH drop induced within-group and interspecies stress propagation, which has the potential to alter community dynamics.

2.4. Abstract

Studies on pH stress in marine animals typically focus on direct or species-specific aspects. This chapter tested the hypothesis that a drop from pH 8.1 to pH 7.6 indirectly affects the intra- and interspecific interactions of benthic invertebrates by means of chemical communication. Fitness-relevant behaviours were observed in small hermit crabs *Diogenes pugilator*, green shore crabs *Carcinus maenas*, and harbour ragworms *Hediste diversicolor* in response to short-term pH drop, and to putative stress metabolites released by either conspecifics or gilt-head sea bream *Sparus aurata* during 30 minutes of acute pH drop. Not only did acute pH drop itself impair the time to find a food cue in small hermit crabs and burrowing in harbour ragworms, but similar effects were observed under exposure to pH drop-induced stress metabolites. Stress metabolites from *S. aurata*, but not its regular control metabolites, also induced avoidance responses in all recipient species. This chapter shows that a short-term acute pH drop, an abiotic stressor, has the capacity to trigger the release of metabolites which induce behavioural responses in conspecific and heterospecific individuals, which can be interpreted as a behavioural cost. The findings that stress responses can be indirectly propagated through means of chemical communication warrant further research to confirm the effect size of the behavioural impairments caused by stress metabolites and to characterise their chemical nature.

2.5. Introduction

Compared to the open ocean, coastal areas and particularly intertidal zones are highly variable environments characterised by abrupt changes in water parameters. This includes fluctuations in pH beyond 0.3 units, the levels predicted for average change related to the process of ocean acidification towards the end of the century (Caldeira and Wickett, 2003; Sabine et al., 2004; IPCC, 2019). While intertidal species may be more resilient to climate change due to their acquired tolerances of pH fluctuations, it also forces them to live more frequently near their physiological tolerance limits (Truchot and Duhamel-Jouve, 1980; Hofmann et al., 2011; Sokolova, 2018; Wolfe et al., 2020). Superimposing ocean acidification on natural pH fluctuations may further increase the variability of organisms' responses (Eriander et al., 2015). Therefore, organisms inhabiting intertidal areas are interesting models to study the effects of short-term pH fluctuations within the IPCC predicted range. A low environmental pH can directly alter animal behaviour through several pathways, which include (i) deviation of energy budgets towards the stress response (Pörtner, 2008), (ii) fleeing to avoid the sources of

stress (Pörtner and Peck, 2010; Abreu et al., 2016), (iii) disrupted information detection and processing leading to impaired decision-making (Briffa et al., 2012; Porteus et al., 2018; Cothran et al., 2021), and (iv) alteration of the chemical signals themselves impacting the sensory environment and the transfer of information (Wyatt et al., 2014; Roggatz et al., 2016, 2019). Behavioural effects triggered by lowered pH are known to occur in different taxonomic groups such as crustaceans (de la Haye et al., 2011), marine ragworms (Bond, 2018), and fish (Munday et al., 2009), although recent research debates both their ubiquitousness and effect size (Clark et al., 2020a, 2020b; Munday et al., 2020; Williamson et al., 2021; Clements et al., 2022). In addition, it should be mentioned that although there is little literature disentangling the behavioural effects of pH drop versus high CO_2, an increasing body of recent research evidenced the role of pH-dependent altered chemical communication (Roggatz et al., 2016; Porteus et al., 2021; Schirrmacher et al., 2021; Velez et al., 2021).

In aquatic environments, where visibility can be limited, infochemicals and chemosensory functions, such as pheromones used for mating (Karlson and Lüscher, 1959a) are crucial for communication (Hardege, 1999; Jordão and Volpato, 2000; Ashur et al., 2017; Saha et al., 2019). However, infochemicals are also a mechanism to signal stress – but stress propagation has mostly been researched within the context of biotic stressors. For example, alarm cues released following mechanical damage from fish epidermal club cells can trigger panic reactions in conspecifics and heterospecifics (Toa et al., 2004; Júnior et al., 2010). Such mechanisms of chemical communication also occur in invertebrates, as evidenced by the reduced out-of-burrow activity of the marine polychaete *Alitta virens* exposed to damaged conspecifics (Watson et al., 2005; Ende et al., 2017). Disturbance cues refer to chemicals that may be stored in gill epithelium or urine, and are released voluntarily or involuntarily by disturbed or startled prey, to induce early antipredator responses in recipients to anticipate potential threats (Bairos-Novak et al., 2017; Goldman et al., 2020a). The central role of chemical communication in the aquatic environment and the recent evidence of its impairment by ocean acidification pinpoints the need for a deeper understanding of such potential environmental modulation of chemical signalling (Chivers et al., 2013).

Overall, though, it is not well understood yet whether abiotic stressors such as pH drop can also induce the release of chemical cues and whether these can propagate the stress response to other individuals. The term “stress metabolites” refers to such compounds released, voluntarily or not, by an organism in response to abiotic stressors.

These can be detected and processed by conspecifics and/or heterospecifics, leading to the induction of a behavioural stress response (Hazlett, 1985). Of note, Draper and Weissburg (2019) defined the "direct effects" of elevated CO_2 on predator-prey interactions as the effects modifying the sensory pathways (cue production and emission by the donor and cue reception and processing by the receiver). Here, the effects of acute pH drop are considered as "direct" when the animal is exposed to the stressor itself, and as "indirect" when the animal is exposed to the stress metabolites released upon pH stress. Both direct and indirect effects may be guided by sensory pathways as well as metabolism in senders and receivers (as defined in Draper and Weissburg, 2019). The signalling of stress responses within or between species by means of stress metabolites is termed "stress propagation" (**Figure 2.1A**). Detecting stress metabolites may allow other individuals to modify their behaviour to avoid a change in the abiotic environment, and communities to coordinate or potentiate their response to ensure survival (Mothersill et al., 2007; Giacomini et al., 2015; Abreu et al., 2016). However, to investigate the function of any pH drop-induced chemical cues, the original stressor (pH drop) must first be removed from the experimental design.

This chapter investigated, within and among species inhabiting the intertidal zone, the indirect effects of acute pH drop through stress metabolites induced by it on fitness-relevant behaviours. Using a full factorial design, this chapter tested the hypothesis that an acute pH drop to end-of-century level (7.6) will both directly (i.e., when the animal is exposed to the abiotic stressor) and indirectly (i.e., when the animal is exposed to the stress metabolites) affect behaviour through the induction of stress metabolites. In this chapter, three marine invertebrates (small hermit crab *Diogenes pugilator*, green shore crab *Carcinus maenas*, and harbour ragworm *Hediste diversicolor*) were exposed to control pH and pH drop in combination with conditioned water from both conspecifics and their potential vertebrate predator, the gilt-head sea bream *Sparus aurata*.

2.6. Methods

2.6.1. Experimental design

Small hermit crabs *Diogenes pugilator* and green shore crabs *Carcinus maenas* were collected in autumn at low tide in the Ria Formosa lagoon (Portugal). Harbour ragworms (*Hediste diversicolor*) were sourced via a local supplier (Valbaits) from the Setubal lagoon (Portugal). Animals were acclimated for one week at pH 8.1 (pH is reported using National Bureau of Standards scale) in large flow-through open-circuit

communal tanks (continuous flow of 0.05 L/min) mimicking natural habitats with natural seawater from the Ria Formosa lagoon at the Ramalhete Marine Station (CCMAR, Faro, Portugal) in a direct CO_2-controlled system, as described in Sordo et al. (2016, 2018) and Gregório et al. (2019), with pCO_2 constantly measured and adjusted. Two system seawater conditions were used, either control pH of 8.1 ± 0.015 or pH drop of 7.6 ± 0.008. Assuming a total alkalinity of 2500 µmol/kg SW, the pCO2 was calculated as 537 µatm and 1922 µatm in the control and pH drop conditions, respectively, according to the CO2calc software (Robbins et al., 2010). Seawater parameters were measured daily at 2.30 pm (mean temperature: 20.16°C ± 1.05°C, mean salinity: 35.67 PSU ± 0.26 PSU, mean dissolved oxygen: 7.55 mg/L ± 0.163 mg/L). A total pool of approx. 100-120 *D. pugilator*, 150-200 *C. maenas*, and over 150 *H. diversicolor* was used during the experimental period, yielding a total of 921 observations. Because no individual marking could be achieved, the reuse of animals in successive behavioural assays was spaced out by circulating animals through recovery tanks after testing, before returning them to their stock population tanks once a day. Animal reuse was randomized across treatments and treatments randomized per day to prevent any confounding effects on the measured behaviours. All experiments were conducted in October 2019, except one independent set of observations (n = 40) in *C. maenas* conducted in September 2018, which was analysed together with the 2019 data with the year treated as a covariate.

A three-way factorial design of pH drop × stress metabolites × metabolite donor species was generated to study the effects of acute pH drop, stress metabolites induced by it, and their combination versus a control containing regular metabolites (control metabolites) (**Figure 2.1B**).

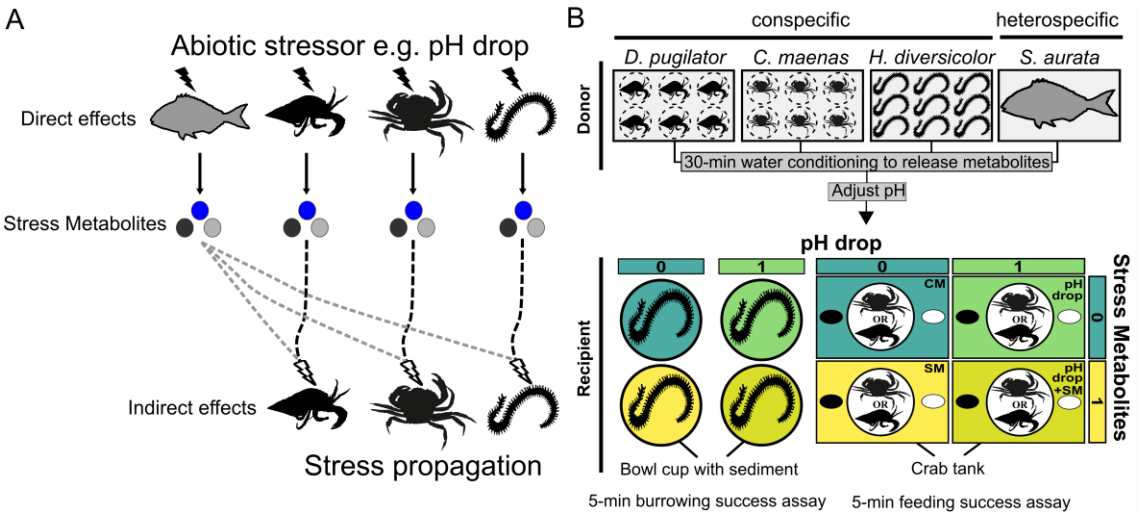

Figure 2.1. Concept of stress propagation and experimental design. A) Concept of stress propagation from pH-stressed donors to naive receivers, themselves stressed by metabolites released by the donors. Solid lines and black flash symbols represent direct pH drop effects. Black and grey dashed lines and white flash symbols represent indirect pH drop effects mediated by stress metabolites (circles) released by conspecifics (black lines) or heterospecifics (grey lines). B) Schematic experimental design showing the presence vs. absence of predictors (pH drop, stress metabolites, donor). Behavioural effects of short-term acute pH drop and stress metabolites it induced were tested in three species: *Diogenes pugilator*, *Carcinus maenas*, and *Hediste diversicolor*. Metabolites were obtained by conditioning donors in either control pH = 8.1 (releasing putative control metabolites), or pH drop = 7.6 (releasing putative stress metabolites), followed by pH adjustments for factorial design yielding four experimental conditions CM, pH drop, SM, and pH drop+SM. Predictors are binary coded as 0 (control metabolites, control pH) and 1 (stress metabolites, pH drop). Metabolites originated from conspecifics or the heterospecific *Sparus aurata*. Behaviour assays for crabs consisted in locating a feeding cue in 300 seconds. Specimens of *H. diversicolor* were placed on top of sediment and burrowing behaviour was recorded for 300 seconds. A range of avoidance behaviours were also recorded. Experimental conditions were CM: control metabolites in control pH, SM: control metabolites in control pH, pH drop: control metabolites in pH drop, pH drop+SM: stress metabolites in pH drop. Animal drawings by A. Murcia and KCWV.

Metabolite donor species were *D. pugilator*, *C. maenas*, *H. diversicolor* (called conspecific donors) and the potential predator *Sparus aurata* (called heterospecific donor). Metabolite donors were conditioned for 30 minutes in seawater at regular pH (pH 8.1, 538 µatm CO_2, putatively inducing control metabolite release), or pH drop (pH 7.6, 1922 µatm CO_2, putatively inducing stress metabolite release). Recipient species were *D. pugilator*, *C. maenas*, and *H. diversicolor*, which received water containing either conspecific or heterospecific metabolites. To achieve the full factorial design, recipient species received either control or stress metabolites and were tested in either control pH (8.1) or pH drop (7.6), by re-adjusting the pH of the conditioned water before each bioassay (with the pH verified with an accuracy of 0.02 units using a portable pH meter). Overall, four different experimental treatments were obtained: (i) putative control metabolites at pH 8.1 (CM), (ii) putative control metabolites at pH 7.6 (pH drop), (iii) putative stress metabolites at pH 8.1 (SM), (iv) and putative stress

metabolites at pH 7.6 (pH drop+SM). Testing conspecific and heterospecific metabolites with three recipient species yielded to a total of twelve treatments. Prior to use in recipient species, conditioned seawater from *H. diversicolor* and *S. aurata* (0.0067 fish/L) was tenfold diluted in fresh system seawater at the desired pH. The effects of undiluted *S. aurata* control metabolites at pH 8.1 in *H. diversicolor* and *D. pugilator* were additionally tested to explore the possibility that stress metabolites are equivalent to highly concentrated control metabolites. See **Table Appendix 2 S1** for further details on treatments.

2.6.2. Metabolite conditioning

To condition water for experiments, each nine harbour ragworms *Hediste diversicolor*, six small hermit crabs *Diogenes pugilator*, six green shore crabs *Carcinus maenas*, or one gilt-head sea bream *Sparus aurata* (~ 880 g) were placed in separate tanks with 0.015 L, 1 L, 5 L, or 15 L of seawater, respectively. Water conditioned by *S. aurata* was provided by the Ramalhete Marine Station. Specimens of *D. pugilator* and *C. maenas* were separated into transparent mesh-bottomed plastic cups to prevent intraspecific interactions while allowing any metabolites to diffuse into the seawater. Specimens of *H. diversicolor* were placed together on top of the sediment into which they tended to burrow individually. Metabolite donor and recipient species couples in the conspecific groups were *D. pugilator/D. pugilator*, *C. maenas/C. maenas*, and *H. diversicolor/H. diversicolor*. Metabolite donor and recipient species couples in the heterospecific groups were: *S. aurata/D. pugilator*, *S. aurata/C. maenas*, and *S. aurata/H. diversicolor*. Conditioning of water with metabolites took place for 30 min at either regular pH (pH 8.1, 537 µatm CO_2, putatively inducing control metabolite release), or pH drop (pH 7.6, 1922 µatm CO_2, putatively inducing stress metabolite release). Conditioned water containing metabolites from *H. diversicolor* and *S. aurata* was tenfold diluted prior use in recipient species. To achieve the full factorial design, control metabolites were tested in pH drop and stress metabolites were tested at control pH. For this purpose, the pH of control metabolite conditioned seawater was reduced to pH = 7.6 (using 0.1 M HCl for control metabolites conditioned by crabs, or by dilution in system water at pH = 7.6 for control metabolites conditioned by *H. diversicolor* and *S. aurata*). On the other hand, the pH of stress metabolite conditioned water was increased to pH = 8.1 (using reef buffer™, Seachem, Georgia, USA, for control metabolites conditioned by crabs; or by dilution in system water at pH = 8.1 for control metabolites conditioned by *H. diversicolor* and *S. aurata*). Addition of reef buffer™ did not alter the

salinity (measured with a salinity meter). The conditioning of the water is summarised in **Table Appendix 1 S1**

2.6.3. Behavioural bioassays

For each of the four conditions, the "time-to-success" was measured as the time to find a feeding cue (1/10 diluted mussel juice) *vs.* a mock (seawater) cue in *D. pugilator* and *C. maenas*, or to bury the head entirely in the sand in *H. diversicolor*. Either *D. pugilator* and *C. maenas* specimens were randomly drawn from acclimatised populations raised in pH-controlled communal tanks (pH = 8.1) and held in the middle of the testing test tank using plastic pipe rings. The feeding cue was prepared by mashing five adult blue mussels (*Mytilus edulis*) and diluting one volume of mussel homogenate in nine volumes of seawater at pH = 8.1. Next, 0.1 mL of ten-times diluted mussel juice was injected using a graduated plastic syringe at either side of the tank (i.e., randomly assigned left or right to the crabs) into an approx. 1 cm^3 yellow synthetic sponge ballasted inside a small metal screw nut. The feeding cue was allowed to diffuse in the seawater for 10 s before the crab was released by lifting the pipe ring. Sets of nine *H. diversicolor* were carefully placed from a holding tub into the centre of each of nine independent test dishes holding conditioned water, and the time to burrow the entire head was measured individually using a stopwatch "laps" function. Behavioural assays were terminated once the animal successfully grabbed the ballasted sponge containing the feeding cue with their pincers (*D. pugilator* and *C. maenas*) or buried its entire head (*H. diversicolor*), or at a maximum time of 300 seconds. Both feeding and burrowing behaviours are tested response variables in crabs (de la Haye et al., 2012; Wang et al., 2018) and ragworms (Bhuiyan et al., 2021) exposed to pH drop. Additionally, avoidance behaviours were binary coded. In *D. pugilator* and *C. maenas*, avoidance behaviours included freezing (suddenly retreating into the shell or attempting to burrow, sudden and lasting arrest in locomotion for at least 120 consecutive seconds or more than 150 seconds in total) and escaping (walking along the walls or retreating into a corner of the tank for at least 120 consecutive seconds or more than 150 seconds in total). Such freeze and escape behaviours indicate danger in crustaceans (Katz and Rittschof, 1993; Perrot-Minnot et al., 2017; Tomsic et al., 2017). In *H. diversicolor*, avoidance behaviours consisted of freezing, which might be accompanied by spread of jaws, sideways-undulating behaviour, and formation of a noticeable slime cap whilst outside the sediment. These behaviours indicate extreme stress in marine polychaetes (Mouneyrac et al., 2003; Burlinson and Lawrence, 2007; McBriarty et al., 2018).

Preliminary experiments (in Autumn 2018, n = 40) showed no effect of the number of conditioned water uses until more than five uses on the time-to-success of *C. maenas* ($p = 0.373$), as well as a disinterest of male *C. maenas* in food cues in the mating period. Experiments were therefore limited to females in *C. maenas*, and each batch of conditioned water was used for at most five behaviour assays before being renewed. The concentration of the diffuse feeding cue from previous tests was considered negligible relative to the freshly added 0.1 mL of feeding cue directly on the ballasted sponge, which is a "hotspot" of food for the tested animals. In addition, conditioning the water with 6-9 animals for 30 min led to the concentration of the conditioning metabolites from the donor dwarfing the negligible concentration of metabolites released by one animal for only 5 min of behavioural assay. Therefore, the feeding cue and the metabolites released by the previous tested animal were considered negligible as the water was reused up to five times. Between each batch of conditioned water, sand in the bioassay tanks was thoroughly rinsed with system water.

The behaviour of *H. diversicolor* was tested using circular plastic bowl cups (H: 5 cm × ⌀: 9 cm) filled with a 1 cm layer of clean fine sand from the Ria Formosa lagoon and 15 mL conditioned seawater resulting in approx. 1 cm seawater layer above the sand. The behaviour of both *D. pugilator* and *C. maenas* was tested in binary choice sport-pitch-like tanks. Tanks used for *D. pugilator* (H: 17 cm × W: 15 cm × L: 25 cm) were filled with 1 L conditioned seawater and a thin (~1 cm) layer of clean fine sand, as *D. pugilator* showed reluctance moving over plastic surfaces without substrate. Test tanks used for *C. maenas* (H: 24 cm × W: 19 cm × L: 37 cm) were filled with 5 L conditioned seawater and were free of sand. Both *D. pugilator* and *C. maenas* tanks were wrapped in black foil to avoid distraction by reflection or light effects. Behavioural experiments were conducted for up to five minutes (300 seconds). Before any experimental behaviour assay, the length of *D. pugilator* shells and the width of *C. maenas* carapaces were measured. Due to practical limitations, *H. diversicolor* specimens were not weighed. In addition, the sex of *C. maenas* was noted based on their abdomen shape with females being selected for the experiment, whereas this was not possible for *D. pugilator* and *H. diversicolor*, for which both sexes were used. All experiments were approved by the Ethical committee of the University of Hull under the Ethics references U020 and FEC_2019_81.

2.6.4. Statistical analysis

Avoidance behaviours were analysed using generalised linear models for logit regression with binomial distribution using the *stats* R package (R Core Team, 2020). Time-to-success was modelled for the time to reach a feeding cue in *D. pugilator* and *C. maenas* or to burrow the head in *H. diversicolor* depending on the three predictors: pH drop, stress metabolites, and donor. Time-to-success data was analysed with a time-to-event analysis (also called survival analysis) using Cox proportional hazard models from the *survival* R package (Therneau and Grambsch, 2000; Therneau, 2021). The event being the success of food cue location (in crabs) or burrowing the head in sediment (in worms), the analysis was hereafter referred to as "time-to-success analysis". The exponentiated estimates (hazard ratios) from the Cox proportional hazard models were expressed as "success ratio". Success ratios were visualised using the *plot_model* function from the *sjPlot* R package (Lüdecke, 2021). The "success probability" (the probability of the feeding or burrowing event occurring at any time over 300s) over time was represented by Kaplan-Meier curves drawn using the *survminer* R package (Kassambara et al., 2020). Animals not reaching the feeding cue or not burying their head were censored and assigned, by convention, the maximum time of "300+".

All statistical models always included the main effects and interaction terms of the binary predictors: pH drop (pH = 8.1 vs. pH = 7.6), stress metabolites (stress metabolites vs. control metabolites), and donor (conspecific vs. heterospecific). Covariates (year, number of water uses, crab size, where relevant; see **Table Appendix 1 S2-3**) were excluded from models when deemed insignificant by at least two model selection methods among the following: an ANOVA Chi-squared test from the *stats* R package (R Core Team, 2020), the Akaike Information Criterion (ΔAIC), and Bayesian Information Criterion (ΔBIC) from the *AICcmodavg* R package (Mazerolle, 2020b). Overall model fit p-values were retrieved from the ANOVA Chi-squared test or the Likelihood ratio test, for generalised linear models and Cox proportional hazard models, respectively. Pairwise comparisons between treatments involved in the interaction term between the three predictors were obtained from statistical models using the *emmeans* R package (Lenth, 2021), wherein false discovery rate p-value adjustments were applied for post-hoc term-wide multiple testing.

In addition to the full factorial design, two separate conditions were tested to better understand the effect of metabolites and discriminate the involvement of pH drop-induced stress metabolites *versus* higher concentrations of control metabolites induced

by a higher metabolism in pH drop-stressed specimens. Therefore, the effects of undiluted control metabolites from *S. aurata* (CM100%) on the feeding response of *D. pugilator* and the burrowing behaviour of *H. diversicolor* were compared to the effects of ten-time diluted treatments of stress metabolites SM and control metabolites CM (from the general factorial design). False discovery rate-corrected pairwise comparisons between SM, CM100% and CM were performed using the *emmeans* R package (Lenth, 2021) after either generalised linear models for logit regression with binomial distribution (escaping response in *D. pugilator* and avoidance response in *H. diversicolor*), or Cox proportional hazard models (time-to-success analysis). The full dataset may include animals tested at most twice over the course of the experimental period, which was addressed by performing random bootstrapping of 50% of the dataset to verify the solidity of the experimental data. All statistical analyses were conducted in R (R Core Team, 2020) using RStudio (RStudio Team, 2020) with a significance threshold of $p \leq 0.05$.

2.7. Results

Time-to-success (**Figure 2.2**) and avoidance (**Figure 2.3**) behaviours were observed in three invertebrate species exposed to pH drop and stress metabolites.

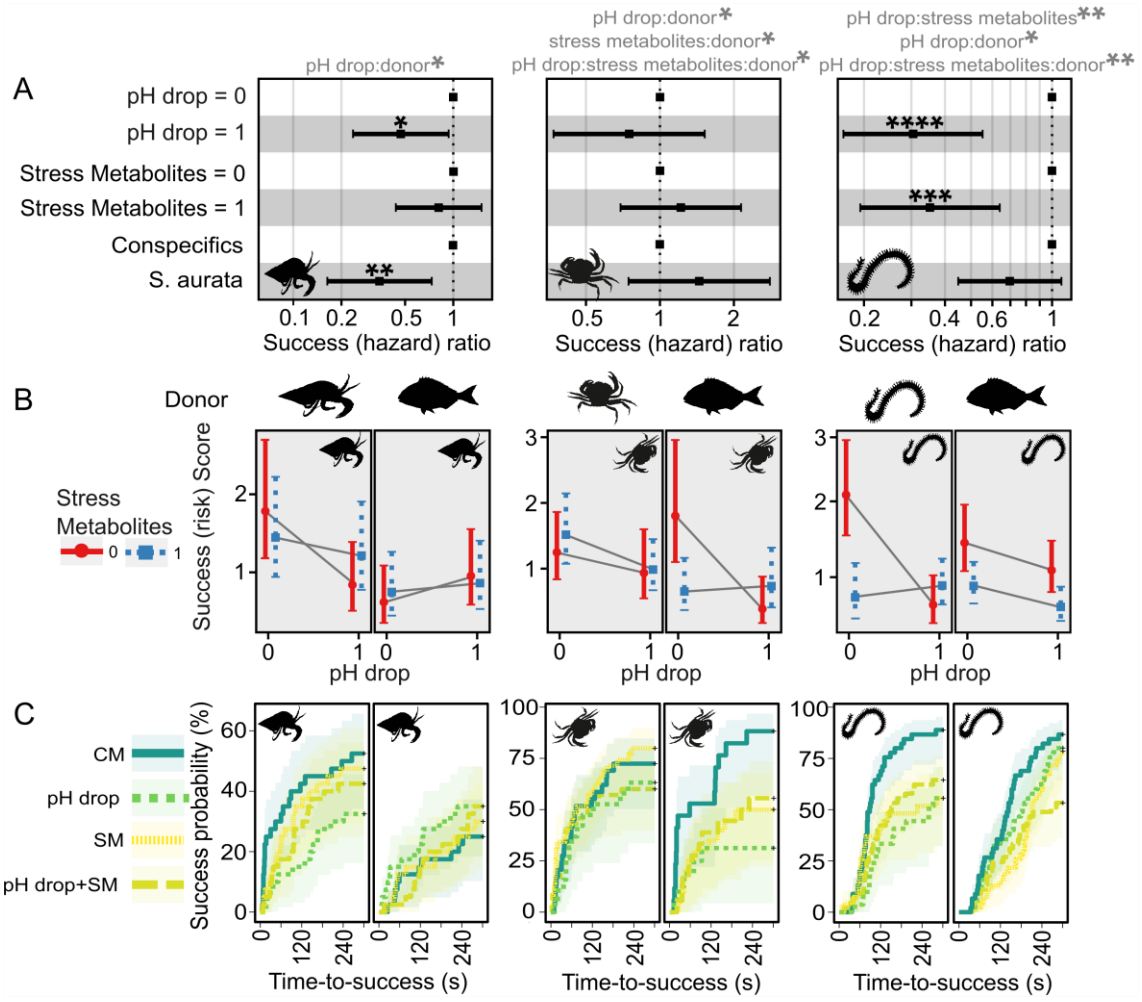

Figure 2.2 Time-to-success is altered by pH drop in *D. pugilator* and by pH drop and stress metabolites in *H. diversicolor*. Effects of predictors (pH drop, stress metabolites, donor) on time-to-success in *Diogenes pugilator*, *Carcinus maenas*, and *Hediste diversicolor*. A) effects of predictors on success ratio (aka hazard ratio with success as event, arbitrary units). Likelihood ratio tests for overall model fit were: *D. pugilator*: p = 0.06; *C. maenas*: p = 0.009; *H. diversicolor*: p < 0.0001). Significant predictors from Cox proportional hazard models are shown with asterisks, and significant interaction terms are shown in grey above the plots. B) Interaction term plot of marginal effects showing predicted success score (aka risk score with success as event, arbitrary units ± confidence interval) split by donor and recipient species. Crossed solid grey lines represent an interacting effect of pH and metabolites. C) Kaplan-Meier curves to visualise success probability (cumulative event) for each experimental condition over time. *: p ≤ 0.05, **: p < 0.01, ***: p < 0.001, ****: p < 0.0001. CM: control metabolites in control pH, pH drop: control metabolites in pH drop, SM: stress metabolites in control pH, pH drop+SM: stress metabolites in pH drop.

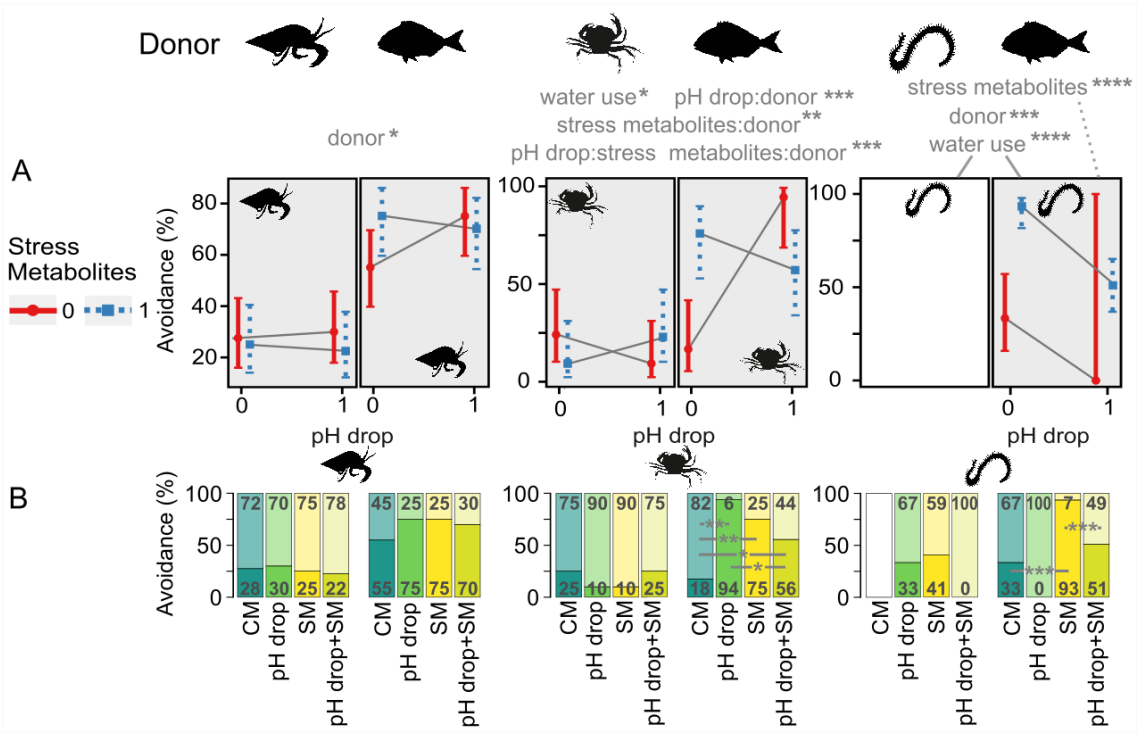

Figure 2.3. Avoidance is altered by stress metabolites from *S. aurata* in *C. maenas* and *H. diversicolor*. Effects of predictors (pH drop, stress metabolites, donor) on the percentage of avoidance behaviour in *Diogenes pugilator*, *Carcinus maenas*, and *Hediste diversicolor*. Avoidance behaviour included freezing and escaping (*D. pugilator* and *C. maenas*), or freezing, curling, flipping, and slime secretion (*H. diversicolor*). A) Split bars represent the presence (dark area) or absence (light area) of avoidance behaviours. Significant main predictors (and their interaction terms) and covariates are shown above plots. Significant pairwise comparisons between treatments in each donor/recipient are shown as horizontal grey lines. *: $p \leq 0.05$, **: $p < 0.01$, ***: $p < 0.001$, ****: $p < 0.0001$. (B) Interaction plot showing the marginal effects on the predicted avoidance percentages (± confidence interval) of stress metabolites and pH drop within the conspecific and heterospecific groups for each species. Crossing solid grey lines represent an interacting effect of pH and metabolites for each donor. The interactive effects of predictors for *H. diversicolor*/*H. diversicolor* are not represented due to the missing CM treatment. Overall effects of donor and water use across the response of *H. diversicolor* (for either donor) are shown with solid lines, whereas the effects of stress metabolites are for *S. aurata*/*H. diversicolor* only (grey dashed line). CM: control metabolites in control pH, pH drop: control metabolites in pH drop, SM: stress metabolites in control pH, pH drop+SM: stress metabolites in pH drop.

2.7.1. Response of *Diogenes pugilator* to pH, stress metabolite, and donor type

The time-to-success analysis was not conclusive for the stress metabolite predictor in *D. pugilator* (**Figure 2.2**, **Table 2.1**, Z = -0.66, p = 0.5073). On the other hand, the Cox proportional hazard model (overall Likelihood ratio test model fit: p = 0.06) found that both pH drop (feeding success ratio = 0.47, Z = -2.14, p = 0.0325) and metabolites from *S. aurata* (feeding success ratio = 0.35, Z = -2.76, p = 0.0058) had significant negative effects on the feeding success ratio of *D. pugilator*. In addition, there was a significant interaction between pH drop and metabolite donor terms on the feeding success of *D. pugilator* (Z = 2.19, p = 0.0289). Overall, pH drop induced a significantly lower success score in the conspecific treatment (**Figure 2.2AB**). Post-hoc analyses

evidenced that all treatments (CM, pH drop, SM, and pH drop+SM) induced similar feeding times in both the conspecific and heterospecific donor groups (**Table 2.2**).

Avoidance responses of *D. pugilator* did not depend on pH drop ($Z = 0.25$, $p = 0.8049$) nor stress metabolites ($Z = -0.25$, $p = 0.7995$, overall Chi-squared test model fit: $p < 0.0001$, Table 2), but were significantly more pronounced when metabolites originated from *S. aurata* (69%) instead of conspecifics (26%, $Z = 2.46$, $p = 0.0139$, **Figure 2.3**, **Table 2.2**). After splitting avoidance behaviour data by donor, pairwise comparisons failed to find differences between the four treatments (CM, pH drop, SM, and pH drop+SM), but confirmed that the donor effect existed across all four treatments (**Figure 2.3**, **Table Appendix 1 S5**). However, partitioning the avoidance behaviour of *D. pugilator* into freezing and escaping responses evidenced that escaping significantly increased with *S. aurata* control metabolites only when tested in pH drop (**Figure 2.4**, **Table Appendix 1 S6-9**).

2.7.2. Response of *Carcinus maenas* to pH, stress metabolite, and donor type

The Cox proportional hazard model (overall Likelihood ratio test model fit: $p = 0.009$) showed that the feeding success ratio of *C. maenas* did not significantly vary with pH ($Z = -0.80$, $p = 0.4247$), metabolites ($Z = 0.68$, $p = 0.4989$), nor donor ($Z = 1.09$, $p = 0.2773$) terms (**Figure 2.2**, **Table 2.1**). Nevertheless, the interaction terms were significant. Post-hoc tests revealed that time-to-success responses were similar across treatments CM, pH drop, SM, and pH drop+SM when *C. maenas* received conspecific metabolites (**Table Appendix 1 S10**). This pattern changed when *S. aurata* was the metabolite donor as evidenced by significantly lower feeding success scores in *C. maenas* exposed to pH drop ($Z = 2.97$, $p = 0.0179$), SM ($Z = 2.48$, $p = 0.0394$), and the trend for pH drop+SM ($Z = 2.20$, $p = 0.0563$), compared to the control CM.

In *C. maenas*, the predictors pH drop ($Z = -1.23$, $p = 0.2195$), stress metabolites ($Z = -1.23$, $p = 0.2195$), and donor ($Z = -0.56$, $p = 0.5785$) did not alter avoidance responses but their interaction terms were significant (overall Chi-squared test model fit: $p < 0.0001$, **Figure 2.3**, **Table 2.2**). Pairwise comparisons showed no differences between the four treatments (CM, pH drop, SM, pH drop+SM) in avoidance patterns of *C. maenas* receiving conspecific metabolites. Conversely, *C. maenas* facing *S. aurata* metabolites while experiencing treatments of pH drop (94%, $Z = -3.60$, $p = 0.0020$), SM (75%, $Z = -3.28$, $p = 0.0031$), and pH drop+SM (56%, $Z = -2.33$, $p = 0.04$) significantly increased their avoidance display compared to control CM (18%). Moreover, pH drop

combined with stress metabolites (pH drop+SM treatment) instead of control metabolites (pH drop treatment) significantly lowered avoidance behaviours (Z = 2.21, p = 0.0405, **Figure 2.3**, **Table Appendix 1 S11**). Partitioning the avoidance behaviour of *C. maenas* into freezing and escaping responses evidenced that escaping explained the avoidance response whereas no clear patterns were observed in the freezing behaviour (**Figure 2.4**, **Table Appendix 1 S12-S15**).

2.7.3. Response of *Hediste diversicolor* to pH, stress metabolite, and donor type

In contrast to crabs, burrowing success responses of *H. diversicolor* did not depend on the donor species (p = 0.1093, **Figure 2.2**,**Table 2.1**). However, the Cox proportional hazard model (overall Likelihood ratio test model fit: p < 0.0001) evidenced that both pH drop (burrowing success ratio = 0.30, Z = -3.91, p < 0.0001) and stress metabolites (burrowing success ratio = 0.35, Z = -3.42, p = 0.0006) terms significantly delayed burrowing time responses of *H. diversicolor*. Significant interactions between the main predictors required to decipher the involvement of within-donor treatment effects (**Table Appendix 1 S16**). Post-hoc tests revealed that pH drop (Z = 3.91, p = 0.0006), SM (Z = 3.43, p = 0.0012), and pH drop+SM (Z = 3.47, p = 0.0012) treatments significantly lowered burrowing success scores compared to the control CM in *H. diversicolor* exposed to conspecific metabolites. Moreover, *H. diversicolor* facing *S. aurata* metabolites had lower burrowing success scores in the pH drop+SM treatment compared to the control CM (Z = 3.35, p = 0.0049).

H. diversicolor displayed more avoidance in response to *S. aurata* metabolites (47%) compared to conspecific metabolites (20%, Z = 1.09, p = 0.0006, overall Chi-squared test model fit: p < 0.0001, **Figure 2.3**, **Table 2.2**). *H. diversicolor* exposed to *S. aurata* metabolites were not affected by pH drop (Z = -0.01, p = 0.9906), whereas stress metabolites induced significantly more avoidance than control metabolites (Z = 4.31, p < 0.0001, overall Chi-squared test model fit: p < 0.0001, Table 2). There were no differences across pH drop, SM, and pH drop+SM treatments in *H. diversicolor* receiving conspecific metabolites (**Table Appendix 1 S17**). Pairwise comparisons revealed that the SM treatment (93%) triggered significantly more avoidance than CM (33%, Z = -4.31, p = 0.0001) and pH drop+SM treatments (51%, Z = 3.92, p = 0.0003) – meaning that pH drop significantly reduced the avoidance behaviours of ragworms to *S. aurata* stress metabolites. Specimens of *H. diversicolor* exposed to *S. aurata* metabolites displayed different avoidance responses in the control treatment CM compared to pH drop (slowed-down burrowing response), SM (sideways-undulating

behaviour with body flips), and pH drop+SM (raised head and spread mouth parts with freezing behaviour in and slowed-down movement with sideways undulating behaviour).

Table 2.1 Effects of pH drop, stress metabolites, and donor on time-to-success. Results of Cox proportional hazard model for the main effects of predictors (pH drop, stress metabolites, donor) on the time-to-success analysis in small hermit crab (*Diogenes pugilator*, n = 320 observations with 120 events of finding a food cue, degrees of freedom = 312), green shore crab (*Carcinus maenas*, n = 189 observations with 122 events of finding a food cue, degrees of freedom = 181), and harbour ragworm (*Hediste diversicolor*, n = 325 observations with 234 events of burrowing head in sediment, degrees of freedom = 317). Unsuccessful observations are censored. Overall significance of the models using Likelihood ratio tests were: *D. pugilator*: p = 0.06; *C. maenas*: p = 0.009; *H. diversicolor*: p < 0.0001). Covariates were dropped from models after analyses of deviance showed that they passed the Chi-squared test (D. pugilator: number of water uses: p = 0.1163, crab size: p = 0.6318; *C. maenas*: number of water uses: P = 0.6104, crab size: p = 0.9995, year: p = 0.3348; H. diversicolor: number of water uses: p = 0.2649). Success ratio (aka hazard ratio) is the exponentiated estimate. SE is the standard error of estimate. Significance ($p \leq 0.05$) is shown in bold.

Predictors	Success (hazard) ratio	Estimate	SE	Z	P
D. pugilator					
pH drop	**0.4702**	-0.7546	0.3530	-2.1378	**0.0325**
stress metabolites	0.8106	-0.2100	0.3167	-0.6631	0.5073
donor	**0.3460**	-1.0613	0.3843	-2.7613	**0.0058**
pH drop:stress metabolites	1.7878	0.5810	0.4858	1.1959	0.2317
pH drop:donor	**3.2842**	1.1891	0.5441	2.1853	**0.0289**
stress metabolites:donor	1.4970	0.4034	0.5326	0.7575	0.4487
pH drop:stress metabolites:donor	0.4168	-0.8752	0.7498	-1.1672	0.2431
C. maenas					
pH drop	0.7490	-0.2890	0.3620	-0.7982	0.4247
stress metabolites	1.2156	0.1953	0.2887	0.6762	0.4989
donor	1.4445	0.3678	0.3385	1.0865	0.2773
pH drop:stress metabolite	0.8674	-0.1422	0.4630	-0.3072	0.7587
pH drop:donor	**0.2870**	-1.2484	0.6312	-1.9777	**0.0480**
stress metabolites:donor	**0.2981**	-1.2102	0.5008	-2.4165	**0.0157**
pH drop:stress metabolites:donor	**6.0273**	1.7963	0.8261	2.1743	**0.0297**
H. diversicolor					
pH drop	**0.3043**	-1.1899	0.3045	-3.9075	**< 0.0001**
stress metabolites	**0.3520**	-1.0442	0.3049	-3.4251	**0.0006**
donor	0.6965	-0.3616	0.2258	-1.6013	0.1093
pH drop:stress metabolites	**3.9914**	1.3841	0.4411	3.1376	**0.0017**
pH drop:donor	**2.4669**	0.9030	0.3816	2.3663	**0.0180**
stress metabolites:donor	1.7318	0.5492	0.3816	1.4390	0.1501
pH drop:stress metabolites:donor	**0.2291**	-1.4736	0.5633	-2.6158	**0.0089**

Table 2.2. Effects of pH drop, stress metabolites, and donor on avoidance behaviours. Results of the binomial generalised linear model for the main effects of predictors (pH drop, stress metabolites, donor) on the avoidance behaviour in small hermit crab (*Diogenes pugilator*, n = 320 observations of finding a food cue, degrees of freedom = 312), green shore crab (*Carcinus maenas*, n = 151 observations of finding a food cue, degrees of freedom = 142), and harbour ragworm (*Hediste diversicolor*, n = 253 observations of burrowing head in sediment, degrees of freedom = 251). Due to missing observations in conspecific control metabolites at control pH in *Hediste diversicolor*, data was analysed with two models. Model 1: effect of donor across all treatments (sample size: 253 observations). Model 2: effects of pH and metabolites in subset receiving *S. aurata* metabolites (sample size: 154 observations). Overall significance of models from Chi-squared analyses of deviance when including only predictors were: *D. pugilator*: $p < 0.0001$; *C. maenas*: $p < 0.0001$; *H. diversicolor*: $p < 0.0001$ (model 1) and $p < 0.0001$ (model 2). Covariates were dropped from models after analyses of deviance showed that they passed the Chi-squared test (*D. pugilator:* number of water uses: $p = 0.5963$, crab size: $p = 0.9158$; *C. maenas:* crab size: $p = 0.2710$). SE is the standard error of estimate. Significance ($p \leq 0.05$) is shown in bold.

Predictors	Estimate	SE	Z	P
D. pugilator				
(Intercept)	-0.9694	0.3541	-2.7380	0.0062
pH drop	0.1221	0.4944	0.2470	0.8049
stress metabolites	-0.1292	0.5086	-0.2540	0.7995
donor	**1.1701**	0.4758	2.4590	**0.0139**
pH drop:stress metabolites	-0.2603	0.7219	-0.3610	0.7185
pH drop:donor	0.7758	0.6919	1.1210	0.2622
stress metabolites:donor	1.0272	0.7022	1.4630	0.1435
pH drop:stress metabolites:donor	-0.8890	1.0039	-0.8860	0.3759
C. maenas				
(Intercept)	-0.2224	0.6725	-0.3307	0.7409
pH drop	-1.1263	0.9173	-1.2279	0.2195
stress metabolites	-1.1263	0.9173	-1.2279	0.2195
donor	-0.4626	0.8326	-0.5556	0.5785
number of water uses	**-0.3077**	0.1556	-1.9772	**0.0480**
pH drop:stress metabolites	2.2527	1.2978	1.7357	0.0826
pH drop:donor	**5.5551**	1.5392	3.6090	**0.0003**
stress metabolites:donor	**3.8799**	1.2465	3.1127	**0.0019**
pH drop:stress metabolites:donor	**-7.5415**	1.9329	-3.9017	**0.0001**
H. diversicolor				
Model 1 (both donors)				
(Intercept)	0.2801	0.3790	0.7391	0.4598
donor	**1.0944**	0.3169	3.4534	**0.0006**
number of water uses	**-0.7745**	0.1462	-5.2980	**< 0.0001**
Model 2 (*S. aurata* donor)				
(Intercept)	-0.6931	0.5000	-1.3863	0.1657
pH drop	-18.8729	1603.1137	-0.0118	0.9906
stress metabolites	**3.3557**	0.7788	4.3086	**< 0.0001**
pH drop:stress metabolites	16.2548	1603.1138	0.0101	0.9919

2.7.4. Partitioning avoidance responses into escaping and freezing in crabs

Partitioning the avoidance responses of crabs into freezing or escaping patterns allowed a better understanding of their locomotion response to predictors (**Figure 2.4**).

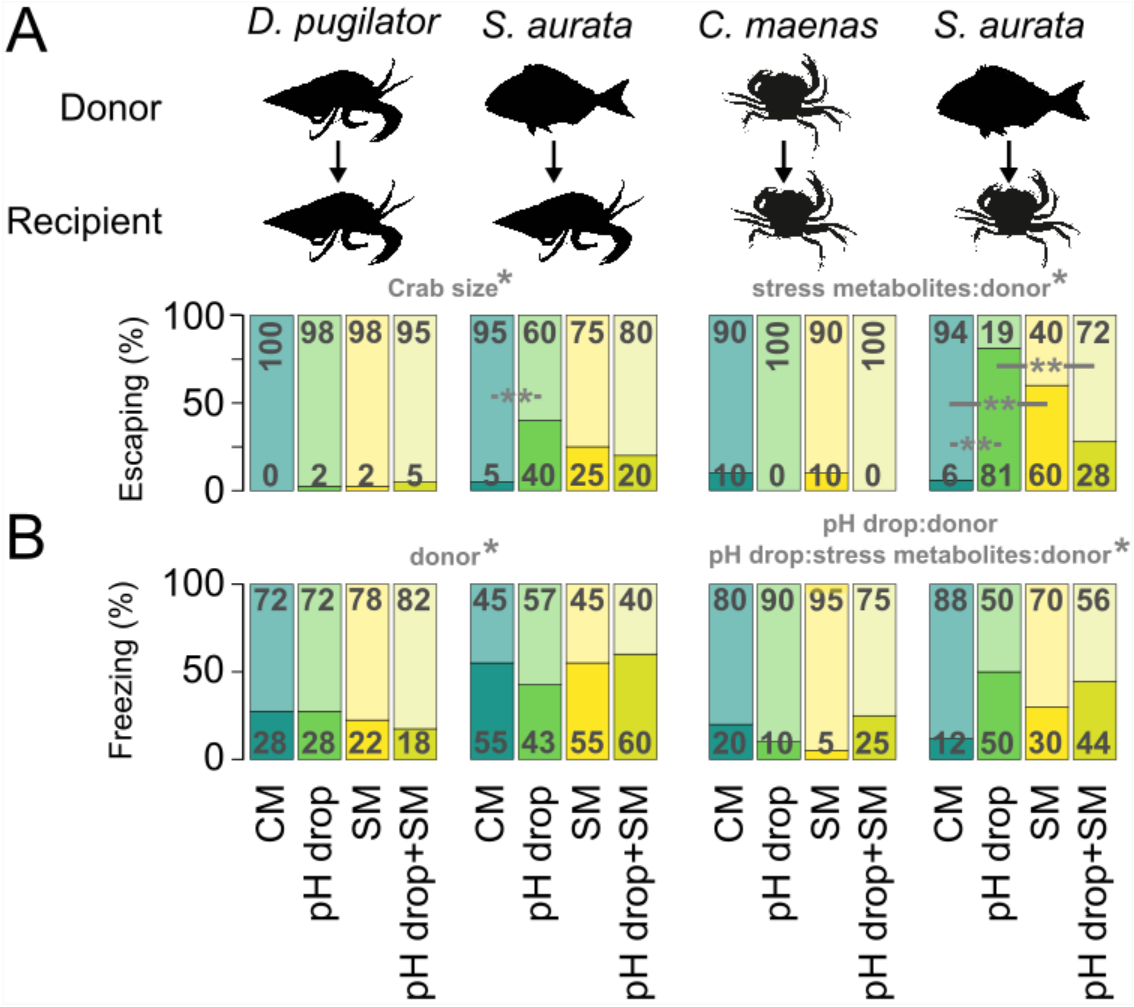

Figure 2.4. Partition of avoidance behaviours into escape and freezing responses in crabs. Percentage of escaping (A) and freezing (B) behaviour in small hermit crab *Diogenes pugilator* and green shore crab *Carcinus maenas* depending on main predictors (pH drop, stress metabolites, and donor). Split bars represent the presence (dark area) or the absence (light area) of escaping and freezing behaviours. Significant main predictors, their interaction terms, and covariates (number of water uses, crab size) are shown above plots. Significant pairwise comparisons between treatments are shown below as horizontal black bars. *: $p \leq 0.05$. Significance was retrieved from binomial generalised linear models. CM: control metabolites in control pH, pH drop: control metabolites in pH drop, SM: stress metabolites in control pH, pH drop+SM: stress metabolites in pH drop.

Apart from *D. pugilator* freezing significantly less in presence of conspecific metabolites (24%) than of *S. aurata* metabolites (53%, $Z = 2.46$, $p = 0.0139$), no significant patterns were observed in the freezing responses of *D. pugilator* (**Table Appendix 1 S7-8**) and *C. maenas* (**Table Appendix 1 S12-13**) to pH drop and stress metabolite predictors. Instead, observed changes in avoidance patterns were mainly attributed to escaping responses. Escaping patterns of *D. pugilator* did not vary with the

pH drop, stress metabolites, nor donor predictors (**Table Appendix 1 S8**) which was also true for specimens that received conspecific metabolites but not *S. aurata* metabolites. Pairwise comparisons revealed that *S. aurata* control metabolites in pH drop induced a significant eightfold increase in escaping (40% in pH drop treatment) in *D. pugilator* compared to control metabolites in control pH (5% in CM treatment, $Z = -3.17$, $p = 0.0091$, **Table Appendix 1 S9**). Furthermore, control metabolites from *S. aurata* increased *D. pugilator* escaping in pH drop ($Z = -3.09$, $p = 0.0079$) but not in control pH ($p = 0.9876$), compared to control metabolites from conspecifics. Stress metabolites from *S. aurata* also significantly increased the escaping of *D. pugilator* compared to conspecific stress metabolites ($Z = -2.35$, $p = 0.0380$). Similarly, the escaping response of *C. maenas* showed that effects of pH drop, stress metabolite, and donor predictors were not significant overall (which held true in specimens exposed to conspecific metabolites) but the "metabolite:donor" interaction term was significant ($Z = 2.06$, $p = 0.0395$, **Table Appendix 1 S14-15**, **Figure 2.4**). However, both pH drop (81%, $Z = -3.49$, $p = 0.0029$) and SM (60%, $Z = -2.82$, $p = 0.0096$) treatments significantly increased escaping behaviours compared to the control CM (6%) in *C. maenas* exposed to *S. aurata* metabolites. The escaping response of *C. maenas* to stress metabolites dropped to 28% in the pH drop+SM treatment compared to the pH drop treatment ($Z = 2.92$, $p = 0.0096$). Of note, pH drop tended to reduce the escaping of shore crabs from *S. aurata* stress metabolites ($Z = 1.95$, $p = 0.0761$). Stress metabolites from *S. aurata* significantly increased escaping compared to that from conspecifics ($Z = -2.98$, $p = 0.0116$).

2.7.5. Confounding effects of covariates

There were confounding effects of covariates on avoidance responses which diminished with time as conditioning water was reused in *D. pugilator* ($Z = -1.98$, $p = 0.0480$) and *H. diversicolor* ($Z = -5.2980$, $p < 0.0001$). Escaping was more pronounced in larger individuals of *D. pugilator* ($Z = 2.49$, $p = 0.0129$, **Figure 2.5A-C**, **Table Appendix 1 S12**).

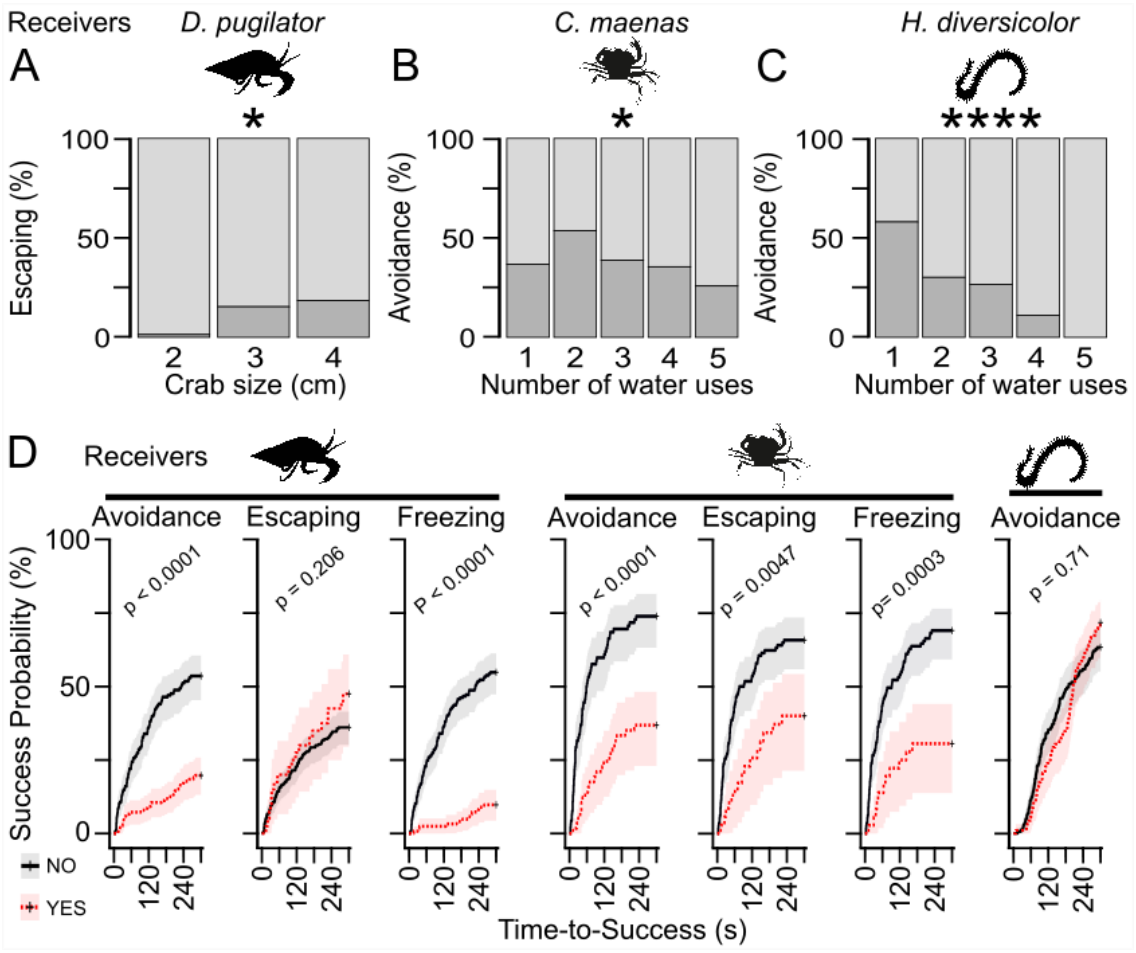

Figure 2.5. Confounding variables and correlations of avoidance behaviour. A) Escaping behaviour of hermit crab *Diogenes pugilator* significantly reduced with crab size (shown here as integer values to represent a continuous range of 2.0 cm to 4.7 cm). The reuse of conditioning seawater significantly decreased avoidance behaviour of shore crab *Carcinus maenas* (B) and avoidance behaviour of ragworm *Hediste diversicolor* (C). Split bars represent the presence (dark area) or the absence (light area) of observed behaviours. Significance was retrieved from binomial generalised linear models. *: $p \leq 0.05$, ****: $p < 0.0001$. D) Kaplan-Meier curves of time-to-success analysis showing the effects of displayed avoidance behaviour on the success probability (cumulative event) over time in *D. pugilator* (left), *C. maenas* (middle), and *H. diversicolor* (right). Avoidance behaviour included freezing and escaping in crabs, and freezing, curling, flipping, and slime secretion in harbour ragworms. Avoidance was also split into freezing and escaping in crabs. P-values represent the significance level comparing the presence vs absence of the studied behaviour on the success ratio according to a Cox proportional hazard model

2.7.6. Relationship between avoidance and time-to-success responses

Cox proportional hazard models were used to assess the relationship between avoidance behaviours and success probability (**Figure 2.5D**). Specimens of *D. pugilator* that displayed an avoidance response had lower feeding success ratios ($p < 0.0001$). This was also true for specimens of *D. pugilator* that froze ($p < 0.0001$) but not for those escaping ($p = 0.2060$). It may be that *D. pugilator* individuals trying to escape the tank went along the walls and eventually found the feeding cue by chance rather than by active foraging (own observations). Avoidance was also associated with lower feeding

success ratios in *C. maenas* ($p < 0.0001$), which held true for both the escaping ($p = 0.0047$) and freezing ($p = 0.0003$) patterns. On the other hand, there was no relationship between the burrowing success ratio and the display of avoidance behaviours in *H. diversicolor*.

2.7.7. Comparison between CM100% and CM or SM

Behavioural observations from different concentrations of sea bream metabolites were used to determine whether the effects of stress metabolites were associated with regularly excreted metabolic wastes (**Figure 2.6**). This positive control experiment could be done in worms and hermit crabs, but not shore crabs due to time limitations during the field experiment. Neither the success ratios nor the percentage of avoidance in *H. diversicolor* and escaping in *D. pugilator* depended on the concentration of sea bream control metabolites as there were no significant differences between CM (diluted to 10%) and CM100% (**Table Appendix 1 S18-19**). On the other hand, SM significantly lowered burrowing success ratios in *H. diversicolor* ($p = 0.0266$), increased avoidance in *H. diversicolor* ($Z = -5.88$, $p < 0.0001$), and increased escaping in *D. pugilator* ($Z = 2.27$, $p = 0.023$) compared to CM100% treatment.

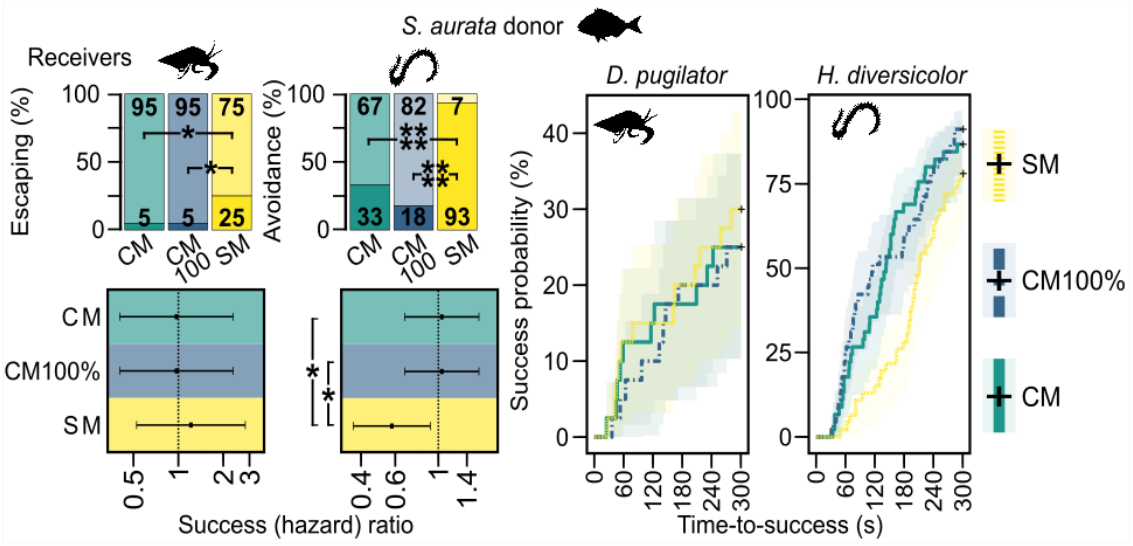

Figure 2.6 Stress metabolites are not concentrated control metabolites. Comparison of concentration and type of metabolites originating from sea bream *Sparus aurata* on fitness-relevant behaviours of hermit crab *Diogenes pugilator* and ragworm *Hediste diversicolor*. Top-left panel shows the % of escaping behaviour in crabs, and avoidance including freezing, curling, flipping, and slime secretion in ragworms (dark area = presence, light area = absence of escaping or avoidance). Bottom-left panel shows time-to-success models (finding feeding cue in crab or burrowing the head in ragworm) with corresponding Kaplan-Meyer curves on the right. Thick lines (with confidence interval as shaded areas) show the probability of success in function of time over 300 seconds. CM: 10-times diluted sea bream control metabolites, CM100%: undiluted sea bream CM. SM: 10-times diluted sea bream stress metabolites. Pairwise comparisons between CM100% and either CM or SM are shown with *: $p \leq 0.05$, ****: $p < 0.0001$.

2.7.8. Validation of effect sizes considering animal reuse

Due to practical limitations, animals could not be individually marked which implied a slight degree of animal reuse (pseudoreplication). Animal reuse was spaced out across treatments by placing specimens in recovery tanks immediately after behavioural assays, although they were returned to the main stock population tanks once a day. Animal reuse was randomised across treatments to prevent any confounding effect on measured variables. However, animals may have been used twice over the course of the experimental period. All statistics reported were measured on the entire sample population as one can argue that in the natural environment, animals would, too, be subjected to repeated challenges. Therefore, pseudoreplication through animal reuse does not depart from realistic conditions. Nevertheless, additional statistical analyses through bootstrapping of the Cox proportional hazard models showed that pseudoreplication did not alter the estimated statistics. Survival analyses were repeated on n = 100 random subsets drawn from the statistical population. **Figure 2.7** shows the distribution of the estimate from the Cox proportional hazard models for the main factor terms (pH drop, SM, and donor) across 100 random bootstraps. This shows that the distribution of term estimates for 50% subsets and empirical term estimates (± standard deviation) for the entire population are similar. Further, bootstrapped average term estimates and empirical term estimates were not statistically different according to one-sample z-tests (**Table Appendix 1 S20**). This additional statistical analysis confirmed the validity of the statistical approach and the accuracy of the estimated effects of pH drop, SM, and donor terms on the time-to-success analysis.

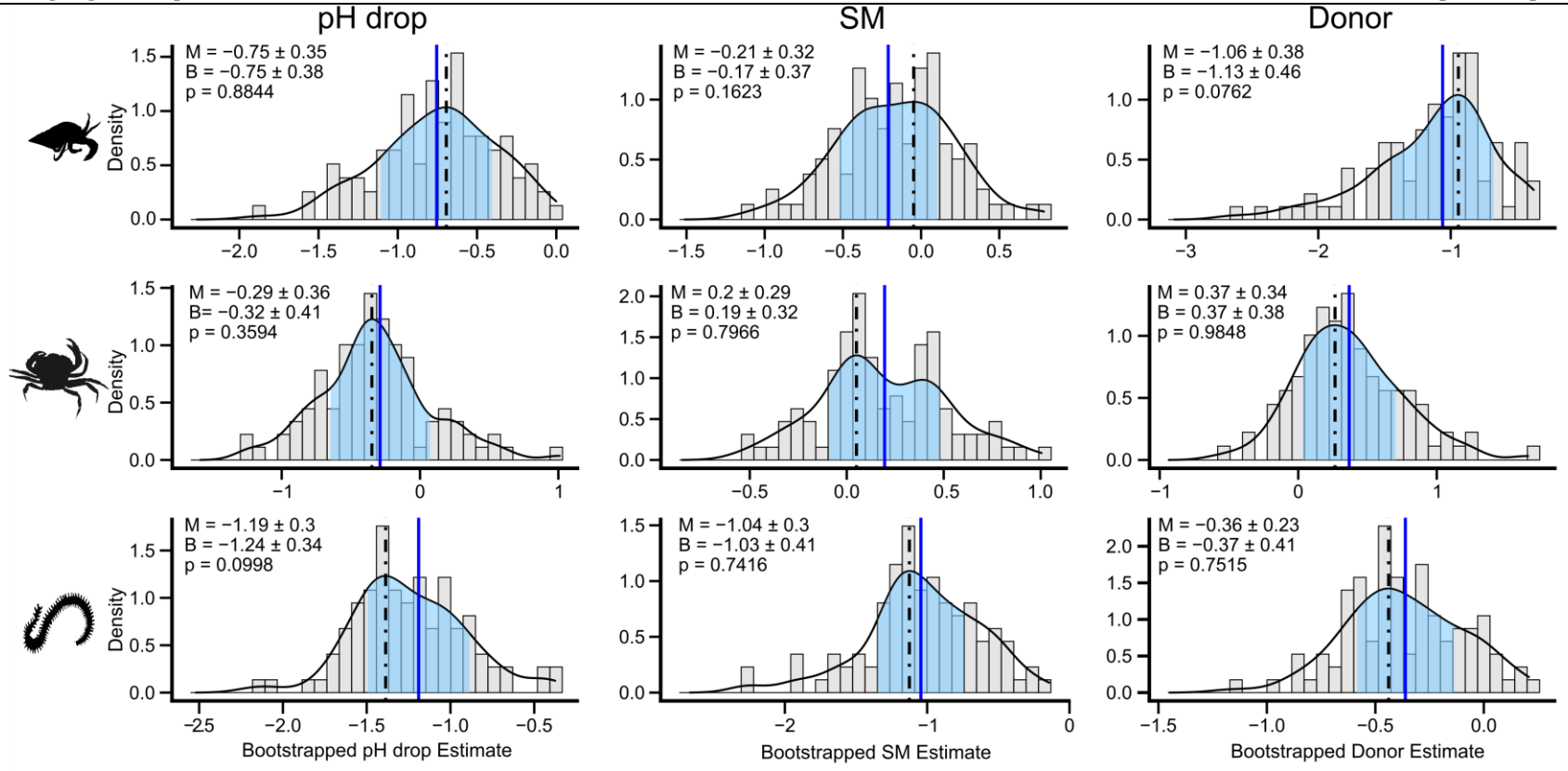

Figure 2.7. Validation of time-to-success analysis model term estimates via bootstrapping. 100 random subsets of 50% of the time-to-success data were drawn from the whole population data to account for pseudoreplication with some individuals that may have been used at most twice. For each subset, a Cox proportional hazard model of pH drop (left) × SM (middle) × donor (right) was computed and the density distribution of the estimate of the main model terms were represented. Top row: small hermit crab *Diogenes pugilator*, middle row: green shore crab *Carcinus maenas*, bottom row: harbour ragworm *Hediste diversicolor*. Averaged bootstrap estimates (black dot-dash lines) from the 50% subsets fall in the range of the empirical estimate values (blue solid lines with standard deviation as blue shade) from the full population. One-sample z-test confirmed that bootstrapped estimates (B.) and empirical models' estimates (M.) are not statistically different (p represents the p-value of the z-test).

2.8. Discussion

2.8.1. Direct effects of pH drop and donor type on fitness-relevant behaviours

Changes in fitness-relevant behaviours to acute pH change can be expected to show high variance and small effect sizes (Clark et al., 2020a), which may therefore require large observational datasets. This chapter used over 900 behavioural observations, and the results reflect a similarly high variance in terms of species-specific responses, donor-dependent effects, as well as sometimes large within-treatment confidence intervals. *Sparus aurata*-conditioned water, whether it contained control metabolites or pH stress-induced metabolites, elicited avoidance in all recipient species which can be attributed to antipredator behaviours. Despite the donor effect, however, much of the remaining behavioural variance was explained by the effects of pH drop and stress metabolites, their interaction, or their interaction with the donor term (**Figure 2**).

Overall, pH drop lowered success ratios in feeding and burrowing in *Diogenes pugilator* and *Hediste diversicolor*, respectively. Such low pH-induced impairments of fitness-relevant behaviours were previously found in hermit crabs *Pagurus bernhardus* and *P. tanneri* and may indicate impaired decision-making (de la Haye et al., 2011, 2012; Kim et al., 2015). Past literature also reported delayed burrowing responses in the harbour ragworm *H. diversicolor* exposed for 28 days to pH drop (Bhuiyan et al., 2021), and an inverse relationship between burrowing and pH in the king ragworm *Alitta virens* (Batten and Bamber, 1996). These behavioural alterations may reflect the cost of acid-base regulation to counteract hypercapnia (Pörtner, 2008), as marine ragworms overexpress the acid-base regulator *Carbonic Anhydrase* (*CA*) at the expense of energy reserves in response to acidification (Freitas et al., 2016; Wage et al., 2016). In the longer term, behavioural costs of an altered burrowing activity may extend to crucial ecological functions as shown by the diminished bioturbation activity of *H. diversicolor* in similar conditions (Bond, 2018). In contrast, *Carcinus maenas* did not delay its feeding response to sudden pH drop in presence of conspecific metabolites, which is in agreement with recent observations of longer-term ocean acidification conditions having weak effect size on marine animal behaviour (Clark et al., 2020a; Clements et al., 2020, 2021, 2022) – although this is debated (Clark et al., 2020b; Munday et al., 2020; Williamson et al., 2021) – including feeding responses in aquatic arthropods (Clements and Darrow, 2018). The resilience to pH stress in female *C. maenas* may be due to their extracellular pH regulatory capacity allowing them to maintain feeding during short-

term assays (Appelhans et al., 2012). Therefore, short-term hypercapnia is not a strong stressor in *C. maenas*, due to its pH-variable intertidal habitat (Fehsenfeld et al., 2011). Other than reduced success ratios, pH drop itself did not induce any avoidance behaviours indicative of stress.

Besides the direct effect of pH drop on behaviour, previous studies on ocean acidification also found contrasting effects of pH drop on predator-prey interactions (Draper and Weissburg, 2019). Here, *C. maenas* showed an increased tendency to escape in response to *S. aurata* control metabolites in pH drop, but not in control pH. Although this was not the main focus of this study, it could mean that pH drop renders predator odour more potent for its prey, for example through pH-dependent changes in odour molecular structure, receptor binding, or information processing (Munday et al., 2009; Roggatz et al., 2016; Schirrmacher et al., 2021).

Overall, the data suggests that a short-term acute pH drop can impair decision-making and predator-prey interactions, and in turn alter fitness-relevant behaviours. Nevertheless, future studies should aim to disentangle the effects of pH drop from that of pCO_2, which ideally also would test short, medium, and long-term responses.

2.8.2. Indirect pH effects on receivers' behaviour through stress propagation

Despite species-specific direct effects of pH drop on behaviour success ratios, this chapter showed that pH drop also has indirect effects on behaviour by altering chemical communication. Stress metabolites released by animals exposed to pH drop altered feeding and burrowing, and increased avoidance behaviours, but the response was donor and recipient species-specific. Responses to stress metabolites in the recipient species were directionally equivalent to those induced by pH drop itself, since it took longer to find a food cue or to burrow the head in the presence of stress metabolites. Although behavioural stress response propagation through chemical communication is well documented for alarm substances and disturbance cues upon predation stress (Giacomini et al., 2015; Abreu et al., 2016; Mathuru, 2016), this chapter shows that chemical communication induced by abiotic stressors such as pH drop can trigger the release of waterborne cues that in turn trigger behavioural stress responses in its recipients. Stress metabolites conditioned by the potential predator *S. aurata* induced more avoidance behaviours, and delayed feeding in *C. maenas* and burrowing in *H. diversicolor*, compared to *S. aurata* control metabolites. Similarly, the presence of

conspecific stress metabolites significantly lowered *H. diversicolor* burrowing success ratio compared to conspecific control metabolites.

On the other hand, *C. maenas* females did not react to conspecific stress metabolites. The different behavioural effect of conspecific stress metabolites between crabs and *H. diversicolor* has several possible explanations ranging from different defence strategies related to stress risk perception and evaluation (Hazlett, 1985; Bairos-Novak et al., 2017, 2018; Goldman et al., 2020b) to different types, concentrations, or ratios of the released chemicals that serve as risk cues (Júnior et al., 2010; Morishita and Barreto, 2011). A pH drop to 7.6 is not a strong stressor in crabs (Fehsenfeld et al., 2011), in agreement with the observed unaffected feeding response to pH drop in *C. maenas*, which may explain the absence of responses to water from pH drop-conditioned *C. maenas* conspecifics. However, the presence of stress metabolites conditioned by *S. aurata* caused a marked drop in success ratios of *C. maenas* at low (but not control) pH, evidenced by significant interaction terms.

Whilst not investigating their chemical structure, this experiment provides insights to characterize novel properties of stress metabolites. Stress metabolites, like disturbance cues, potentially consist of regularly excreted metabolites such as urea and ammonia (Bairos-Novak et al., 2017; Shrivastava et al., 2019). The fact that the behavioural responses of *H. diversicolor* and *D. pugilator* remained unchanged even when using undiluted control metabolites indicates that stress metabolites are not just up-concentrated control metabolites (at least in the tested range of tenfold control metabolites), or that the cocktail of chemicals contains much higher ratios of stress cues relative to control cues. Avoidance behaviours by both *C. maenas* and *H. diversicolor* became somewhat less pronounced with subsequent water uses, suggesting that the recipients may be able to discriminate degraded versus fresh metabolites and react accordingly to the degree of threat they may indicate (Fuselier et al., 2009; Bairos-Novak et al., 2018). This shows that stress metabolites induced by pH drop are either not identical with metabolites released in normal pH, and/or are at least more than tenfold higher concentrated than control metabolites.

The avoidance behaviours recorded in this study are known indicators of stress. *S. aurata* stress metabolites elicited atypical freezing, eversion of the proboscis, mucus secretion, flipping and sideways-undulating behaviours in *H. diversicolor*, which were previously described as indicators for a physiological stress response following

exposure to copper sulphate (Burlinson and Lawrence, 2007), antiparasitic drugs (McBriarty et al., 2018), and trace metals (Mouneyrac et al., 2003). There were increased freezing and escaping behaviours in crabs, which indicates a stress response in crustaceans (Katz and Rittschof, 1993; Perrot-Minnot et al., 2017; Tomsic et al., 2017). The finding that *S. aurata* stress metabolites induced such responses in potential prey species suggests that responses to disturbance cues do not depend on the "audience", similar to what has been observed in tadpoles (Bairos-Novak et al., 2020).

A directionally similar response to pH drop and to the stress metabolites it induces shows that pH drop can have indirect effects through stress propagation, by which animals directly experiencing environmental stressors negatively influence fitness-relevant behaviours of community members. The stress propagation towards naive conspecific individuals might constitute a "positive stress feedback loop". This was first observed by Hazlett (1985) after freshwater crayfish exposed to water conditioned by heat-stressed conspecifics displayed increased alertness, after returning the conditioned water to normal temperature. Similar indirect effects through chemical signalling from stressed donors towards unstressed, naive recipients exposed to the water conditioned by the directly stressed donors but not to the stressor itself, were also shown in response to different types of biotic stressors such as mock predator chase (Toa et al., 2004; Giacomini et al., 2015), handling (Barcellos et al., 2011), and acute fasting (Abreu et al., 2016), to physical injury including irradiation (Mothersill et al., 2007), and to predation (Frisch, 1938; Mathuru et al., 2012; Oliveira et al., 2013). Last, the data suggested that pH drop weakened the response of *H. diversicolor* and *C. maenas* to stress metabolites (but potentiated that of control metabolites) from *S. aurata*, which warrants further investigation.

2.8.3. Conclusions and Perspectives

This chapter shows that short-term pH drop of a similar magnitude of that experienced within the intertidal zone, but also aligned to end-of-century predicted average values (Chavez et al., 2017; Landschützer et al., 2018), had negative consequences on fitness-relevant behaviours in harbour ragworm *H. diversicolor* and small hermit crab *D. pugilator*. Additionally, the data evidence that pH drop events also impede the same behaviours in the same way indirectly via chemical communication, albeit these effects depended on donor and recipient species. Sea bream *S. aurata* and ragworm *H. diversicolor* stressed by pH drop released stress metabolites which possibly differ from control metabolites and negatively affect fitness-relevant behaviours in

metabolite recipients. Stress metabolites induced similar avoidance behaviours as those exhibited under physiological stress, meaning that a stress response was propagated from donor to recipient. These negative indirect behavioural effects of pH drop warrant further study, especially as the results were inconclusive with regards to the combined treatments of low pH and stress metabolites. Short-term pH drops thus involve behavioural additionally to metabolic trade-offs, which is also of interest for understanding natural and aquaculture systems under ocean acidification combined with tidal pH fluctuations. One potential limitation of the experimental design was that animals could not be individually marked. Despite circulating animals to recovery tanks to limit animal reuse, this may have led to a small degree of animal reuse wherein the full dataset may include animals tested at most twice over the course of the experimental period. Nevertheless, random bootstrapping of 50% of the dataset showed that the outcomes of the time-to-event analysis remain unchanged even if only half of the observations are analysed, which confirms the validity of the experimental data. Whether or not pseudoreplication is present in ecological studies has been subject to debate (Davies and Gray, 2015), but owing to the large number of observations, animal reuse had no effect on model outcomes and effect sizes are likely not overestimated. Given the potential high ecological significance of indirect negative effects of pH fluctuations on population fitness, and to address the reproducibility crisis (Baker, 2016), studies aiming to replicate results from this chapter should aim to further optimise the experimental design with better technical equipment including automatic behaviour video tracking to investigate stress propagation. The results from this chapter open three important questions: (i) whether stress propagation is a widespread and innate mechanism existing in other species and at embryonic stages, (ii) whether stress propagation can be activated by other types of abiotic stressors, and (iii) the identification of molecular mechanisms causing stress propagation. To address these questions, the next chapters used zebrafish embryos and heat stress to unravel the molecular basis of abiotic stress-induced stress propagation.

Chapter 3. Thermal stress induces a positive phenotypic and molecular feedback loop in zebrafish embryos

3.1. Significance statement

This second experiment further explored, in the laboratory, the findings from Chapter 2 that abiotic stressors induce stress propagation. Here, Chapter 3 shows that another abiotic stressor, repeated high temperatures, can induce stress responses in conspecifics not directly exposed to it. This chapter extends the concept of abiotic stress propagation to heat stress, freshwater species, and the life stage of embryogenesis, which suggests that it is an innate and widespread mechanism.

3.2. Graphical abstract

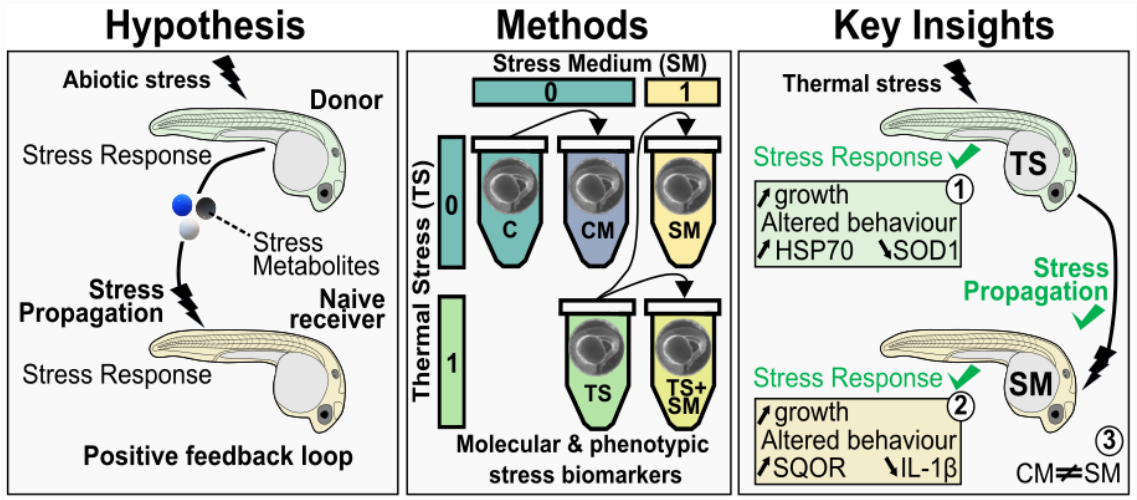

3.3. Highlights

- Repeated sublethal thermal stress induces a stress response in zebrafish embryos.
- Stressed embryos chemically signal stress to naive conspecifics via the medium.
- Directly and indirectly stressed embryos show similar behaviour and faster growth.
- Stress medium receivers have altered immune and antioxidant gene expression.

3.4. Abstract

Aquatic organisms must cope with both rising and rapidly changing temperatures. These thermal changes can affect numerous traits, from molecular to ecological scales. Biotic stressors are already known to induce the release of chemical cues which trigger behavioural responses in other individuals. In this chapter, I infer whether repeated heat events, as an abiotic stressor, may similarly induce stress-like responses in individuals not directly exposed to the stressor. To test this hypothesis, zebrafish (*Danio rerio*) embryos were exposed for 24 hours to fluctuating thermal stress, to medium in which another embryo was thermally stressed before ("stress medium"), and to a combination of these. Growth, behaviour, expression of molecular markers, and of whole-embryo cortisol were used to characterise the thermal stress response and its propagation between embryos. Both fluctuating high temperature and stress medium significantly accelerated development, by shifting stressed embryos from segmentation to pharyngula stages, and altered embryonic activity. Importantly, I found that the expression of sulfide:quinone oxidoreductase (*sqor*), the antioxidant gene *sod1*, and of interleukin-1β (*il-1β*) were significantly altered by stress medium. This chapter illustrates the existence of positive thermal stress feedback loops in zebrafish embryos where heat stress can induce stress-like responses in conspecifics, but which might operate via different molecular pathways. If similar effects also occur under less severe heat stress regimes, this mechanism may be relevant in natural settings as well.

3.5. Introduction

Fish are ectothermic vertebrates susceptible to changes in the thermal environment, particularly to higher temperatures close to their upper thermal limits (Morgan et al., 2001; Araújo et al., 2013; Paaijmans et al., 2013). Early developmental stages have narrower thermal ranges than adults (Skjærven et al., 2014). Temperature regimes during development have irreversible effects as they modulate subsequent stages. Examples of persistent effects of temperature changes during development include alterations of swimming performance and cardiac anatomy (Dimitriadi et al., 2018), masculinisation (Ribas et al., 2017) and increased mortality (Hosseini et al., 2019). Together these can shape the future trajectory of populations, as global warming is characterised by both greater thermal variability, and more extreme thermal events of longer duration and higher magnitude (Vasseur et al., 2014; Pörtner et al., 2019).

Zebrafish (*Danio rerio*) is an emerging model organism to study the effects of thermal stress (Clark et al., 2011; Long et al., 2012; Brown et al., 2015; Luu et al., 2021). Adult zebrafish are eurythermal, naturally tolerating a wide range of temperatures (16.5-38.6°C) with optimal temperature around 27-28.5°C. They may face natural thermal variations of ~5°C daily, and from 6 to 38°C seasonally (Engeszer et al., 2007; Spence et al., 2008; López-Olmeda and Sánchez-Vázquez, 2011). However, early stages of zebrafish only tolerate minimum temperatures of 22-23°C and maximum temperatures of around 32°C to develop normally (Schirone and Gross, 1968; Schnurr et al., 2014; Pype et al., 2015). These warm-adapted fish are living near their upper thermal limit and may be among the "losers" of climate change (Somero, 2010). Of note, the thermal biology of zebrafish is conserved in laboratory populations, in spite of laboratory domestication, which makes them an adequate model organism to investigate the effects of thermal challenges in the laboratory (Brown et al., 2015; Morgan et al., 2019) – although recent research shows that laboratory zebrafish lost thermal plasticity and have narrower thermal tolerances than wild strains (Morgan et al., 2022).

Heat-stressed zebrafish larvae display anxiety-like behaviours (Bai et al., 2016), transient hyperactivity (Yokogawa et al., 2014), and an altered embryonic development (Hallare et al., 2005; Schröter et al., 2008; Long et al., 2012; Hall and Warner, 2021). At the molecular level, heat stress leads to the accumulation of reactive oxygen species (Vinagre et al., 2012; Madeira et al., 2016b), and to changes in the hypothalamic-pituitary-interrenal (HPI) axis (Alsop and Vijayan, 2009b) and global gene expression patterns (Long et al., 2012; Logan and Buckley, 2015; Ribas et al., 2017). For example, the expression of Cu/Zn-superoxide dismutase I (*sod1*) and sulfide:quinone oxidoreductase (*sqor*) is modulated by temperature and hypoxia in zebrafish embryos (Long et al., 2012, 2015; Icoglu Aksakal and Ciltas, 2018). The innate immune system is also challenged by both high temperatures and thermal fluctuations in teleost early stages (Zhang et al., 2018; Mariana and Badr, 2019). For instance, interleukin-1β (*il-1β*), a gene central to stress and immune responses (Vitkovic et al., 2000; Metz et al., 2006; Goshen and Yirmiya, 2009), is upregulated in zebrafish embryos exposed to high temperatures (Icoglu Aksakal and Ciltas, 2018).
Largely overlooked to date, however, is the question of whether the response to thermal stress can be transmitted to other individuals. Fish use chemical communication to alert others of a threat using so-called "alarm cues", released after skin damage, or "disturbance cues", released without injury when being startled by biotic stressors

(Jordão and Volpato, 2000). Exposure to predation-induced disturbance cues elicits stress-like responses in fish (Jordão and Volpato, 2000; Toa et al., 2004; Ferrari et al., 2008; Barcellos et al., 2011, 2014; Bett et al., 2016), including zebrafish (Barcellos et al., 2014). Importantly, even early developmental stages of fish are capable of such chemical communication as they respond to alarm cues (Oulton et al., 2013; Atherton and McCormick, 2015, 2017; Poisson et al., 2017). Typically, stress induces the release of metabolites into the environment such as cortisol (McGlashan et al., 2012; Barcellos et al., 2014), CO_2 (McGlashan et al., 2012), respiratory by-products, catecholamines, or nitrogenous metabolic compounds such as urea (Hubbard et al., 2003; Giaquinto and Hoffmann, 2012; Bairos-Novak et al., 2017; Henderson et al., 2017).

Despite the wealth of information on such biotic stress-induced stress propagation, this phenomenon is only known for a few abiotic stressors, such as low pH or acute fasting (Abreu et al., 2016; Chapter 3). Evidence of transmission of heat-induced stress between conspecifics comes mainly from a single experiment in crayfish (Hazlett, 1985). In this chapter, I tested the hypothesis that thermal stress induces cues conferring signals of thermal stress to naive receivers, in which they elicit a response (**Figure 3.1A**).

In contrast to alarm and disturbance cues induced by biotic stressors, I introduced the term "stress metabolite" to refer to such cues putatively induced by abiotic stress. To test this hypothesis, zebrafish embryos were exposed to independent and combined treatments of thermal stress and medium putatively containing stress metabolites induced by thermal stress. Zebrafish embryos were exposed to thirteen heat peaks of +5°C above control temperatures (27°C) within the 24 hours of the segmentation period. This thermal regime was intended to elicit a high stress response in zebrafish embryos. Zebrafish embryo behaviour, growth rate, and expression of genes involved in the immune response (*il-1β*) and antioxidant pathways (*sod1*, *sqor*) were investigated, alongside an assessment of heat stress-induced HSP70 and the levels of whole-embryo cortisol. The three main expectations were that (i) fluctuating high temperatures, similar to constant higher temperatures, trigger developmental, behavioural and molecular stress responses in zebrafish embryos, and that (ii) these responses can be propagated to naive receiver embryos through stress medium, which are however (iii) not elicited by neither fresh nor control medium.

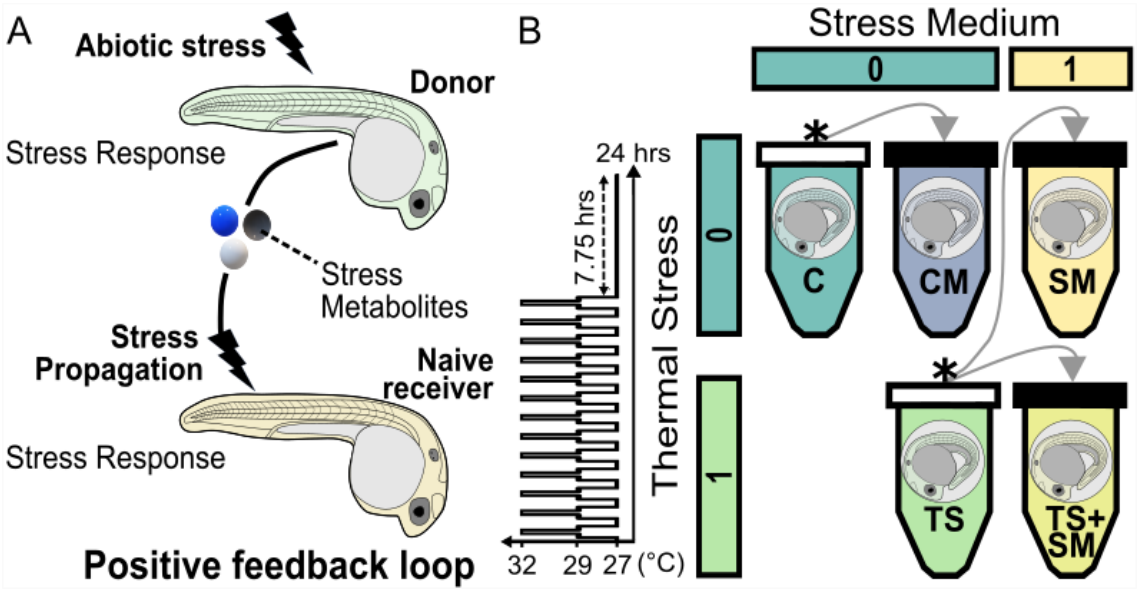

Figure 3.1. Overview of concept and experimental design. A) The hypothesis is that abiotic stress triggers the release of stress metabolites following a heat stress response, and that these stress metabolites signal a threat to naive receivers, in which they initiate an indirect stress response. Stress is propagated from directly exposed individuals towards naive conspecifics, thereby constituting a positive feedback loop. B) In a two-way factorial design (represented by 0 and 1 for factor levels), zebrafish embryos (*Danio rerio*) were exposed to either fluctuating thermal stress (inset diagram) followed by a recovery period (dashed arrow line) or constant control temperature (27°C), in combination with fresh E3 medium or stress medium containing putative stress metabolites produced by one previously thermally-stressed embryo. An additional treatment was incubated at 27°C in a control medium containing metabolites from an embryo previously exposed to control conditions. Plain grey arrows indicate medium transfer from donor embryos (black asterisks) to receiver embryos (plain black tube caps). CM: control medium, C: control, SM: stress medium, TS: thermal stress, TS+SM: thermal stress + stress medium.

3.6. Methods

3.6.1. Animals

Adult zebrafish (*Danio rerio*) were raised within their range of tolerance (25°C, 12 hrs light/12 hrs dark cycle, pH = 7.6, salinity = 1) at the Aquarium facility of the University of Hull. The zebrafish strain was an outcrossing, non-laboratory strain obtained from a local pet store (PET) and raised at the University of Hull for only few generations. Adult zebrafish were fed twice daily an alternate diet of Gamma Mini Bloodworm Blister (Tropical Marine Centre, UK) and Daphnia Plus Vitamins (JMC Aquatics, UK). Plastic trays half-filled with marbles and covered with plastic plants were left overnight in the fish tank for breeding purposes. Marbles mimicked a natural spawning substrate and prevented cannibalism on eggs (Nasiadka and Clark, 2012). Adult fish were randomly selected and allowed to rest for at least two days between breeding events to limit parental effects on the embryos. In the morning, eggs were collected using a plastic Pasteur pipette and transferred into the laboratory. Eggs were

rinsed in 1X E3 medium (Cold Spring Harbor Laboratory Press, 2011) containing 1% methylene blue. Experimental treatments were conducted on embryos collected at different times throughout the year 2019 but with similar breeding stocks kept in constant conditions. All experiments were approved by the Ethical committee of the University of Hull (Ethics reference U144b).

3.6.2. Experimental design

Just before the beginning of experimental treatments, several eggs were photographed to estimate the median initial stage. Embryos were observed under a stereomicroscope (ZEISS SteREO Discovery.V8, Carl Zeiss) mounted with an Axiocam 105 Color camera (Carl Zeiss) and coupled with the ZEN lite software (Carl Zeiss). Exposure began around the blastula stage (median stage: 2.75 hpf, at 512-cells). Fertilised healthy embryos (with chorion) were selected and individually placed into 0.2 mL PCR tubes pre-filled with 200 µL of 1X E3 medium (Cold Spring Harbor Laboratory Press, 2011).

In a two-way factorial design, embryos were exposed to different combinations of the two factors, thermal stress (TS) and medium conditioned with putative stress metabolites. The term “stress medium” (SM) describes this thermal stress-conditioned medium. One may argue that any observed effects of stress medium may be due to regularly excreted metabolites, which could accumulate towards the end of each treatment independently of thermal stress. This warranted the use of an additional control, the “control medium” (CM), that is, medium that had previously hosted control embryos and containing putative regular metabolites in the absence of heat stress, to see whether CM could produce similar outcomes as TS or SM. Embryos were exposed to either thermal stress or control temperature protocols within a thermocycler, incubated in fresh, control, or stress medium. All experimental treatments are detailed in **Figure 3.1B** and **Table Appendix 2 S1**. The thermal stress protocol spanned 16.25 hrs, divided into thirteen 75-min series of temperature fluctuations between 27, 29, 32, 29, and 27°C, with each temperature step being maintained for 15 min. Thermal stress mimicked +5°C temperature peaks over zebrafish optimal temperature (a total of n = 13 peaks) reaching the sublethal temperature of 32°C (Scott and Johnston, 2012). While not replicating realistic conditions of heatwaves, the choice of this thermal regime aimed to elicit maximal responses to repeated exposure to sublethal stress in early embryos at the crucial time of somitogenesis. A recovery period of 7.75 hrs at 27°C followed the fluctuating temperature period to reach a total incubation time of 24 hrs. The control

temperature protocol was a steady 27°C for 24 hrs. E3 media following control or thermal stress conditions were reused for "control medium" and "stress medium" treatments, respectively. In total this yielded five treatments: control (C, control temperature protocol with fresh medium), control medium (CM, control temperature protocol with reused medium from C), thermal stress (TS, thermal stress protocol with fresh medium), stress medium (SM, control temperature protocol with reused medium from TS), and thermal stress + stress medium (TS+SM, thermal stress protocol with reused medium from TS). Conditioned media were immediately re-used for treatments containing putative stress or control metabolites, respectively. As development in zebrafish accelerates with higher temperature (Kimmel et al., 1995), but decelerates with darkness (Bucking et al., 2013; Villamizar et al., 2014), additional control embryos were monitored after longer incubation times: 31 hrs (C31), 37 hrs (C37), and 46 hrs (C46), which yielded eight conditions in total. These times were adjusted for darkness-raised embryos to reach the stages of prim-6 (25 hpf), prim-16 (31 hpf), and late pharyngula (35-42 hpf), respectively (**Figure 3.2**). Initial, final, and total exposure times were used to standardise each procedure. After incubation, transparent embryos were deemed alive and kept for subsequent steps.

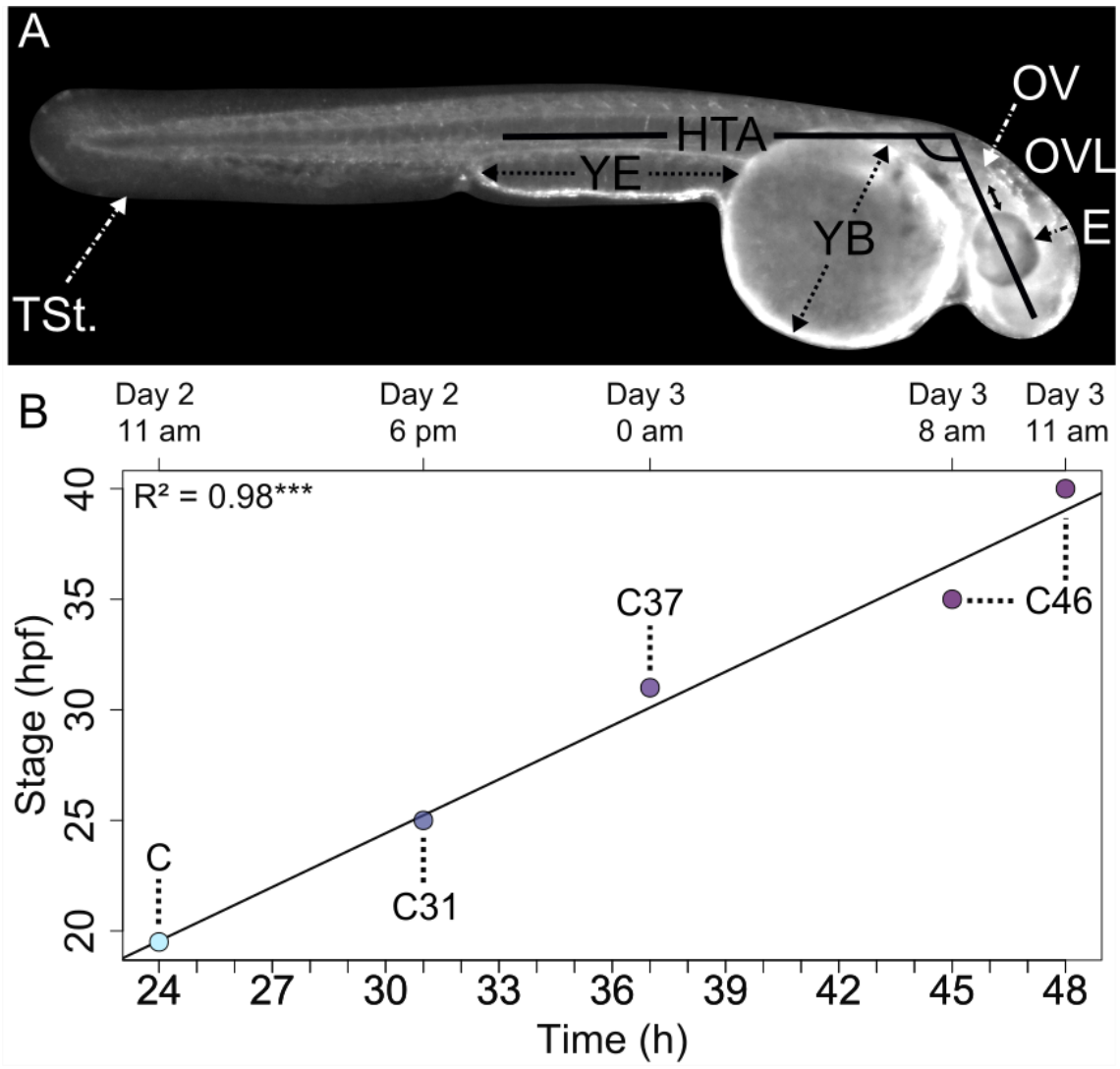

Figure 3.2. Optimisation of exposure times to reach different final stages. Stages expressed in hours post fertilisation (hpf). A) Example onset image (modification: manually contoured and enhanced contrast) of control embryo in late pharyngula stage (35-42 hpf) with criterion used for staging according to Kimmel et al. (1995): head-trunk angle (HTA), ratio between yolk ball (YB) and yolk extension (YE), otic vesicle length (OVL) defined as the distance between the eye (E) and otic vesicle (OV), and the strengthening of the tail (TSt.). B) Developmental delay in complete darkness as shown by the mismatch between time of exposure (hours) and final stage (hpf). Control embryos were raised in darkness with different incubation times: 24 hrs (C), 31 (C31), 37 (C37), and ~46 hrs (C46) to reach the stages of 21-somite (19.5 hpf), prim-6 (25 hpf), prim-16 (31 hpf), and late pharyngula (35-42 hpf).

3.6.3. Developmental and Behavioural Analysis

Phenotypes were observed for all eight treatments. Embryos were placed in a watch glass vial and videoed by small batches using the camera setup for 20 seconds. Embryos were placed under light (similar intensity across measurements) to elicit a startle-like response after exposure in darkness. Behavioural data was analysed using Danioscope (Noldus). Where possible, several videos were recorded for each embryo clutch, and behavioural measurements were averaged for each individual embryo. Behavioural analyses were conducted on video-length standardised data: burst counts

per minute and burst activity percentages (percentage of the time, from the total measurement duration, the embryo was moving). Final embryonic stages were estimated following Kimmel et al. (1995) from several photographs of embryos within their chorions using the criteria somite number, yolk extension to yolk ball ratio, presence and morphology of otoliths, tail aspect, presence of lens primordium, presence and position of the cerebellum relatively to the eyes, and pigmentation. The growth index was calculated as in **Equation 3.1**.

$$\Delta hpf/hr = \frac{\text{embryo final stage (hpf)} - \text{batch median initial stage (hpf)}}{\text{batch exposure time (hr)}} \qquad \textbf{Equation 3.1}$$

Statistical analyses were conducted in RStudio (RStudio Team, 2020). Outlier behavioural values were excluded using Tukey's fence method with a 1.5 interquartile range cut-off (Tukey, 1977). The effects of two-way predictors (stress medium and thermal stress) were evaluated across the C, TS, SM, and TS+SM treatments. Shapiro-Wilk and Levene's tests were used to evaluate normality and homogeneity of variances, respectively. Normalisation methods were compared using the *BestNormalize* R package (Peterson and Cavanaugh, 2020). The growth index was normalised using an order normalising transformation (Shapiro-Wilk's $p = 0.98$, Levene's $p = 0.27$), and analysed by a two-way ANOVA with thermal stress and stress medium as predictors, followed by post-hoc pairwise Student's t-tests between control C and each experimental condition. Burst activity percentages, burst counts per minute, and final stages (in hpf) could not be normalized and were analysed for the effects of both predictors using nonparametric Scheirer-Ray-Hare tests from the *rcompanion* R package (Mangiafico, 2021), followed by pairwise post-hoc Wilcoxon-Mann-Whitney tests. Final embryonic developmental periods were coded as either segmentation or pharyngula and analysed for the effects of thermal stress and stress medium as factors and initial stages as covariate using a generalised logistic model. This was followed by pairwise post-hoc comparisons using the *emmeans* R package (Lenth, 2021). Pairwise tests also compared all response variables of CM against C and SM. To determine whether behavioural effects of treatment were related to developmental acceleration, behavioural responses of control embryos (C) were compared to that of older control embryos (C31, C37, C46) using Kruskal-Wallis tests. Behaviour responses of embryos from stress medium and thermal stress treatments were also compared against that of control embryos incubated for longer times using pairwise Wilcoxon-Mann-Whitney

tests. Pairwise comparisons were corrected for multiple testing using Bonferroni adjustments. Additional to temperature and stress medium as the main predictors, the effects of confounding factors were assessed. Because experiments were repeated on different days, median initial stages slightly differed across batches with CM treatments starting in average at 2.75 hpf (512-cell) and thus were somewhat older than in C and SM conditions that started at 2 hpf in average (64-cell). However, median initial stages in SM (2 hpf), TS (3.08 hpf), and TS+SM (2.25 hpf) treatments were not statistically different compared to control embryos (2 hpf, all $p > 0.05$). The effects of batch median initial stages on behavioural responses were analysed using Kruskal-Wallis tests. Effect sizes were expressed as Cohen's |d| obtained from the *effsize* R package (Torchiano, 2016) when comparing two groups, or according to Lenhard and Lenhard (2016) for two-way models. Effect sizes were based on thresholds given in Sawilowsky (2009): very small: $|d| > 0.01$, small: $|d| > 0.2$, medium: $|d| > 0.5$, large: $|d| > 0.8$, very large: $|d| > 1.20$, huge: $|d| > 2.0$.

3.6.4. Oxygen and pH measurements

For a subset of embryos, embryo media were sampled before and after each treatment exposure, to measure pH and O_2 saturation levels that could impact embryos in conditioned media. In a preliminary set of experiment[1], oxygen levels were measured using the Unisense oxygen sensor which consisted of the Oxygen measuring system 1-CH (OXY METER, Unisense) combined with the Oxygen Microsensor 200 μm (OX-200, Unisense) and read using the SensorTrace Logger (STLOGGER, Unisense). The oxygen electrode was prepared 2 hours before use to ensure pre-polarisation. The device was calibrated once the signal was stable for 10 minutes. The calibration was performed by filling the calibration chamber (CAL300, Unisense) with 300 mL of calibration solutions: one 100% oxygen saturated 1X E3 medium sample and one 0% oxygen 1X E3 medium sample. The 100% saturated calibration solution was saturated with oxygen via bubbling for 5 minutes using an attached air pump. The 0% saturated calibration solution was made anoxic by bubbling using nitrogen gas. The calibration was set once the reading of the calibration solution was stable. After calibration, oxygen levels were measured in the embryo medium obtained from experimental conditions. As the microprobe oxygen method above was not available for my experiments, oxygen levels were additionally routinely verified on larger volumes (1.5 to 2 mL of pooled embryo

[1]Oxygen measurements using Unisense were performed by Victoria Scott in preliminary work prior to the commencement of my experiments.

medium) from 2 min-long measurements in a 5 mL glass vial equipped with an oxygen sensor spot (OXSP5, sensor code: SC7-538-193, Pyroscience GmbH) and connected to the FireSting O_2 Fiber Optic Oxygen Meter (FSO2-4, Pyroscience GmbH) and Oxygen Logger software (Pyroscience GmbH). pH levels were measured using a pH electrode (Mettler Toledo™ Specialty Series pH and pH/ATC Combination Electrodes: InLab™ Flex-Micro pH; #11324213; Fisher Scientific) connected to the Fisherbrand™ accumet™ AB150 pH Benchtop Meters (#12880633; Fisher Scientific). Three-point calibrations (pH 4.0, pH 7.0, pH 10.0) were done before each new series of measurements. pH levels were assessed by immersing the sensor in at least 1 mL of embryo medium and values were noted after 10-second stabilisation. pH sensors were rinsed with ultrapure water between each sample measurement. Of note, pH and oxygen level measurements were limited because the experimental design required to keep the conditioned medium for treatments.

3.6.5. Gene expression

Gene expression was measured in CM, C, SM, TS, and TS+SM treatments (n = 3 replicate pools each representing the average gene expression of 60 embryos per treatment i.e., a total of 180 embryos per treatment). Embryos were snap-frozen at -80°C immediately after experimental treatments. Total RNA was extracted using the High Pure RNA Isolation Kit (cat. n° 12033674001, Sigma-Aldrich Company Ltd., Missouri, USA) following the manufacturer's recommendations, with small adjustments for optimisation: (i) 400 µL of lysis/binding buffer (in two steps of 100 µL and 300 µL with 15 min incubation in ice for optimal tissue disruption) were added to 1.5 mL tubes and embryos were manually homogenised for 30-45 s using plastic pestles (pre-cleaned with RNAse-away and 75% ethanol). (ii) Total RNA was eluted in 50 µL Elution Buffer and centrifuged 1 min at 8,000 rpm. Eluted RNA was passed another time through the column and the centrifugation repeated to enhance extraction yields. For each reaction, 11 µL were aliquoted for triple-assessment of RNA quality whilst the remaining volume was immediately stored at -80°C until further processing to limit RNA degradation. RNA integrity was assessed by observing clear 28S and 18S bands in electrophoresis (70V for approx. 1 hr) by loading samples pre-mixed in 1/5 v/v loading dye (Gel Loading Dye Purple, 6X, New England Biolabs) in a 1% agarose gels in 1X Tris/Borate/EDTA buffer (dilution of 10X TBE, Fisher Bioreagents, in ultrapure water) with 1/30,000 v/v GelRed Nucleic Acid Stain 10,000X in DMSO (Cambridge Bioscience) observed using the Bio-Rad ImageLab. Total RNA was quantified using the

Qubit® fluorometer and Qubit RNA BR Assay Kit (Invitrogen). RNA purity was assessed using the NanoDrop 1000 spectrophotometer (Thermo Scientific). Ratios ranged within [2.03-2.30] and [1.98-2.22] for 260/280 and 260/230 ratios, respectively. Total RNA was deemed suitable for further processing.

From total RNA samples, mRNAs were randomly reverse-transcribed in a 20 µL reaction for a final concentration of 16 ng/µL using the Superscript II™ Reverse Transcriptase kit (Invitrogen, Life Technologies Ltd.). For each reaction, 320 ng of RNA were combined with 1 µL of oligodT (Nanoscript Precision™ OligoDT primer mix, Primer Design), 1 µL of nucleotides (dNTP mix, 10 mM each), and molecular grade water up to a total volume of 13 µL. The preparation was incubated 5 min at 65°C and immediately chilled on ice. Four microliters of 5X First Strand Buffer and 2 µL of 0.1 M DTT (Invitrogen, Life Technologies Ltd.) were added to each reaction. After incubation at 42°C for 2 min, 1 µL of Superscript II™ Reverse Transcriptase (Invitrogen, Life Technologies Ltd.) was added. No Reverse Transcription (NRT) reactions served as negative controls, prepared by replacing the enzyme by molecular grade water. cDNA was then synthesised for 50 min at 42°C and the reaction terminated by 15 min at 70°C. The success of the cDNA synthesis was checked (i) by 1% agarose gel electrophoresis and (ii) by conventional PCR with previously optimised custom primers for elongation factor alpha 1 (*eef1a1l1* – here referred to as *ef1-a*, GenBank: NM_131263, forward primer: 5'-GATGCACCACGAGTCTCTGA-3'; reverse primer: 5'-TGATGACCTGAGCGTTGAAG-3') and Cu/Zn-superoxide dismutase (*sod1*, GenBank: Y12236, forward primer: 5'-CGTCTGGCTTGTGGAGTGAT-3'; reverse primer: 5'-TAATGTCAGCGGGCTAGTGC-3'). The PCR program consisted of 5 min at 95°C followed by 40 cycles of 30 s at 95°C, 30 s at 62°C, and 30 s at 72°C, 1 min at 60°C and a final elongation of 5 min at 72°C. PCR reactions were loaded in a 2% agarose gel in 1X TBE alongside 100p DNA ladder (New England Biolabs). The presence of one sharp band in +RT and the absence of amplicon in NRT samples validated the cDNA integrity. Sharp bands were observed when loading cDNA from 0.16 ng to 32 ng in 20 µL of PCR reaction, which justified dilution of cDNA samples for qPCR. Fourfold diluted cDNA samples (4 ng/µL) were then prepared in molecular grade water and stored at -20°C until used in qPCR.

TaqMan® Gene Expression Assays (Thermo Fisher Scientific) and 2X qPCR Bio Probe Hi-ROX (PCRBiosystems) were used to quantify the expression of three genes of interest (GOIs): sulfide:quinone oxidoreductase (*sqor*, TaqMan® assay ID:

Dr03122210_m1), superoxide dismutase 1 (*sod1*, TaqMan® assay ID: Dr03074067_m1), and interleukin-*1β* (*il-1β*, TaqMan® assay ID: Dr03114368_m1). Two reference genes (eukaryotic translation elongation factor 1 alpha 1, like 1, *eef1a1l1* – here referred to as *ef1-a*, TaqMan® assay ID: Dr03432748_m1; and actin, beta 1, *actb* – here referred to as *β-actin*, TaqMan® assay ID: Dr03432610_m1) were chosen for normalisation. The compatibility of the universal probe kit 2X qPCR Bio Probe Hi-ROX (PCRBiosystems) with each TaqMan® probe was assessed after successful amplification in conventional PCR. For this, half reactions were prepared with 2 µL of diluted cDNA samples (4 ng/µL), 0.5 µL of 20× TaqMan® Gene Expression Assay, and 5 µL of 2X qPCR Bio Probe Hi-ROX. The PCR program was as follows: 5 min at 50°C followed by 40 cycles of 15 s at 95°C and 1 min at 60°C. PCR samples were loaded in 2% agarose gels in 1X TBE. Sharp bands were observed for diluted cDNA samples and NRT samples did not result in amplification. Gene expression was subsequently measured in quantitative PCR with methods based on TaqMan® Gene Expression Assays (Thermo Fisher, available at http://tools.thermofisher.com/content/sfs/manuals/cms_041280.pdf). Each 20 µL qPCR reaction contained 16 µL of a master mix made of 10 µL of 2X qPCR Bio Probe Hi-ROX (PCRBiosystems), 1 µL of 20× TaqMan® Gene Expression Assay, and 5 µL of molecular grade water. Each qPCR reaction was completed with 4 µL of cDNA template at 4 ng/µL. No template Control (NTC) and NRT reactions were added and validated the procedure as they were not expressed or at > 5 cycle thresholds (C_T) after the lowest sample. Standard runs (2 hrs) of qPCR consisted of 2 min at 50°C, 10 min at 95°C, followed by 40 cycles of 15 s at 95°C and 1 min at 60°C. Gene expression was analysed using the StepOnePlus™ Real-Time PCR System coupled with the StepOne™ software v2.3 (Applied Biosystems™). Sample maximisation strategies (as many samples as possible for one gene measured in the same plate) were used to limit run-to-run variation (Hellemans et al., 2007). Reference gene stability was verified using RefFinder (Xie et al., 2012) (available online at https://www.heartcure.com.au/reffinder/, accessed January 2020). GeNorm (Vandesompele et al., 2002), NormFinder (Andersen et al., 2004), and BestKeeper (Pfaffl et al., 2004) algorithms were used to assess the suitability of reference genes. GeNorm expression stability value M was below 0.5 and 1.5 (M = 0.164 for ef1-α and geometric mean, M = 0.239 for β-actin), which indicated stable reference genes (D'haene and Hellemans, 2010; Sarker et al., 2018). Standard deviations of cycle threshold were around 1 (SD Ct ef1-α = 1.011, SD Ct β-actin = 1.098, SD Ct geometric mean = 1.042), which was deemed stable (Pfaffl et al., 2004).

The geometric mean of both reference genes improved the stability value in normFinder (*ef1-a*: 0.243, *β-actin*: 0.264, geometric mean: 0.082) and was used to normalise expression values. Cycle thresholds of samples that were run on different plates were expressed as calibrated C_T values (Vermeulen et al., 2009) relative to one or two plate intercalibrators (IRC) to account for plate-to-plate differences. The relative gene expression was expressed as log fold-change (LFC) (Livak and Schmittgen, 2001) as shown in **Equation 3.2** and **Equation 3.3**.

$$\Delta\Delta CT = (C_T\ GOI - C_T\ ref_{Treatment}) - (C_T\ GOI - C_T\ ref_{Control}) \qquad \textbf{Equation 3.2}$$

$$LFC = \log_2{}^{-\Delta\Delta CT} \qquad \textbf{Equation 3.3}$$

The qPCR assay using TaqMan® probes did not necessitate amplification efficiency calculation, as per the manufacturer's Application Note, (Applied Biosystems, 2006). The effects of stress medium and thermal stress on the $Log_2\ 2^{-\Delta\Delta CT}$ values were investigated using the *eBayes* and *lmFit* functions within the *limma* package (Ritchie et al., 2015) within the *Bioconductor v.3.11* (Ihaka and Gentleman, 1996) R environment. Next, pairwise post-hoc comparisons on C vs SM, TS, or TS+SM, and CM vs C or CM were performed using pairwise moderated t-tests with Bonferroni adjustments. Effect sizes (Cohen's |d|) were calculated as before (see section **3.6.3**).

3.6.6. Heat Shock Proteins and Cortisol

To verify that the thermal stress treatment caused heat stress to embryos, two common heat stress biomarkers were quantified in embryos: protein levels of heat shock protein 70 (HSP70)[2] and whole-body cortisol levels. Stress biomarker levels were measured in C, SM, TS, and TS+SM. An additional control (C31) was used for the HSP70 quantification. In this protocol, eggs were sanitised using bleach baths (Westerfield, 2000) after collection at 0 dpf to avoid unwanted microbial contamination whilst avoiding the use of methylene blue, which might have otherwise affected enzymatic and colorimetric measurements. Embryos were placed in a small tea strainer and transferred through a series of small petri dish (⌀: 35 mm) filled with ~9 mL of medium in the following order: bleaching medium, 1X E3 embryo medium, bleaching medium, and 1X E3 embryo medium (twice). The bleaching medium contained 0.004%

[2]Western Blots (and their methodological description) for the HSP analysis were done by Quentin Rodriquez-Barucg and supervised by Pedro Beltran-Alvarez. I analysed the final data.

bleach, by diluting 10-13% active sodium chloride in fresh 1X E3 embryo medium. Embryos were sanitised by gentle swirling during 3-4 minutes in each bath, followed by thorough rinsing in clean 1X E3 embryo medium, before the embryos were placed in a new petri dish in clean 1X E3 embryo medium free of bleach carry-over.

At the end of the exposure, three pools of 20 embryos per treatment (i.e., a total of 60 embryos per treatment) were sampled and immediately euthanised by snap-freezing at -80°C in sterile 1.5 mL microcentrifuge tubes. This pool sampling captured the average amount of expressed protein or cortisol content of 20 embryos per replicate. Cortisol was extracted from zebrafish embryos using methods adapted from Wilson et al. (2013). Embryos were homogenised in 100 µL ice-cold v/v solution of pre-autoclaved 1X PBS (Dubelco A, Oxoid™ Phosphate Buffered Saline Tablets, BR0014G) and methanol (34860, Sigma-Aldrich) for approx. 30 seconds using plastic pestles and brief vortexing. The manual pestle homogenisation was repeated another time following 15 min of incubation in ice to optimise embryo lysis. Homogenates were then sonicated in ice for 5 min (high intensity with 5 × 30 sec intervals) using the Bioruptor Sonicator (Diagenode) before being incubated for 1 hour at 4°C at 10 revolutions per minute on a rotary shaker. Next, lysates were centrifuged at 13,000 g for 5 min. At this step, samples were randomised (using a R script for random sorting) for blind analysis. Twenty microliters of this supernatant were aliquoted to a separate tube (for total protein quantification for normalisation). The remaining volume of supernatant (~80 µL) was transferred to a new sterile 1.5 mL microcentrifuge tube and evaporated until complete dryness (approx. 45 to 90 min) at room temperature under nitrogen flow. Pellets were reconstituted in 125 µL ice-cold ELISA assay reagent buffer (Salivary Cortisol ELISA kit 1-3002, Salimetrics) and resuspended by vortexing before being stored at -80°C. Resuspended samples were split in half for quantification of cortisol and HSP70 using ELISA and western blotting, respectively.

Cortisol extraction recovery rates (71.3% ± 7.32%, n = 4) were validated by spiking 100 µL of ice-cold v/v PBS/methanol with 20 µL of 100 pg/µL cortisol standard, obtained by a tenfold dilution series from a 1 µg/µL cortisol standard stock solution containing 10.9 mg of H0396 (Sigma, 92 mg hydrocortisone per g powder) in 1 mL of molecular grade water. Total protein concentrations were measured in the 20 µL of aliquoted PBS/Methanol lysate using the Qubit™ Protein Assay Kit. To determine whether Qubit measurements were impacted by methanol, a 2 mg/mL Bovine Serum Albumin (BSA) standard was diluted to 1 mg/mL in 50% methanol, which was then

diluted in ice-cold PBS/methanol (v/v) at the following concentrations: 0.75 mg/mL, 0.50 mg/mL, 0.25 mg/mL, 0.125 mg/mL, and 0.05 mg/mL. Methanol showed no effect on the Qubit quantification given that the Qubit values were correlated with the standard input ($r^2 = 0.999$). This confirmed the suitability of the Qubit™ Protein Assay kit for protein quantification of zebrafish embryos in PBS containing up to 50% methanol. Cortisol concentrations were interpolated from the standard curve which was computed as a 4-parameter nonlinear regression curve using the online calculator mycurvefit.com (accessed 25/03/2021, $r^2 = 0.9998$, p = 0.0004, F = 2,256, **Figure 3.3**).

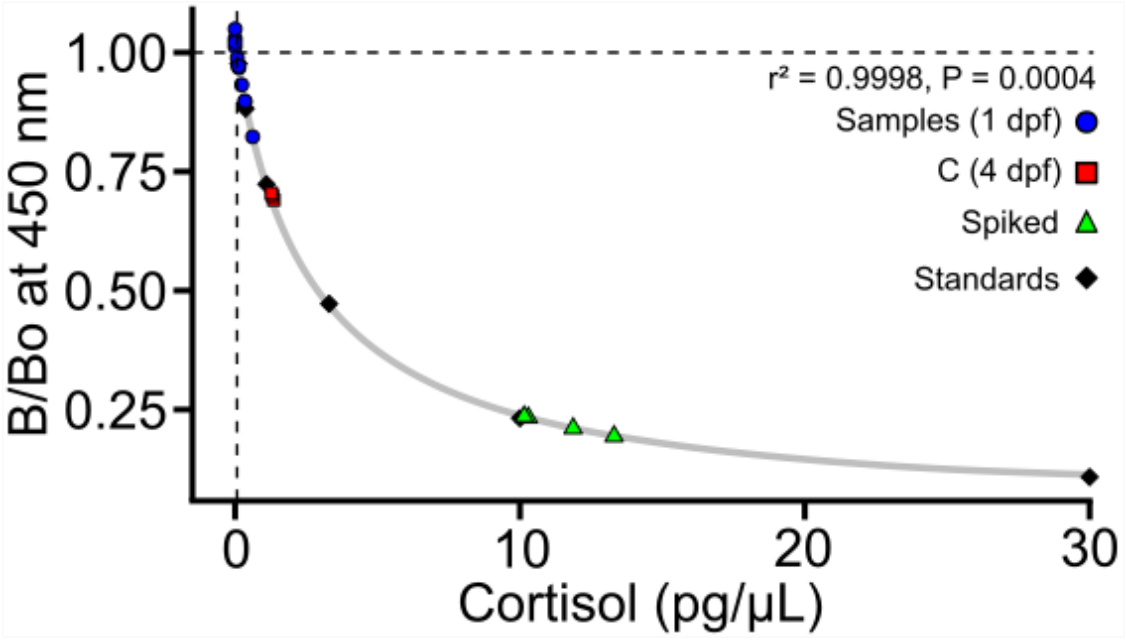

Figure 3.3. Validation of cortisol assay. Standard curve of cortisol assay (grey line) of the blank-corrected cortisol absorbance (B/Bo, at 450 nm) in function of cortisol standards (pg/µL). Standard curve replicated using the four-parameter nonlinear regression equation computed by mycurvefit.com (equation fit given in top-right corner). Values from embryos at 1 day post fertilisation (dpf, blue circles, n = 12) were interpolated from the standards (black diamonds, n = 6). Four samples with values outside the detection range (0.07 pg/µL, dashed lines) were arbitrarily replaced by "0 pg cortisol/µL per µg/µL protein". Positive controls of zebrafish embryos at 4 dpf are shown for reference (red squares, n = 3). Extraction efficiency was estimated as 71% ± 9% using samples spiked with a known cortisol concentration (16 pg/µL, green triangles, n = 4).

Cortisol concentrations were standardised to total protein concentrations as pg cortisol/µL per µg/µL protein. Because n = 4 samples (out of 12) were lower than the detection range, their values were arbitrarily assigned as "0 pg cortisol/µL per µg/µL protein". This required to perform a more "qualitative" analysis to determine whether the cortisol concentration and the out-of-range samples were related to experimental treatments. This was done using a two-factorial nonparametric Scheirer-Ray-Hare test from the *rcompanion* R package (Mangiafico, 2021). Due to the low levels of cortisol in 1-dpf embryos which have been reported in previous studies (Alsop and Vijayan, 2008;

Wilson et al., 2013), the assay was validated by measuring cortisol in a positive control, that is, embryos at 4 dpf, for reference.

Western blot analyses were used to quantify HSP70 protein levels in zebrafish embryos. Proteins were separated by SDS-PAGE in 12% gels alongside a protein marker (#26619, Thermo Fisher). Proteins were transferred to a polyvinylidene fluoride membrane (PVDF, GE Healthcare) at 110 mA for 1 h. Membranes were blocked in 5% milk powder in TBST (50 mM Tris-HCl, 150 mM NaCl, 0.05% Tween-20, pH = 7.4) for 1 h and probed overnight at 4◦C with primary HSP70 antibody (#11565722 Fisher Scientific UK), diluted in 5% milk in TBST at 1:1000 dilution. After three washes with TBST, membranes were incubated with HRP-conjugated secondary antibody (Dako, Beijing, China) for 1 h at room temperature, washed, and signals were visualised by incubation with HRP substrate (Millipore, Burlington, MA, USA). Ponceau staining was used as a total loading control. Membranes were incubated in Ponceau for 10 minutes at room temperature and then washed in water for 20 minutes. Two bands were used to quantify the amount of protein and normalise the data. Protein levels were quantified using ImageJ (National Institute of Health, Bethesda, MD, USA. http://rsb.info.nih.gov/ij) (Schneider et al., 2012). One table-wide outlier (6.7% of a total of 15 values) amongst data of normalised HSP70 protein levels was detected using a Grubbs' test ($G = 2.78$, $U = 0.41$, $p = 0.006$). This resulted in a sample of $n = 3$ biological replicates in TS, SM, TS+SM, and C31, and $n = 2$ in the treatment C. This led to considering a pooled population of C31 (prim-6 after 31 hours of exposure to be stage-matched to median stages in SM, TS, and TS+SM) and C (after 24 hours of exposure) as the control ($n = 5$) of mixed stages similar to that reached by stressed embryos. HSP70 values failed normality assumption following a Shapiro-Wilks test, thus a nonparametric two-way Scheirer-Ray-Hare test from the *rcompanion* R package (Mangiafico, 2021) was used to model the effects of thermal stress and stress medium predictors on the protein level of HSP70 across all five treatments.

3.7. Results

3.7.1. Phenotypic effects of thermal stress and its propagation

The phenotypic effects of fluctuating thermal stress and of stress medium treatments were analysed (**Figure 3.4A-F**). Embryonic growth indices were significantly accelerated by the factors stress medium (small effect size, $F = 6.291$, $p = 0.0128$), thermal stress (large effect size, $F = 75.502$, $p < 0.0001$), and their combination

(very large effect size, F = 7.498, p = 0.0067, **Figure 3.4A**, **Table Appendix 2 S2**). Post-hoc tests revealed that TS (t = -7.9874, p < 0.0001), SM (t = -3.6784, p = 0.0012), and the combined treatment TS+SM (t = -7.2413, p < 0.0001) all accelerated growth, compared to the control C (**Table Appendix 2 S2**). The control medium containing regularly excreted metabolites excluded the role of oxygen saturation and pH as confounding variables. These levels were also independently measured at the beginning of treatments and in all cases fell within zebrafish natural tolerance ranges, with pH and oxygen levels ranging between [6.54-7.84] and [6.5-10.6 mg/L], respectively (Strecker et al., 2011; Zahangir et al., 2015). This chapter explored whether stress medium, that is, the conditioned medium of embryos exposed to thermal stress, evoked different effects compared to control medium. Embryonic growth in CM was compared to growth in C and SM. Embryos in CM grew slightly slower than control embryos (t = 2.3472, p = 0.0418) and much slower than embryos in SM (t = -6.7215, p < 0.0001, **Figure 3.4A**, **Table Appendix 2 S2**). As a consequence of faster growth, thermally-stressed embryos TS (H = 71.096, p < 0.0001) and the interaction of TS+SM (H = 6.074, p = 0.0137) led to significantly older embryonic stages (**Figure 3.4B**, **Table Appendix 2 S3**). Embryos stressed by SM (W = 611.5, p = 0.0056), TS (W = 766.5, p < 0.0001), and TS+SM (W = 526.5, p < 0.0001) treatments were at a median stage of 25 hpf (prim-6) whereas control embryos were 22-hpf old (26-somite, **Figure 3.4C**). Embryos in CM were also at a stage of 22-hpf, similar to C, but which is significantly younger than SM (W = 699, p = 0.0015). Kimmel et al. (1995) classified two embryonic periods as segmentation (10-22 hpf) and pharyngula (24-48 hpf). Heat (Z = -7.035, p < 0.0001), stress medium (Z = -3.255, p = 0.0011), and the interaction term (Z = 2.897, p = 0.0038) significantly shifted the timing of entrance into the pharyngula period (**Figure 3.4C**, **Table Appendix 2 S4**). Most embryos were in pharyngula period after treatment with SM (Z = -3.255, p = 0.0034), TS (Z = -7.035, p < 0.0001), and the combined treatment TS+SM (Z = -5.804, p < 0.0001) against only a quarter in C. The percentage of embryos in the pharyngula period in CM did not significantly vary compared to control but was significantly lower than in SM (Z = 3.456, p = 0.0005). Final stages (χ^2 = 104.49, Spearman's ρ = 0.25, both statistics with p < 0.0001) and final periods (Z = -2.5211, p = 0.0117) were however also significantly dependent on median initial stages. In summary, the growth acceleration in TS, SM, and TS+SM was accompanied by a median advancement in embryonic stages of 3 to 9 hours, resulting in a switch from the segmentation to the pharyngula stage, compared to controls C and CM.

The behaviour of embryos was investigated in response to acute light (**Figure 3.4E-F**). Burst activity percentages were significantly lowered by both predictors stress medium ($H = 9.3222$, $p = 0.0023$) and thermal stress ($H = 17.008$, $p < 0.0001$), whereas the interaction term was not significant ($H = 1.8193$, $p = 0.1774$, **Table Appendix 2 S5**). Post-hoc comparisons showed that embryos treated with SM ($W = 1{,}387$, $p = 0.0018$), TS ($W = 3{,}548$, $p = 0.0003$), and TS+SM ($W = 2{,}455$, $p < 0.0001$) all displayed lower burst percentages compared to control C. Embryos exposed to CM showed an even stronger decline in burst activity percentages compared to C ($W = 3{,}287$, $p < 0.0001$) and SM ($W = 1{,}745$, $p < 0.0001$, **Table Appendix 2 S5**). In addition to the effects of both factors (thermal stress and stress medium), burst activity percentages significantly decreased with initial stages (Spearman's $\rho = -0.33$, $p < 0.001$) across all treatments. However, burst activity percentages did not correlate with final stages (in hpf, Spearman's $\rho = -0.08$, $p = 0.1627$) nor growth indexes (Spearman's $\rho = 0.04$, $p = 0.5027$, **Table Appendix 2 S5**).

Considering the stress-induced growth acceleration, stage-dependent effects of behaviour were investigated in control embryos incubated for 24, 31, 37, or 46 hrs. Burst activity percentages significantly decreased with development in control embryos raised for 31, 37, and 46 hrs compared to those incubated for 24 hrs ($X^2 = 99.639$, $p < 0.0001$, Spearman's $\rho = -0.70$, $p < 0.0001$, **Figure 3.4E**, **Table Appendix 2 S6**). Moreover, pairwise tests showed that embryos with development accelerated by TS, SM, and TS+SM treatments were significantly more active than control embryos reaching the same median stage of prim-6 in C31 ($p < 0.0001$, **Figure 3.4E**, **Table Appendix 2 S6**). All patterns were similar for the burst counts per minute data (**Figure 3.4F**). Treatments had no obvious effect on mortality.

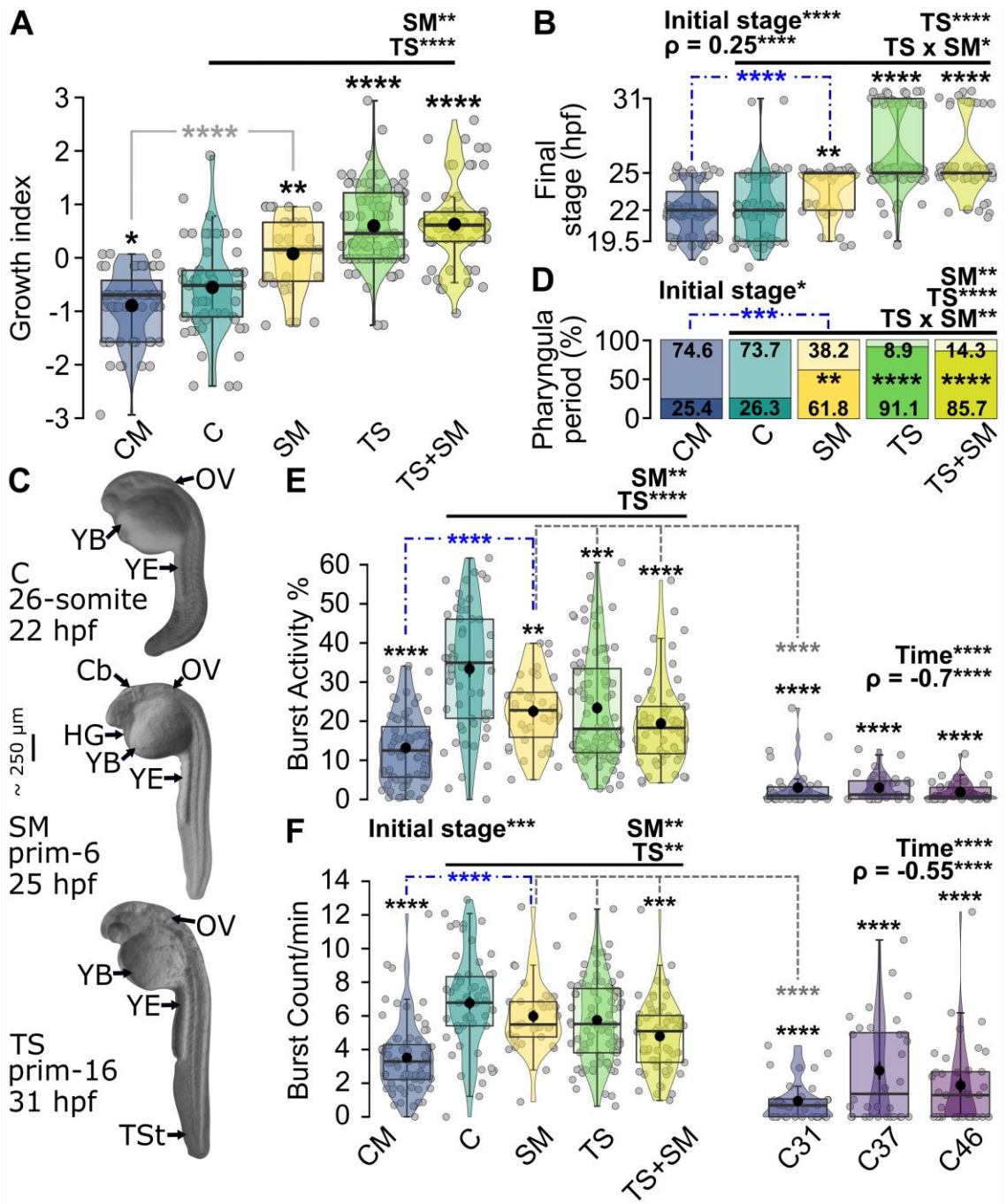

Figure 3.4. Thermal stress and stress medium accelerate growth and cause hypoactivity. A) Growth index stage at 1 day post fertilisation (dpf). B) Final stage in hrs post fertilisation (hpf). C) Representative images (image modification: manually detoured) of advanced development in stressed embryos in stress medium (middle) and thermal stress (right), compared to control (left). OV: otic vesicle; YE/B: yolk extension and ball; Cb: cerebellum; HG: hatching gland; TSt.: straight tail. D) % of embryos in pharyngula (25-42 hpf, dark areas) or segmentation (18-22 hpf, light areas). E) Burst activity % and F) burst count per minute. Boxes show median and 25%-75% quartiles. Whiskers are min/max values within 1.5 IQR. Jittered raw data given as grey circles. Black dots show mean ± SE. Significant 2-way model predictors (thermal stress and stress medium) are shown above horizontal black bars. Significant post-hoc tests compare conditions vs C (black asterisks), SM vs CM (blue dot-dash bars/asterisks), or stressed embryos (SM, TS, TS+SM) vs C31 (dark grey dashed bars/asterisks). Treated embryos were incubated from 2.75 hpf for 24 hrs in CM: control medium (n = 67), SM: stress medium (n = 34), TS: thermal stress (n = 90), and TS+SM (n = 56). Control embryos were incubated for 24 (C, n = 57), 31 (C31, prim-6, n = 32), 37 (C37, n = 32), and 46 (C46, n = 37) hrs to account for time effect on behaviour (Kruskal-Wallis/correlation statistics shown in top-right in E-F). *: $p \leq 0.05$, **: $p \leq 0.01$, ***: $p \leq 0.001$, ****: $p \leq 0.0001$.

3.7.2. Effects of heat and stress medium on stress-related gene expression

Increased HSP70 protein levels in heat-treated embryos confirmed that repeated exposure to 32°C caused heat stress (**Figure 3.5A**, **Table Appendix 2 S7**), validating the experimental design to investigate stress propagation. In contrast, neither thermal stress nor stress medium altered cortisol levels (**Figure 3.5B**, **Table Appendix 2 S8**). Next, the whole-embryo expression of three stress-inducible candidate genes (*il-1β*, *sod1* and *sqor*) was analysed (**Figure 3.5C-D**, **Table 3.1**). Heat treatments were not a significant predictor variable for the expression of *il-1β*, *sod1*, and *sqor*. Pairwise comparison showed that *sod1* expression was slightly lowered in the TS treatment compared to the fresh medium control C (with marginal significance, t = 2.76, p = 0.045). Comparing the molecular responses between CM and SM helped determining whether stressed and unstressed embryos have different profiles. Contrary to thermal stress, stress medium treatment did not increase HSP70 levels (**Figure 3.5**A, **Table Appendix 2 S7**), but stress medium significantly reduced *il-1β* expression (very large effect size, t = 2.28, p = 0.038) and increased *sqor* expression (huge effect size, t = -3.54, p = 0.003) compared to fresh medium. There were greater differences in the expression of *il-1β*, *sod1*, and *sqor* between CM and treated embryos (i.e., SM, TS, and TS+SM), than between C and treated embryos (**Figure 3.5C-E**). Pairwise tests between CM and SM conditions revealed significant differences in *sod1* (very large effect size, t = -2.64, p = 0.034), *il-1β* (very large effect size, t = 2.62, p = 0.034) and a trend for difference in *sqor* expression (p = 0.08; **Table Appendix 2 S8**-**S9**), indicating that SM and CM have distinct molecular profiles. The gene expression data suggested that incubation in the stress medium of previously heat-stressed embryos altered the antioxidant and immune responses in receiver embryos.

Table 3.1. Effect of thermal stress and stress medium on gene expression. Effects of model terms (thermal stress and stress medium) on the expression of *il-1β*, *sod1* and *sqor* were obtained via moderated t-tests (t-statistic). B describes the log-odds of gene expression. Effect size (Cohen's |d|) is interpreted according to Sawilowsky (2009). Significant terms ($p \leq 0.05$) are shown in bold.

Model terms	t	B	P	|d|	Effect size
il-1β					
Thermal Stress	1.03	-4.70	0.310	0.49	medium
Stress Medium	2.28	-3.95	**0.038**	**1.20**	**very large**
sod1					
Thermal Stress	1.65	-4.27	0.108	1.08	large
Stress Medium	0.32	-6.16	0.757	0.17	small
sqor					
Thermal Stress	-0.17	-4.99	0.869	0.11	small
Stress Medium	-3.54	-1.67	**0.003**	**2.43**	**huge**

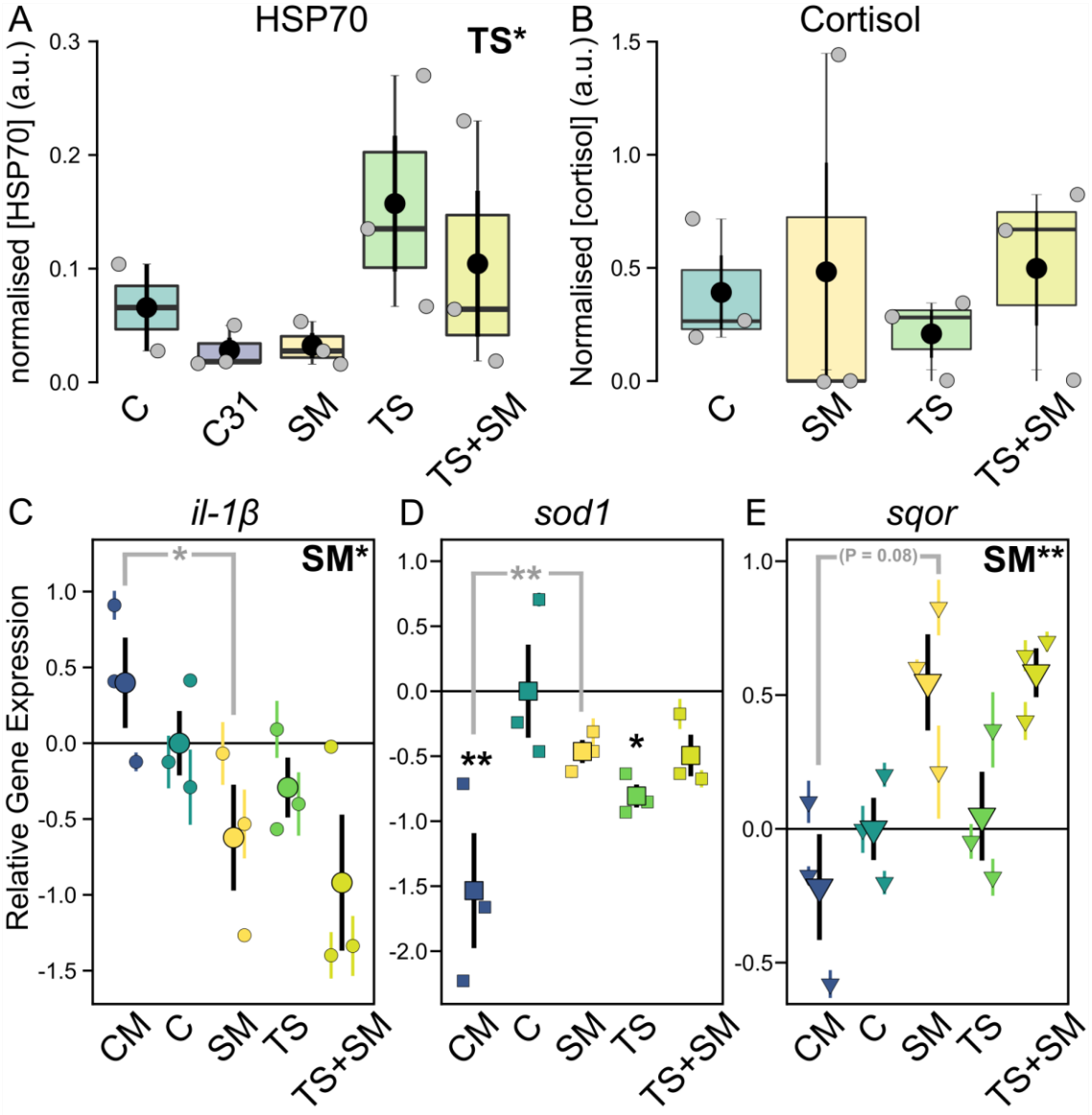

Figure 3.5. Stress medium alters stress-related gene expression of zebrafish embryos. Molecular data at 1 day post fertilisation (dpf) after 24 hr-long exposure in stress medium and thermal stress factorial design. A) Protein expression of heat shock protein 70 (HSP70) normalised to total protein loading (arbitrary units, a.u.). C and C31 were used as a pooled control due to excluded significant table-wide outlier in C. B) Whole-embryo cortisol concentrations (pg/µL normalised to protein concentration, a.u). Concentrations lower than the detection range were assigned as "0 a.u.". C) Interleukin-1β (*il-1β*, immune response). D) superoxide dismutase 1 (*sod1*, antioxidant response). E) sulfide:quinone oxidoreductase (*sqor*, metabolism and antioxidant response). Jittered symbols represent mean Log $2^{-\Delta\Delta CT}$ ± SE (coloured bars) biological replicate values. Black symbols represent mean Log $2^{-\Delta\Delta CT}$ ± SE (black bars) treatment values relative to control averages (black horizontal lines). Annotations on top right corners show the factorial effects of thermal stress (TS) and stress medium (SM) on C, SM, TS, TS+SM. Black asterisks above mean values show pairwise comparisons against control C. Comparisons between CM and SM are shown by grey asterisks. Each sample is a biological replicate pool representing the average expression of 20 (A-B) or 60 (C-D) embryos. Boxes show median and 25%-75% quartiles, and whiskers are min/max values within 1.5 IQR. Jittered raw data given as grey circles. Black dots show mean ± SE values of each treatment. C: control, SM: stress medium, TS: thermal stress, TS+SM: thermal stress + stress medium. After 24 hours, embryos are at the median stage of or 22-somite (C, CM) or prim-6 (SM, TS, TS+SM), and after 31 hours (C31, positive control), control embryos are stage-matched to prim-6.

3.8. Discussion

3.8.1. Repeated heat stress induce a stress response in zebrafish embryos

The overarching aim of this work was to investigate whether zebrafish embryos can propagate aspects of their response to fluctuating heat stress to naive receiver embryos through conditioned media. The data showed that embryos were indeed heat-stressed by repeated exposure to 32°C, through higher HSP70 protein expression, indicating stress (Hallare et al., 2005). Heat-stressed embryos grew faster than control embryos, which is consistent with previous reports (Long et al., 2012; Schnurr et al., 2014). This may in turn favour the premature hatching of smaller larvae (Cingi et al., 2010; Schmidt and Starck, 2010). Heat-stressed embryos were less active than control embryos incubated for 24 hrs but were hyperactive compared to control embryos developed to the same stage of prim-6. The results support previous observations that heat stress triggers higher behavioural activity in developing zebrafish compared to the stage-matched control (Gau et al., 2013; Yokogawa et al., 2014). Such behavioural alterations may be explained by (i) energy trade-offs between behaviour, growth, and the metabolic costs of stress response (Barton and Iwama, 1991; Simčič et al., 2015), as well as (ii) temperature-dependent molecular changes in gene expression, epigenetic gene regulation, or post-translational modification related to behaviour, potentially involving circadian clock and neurodevelopmental genes (López-Olmeda and Sánchez-Vázquez, 2011; Colson et al., 2019).

The gene expression of *il-1β* and *sqor* remained unchanged in heat-stressed embryos. This contrasts with previous findings of *sqor* upregulation in response to thermal and hypoxic stresses (Long et al., 2012, 2015; Guo et al., 2016; Xia et al., 2018) and of heat-induced increased *il-1β* levels in adult black rockfish *Sebastes schlegelii* (Lyu et al., 2018) and zebrafish embryos (Icoglu Aksakal and Ciltas, 2018). Heat stress usually triggers an upregulation of *sod1* (Mahanty et al., 2016; Liu et al., 2018). In contrast, fluctuating thermal stress in this study reduced *sod1* expression compared to the control. These deviating results may result from measuring *sod1* expression not immediately after the cessation of thermal fluctuations. These inverted gene expression patterns under fluctuating as compared to constant thermal stress, might be related to energetic depletion as a result of the thermal cycles (Schaefer and Ryan, 2006; Alfonso et al., 2020). Repetition of heat stress also attenuated the response of heat shock proteins at the mRNA level in lake whitefish (*Coregonus clupeaformis*) embryos (Whitehouse et al., 2017; Sessions et al., 2021). However, HSP70 protein levels remained upregulated

by heat stress in this experiment. As gene expression varies with ontogeny during zebrafish embryogenesis (Mathavan et al., 2005), there may be a cofounding effect in gene expression aligned to the developmental acceleration in heat treatments. Collectively, the data confirms that fluctuating thermal stress induced a stress response in zebrafish embryos at the gene (marginally in *sod1* when compared between TS and C treatments), protein (HSP70), and phenotypic (growth, behaviour) levels. As cortisol is a biomarker for heat stress (Sadoul and Geffroy, 2019), one might expect that a stress-induced accelerated growth may also trigger an earlier onset of the cortisol stress response. However, cortisol levels remained unchanged in zebrafish embryos exposed to all treatments compared to control (**Figure 3.5B**, **Table Appendix 2 S8**), in line with previous literature reporting a cortisol stress response no earlier than 2-4 dpf in zebrafish (Alderman and Bernier, 2009; Alsop and Vijayan, 2009b; Eto et al., 2014).

3.8.2. Heat induces a positive stress feedback loop in naive receiver embryos

It is well-known that animals can chemically communicate their state of distress to others, although predation stress has traditionally received the most attention (Jordão and Volpato, 2000; Barcellos et al., 2014). Here, fluctuating thermal stress indirectly negatively affected naive conspecifics, with a similar directionality of effects compared to thermal stress itself: this could be described as a positive feedback loop (**Figure 3.1**). A feedback loop is defined as the outcome of a process which influences a future process within a system. Negative feedback loops are used to maintain homeostasis, while positive feedback loops amplify the outcome of the initial reaction.

First, embryos grew faster when subjected to stress medium obtained from heat-stressed embryos, reaching similar stages to those of heat-stressed embryos. Such "catch-up" synchronous growth has been shown in egg-clustered embryos of several species and indicates the presence of embryo-embryo communication (Colbert et al., 2010; McGlashan et al., 2012). Supporting this idea, there were also consistent differences between embryos incubated in fresh E3 medium compared to regularly excreted control metabolites. Usually this communication serves to maximise energy costs against potential threats and to potentially facilitate group emergence (Colbert et al., 2010; McGlashan et al., 2012; Aubret et al., 2016).

Second, stress medium triggered behavioural hyperactivity compared to control embryos reaching an equivalent stage (prim-6) and the control medium containing regular metabolites, but not the fresh medium control. These results are in agreement

with higher activities in rainbow trout embryos facing alarm cues (Poisson et al., 2017) but depart from lower behaviour activities in 24-hpf zebrafish embryos exposed to conspecific alarm cues (Lucon-Xiccato et al., 2020). This suggests that behaviours depend on the type of cue and the species. Such behavioural alterations were observed in adult zebrafish exposed to low pH and fasting stress-induced cues (Abreu et al., 2016), but also in Chapter 2 in adult marine invertebrates in presence of cues from low pH-stressed individuals.

Third, stress medium conditioned by heat-stressed embryos induced changes in gene expression patterns in naive receivers. Interleukin *il-1β* was significantly downregulated in stress medium treatments. The observed stress medium-mediated inhibition of *il-1β* suggests that one of its inhibitor stress hormones, such as adrenaline and the adrenocorticotropic hormone (Castillo et al., 2009; Castro et al., 2011), or heat shock factor 1 (HSF1) (Cahill et al., 1996) – but not cortisol which remained unchanged here – could be upregulated by stress medium. Intriguingly, the expression of immune genes may be associated with behavioural changes in zebrafish, since highly responsive fish also have higher *il-1β* expression (Kirsten et al., 2018). This may indicate a functional link between decreased *il-1β* expression and hypoactivity in stress medium-treated embryos compared to embryos incubated in fresh medium for 24 hours.

On the other hand, *sqor* expression was significantly upregulated by stress medium. *sqor* emerged as a novel candidate biomarker from recent transcriptomics studies of thermal and oxidative stress (Long et al., 2012, 2015; Guo et al., 2016; Xia et al., 2018; Wollenberg Valero et al., 2021). *sqor* is involved in the metabolism of hydrogen sulphide (H_2S), concentrations of which are toxic at supraphysiological levels, by regulating its neuromodulatory and biological roles (Chao et al., 2012; Jackson et al., 2012; Horsman and Miller, 2016; Augustyn et al., 2017; Rose et al., 2017). Interestingly, *sqor* and H_2S may be involved in the response to oxidative stress through increasing glutathione levels (Yonezawa et al., 2007; Kimura et al., 2010) and by mediating the antioxidant effects of Coenzyme Q10 (CoQ10) (Kleiner et al., 2018). There is evidence that *sqor* maintains ATP production (Quinzii et al., 2017) and has been proposed as a growth-related candidate gene (Zhuang et al., 2020). Kleiner and colleagues (2018) found that an increase of SQOR may prevent oxidative stress by facilitating the antioxidant effects of CoQ10. Reversely, a downregulation of *sqor* may reflect deficiency of its coenzyme CoQ10, which in turn alters the sulphide metabolism leading to accumulated H_2S levels and depletion of glutathione, that may cause oxidative

damages (Luna-Sánchez et al., 2017; Quinzii et al., 2017; Ziosi et al., 2017). Therefore, the upregulation of *sqor* under stress medium treatment could have multiple functions, from metabolising toxic levels of H_2S to restoring both ATP and GSH levels in response to stress propagation from a conspecific. Collectively, the molecular data may indicate impaired immune and antioxidant responses in embryos exposed to stress medium. Nevertheless, the molecular patterns, both at the gene (*sod1*, *sqor*, *il-1β*) and protein (HSP70, **Figure 3.5A**) levels suggest that the molecular pathways of action may differ between heat-stressed versus stress medium-conditioned embryos. Therefore, further work is needed to better understand the molecular pathways activated by the stress medium in comparison with thermal stress. Whilst an experimental limitation was that it only used a limited number of replicate pools of 60 embryos each to statistically compare the transcript levels, it should be emphasized that pooled sampling allows for high confidence in averaged gene expression measurements (Schlötterer et al., 2014; Takele Assefa et al., 2020).

3.8.3. Stress and control media induce distinct feedback mechanisms

Embryos exposed to control medium conditioned by control embryos developed slower than embryos exposed to fresh E3 medium only. These effects on development were mirrored by the expression patterns of the three investigated genes, which differed between control medium and experimental stress treatments. The behavioural response to stress medium was also different to that induced by the control medium, corroborating previous studies where metabolites from undisturbed versus stressed donors induced different responses in several species (Bett et al., 2016; Bairos-Novak et al., 2017). However, activity was much higher in control embryos from fresh E3 medium than in embryos incubated in control medium. This finding may indicate that behaviours of zebrafish embryos are tightly controlled by the nature of their chemical environment (vs. relaxed in the absence of any cues), lending additional support to chemical communication as a parameter relevant to thermal changes.

Lastly, the similarity in development and behaviour in combined thermal stress plus stress medium treatments, together with a larger effect size, indicate that thermal stress and stress medium may individually saturate the phenotypic reaction norms, which cannot be further altered in the combined treatment. Conversely, the gene expression and HSP70 analyses revealed a difference in molecular responses between the two independent factors, thermal stress and stress medium. To better understand

these contrasting synergistic vs. independent effects of thermal stress and stress medium, gene expression was compared at a global scale in Chapter 4.

3.9. Conclusion

To conclude, this chapter indicates that heat-stressed zebrafish embryos induced a stress-like response in naive conspecifics that have not been directly exposed to thermal stress, which is measurable from molecular to phenotypic levels. This phenomenon warrants designation as a positive feedback loop. If such positive feedback loops also exist in response to naturally occurring thermal fluctuations, this may have implications in the context of climate change or in high-density settings such as aquaculture. Further investigations should focus on the identification of stress metabolites potentially responsible for this stress propagation, their molecular consequences at an individual level, as well as longer-term consequences for populations and ecosystems. To address these questions, Chapter 4 will characterise the nature of stress metabolites and the molecular basis of stress propagation, whilst Chapter 5 will investigate the effect of stress propagation in a mutagenic environment.

Chapter 4. Heat induces multi-omic and phenotypic stress propagation in zebrafish embryos and larvae

4.1. Significance statement

Aquatic animals utilise chemicals to mediate adaptive behaviours. For instance, predated fish release chemical cues that elicit antipredatory responses in naive receivers. Chapter 2 and Chapter 3 evidenced that this concept is not limited to biotic stress since abiotic factors such as heat and acidification also cause stress propagation. Using multi-omic data, Chapter 4 uncovers the molecular basis of stress propagation towards naive receivers. I propose that heat activated molecular stress responses, leading to the release of distinct stress metabolite classes into the environment. These stress metabolites altered the transcriptome of receivers, resulting in faster development and hypoactivity. Heat combined with stress metabolites had the largest effect, highlighting that abiotic stress, experienced both directly and indirectly, can alter chemical communication and affect early development.

4.2. Graphical Abstract

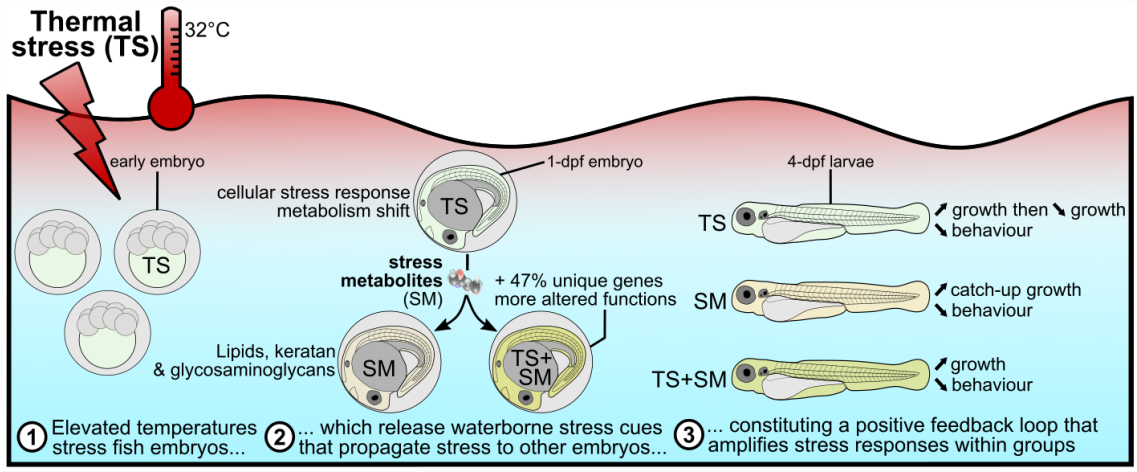

4.3. Highlights

- Repeated heat stress induced a cellular and cortisol stress response and altered the phenotype of zebrafish embryos and larvae.
- Heat-stressed developing zebrafish released stress metabolites enriched in lipids and sulphur-containing compounds that altered the transcriptome and behaviour, and accelerated development, in naive receivers.
- In combination, heat and stress metabolites induced 47% distinct differentially expressed genes, with many related to organ development.
- Stress propagation was characterised by similar behavioural outcomes, but distinct molecular pathways, in response to heat stress experienced either directly or indirectly via stress metabolites.

4.4. Abstract

The previous chapters pioneered the concept that abiotic stress induces a chemical stress propagation towards naive receivers. This chapter provides a comprehensive picture of the molecular basis of such stress propagation by integrating multi-omic and phenotypic data. Repeated heat peaks elicited a molecular stress response and a burst of accelerated growth followed by a slow-down in concert with hypoactivity. Excreted metabolomes of heat stress and control media revealed several candidate stress metabolites including sulphur-containing compounds and lipids. These stress metabolites elicited transcriptomic changes in naive receivers related to immunity, extracellular signalling, keratinisation, glycosaminoglycan/keratan sulphate, and lipids. Consequently, receivers experienced accelerated catch-up growths and reduced swimming performances. The combination of heat and stress metabolites accelerated embryo development the most, mediated by apelin signalling. This chapter confirms that heat stress can be propagated towards naive receivers via stress metabolites, inducing phenotypes comparable to directly heat-stressed zebrafish, but through distinct molecular pathways. An independent experiment using non-laboratory and group-exposed zebrafish line confirmed that glycosaminoglycan-related genes functionally connected to candidate stress metabolites are differentially expressed in receivers, suggesting the involvement of *Schreckstoff*, raising the possibility for further stress propagation. Heat-induced stress metabolites may therefore have ecological and animal welfare implications in wild and farmed aquatic populations in a changing climate.

4.5. Introduction

Temperature is the abiotic "master" factor (Brett, 1971) regulating the biology of ectotherms (Beitinger et al., 2000; López-Olmeda and Sánchez-Vázquez, 2011). Heat stress alters a wide range of responses in fish, from gene expression (Long et al., 2012) to development (Hallare et al., 2005; Schröter et al., 2008) to population dynamics (Alfonso et al., 2020). The type of heat stress also matters: single and repeated periods of stress can induce different gene expression patterns as well as distinct behavioural responses (Otsuka et al., 2022). Repeated thermal conditioning can impair the ability to restore homeostasis (Clark et al., 2011) and alter the response to subsequent heat stress by attenuating the corticosteroid (Ouchi et al., 2020) and heat shock (Whitehouse et al., 2017; Sessions et al., 2021) pathways. For example, the marine medaka *Oryzias latipes* increased or suppressed its locomotor activity in response to single and repeated heat stress, respectively (Otsuka et al., 2022). Nevertheless, other studies showed that fish can maintain their thermal tolerances despite multiple heating events (Bard and Kieffer, 2019). There is also a growing concern about the response of fish embryos to heat due to their narrow thermal tolerance (Pörtner and Farrell, 2008; Martin et al., 2020), and about lasting effects on adult stages through early thermal conditioning (Scott and Johnston, 2012). This marks early development as a vulnerable (Dahlke et al., 2020a) "bottleneck" stage for fish populations (Madeira et al., 2016b) when it comes to heat stress.

Heat stress responses at the molecular and behavioural levels are well studied in aquatic species, but its effect on chemical communication is little studied. Previous studies on communication have focused mostly on cues released upon biotic factors such as injury (Barbosa Júnior et al., 2010; Barreto et al., 2010), decay (Hussain et al., 2013; Kermen et al., 2020), disturbance cues in uninjured animals presented with a predator (Bairos-Novak et al., 2017; Goldman et al., 2019, 2020a, 2020b), manual chasing and handling, or fasting (Barcellos et al., 2011, 2014; Abreu et al., 2016; Bett et al., 2016). However, to date, only a few studies have shown that animals communicate abiotic-induced factors to each other (Hazlett, 1985). Previous chapters confirmed that abiotic stress such as heat or low pH also elicits the release of olfactory cues, termed "stress metabolites". Chapter 3 evidenced that stress metabolites elicit similar phenotypic responses as heat stress itself in naive receivers, which are the characteristics of a positive feedback loop.

Zebrafish (*Danio rerio*) is commonly used as an experimental model, including for behavioural assays (Tegelenbosch et al., 2012) and "omics" approaches (Scholz et al., 2008). Adult zebrafish tolerate water temperatures ranging 6-39°C (Spence et al., 2008; Gerlai, 2013) whilst zebrafish embryos develop normally in the 22-32°C range (Schirone and Gross, 1968; Schnurr et al., 2014; Pype et al., 2015), with an optimum around 28 ± 1°C (Schmidt and Starck, 2010; Pype et al., 2015; Delomas and Dabrowski, 2018). The phylotypic stage, from 10 hpf to 24-30 hpf in zebrafish embryos (Irmler et al., 2004), is defined as the mid-embryogenesis period with a conserved anatomical plan during which important body structures develop (Irie and Kuratani, 2014). The phylotypic period is not modularised during zebrafish early embryogenesis, which means that traits can be influenced by temperature, resulting in an altered morphology (Schmidt and Starck, 2010). Importantly, the thermal biology of zebrafish is conserved in laboratory conditions, which makes it a suitable model for investigating climate-related questions (Morgan et al., 2019), such as the mechanistic basis of heat stress perception. Zebrafish embryos produce alarm cues (Cao and Li, 2020) and innately react to extracts of crushed conspecific larvae with a decreased activity as early as 12 and 24 hpf (Lucon-Xiccato et al., 2020). This early ability to detect cues is in line with observations of kin and alarm odour recognition in damselfish embryos (Atherton and McCormick, 2015, 2017), predator recognition in rainbowfish embryos (Oulton et al., 2013), predator and conspecific odours in cichlid embryos (Nelson et al., 2013), and alarm cues reaction in juvenile rainbow trout (Poisson et al., 2017). Altogether, there is evidence that fish, including zebrafish at early embryonic stages, can detect and discriminate stress chemical cues.

There is evidence that natural chemical communication is often mediated by a cocktail of compounds (Parra et al., 2009; Mathuru et al., 2012; Stensmyr and Maderspacher, 2012). However, abiotic stress-induced chemical communication has previously been studied using mainly phenotypic and physiological endpoints (Crane et al., 2022). Consequently, the biological compound bouquets mediating specifically heat stress-related communication, and their molecular pathways of action, are not yet known. This chapter investigates the molecular response of zebrafish embryos exposed to thermal stress and to heat stress-induced metabolites using metabolomics and transcriptomics. I hypothesised that (i) the metabolome excreted by control and heat-stressed zebrafish embryos differ from each other; (ii) there may be similarities between the transcriptomic signatures of embryos exposed to heat stress and to stress metabolites,

(iii) that stress metabolites activate chemosensory perception genes, and (iv) both heat-stressed and indirectly stressed individuals differ in growth patterns and behaviour from controls. (vi) Laboratory strains of zebrafish may perform differently to their wild counterparts (Morgan et al., 2022), and embryos in clutches may react differently than single embryos in tubes. Similar molecular responses to stress metabolites are expected in group-raised outcrossed zebrafish embryos, but perhaps with different magnitudes.

4.6. Methods

4.6.1. General experimental design

Zebrafish embryos were collected by breeding adult zebrafish at the University of Hull. Embryos were collected in the morning, cleaned in fresh 1X E3 medium (Cold Spring Harbor Laboratory Press, 2011) and rinsed by bleaching. Developmental stages were measured in hours post fertilisation (hpf) according to Kimmel et al. (1995). Two temperature protocols were used, either (i) a control constant temperature of 27°C, or (ii) repeated temperature fluctuations from 27 to 32°C (see section 4.6.2). Embryos were incubated in E3 medium (i) free of any putative metabolites ("fresh medium"), (ii) medium containing "stress metabolites" released by heat-stressed donors, or (iii) medium containing "control metabolites" released by control donors (see section 4.6.3). A factorial design for the two factors "temperature" and "stress metabolites" (**Figure 4.1A**), yielded four experimental treatments: fresh medium at 27°C (control C), fresh medium with thermal stress (TS), medium containing stress metabolites at 27°C (SM), and medium containing stress metabolites with thermal stress (TS+SM). A fifth condition was the control medium containing control metabolites (CM) released by control individuals (C). Comparing SM and C to the additional control CM aimed to assess whether regular metabolites in higher concentrations are responsible for any observed effect of stress metabolites. Individuals in C and TS were metabolite donors for treatments CM and SM (which were the metabolite receivers). Five different endpoints were measured at different time points, which yielded (1) cortisol, (2) transcriptomic, (3) metabolomics, (4) multi-omics, and (5) phenotypic data (**Figure 4.1B**). Additionally (6), the gene expression of candidate genes was measured[3] in response to SM in group-exposed, non-laboratory outcrossing pet store (PET) embryos (**Figure 4.1C).**

[3] This analysis was done by T. Emagbetere (see section 4.6.10)

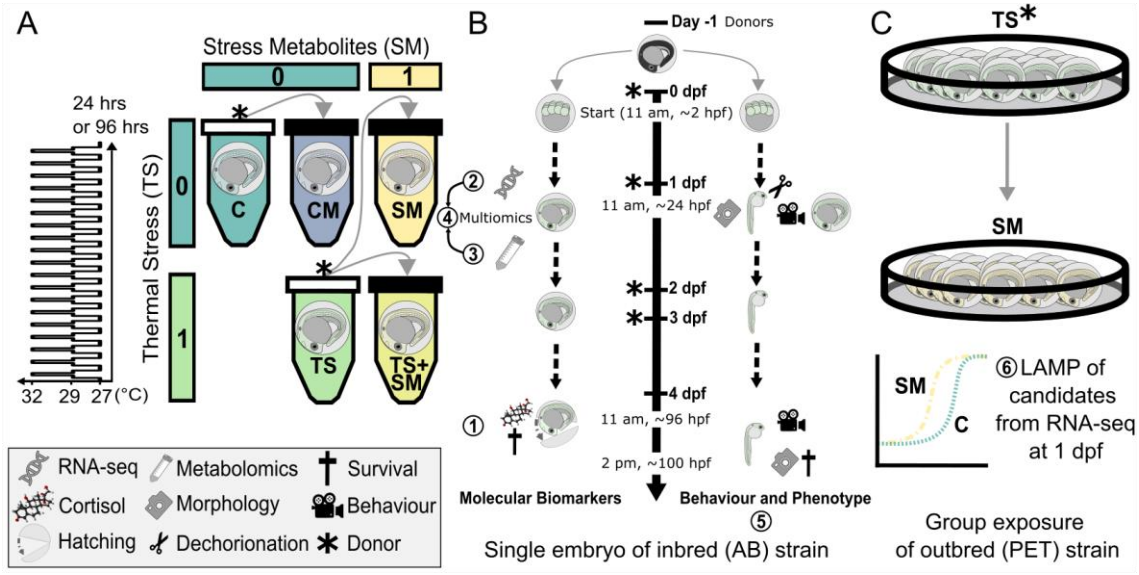

Figure 4.1. Scheme of experimental design. A) Zebrafish embryos at < 3 hours post fertilisation (hpf) were incubated according to a two-way factorial design represented by two predictors: thermal stress (0 = control temperature of 27°C, 1 = repeated thermal stress at sublethal temperature of 32°C as shown in left graph) and stress metabolites (0 = fresh medium free of metabolites, 1 = stress metabolites released by individuals exposed to thermal stress). Treatments were CM: control metabolites at 27°C, C: control in fresh medium at 27°C, SM: stress metabolites at 27°C, TS: fresh medium in thermal stress, TS+SM: stress metabolites in thermal stress. Grey arrows indicate medium transfer from metabolite donor (✱ symbols and white tube caps) to metabolite receiver (plain black tube caps). B) Endpoints: embryos and larvae were sampled for both molecular (RNA-sequencing of embryos and metabolomics of medium at 1 dpf and cortisol and HSP70 at 4 dpf) and phenotypic (1 dpf and 4 dpf) endpoints (circled numbers 1-5). C) Confirmatory experiment with Loop-Mediated Isothermal Amplification (LAMP) data of candidate genes found in RNA-seq in social groups of 20 embryos incubated in stress metabolites (SM) or fresh medium (C) until 1-dpf. Endpoints 1/2/5 utilised a laboratory inbred (AB) and endpoints 3/6 an outbred (PET) zebrafish.

4.6.2. Temperature protocols

For both temperature protocols, embryos and larvae were incubated in 0.2 mL PCR wells placed in darkness in a thermocycler with a closed lid. Of note, constant darkness delays the normal zebrafish embryonic development (Villamizar et al., 2014), and the observed results have to be interpreted in this respect. For the repeated heat peaks treatment, every twenty-four hours of thermal stress protocol consisted of temperature fluctuations between 27, 29, 32, 29, and 27°C, with each temperature step being maintained for 15 min. This thermal stress mimicked +5°C temperature peaks over zebrafish embryo optimal temperature and reached a sublethal temperature of 32°C (Scott and Johnston, 2012). This temperature protocol aimed to impose many heat peaks within a short timeframe to better understand the molecular mechanism of stress responses. Depending on the endpoint as described below, zebrafish embryos and larvae experienced up to 19 heat peaks per 24 hours until they reached either 1 dpf (metabolomics of medium, RNA-seq, phenotype data) or 4 dpf (cortisol and HSP70,

phenotype data). For the metabolomics data (endpoint 3), zebrafish embryos were exposed for 24 hours to a total of n = 13 heat peaks for 16 hours and 15 min followed by 7 hours and 45 min of recovery at 27°C, resulting from the experimental design of Chapter 3. Of note, for the confirmatory experiment of endpoint 6, heat-stressed donors were exposed in darkness to a constant 32°C in petri dishes.

4.6.3. Embryo medium

Embryo medium (Cold Spring Harbor Laboratory Press, 2011) was prepared by dissolving 34.8 g NaCl, 1.6 g KCl, 5.8 g $CaCl_2 \cdot 2H_2O$, and 9.78 g $MgCl_2 \cdot 6H_2O$ in ultrapure water to a final volume of 2 litres. The pH was adjusted to pH = 7.2 with NaOH and the solution was autoclaved and stored at 4°C. The working solution of 1X E3 embryo medium was prepared by 1:60 dilution of the 60X stock ultrapure water. For the metabolomic experiment, the embryo medium was prepared with autoclaved fish system water instead of ultrapure water.

Embryo media were in the range of pH 7-8.1 after 24 hours of incubation, which falls into the range of zebrafish embryos (Engeszer et al., 2007; Lawrence, 2007; Zahangir et al., 2015). At the end of incubation at 1 dpf, triplicate samples of ~800 µL (170 µL per 5-6 individual embryos) of medium were collected, along with a blank consisting in fresh E3 medium, from control and heat-stressed embryos at the end of C and TS protocols and stored in centrifuge tubes at -80°C until further processing for ammonia measurements. Levels of NH_3 were measured at 340 nm on a Libra S12 spectrophotometer using the Ammonia Assay Kit (AA0100, Sigma-Aldrich), following the manufacturer's recommendations.

4.6.4. Fish husbandry, breeding, and zebrafish embryos handling methods

Zebrafish embryos for endpoint 3 (metabolomics of medium) and 6 (LAMP) were obtained from a stock of adult fish raised in-house for several generations after purchase from a local pet-store supplier (PET line). Zebrafish embryos and larvae used in endpoints 1 (cortisol), 2 (RNA-seq), and 5 (phenotype) were obtained from a breeding stock of adult zebrafish (*Danio rerio*, AB strain) from the Universities of Sheffield and Cambridge (UK). The reason for this was to limit genetic variation in the embryos sampled for RNA-sequencing by using true-breeding embryos from the AB zebrafish line. Fish stocks were maintained at the University of Hull in a temperature-controlled room kept at 27°C with 14:10 hour light:dark cycle. Fish were fed twice a day an alternate diet of mini-bloodworm, daphnia, and dried flakes. Fish were maintained in

appropriate male-to-female ratios for breeding purposes and the fish population was renewed by inhouse breeding.

Breeding was completed by placing plastic trays half-filled with marbles and covered in plastic plants on the afternoon before. Eggs were collected at 10 am in the morning, after the beginning of the light cycle. Zebrafish embryos were collected using plastic pipettes and placed in plastic jars before being transferred to the laboratory. Zebrafish embryos were cleaned 3-5 times in fresh 1X E3 embryo medium to remove organic matter. Next, zebrafish embryos were placed in a small tea strainer immersed for 3-4 minutes, with gentle swirling, in small petri dishes (⌀: 35 mm) filled with ~9 mL of medium in the following order: (1) bleaching medium, (2) 1X E3 embryo medium, (3) bleaching medium, (4) 1X E3 embryo medium, and (5) 1X E3 embryo medium. Bleaching medium consisted in 0.004% bleach in 1X E3 embryo medium which was prepared by diluting 10-13% active sodium chloride in fresh 1X E3 embryo medium. Under a stereomicroscope (Zeiss), zebrafish embryos were then carefully moved to a petri dish (⌀: 90 mm) in fresh 1X E3 embryo medium. Viable embryos (at least 2-cells stage i.e., 0.75 hours post fertilisation and no more than high stage i.e., 3.3 hpf; with no visible deformation nor chaotic cell division) were carefully pipetted into 0.2 mL PCR wells pre-filled with the appropriate experimental medium for experimental treatments, ensuring to add no more than a few microliters (estimated < 5% of final volume) of additional medium.

4.6.5. Endpoint 1: Cortisol and heat shock response in 4-dpf larvae

To determine which time point was best to assess the cortisol stress response, the time course of cortisol expression was measured in control zebrafish at 1, 2, 3, and 4 dpf. Control individuals were incubated in clutches at 27°C, with natural light conditions (approx. 14:10 hour light:dark), in ~10 mL of 1X E3 medium. Zebrafish (PET line) were pooled into groups of 40 embryos per sample (n = 3 pooled samples per time point). After cortisol extraction (see methods below), it was confirmed that cortisol was recoverable and detectable, within the range of an ELISA assay, in 4-dpf larvae.

Following this optimisation, zebrafish were continually exposed to C, CM, TS, and SM treatments from 0 to 4 dpf. Embryo medium was renewed once a day by either fresh embryo medium (C and TS) or reused medium from donor embryos (CM and SM). Survival and hatching were monitored once a day at 11 am. At 4 dpf, viable larvae were snap-frozen at -80°C until further processing for cortisol analysis. Experimental

treatments were repeated several times using independent clutches and sampled larvae were distributed equally into biological replicates to limit any batch effects, until 60 larvae per biological replicate were obtained for each treatment (n = 3 samples per treatment, total of 180 larvae per treatment). Cortisol was extracted from pooled larvae samples using a method modified from Wilson et al. (2013), and measured blindly via an ELISA assay, similar to section 3.6.6 in Chapter 3. Briefly, larval samples were homogenised in 100 µL PBS/Methanol, sonicated, and incubated on a rotary shaker at 4°C. Before nitrogen evaporation, 20 µL of lysate were aliquoted and fourfold diluted in PBS for total protein quantification using the Qubit™ Protein Assay Kit (Thermo Fisher Scientific). The remaining volume of supernatant was evaporated at room temperature under nitrogen flow until complete dryness and the pellet was reconstituted in 62 µL ice-cold ELISA assay reagent, resuspended by vortexing, and stored at -80°C until cortisol quantification. Cortisol extraction recovery rates were estimated at 90.9% ± 10.8% (n = 3) using cortisol standards as described in section 3.6.6. Absorbance values were read at 450 nm with a reference at 490 nm using the BioTek ELX808 plate reader (NorthStart Scientific Ltd). Cortisol concentrations were calculated from a standard curve modelled as a four-parameter nonlinear regression using the online calculator mycurvefit.com (accessed 25/03/2021, $r^2 = 0.9999$, $p = 0.0001$, $F = 8,332$). Cortisol concentrations were normalised to total protein concentrations. Cortisol concentrations were transformed using the Lambert transform function from the *bestNormalize* R package (Peterson and Cavanaugh, 2020). Transformed values passed the normality and homoscedasticity assumptions (Shapiro-Wilk's test $p = 0.2$, Breusch-Pagan's test $p = 0.08$) and were compared across treatments using a one-way ANOVA. Post-hoc pairwise comparisons with false discovery rate p-value adjustment were computed using the *emmeans* v1.7.2 R package (Lenth, 2022) in R v4.0.2 (R Core Team, 2020).

HSP70 measurements[4] were obtained from the fourfold-diluted supernatants saved before cortisol extraction. Briefly, samples were incubated with Laemmli buffer, boiled for 10 min, and 15 µg proteins were resolved through a 10% SDS-PAGE gel. Proteins were transferred to nitrocellulose membranes and blotted for HSP70 using specific antibodies (#11565722, Fisher Scientific). Chemiluminescence signals were acquired using a ChemiDoc Imaging System (Bio-Rad). Membranes were stained with Ponceau S for loading control normalisation. Quantification of signals was done using Image J (U. S. National Institutes of Health, Bethesda, Maryland, USA,

[4]Analysis performed by Linsey Malcolm, Kathleen Bulmer, and Pedro Beltran-Alvarez.

https://imagej.nih.gov/ij/). HSP70 intensities (validated in a second replicate) were normalised independently against the intensity of two separate Ponceau bands, and the average of these two ratios was then calculated. This was a blind analysis, where the experimenter did not know the identity of the samples. HSP70 protein levels were compared across treatments using a one-way ANOVA as values passed the residual normality and homoscedasticity assumptions.

4.6.6. Endpoint 2: 1-dpf transcriptomic responses to heat and stress metabolites

The transcriptomic response to thermal stress and stress metabolites was characterised by exposing zebrafish embryos to treatments C, TS, SM, and TS+SM from < 3.3 hpf for 24 hours. At the end of the exposure, viable zebrafish embryos still in their chorion were pooled into groups of 20 and processed for RNA-sequencing (n = 3 biological replicates of 20 embryos, i.e., total of 60 embryos per treatment). Embryo pools were immediately snap-frozen at -80°C. Pooled samples were randomised prior to the RNA extraction for blind sample preparation and analysis. Total RNA was extracted using the TRIzol method following the manufacturer's recommended protocol, followed by a DNAse I digestion step (#10792877, Invitrogen™ TURBO DNA-free™ Kit) and a sodium acetate clean-up. For this purpose, 0.1 mL of TRIzol reagent were added and embryos were homogenised using a plastic pestle for approx. 30 sec on ice. Further 0.4 mL of TRIzol were added to the samples, followed by another approx. 20 sec of homogenisation on ice using a plastic pestle. To ensure that tissues were fully homogenised in TRIzol, samples were passed several times through a 200 µL pipette tip. Homogenates were centrifuged 10 min at 12,000 g to discard fat and debris, after which the supernatant was transferred to a new tube. TRIzol homogenates were incubated 5 min at room temperature to dissociate the nucleoprotein complex. Next, 0.2 mL of molecular grade chloroform:isoamyl alcohol 24:1 (#327155000, Acros Organics) were added to homogenates before vigorous shaking. Samples were incubated 15 min at room temperature. Samples were centrifuged 15 min at 12,000 g at room temperature before the upper RNA-containing aqueous layer was transferred to a new tube. Next, 0.25 mL molecular grade isopropanol (99.5% #184130010, Acros Organics) were added, and samples were mixed by several inversions before being left to incubate 10 min at room temperature. Samples were centrifuged 10 min at 12,000 g at room temperature (to prevent salt precipitation) to pellet the RNA. The supernatant was discarded. RNA pellets were cleaned three times in ethanol by resuspending in 0.5 mL molecular grade ice-cold 75% ethanol, centrifuging 5 min at 10,000 g at 4°C, and discarding the ethanol

phase. Excess ethanol was removed using a pipettor and evaporated by air-drying at room temperature for approx. 3 min and at 55°C on a block heater for 2 min. Next, RNA pellets were resuspended in 70 µL molecular grade water and heated for 5 min at 55°C with regular vortexing. DNA was removed by a routine DNAse I treatments (#10792877, Invitrogen™ TURBO DNA-free™ Kit). For this purpose, 0.1 volumes of 10X Turbo DNAse Buffer and 1 µL DNAse enzyme were added to the RNA and gently mixed before 20-min incubation times at room temperature. 0.1 volumes of DNAse inactivation reagent were added before 5-min incubation times at room temperature with regular mixing by flicking the tubes. Samples were centrifuged for 90 sec at 10,000 g at room temperature. Next, 80 µL of DNA-free RNA solutions were transferred to a new tube and samples placed on ice. RNA samples were purified using sodium acetate protocol modified from Walker and Lorsch (2013) to remove impurities such as phenol and protein contamination. A stock of 3M sodium acetate was prepared by adding 12.3 g of sodium acetate anhydrous (#BP333-500, Fisher scientific) in 7.6 mL glacial acetic acid (#A/0360/PB15, Fisher scientific, to adjust the pH to 5.2) and completing the volume to 50 mL in molecular grade water before autoclaving the solution. Next, 0.1 volumes of ice-cold 3M sodium acetate and 2.5 volumes of ice-cold molecular grade absolute ethanol were added to RNA samples. Samples were left to incubate at -20°C for 2 hours and RNA was pelleted at 12,000 g for 15 min at 4°C. Next, the supernatant was carefully removed, and the RNA pellet washed three times by adding 200 µL ice-cold molecular grade 75% ethanol, letting the pellet soak for 2 min (in ice) before centrifuging 2 min at 12,000 g at 4°C, and removing the ethanol supernatant. Purified RNA was resuspended in 75 µL molecular grade water by heating 2 min at 55°C on a block heater. Aliquots of 10 µL were taken for quality and quantity assessment, whilst the remaining 65 µL were stored at -80°C before being sent in dry-ice to Edinburgh Genomics for RNA-sequencing. RNA purity ratios were assessed using the NanoDrop 1000 Spectrophotometer. All RNA samples contained 65 µL with ≥ 1,200 ng RNA, and sufficient purity as shown by 260/280 and 260/230 ratios respectively > 1.9 and > 1.5.

Total RNA samples were further analysed at the Edinburgh Genomics facility using a Bioanalyser to obtain the RNA integrity number (RIN). Libraries were prepared with the TruSeq stranded mRNA kit and sequenced by Illumina NovaSeq 6000, 50PE sequencing. Due to some samples having low RIN and cDNA concentrations, polyA bead clean-up was performed on cDNA libraries that did not meet the minimum

requirements. The samples of highest quality were sequenced on the same lane whilst lower quality samples were run on another flow-cell lane. Raw read data were returned to me in .fastq format. The RNA-seq analysis was performed on the VIPER High-Performance Computing facility hosted at the University of Hull. Read quality was assessed using *FASTQC* v0.11.9 (https://www.bioinformatics.babraham.ac.uk/projects/fastqc/). Reads were filtered and trimmed to remove polyG, polyX, and Illumina adapter sequences using *fastp* v0.23.1 (Chen et al., 2018) with deduplication disallowed (*--adapter_fasta adapters.fasta --dup_calc_accuracy 3 --trim_poly_g --trim_poly_x*). Reads were reassessed for quality control using *fastp* and *FASTQC*. The absence of PCR-biased duplication was assessed using the R package *DupRadar* v1.18.0 (Sayols et al., 2016). Only one sample with the lowest RNA integrity (RIN = 4.5), no library clean-up, and ran on the low-quality lane, showed technical PCR bias of reads with 33% duplication rates. However, there were no differences in duplication rates ($p = 0.5662$) nor RIN ($p = 0.9367$) between treatments which led me to deciding that all samples should be treated the same without deduplication (**Figure 4.2A-B**).

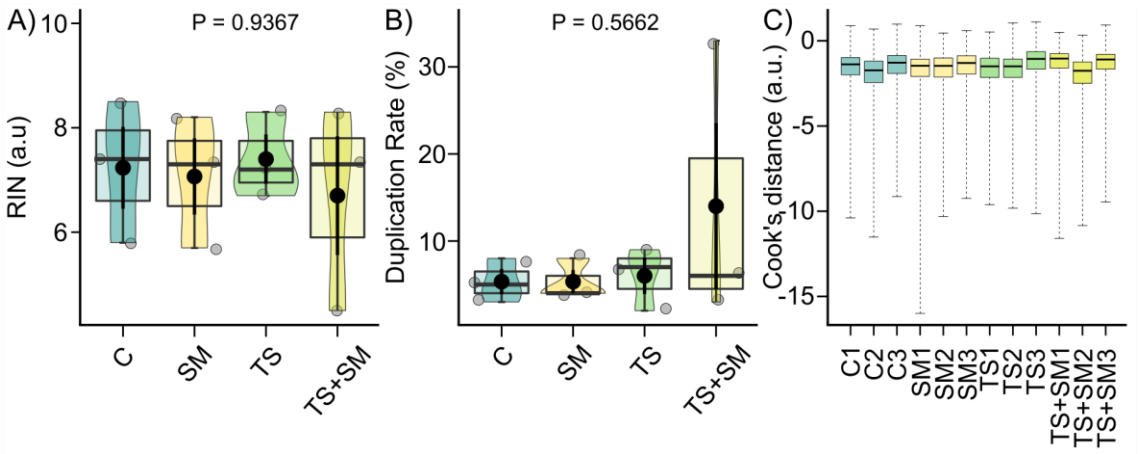

Figure 4.2. Quality control of RNA-seq data. A) RNA Integrity Number (RIN) of RNA samples. B) duplication rates of reads. C) Cook's distance representing the homogeneity of the gene expression variance across samples. There was no evidence that RIN, duplication rates, and Cook's distances had any effect on treatments which justified to ignore these covariates in the gene expression analysis. Boxes show median and 25%-75% quartiles, and whiskers are min/max values within 1.5 IQR. Jittered raw data given as grey circles. Black dots show mean ± SE values of each treatment.

Next, the splice-aware mapper *STAR* v2.6.1 (Dobin et al., 2013) was used to align reads to the zebrafish genome (primary genome assembly GRCz11.104). The genome index was generated with *STAR* default options. Reads were counted by genes (--runMode *alignReads* –quantMode *TranscriptomeSAM GeneCounts* –outSAMtype *BAM SortedByCoordinate* –outSAMunmapped *None* –outSAMattributes *Standard*) to

generate read count tables. Alignment statistics were obtained with *STAR* and *samtools*. Differential gene expression analyses were performed using *DESeq2* v1.28.1 (Love et al., 2014) in R v4.0.2 (R Core Team, 2020) in *Bioconductor* v3.11 (Morgan, 2021). Gene expressions were analysed by using "treatment" as a single factor in the matrix design. Pairwise comparisons (SM, TS, and TS+SM versus control C) were retrieved from the *results* function with the "*cooksCutoff*" option disabled since there was no evidence of extreme outlier (**Figure 4.2C**). The Principal Component Analysis was represented after regularised logarithmic (*rlog*) transformation using the *plotPCA* function (**Figure 4.2D**). Differentially expressed genes (DEGs) were visualised on volcano plots using the *EnhancedVolcano* package v1.6.0 (Blighe et al., 2020). Gene names were converted using the *biomaRt* R package v2.44.4 (Durinck et al., 2005, 2009). I reasoned that heat stress would induce whole-body transcriptomic changes, hence multiple testing-adjusted p-values (p-adj < 0.05, controlling for false positives) were used to subset genes with evidence for altered expression in the functional enrichments. On the other hand, stress metabolites were expected to activate a more local transcriptomic response – similar to kairomones (Oliver et al., 2022) – which were explored via the criterion of raw p-values ($p < 0.01$). Genes subsets by biological process gene ontology (GO) terms obtained using *topGO* v2.40.0 (Alexa and Rahnenfuhrer, 2020) were analysed to investigate the effect of TS and SM respectively on genes related to heat stress (GO:0009408) and chemosensory perception (GO:0007606) with GO term-wide false discovery rate p-value adjustments. The functional enrichment for GO terms (BP: biological processes, MF: molecular functions, and CC: cellular components), Kyoto Encyclopedia of Genes and Genomes (KEGG), and Reactome pathways were performed using the *Gostat* v2.54.0 (Falcon and Gentleman, 2007), *clusterProfiler* v3.16.1 (Yu et al., 2012), and *ReactomePA* 1.32.0 (Yu and He, 2016) R packages, respectively. Relevant information about specific DEGs was retrieved from the Zebrafish Information Network (Ruzicka et al., 2019). In addition, when annotating the SM-responsive DEGs in the ZFIN database, it was noticed that several of them were previously mentioned in a publication by Elkon et al. (2015). Therefore, the published dataset from Elkon et al. (2015) was used to identify genes expressed both in SM and hair cells of the lateral line system of 5-dpf zebrafish embryos[5].

[5]Katharina Wollenberg Valero did the scoring of DEGs in hair cells.

4.6.7. Endpoint 3: Metabolomic characterisation of stress metabolites

4.6.7.1 Experimental design

The medium in which heat-stressed embryos were exposed was used for a metabolomic analysis to characterise stress metabolites released upon thermal stress. The protocol and samples resulted from Chapter 3, where the heating protocol consisted of thirteen heat peaks was followed by a recovery period of 7 hours and 45 min at 27°C until 24 hours of treatment were reached. Embryo media from donor treatments (C and TS) at the end of control thermal protocol (i.e., control medium containing control metabolites CM) or thermal stress protocol (i.e., stress medium containing stress metabolites SM) were collected for metabolomic identification of metabolites released within the medium samples. To account for contaminants from the embryo medium stock and microbial compounds, a blank was prepared by incubating fresh medium without embryos for 24 hours using the control thermal protocol. 170 µL of medium from 60 embryos were collected and filtered through centrifuge tube filters (Costar® Spin-X®, 0.45 µm Pore CA Membrane) to yield one pooled sample of approx. 10 mL medium for CM, SM, and the blank.

4.6.7.2 LC-MS/MS and raw data preprocessing[6]

The LC-MS/MS analysis and raw data pre-processing were performed at the Metabolomics & Proteomics facility of the University of York. Each pooled embryo medium (SM, CM, or blank) was split into three technical replicates for a total of 9 runs for each ionization mode (positive and negative). Two microlitres of provided samples were injected onto a Waters HSS T3 100 mm × 2.1 mm (1.8 µm particle) column, using an Acquity I-Class UPLC system. Compounds were eluted over a 9 min gradient of water/acetonitrile/ 0.1 % (v/v) acetic acid at column temperature of 40°C and a flow rate of 0.5 mL/min. The column was conditioned with six runs of pooled samples before acquiring usable data. Each sample was injected twice, for separate positive and negative ESI mode analysis on a Thermo Tribrid Fusion Orbitrap MS system. Data was collected between 0.5 and 8.5 min, in data-dependent MS2 mode. This collected high-resolution MS1 data (60000 FWHM at m/z 200), and low resolution MS2 scans in both CID and HCD modes. The MS1 data (approx. 2 scans/s) was used for feature picking and quantification. Acquired Thermo .raw files were converted to 32-bit precision centroided .mzML files using *MSConvert* version 3.0.20023-2701dc40b. These were

[6]This was conducted off-site by the technical staff of Metabolomics & Proteomics facility of the University of York.

then processed using bespoke R scripts (R 4.0.3 64-bit in Linux environment). Briefly, features were selected using the *xcmsSet*() function from the *xcms* R package v3.12.0 (Smith et al., 2006), with the following parameters: method = "centWaveWithPredictedIsotopeROIs", ppm = 5, snthresh = 10, peakwidth = c(3, 30), prefilter = c(3, 1000), integrate = 2, mzdiff = -0.1. Features were then grouped, and missing values imputed using derived *xcms* functions. Feature relationships were identified using the *CAMERA* R package v1.33.3, (Kuhl et al., 2012), and candidate formulae calculated using the *rcdk* R package v3.5.0 (Guha, 2007; Voicu et al., 2020). Where appropriate, MS2 spectra were extracted using bespoke scripts, and data tables and plots generated using adapted R functions. Using bespoke R scripts, the annotated features were identified and assigned a unique identifier (hereafter, "masstag") informing the monoisotopic mass m/z and retention time in seconds. There was respectively n = 3,345 and n = 2,238 masstags in the positive and negative ionisation modes, yielding a grand total of n = 5,583 masstags.

4.6.7.3 Compound annotation, filtering, and biomarker identification

Next, masstags were automatically annotated using available libraries. First, masstags were automatically matched against a custom list of n = 30 potential candidate compound references (**Table Appendix 3 S1**). Second, the web-based platform *MetaboAnalyst* v5.0 (Pang et al., 2021) was used for automatic matching of masstags to known compounds using the "Functional Analysis of MS peaks" module. For each negative and positive mode of the nine samples from the three media (CM, SM, and blank), raw peak intensity data was entered with retention times in seconds and mass tolerance of 5 ppm. The data was left unfiltered (recommended for n features < 5,000), sample-normalised by median (negative mode) or sum (positive mode), cube-root transformed, and auto-scaled (i.e., mean-centred and divided by the standard deviation of each variable). Matched compounds were retrieved from the *mummichog* v2.0 algorithm with a custom currency metabolite exclusion list for common contaminants (water, proton, oxygen, NADPH, NADP, NADH, NAD, carbon dioxide) whilst including all available adducts in positive and negative modes. In order to maximise the compound matching, the *mummichog* algorithm was repeated using all available libraries from the following animal species: the zebrafish *Danio rerio* (MetaFishNet or MFN library covering KEGG zebrafish model, human BiGG and Edinburgh Models) for fish (Li et al., 2010); the human *Homo sapiens* (MTF library covering KEGG, BIGG, and Edinburgh Model databases), the mouse *Mus musculus* (KEGG and BioCyc), the

rat *Rattus norvegicus* (KEGG), the cow *Bos taurus* (KEGG) for mammals; the chicken *Gallus* (KEGG) for birds; the fruit fly *Drosophila melanogaster* (KEGG, BioCyc) for insects; and the nematode *Caenorhabditis elegans* (KEGG). After filtering duplicates, this yielded a grand total of 217 and 281 unique matched compounds from the *mummichog* algorithm in the negative and positive modes, respectively. To exclude the masstags predominantly present in the blank, a threshold cut-off was defined relative to the average intensity of a given masstag m/z in the blank $Intensity_{Blank}^{m/z}$ as shown in **Equation 4.1**.

$$\text{Cut} - \text{off} = 2 \times (mean\ Intensity_{Blank}^{m/z} + 3 \times SD\ Intensity_{Blank}^{m/z}) \quad \textbf{Equation 4.1}$$

Masstag intensities were blank corrected (BC, **Equation 4.2**) and their intensity expressed as blank corrected percent total relative to the sum of masstag areas per sample (BCP, **Equation 4.3**).

$$BC_{m/z} = Area_{Masstag}^{Sample} - Cutoff_{m/z} \quad \textbf{Equation 4.2}$$

$$BCP_{m/z} = 100 \times \frac{BC_{m/z}}{\sum_{i=1}^{per\ sample} BC}) \quad \textbf{Equation 4.3}$$

Because the analysis only used one pooled biological replicate (pooled medium sample from 60 embryos) but with technical replicates, I aimed to avoid pseudo-replication bias and therefore did not use statistical analysis of significance between CM and SM. Instead, each sample was assumed to represent a high confidence average of the metabolome excreted by 60 embryos per treatment. The data was first filtered to account for signal-to-noise ratio by only selecting masstags with intensities over the threshold cut-off in at least three samples out of six technical run replicates (n = 3 in CM, n = 3 in SM). This narrowed the potential biomarkers of SM and CM media to n = 89 unique masstags from the positive and negative modes altogether. Second, the biomarkers were assigned to either SM or CM based on which group their average blank corrected percent total intensity was highest. Third, the absolute differences between the blank corrected percentage intensities in CM and SM media were calculated to identify stress and control biomarkers (B), with higher B values indicating suitable biomarkers for either condition (**Equation 4.4)**.

$$B = |BCP_{m/z}^{CM} - BCP_{m/z}^{SM}| \quad \textbf{Equation 4.4}$$

To complement the annotation of all 89 masstags, they were manually matched with available online databases using their m/z masses. The two main databases were used, with all available positive and negative ion adducts and a tolerance threshold of ± 0.0005 m/z: the Direct Infusion Metabolite database (O'Shea et al., 2018) and the Metabolomics Workbench (The Metabolomics Workbench available at https://www.metabolomicsworkbench.org/, using three available options: reference set of metabolite species, *RefMet*; the Metabolomics Workbench Metabolite database with a m/z value; and the untargeted metabolite search option). Additional manual annotations using the narrowest available mass tolerance range were retrieved from other databases including the metabolomic Fiehn lab's LipidBlast database (Kind et al., 2013), The LIPID MAPS® Lipidomics Gateway (https://www.lipidmaps.org/), UniProt (UniProt Consortium, 2019), MassBank Europe (https://massbank.eu/MassBank/), mzCloud (https://www.mzcloud.org/), as well as a general screening of the available literature and supplemental data therein. This manual screening of > 5,000 entries identified approx. 2,500 possible hits (including within and cross-database duplicates). Each potential hit was assigned a compound name and its identifier from common chemical registries (of which PubChem, Human Metabolome DataBase or HMDB, and KEGG). Next, the literature and publicly available metabolome information corresponding to each possible hit was thoroughly screened (HMDB, KEGG, Food database, PubChem-associated literature, clinical trials, and patents; literature search; ChEBI, MetaCyc, KNApSAcK) to enhance the compound annotation by removing potential hits not likely to be found in zebrafish embryos exposed. For this purpose, the exclusion criterions were: no biological records, fungal, bacterial or plant metabolites, xenobiotic metabolites, or industrial or pharmaceutical use. On the other hand, the inclusion criterions were that the potential hits were previously found in metazoan species, are known as general metabolites, or could not be disregarded using the exclusion criterions. It should be acknowledged that although this filtering may be subjective, it mainly aimed to limit the risks of associating masstags to compounds unlikely to be excreted by zebrafish embryos exposed to TS and C.

4.6.7.4 Metabolite functional enrichment

Possible hits were annotated with their IUPAC International Chemical Identifiers (InChI or InChI Key), which were used for automatic structure-based ChemOnt

chemical taxonomy classification using the *ClassyFire* algorithm (Djoumbou Feunang et al., 2016) (available at http://classyfire.wishartlab.com/queries/new or https://cfb.fiehnlab.ucdavis.edu/, last accessed April 2022). I reasoned that because one cannot assign a unique metabolite per masstag amongst several isomer candidates, one should use only one compound per level of classification to prevent redundancy in the functional enrichment and to prevent bias towards subclasses for masstags that match several known compounds. Therefore, where relevant (i.e., if there were possible hits and different chemicals sharing the same classification), one compound per subclass (or class and superclass when compounds were not classified to the subclass level) per masstag that had either a KEGG or HMDB identifier was selected as a representative compound for the functional enrichment. This yielded 135 representative compounds used for both chemical structure (subclass) and KEGG pathways (Kanehisa and Goto, 2000) functional enrichment using the *MetaboAnalystR* v3.0 R package (Pang et al., 2020). Functional enrichments were performed for SM- and CM-specific filtered metabolites separately, with Holm's p-value correction for multiple testing.

4.6.8. Endpoint 4: Multi-omic integrative analyses

Next, the transcriptome and excreted metabolome data were integrated into two joint analyses. First, the Joint Pathway from MetaboAnalyst was used to explore the enriched KEGG pathways. Only the representative hits of the stress medium were used in the joint pathway analysis to avoid an artificial bias as masstags could have several hits with the same ChemOnt classification. The Joint Pathway analysis looked for the enriched KEGG pathways using a hypergeometric test using MetaboAnalyst v.5.0 (Pang et al., 2021), (https://dev.metaboanalyst.ca/MetaboAnalyst/upload/JointUploadView.xhtml, accessed February 2022 – options were set to: organism: *Danio rerio*; Metabolomic type: "targeted (compound list)"; ID type: "official gene symbol" and "compound name"; topology measure: "degree centrality"; integration method: "combine queries", pathway database: "metabolic pathways"). Second, the compound-protein interactions (CPI) were identified via the STITCH database using Cytoscape v.3.9.0 (Shannon et al., 2003). Out of the 202 unique possible metabolites in SM, several compounds (proteins, lipids, and polypeptides; with non-standard identifiers) could not be searched in STITCH and were removed, leaving 46 compounds that were manually searched in the online version of STITCH (http://stitch.embl.de/, accessed February 2022). There were n = 26 compounds that existed in the STITCH database, which were used for the CPI analysis.

I reasoned that the significant genes in TS may lead to the synthesis and release of stress metabolites in the stress medium, and that the stress metabolites would initiate a transcriptome response in embryos of the SM treatment. Therefore, the joint pathway and CPI analyses were performed twice by combining the candidate stress metabolites with genes of either SM or TS. To optimise the readability of the networks, the CPI analyses for TS (n = 136 identifiers with 106 DEGs + 26 compounds) and SM (n = 108 identifiers with 79 DEGs + 26 compounds) were performed at confidence score cut-off of 0.7 and 0.4, respectively, with the following options: network type: full STRING network; no additional interactors, no singletons. See **Figure 4.3A** for a schematic design of the metabolomic experiment.

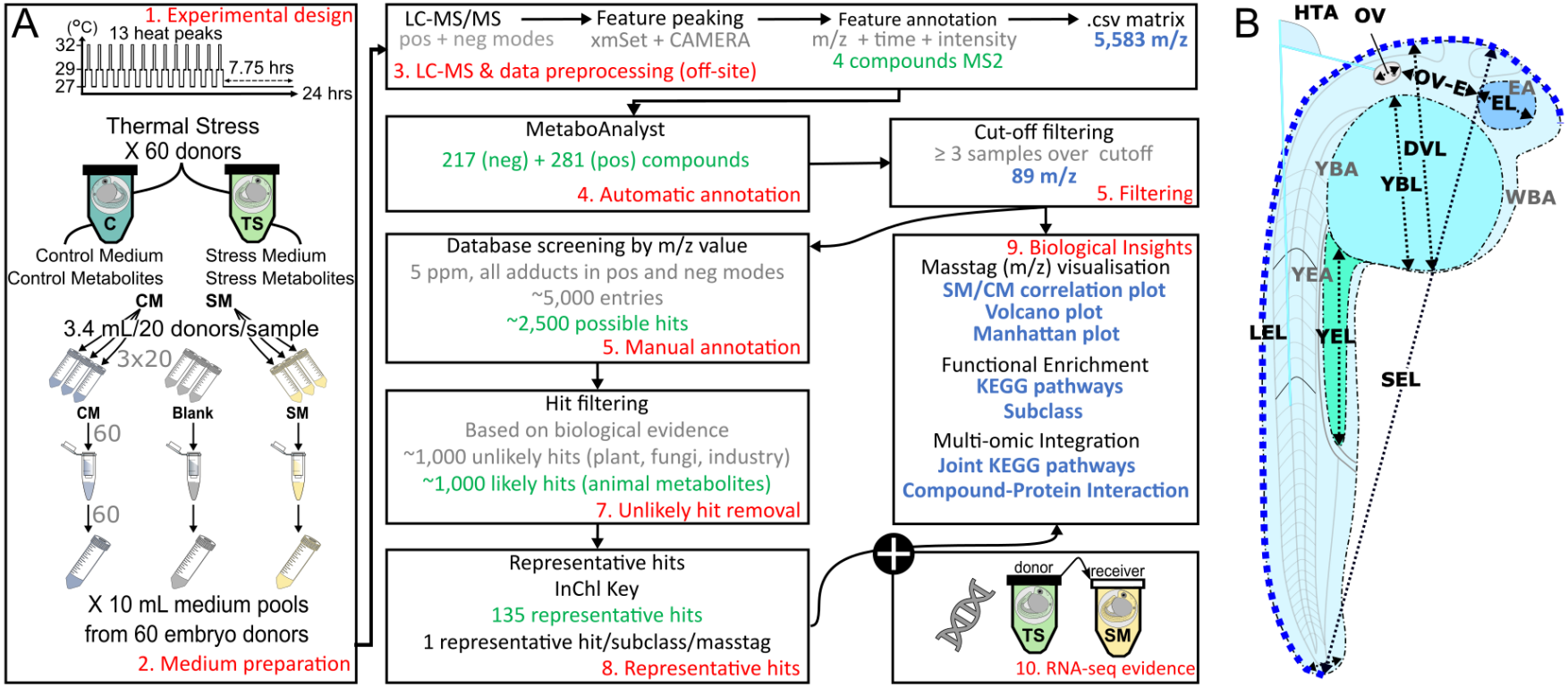

Figure 4.3. Schematics of multi-omic and imaging analyses. A) Schematics of multi-omic analysis. Red font: steps 1 to 10 of multi-omic analysis. Green font: compound identification. Blue font: masstag (m/z) data. Multi-omic analyses integrate data from donors (TS) and receivers (SM) of stress metabolites using RNA-seq and metabolomics. In the left-most panel, the pooling steps of medium from 60 embryos is shown with grey font. B) Measurements of zebrafish embryos and larvae quantified in Image J. Lengths (dashed lines) and areas (dot-dashed lines) are shown in black and grey font, respectively. LEL: longest embryo length, SEL: shortest embryo length, YEL: yolk extension length, YBL: yolk ball length, OV: otic vesicle, OV-E: otic vesicle to eye length. OVL is the ratio OV-E/OV. EL: eye length, DVL: dorsal-ventral length, YEA: Yolk extension area, YBL: yolk ball area, WBA: whole-body area. HTA is the head-trunk angle formed between the cyan blue lines. Criteria are based on Kimmel et al. (1995).

4.6.9. Endpoint 5: Phenotypic response in 1-dpf and 4-dpf zebrafish

A range of phenotypic parameters was measured in zebrafish at 1 dpf and 4 dpf in all five treatments, both within and outside of their chorions. All conditions were tested on the same day using the same clutch to prevent batch effects; and this was repeated twice. Control and stress metabolites, respectively, were obtained from one-day older donors raised within their chorion in C and TS. Embryos were collected around 10 am, cleaned through bleaching as described before, and selected under the stereomicroscope. Embryos were then individually exposed to treatments within their chorion from 0 dpf to 1 dpf. After 24 hours, embryos were removed from their individual wells and placed in watch glasses with a small amount of their medium. Next, light-induced startle responses were videoed under the stereomicroscope for 30 seconds. Embryos were then gently manually dechorionated under the stereomicroscope using Dumont n°5 forceps and individually imaged in lateral view on a microscope slide with a micrometre scale, before being placed in new individual wells pre-filled with 200 µL of experimental medium. Experimental conditions were maintained until 4 dpf. At 2 and 3 dpf, 180 µL of medium were replaced with either fresh or conditioned media. All embryos and larvae were monitored daily for hatching and survival.

At 4 dpf (96 hpf at 12 am), larvae were moved to a temperature-controlled room at 25°C for swimming assays. Larvae were gently individually transferred into flat-bottom wells of 35 mm diameter pre-filled with 3 mL of fresh embryo medium pre-warmed at 27°C. The starting temperature was measured using a small portable thermometer. A Canon 1,200D camera was used to record swimming behaviours. The 6-well plate was positioned at the centre of a photo box. Larvae were allowed to settle for 30 seconds after being placed in their swimming wells before the video started. The swimming assay consisted of touching the head of the larvae with the loop of an inoculating needle to record the touch-evoked swimming behaviour. One escape response was triggered every 20 seconds with three repeats per larva to measure their stamina. Once all videos were completed, 4-dpf larvae (100 hpf) were imaged on a microscope slide with a micrometre scale. Both imaging and videoing were conducted with treatments randomised and blind to the experimenter and with treatment alternation to limit the effects of the time of day.

All images and videos were automatically bulk renamed and randomised (using Bulk Rename Utility v3.4) for a blind analysis. In Image J v1.53e (Schneider et al., 2012), images were calibrated to scale to measure lengths (mm) and areas (mm^2) of

several phenotypic characters (**Figure 4.3B**) from Kimmel et al. (1995). For 1-dpf embryo, these were: shortest embryo length (SEL, shortest embryo length from head to tail), longest embryo length (LEL, segmented line in the anterior-posterior axis from the epiphysis in the middle of the head to the tail), yolk ball length (YBL) and area (YBA), yolk extension length (YEL) and area (YEA), tail width (TW, cross section of the caudal fin in dorsal-ventral axis where the notochord ends), eye length (EL) and area (EA), dorso-ventral length (DVL, longest dorso-ventral cross section in the yolk ball region), and whole-body area (WBA). In addition, several staging indices were used to estimate embryonic developmental stages, including the head-trunk angle (HTA, adjacent angle to the angle formed between a line crossing through the middle of the eye and the otic vesicle and the line parallel to the notochord between the 5^{th} and 10^{th} somites), the otic vesicle length (OVL, i.e. how many more otic vesicles would fit between the otic vesicle and the eyes), and yolk extension-to-yolk ball ratios (YE/YB). Embryo staging was also guided by binary coding for the presence of features such as the eye primordium (≥ 19.5 hpf), two clear otoliths (≥ 22 hpf), the hatching gland (≥ 22 hpf), the cerebellum formation (≥ 25 hpf) and its migration towards the head (≥ 31 hpf), or the tail strengthening (≥ 31 hpf). In 4-dpf larvae, the EL, SEL, DVL, TW, and WBA were measured.

Videos of acute light-evoked startle responses of 1-dpf embryos within their chorions were analysed using Danioscope (Noldus) to quantify burst counts per minute and burst activity percentages. The touch-evoked swimming behaviour at 4 dpf was analysed in Kinovea v0.9.5 (Charmant and Contributors, 2021). The total distance and number of swimming burst events were measured following each of three stimuli for the entire video. Next, speed and acceleration following the 1^{st} and 3^{rd} (last) stimuli were monitored at each frame for the first complete burst defined as when larvae reached full immobility (0 m/s) for at least two consecutive frames regardless of subsequent bursts. Comparing responses between the first and last touches allowed me to calculate delta total distances to estimate the stamina of larvae. However, since Welch's adjusted t-tests showed that there were no significant differences between the 1^{st} and 3^{rd} stimuli for the mean acceleration ($t = -0.014825$, $df = 284.08$, p-value = 0.9882) and mean speed ($t = 0.98882$, $df = 313.8$, p-value = 0.3235), the data were averaged across the first and last stimuli.

All phenotypic data analyses were conducted in R v4.0.2 (R Core Team, 2020) using Rstudio v1.3.1056 (RStudio Team, 2020) with *ggplot2* v3.3.5 (Wickham, 2016)

for graphs. Outliers were excluded using repeated Grubbs' tests for one outlier from *outliers v0.14* (Komsta, 2011). For each response variable, models were fitted to estimate the effects of (i) thermal stress and stress metabolites across the two-way factorial design (C, SM, TS, TS+SM), followed by pairwise post-hoc comparisons relative to control C, and (ii) of media by post-hoc comparing CM to C and SM. Covariates were included when there was evidence of their significance for the model according to the Akaike Information Criterion calculated using the *aictab* function from the *AICcmodavg* v2.3-1 R package (Mazerolle, 2020a) to sort possible models by delta AICc, the *stepAIC* function from the *MASS* v7.3-51.6 R package (Venables and Ripley, 2002) to estimate the best model from the full model; and the *drop1* function (*stats* R package) to estimate whether any terms could be dropped. Since embryos were not fixed in agarose for imaging, approx. 30% of the images could not capture the otic vesicle which prevented the measurement of several variables of interest. Therefore, only complete cases (n = 114 out of 157 embryos) were retained for a multivariate analysis using a PERMANOVA using the *adonis* function from the *vegan* v2.5-7 R package (Oksanen et al., 2020). Morphology data was represented by a principal component analysis (PCA) of treatment groups using the *ggbiplot* v0.55 (Vu, 2011) and *prcomp* R functions. All pairwise comparisons were corrected by Tukey's method for false discovery rates. If necessary, data were normalised using *BestNormalize v1.8.2* (Peterson and Cavanaugh, 2020). The normality of model residuals was assessed using Shapiro-Wilks' tests. Studentized Breusch-Pagan tests from the *lmtest* v0.9-38 R package (Zeileis and Hothorn, 2002) were used to test the homoscedasticity of model residuals. Continuous data of the two-way factorial design were analysed by ANOVAs for parametric data or Scheirer-Ray-Hare tests – *rcompanion* v2.4.1 R package (Mangiafico, 2021) – for non-parametric data. Binary data were analysed using generalised linear models (GLMs) with binomial distribution. 4-dpf swimming burst count data were analysed using GLMs with negative binomial distribution from *MASS* (Venables and Ripley, 2002), as this distribution best fitted the data according to the *fitdistrplus* v1.1-6 R package (Delignette-Muller and Dutang, 2015). The swimming burst data analysis was double-checked with a two-group equal density test from the *sm* v2.2-7.7 R package (Bowman and Azzalini, 2021). Pairwise comparisons were retrieved from models (ANOVAs and GLMs) using the *trt.vs.ctrl* argument of *emmeans* v1.7.2 (Lenth, 2022), Wilcoxon-Mann-Whitney tests (non-parametric data), or *pairwiseAdonis* v0.4 (Martinez Arbizu, 2017) (PERMANOVAs). Effect sizes of model terms were represented by Cohen's |d| values, approximated as $d = 2 \times f$ (Cohen, 1988) from

Cohen's f values from *effectsize v0.6.0.1* (Ben-Shachar et al., 2020). Effect sizes were interpreted according to Sawilowsky (2009) as tiny ($|d| < 0.1$), very small ($|d| > 0.1$), small ($|d| > 0.2$), medium ($|d| > 0.5$), large ($|d| > 0.8$), very large ($|d| > 1.20$), and huge ($|d| > 2.0$). Phenotypic data were interpreted using $p < 0.05$ for significant evidence whilst considering $p \leq 0.08$ as "trends with weak evidence".

4.6.10. Endpoint 6: candidate genes in outcrossing group-exposed embryos[7]

Three sets of 20 embryos each obtained from an outcrossing strain (PET) of zebrafish maintained at the University of Hull since 2018. Embryos were exposed in groups in petri dishes for 24 hrs to either fresh E3 medium or SM (n = 60 embryos per sample, 250 µL medium per embryo). Stress metabolites were obtained from heat-stressed donors raised in darkness and experiencing constant thermal stress of 32°C from 0 to 1 dpf. Total RNA was extracted from 4 such pools per treatment as previously described. Fluorometric LAMP (Loop-mediated isothermal amplification reactions) were performed according to manufacturer's protocol (NEB #M1708S) with primers designed for selected RNA-seq DEGs: chitin synthase 1 (*chs1*), lactate dehydrogenase A4 (*ldha*), olfactory receptor class A related 3 (*ora3*, a V1R-like vomeronasal chemoreceptor), otoferlin a (*otofa*), proteoglycan 4a (*prg4a*), and toll-like receptor 18 (*tlr18)*. Reactions were run in technical triplicate on a StepOne qPCR machine. Gene expression was quantified using the $-\Delta\Delta C_T$ method (Livak and Schmittgen, 2001) which represented the time to reach the threshold (C_T with each cycle lasting 1 min) normalised to β-Actin as housekeeping gene and scaled to control values. Gene expressions were compared using Student's t-tests.

4.7. Results

4.7.1. Heat, but not stress metabolites, increases cortisol in 4-dpf larvae

Cortisol plays a central role in the hypothalamic-pituitary-interrenal (HPI) axis stress response. First, a cortisol increase was confirmed between 1 and 4 dpf in control zebrafish (**Figure 4.4A-B**). Cortisol was then measured at 4 dpf in control (C) and heated (TS) donors and their respective receivers CM and TS. A one-way ANOVA showed that cortisol concentrations significantly varied across treatments ($F = 14.35$, $p = 0.0014$, **Figure 4.4C**). Post-hoc pairwise comparisons revealed that TS significantly increased cortisol levels by 92% compared to control C ($t = -4.86$, $p = 0.0055$, huge

[7]Laboratory experiments by Timothy Emagbetere. Code for LAMP data processing by Adam Bates. I conducted statistical analysis & graphs on final processed data.

effect size = 6.17). On the other hand, incubation media did not have an effect as there were no differences between C and CM (t = -1.48, p = 0.4895), or SM (t = 1.38, p = 0.5453). There was only weak evidence for a trend (t = 2.86, p = 0.0812, very large effect size = 1.85) of higher cortisol levels in CM compared to SM. Therefore, cortisol profiles were regulated by heat stress whilst medium had no effect.

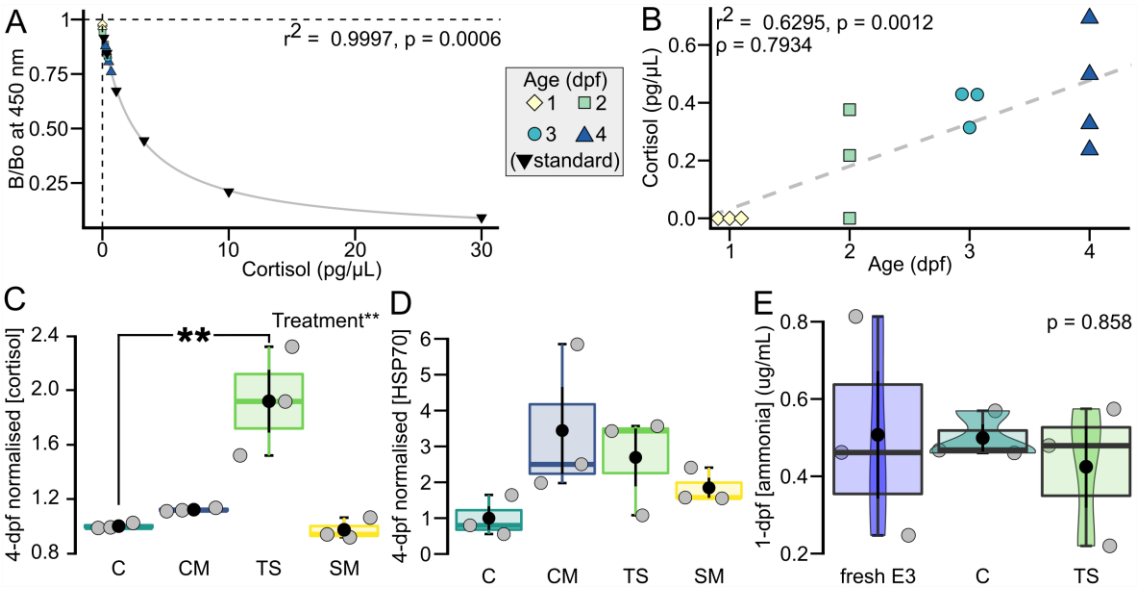

Figure 4.4. Cortisol, HSP70, and ammonia are not involved in stress propagation. A) Optimisation of cortisol assay showing extraction method works best with larvae at 4 days post fertilisation (dpf, dark-blue triangles). Four-parameter nonlinear standard curve (grey line, fit in top-right corner) of cortisol assay of the blank-corrected cortisol absorbance (B/Bo, at 450 nm) in function of cortisol standards (pg/µL). Values from control zebrafish at 1, 2, 3, and 4 dpf (coloured shapes, n = 13 samples of 40 individuals each) were interpolated from standards (black diamonds, n = 6). Values outside detection range (0.07 pg/L, dashed lines) were replaced by 0 pg/µL. B) Comparison of cortisol levels in zebrafish from 1 to 4 dpf. Fit and significance of linear regression (slope: grey dashed line) are shown in top-left corner. C) Thermal stress induces a cortisol stress response at 4 dpf in zebrafish larvae (F = 14.35, p = 0.0014). Cortisol was normalised to protein content and rescaled to control mean (arbitrary units). D) 4-dpf protein expression of heat shock protein 70 (HSP70) normalised to total protein loading (Ponceau staining) and control mean (arbitrary units). Cortisol and HSP70 measurements are from the same samples with n = 3 replicates of 60 larvae, total of 180, per treatment. E) Ammonia levels measured in media after 24 hours of incubation (n = 3 replicates of 5-6 embryos). Boxes show median and 25%-75% quartiles, and whiskers are min/max values within 1.5 IQR. Jittered raw data given as grey circles. Black dots show mean ± SE values of each treatment. Pairwise comparisons are shown with *: $p \leq 0.05$, **: $p \leq 0.01$. E3: fresh medium without zebrafish, C: control in fresh medium at 27°C; CM: control metabolites at 27°C; TS: thermal stress in fresh medium; SM: stress metabolites at 27°C.

However, the expected heat shock protein response was inhibited by repeated heat stress after experiencing 76 (19 peaks per day for four days) peaks at sublethal temperatures at 4 dpf since there were no differences in protein levels of HSP70 between treatments (F = 1.9271, p = 0.2038, **Figure 4.4D**).

4.7.2. Heat stress altered the whole-body transcriptome of 1-dpf embryos

The principal component analysis of RNA-seq data did not show evidence that samples clustered by treatments across either of the first two variance axes (PC1 = 51% and PC2 = 16% of variance, respectively, **Figure 4.5A**). Nevertheless, the effect of thermal stress was uncovered by the multidimensional analysis on the second and third axes (PC3 = 9.97%, **Figure 4.5B-C**).

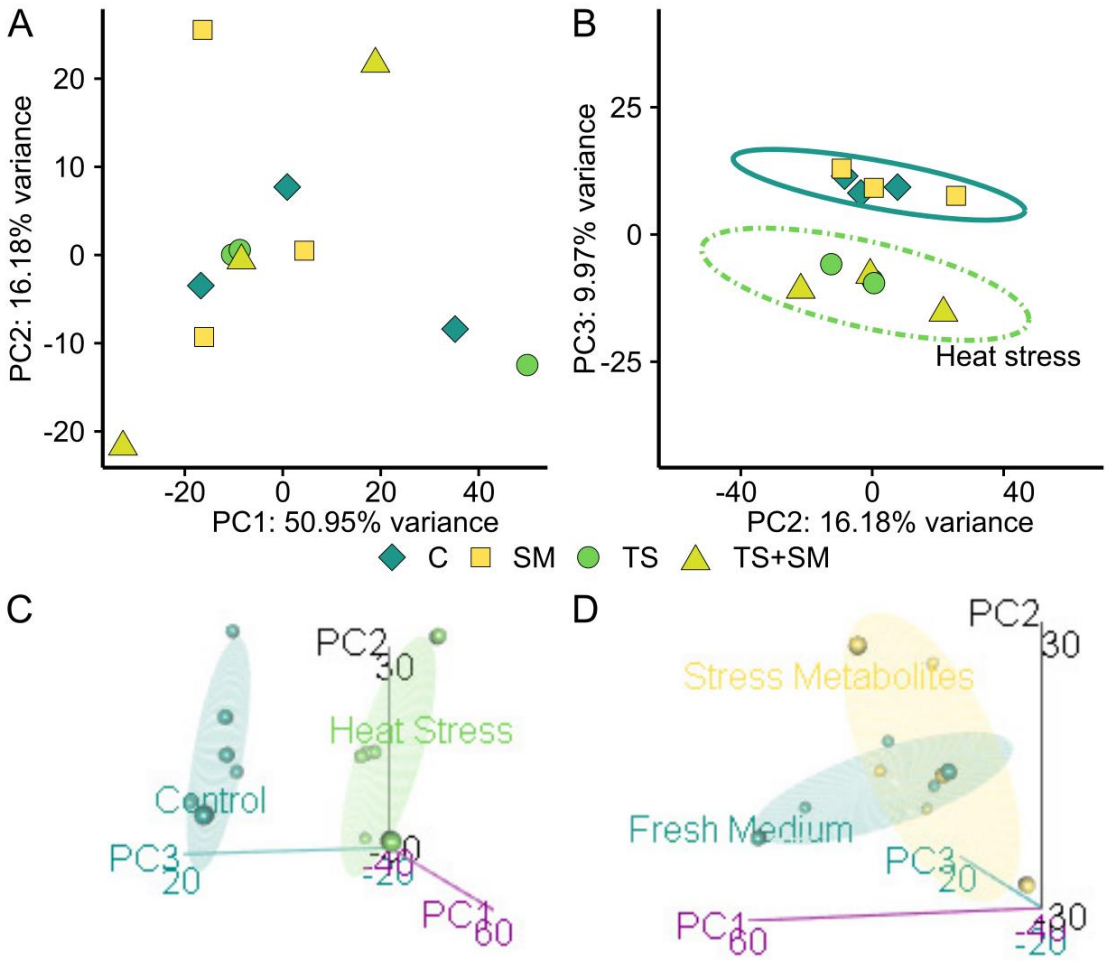

Figure 4.5. Principal Component Analysis of RNA-seq. A) Axes 1 and 2 and B) 2 and 3 of the principal component analysis (PCA) in 2D representation. Ellipses show the 95% interval confidence of centroids of heat stress (green dot-dash lines, n = 6 samples) and 27°C (blue solid lines, n = 6 samples). Medium effect is not evident on the first three axes and is not represented. C) 3D representation of the PCA showing the effect of heat stress term (green ellipse) versus control temperature (blue ellipse). D) PCA showing the effect of stress metabolites term (yellow ellipse) versus fresh medium (blue ellipse). C: control in fresh medium at 27°C, SM: stress metabolites at 27°C, TS: fresh medium in thermal stress, TS+SM: stress metabolites in thermal stress.

Consequently, repeated heat stress induced n = 369 DEGs ($p \leq 0.01$) as shown in the volcano plot (**Figure 4.6A**). The three genes with largest effect size and log fold-change |LFC| > 3 were *atp2a1l* (ATPase sarcoplasmic/endoplasmic reticulum Ca^{2+}

transporting 1, like), *crygm2d18* (crystalline, gamma M2d18), and *matn3a* (matrilin 3a). Two paralogues of gamma-glutamylamine cyclotransferase, tandem duplicate (*ggact.2* and *ggact.3*) were the two most heat-inhibited genes, with 98% fewer transcripts than in control embryos. Functional enrichments (for Biological Processes, KEGG, and Reactome pathways) were conducted for the top 106 genes with the strongest evidence of heat stress-induced transcriptomic alteration (p-adj ≤ 0.05), most of which were upregulated (n = 90 genes with fold change FC > 1.5) whilst a few were downregulated (n = 16 genes). This evidenced that heat stress induced transcriptomic changes in (i) embryonic development (eyes, muscles, and somites), (ii) the heat stress response, and (iii) the metabolism of sugars, amino acids, purine, and energy intermediates (ATP and pyruvate, **Figure 4.6D, Figure Appendix 3 S1**).

The most significantly enriched biological processes were associated with eye development, as evidenced by the terms "*lens development in camera-type eye*" (GO:0002088) and "*visual perception*" (GO:0007601). These gene ontology (GO) terms mostly involved six genes linked to the lens and cornea proteins, crystallin alpha (*cryba1*, *cryba1l1*, *cryba2a/b*, and *crybb1l1/2*), and eight crystallin gamma genes (*crygm2d8/10/13/17/18/20*, *crygmx*, and *crygmxl2*). Other development-related functions included GO terms such as "*multicellular organism development*" (GO:0007275), "*animal organ development*" (GO:0048413), "*developmental process*" (GO:0032502), "*somite specification*" (GO:0001757), and "*muscle fibre development*" (GO:0048747). Reactome pathway enrichment also indicated an alteration of muscle-related gene expression with the term "*striated muscle contraction*". Further, muscle development in heat-stressed embryos was associated with elevated transcript levels of three paralogues of actinidin (*and1/2/3*), as well as myosin *myhz2* (myosin heavy polypeptide 2, fast muscle specific), but also three myozenin genes (*myoz1a/1b/3a*). On the other hand, there was evidence that the gene expression of myogenin (*myog*) and myosin 7 (*CU633479.2*) were significantly inhibited by high temperatures.

Analysing genes within the Biological Process GO term "*response to heat*" (GO:0009408) provided strong evidence that there was an over threefold upregulation of four genes related to the heat shock response, namely *hsp90aa1.2* (heat shock protein 90, alpha, cytosolic, class A member 1, tandem duplicate 20), *hsp70.3* (heat shock cognate 70-kDa protein, tandem duplicate 3), *hspa8b* (heat shock protein family A [Hsp70] member 8b), and *hsc70* (heat shock cognate 70). The transcriptional upregulation of members of the heat shock response explained why "*cellular response*

to heat" (GO:0034605) as well as "*cellular response to heat stress*" and "*regulation of HSF1-mediated heat shock response*" were amongst the most significantly enriched functions in heat-stressed embryos compared to control (**Figure 4.6A/D,**). Functions associated to protein refolding (e.g., GO:0042026; GO:0034620) were also significantly enriched by *hsp90aa1.2, hsp70.3, hspa8b,* and *hsc70*.

The third major GO term category with significant functional enrichment covered several metabolism and energy pathways, such as the regulation of adenosine diphosphate (ADP, GO:004603), triphosphate (ATP, GO:0046034), and glycolysis (GO:0006096). Notably, heat activated several transcripts of enolase (*eno1a* and *eno3*), glyceraldehyde-3-phosphate dehydrogenase, spermatogenic (*gapdhs*) but also genes with a kinase activity such as phosphoglycerate kinase 1 (*pgk1*) and pyruvate kinase M1/2b (*pkmb)*. Additional functional enrichment for Reactome and KEGG pathways confirmed that high temperatures altered the metabolism of ADP/ATP, glucose (e.g., "*gluconeogenesis/glycolysis*", "*pentose phosphate metabolism*"), amino acids, as well as pyruvate.

In addition, network analyses revealed a strong functional interconnectivity between the DEGs of TS (**Figure 4.7A**, CPI enrichment $p < 0.0001$, 64 edges observed vs. 5 expected edges). A cluster of co-upregulated genes was assigned to the GO term "*metabolism of carbohydrates*" (GO:0005975): *pgk1*, *gpia, eno1a*, *eno3*, *ldha,* and *gapdhs*. Another cluster grouped five transcription regulators (GO:0000122) of the GO terms "*segmentation*" (GO:0035282) and "*somite development*" (GO:0061053): *mespab*, *her1/7, ripply2,* and *tbx6* (**Figure 4.7A).**

In summary, this shows that heat stress induced transcriptomic changes in embryonic development (of the eyes, muscles, and somites), the metabolism of sugars, amino acids, purine, and energy intermediates (ATP and pyruvate), as well as the heat stress response.

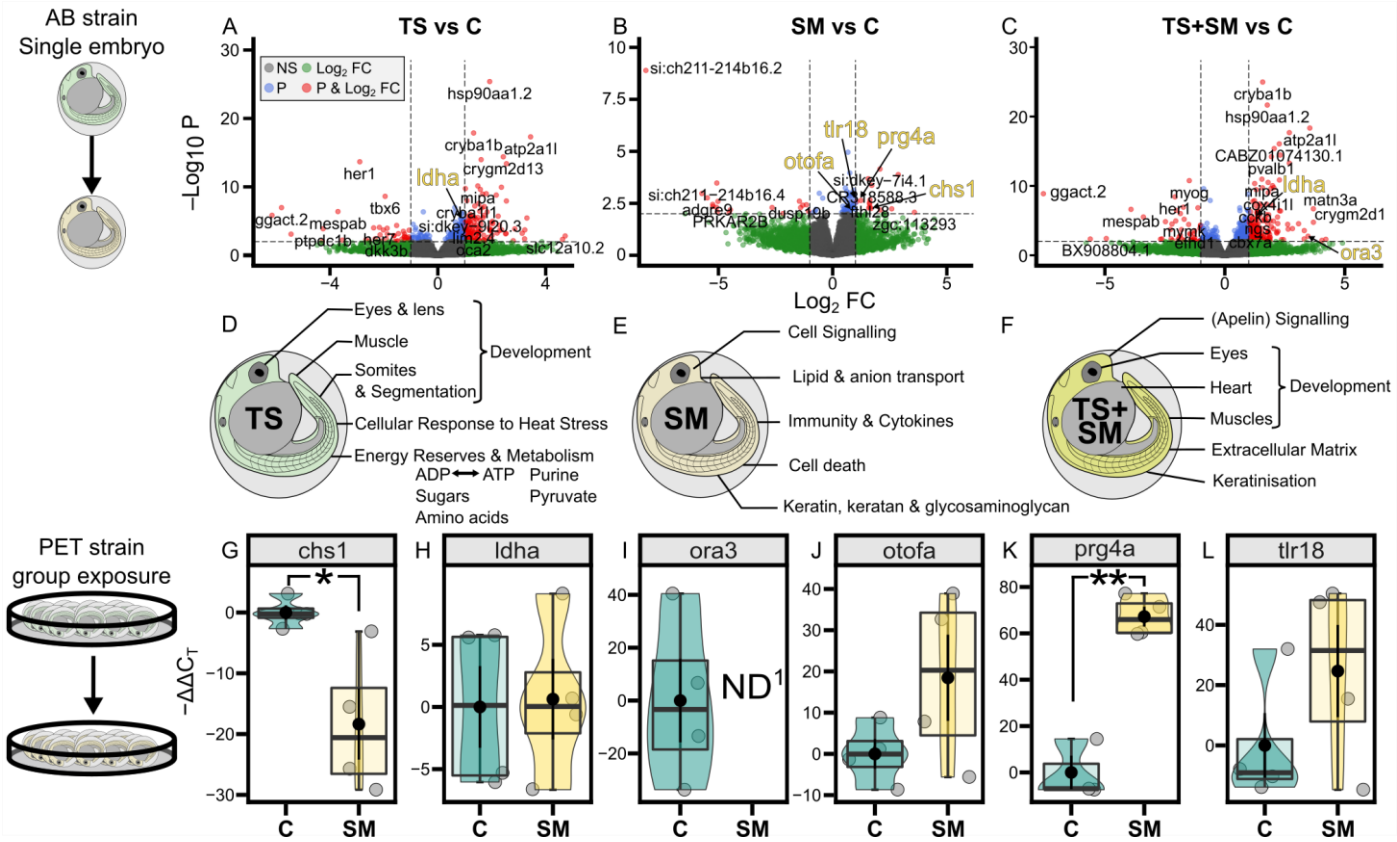

Figure 4.6. Thermal stress and stress metabolites alter the transcriptome and its functions in 1-dpf zebrafish embryos. Top row: volcano plots showing the differentially expressed genes in response to (A) thermal stress (TS), (B) stress metabolites (SM), and (C) their combination TS+SM compared to control C. Genes of interest are shown in red when they have significant raw p-values (above horizontal line) and an absolute fold change (FC, representing the effect size) greater than 2 (|log 2 FC| > 1, vertical lines). DEGs left to the left vertical line and right to the right vertical line are respectively significantly underexpressed and overexpressed compared to the control C. Middle row: gene functional categories from KEGG, Reactome, and GO Biological Process analysis for (D) TS, (E) SM, and (F) those uniquely present in the combined treatment TS+SM. Top and middle row show transcriptomic data from individually-raised AB strain embryos. Bottom rows Loop-Mediated Isothermal Amplification (LAMP) data of candidate genes associated with stress metabolites showing the gene expression ($-\Delta\Delta C_T$) in C and SM in more realistic environmental conditions (genetically diversified outbred pet-store PET strain raised in groups). *chs1*: chitin synthase 1, *ldha*: lactate dehydrogenase A4, *ora3*: olfactory receptor class A related 3, *otofa*: otoferlin a, *prg4a*: proteoglycan 4a, *tlr18*: toll-like receptor 18. [1]ND: mRNA amplification non-detected suggesting a depletion of *ora3* in SM. Student's t-tests compared SM to C with significant comparisons shown by horizontal bars with *: $p \leq 0.05$, **: $p \leq 0.01$. In G-L, jittered raw data given as grey circles. Black dots represent the mean ± SE values of each treatment. Treatments were SM: stress metabolites at 27°C, TS: fresh medium in thermal stress, and TS+SM: stress metabolites in thermal stress, compared to C: control in fresh medium at 27°C.

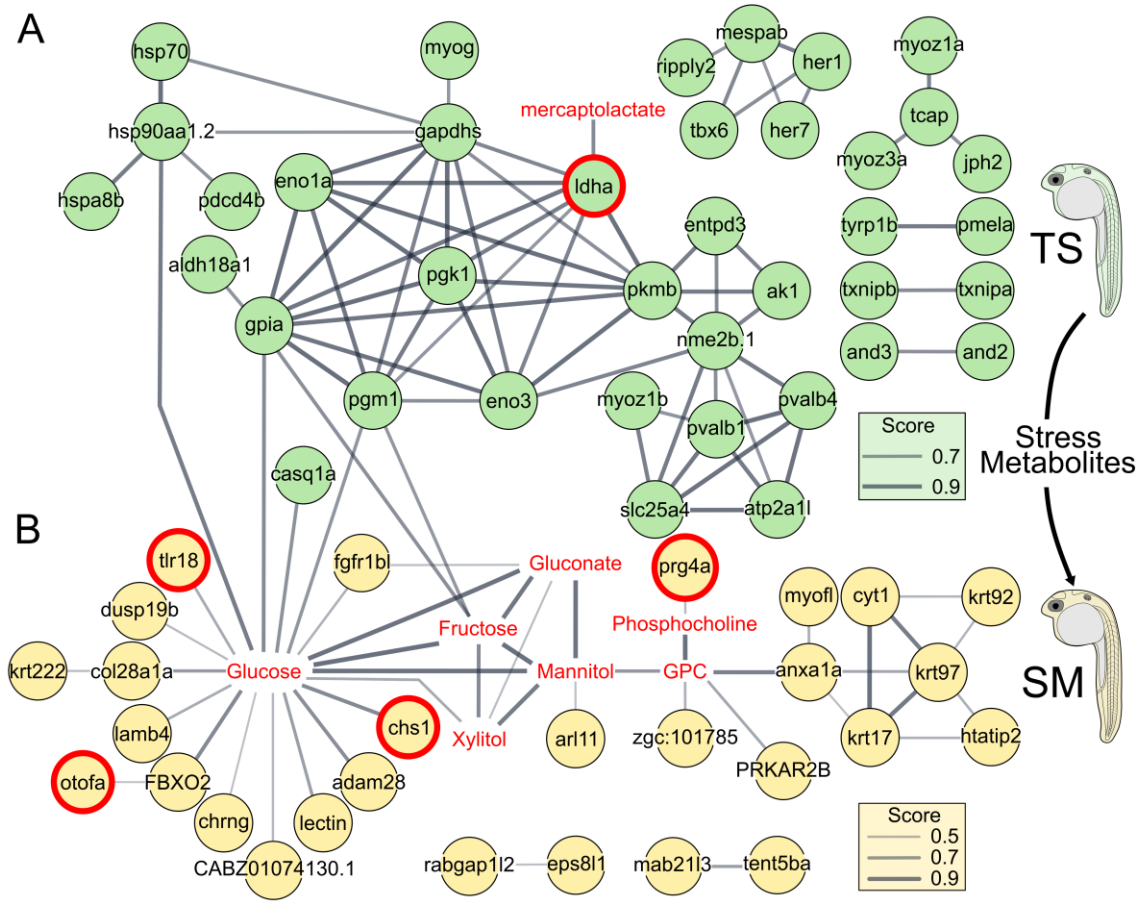

Figure 4.7. Heat-induced DEGs are functionally connected to stress metabolites, which interact with the transcriptome of receivers. Compound-Protein Interaction (CPI) network analysis of significant differentially expressed genes (circles) of TS (top row, A) or genes of SM (bottom row, B) and stress metabolite compounds (in red without circle). Line width represents the increasing confidence score with a minimum threshold of 0.7 (TS) or 0.4 (SM). Computed and drawn independently for A and B in STITCH using Cytoscape and merged in Inkscape. A: CPI enrichment $p < 0.0001$, 64 edges observed vs. 5 expected edges. B: CPI enrichment $p < 0.0001$, 14 CPI edges observed vs. 3 expected. GPC: glycerophosphocholine. Treatments were SM: stress metabolites at 27°C and TS: fresh medium in thermal stress compared to C: control in fresh medium at 27°C. Genes with red bold circles were also measured in LAMP.

4.7.3. Stress metabolites induced a localised transcriptomic response in embryos

The transcriptomic response to stress metabolites was less pronounced compared to the whole-body response to heat stress; with the only visible difference being that SM and C treatments were partitioned on different, orthogonal planes on the three-dimensional analysis (**Figure 4.5D)**. Comparing the treatment SM to the control C revealed that 79 transcripts had raw p-values lower than 0.01 (**Figure 4.6B)**. Respectively 45 and 15 of these were up- or downregulated in SM compared to C. The gene *si:ch211-214b16.2* (ENSDARG00000102593, significant after p-value adjustment) was downregulated by 99.7% by stress metabolites. *si:ch211-214b16.2* is likely an ortholog of the gene *NOD2* (nucleotide binding oligomerization domain containing 2) identified as the orthogroup *45875at7898* at Actinopterygii level by OrthoDB v10.1

(Zdobnov et al., 2021). Genes belonging to the GO term "*chemosensory perception*" (GO:0007606) were not significantly enriched. Instead, the transcriptomic response to SM was related to five wider categories: extracellular signalling, (phospho-) lipid and anion transport, keratinisation, the metabolism of glycosaminoglycan and keratan, but also the immune response involving interleukin cytokines and apoptosis (**Figure 4.6B, Figure Appendix 3 S2A-C**). The cytokine-related GO terms (e.g., GO:0001816) were associated with the genes *anxa1a* (*annexin A1a*) and *scamp5a* (*secretory carrier membrane protein 5a*). The GO term "*intracellular signal transduction*" had the highest gene count (GO:0035556, n = 8 genes: *adgre9*, *dusp19b*, *eps8l1a*, *map3k15*, *si:ch211-214b16.2*, *si:ch73-50f9.4*, *si:dkey-7i4.1*, and *traf3ip2l*) and included the most upregulated gene *si:ch211-214b16.2 (NOD2* ortholog). Moreover, the genes *fthl28* (*ferritin, heavy polypeptide-like 28*) and *tlr18* (*toll-like receptor 18*) led to the enrichment of the cell death-related Reactome terms "*ferroptosis*" and "*necroptosis*". There was evidence that one set of genes initiated the pathways of glucosamine and glycosaminoglycans (e.g., "*chitin biosynthetic process*" – GO:0006031, "*keratinization*", and "*keratan sulfate/keratin metabolism*"). These genes included the upregulated keratin genes (*krt97/17*) and chitin synthase 1 (*chs1*), the downregulated carbohydrate sulfotransferase 2b (*chst2b*), but also a proteoglycan *prg4a*. Further, several other keratin genes (*krt92/222*) and cytokeratin *cyt1* (type I cytokeratin, enveloping layer) were upregulated in SM. Several terms associated with anion and lipid transport were also enriched such as "*phospholipid transport*" (GO:0015914), "*lipid localisation*" (GO:0010876), and "*anion transport*" (GO:0006820) which included genes such as *anxa1a* (annexin 1a), *best1* (bestrophin 1), *bscl2l* (BSCL2 lipid droplet biogenesis associated, seipin, like), *pitpnc1b* (phosphatidylinositol transfer protein cytoplasmic 1b), and *xkr8.2* (XK related 8, tandem duplicate 2). Remarkably, the DEGs in SM are also significantly upregulated in zebrafish lateral line hair cells in 5-dpf larvae, relative to their expression in neighbouring epidermis cells (z-score = 8.71505; $p < 0.0001$, **Figure Appendix 3 S2D**). This comparison again highlighted *xkr8.2*, which is the highest upregulated gene in both hair cells and SM (LFC = 1.68) compared to non-hair cells, and is a scramblase involved in the enriched GO term "*membrane phospholipid transport"* (GO:0015914). SM-responsive genes were also significantly ($p < 0.0001$, 14 CPI edges observed vs. 3 expected) functionally connected in a network (**Figure 4.7B**) which supports the biological relevance of the measured response.

4.7.4. Heat stress and stress metabolites induce few similar genes and have unique effects in combination

Only nine genes were common to both TS and SM conditions compared to control C. Genes upregulated in both conditions were associated with eye development (*cryba1b*), the immune response (*tcima, transcriptional and immune response regulator a*), chloride transmembrane transport (*bestrophin 1, best1*), and cell death (*fthl28*). In contrast, *Gamma-glutamyl amino cyclotransferase B, ggact.2* was inhibited by TS but activated in SM. In the natural environment, if heat stress occurs, SM would increase simultaneously. Therefore, the transcriptomic response was explored in the combined TS+SM treatment (**Figure 4.6C)**. This revealed that the transcriptome of embryos in TS+SM was mainly driven by heat stress since 49% DEGs (78/159) were shared with TS (**Figure 4.8A**), and functions were largely similar to those in TS (**Figure 4.8B, Figure 4.9C**).

However, the combined treatment also up-regulated by elevenfold one olfactory gene, the taste receptor *ora3* (*olfactory receptor class A related 3*, LFC = 3.47, GO term-wide p-adj = 0.0412). Moreover, 47% of DEGs (75/159 with p-adj < 0.05, **Figure 4.8A**) were uniquely up- or down-regulated in TS+SM, suggesting an interaction between the SM and TS factors causing a different response than either factor by itself. There were additional functions unique to TS+SM, ascribed to developmental processes (eyes, heart, muscles), interestingly involving apelin signalling (which includes five genes *acta2, si:ch211-286b5.5, mef2aa, ryr2a, map1lc3cl*; **Figure 4.6F** and **Figure 4.8C-E**). Additional comparisons of TS+SM against SM (**Figure 4.9A**) or TS (**Figure 4.9B**) helped to determine the effects of combined versus single stressors. One candidate gene that was significantly altered by TS+SM compared to SM was *olfcb1* (*olfactory receptor C family, b1*, LFC = 2.30, p-adj < 0.0001, **Figure 4.9A**). This suggests that heat in combination with SM affects chemosensation. Comparing TS+SM to the TS treatment showed that the addition of stress metabolites altered another 32.5% novel biological processes terms, 37.5% Reactome pathways, and 16.7% KEGG pathways (**Figure 4.9D-E**). Altogether, the combined treatment TS+SM provided evidence that there were interacting non-additive effects between heat and stress metabolites when in combination.

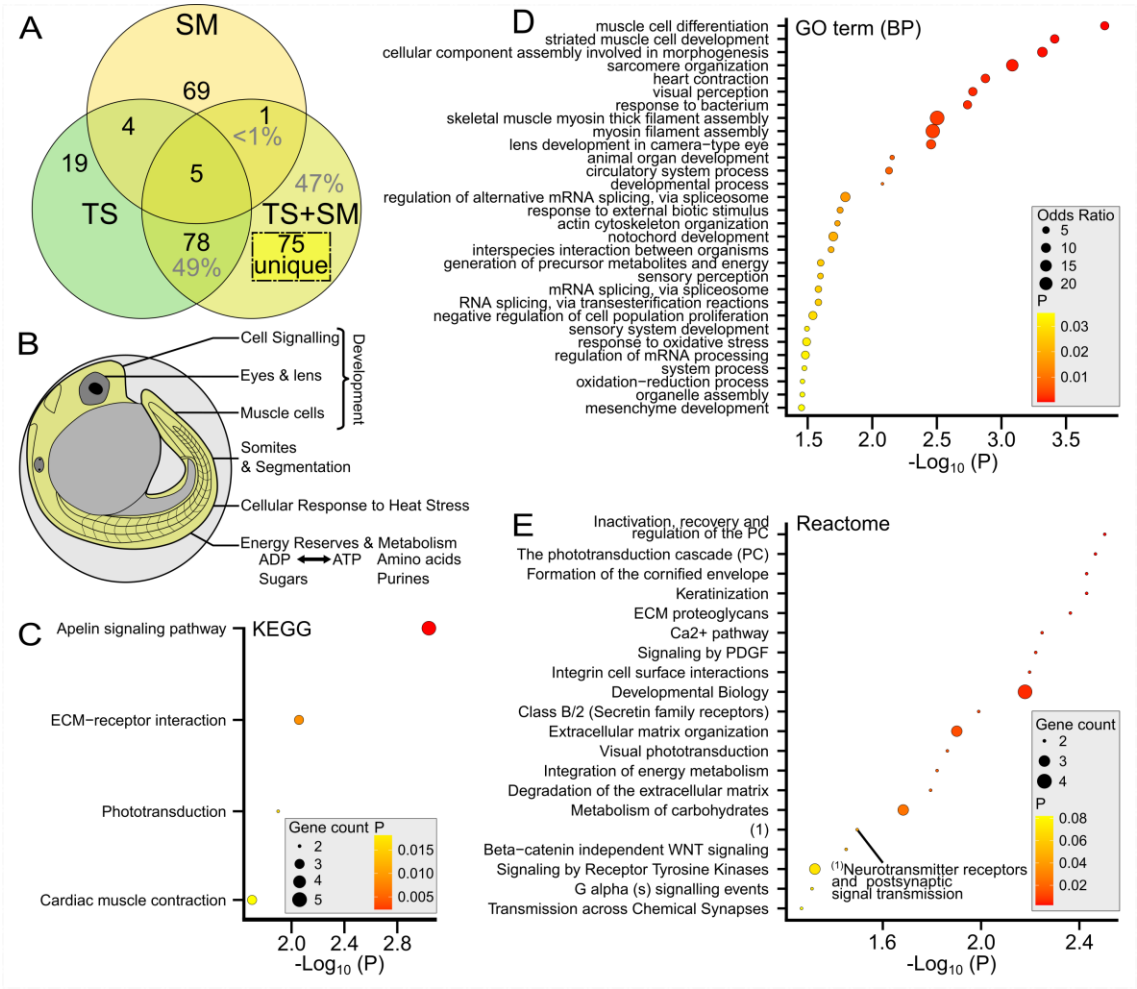

Figure 4.8. Stress metabolites combined with heat in TS+SM alter unique genes and functions. A) Venn diagram showing the differentially expressed genes shared for each treatment compared to the control C. B) gene functional categories from KEGG, Reactome, and GO Biological Process analysis for all n = 159 DEGs of TS+SM. In C, D, and E, genes that are present in TS+SM only (compared to C, n = 75 genes) were retrieved for functional enrichments as they indicate an interactive effect of TS and SM on (C) biological processes gene ontology terms, D) KEGG pathway, and E) Reactome pathways. All represented terms have ≥ 2 gene counts and are ranked by decreasing significance.

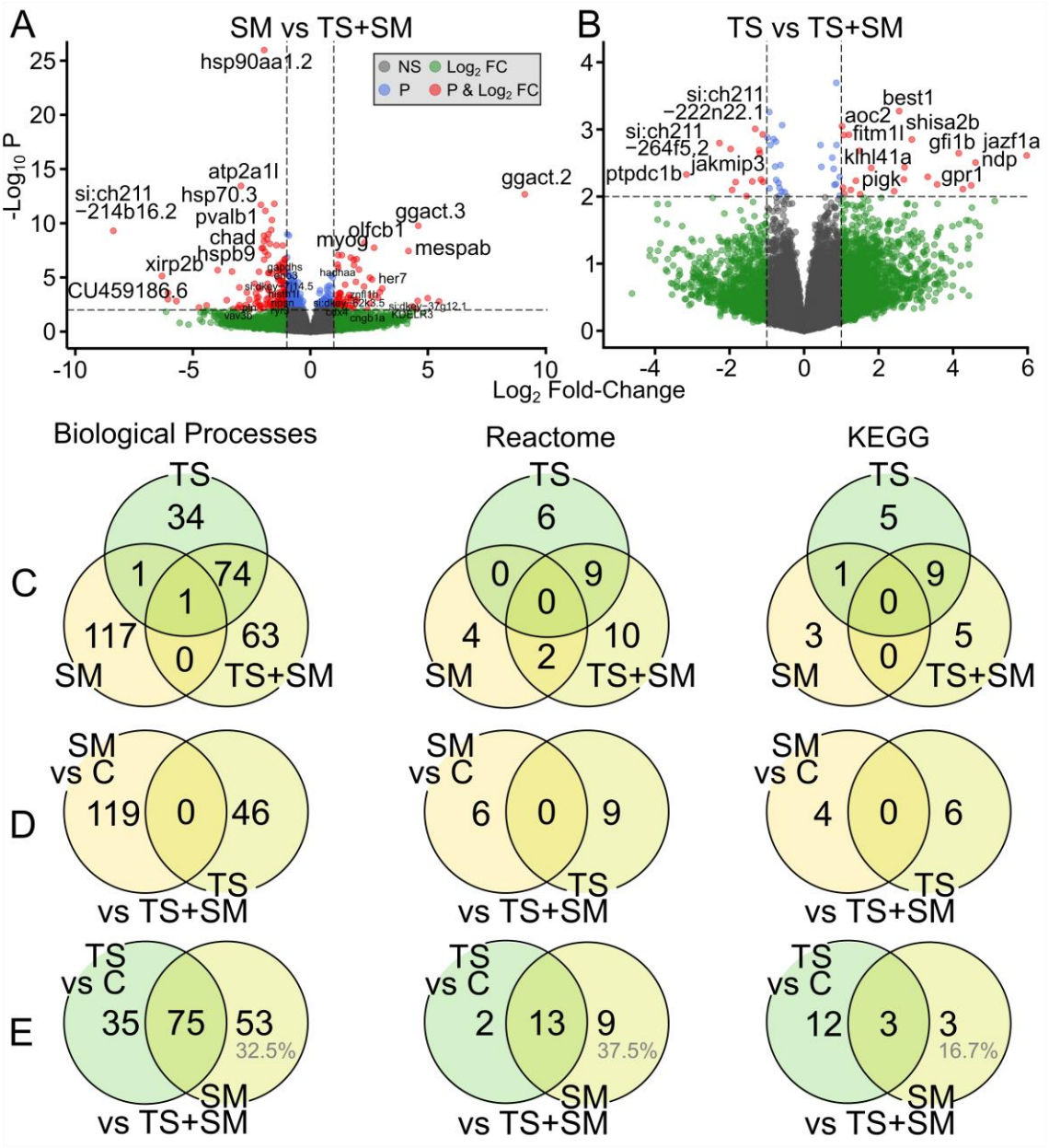

Figure 4.9. Heat and Stress metabolites induce a non-additive effect on TS+SM transcriptome. Volcano plot of the differentially expressed genes of (A) SM vs TS+SM and (B) TS vs TS+SM. Genes in red have significant raw p-values (above horizontal line) and an absolute fold change (FC, representing the effect size) greater than 2 (|log 2 FC| > 1, vertical lines). DEGs left to the left vertical line and right to the right vertical line are respectively significantly underexpressed and overexpressed compared to the control C. Venn Diagrams of significant ($p < 0.05$, $n \geq 1$ gene/term) biological process gene ontology terms (left), Reactome (middle), and KEGG pathways (right) that are shared between treatments (C) TS, SM, TS+SM compared to the control C, (D) SM versus C and TS versus TS+SM , and (E) TS versus C and SM versus TS+SM. If there were no interactive effects of TS and SM, one would expect a strong redundancy and shared partitions. In A, B, and C, partitions unique to TS+SM indicate interaction effects in combined treatment TS+SM compared to single treatments TS and SM.

4.7.5. Stress and control media show distinct excreted metabolome profiles

The excreted metabolomes contained 89 metabolites which were matched to 658 possible compounds (**Figure 4.10A, Figure Appendix 3 S3).** Correlating masstag intensities in SM and CM showed that metabolites were either present in both media in varying concentrations, or were uniquely secreted in either CM or SM (dubbed "CM cloud" and "SM cloud", **Figure 4.10A**, **Table Appendix 3 S3**). Two different masstags were assigned to 3'-mercaptolactate (SM12 and SM21). Several candidate chemicals from alarm/disturbance cue studies (**Table Appendix 3 S3**) were unexpectedly more concentrated in control medium compared to stress medium (e.g. hypoxanthine – $C_5H_4N_4O$ – a derivative similar to hypoxanthine-3-N-oxide – $C_5H_4N_4O_2$ – as well as trigonelline or homarine, cysteine, or acetylcholine, **Table Appendix 3 S3**). Representative compounds of each identified masstag were used for functional subclass and KEGG pathway enrichments (**Figure 4.11**). Representative control metabolites were mainly associated with amino acids (e.g., CM8 proline, CM14 L-tyrosine), catechols, purine ribonucleoside monophosphate (e.g., CM6 adenosine monophosphate), and dipeptides. Representative stress metabolites, in contrast, were mostly associated with sulphur-containing carbothioic S-acids (organosulfur compounds), and lipids including O-acylglycerol-phosphates, fatty acids, and glycerophospholipids. Representative stress metabolites were mainly ascribed to lipid-like molecules such as glycerophosphocholine and phosphocholine, and "*organic oxygen compounds*", whereas control medium contained molecules which had a more diverse chemical classification, and were mainly "*organic acids and derivatives*" and "*nucleosides, nucleotides, and analogues*" (**Figure 4.10B-C, Table Appendix 3 S3**). Several compounds did not have a ChemOnt classification but were likely proteins (SM1, SM4, SM19, SM23) or polyamines (SM7).

Since ammonia is a candidate compounds functioning as disturbance cue, I asked whether ammonia may also play a role as a stress metabolite. A one-way ANOVA did not detect differences in ammonia levels between media that had contained control, heat-stressed, or no embryos ($F = 0.157$, $p = 0.8580$) with all treatments having similar levels compared to fresh 1X E3 medium (**Figure 4.4E**). Therefore, ammonia is unlikely to function as a stress metabolite.

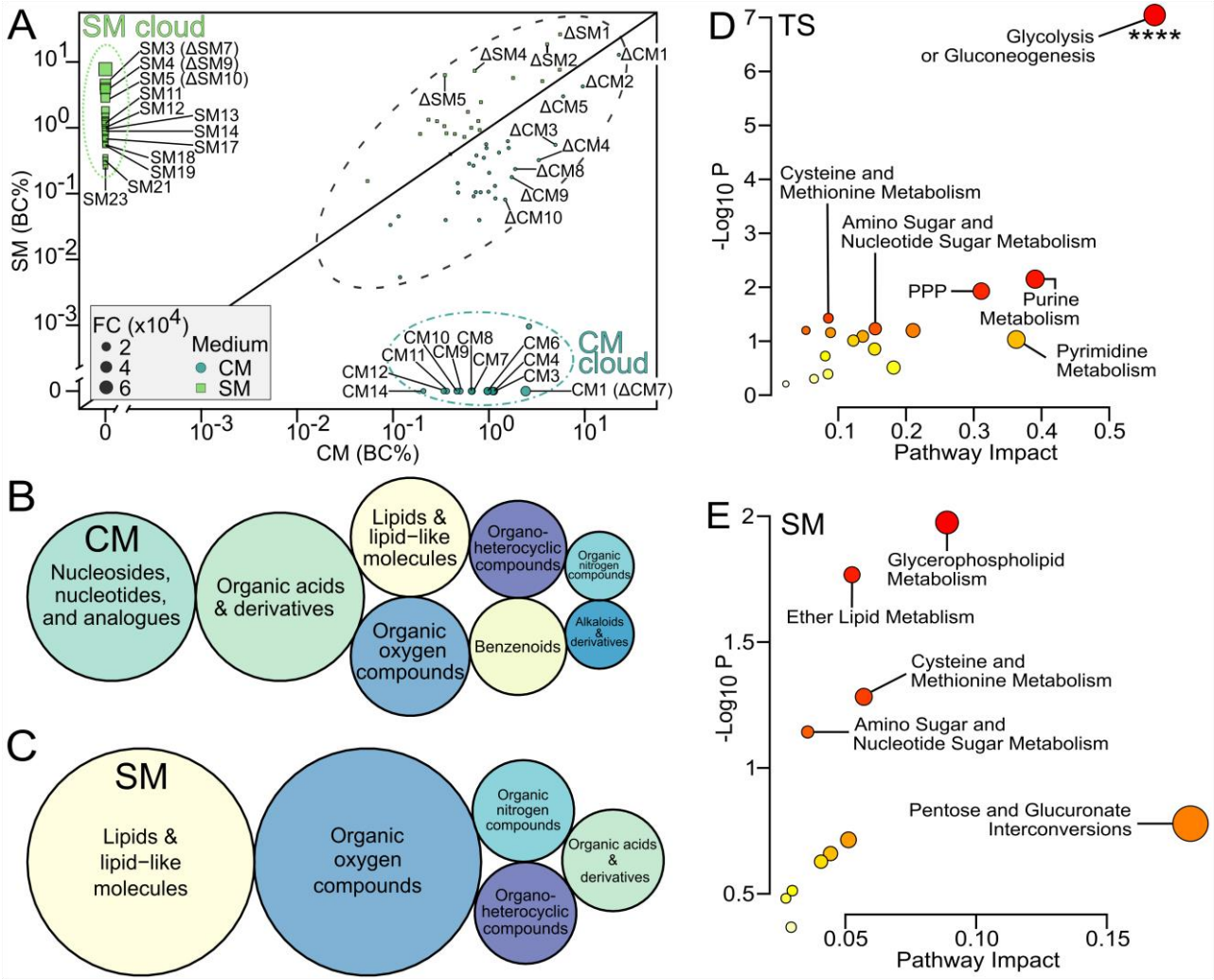

Figure 4.10. Multi-omic evidence that heat stress induces stress metabolites that differ from control metabolites. A) Correlation plot showing filtered (n = 89) masstags that are possible biomarkers of control metabolites CM (blue circles, bottom right) and stress metabolites SM (green squares, top left) groups. Data is presented as blank corrected total percent intensity (BC%). Masstags inside the black dotted ellipse are unlikely to be biomarkers of SM or CM since they are present in both conditions. Masstags inside the dot-dashed blue and dashed green ellipses represent CM and SM-specific biomarkers, respectively. FC: fold-change between SM and CM where the numerator is the medium with the highest concentration for each compound. Labels show the masstags with possible hits amongst the top 23 compounds of SM and top 14 compounds of CM based on fold-change (see **Table Appendix 3 S3** for associated chemicals) and top 10 compounds based on difference between SM and CM (delta Δ identifiers). Superclasses of representative hits for the biomarkers of (B) CM and (C) SM. Bubble sizes are proportional to counts of superclasses per medium type. Candidate cause-and-effect pathways derived from multi-omic analysis of KEGG pathways integrating the representative hits of the stress metabolites with the differentially expressed genes of (D) TS or (E) SM. The top five most evident pathways are given within plots, respectively. Significant terms are shown by **** (p-adj ≤ 0.0001). PPP: pentose phosphate pathway.

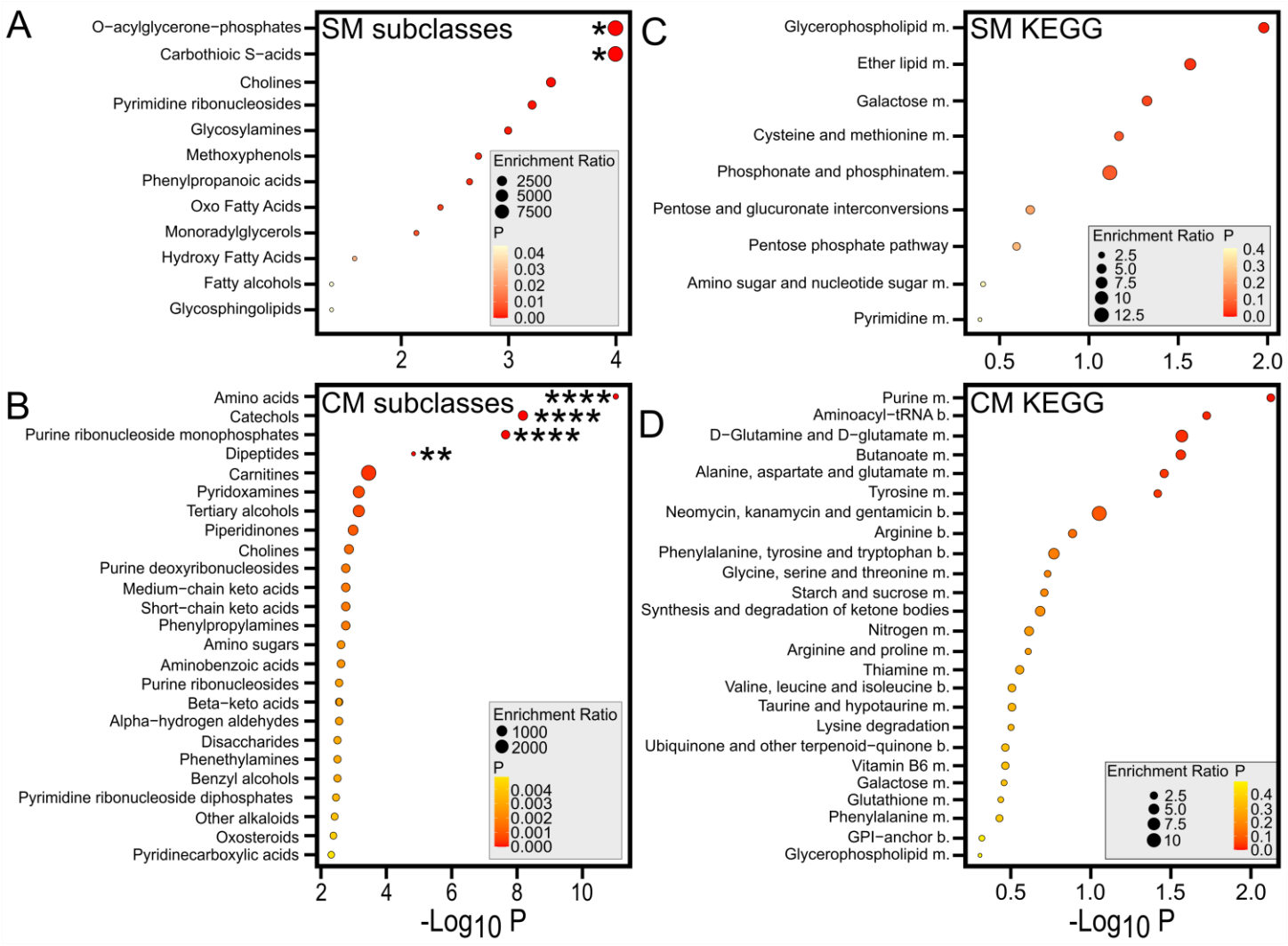

Figure 4.11. Stress metabolites and control metabolites differ in classes. Subclasses (left) and KEGG pathways (right) functional enrichment for the representative compounds of SM (top row) and CM (bottom row) biomarkers. Only representative compounds assigned to known chemicals were used for the excreted metabolome functional enrichment. Raw p-values are shown. Significant pathways after Holm's p-value correction are shown with *: $p \leq 0.05$, **: $p \leq 0.01$, ****: $p \leq 0.0001$. Abbreviations: b.: biosynthesis, GPI: Glycosylphosphatidylinositol, m.: metabolism.

4.7.6. Multi-omic analysis uncovers sender-receiver gene-metabolite candidate pathways

Since (i) the DEGs of heat-stressed donors (TS vs C) putatively lead to the synthesis and/or release into the environment of stress metabolites (SM), which (ii) may in turn alter the transcriptome of receivers (DEGs from SM vs C), these data sets were integrated into multi-omic joint analyses. The joint pathway analysis evidenced that stress metabolite donors in TS were significantly enriched for "glycolysis/gluconeogenesis" (**Figure 4.10D**). Stress metabolite receivers, in contrast, were enriched, albeit with weak evidence (raw $p \leq 0.07$ but FDR > 0.05), for “glycerophospholipid”, “ether lipid”, “cysteine and methionine”, and “amino sugar metabolism” pathways (**Figure 4.10E**). The compound-protein interaction (CPI) network evidenced a strong connectivity of stress metabolite compounds with DEGs of either TS (64 CPI edges observed vs. 5 expected edges, $p < 0.0001$) or SM (14 CPI edges observed vs. 3 expected, **Figure 4.7**). For instance, *ldha* (Lactate dehydrogenase A4) was linked to 3'-mercaptolactate in donors (**Figure 4.7A**) whereas in receivers many genes, including *tlr18* (toll-like receptor 18), *chs1* (chitin synthase 1), and *otofa* (otoferlin A), linked to glucose, whilst *prg4a* (proteoglycan 4a) was associated with phosphocholine (**Figure 4.7B**).

4.7.7. Both heat stress and stress metabolites alter development and behaviour

Several binary phenotypic variables were measured in developing zebrafish over the course of four days of stress exposure. Heat stress ($F = 30.1$, $r^2 = 0.25$, $p = 0.001$), but neither stress metabolites ($F = 0.16$, $p = 0.7610$) nor the interaction term ($F = 2.34$, $p = 0.1320$), altered the phenotype of 1-dpf embryos according to the PERMANOVA (**Table Appendix 3 S4**). This effect was evident on the PCA with the first axes (PCA1 = 34.1% of variance) discriminating thermal stress (TS and TS+SM) from control temperature (**Figure 4.12A)**. Testing individual variables confirmed that, at 1 dpf, thermal stress significantly increased whole-embryo lengths (**Figure 4.12C**), but also the absolute lengths of their eye and yolk elongation. On the other hand, heat stress decreased the head-trunk angle and otic vesicle length (see PCA loadings in **Figure 4.12A)**, and the percentage of defects (**Figure 4.13D**). Thermal stress also significantly accelerated the aging of embryos (median stage: 31 hpf, $H = 50.36$, $p < 0.0001$, very large effect size = 1.47) compared to control C (median stage: 25 hpf) within the first 24 hours of development (**Figure 4.13A**). Therefore, heat-stressed embryos reached the pharyngula stage earlier ($z = -2.67$, $p = 0.0076$, **Figure 4.13E**). Conversely, stress

metabolites had no effect on development at 1-dpf. Light-induced startle responses of 1-dpf embryos showed that the percentage of moving embryos did neither vary with heat ($z = -1.28$, $p = 0.2011$) nor with stress metabolites ($z = 1.02$, $p = 0.3088$). Because over half (52.4%) of the embryos did not move during the behaviour assay, the burst count per minute was re-analysed only for active embryos (**Figure 4.12B**). Heat stress ($t = 18.15$, $p < 0.0001$), but neither stress metabolites ($t = 0.29$, $p = 0.5891$) nor their interaction ($t = 0.07$, $p = 0.7872$), significantly reduced burst counts per minute during the 1-dpf startle response (**Figure 4.12B, Table Appendix 3 S5-6**). Of note, there was a marginal decrease in the percentage of moving embryos in SM (34.7%) compared to CM (57.1%, $t = 1.77$, $p = 0.0552$, Figure 4.13B); albeit those that moved tended to have higher burst counts per minute in SM compared to CM ($z = -2.21$, $p = 0.0821$, **Figure 4.12B**). On the other hand, the burst percentage activity remained unchanged by either treatment (**Figure 4.13C**).

In contrast, 4-dpf zebrafish larvae grew significantly longer in the presence of stress metabolites ($t = 4.80$, $p = 0.0304$, small effect size = 0.35) but not with thermal stress ($t = 1.91$, $p = 0.1692$) nor the interaction term ($t = 0.11$, $p = 0.7353$, **Figure 4.12D**). However, statistically accounting for the large effect size of batch ($d = 1.10$, $t = 38.33$, $p < 0.0001$) and its interaction with heat ($t = 5.51$, $p = 0.0206$) revealed a marginal increase in 4-dpf body length with thermal stress in one batch of larvae. Larvae in TS+SM had longer 4-dpf body lengths compared to control larvae ($t = 2.41$, $p = 0.0520$, **Figure 4.12D**).

The contrasting results between 1- and 4-dpf body lengths led to performing an additional ANOVA analysis on the growth increment from 1 to 4 dpf. This revealed that both heat and stress metabolites significantly altered the increment of growth (ΔSEL) between 1 and 4 dpf, but in opposite directions (**Figure 4.12E**, **Table Appendix 3 S7**). Heat-stressed larvae had a lower ΔSEL ($t = 20.99$, $p < 0.0001$, large effect size = 0.81) whereas those experiencing stress metabolites accelerated growth from 1 to 4 dpf ($t = 6.65$, $p = 0.0112$, small effect size = 0.43) and slightly surpassed the TS treatment in average final length at 4 dpf (**Figure 4.12D-E**). There was also a significant decrease in ΔSEL in TS compared to C ($t = -3.34$, $p = 0.0034$). ΔSEL was however similar in CM compared to SM ($p = 0.3133$) and C ($p = 0.9307$). The pattern of slower growth with high temperature between 1 and 4 dpf was confirmed for the eye length increment (ΔEL) which tended – albeit not significantly ($t = 3.29$, $p = 0.0724$) and mainly in one batch – to marginally decrease with thermal stress (**Figure 4.13H**). Heat stress also slowed the

mean acceleration (t = 4.26, p = 0.0412, small effect size = 0.34), and the treatment TS marginally reduced mean speeds compared to C (t = -2.74, p = 0.0212) in 4-dpf touch-evoked swimming assay (**Figure 4.13I-K**). Larvae incubated in stress metabolites had fewer burst counts compared to fresh medium (t = -2.1, p = 0.0381, **Figure 4.12F**), and the fewest burst counts of all treatments. At 4 dpf, larvae incubated in CM tended to swim longer distances than those in SM (t = -2.22, p = 0.058, **Figure 4.13K**).

Both mortality (**Figure 4.13F**) and hatching (**Figure 4.13G**) were recorded in over 1,000 individuals across more than 30 batches. There were no significant differences in mortality across treatments (analysis of deviance's p = 0.0951) with an average survival of 92%, which confirmed that all experimental protocols were sublethal. Next, there were no significant differences in hatching percentages between C and SM (z = 0.3765, p = 0.7066). On the other hand, hatching was significantly earlier in TS (43%) compared to C (25%, z = -5.79, p < 0.0001), but also high in CM (63%) compared to C (z = 9.52, p < 0.0001) and SM (33%, z = 9.03, p < 0.0001). In order to validate the reproducibility of the stress propagation experiments, the behaviour patterns of the 1-dpf startle response were compared between two strains of zebrafish: outcrossing PET (data from Chapter 3) and inbred AB (data from Chapter 4). This showed that the startle response of control embryos from the outcrossing PET line was significantly higher compared to AB embryos (t = 3.21, p = 0.0022), suggesting strain-specific differences. However, the general behavioural patterns of the effect of treatments were similar in the experiments from Chapter 3 and Chapter 4 (**Figure 4.14**) which brings additional confidence to the validity of the effects of stress metabolites on zebrafish embryos.

4.7.8. Stress metabolites also exist in group-raised non-laboratory embryos

An independent experiment utilising outcrossing non-laboratory (PET) group-raised zebrafish embryos aimed to confirm, through the LAMP method, the role of candidate genes from the RNA-seq data in the response to stress metabolites (SM vs C treatments). First, lactate dehydrogenase A4 (*ldha*), overexpressed in both TS and TS+SM in the RNA-seq data, was not altered in response to group-induced stress metabolites (t = -0.14, p = 0.8960, **Figure 4.6H, Table Appendix 3 S8**). Two candidate genes involved in sensory perceptions (*otofa*, expressed in lateral line hair cells) and immunity (*tlr18*) were not significantly altered by group-induced stress metabolites, albeit both followed the same upregulation patterns as those previously found in AB embryos (**Figure 4.6J, L, Table Appendix 3 S8**). Conversely, stress metabolites from

heat-stressed group-raised PET embryos significantly upregulated *prg4a* (t = -8.01, p = 0.0026, |d| = 6.52, "huge" effect size) and downregulated *chs1* (t = 3.08, p = 0.0487, |d| = 2.18, "huge" effect size, **Figure 4.6G, K, Table Appendix 3 S8**), which matched the RNA-seq data of isolated AB embryos exposed to SM for *prg4a* (LFC = 1.24) but not for *chs1* (LFC = 1.64). One chemosensory candidate gene, *ora3* (olfactory receptor class A related 3), was expressed in control embryos but not detected in SM, suggesting its depletion in all embryos exposed to stress metabolites (**Figure 4.6I)**. Of note, another candidate gene identified in Chapter 3, sulfide:quinone oxidoreductase (*sqor*) was significantly downregulated by stress metabolites in group-raised PET zebrafish embryos (Student's t-test t = 4.783, p = 0.0032, **Figure Appendix 3 S4D**).

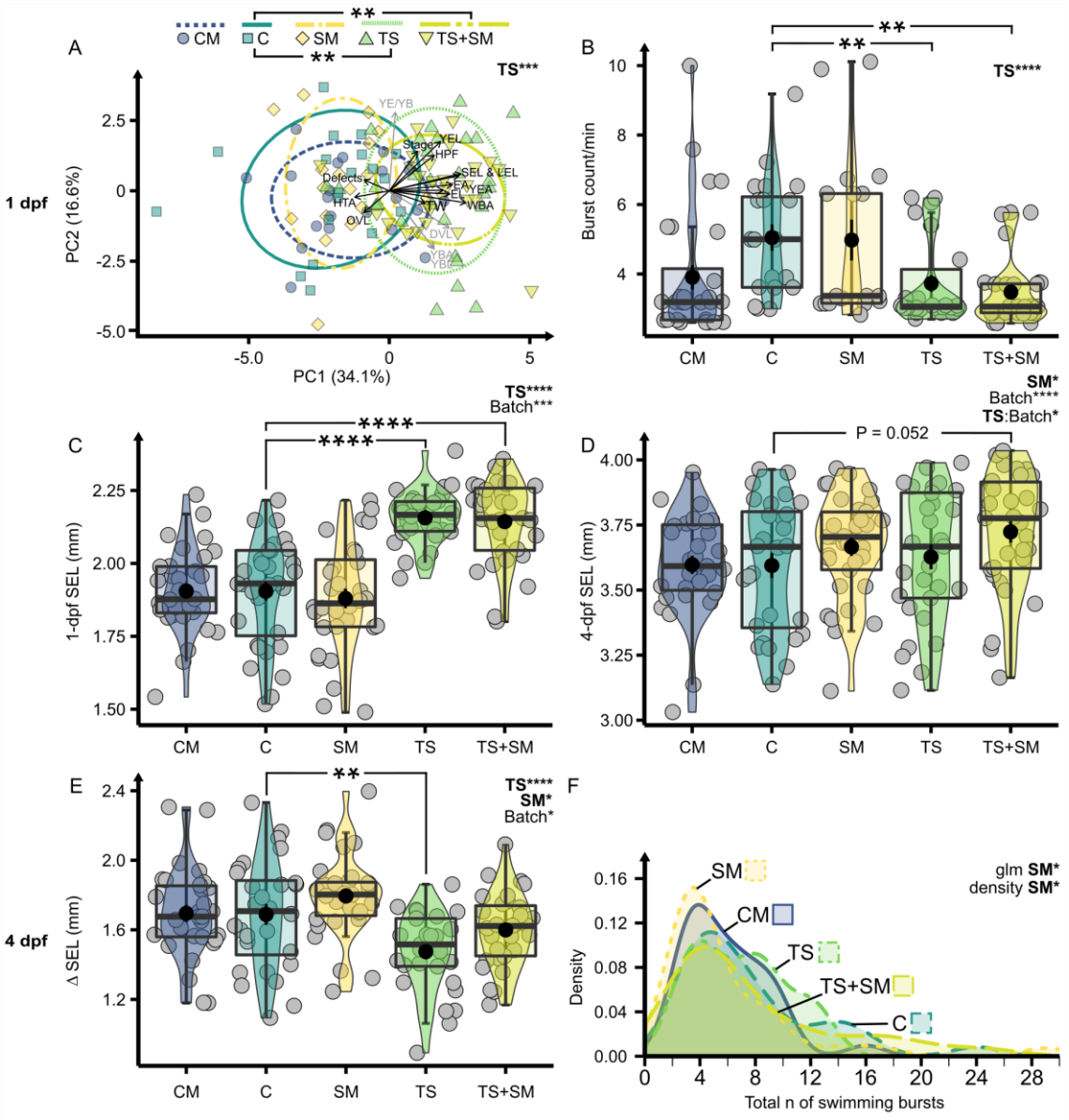

Figure 4.12. Thermal stress and stress metabolites alter development and behaviour in developing zebrafish. A) PCA of 1-dpf morphology. HPF: final stage in hours post fertilisation, Stage: % in segmentation or pharyngula, EA: eye area, EL: eye length, DVL: dorsal-ventral length, HTA: head-trunk angle, LEL: longest embryo length, OVL: otic vesicle length, SEL: shortest embryo length, WBA: whole-body area, YBA/L: yolk ball area/length, YEA/L: yolk extension area/length, YE/YB: yolk extension/yolk ball ratio. Individual variables significantly altered by thermal stress are shown by black arrows. B) Burst count per minute in active 1-dpf embryos. C) SEL (mm) increment from 1 to 4 dpf. D) Mean acceleration (m/s²) of the 1st complete burst following 1st and 3rd touch stimuli. E) Density distribution of total burst count and total distance in cm (F) after three touch stimuli. Effects of thermal stress and stress metabolites across the two-way factorial design (C, SM, TS, TS+SM) were computed using PERMANOVA (A), ANOVA (B-D, F), or negative binomial generalised linear model (E, confirmed by a density test) with significant predictors and covariates ("batch") reported on top-right corners. Pairwise tests with FDR p-value correction compared CM to C and SM, or C to SM, TS, and TS+SM, with significant comparisons shown by horizontal bars. *: $p \leq 0.05$, **: $p \leq 0.01$, ***: $p \leq 0.001$, ****: $p \leq 0.0001$. Boxes show median and 25%-75% quartiles, and whiskers are min/max values within 1.5 IQR. Jittered raw data given as grey circles. Black dots show mean ± SE values of each treatment. Treatments were CM: control metabolites at 27°C, C: control in fresh medium at 27°C, SM: stress metabolites at 27°C, TS: fresh medium in thermal stress, TS+SM: stress metabolites in thermal stress.

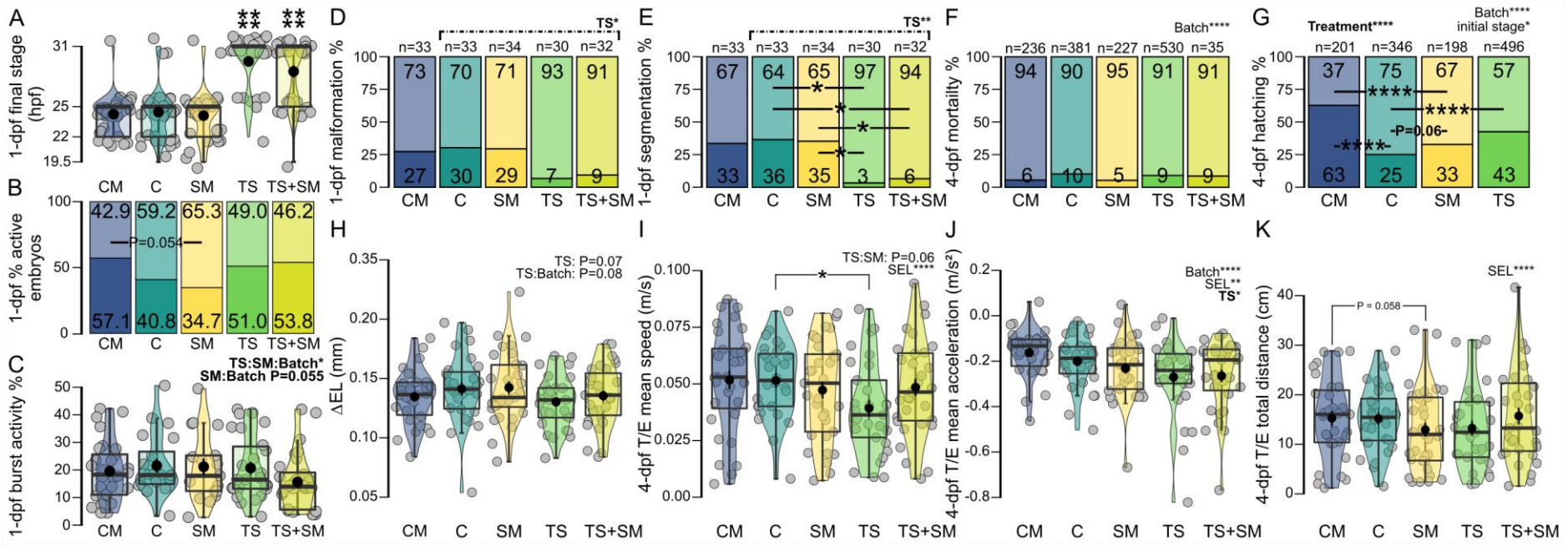

Figure 4.13. Stress alters development, hatching, and swimming in developing zebrafish. A) Final median stage in hours post fertilisation (hpf) at 1 day post fertilisation (dpf). B) % of 1-dpf embryos moving (dark areas) or not (light areas) under acute light change. C) Burst activity % of the startle response at 1-dpf for active embryos. D) % of embryos showing malformations (dark areas) or not (light areas) at. 1 dpf. E) % of 1-dpf embryos in segmentation (dark areas) or pharyngula (light areas). F) % dead (dark areas) or surviving (light areas) 4-dpf larvae. G) % hatched (dark areas) or unhatched (light areas) 4-dpf larvae. H) Delta eye length (ΔEL, mm) from 1 to 4 dpf. G) mean speed (m/s) and mean acceleration (I) averaged after the 1st and 3rd stimuli in the 4-dpf touch-evoked (T/E) assay. H) Total distance (cm) after three stimuli in the T/E assay. 2-way model effects (thermal stress × stress metabolites) across C, TS, SM, and TS+SM are shown in top right corners. Significant treatment and covariate effects (batch, initial stage, month, embryo length SEL) are reported above plots. Significant pairwise comparisons are shown by horizontal bars. *: $p \leq 0.05$, **: $p \leq 0.01$, ***: $p \leq 0.001$, ****: $p \leq 0.0001$. CM: control metabolites at 27°C (n = 31), C: control in fresh medium at 27°C (n = 28), SM: stress metabolites at 27°C (n = 33), TS: fresh medium in thermal stress (n = 29), TS+SM: stress metabolites in thermal stress (n = 31). Boxes show median and 25%-75% quartiles, and whiskers are min/max values within 1.5 IQR. Jittered raw data given as grey circles. Black dots show mean ± SE values of each treatment. Samples sizes of D-G are shown above treatments. In F-G, mortality and hatching were recorded over 1,000 embryos across > 30 batches.

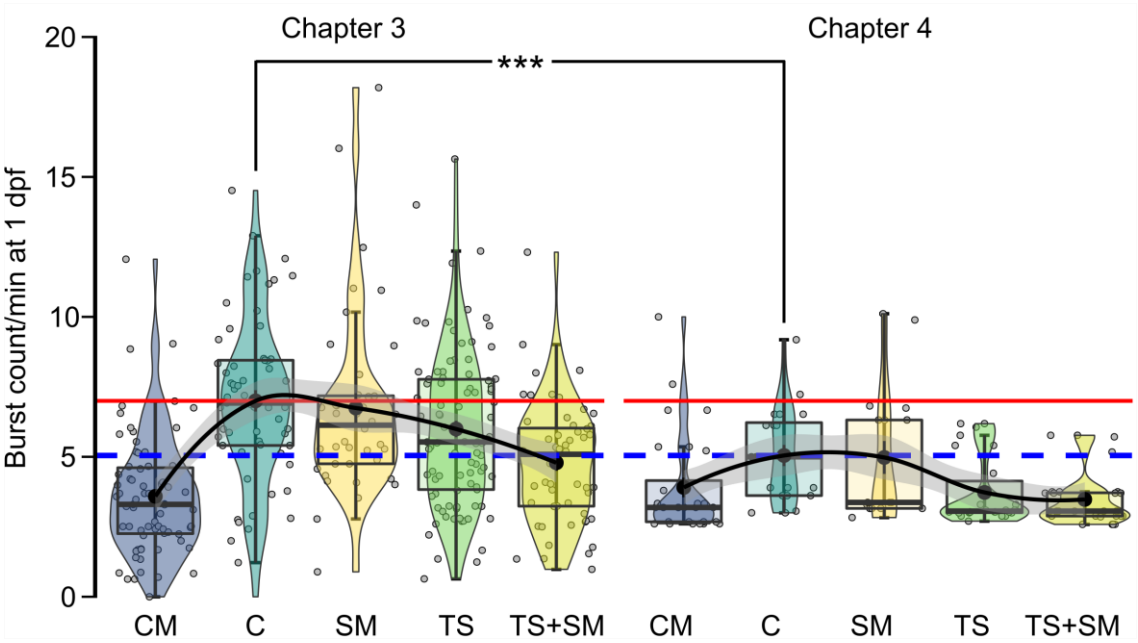

Figure 4.14. Cross-chapter validation of altered behaviours in treatments in zebrafish embryos. Chapter 3: PET strain, with 16 hours and 15 min of heat protocol followed by 7 hours and 45 min of recovery period (redrawn from Chapter 3). Chapter 4: AB strain, 24 hours of heat protocol. Inactive embryos were removed in Chapter 4. Both chapters tested the acute light-induced startle response at 24 hours. Smoothed lines were added on the arbitrary basis of the gradual developmental effects (in order of increasing final age: CM, C, SM, TS, TS+SM) shown in study 1 and show similar patterns in either study. Asterisks represent the comparison of controls (Welch's modified t-test). Boxes show median and 25%-75% quartiles, and whiskers are min/max values within 1.5 IQR. Jittered raw data given as grey circles. Black dots show mean ± SE values of each treatment. CM: control metabolites at 27°C, C: control in fresh medium at 27°C, SM: stress metabolites at 27°C, TS: fresh medium in thermal stress, TS+SM: stress metabolites in thermal stress.

4.8. Discussion

The aim of this work was to elucidate the molecular aspects of heat-induced stress propagation in developing zebrafish. This experiment confirmed that repeated heat peaks altered a range of different aspects of the biology of zebrafish embryos and larvae. Heat stress altered molecular profiles leading to developmental changes, and earlier hatching. In contrast to studies reporting a higher activity upon heat stress (Gau et al., 2013; Yokogawa et al., 2014), developing zebrafish displayed behavioural hypoactivity, with changes possibly mirrored by the transcriptome enrichment of muscle genes and functions. Of note, Chapter 3 reported that over-developed stressed embryos after 24 hours of exposure were more active than stage-matched controls, but such positive control was not used in Chapter 4. The cortisol stress response onset was confirmed to occur around 2-4 dpf in zebrafish (Alsop and Vijayan, 2008, 2009b; Alderman and Bernier, 2009; Eto et al., 2014). The central role of glucocorticoids in muscle growth, hatching, and behaviour (Wilson et al., 2013, 2016; Sadoul and Vijayan, 2016) may explain the concomitant increase in cortisol and the decrease in locomotor activity

observed here. The upregulation of heat shock protein (HSPs) transcripts and cortisol confirmed that repeated heat stress induced a (cellular and heat) stress response (Iwama et al., 2004; Sadoul and Geffroy, 2019). Similarly, overregulated *hsp90a* transcripts were found in marine medaka *O. latipes* upon repeated thermal stress (Shimomura et al., 2019). Higher HSPs levels might be a strategy to prepare for reaching the upper thermal limit (Manzon et al., 2022) and are associated with adaptation to abiotic stress in vertebrates (Wollenberg Valero et al., 2021). However, elevated basal mRNA levels of HSPs may in turn attenuate the heat shock response (HSR) induction to subsequent acute stress exposure (Whitehouse et al., 2017; Sessions et al., 2021). Supporting this, the HSR response was no longer present in 4-dpf larvae having experienced 76 peaks at 32°C, which suggests either failure to mount the HSR or habituation to higher temperatures.

Heat stress induced changes in glucose, pyruvate, and ADP/ATP metabolism, indicating mobilisation of energy reserves. Likely due to the observed aging under heat stress, developmental transcriptome dynamics were also altered (Mathavan et al., 2005; Aanes et al., 2014; Rauwerda et al., 2017). As a consequence, heat-stressed embryos were developmentally older and grew longer at 1 dpf, in accordance with previous studies (Hallare et al., 2005; Schröter et al., 2008; Schmidt and Starck, 2010) and with Chapter 3. However, a subsequent slow-down of development occurred from 1 to 4 dpf. This observation conforms to the temperature-size rule stating that, with warming, fish grow faster during early stages but become smaller adults (Wootton et al., 2022). Such findings in embryos at the phylotypic stage of pharyngula, which is most conserved across vertebrates (Irie and Kuratani, 2014), may be relevant for other species.

Only a few prior studies have already characterised stress (including heat) induced whole-body metabolome profiles in fish (Samuelsson and Larsson, 2008; Sun et al., 2018; Song et al., 2019; Rosdy et al., 2021), but they have not focused on cue secretion into the environment. A major finding of this chapter was that heat induced the release of stress metabolites into the medium, which differed from control metabolites released by unstressed embryos, supporting recommendation from the literature to consider cues from unstressed individual as a control condition (Crane et al., 2022). Here, heat-stressed zebrafish embryos showed profound changes in energy-related metabolome and transcriptome pathways (**Figures 4.6/4.10/4.11**). A multi-omic compound-protein interactome evidenced functional network links between heat-induced genes and the excreted metabolome containing stress metabolites released into the medium.

Interestingly, several candidate chemicals (e.g. trigonelline, homarine, hypoxanthine-3-N-oxide) previously identified as alarm cues (Parra et al., 2009; Poulin et al., 2018) were more concentrated in the control medium. In contrast, stress metabolites were mainly ascribed to two compound superclasses: "*organic oxygen compounds*" and "*lipids and lipid-like molecules*".

Carbohydrates within stress metabolites may originate from heat-induced metabolic activity such as glycolysis (Karakach et al., 2009). The multi-omic analysis highlighted that the pentose phosphate pathway (PPP, including deoxyribose, *gpia,* and *pgm1*), a major cellular redox mechanism (Stincone et al., 2015), was altered in response to heat. Organosulfur compounds (such as 3-mercaptolactate or 2-oxo-4-methylthiobutanoic acid) were a main component of the organic oxygen compounds classification. Multi-omic analysis of stress metabolites with DEGs in receivers revealed "*Cysteine and Methionine metabolism*" as an important altered pathway, lending support to a functional relationship between secreted organosulfur compounds and receiver responses. 3-mercaptolactate is part of the cysteine transamination pathway, and synthesised by the heat stress-induced lactate dehydrogenase gene (Sörbo, 1987; Andreeßen et al., 2018). Lactate dehydrogenase was likewise found to be upregulated by heat stress in tissue of rockfish *Sebastes schlegelii* (Song et al., 2019). Organosulfur compounds have a role as cues in chemical ecology for instance in fox urine (McLean et al., 2021), attractants in insects (Cortez et al., 2017), and urinary pheromones in cats (Miyazaki et al., 2006), and therefore warrant further study.

In addition, stress metabolites predominantly contained a range of lipids, including fatty acyls, glycerolipids, sphingolipids, glycerophospholipids, and steroid esters. The multi-omic analysis found "*glycerophospholipid metabolism*" and "*ether lipid metabolism*" as the two major KEGG pathways enriched between stress metabolites and receiver transcriptomes. Previous lipidomic studies demonstrated a role of lipids, particularly sphingolipids, in protecting the cell from heat damage and acting as messengers (Balogh et al., 2013; Török et al., 2014). Differential vulnerability of lipid classes to reactive oxygen species leads to temperature-controlled membrane lipid remodelling (Hazel, 1995; Crockett, 2008). For instance, the proteome of adult zebrafish shows such changes in lipids following heat stress at 34°C for 21 days (Nonnis et al., 2021) and crucian carp (*Carassius carassius*) release phosphatidylethanolamines upon alkalinity stress (Sun et al., 2018). Two notable glycerophospholipids amongst stress metabolites were phosphocholine and

glycerophosphocholine. Olive Flounder *Paralichthys olivaceus* exposed to heat stress also displayed elevated tissue levels of phosphocholine and glycerophosphocholine (Kim et al., 2019), which may originate from temperature-induced breakdown of phosphatidylcholine in the cell membranes (Karakach et al., 2009). A possible role for lipids in chemical communication is likewise documented (Watson et al., 2009; Hay, 2010). For instance, mating in reptiles may depend on epidermal skin lipids (Goldberg et al., 2017; Andonov et al., 2020) and migratory behaviours in sea lamprey are regulated by larval-released fatty acid-derivatives (Li et al., 2018). Bile contains phospholipids, mainly phosphatidylcholines (Reshetnyak, 2013) which form the micelles containing bile salts (Hashim Abdalla et al., 2011) metabolised in the liver and excreted into the environment to trigger chemical communication (Velez et al., 2009; Li et al., 2013b; Buchinger et al., 2014). Lastly, in zebrafish embryos, these lipids may also originate from the yolk sac, being the most common membrane lipids (van der Veen et al., 2017). Since membrane lipids such as phosphatidylcholine are known not only as cellular signalling molecules, but also as conveying group identity between newly hatched catfish (*Plotosus lineatus*) (Matsumura et al., 2007), this could support a role for heat-mediated change in composition of membrane lipids as heat-stress related signalling molecules. For instance, the lipid-related gene *xkr8.2* is upregulated by stress metabolites, and is also active within zebrafish lateral line hair cells (Elkon et al., 2015), which may play a role in chemical communication (Desban et al., 2022). Its human orthologue *xkr8* flips phospholipids between the inner and outer membrane layers (Sakuragi et al., 2021), so it could be used by receivers to interact with lipid stress metabolites. Further compounds active as stress metabolites could be peptides or proteins (Wyatt, 2014; Ferrier et al., 2016) but which could be not characterised further. However, one compound was identified as a tripeptide (SM13, **Table Appendix 3 S3**). Tripeptides are important for chemical communication (Wyatt, 2014) such as oyster larval settlement (Zimme-Faust and Tamburri, 1994). Additionally, several stress metabolites were matched in Metabolomics Workbench with studies investigating stress, cancer, disorders, and infection, and/or in biofluids and excretions in several animal species, which hints at their role as stress biomarkers and chemical signals in several species. On the other hand, ammonia was unlikely to function as stress metabolite, since all treatments had similar NH_3 levels, and likewise pH levels were in the range of zebrafish embryos' tolerance.

As an outcome of this process, heat-stressed individuals propagated stress towards naive receivers. Molecular and phenotypic effects of stress metabolites included accelerated development and impaired behavioural activity as previously found for alarm cues (Lucon-Xiccato et al., 2020; Jesuthasan et al., 2021) and for stress metabolites in Chapter 3. These phenotypic effects were similar to those induced by heat itself, but developmental acceleration in response to stress metabolites could only be measured at 4 dpf. This could have been caused by either an age-dependent onset of cue-induced receptors (Fore et al., 2020; Lucon-Xiccato et al., 2020), or by developmental constraints during the mid-embryogenesis phylotypic stage limiting the scope for plasticity (Irmler et al., 2004; Irie and Kuratani, 2014).

In contrast, while heating induced a large spike in whole-body cortisol, stress metabolites did not. Stress metabolites also initiated a suite of cellular signalling pathways different from those induced by heat. The most significantly downregulated gene in stress metabolite receivers was *si:ch211-214b16.2* (NOD2 ortholog) which is involved in intracellular signal transduction (Alliance of Genome Resources Consortium, 2020) and in the activation of apoptotic and immune pathways (Deshmukh et al., 2009; Kriventseva et al., 2019; Kuss-Duerkop and Keestra-Gounder, 2020). Further immune and apoptosis responses were induced via *fthl28* and *tlr18. tlr18* is a fish-specific toll-like receptor expressed in the skin, regulated by both pathogen challenge and lipopolysaccharides (Quiniou et al., 2013; Shan et al., 2018; Trung et al., 2021), and may be homologous to the mammalian *tlr1* which binds lipopeptides (Nie et al., 2018). Therefore, *tlr18* may be directly responsive to lipid stress metabolites present in the medium. A (non-significant) increase of *tlr18* was independently confirmed in the stress medium of group-exposed PET line zebrafish (**Figure 4.6L**). Corroborating these results, brain transcriptomes of three-spine stickleback *Gasterosteus aculeatus* exposed to predator and alarm odours were also enriched for apoptosis, immune, and signalling pathways (Sanogo et al., 2011).

Moreover, several genes related to development such as keratins were activated by stress metabolites, which may explain the observed developmental acceleration in this treatment at 4 dpf. In addition to hypoxanthine 3-N-oxide ($C_5H_4N_4O_2$), for which here its derivative hypoxanthine ($C_5H_4N_4O$) was found in the control condition, *Schreckstoff* also contains other components such as extracellular polysaccharides (glycosaminoglycans), presumably but not exclusively chondroitin sulfate (Mathuru et al., 2012), and mucin proteins. The second major glycosaminoglycan in zebrafish with

20% prevalence is keratan sulfate (Souza et al., 2007). Keratan sulfate is bound to proteoglycan, another component of the mucus layer next to mucins. This chapter showed that stress metabolites secreted from heat-stressed embryos contained many sugars and, albeit they could not be identified, potentially also the constituents of keratan sulfate 3GalB1-4GlcNAcB1. Stress metabolites significantly upregulated proteoglycan 4 (*prg4a*) and altered two transcripts involved in keratan sulfate biogenesis (*chs1* and *chst2b*) in receiver embryos, both in AB and PET line experiments. This lends support to proteoglycan 4 and keratan sulfate as components of *Schreckstoff*, but since this was observed in receivers not senders of heat stress metabolites, it could mean that naïve receivers of stress metabolites may themselves propagate the release of *Schreckstoff* as a social anxiety cue to more embryos in a developing clutch. Of note, the complete inhibition of the chemosensory receptor *ora3* (olfactory receptor A like 3) in embryos group-exposed to SM suggests receptor depletion upon involvement in SM detection. On the other hand, sulfide:quinone oxidoreductase (*sqor*) and interleukin-1β (*il-1β*), which were candidates of stress metabolites pathways in isolated wild-type PET embryos (Chapter 3), were not altered by SM in isolated inbred AB embryos (RNA-seq data, **Figure Appendix 3 S4A-C**) but *sqor* was significantly downregulated in group-raised wild-type PET embryos, which warrants further research regarding sulphur-signalling-related genes.

Therefore, the data from Chapter 4 confirms the findings from Chapter 3 that heat stress can be propagated to conspecific receivers through stress metabolites, inducing similar phenotypic outcomes and molecular mechanisms related to growth acceleration. Chapter 4 also highlights mechanistic differences of indirect stress propagation compared to the direct heat exposure, such as the absence of the cortisol and HSP responses and the use of different signalling pathways (**Figure 4.15**).

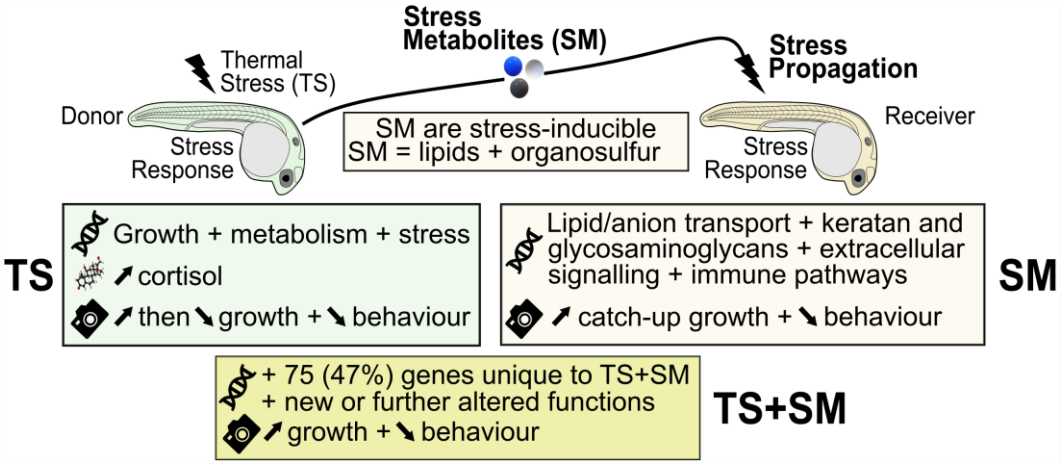

Figure 4.15. Conceptual summary of heat-induced stress propagation. Heat-exposed zebrafish embryos transmit stress to naïve receivers through stress metabolites, which mount a similar phenotypic response through distinct molecular pathways. When combined, heat alters the function of stress metabolites by inducing an interactive effect potentiating the stress response.

A similar mode of stress propagation induced by an abiotic stressor (electric shock) has been identified in *Drosophila*, where volatile alkanes were the signal carriers (Yost et al., 2021). Altogether, the results from this chapter show that heat stress elicited stress propagation to naive receivers, in line with the pilot experiments from Chapters 2 and 3, and with similar patterns, although some differences may be related to modifications in the stress protocol as well as zebrafish strain-dependent effects (Abel, 1992; Quadros et al., 2016, 2018) (**Figure 4.14**).

In support to these findings, the confirmatory experiment utilising an outbred non-laboratory zebrafish strain, raised in groups rather than individually, showed that stress metabolites existed in this social context and again altered gene expression of chitin synthase *chs1* and proteoglycan *prg4a* which are functionally associated with two stress metabolite candidates, glucose and phosphocholine, respectively (**Figure 4.7B**). Unexpectedly, stress metabolites inhibited the expression of the candidate olfactory receptor *ora3*. Fish *ora* genes encode vomeronasal V1R receptors, expressed in olfactory receptor cells and the olfactory epithelium, that may detect semiochemicals such as pheromones and bile (Saraiva and Korsching, 2007; Johansson and Banks, 2011; Ota et al., 2012; Saraiva et al., 2015; Cong et al., 2019; Alliance of Genome Resources Consortium, 2020; Zhang et al., 2020). The downregulation of *ora3* may indicate a receptor depletion 24 hours after first experiencing stress metabolites and suggests the involvement of the sensory perceptions in stress propagation. The different experiments

from Chapter 2, Chapter 3, and Chapter 4 indicate that stress metabolites may be a widespread mechanism although its effect size and controlling factors (density, timepoints, species, strain, etc) will require further investigation.

Outside of the laboratory, high-density population scenarios such as developing fish clutches exposed to heat would experience stress metabolites simultaneously with heat, leading to combined exposure. Here, the combined treatment revealed that these larvae grew the most of all treatments and also had the lowest behavioural activity. While heat was the predominant driver of this transcriptome, it also showed unique responses compared to the heat-only treatment, catalysed through the addition of stress metabolites. These involved differential expression of two chemosensory (vomeronasal receptor-like) genes, V1R/*ora3* and V2R/*olfcb1,* which supports the hypothesis that stress metabolites may be detected by chemoreceptors. In contrast to its downregulation by stress metabolites in group-raised outcrossing embryos, *ora3* was upregulated by the combined treatment TS+SM in isolated true-breeding embryos. Interestingly, the gene *olfcb1* was upregulated in SM compared to TS+SM, and is involved in the detection of amino acids (Zhang et al., 2022) and the chemically-induced fright reaction in fish (Yang et al., 2019). The combined treatment TS+SM also altered genes involved in developmental acceleration via five genes in the apelin signalling pathway (*acta2, si:ch211-286b5.5, mef2aa, ryr2a, map1lc3cl*). Apelin signalling is a type of environmental signal processing with a wide array of physiological effects such as angiogenesis, renal fluid homeostasis, energy metabolism, immune response, embryonic development, and the neuroendocrine stress response (Chapman et al., 2014), which hints at activation of the sympathetic nervous system SNS (Drougard et al., 2014) and the emergence of chronic stress (Vashist and Marion Schneider, 2014). Such positive stress feedback loops warrant further study due to the ever-increasing occurrences of diel and seasonal heat events. Altogether, the data from Chapters 2, 3, and 4 demonstrated that stress propagation exists in several aquatic species. Next, Chapter 5 will ask what the consequences of abiotic stress and stress propagation are when animals encounter a highly stressful mutagenic environment.

Chapter 5. Consequences of directly- and indirectly-experienced heat stress in a mutagenic environment

5.1. Significance statement

The previous chapters showed that abiotic stress induces stress responses directly in aquatic animals but also indirectly in their conspecifics. This chapter shows that early stress – either experienced directly in donors or indirectly in receivers of stress cues – nonlinearly alters larval fitness in a mutagenic environment. This chapter reveals the significance of stress propagation for fitness responses in aquatic animals exposed to mutagens found in natural environments.

5.2. Graphical Abstract

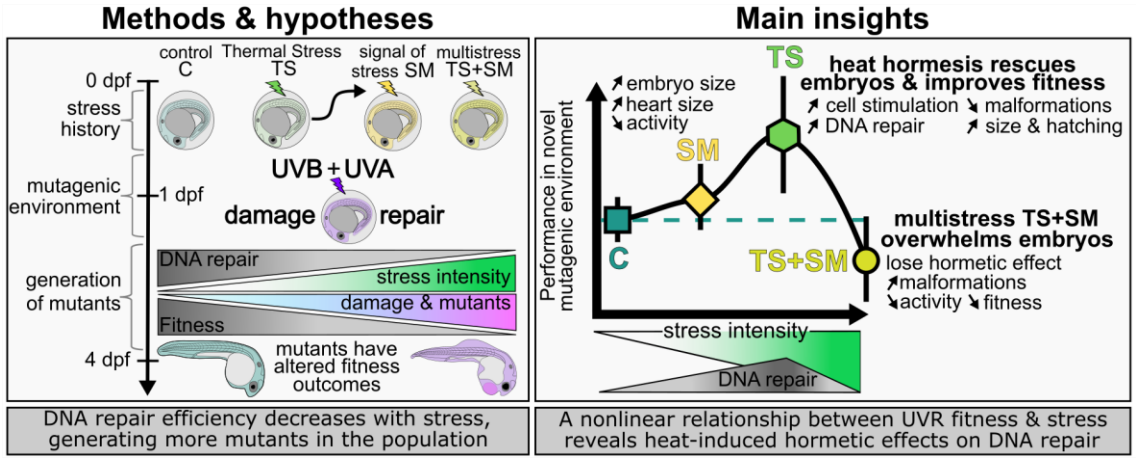

5.3. Highlights

- Heat stress had a hormetic (protective) effect against UV damage by stimulating the heat shock response, antioxidants, and DNA repair.
- The heat hormetic effect rescued embryos from UV damage by lowering malformations and accelerating development.
- Heat-stressed embryos released stress metabolites which initiated keratin, immune, and cellular structuring responses in receivers, in turn accelerating growth but without reducing malformations
- Heat combined with stress metabolites overwhelmed embryos in response to UV radiations, reducing their fitness-related performances.
- Heat stress during early embryogenesis leads to differential fitness outcomes, with a nonlinear relationship with stress intensity.

5.4. Abstract

Climate change increases both the frequency and duration of heat events. Direct negative effects of such heat stress may be exacerbated through heat-induced stress propagation (via stress metabolites) between aquatic animals. Whilst early life stages are vulnerable to stress-induced damage, they also deploy cellular mechanisms to protect cells against their naturally mutagenic environment. Little is known about the fate and performance of fish embryos which have experienced direct or indirect heat stress in a mutagenic environment. Natural environmental mutation rates are, however, typically low, which poses an observational challenge. To circumvent this, zebrafish embryos were here exposed to three treatments consisting of direct heat, indirect heat-induced stress metabolites, and heat combined with heat-induced metabolites before undergoing a UVB/UVA damage/repair assay to mimic a mutagenic environment. Indirect heat stress altered keratin and cell structuring-related genes in receivers, leading to longer larvae with over-developed pericardial widths, which were behaviourally hypoactive. Heat stress had a hormetic effect by stimulating the cellular stress response, and presumably facilitating DNA repair, which rescued larvae from subsequent UV damage and improved their fitness. Heat stress combined with stress metabolites emitted by heat-stressed conspecifics, however, overwhelmed embryos, which annihilated the hormetic effect, generated mutants, and lowered overall fitness indicators. Overall, this chapter revealed a nonlinear relationship between stress intensity and fitness performances in a mutagenic environment. Whilst generated in the laboratory, these findings provide an important baseline to understanding the consequences of thermal stress history in the natural environment, where direct and indirect heat stress co-occur.

5.5. Introduction

In an era of fast-paced climate change, anomalies in the thermal environment such as extreme temperatures are more frequent (IPCC, 2019, 2022). Such heat events have catastrophic implications for ectotherms, which may experience sharp declines in fitness (Jørgensen et al., 2022). Aquatic ectotherms, such as zebrafish (Engeszer et al., 2007), spawn in shallow waters where offspring are exposed to high temperatures and to environmental mutagens such as ultraviolet radiation (UVR) (Dahms and Lee, 2010).

Early life stages of animals that develop outside the maternal body (such as most fish) are more vulnerable to both UVR (Zagarese and Williamson, 2001; Dahms and

Lee, 2010) and heat stress (Dahlke et al., 2020a, 2020b). Since early-life exposure to UVR lowers fitness in later stages (Ceccato et al., 2016; Lundsgaard et al., 2022), understanding the effects of heat stress and UVR on developing stages is an important avenue of research. There is a rising concern regarding the combined effects of thermal stress and environmental UVR (Cramp et al., 2014), as past studies found that abiotic stressors, such as high temperatures, combined with UVR can lead to additive, synergistic, or antagonistic effects on the biology of fish (Cramp et al., 2014; Icoglu Aksakal and Ciltas, 2018; Alves and Agustí, 2020). For instance, heat may denature DNA repair proteins (Lupu et al., 2004; Alton and Franklin, 2012) and lower energy investment allocated to DNA repair (Berger et al., 2017). However, these studies primarily investigated the effects of heat simultaneous to UVR, which due to temperature-dependant activation of DNA repair proteins can obscure the casual factors for repair, whilst less is known about the effects of heat stress history *prior* to UV-induced DNA damage/repair. A lowered DNA repair capacity may increase DNA damage, which would affect fitness and survival. In addition, aquatic animals can integrate signals (dubbed "stress metabolites") released by heat-stressed zebrafish, which alter their phenotypes despite not experiencing heat stress first-hand (Feugere et al., 2021a, 2021b). Therefore, social species may have amplified stress responses to heat through chemical communication, but the consequences of which are little studied.

UV-induced damage is caused by both UVA (315-400 nm) and UVB (280-315 nm) radiation (Dahms and Lee, 2010; Rastogi et al., 2010). UVR causes damage to lipids, proteins, and DNA (Alves and Agustí, 2020). UVB directly alters DNA through absorption, whereas UVA also induces indirect damage via oxidative stress (Griffiths et al., 1998; Pourzand and Tyrrell, 1999; Sinha and Häder, 2002). The main UV-induced DNA lesions are cyclobutane pyrimidine dimers (CPDs) and pyrimidine-pyrimidone 6-4 photoproducts (6-4PPs) (Sinha and Häder, 2002; Rastogi et al., 2010). Other DNA damages include misincorporated, modified, missing, and mispaired bases (Griffiths et al., 1998; Rastogi et al., 2010). UVR produces single (SSB) and double (DSB) DNA strand breaks leading to genetic information loss, mutations, or cytotoxicity by preventing replication or altering gene expression (Dahms and Lee, 2010; Rastogi et al., 2010).

Cells remove such insults to DNA through the DNA damage response (DDR) (Chatterjee and Walker, 2017). Photoprotective pigments and antioxidants protect from damage whereas repair systems remove macromolecule damage (Dahms and Lee, 2010;

Rastogi et al., 2010). The p53-pathway arrests the cell cycle to allow time for repair (Williams and Schumacher, 2016) utilising three major routes: photoreactivation, excision repair, and recombination. Most DNA damage is attributable to UVB whilst UVA activates photorepair (Sinha and Häder, 2002; Dong et al., 2008). Photoreactivation or photoenzymatic repair (PER, light repair excited by UVA and light) involves photolyases that directly reverse damaged bases by removing CPDs and 6-4PPs (Rastogi et al., 2010; Banaś et al., 2020). Excision repair (dark repair) substitutes damaged DNA with new nucleotides either by base excision repair (BER) or nucleotide excision repair (NER), which respectively remove small or bulky lesions (Griffiths et al., 1998; Dahms and Lee, 2010; Rastogi et al., 2010). Mismatch repair (MMR) removes mispaired bases to improve replication fidelity (Jiricny, 2013). SSBs are repaired through NER, BER, and MMR routes whilst DSBs are removed through homologous recombination and non-homologous end joining (Rastogi et al., 2010; Minten and Yu, 2019). Last, damaged cells may be removed through p53-mediated apoptosis pathways (Wang, 2001). Failure to mount such protective and repair responses to UVR will impair immunity (Salo et al., 2000; Banerjee and Leptin, 2014; Cramp et al., 2014), behaviour and physiology in fish (Hurem et al., 2018), leading to severe defects such as embryonic malformations, impaired hatching, and ultimately to increased mortality (Alves and Agustí, 2020). Additional to DNA damage, UVR may induce inheritable epigenetic changes such as histone modification (Shen et al., 2017; Reardon et al., 2022).

Zebrafish, including embryos, possess a competent repair system to remove UVB-induced DNA lesions (Dong et al., 2007, 2008; Sussman, 2007; Pei and Strauss, 2013). For instance, light- and UVA-activated photolyase enzymes efficiently photorepair CPDs and 6-4PPs formed during UVB exposure, rescuing zebrafish embryos from morphological defects (Dong et al., 2007, 2008). This makes zebrafish embryos a suitable model to study the effect of heat stress history on DNA repair (Pei and Strauss, 2013). This chapter asked whether heat stress, experienced directly or indirectly via stress metabolites, affects DNA repair capacities and fitness-relevant outcomes in a mutagenic environment. I expected that both strong and direct (heat stress) and weaker and indirect (heat-induced stress metabolites) stressors weaken the protective and reparative responses to UVR in a mutagenic environment, and that this would be further disrupted in the combined treatment. I hypothesised that, by limiting DNA repair, heat stress history would increase the proportion of mutants and lower fitness performances.

5.6. Methods

5.6.1. General experimental design

Zebrafish embryos (AB line) were obtained from a stock population at the University of Hull. Eggs were collected in the morning, thoroughly cleaned in fresh 1X E3 medium, and further cleaned by bleaching. Fish husbandry, breeding, and zebrafish handling methods were the same as in Chapter 4 (see section 4.6.4). All experiments were approved by the Ethics committee of the University of Hull (FEC_2019_194 Amendment 1).

This chapter aimed to explore the effect of stress treatments from Chapter 4 (see section 4.6.1) on DNA repair dynamics. Specifically, it aimed to evaluate the effects of thermal stress (TS) and stress metabolites (SM) released by conspecifics upon thermal stress on the capacity for DNA repair using RNA-sequencing and a panel of phenotypic analyses (**Figure 5.1**).

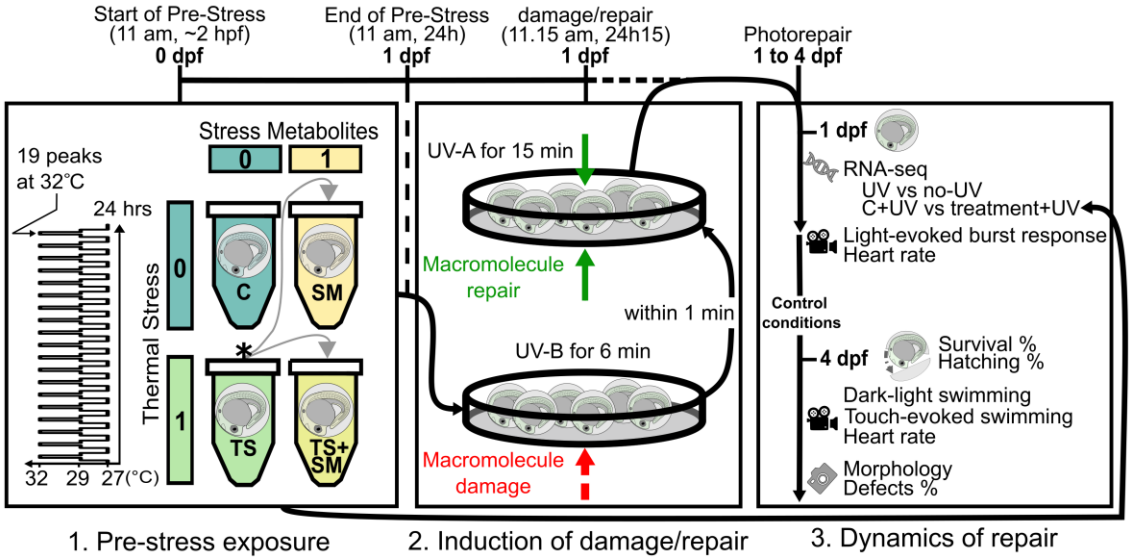

Figure 5.1. Scheme of experimental design. Left: zebrafish embryos were exposed to heat stress history consisting of repeated thermal stress (see diagram of heat peaks), or stress metabolites induced by it. This yielded four treatments of donor (*) and receiver (grey arrows) embryos: control (C), thermal stress (TS), stress metabolites (SM) in control temperature, stress metabolites in thermal stress (TS+SM). Middle: At 1 day post fertilisation (dpf), embryos experienced successive macromolecule damage (UVB for 6 min, short-dash red arrow) and macromolecule repair (UVA for 15 min plain green arrows). Right: zebrafish embryos were either immediately sampled for RNA-sequencing at 1 dpf (with or without UV) or incubated in control conditions for phenotypic analyses from 1 to 4 dpf. Symbols represent endpoints: gene expression (DNA symbol), morphology (photo camera), hatching (opened chorion), behaviour (video camera), survival (cross) within the chorion until 4 dpf or after dechorionation (scissors) at 4 dpf.

For this purpose, zebrafish embryos were exposed, starting during the cleavage period (2 hpf to 3.3 hours post fertilisation – hpf) to the control C or stress treatments

TS, SM, and TS+SM (in the following also called "stress history") for 24 hours similar to in Chapter 4. At the end of the exposures, survival rates were monitored, and viable embryos were placed into small petri dishes (⌀: 35 mm) by treatment groups in their incubation media and were subjected to a UVB/UVA damage/repair assay (**Figure 5.1**). This assay induced deleterious mutations through UVB exposure followed by UVA-induced DNA repair. UV exposure treatments were labelled C+UV, TS+UV, SM+UV, and TS+SM+UV.

5.6.2. UVB + UVA protocols

The methods were adapted from Dong et al. (2007) who showed complete recovery of UVB-induced alterations by UVA-activated photorepair in zebrafish embryos. UVA and UVB protocols were optimised so that larvae survived up to 5 days with > 75% survival whilst showing obvious teratogenic effects, on which differences in phenotypes may be observed between treatments.

For this purpose, a small number of control zebrafish embryos (PET strain) were raised in control conditions (27°C in petri dishes in natural light conditions) and exposed at 24 hpf to different durations and intensities of UVB and UVA. First, exposing embryos to UVB for 3, 6, or 9 min determined the best UVB exposure as 6 min because 9 min induced too much death and strong defects that were not recovered. Next, 24-hpf control embryos were exposed to UVB only (6 min; one bottom-up source), UVA only (28 min; one bottom-up source), UVB+UVA. At 3 dpf, half the embryos from UVA were exposed to UVB (UVA+UVB group) to test how late the defects can be induced. This preliminary experiment showed that UVB induces mortality and aberrant phenotypes when applied at either 1 dpf (UVB+A) or 3 dpf (UVA+B, **Table Appendix 4 S1**). These deformities included pericardial edema, no caudal fin formation, developmental delay, yolk ball and yolk extension alteration, or lateral fin alteration (**Figure 5.2A**). These UVB-induced defects were less severe, delayed, or rescued in embryos subsequently exposed to UVA at 1 dpf. Such UVB+A treatment prevented mortality up to 4 dpf (**Figure 5.2A**, **Table Appendix 4 S1**). There were no defects caused by UVA only.

In order to catch transcriptomic changes occurring just after UVA repair, there should not be too much delay after the UV treatments, since DNA damage not repaired within 2 hours may be irreversible in zebrafish embryos (Dong et al., 2008). Hence, a protocol of 15 min of double-source bottom-up/top-down UVA exposure was used

instead of 28 min of single-source bottom-up UVA exposure. To test this protocol, control embryos were kept in control conditions (control C) or were exposed to UVB (6 min) alone or followed by UVA (15 min with 2 sources) at 24 hpf. This small set of preliminary data (n = 26-29 embryos/treatment) showed that 15 min of this UVA protocol was sufficient to partially recover from UVB-induced defects as evidenced by decreased mortalities and increased hatching rates – although few embryos still presented pericardial edema, tail malformation, or spine curvature in UVB+UVA treated embryos (**Table Appendix 4 S2**, **Figure 5.2B**). Therefore, 15 min of double-source UVA exposure was selected to capture DNA repair transcriptomic changes in zebrafish embryos. To estimate more finely the UVA-activated recovery from UVB-induced malformations, one last optimisation experiment compared the ratios of dead, aberrant, or healthy embryos in C, UVB (6 min, bottom-up source), and UVB+A (15 min, double source) conditions. The successful photorepair effect of UVA was confirmed by significantly increased ratios of healthy embryos in UVB+UVA (n = 14/21, 61%), to similar levels as in the control (n = 19/21, 90%, $\chi^2 = 0.76$, p-adj = 0.3840), compared to UVB (n = 0/24, 0%, $\chi^2 = 14$, p-adj= 0.0004). Embryos exposed to UVB+UVA (n = 23/23, 100%) increased their survival rates to similar levels as in the control (n = 21/21, 100%, $\chi^2 = 0.1$, p-adj = 0.763), compared to embryos exposed to UVB alone (n = 14/24, 58%, $\chi^2 = 5.12$, raw p = 0.0236, p-adj = 0.0708, **Table Appendix 4 S3**). Overall, UVB and UVA optimisation protocols showed that UVA (15 min, double source) rescued embryos from UVB-induced defects (6 min, single source) with no mortality and a significant increase in healthy embryos.

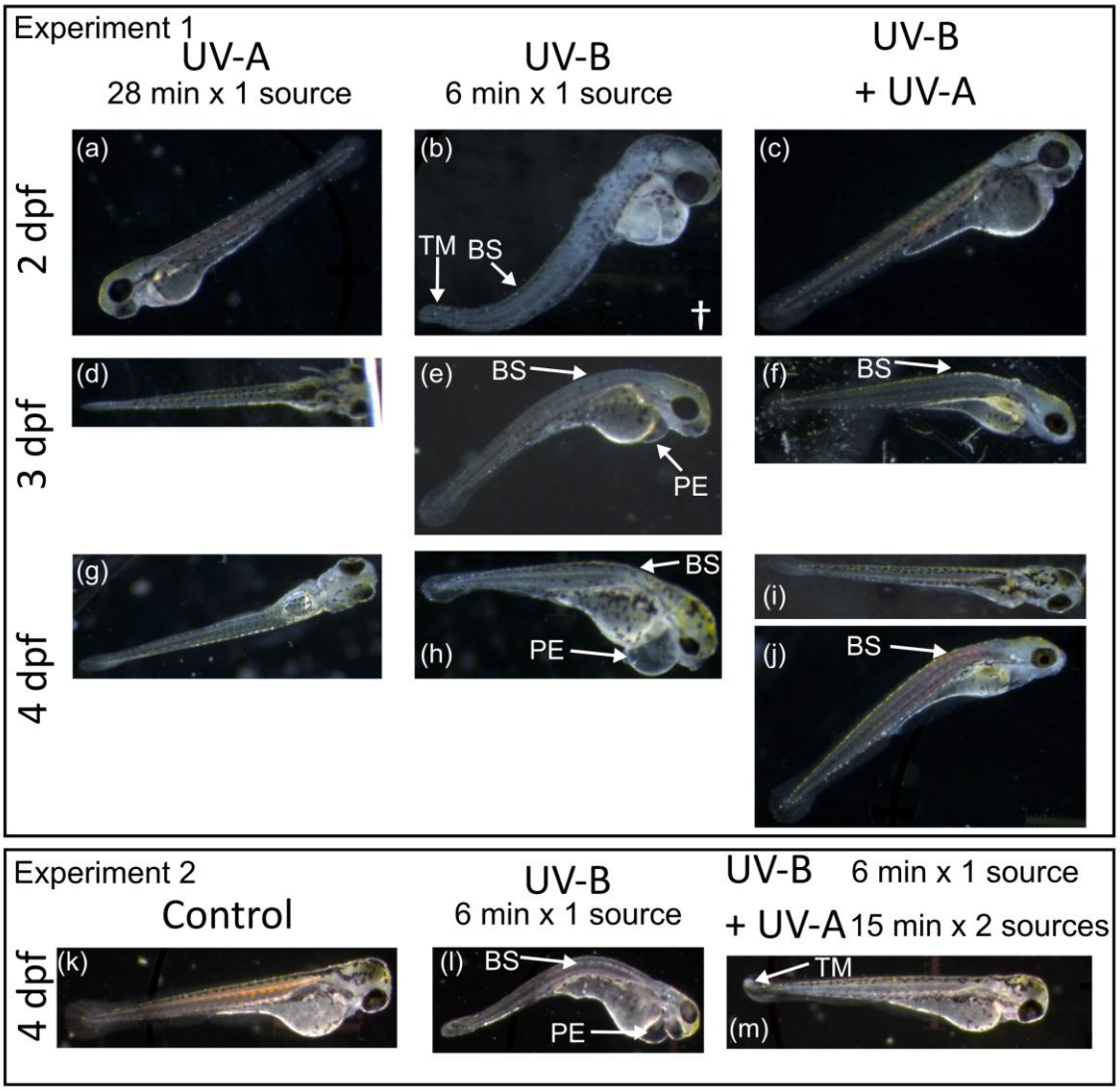

Figure 5.2 UVA exposure repairs UVB-induced DNA damage. Top: experimental optimisation 1. Exposure to UVA, UVB, and UVB+A treatments in zebrafish embryos at 2 (a-c), 3 (d-f), and 4 (g-j) days post fertilisation (dpf). UVA: 28 min of bottom-up (1 UVA source) exposure (a, d, g), UVB, 6 minutes of bottom-up exposure (b, e, h), and UVB+A: UVB exposure followed by immediate UVA exposure (c, f, i, f). Defects included tail malformation (TM, showing reduced cross-section of the tail), bent spine (BS), and pericardial edema (PE). (i) and (j) show complete (no defects) and partial (non-lethal defects) UVA-induced recovery from UVB-induced deleterious effects. Bottom: experimental optimisation 2 where UVA-induced DNA repair lasted 15 min from two UVA sources and showing a strong recovery of UVB-induced damages with non-lethal defects.

The final, optimised UV exposure protocol was as follows: zebrafish embryos were centred in their Petri dish (⌀: 30 mm, with ~5 mL of fresh embryo medium) and exposed in darkness for 6 min on top of a transilluminator (GelVue GMV20, Syngene LTD) equipped with 6 UVB bulbs (peak of 306 nm UVB, 8 watts lamp wattage, 1.6-watt ultraviolet output, Sankyo Denki G8T5E). Next, zebrafish embryos were immediately transferred (within 1 min) to the UVA setup which consisted of a 15-min exposure in a double-source "sandwich" system of ultraviolet lamps (365 nm UVA, Spectroline ENF-240C/FE) comprised of both one bottom-up (direct contact against the

bottom of the Petri dish) and one top-down (11 mm away from embryos due to the height of the petri dish) UVA sources. Of note, the UVA setup was placed under natural light which also excites DNA repair (Essen and Klar, 2006). The chosen timing (6 min UVB + 15 min UVA) aimed to allow the expression of DNA repair mechanisms at the time of embryo sampling for RNA-sequencing (within 15 min after the end of the UVB+A exposure, and within 30 min after beginning UVB irradiation). Zebrafish embryos were either immediately sampled at 24 hpf for RNA-sequencing or maintained in control conditions (incubation in darkness at 27°C in fresh embryo medium) until 4 dpf for phenotypic analyses (see below).

5.6.3. RNA-sequencing

1-dpf zebrafish embryos were sampled immediately after UVB+A exposure. Sampling, sequencing, and read processing were performed as described in Chapter 4 (see section 4.6.6). Briefly, total RNA was extracted using TRIzol followed by DNAse and sodium acetate clean-up. Total RNA samples were quality checked using a Nanodrop 1000, agarose gels, and a Bioanalyzer. cDNA libraries were prepared with the TruSeq stranded mRNA kit, cleaned, and sequenced by Illumina NovaSeq 6000, 50PE sequencing at the Edinburgh Genomics facility (see section 4.6.6). *FASTQC* v0.11.9 was used to assess read quality before and after filtering and trimming. PCR-biased read duplication was analysed in RNA samples from UV-treated embryos using the R package *DupRadar* v1.18.0 (Sayols et al., 2016). For this purpose, duplication rates were compared in raw reads, reads filtered using *Trimmomatic* (Bolger et al., 2014) without deduplication, and reads filtered with deduplication by *fastp* (Chen et al., 2018). Most reads from UV-treated embryos had intercepts higher than ~35%, indicating that lowly expressed reads had a PCR duplication bias highlighting the need for deduplication. Deduplication using *fastp* increased read quality by lowering duplication rate intercepts to normal levels of < ~0.04% for lowly expressed reads (**Figure Appendix 4 S1**). Reads filtered, trimmed, and deduplicated using *fastp* v0.23.1 were utilised for the analysis. Reads were aligned and genes counted using *STAR* v2.6.1 (Dobin et al., 2013). *DESeq2* v1.28.1 (Love et al., 2014) was used for differential expression analyses in *Bioconductor* v3.11 (Morgan, 2021) and *R* v4.0.2 (R Core Team, 2020).

Taking advantage of a three-way factorial design of thermal stress × stress metabolites × UV (see non-UV samples from Chapter 4), two statistical approaches were used to assess the effects of heat stress history on the response to UVR. The

effects of all three treatments SM+UV, TS+UV, and TS+SM+UV were compared to C+UV. The effect of the combined stressors was explored by comparing SM+UV and TS+UV to TS+SM+UV. The treatment-specific transcriptomic response to UV was also compared for each UV versus no-UV pair, that is C vs C+UV, TS vs TS+UV, SM vs SM+UV, and TS+SM vs TS+SM+UV. Next, the magnitude of change (absolute log fold change, LFC) and gene expression ratios in response to UV were compared in a two-way design of thermal stress × stress metabolites across C+UV, SM+UV, TS+UV, and TS+SM+UV. This analysis was repeated with GO-term wide p-value adjustment within subsets of genes from four candidate pathways: "*DNA repair"* (GO:0006281), "*protein folding"* (GO:0006457), "*macromolecule methylation"* (GO:0043414), and "*regulation of gene expression, epigenetic*" (GO:0040029). Principal Component Analyses of regularised logarithmic (*rlog*) transformed data were explored using the *prcomp* R function. The differentially expressed genes (DEGs) were visualised on volcano plots with the *EnhancedVolcano* R package v1.6.0 (Blighe et al., 2020). DEGs were considered significant when p-adj < 0.05 and |FC| ≥ 1.5 (|LFC| > 0.58). Gene identifiers were cross-database-converted using the *biomaRt* R package v2.44.4 (Durinck et al., 2005, 2009) and mapped to GO terms using the *topGO* v2.40 (Alexa and Rahnenfuhrer, 2020) and *org.Dr.eg.db* v3.11.4 (Carlson, 2020) R packages. *GOstat* v2.54.0 (Falcon and Gentleman, 2007) (hypergeometric test), *clusterProfiler* v3.16.1 (Yu et al., 2012), and *ReactomePA* 1.32.0 (Yu and He, 2016) R packages respectively identified functionally enriched GO terms, Kyoto Encyclopedia of Genes and Genomes (KEGG) pathways, and Reactome pathways. Terms were considered significantly enriched when p-adj < 0.1 and gene count ≥ 2.

5.6.4. Phenotypic experiments

Phenotypic measurements consisted of imaging and videoing for heart rate, burst activity, and swimming performance at several time points. To account for possible batch effects, embryos from the same clutch were observed for all treatments, and separate embryo medium donor groups were raised on the previous day (but not used in phenotypic analyses) to obtain fresh stress metabolites for SM and TS+SM. Zebrafish larvae were monitored for hatching and for survival by transparency (i.e., white/cloudy eggs were deemed dead whereas clear eggs were assessed as alive, confirmed by later observing heart beats under the stereomicroscope).

After treatments and UVB+A exposure, 1-dpf zebrafish embryos were moved per treatment groups into small glass dishes to record their startle responses. Zebrafish

embryos within their chorion were videoed for burst activity (for 15 s under the stereomicroscope after switching the underneath light source to 50% intensity to induce the startle response) by batches of 4-5 embryos in small glass wells with fresh embryo medium, with treatment alternation and blind to the experimenter. Next, embryos were placed in individual wells with 200 µL of fresh embryo medium for control conditions (incubation in darkness at 27°C in fresh embryo medium) until 4 dpf. Zebrafish were monitored for hatching and survival until 4 dpf. After 31 hours (6 hours after UV treatment, 1 dpf on late evening) each chorionated embryo was removed from its individual well, carefully placed using a plastic pipette into a watch glass in a small volume of embryo medium and videoed for 15 s using the stereomicroscope for heart rate monitoring. Zebrafish embryos were then returned to their wells at which point their medium was replaced with 180 µL of fresh embryo medium. Zebrafish were also monitored at 2 and 3 dpf at 11 am at which point their media were replaced with 180 µL of fresh embryo medium. At 4 dpf, zebrafish larvae that did not naturally hatch were manually dechorionated using fine forceps (Dumont n°5) before being returned to their individual wells. Larvae were allowed to recover in control conditions for 2 hours after dechorionation. At 5 pm on 4 dpf (102 hours of experimental exposure), zebrafish larvae were videoed for swimming assays using a Canon 1,200D camera set at 25 frames per second. Zebrafish larvae were tested 6 at a time by placing each larva individually in one well of a 6-well plate filled with 3 mL of pre-heated fresh embryo medium. Zebrafish larvae were left for five minutes in darkness and immediately videoed for two minutes once artificial light was applied to induce a startle-like response (dark-light swimming behaviour). Next, larvae were videoed for a touch-evoked swimming behaviour which consisted in three consecutive touches on the head, every ten seconds, using the loop of an inoculating needle. The embryo medium was changed between each larva. At the end of the swimming assay, after 105 hours of treatment (8 pm on day 4), zebrafish larvae without their chorion were carefully moved onto a microscope slide labelled with a micrometre for imaging under the stereomicroscope. Larvae were carefully moved into a watch glass in a small volume of embryo medium and videoed for 15 s using the stereomicroscope for 15 s to acquire 4-dpf heart rate videos. In all phenotypic analyses, treatments were alternated to limit time effect on swimming behaviours, and blind to the experimenter to limit experimental bias. Images and videos were randomised for blind data acquisition analyses using Bulk Utility Rename v3.4. Videos of startle response at 1 dpf and heart rates at 1 and 4 dpf were analysed using Danioscope (Noldus). 4-dpf swimming videos were analysed using

Kinovea v0.9.5 (Charmant and Contributors, 2021) to obtain distances and moving times from which speed was calculated, as well as swimming burst counts. Fatigability was measured as the delta of measurements between the 1st and 3rd (last) stimuli in the touch-evoked response. Images were analysed using Image J v1.53e (Schneider et al., 2012) after calibration to a micrometre scales to measure lengths (mm) of several morphology characters: whole-body, eye, yolk ball, yolk extension, pericardial and tail width lengths (**Figure 5.3**).

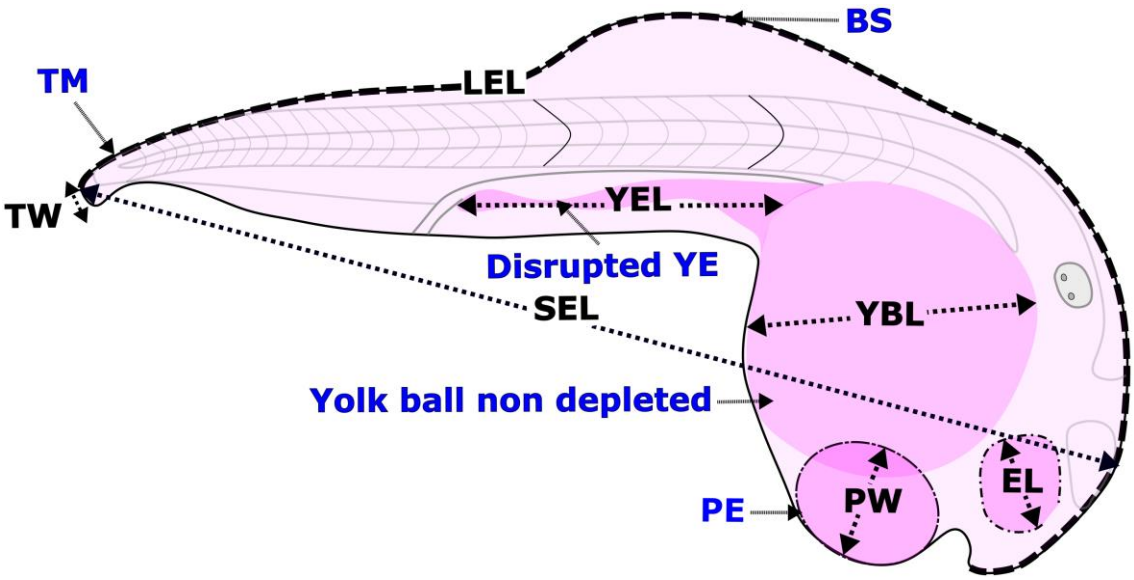

Figure 5.3. Screening of malformations in larvae exposed to stress and UVR. Lengths (dot lines) were eye length (EL), yolk ball length (YBL), yolk extension length (YEL), longest embryo length (LEL), shortest embryo length (SEL), pericardial width (PW) and tail width (TW). HTA: heat-trunk angle. Defects (blue font) were binary coded for tail malformation (TM), disrupted yolk extension (YE), yolk ball non-depleted, bent spine (BS), and pericardial edema (PE).

5.6.5. Statistical analysis

All statistical analyses were performed in R v4.0.2 (R Core Team, 2020) in RStudio v1.3.1056 (RStudio Team, 2020) and graphs were drawn mainly with the *ggplot2* v3.3.5 R package (Wickham, 2016). Gene expression binary data were analysed using Chi-squared tests from *rstatix* v0.7.0 (Kassambara, 2021) using *chisq_test* for model terms and *pairwise_chisq_gof_test* for pairwise post-hoc treatment comparisons. Gene expression linear models were represented with *ggscatter* from *ggpubr* v0.4.0 (Kassambara, 2020). Binary phenotypic data were analysed using generalised linear models with binomial data. Parametric numerical data were analysed using two-way ANOVAs followed by pairwise post-hoc tests using *emmeans* v1.7.3 (Lenth, 2022), after transformation using *BestNormalize* v1.8.2 (Peterson and Cavanaugh, 2020; Peterson, 2021) where necessary and possible. Model assumptions were verified using

Breusch-Pagan tests for heteroskedasticity from *lmtest* v0.9-38 (Zeileis and Hothorn, 2002) and Shapiro-Wilks Test for normality of residuals. Non-parametric numerical data were analysed using Scheirer-Ray-Hare tests from *rcompanion* v2.4.1 (Mangiafico, 2021) followed by pairwise Wilcoxon-Mann-Whitney post-hoc tests from *rstatix* v0.7.0. All post-hoc comparisons were corrected for multiple testing. Effect sizes were computed using *effectsize* v0.6.0.1 (Ben-Shachar et al., 2020) and categorised according to Sawilowsky (2009). Because both behavioural and morphological alterations were outcomes of treatments, correlation statistics were verified between phenotypic variables using *corrplot* v0.92 (Wei and Simko, 2021). PERMANOVAs were performed through the *adonis* function from *vegan* v2.5-7 (Oksanen et al., 2020) followed by pairwise PERMANOVAs from *pairwise.adonis* function from *pairwiseAdonis* v0.4 (Martinez Arbizu, 2017). Principal Component Analyses of 1-dpf and 4-dpf data were conducted using *prcomp* which allowed to retrieve data from the first two variance contributors (PC1 and PC2). Multivariate data were visualised using *ggbiplot* v0.55 (Vu, 2011). Model terms were visualised using the *plot_model* function from *sjPlot* v2.8.10 (Lüdecke, 2021) and trends were represented by smoothed *loess* lines using *stat_smooth* from *ggplot2*.

5.7. Results

The overarching aim of this study was to investigate the transcriptomic and phenotypic effects of direct and indirect heat stress history on the repair capacity following UV-induced damage.

5.7.1. Confirmatory results: stress metabolites propagated stress to conspecifics

5.7.1.1 Effect of heat and stress metabolites combined with UV compared to C+UV

First, the transcriptomic response was compared between heat and stress metabolite treatments following UV exposure (C+UV vs TS+UV vs SM+UV vs TS+SM+UV, **Figure 5.4**).

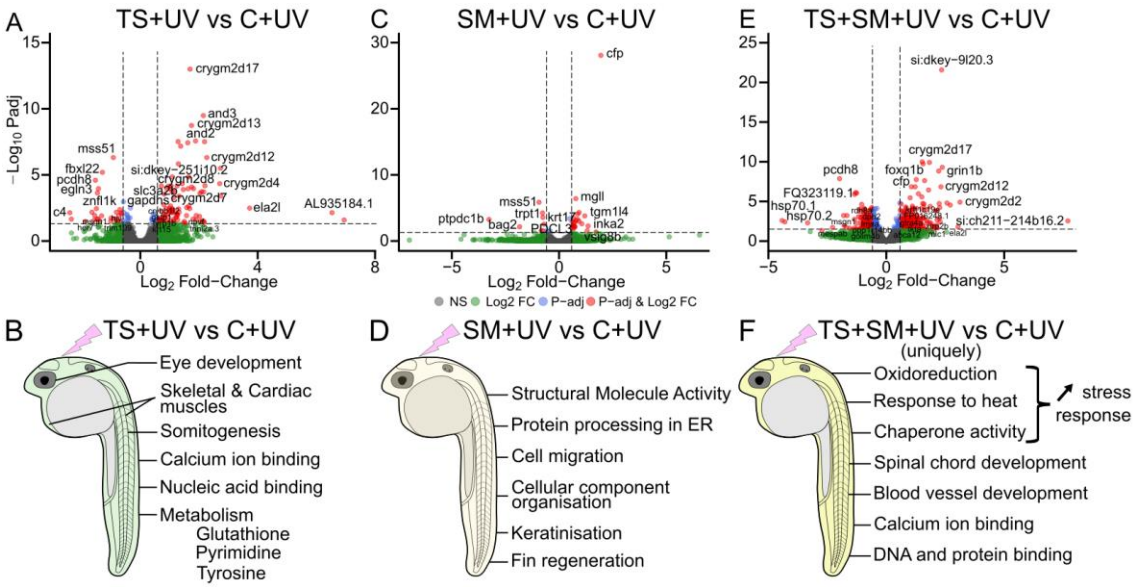

Figure 5.4. Heat stress and stress metabolites followed by UVR alter important molecular pathways. Volcano plots (upper row) showing the differentially expressed genes in response to (A) thermal stress (TS+UV vs C+UV), (C) stress metabolites (SM+UV vs C+UV), and (E) their combination (TS+SM+UV vs C+UV). Genes of interest are shown in red when significant (p-adj < 0.05, |FC| > 1.5). DEGs left of the left vertical line and right of the right vertical line are respectively significantly underexpressed and overexpressed compared to the control C+UV. Functional enrichments (bottom row) of transcriptomic response to TS+UV (B), SM+UV (C), and TS+SM+UV (F) compared to C+UV. Only main enriched terms of Gene Ontology of Biological Processes and Molecular Functions, KEGG and Reactome pathways are shown.

Despite two outlier samples along PC1 (58.1% variance), heat stress clearly clustered the samples together along PC2 (11.3% variance) and PC3 (7.9% variance) whilst the effect of stress metabolites was more subtle (**Figure 5.5B-C)**. The treatment TS+UV significantly altered 133 genes compared to C+UV (**Figure 5.4A**). These genes were functionally enriched for biological processes of eye development (GO:0001654), somitogenesis (GO:0001756), skeletal and cardiac muscle (GO:0060048), as well as molecular functions associated with calcium ion (GO:0005509) and nucleic acid (GO:0001067) binding. The genes associated with eye development were strikingly numerous (n = 23 crystallin β and γ genes with an average FC = 3.24). Interestingly, the genes induced by TS+UV tended to be involved in TGF-β signalling pathway (dre04350), as well as in the metabolism of tyrosine (dre00350), glutathione (dre00480 incl. glutathione S-transferase pi 1, *gstp1*), and pyrimidine (dre00240) (**Figure 5.4B**, **Figure 5.5D**).

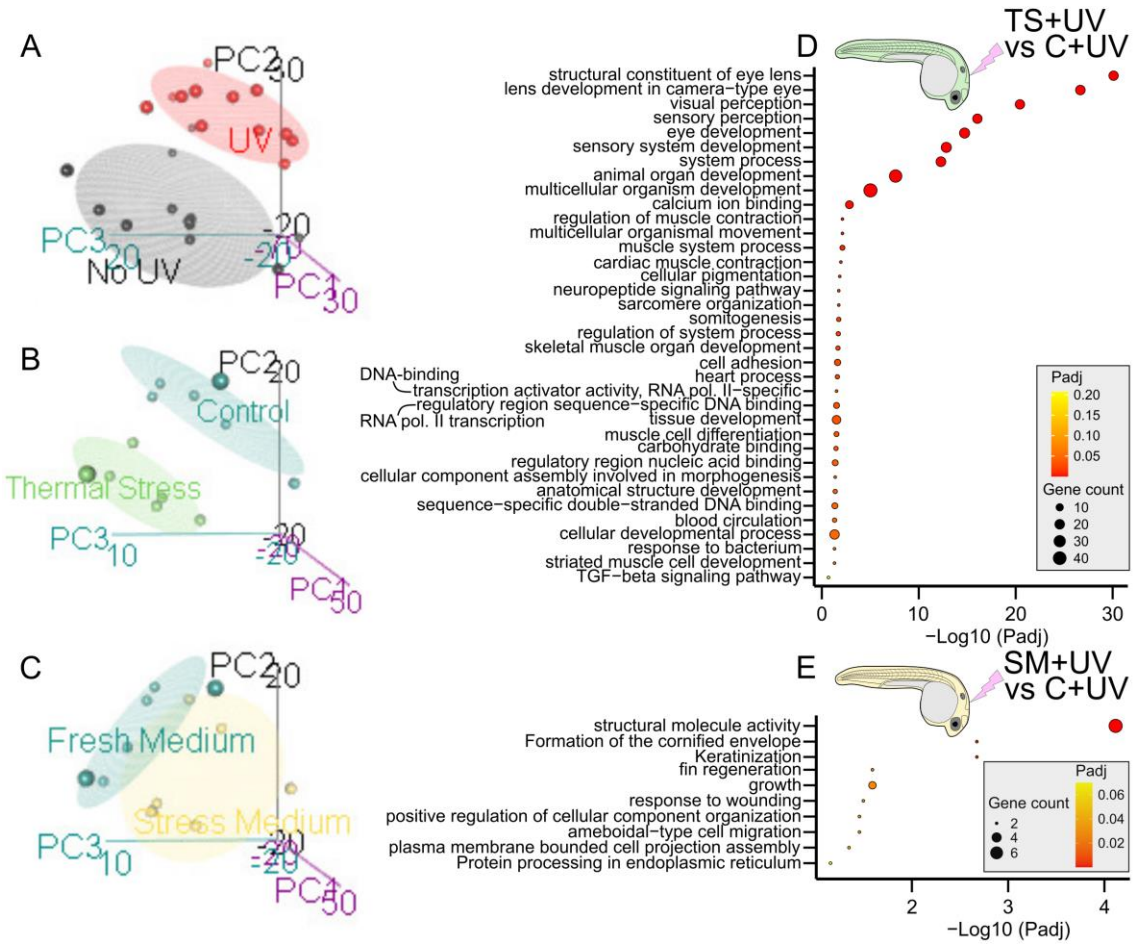

Figure 5.5. UVR, heat, and stress metabolites, alone or in combination, altered the transcriptome of zebrafish embryos. A) UV (red ellipse and dots, n = 12) versus no-UV (black ellipse and dots, n = 12) samples. B) Thermal stress (green ellipse and dots, n = 6) versus control temperature (27°C, blue ellipse and dots, n = 6) within UV-treatment. C) Stress metabolites (yellow ellipse and dots, n = 6) versus control temperature (27°C, blue ellipse and dots, n = 6) within UV-treatment. Principal component analysis (PCA) showing the sample composition along the first three axes of the spectral decomposition (*prcomp*) of the regularised log transformed variance of the read count data. Heat stress (D) and stress metabolites (E) followed by UV alters important molecular pathways. Top functionally enriched terms (based on highest gene count/term with n ≥ 2 genes/term) of the differentially expressed genes found in TS+UV (D) and SM+UV (E) compared to C+UV. Terms are sorted by decreasing significance and show Gene Ontology of Biological Processes and Molecular Functions, KEGG and Reactome pathways.

On the other hand, the 31 genes significantly altered (|FC| > 1.5, p-adj < 0.05) by stress metabolites (SM+UV vs C+UV, **Figure 5.4C**) were associated with fin regeneration (GO:0031101), keratinisation (DRE-6805567), structural molecule activity (GO:0005198), and protein processing in the endoplasmic reticulum (dre04141, **Figure 5.4D**, **Figure 5.5E**). Interestingly, genes of SM+UV involved three keratin orthologues (krt5/17/92) and two cytokeratins (*type I cytokeratin, enveloping layer*, cyt1; and cyt1 like, *cyt1l*). In SM+UV vs C+UV, the gene *ptpdc1b* (protein tyrosine phosphatase domain containing 1b) was markedly downregulated (LFC = -3.27) whilst two genes involved in immune response were largely upregulated: *cfp* (complement factor

properdin, FC = 3.86) and *vsig8b* (V-set and immunoglobulin domain containing 8b, FC = 3.3). Of note, chemosensation (GO:0007606) was not altered in response to SM+UV.

The multistress treatment TS+SM+UV altered the expression of 408 genes compared to C+UV which is significantly higher than UV treatments combined with heat (TS+UV: n = 133, χ^2 = 140.0, p-adj < 0.0001) or stress metabolites (SM+UV: n = 31, χ^2 = 324.0, p-adj < 0.0001) alone. The genes of TS+SM+UV were partially (n = 94, 20.4%) ascribed to the response to temperature (**Figure 5.6A**). Twelve genes were significantly altered, with the same expression direction, by both SM+UV and TS+SM+UV which brings additional evidence of their role in stress metabolites-induced responses, with again *cfp* (complement factor properdin) and two cytokeratins *cyt1* and *cyt1l*. There were however another 299 (65.9%) genes unique to the combined treatment TS+SM+UV suggesting an altered response when combining stress metabolites with heat (**Figure 5.4E**, **Figure 5.6A**). These genes unique to TS+SM+UV were involved in temperature response (GO:0009266), oxidoreduction (GO:0055114), folding activity (GO:0051082), calcium ion binding (GO:0005509), DNA binding (GO:0003700), but also in spinal cord (GO:0021510) and blood vessel (GO:0001568) development – but not with chemosensation (**Figure 5.4F**, **Figure 5.6B**).

Next, the transcriptomic response to multistress TS+SM+UV was compared to that of SM+UV (**Figure 5.6C**) and TS+UV (**Figure 5.6D**). If heat and stress metabolites do not have interacting effects, then one would expect that comparing TS+SM+UV to SM+UV would be equivalent to comparing TS+UV to C+UV for the heat stress term, whereas comparing TS+SM+UV to TS+UV would be the same as comparing SM+UV to C+UV for the stress metabolites term. However, such comparisons showed that TS+SM+UV vs SM+UV induced another 65 genes (31%) not found in TS+SM vs C+UV (**Figure 5.6E**) and that TS+SM+UV vs TS+UV was associated with 19 genes (38%) not found in SM+UV vs C+UV. This supports the hypothesis that heat, and stress metabolites exert interactive effects when in combination, distinct to their individual effects. Still, 8 genes were found both in SM+UV vs C+UV and in TS+SM+UV vs TS+UV, lending support for their role in the response to stress metabolites. These included two keratins *krt5/krt17*, *cpf*, *foxq1b*, and *scel* but also *si:ch73-70o10.1* and *si:dkey-9l20.3* (**Figure 5.6F**).

5.7.1.2 Comparing the common genes altered by stressors, with and without UV

Next, the findings from Chapter 4 were validated by cross comparing the genes altered by stressors with and without UV in a "meta-analysis". Compared to control, with and without UV, heat altered 48 genes in both studies with similar fold-changes ($r = 0.96$, $p < 0.0001$, **Figure 5.7A**). These genes were mostly related to developmental processes of the eyes (several crystallin β and γ genes), muscles, and cartilages; as well as calcium binding (**Figure 5.7A**).

Seven genes were found in both SM vs C and SM+UV vs C+UV, including three genes related to keratin (*krt17/92* and *cyt1*), epidermis (epidermis growth factor e*ps8l1a* and sciellin *scel*), transglutaminase (*tgm1l4*), and cell-matrix adhesion (*si:dkey-9l20.3*) (**Figure 5.7B**). Genes associated to stress metabolites alone participated in cell structures and movement (e.g., "structural molecule activity", "keratinisation", "cell matrix adhesion", **Figure 5.7B**).

There were 59 genes found in TS+SM compared to control, with and with UV, most of which were similar to TS alone (**Figures 5.7B-5.8B**). Since heat explained most of the response to TS+SM, I explored the genes related to stress metabolites and/or the interacting effect of heat with stress metabolites by retrieving genes common to (TS+SM vs C) and (TS+SM+UV vs C+UV) but not found in neither in (TS vs C) nor (TS+UV vs C+UV). This showed that 14 genes were repeatedly associated to TS+SM but not explained by heat alone (**Figure 5.7D**). The functional enrichment evidenced that these genes play a role in muscle cells (myocyte enhancer factor 2d *mefd* and myomaker, myoblast fusion factor *mymk*), protein dimerization and DNA binding (*mef2d* and T-cell acute lymphocytic leukemia 1 *tal1*), apelin signalling (*gngt1/mef2d*) as well as neurotransmission (cholinergic receptor *chrng* and *gngt1,* **Figure 5.7D**).

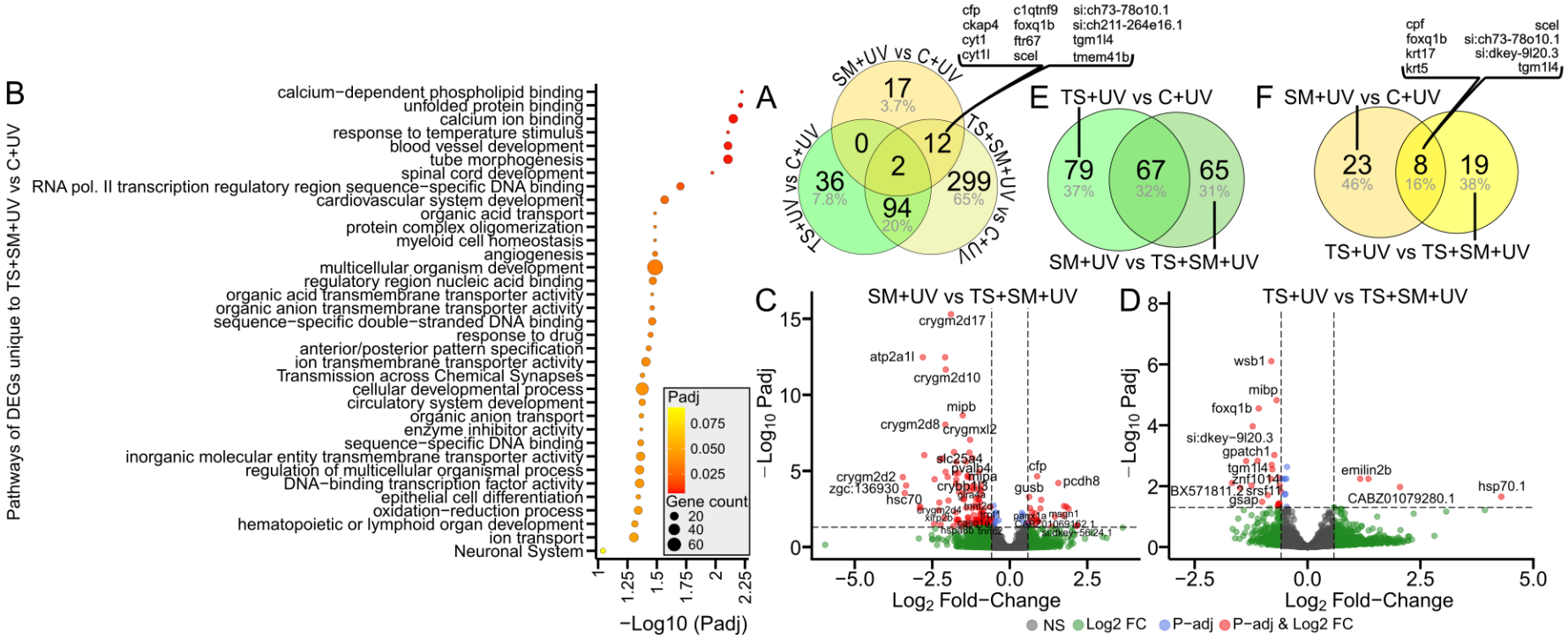

Figure 5.6. Heat stress altered the transcriptomic response to stress metabolites. A) Venn diagram of DEGs in treatments compared to C+UV showing a large portion of genes unique to TS+SM+UV. B) Top 30 (based on highest gene count/term with n ≥ 2 genes/term) functionally enriched terms of the 299 differentially expressed genes found only in TS+SM+UV. Terms show biological processes and molecular functions GO terms, KEGG and Reactome pathways. Volcano plots of D) SM+UV vs TS+SM+UV and F) TS+UV vs TS+SM+UV. Venn diagrams of genes associated with C) thermal stress between TS+UV vs C+UV and SM+UV vs TS+SM+UV, or with E) stress metabolites between SM+UV vs C+UV and SM+UV vs TS+SM+UV. If there was no interaction effect between TS and SM, one would expect the same genes to be differentially expressed when comparing treatments (SM+UV and TS+UV) to C+UV or TS+SM+UV. Rather, large unique percentages in Venn diagrams evidence an interaction of heat and stress metabolites. Volcano plots show differentially expressed genes in red when significant (p-adj < 0.05, |FC| > 1.5). DEGs left to the left vertical line and right to the right vertical line are respectively significantly underexpressed and overexpressed compared to TS+SM+UV.

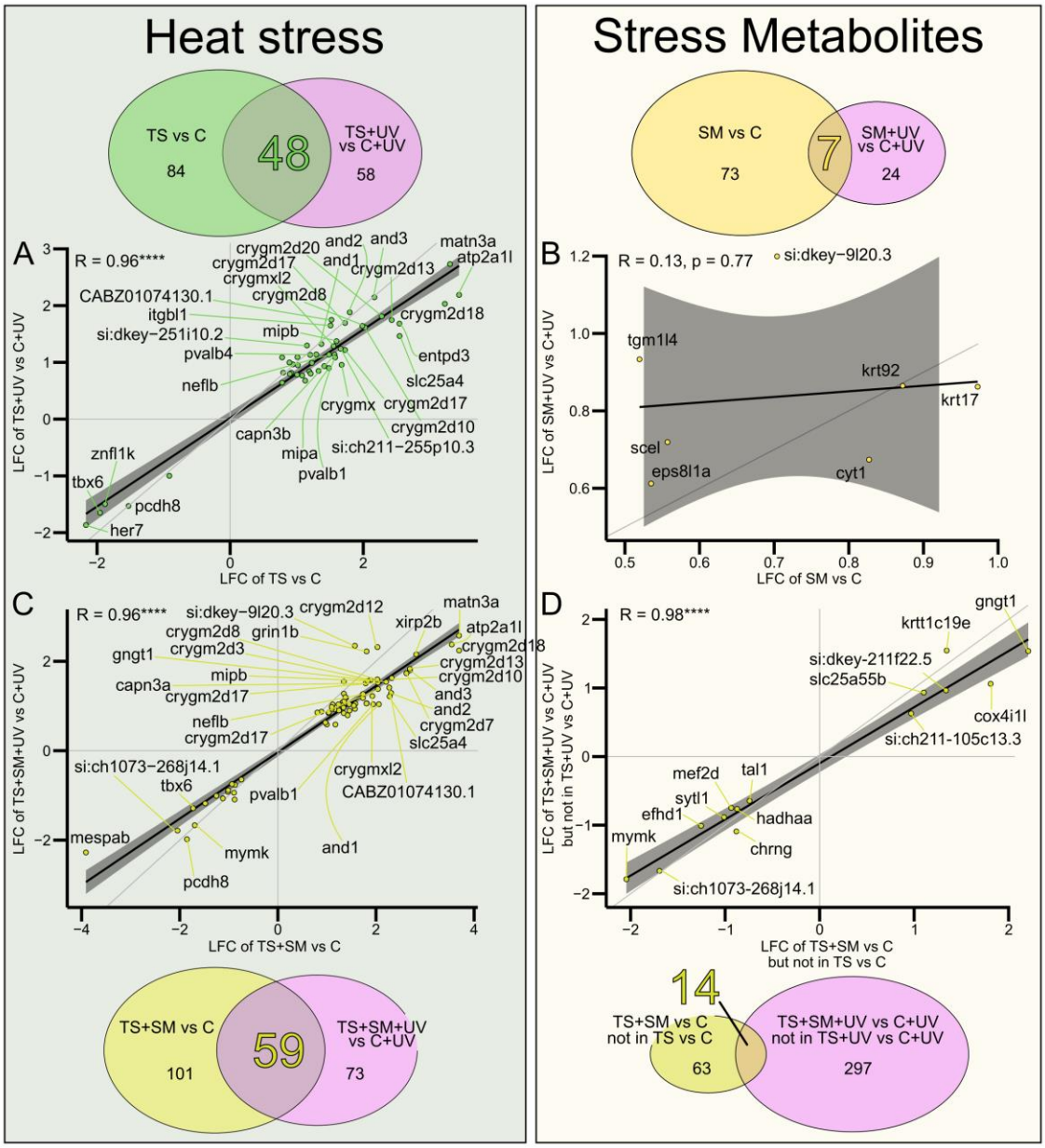

Figure 5.7. Heat and stress metabolites, alone and combined, with and without UV, altered the transcriptome of zebrafish embryos. Comparison of the genes altered by (A) heat stress common to TS vs C and TS+UV vs C+UV, (B) stress metabolites common to SM vs C and SM+UV vs C+UV, and (C) stress metabolites combined with heat stress common to TS+SM vs C and TS+SM+UV vs C+UV. In (D), the transcriptome associated with stress metabolites and/or the interaction effect of TS+SM is shown by the genes common to TS+SM vs C and TS+SM+UV vs C+UV but not induced by heat stress as they are not found in TS vs C and TS+UV vs C+UV. Correlation plots represent genes from shared portions. The cross comparison shows the genes mainly associated with heat stress (left) and stress metabolites (right) in samples with and without UV.

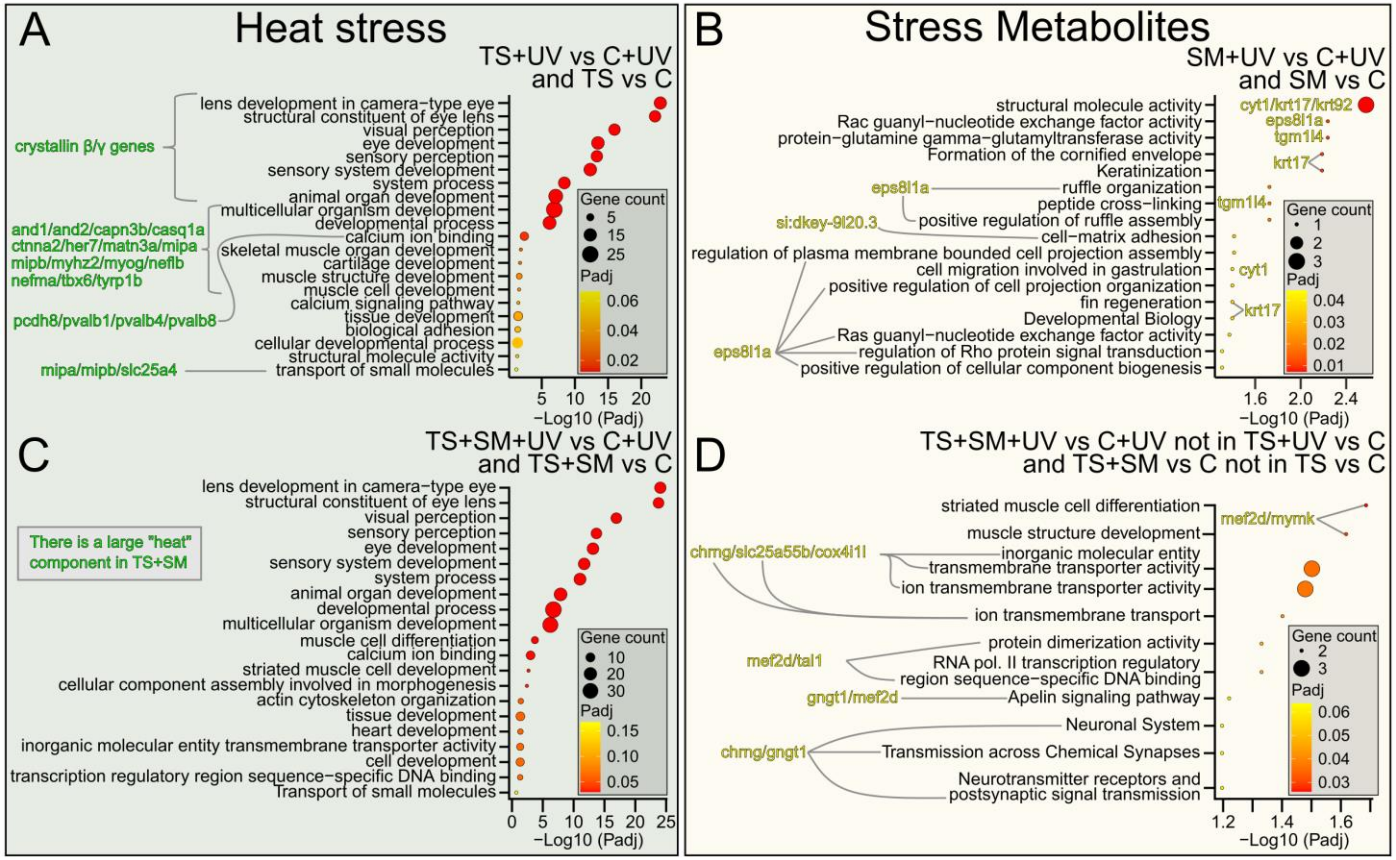

Figure 5.8. Heat altered development whilst stress metabolites induced structural and signalling functions. Functional enrichment of the genes altered by (A) heat stress common to TS vs C and TS+UV vs C+UV, (B) stress metabolites common to SM vs C and SM+UV vs C+UV, and (C) stress metabolites combined with heat stress common to TS+SM vs C and TS+SM+UV vs C+UV. The functional enrichment of the transcriptome associated with stress metabolites and/or the interaction effect of TS+SM is shown in (D) by the genes common to TS+SM vs C and TS+SM+UV vs C+UV but induced by heat stress as they are not found in TS vs C and TS+UV vs C+UV. The cross comparison shows the functions associated with heat stress (left) and stress metabolites (right) in samples with and without UV. Functions combine the top terms of gene ontology for biological processes and molecular functions, and KEGG and Reactome pathways).

5.7.2. A common response to UV exposure existed in all treatments

Next, the response to UVR was analysed for each treatment by comparing treatments followed by UV with their non-UV treated counterparts (C vs C+UV, SM vs SM+UV, TS vs TS+UV, and TS+SM vs TS+SM+UV). Samples clustered by UV treatment along 12% of the variance on PC2 (**Figure 5.5A**). Out of 1013 UV-responsive genes, 127 (12.5%) genes had similar directionality and expression levels in all four treatments in response to UV (**Figure 5.9A-B, Figure 5.10A, Table Appendix 4 S4**). These genes functionally enriched for macromolecule alteration, damage checkpoints, p53- and NF-κB-dependent pathways, immune-response cascades, apoptosis, as well as eye development (**Figure 5.9A** summarised in **Figure 5.10C**). Two major terms involved the metabolism and biosynthesis of macromolecules (GO:0044260; GO:0009059). Several terms were associated with the processing of ribosomes (e.g., dre03010) covering c.a. 30 genes coding for ribosomal protein subunits which expression dropped by approx. 50% in all four treatments in response to UVR. These ribosomal proteins also accounted for the processing of ribosomal RNA (rRNA, GO:0019843) and non-coding RNA (ncRNA, GO:0034660), as well as mRNA surveillance (R-DRE-927802, "Nonsense-Mediated Decay (NMD)"). UV treatments also activated cell cycle DNA damage checkpoints and repair (e.g., KEGG pathway "p53-Dependent G1/S DNA damage checkpoint" and "Nucleotide Excision Repair – NER"). Several terms were linked to NF-κB and immune pathways involving toll-like receptors (TLRs), interleukins, and tumour necrosis factors (TNF), albeit only a few genes ascribed to these functions such as *nfkbiab* (nuclear factor of kappa light polypeptide gene enhancer in B-cells inhibitor, alpha b), *sqstm1* (sequestosome 1), *ubb* (ubiquitin B), *rps27a* (ribosomal protein S27a), *fosab* (v-fos FBJ murine osteosarcoma viral oncogene homolog Ab), *rack1* (receptor for activated C kinase 1), and *ccne1* (cyclin E1). Furthermore, UVR altered the transcription of several chaperone proteins associated with protein refolding and binding (e.g., GO:0051082). These chaperones included four heat shock proteins: *hsp70.2*, *hsp70l*, *hsp90ab1*, and *hspa8*. Both heat shock cognate proteins *hsp70.2* and *hsp70l* were drastically upregulated, whilst *hsp90ab1* and *hspa8* were downregulated by approx. 50%, in all four treatments in response to UVR.

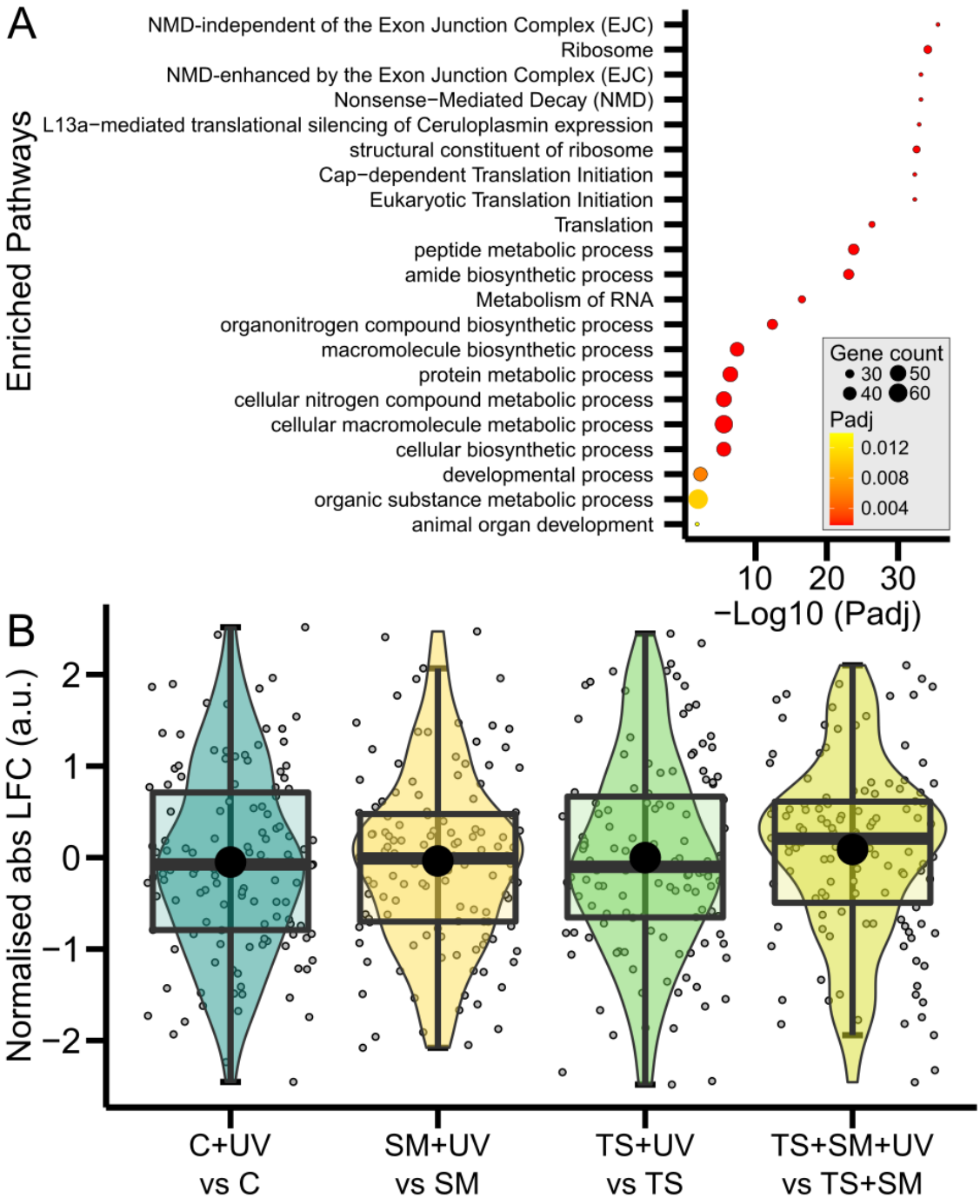

Figure 5.9. The common response to UVR in all treatments. A) Top enriched terms (with highest gene count/term) of Biological Processes, Molecular Functions, KEGG and Reactome pathways sorted by decreasing significance shared by all four UV treatments (C, SM, TS, TS+SM) compared to their non-UV pairs. B) The genes shared by all four treatments in response to UV show the same expression levels. Box-Cox normalised absolute log-fold change (LFC) values in function of treatments do not vary with stress metabolites ($F = 0.32$, $p = 0.5720$) nor heat ($F = 0.96$, $p = 0.3271$) nor their interaction ($F = 0.19$, $p = 0.6645$) according to an ANOVA. Treatments were C: control in fresh medium at 27°C, SM: stress metabolites at 27°C, TS: fresh medium in thermal stress, TS+SM: stress metabolites in thermal stress. All treatments are compared to their non-UV pairs.

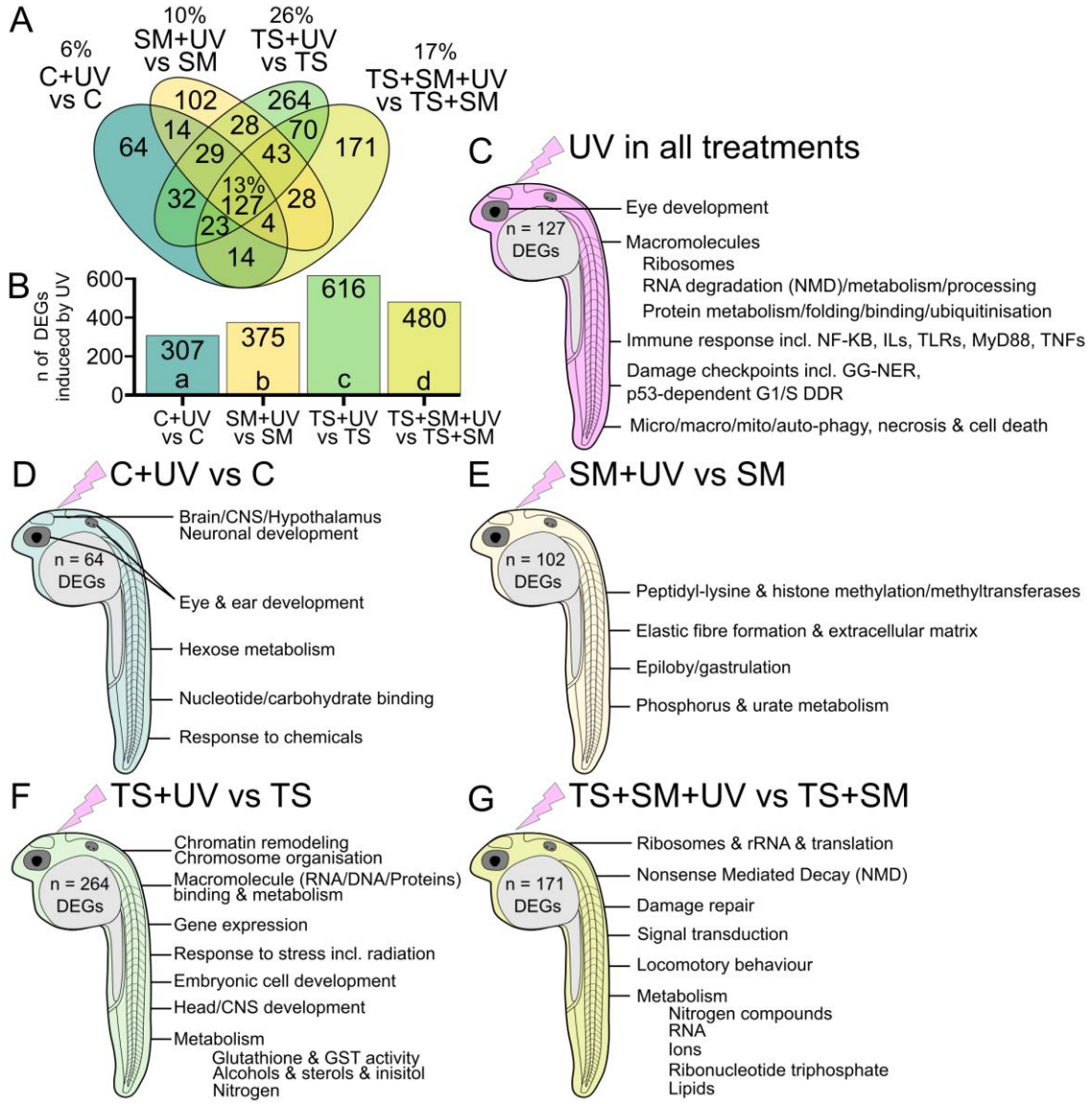

Figure 5.10. Heat stress history potentiated the transcriptomic response to UV exposure and induced a unique transcriptomic response to UV with different biological signatures. Transcriptomic signature of each of the four UV treatments (C, SM, TS, TS+SM) compared to their non-UV pairs. A) Venn diagram and B) counts of DEGs (p-adj < 0.05 and |FC| > 1.5) in response to UV in each treatment. Different letters depict significant pairwise differences in gene counts. Functional enrichment of the genes (C) shared by all four treatments, or (D) unique to C+UV vs C, (E) unique to SM+UV vs SM, (F) unique to TS+UV vs TS, and (G) unique to TS+SM+UV vs TS+SM. Enrichments show the top enriched terms (with highest gene count/term) of Biological Processes, Molecular Functions, KEGG and Reactome pathways sorted by decreasing significance from lists of significant genes (p-adj < 0.05 and |FC| > 1.5). Treatments were C: control in fresh medium at 27°C, SM: stress metabolites at 27°C, TS: fresh medium in thermal stress, TS+SM: stress metabolites in thermal stress, all compared to their non-UV pairs. CNS: central nervous system; DDR: DNA damage response: ILs: interleukins, GG-NER: global genome nucleotide excision repair; GST: glutathione-s-transferase; NMD: nonsense mediated decay; TNFs: tumour necrosis factors; TLRs: toll-like receptors.

5.7.3. Heat stress history potentiated the response to UVR with unique signatures

Additional to the shared response to UVR, the treatment-specific transcriptomic signatures affecting the response to UVR were explored. Stress history treatments strikingly increased the number of UV-responsive genes in SM+UV (n = 375, $\chi^2 = 6.78$,

p = 0.0092), TS+UV (n = 616, χ^2 = 103.0, p < 0.0001), and TS+SM+UV (n = 480, χ^2 = 38.0, p < 0.0001), compared to control C+UV (n = 307, **Figure 5.10B**). The combined treatment TS+SM+UV also significantly increased and decreased the number of significant genes compared to SM+UV (χ^2 = 12.9, p = 0.0007) and TS+UV (χ^2 = 16.9, p = 0.0007), respectively. Compared to C+UV (n = 64 genes, 6.32%), the proportion of treatment-specific UV-responsive genes increased by 60% in SM+UV (n = 102 genes, 10.1%, χ^2 = 8.7, p = 0.0032), more than doubled in TS+SM+UV (n = 171, χ^2 = 48.7, p < 0.0001), and more than quadrupled in TS+UV (n = 264, χ^2 = 122.0, p < 0.0001, **Figure 5.10A**). The combined treatment of heat and stress metabolites TS+SM+UV again induced significantly more and fewer pronounced treatment-specific UV-induced DEGs compared to SM+UV (χ^2 = 17.4, p < 0.0001) and TS+UV (χ^2 = 19.9, p < 0.0001), respectively.

The 64 genes unique to C+UV vs C, which represent the general response to UVR, were associated with eye/ear development, neuron development in the brain (hypothalamus and central nervous system), hexose metabolism (GO:0019318), "response to chemicals" (GO:0042221, including for example peroxiredoxin *prdx1* and another heat shock protein, *hsp90aa1.2*), and nucleotide/carbohydrate binding (**Figure 5.10D**, **Figure Appendix 4 S2A**). The 102 genes unique to SM+UV vs SM were significantly enriched for peptidyl-lysine methylation (GO:0018022) with three notable genes, *eef1akmt2* (EEF1A lysine methyltransferase 2), *smyd1b* (SET and MYND domain containing 1b), and *suv39h1a* (SUV39H1 histone lysine methyltransferase a, **Figure 5.10E**, **Figure Appendix 4 S2B**). The 264 genes unique to TS+UV vs TS were primarily associated with the regulation of gene expression (GO:0010467) and RNA metabolism (e.g. GO:0016070), brain and CNS development (e.g. GO:0007417), response to stimulus including radiation (e.g. GO:0009314), which may lead to the metabolism of glutathione (GO:0006749 including several glutathione S-transferases *gstt1b*, *gstp1*, *gsto2*, and *gstk2*), and inositol (GO:0032958) and cholesterol (genes in sterols/alcohols GO terms, GO:0016125/GO:0006066, **Figure 5.10F**, **Figure Appendix 4 S2C**). The 171 genes altered only in TS+SM+UV vs TS+SM were mainly associated with metabolism, particularly of ribonucleotides (GO:0009259) and nucleotide di/triphosphates, the homeostasis of ions (e.g. GO:0055080), signal transduction, but also further ribosomal deactivation (with 28 more rRNA downregulated) and nonsense-mediated decay (NMD, **Figure 5.10G**, **Figure Appendix 4 S2D**). Of note, TS+SM+UV also induced several locomotory and swimming behaviour genes (GO:0007626),

namely *atoh7* (atonal bHLH transcription factor 7), *gdpd5a* (glycerophosphodiester phosphodiesterase domain containing 5a), *htr2cl1* (5-hydroxytryptamine (serotonin) receptor 2C, G protein-coupled-like 1), *pleca* (plectin a), and *pogza* (pogo transposable element derived with ZNF domain a).

5.7.4. Candidate pathways of UV-induced damage and repair

Heat stress history-dependent responses to UVR were further explored within candidate pathways associated with macromolecule processing: "RNA integrity", "DNA repair" (GO:0006281), "protein folding" (chaperone response, GO:0006457), "regulation of gene expression, epigenetic" (GO:0040029), and "macromolecule methylation" (GO:0043414, **Table Appendix 4 S4**).

5.7.4.1 RNA integrity

UVB+A exposure degraded RNA as evidenced by the significantly lowered RNA integrity number ($F = 6.44$, $p = 0.0195$). However, there were no effects of heat ($F = 0.01$, $p = 0.9192$) nor stress metabolites ($F = 0.18$, $p = 0.6750$) on RNA integrity (**Figure** 5.11, **Table Appendix 4 S5**).

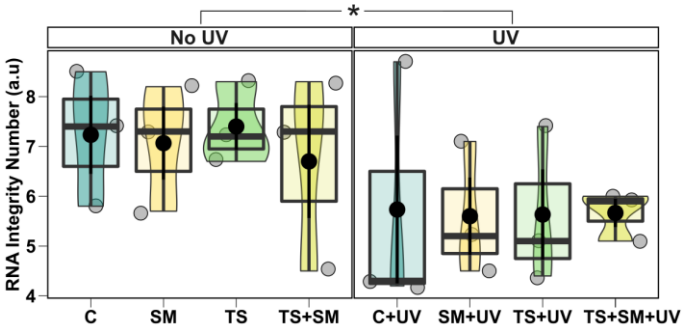

Figure 5.11. UV exposure, but not stress history from neither heat nor medium, degraded RNA integrity. C: control in fresh medium at 27°C, SM: stress metabolites at 27°C, TS: fresh medium in thermal stress, TS+SM: stress metabolites in thermal stress, all without (left, "no UV") or with UVB+A ("+UV", right). *: $p < 0.05$.

5.7.4.2 DNA repair

Two DNA repair genes, namely *eya1* (EYA transcriptional coactivator and phosphatase 1) and *fancf* (FA complementation group F), were respectively down- and up-regulated in all treatments in response to UVR (**Figure 5.12A-B**). There were more significant UV-responsive genes associated with DNA repair in response to heat stress ($n = 19$ genes, $\chi^2 = 5.54$, $p = 0.0186$) compared to control temperature ($n = 7$ genes), whilst stress metabolites had no effect ($\chi^2 = 0.0$, $p = 1.0000$, **Figure 5.12A-B**). Heat stress ($H = 4.23$, $p = 0.0397$ – albeit with a "very small effect size" $|d| = 0.11$), but not stress metabolites ($H = 0.49$, $p = 0.4849$), significantly increased the magnitude of mRNA expression of DNA repair genes (Figure 5.12C, **Table Appendix 4 S4**). The

initial hypothesis was that stress history would limit DNA repair capacities in response to UVR, but unexpectedly, TS+UV altered 7 DNA repair genes that were not found in C+UV. Six such genes were upregulated, namely *adprhl2* (ADP-ribosylhydrolase like 2), *cry5* (cryptochrome circadian regulator 5), *nthl1* (nth-like DNA glycosylase 1), *prmt6* (protein arginine methyltransferase 6), *rmi2* (RecQ mediated genome instability 2), and *ube2al* (ubiquitin conjugating enzyme E2 A, like), whereas *zfyve26* (zinc finger, FYVE domain containing 26) was downregulated by TS+UV. One DNA repair gene, *apex2* (Apurinic/Apyrimidinic Endodeoxyribonuclease 2), was significantly upregulated in all heat stress history conditions but not in C+UV (**Figure 5.12B**). Furthermore, several DNA repair genes deviated from the expected 1-to-1 ratio of identical expression evidencing perturbations of the DNA repair pathway by stress history compared to C+UV (**Figure 5.12D-F**).

5.7.4.3 Chaperone proteins

The protein folding activity (GO:0006457) was consistent in response to UVR in all treatments, when comparing the chaperone activity gene expression in UV vs non-UV pairs. There were 7 genes shared by all four treatments, including three HSPs (*hsp70l*, *hsp90ab1*, and *hspa8*), but also *dnajb1b* (DnaJ heat shock protein family [Hsp40] member B1), *ppiaa* (peptidylprolyl isomerase Aa), *tbcc* (tubulin folding cofactor C), and *zgc:122979* (i.e. also an HSP 40 kD with its human orthologue being DNAJB5) (**Figure 5.13A-B**). The proportion and the expression magnitude of UV-induced protein folding genes were not altered by heat (Chi-squared test of proportion: $\chi^2 = 1.47$, $p = 0.2250$; ANOVA test of LFC: $F = 0.2$, $p = 0.6736$) and medium (Chi-squared test of proportion: $\chi^2 = 0.02$, $p = 0.8930$; ANOVA test of LFC: $F = 0.0$, $p = 0.9862$, **Figure 5.13A-C**, **Table Appendix 4 S4**). However, compared to C+UV vs C, TS+SM+UV vs TS+SM led to a drastic drop – sometimes losing their significance – in the magnitude of expression of several hallmark genes of the general UV-induced response in C+UV, such as *hsp70.3* (heat shock cognate 70-kd protein, tandem duplicate 3), *hsp90aa1.2*, *fkbp1b* (FKBP prolyl isomerase 1B), as well as *dnajb1*and *dnaja1b* (**Figure 5.13F**). Particularly, *hsp70l* increased by 200-fold in C+UV compared to C, but only 6-fold in TS+SM+UV compared to TS+SM, indicating a 30-fold drop in its expected UV induction.

5.7.4.4 Methylation

Overall, macromolecule methylation (GO:0043414) remained stable in all treatments in response to UVR as there heat and medium factors had no effects in neither the proportion of genes (heat: $\chi^2 = 0.29$, $p = 0.5930$; medium: $\chi^2 = 1.14$, $p = 0.2850$) nor their transcription magnitude (albeit a trend for heat: $F = 2.75$, $p = 0.0981$; but not stress metabolites: $F = 0.31$, $p = 0.5772$, **Figure 5.14A-C**, **Table Appendix 4 S4**). However, there was a marginal effect of stress metabolites on methylation, as they activated *suv39h1a* (suppressor of variegation 3-9 homolog 1a) and repressed *smyd1b* (SET and MYND domain containing 1b, **Figure 5.14A-B, D**) which were not found in C+UV.

5.7.4.5 Epigenetic

In response to UVR, stress metabolites ($\chi^2 = 5.0$, $p = 0.0253$), but not heat stress ($\chi^2 = 0.2$, $p = 0.6550$), activated several epigenetic regulators (GO:0040029, Figure 5.15A). There were four genes found in stress metabolites treatments otherwise not present in C+UV: *bmi1b* (bmi1 polycomb ring finger oncogene 1b), *srrt* (serrate RNA effector molecule homolog), as well as two histone linkers, *h1-0* and *si:ch73-368j24.12* (human ortholog: H1.5 linker histone). Stress metabolites also altered the normal UV-induced epigenetic gene expression since the expected 1-to-1 correlation between SM+UV and C+UV was perturbed ($R = 0.18$, $p = 0.098$, Figure 5.15A). Of note, heat marginally tended ($p < 0.1$) to increase the magnitude of gene expression of epigenetic processes (**Figure 5.15B**, **Table Appendix 4 S4**).

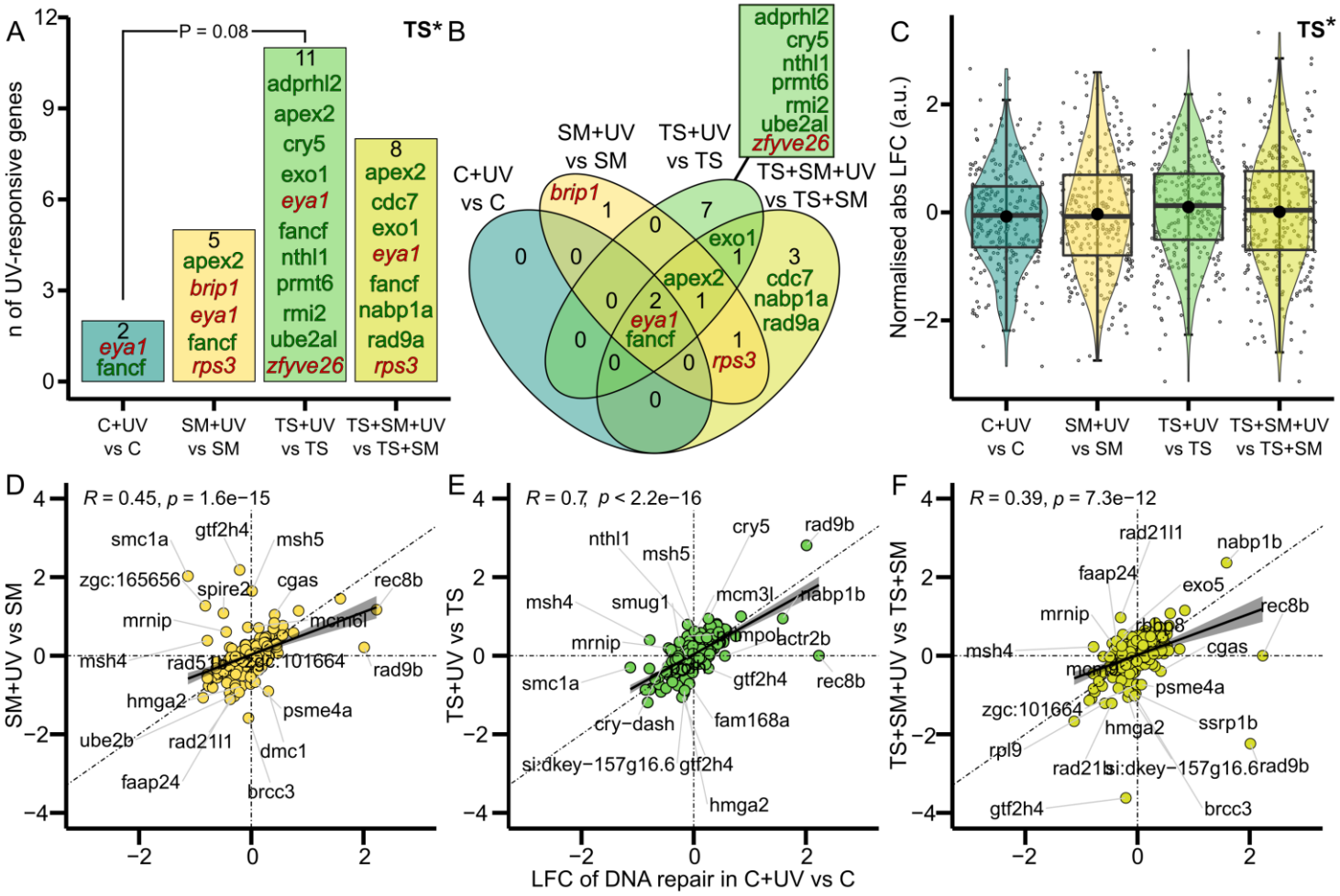

Figure 5.12. Heat potentiated, and stress deviated, the UV-induced transcriptomic DNA repair response. A) Counts and B) Venn diagram of DEGs from DNA repair (GO:0006281, 288 total genes) in each treatment in response to UVR. Dark green and italicised dark red font respectively indicates up- and downregulation (GO-term wide p-adj < 0.05 and |FC| > 1.5). C) Magnitude (normalised absolute log FC, LFC) of UV-induced DNA repair gene expression. Heat stress (TS) is a significant predictor shown on top-right corners in A (χ^2 test) and C (Scheirer-Ray-Hare test) with *: p < 0.05. Bottom row: LFC of gene expression in DNA repair pathway in response to UVR in (D) SM, (E) TS, and (F) TS+SM treatments (y-axes) compared to C (x-axes). The null hypothesis is that UV responses are similar for all treatments, following 1-to-1 ratios (diagonal lines). Solid black lines and shaded areas depict linear fits and confidence intervals. Labels show top 20 genes with the most pronounced deviation relative to C. C: control in fresh medium at 27°C, SM: stress metabolites at 27°C, TS: fresh medium in thermal stress, TS+SM: stress metabolites in thermal stress all compared to their non-UV pairs.

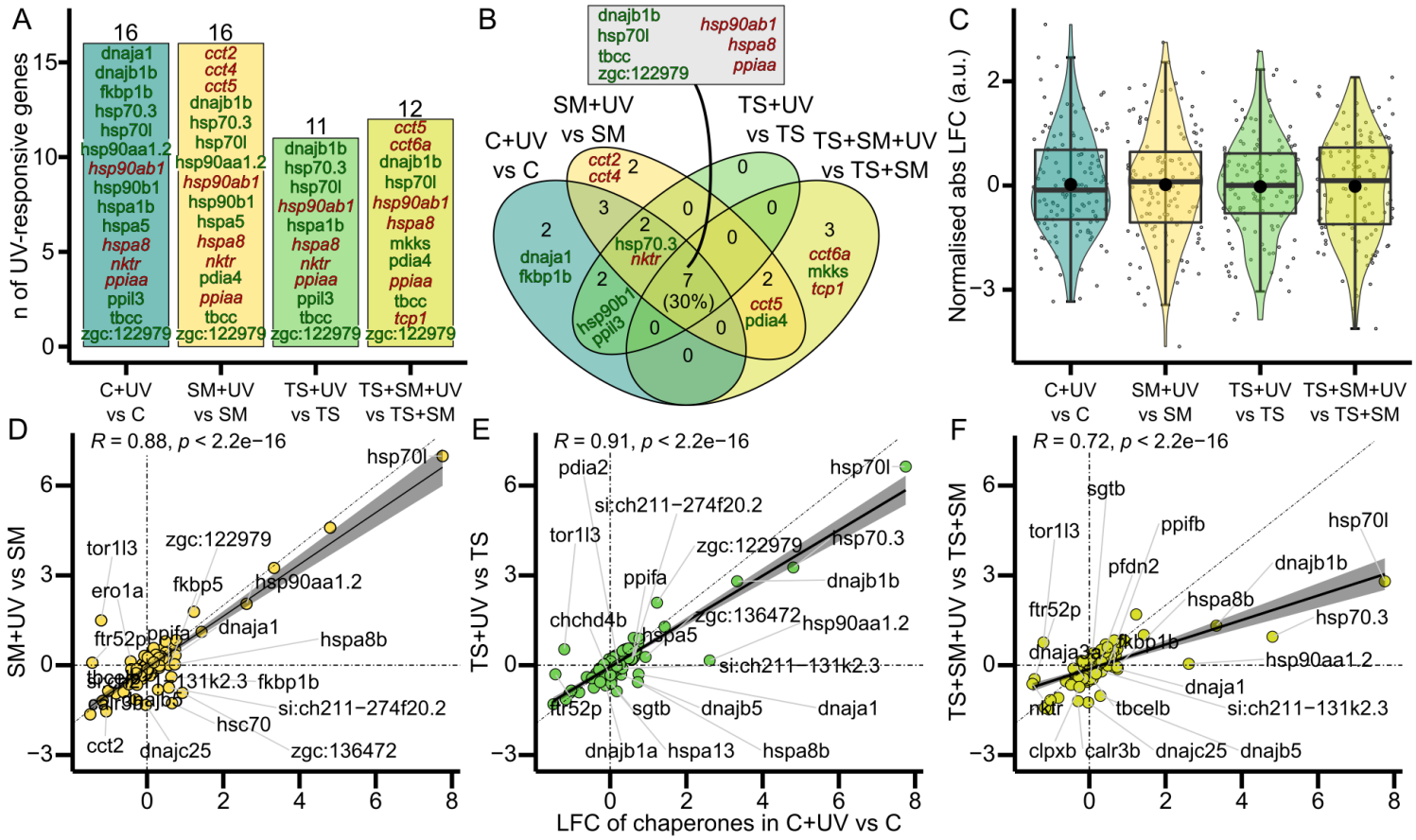

Figure 5.13. Multistress TS+SM dampened the normal chaperone response to UVR for a few genes. A) Counts and B) Venn diagram of significant genes from protein folding (GO:0006457, n = 125 genes) in each treatment in response to UVR. Non-italicised dark green and italicised dark red gene names respectively indicate up- and downregulation (GO-term wide P-adj < 0.05 and |FC| > 1.5). C) Magnitude of UV-induced protein folding gene expression change represented by the normalised absolute log-fold change (LFC). Model terms (heat × medium) are not significant in A (χ^2 test) and C (Scheirer-Ray-Hare test). Bottom row: $\log_2$ FC of protein folding genes in (D) SM+UV-SM, (E) TS+UV vs TS, and (F) TS+SM+UV vs TS+SM (y-axes) compared to C+UV vs C (x-axes). The null hypothesis is that the UV-induced response is similar for all treatments, following 1-to-1 ratios (diagonal lines). Solid black lines and shaded areas depict linear fits and confidence intervals. Labels indicate the top 20 genes with the most pronounced deviation relative to C. Treatments were C: control in fresh medium at 27°C, SM: stress metabolites at 27°C, TS: fresh medium in thermal stress, TS+SM: stress metabolites in thermal stress all compared to their non-UV pairs.

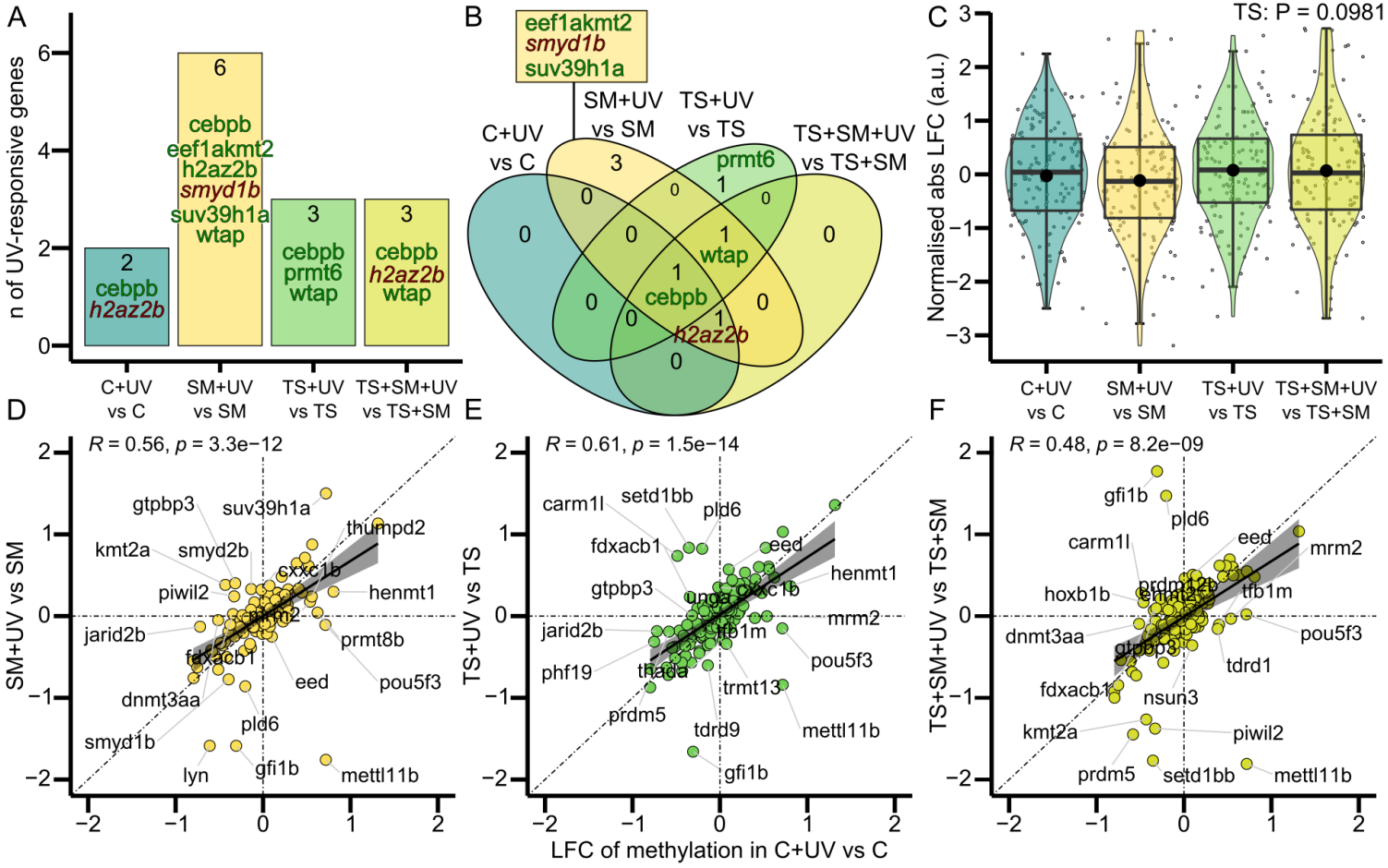

Figure 5.14. Stress metabolites altered the methylation response to UV. A) Counts and B) Venn diagram of significant genes from methylation (GO:0043414, n = 131 genes) in each treatment in response to UV. Non-italicised dark green and italicised dark red gene names respectively indicate up- and downregulation (GO-term wide P-adj < 0.05 and |FC| > 1.5). C) Magnitude of UV-induced methylation gene expression change represented by the normalised absolute log-fold change (LFC). Model terms (heat × medium) are not significant in A (χ^2 test) and C (ANOVA, albeit a trend for heat). Bottom row: $\log_2$ FC of methylation genes in (D) SM+UV-SM, (E) TS+UV vs TS, and (F) TS+SM+UV vs TS+SM (y-axes) compared to C+UV vs C (x-axes). The null hypothesis is that the UV-induced response is similar for all treatments and respects a 1-to-1 ratio (diagonal lines). Solid black lines and shaded areas depict linear fits and confidence intervals. Labels indicate the top 20 genes with the most pronounced deviation relative to C. C: control in fresh medium at 27°C, SM: stress metabolites at 27°C, TS: fresh medium in thermal stress, TS+SM: stress metabolites in thermal stress all compared to their non-UV pairs.

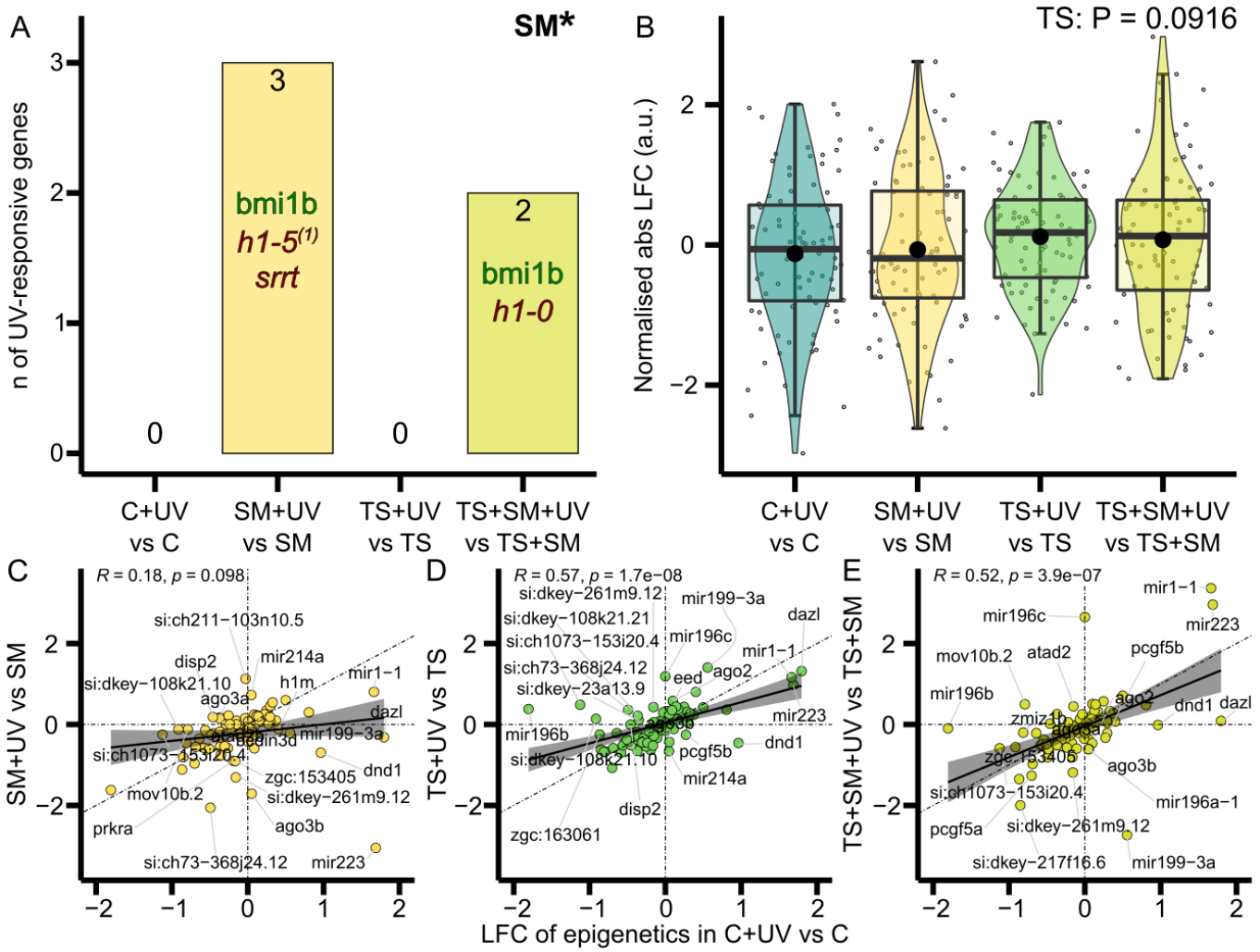

Figure 5.15. Stress metabolites activated epigenetic processes in response to UVR. A) Counts of significant epigenetic genes (GO:0040029, n = 84 genes) in each treatment in response to UVR. Non-italicised dark green and italicised dark red gene names respectively indicate up- and downregulation (GO-term wide p-adj < 0.05 and |FC| > 1.5). B) Magnitude of UV-induced epigenetic gene expression change shown by the normalised absolute $\log_2$ FC. Stress metabolites induced more epigenetic genes in A (χ^2 test) and heat tends to increase LFC in C (Scheirer-Ray-Hare test). Bottom row: $\log_2$ FC of epigenetic genes in (C) SM+UV-SM, (D) TS+UV vs TS, and (E) TS+SM+UV vs TS+SM (y-axes) compared to C+UV vs C (x-axes). The null hypothesis is that the UV-induced response is similar for all treatments and respects a 1-to-1 ratio (diagonal lines). Solid black lines and shaded areas depict linear fits and confidence intervals. Labels indicate the top 20 genes with the most pronounced deviation relative to C. C: control in fresh medium at 27°C, SM: stress metabolites at 27°C, TS: fresh medium in thermal stress, TS+SM: stress metabolites in thermal stress all compared to their non-UV pairs. (1) human ortholog of si:ch73-368j24.12.

5.7.5. Heat rescued embryos, stress metabolites induced hypoactivity, and TS+SM overwhelmed rescuing capacities

Next, I asked how heat stress history combined with UVR translated into long-lasting whole-organism phenotypic alterations by measuring a range of several phenotype responses 1 and 3 days following the exposure to stress and UVR.

5.7.5.1 Stress had no effect on mortality and heat advanced hatching upon UVR

There were no differences in mortalities with heat stress ($z = 0.24$, $p = 0.8079$), stress metabolites ($z = 0.17$, $p = 0.8618$), and their interaction term ($z = -0.24$, $p = 0.8125$), as > 95% of embryos survived the UVB+UVA exposure regardless of treatments (**Figure 5.16A, Table Appendix 4 S6**). Heat stress ($z = 2.8$, $p = 0.0051$) significantly facilitated hatching at 4 dpf with a significant increase from 11% hatched embryos in C+UV to 50% in TS+UV ($z = -2.8$, $p = 0.0306$), whilst stress metabolites ($z = 0.32$, $p = 0.7528$) had no effect on hatching (**Figure 5.16B, Table Appendix 4 S6**).

5.7.5.2 Heat rescued embryos from UVR

Although heat ($F = 1.75$, $p = 0.1891$) and medium ($F = 0.37$, $p = 0.5424$) factors were not significant predictors of growth, there was a significant effect of the interaction term ($F = 16.1$, $p = 0.0002$) on embryo length at 4 dpf. As a result, embryos in SM+UV ($t = -2.3$, $p = 0.0491$) and TS+UV ($t = 3.8$, $p = 0.0016$) were significantly longer than in control C+UV (**Figure 5.16G, Table Appendix 4 S7**). Conversely, embryos in multistress treatment TS+SM+UV grew smaller than in TS+UV ($t = 3.3$, $p = 0.0035$) with a similar trend relative to SM+UV ($t = 1.9$, $p = 0.0937$, **Figure 5.16G**). Stress metabolites ($F = 4.9$, $p = 0.0287$), heat ($F = 2.9$, $p = 0.0945$ – albeit a trend), and their interaction ($F = 4.8$, $p = 0.0317$) significantly altered the 4-dpf embryo size-normalised pericardial width (**Figure 5.16J, Table Appendix 4 S7**). Post-hoc comparisons revealed that embryos in TS+UV had significantly smaller pericardial widths relative to their whole-body sizes, compared to C+UV ($t = 2.91$, $p = 0.0104$ and SM+UV ($t = 2.87$, $p = 0.0104$), indicative of a protective effect against heart edema. However, this edema-limiting protective effect disappeared in the multistress treatment TS+SM+UV in which embryos had wider pericardia compared to TS+UV ($t = -3.11$, $p = 0.0104$, **Figure 5.16J**). Coincidently, embryos experiencing heat stress ($z = -3.3$, $p = 0.0010$), but not stress metabolites ($z = -1.6$, $p = 0.1190$), showed fewer pericardial edema at 4 dpf (Figure 5.16C**, Table Appendix 4 S6**). The significant interaction term ($z = 2.6$, $p = 0.0093$) revealed a significant and strong decrease of pericardial edemas only in TS+UV

(32%, z = 3.3, p = 0.0059) compared to C+UV (82%, **Figure 5.16C**). Embryos exposed to TS+UV also had the lowest defect score (sum of binary code individual defects) albeit not significant relative to C+UV (**Figure 5.16I, Table Appendix 4 S7**). Heat stress (F = 8.27, p = 0.0051), but not stress metabolites (F = 0.01, p = 0.9071) nor the interaction term (F = 0.94, p = 0.3349), significantly increased eye-to-body size ratios following exposure to UVR. The multistress treatment TS+SM+UV tending to have increased such ratios relative to C+UV (t = -2.29, p = 0.0735) and SM+UV (t = -2.68, p = 0.0522, **Figure 5.16H, Table Appendix 4 S7**).

Interestingly, in addition of the growth and hatching benefits of the TS+UV treatment, there was several hints that embryos in TS+UV performed better in the behavioural assays at 4-dpf compared to other treatments. Indeed, embryos in TS+UV always (despite not being significant in the post-hoc comparisons) displayed the highest swimming performances. This held true for the dark-light response with embryos in TS+UV having the highest number of active embryos (74% compared to ≤ 50% in C+UV, SM+UV, TS+SM+UV, **Figure 5.16D**), the highest mean activity percentage (**Figure 5.16K**), the longest distance swam (**Figure 5.16L**), the highest median burst count (**Figure 5.16M**), and the highest mean speed (**Figure 5.16N**). Similarly, embryos in TS+UV had the longest total distance and the highest mean swimming speed in response to touch stimuli at 4 dpf (**Figure 5.16O-P**).

In most cases, swimming performances were positively associated with embryo sizes but negatively correlated with pericardial edema, size-normalised pericardial width, and defect scores (**Figure 5.16** – all of which were morphological consequences of exposure to TS+UV). Of note, defect scores (ρ = -0.65, p < 0.05) and pericardial edemas (ρ = -0.5, p < 0.05) were negatively associated with embryo length. This indicates a mechanism of action by which heat limited damage in response to UVR, in turn correlating with better behavioural fitness outcomes. However, TS did not rescue embryos from swimming fatigability after three stimuli in the touch-evoked assay (**Table Appendix 4 S10**), nor heart rates at 1 and 4 dpf (**Table Appendix 4 S11**), which were similar across all treatments (**Figure Appendix 4 S3**).

5.7.5.3 Heat and stress metabolites induced hypoactivity at 1 dpf

Both heat stress (H = 38.1, p < 0.0001) and stress metabolites (H = 3.96, p = 0.0465), but not their interaction (H = 1.15, p = 0.2832), significantly reduced acute light-induced burst activity percentages in 1-dpf embryos (**Figure 5.16E, Table**

Appendix 4 S8). Post-hoc tests evidenced that TS+UV ($W = 457$, $p = 0.0009$) and TS+SM+UV ($W = 661$, $p < 0.0001$) significantly reduced burst activity percentages compared to C+UV (**Figure 5.16E**). This pattern was similar for the 1-dpf burst counts per minute which was significantly reduced by heat stress ($H = 6.55$, $p = 0.0105$) and stress metabolites ($H = 7.82$, $p = 0.0052$) but not their interaction ($H = 2.2$, $p = 0.1378$, **Figure 5.16F, Table Appendix 4 S8**).

5.7.5.4 Stress metabolites induced hypoactivity at 4 dpf

Stress metabolites ($H = 3.86$, $p = 0.04955$) significantly reduced the burst activity percentage in the dark-light swimming behaviour assay (**Figure 5.16K, Table Appendix 4 S9**). Stress metabolites also tended to lower both dark-light swimming burst counts ($H = 3.37$, $p = 0.0663$) and touch-evoked average swimming speeds ($F = 3.64$, $p = 0.0599$) at 4 dpf, despite the positive effects ($\rho = 0.4$, $p < 0.0001$, **Figure 5.16C, Table Appendix 4 S10**) of embryo sizes (which, as mentioned above, were increased in SM+UV).

5.7.5.5 Embryos in multistress treatment TS+SM performed worst in UVR

Whilst both TS+UV and SM+UV induced faster growth, embryos in TS+SM+UV lost this developmental effect and grew smaller compared to TS+UV ($t = 3.3$, $p = 0.0035$) and SM+UV ($t = 1.89$, $p = 0.0937$ – albeit a trend), to similar sizes as in the control C+UV ($t = -0.32$, $p = 0.7474$, **Figure 5.16G**). Edema-protective effects evidenced in TS+UV were lost in TS+SM+UV ($t = -3.11$, $p = 0.0104$), which had pericardial widths similar to the control C+UV ($t = -0.35$, $p = 0.8889$, **Figure 5.16C**). Likewise, the proportion of embryos with pericardial edemas doubled in TS+SM+UV compared to TS+UV (although not significant, $z = -2.12$, $p = 0.1008$, **Figure 5.16C**). Defect scores of embryos in TS+SM+UV were also higher than in TS+UV ($W = 116$, $p = 0.0490$, **Figure 5.16I, Table Appendix 4 S7**). Post-hoc tests evidenced that TS+SM+UV had the lowest 1-dpf burst activity percentages compared to TS+UV ($W = 383$, $p = 0.005$, **Table Appendix 4 S8**). Similarly, TS+SM+UV resulted in the lowest burst counts per min in the 1-dpf startle response compared to all other treatments – themselves not different from one another (**Figure 5.16A**). The 4-dpf swimming assays also tended to show that embryos in TS+SM+UV performed worst, and were hypoactive, compared to those incubated in TS+UV, both for the dark-light and touch-evoked responses (**Figure 5.16**). Overall, this evidenced that the multistress treatment TS+SM+UV induced more defects and negative outcomes compared to TS+UV.

5.7.5.6 Nonlinear relationship between fitness responses and heat stress history

The statistical analysis of individual variables suggested that (i) TS treatment ameliorated performances at 4 dpf, (ii) heat stress experienced indirectly through SM altered epigenetic and methylation profiles associated with phenotypic changes, and that (iii) TS+SM+UV had the lowest performances at 1 dpf compared to C+UV and at 4 dpf compared to TS+UV. This would mean that the relationship between the performance in response to UV and the intensity of heat stress history is nonlinear. To verify this hypothesis, another set of analyses involved separate multivariate analyses (PERMANOVAs) of the data at 1 dpf and 4 dpf (**Figure 5.17A-B**). The reason to perform separate analyses at 1 and 4 dpf was to account for age-specific responses to UV.

The PERMANOVA confirmed a significant effect of heat ($F = 28.0361$, $p = 0.001$), stress metabolites ($F = 9.14$, $F = 0.001$), and their interaction term ($F = 3.33$, $p = 0.046$) on the multivariate behavioural response to the light-induced startle response at 1 dpf (**Table Appendix 4 S12**). Pairwise post-hoc comparisons further evidenced a significant difference between TS+UV ($F = 7.78$, $p = 0.006$) and TS+SM+UV ($F = 34.74$, $p = 0.006$) compared to C+UV. In addition, the response of TS+SM+UV significantly differed compared to SM+UV ($F = 17.99$, $p = 0.006$) and TS+UV ($F = 8.27$, $p = 0.024$, **Table Appendix 4 S12**). These effects were apparent when representing the centroids of the coordinates from the first two variance contributors of the principal component analysis, showing that heat treatments differed from control temperature conditions, with the addition of stress metabolites in TS+SM+UV accentuating these differences further (**Figure 5.17A**). Regarding the 4-dpf multivariate data, on the other hand, only TS+UV was significantly distinct from C+UV ($F = 5.62$, $p = 0.03$) and tended to marginally differ from both SM+UV ($F = 4.72$, $p = 0.078$) and TS+SM+UV ($F = 4.69$, $p = 0.066$, **Table Appendix 4 S12**). This was confirmed by the centroid of TS+UV being distant from other treatments along PC1 (40.3% of the variance) of the principal component analysis, with TS+UV being associated with higher fitness-relevant scores along PC1 at 4 dpf after recoding the variables so that higher values indicate an advantage for fitness (**Figure 5.17B**).

Since PC1 respectively represented 70.7% and 40.3% of the multidimensional variance at 1 and 4 dpf, it can be used as a "fitness score" (where higher values along PC1 indicate better fitness outcomes, as represented by loading directions in **Figure 5.17**) representing the general outcome of the response to UVR in all treatments.

Pairwise comparisons confirmed that TS+SM+UV had significantly lowest fitness scores (i.e. lowest activity levels in response to an acute light change) at 1 dpf compared to C+UV ($t = 5.92$, $p < 0.0001$), SM+UV ($t = 5.72$, $p < 0.0001$), and TS+UV ($t = 4.22$, $p < 0.0001$, **Table Appendix 4 S12**). A *loess* smoothed trend line confirmed the lowest fitness score in TS+SM+UV (**Figure 5.17C**). However, TS+UV was the most different treatment at 4 dpf, with an increased 4-dpf fitness score compared to C+UV ($t = -3.47$, $p = 0.0049$), SM+UV ($t = -2.54$, $p = 0.0257$), and TS+SM+UV ($t = 3.05$, $p = 0.0094$), trends that were confirmed by *loess* smoothed lines (**Table Appendix 4 S12**, **Figure 5.17D**).

These PERMANOVAs and ANOVAs of PC1 data helped to confirm the trends seen in individual variable analyses: embryos in TS+SM+UV performed worse at 1 dpf compared to all other treatments, and worse than TS+UV at 4 dpf; whilst TS+UV had the highest fitness advantage at 4 dpf. Next, averaging 1-dpf and 4-dpf fitness scores (i.e., PC1 values) helped summarising the overall outcome of the response to UV in zebrafish embryos and larvae. Zebrafish in TS+UV had the highest average fitness score, which was significantly higher than C+UV ($t = -2.51$, $p = 0.0422$) and TS+SM+UV ($t = 3.9$, $p = 0.0010$). TS+SM+UV also tended to have lower fitness scores compared to C+UV ($t = 1.76$, $p = 0.0983$) and SM+UV ($t = 2.24$, $p = 0.0550$, **Table Appendix 4 S12**, **Figure 5.17E**). The *loess* smoothed trend line of the average fitness score confirmed that the fitness outcome in response to UVR peaked if embryos experienced TS alone but dropped in embryos that were exposed to the multistress treatment TS+SM (**Figure 5.17E).** Therefore, these additional analyses confirmed the nonlinear relationship between heat stress history intensity and the fitness response to UVR.

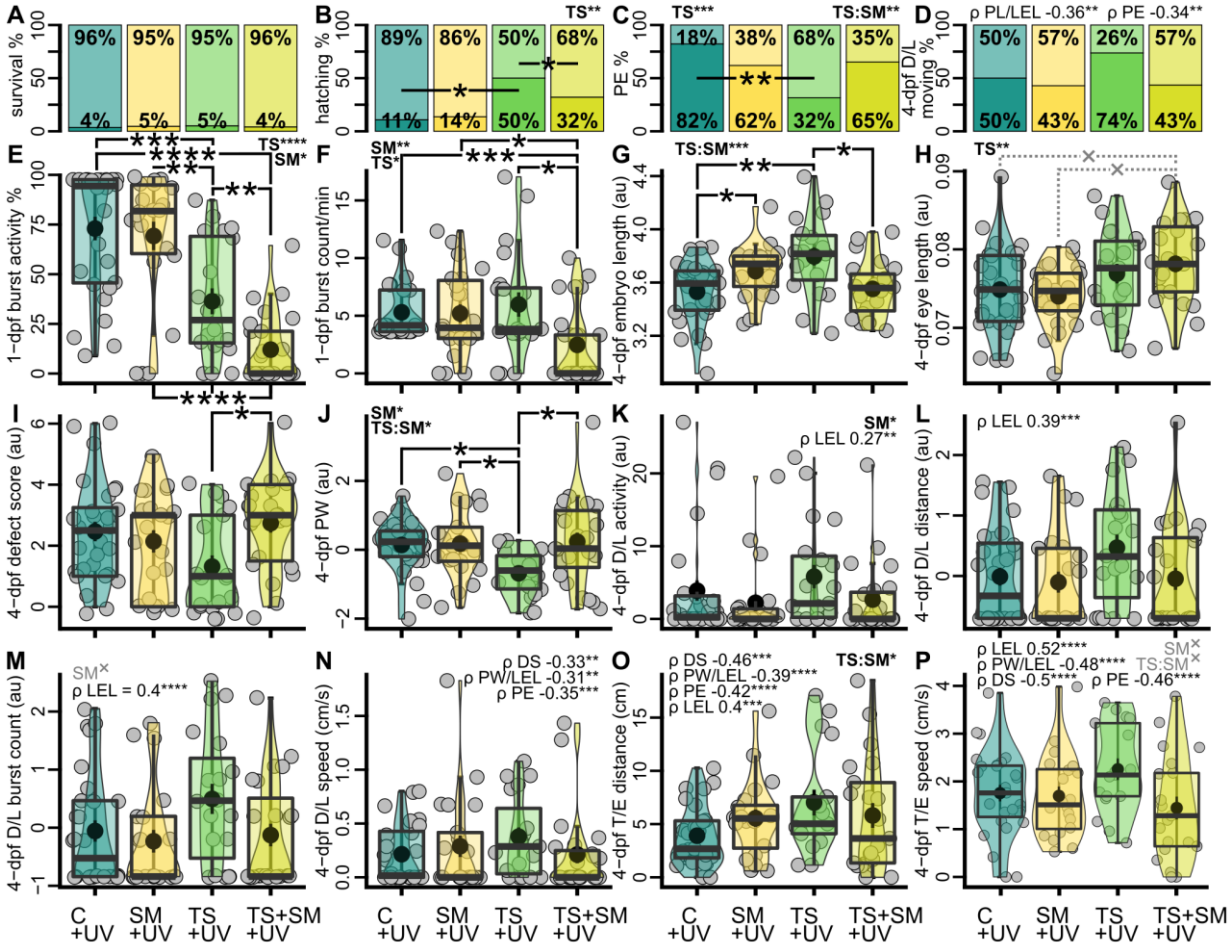

Figure 5.16. Stress metabolites impaired behaviour whilst heat tended to facilitate swimming through better repair. Behaviour and fitness outcome at 1 day and 4 days post fertilisation (dpf). Values in arbitrary units (au) are transformed to fit parametric assumptions. A) % of dead (bottom dark areas) or surviving (top light areas) 4-dpf larvae. B) % hatched (bottom dark areas) or unhatched (top light areas) 4-dpf larvae. C) % 4-dpf larvae with (bottom dark areas) or without (top light areas) pericardial edemas (PE). D) % moving embryos in 4-dpf dark-light behaviour (D/L) assay. E) Burst activity % and (F) burst count per min in response to light stimulus in 1-dpf embryos. G) 4-dpf embryo length. H) 4-dpf embryo size-standardised eye length. (I) 4-dpf defect score. (J) 4-dpf embryo size-standardised pericardial width (PW). (K) Swimming activity (moving time to tested time ratio), (L) total distance (M) number of bursts accelerations, (N) mean speed (cm/s), in the 4-dpf D/L assay. O) Total distance and (P) mean speed in the 4-dpf touch-evoked (T/E) swimming assay. Significant two-way model terms (heat × medium symbolised TS and SM) are shown in bold in top corners following analyses of deviance (binary generalised linear models), variance (ANOVAs) or Scheirer-Ray-Hare tests. Significant correlations with covariates are shown by ρ symbolising Pearson's coefficient. DS: defect score, LEL: longest embryo length, PW: pericardial width, PE: pericardial edema. Pairwise comparisons are shown with horizontal bars. Treatments were C+UV: control in fresh medium at 27°C, SM+UV: stress metabolites at 27°C, TS+UV: fresh medium in thermal stress, TS+SM+UV: stress metabolites in thermal stress (all followed by UV exposure). X: trends ($p < 0.08$, in grey), *: $p \leq 0.05$, **: $p \leq 0.01$, ***: $p \leq 0.001$, ****: $p \leq 0.0001$.

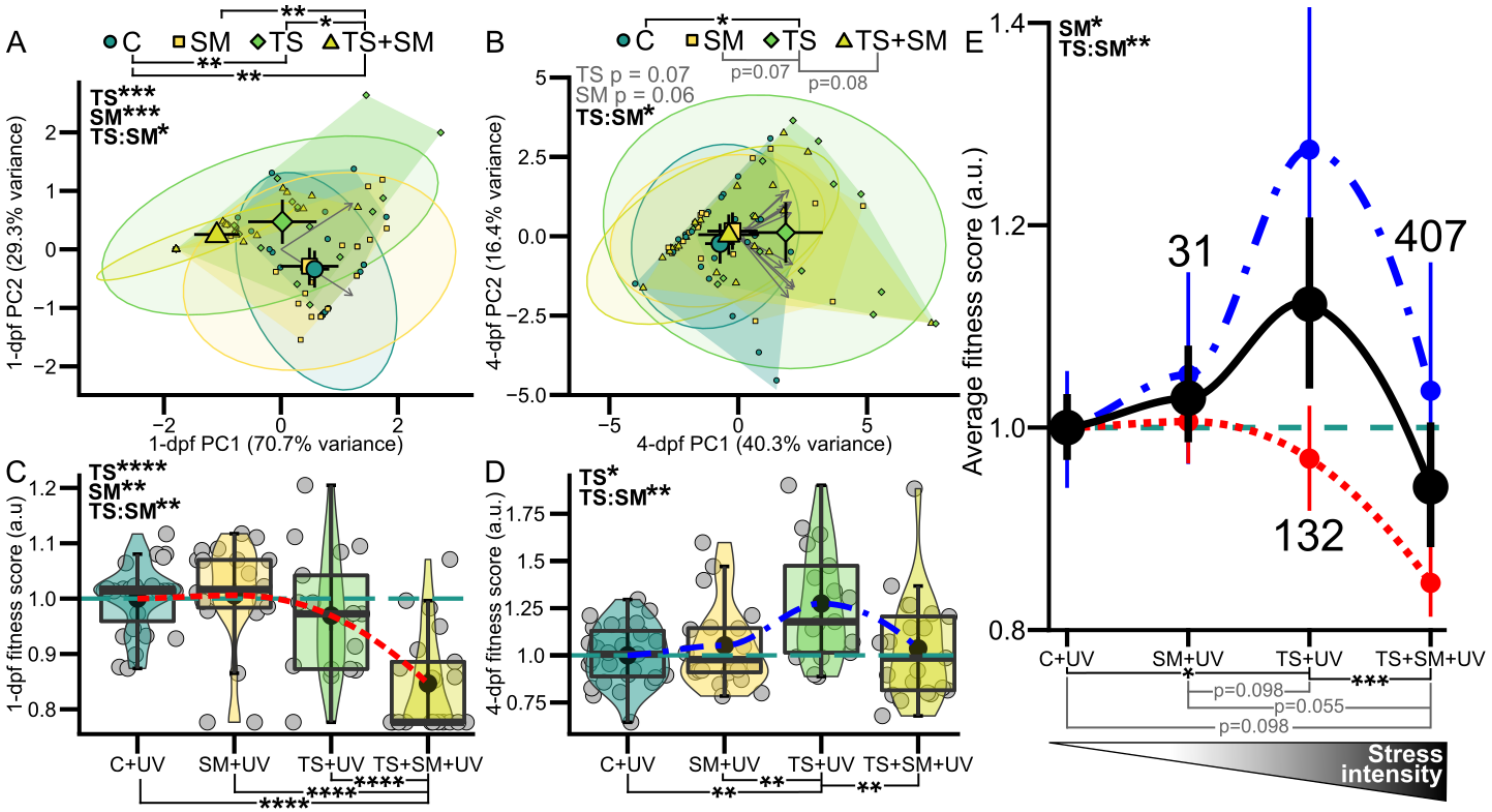

Figure 5.17. Nonlinear response to UVR with heat stress history: TS outperformed C and TS+SM. Principal Component Analysis of phenotypic outcomes at 1 (A) and 4 (B) dpf. Variables were recoded to indicate better outcomes with centroids associated with higher values along PC1 tending to have increased fitness outcomes. Large and small coloured symbols show centroids (± 95% confidence interval, CI) and individual scores, respectively. Ellipsoids show 95% normal confidence interval probabilities. Polygons are convex hulls showing the smallest area clustering all samples per treatment. Given the large variance explained by first x-axes, PC1 scores (dubbed "fitness score" in arbitrary units) were used in follow-up ANOVAs at 1 (C) and 4 (D) dpf. Data were scaled to control values (dashed blue horizontal lines) for neatness. Red dotted and blue dot-dashed lines are smoothed *loess* trends. In E), the average control-standardised PC1 score from 1 and 4 dpf is shown as a function of an increasing stress intensity with dots showing means ± 95% CI. Smoothed *loess* trends are shown by black solid line (average PC1 score), dot-dashed blue line (4-dpf PC1 score ± 95% CI) and dotted red line (1-dpf PC1 score ± 95% CI). Numbers in E show how many genes were altered compared to C+UV. Significant 2-way model terms (PERMANOVAs in A-B and ANOVAs in C-E) are shown in top-left corners with TS = thermal stress and SM = stress metabolites. Post-hoc comparisons are shown with horizontal bars. Trends ($p < 0.1$) are shown in grey. Treatments were C+UV: control in fresh medium at 27°C, SM+UV: stress metabolites at 27°C, TS+UV: fresh medium in thermal stress, TS+SM+UV: stress metabolites in thermal stress. *: $p \leq 0.05$, **: $p \leq 0.01$, ***: $p \leq 0.001$, ****: $p \leq 0.0001$.

5.8. Discussion

This chapter explored the effects of direct and indirect heat stress history on the UVA-catalysed capacity to cope with UVB-induced damage in zebrafish embryos and larvae. Heat stress experienced indirectly through stress metabolites stimulated some molecular pathways, such as methylation and epigenetic responses, which accelerated growth but impaired larval heart development and behaviour. Direct heat stress improved DNA repair and stimulated cells, which improved fitness-relevant performances and rescued larvae from UVR damage. However, heat stress combined with stress metabolites overwhelmed larvae and annihilated the heat protective effect, lowering their fitness-relevant responses.

5.8.1. UV-induced cellular damage

UVR is known to cause oxidative stress that is toxic to lipids, antioxidants, ribosomes, proteins, and nucleic acids (Iordanov et al., 1998; Dahms and Lee, 2010; Hurem et al., 2018) (**Figure 5.18A**). In this experiment, UVR altered the metabolism of macromolecules (ribosomes, mRNA, protein), DNA checkpoints, and organ development. Many ribosomal subunits were inhibited by UVR, contrasting with previous studies finding a UV-induced ribosome synthesis (Casati and Walbot, 2004; Tsai et al., 2009). The unfolded protein response and ubiquitination protect proteins and remove damaged ones (Simon et al., 1995; Bianchi et al., 2015), which likely explains their activation in response to UVR in this study. UVR lowered RNA integrity and activated nonsense-mediated mRNA decay as well as DNA checkpoints, indicating that UVR damaged nucleic acids. The DNA repair response involved *fancf* and *eya1* in all treatments. *fancf* stabilises the Fanconi Anaemia complex which recruits DNA repair genes upon DNA damage (Grompe and D'Andrea, 2001; Kowal et al., 2007; Yao et al., 2015). Upregulating only one DNA repair gene, *fancf*, suggests a minimal DNA repair response to UVR in control embryos. Moreover, *eya1* is a DNA repair-promoting UV-inducible enzyme, that was here downregulated by UVR, indicative of genotoxicity (Cook et al., 2009; Farrell et al., 2011; Zhou et al., 2017). Therefore, UVR altered most cell components, leading to the activation of autophagy pathways to remove damaged macromolecules (Sample and He, 2017). These cellular effects were observable at the organismal level in the form of impaired larval phenotypes, resulting in hypoactivity, teratogenicity, and reduced hatching, as previously reported in zebrafish embryos (Charron et al., 2000; Hurem et al., 2018).

5.8.2. Heat stress had a hormetic effect protecting embryos from UVR

Heat-stressed larvae grew longer with fewer heart malformations, better swimming performances, and earlier hatching, evidencing that heat rescued embryos from UVR. The data do not support the initial hypothesis that heat-stressed individuals would be disadvantaged in a mutagenic environment. Instead, the results support the concept of "hormesis", which refers to beneficial stimulating effects of low-dose stress (Calabrese and Baldwin, 2002; Costantini et al., 2010). In this chapter, the heat hormetic effect rescuing embryos from UVR likely resulted from heat activation of defence mechanisms, which protected against and/or repaired irradiation damage. Comparing transcriptomic responses of heat-stressed embryos before and after the UVR damage/repair assay suggests that hormesis was mediated through (i) a stage-dependent increased tolerance, and by stimulating (ii) antioxidants, (iii) the heat shock response (HSR), and (iv) DNA repair (**Figure 5.18A)**.

5.8.2.1 Stage-dependent tolerance may protect older heat-stressed embryos from UVR

Due to temperature-dependent developmental acceleration, heat-stressed embryos were six hours older than control embryos that were still undergoing segmentation when UVR started (Chapter 4). Mature fish are more resistant to UVR than embryos and larvae, likely through a protective role of pigmentation (Charron et al., 2000; Dahms and Lee, 2010; Alves and Agustí, 2020). Heat treatment upregulated two genes (*tyrp1a/b*) involved in melanin synthesis (Braasch et al., 2009; Krauss et al., 2014), which may shield cells from irradiation (Brenner and Hearing, 2008). Overdeveloped heat-treated embryos may also have benefited from energy supply provided by the yolk sac (Sant and Timme-Laragy, 2018). Likewise, heat upregulated several genes involved in glycolysis (e.g., *gapdh*, *gpia*, *pkmb*) and energy metabolism (Chapter 4). Heat-stressed embryos may therefore have mobilised energy to fuel ATP-dependent mechanisms such as nucleotide excision repair (Reef et al., 2009) and mismatch repair (Jiricny, 2013; Groothuizen and Sixma, 2016). Supporting this, heat-stressed embryos were hypoactive immediately after UVR exposure, suggesting that they redirected energy towards UV-coping strategies.

5.8.2.2 "Preparation for oxidative stress" protected heat-stressed embryos from ROS

Antioxidants may mediate hormesis via the "preparation for oxidative stress" (POS) strategy, which is an adaptive physiological mechanism upregulating antioxidants to confer tolerance against stress-induced reactive species (Costantini et al.,

2012; Oliveira et al., 2018; Giraud-Billoud et al., 2019). Supporting this, heat stress upregulated several glutathione-s-transferases (GSTs) in response to UVR damage/photorepair assay. GSTs control glutathione levels, which protects against UVA damage and detoxifies cells by removing toxic lipid, DNA, and protein oxidation products (Griffiths et al., 1998; Hayes and McLellan, 1999; Hayes et al., 2005; Dusinska et al., 2012). Likewise, TS+UV downregulated *txnipb* (thioredoxin interacting protein b), which may have helped translocating thioredoxin into the nucleus to limit DNA damage (Ogata et al., 2013; Chen et al., 2020). Therefore, antioxidants such as GSTs and *txnipb* likely protected heat-treated embryos from UV-induced oxidative stress.

5.8.2.3 Heat limited protein stress via the heat shock and ubiquitin-proteasome systems

The heat shock response (HSR) may mediate hormesis by limiting molecular damage (Jantschitsch and Trautinger, 2003; Rattan, 2006). Heat stress initiated the HSR at 1 dpf by upregulating HSP transcripts and HSP70 protein levels (Chapters 3 and 4). Heat preconditioning may provide embryos with a reserve of HSPs ready to be translated once exposed to UVR. HSPs also are key modulators of DNA repair genes, which may in turn favour cell survival (Sottile and Nadin, 2018). Furthermore, heat activated the ubiquitin-proteasome system (UPS, involving several ubiquitin, e.g. *ube2al*, *otulina*, *igs15*, and *otud7b*), which plays a central role in DNA repair (Sakai et al., 2020).

5.8.2.4 Heat stress improved the efficiency of DNA repair upon UVR

Unexpectedly, heat stress improved DNA repair efficiencies in the UVR damage/photorepair assay. These findings agree with increased DNA repair rates observed at high temperature in daphnia (MacFadyen et al., 2004), tadpole (Morison et al., 2020), and zebrafish embryos (Chien et al., 2020). DNA damage not repaired within 2 hours are irreversible in zebrafish embryos (Dong et al., 2008), suggesting that the transcriptome captured approx. 30 min after initiating UVR played a key role in mediating hormesis. Whilst control embryos activated one DNA repair gene (*fancf*), heat upregulated several DNA repair genes, such as *adprhl2, apex2, cry5, exo1, nthl1, rmi2,* and *ube2al,* all of which likely helped heat-stressed embryos to limit single- and double-strand DNA break (**Figure 5.18A, Table 5.1**). Likewise, heat stress activated the biosynthesis of inositol phosphate, which is known to stimulate double-strand break repair through non-homologous end joining (Hanakahi et al., 2000).

Table 5.1. Heat stress facilitates DNA repair, rescuing embryos from UV-induced DNA damage. [1] Ghosh et al. (2018); [2] Lanza et al. (2021), Subramanian et al. (1998), Zaksauskaite et al. (2021); [3] Tamai et al. (2004), Hirayama et al. (2009), Weger et al. (2011), Banaś et al. (2020); [4] Goellner et al. (2015); [5] Das et al. (2020); [6] El-Andaloussi et al. (2006), Zhao et al. (2016), Chen et al. (2022); [7] Xu et al. (2008), Hudson et al. (2016), Patel et al. (2017); [8] Cukras et al. (2014), Brinkmann et al. (2015), Stewart et al. (2016).

Gene	Role	Ref.
adprhl2	Prevents cell death by removing poly-ADP ribose accumulated following oxidative stress	[1]
apex2	Limits DNA damage by preventing the stabilisation of UV-induced DNA cleavage	[2]
cry5	A 6-4 photolyase involved in UVA-activated photorepair that removes DNA lesions such as 6-4 photoproducts (6-4PPs) and is responsible for light-induced tolerance to UVB in zebrafish embryos	[3]
exo1	Mediates a faster DNA mismatch repair (MMR) pathway	[4]
ntlh1	Cleaves oxidative pyrimidine damage during base excision repair (BER)	[5]
prmt6	A methyltransferase that can prevent apoptosis and rescue embryogenic defects, and regulate DNA polymerase and DNA repair genes	[6]
rmi2	Promotes genome stability as part of the Bloom syndrome (BLM) complex, involved in homologous repair (HR)	[7]
ube2al	E2 ubiquitin-conjugating enzymes such as *ube2a* mediate protein ubiquitination promoting DNA repair and genome integrity	[8]

5.8.2.5 Heat stress caused epigenetic changes

Furthermore, heat stress slightly increased (but with $p < 0.1$) the expression of transcripts involved in epigenetics and methylation. Methylation can transmit the heat hormetic effect to later life stages and subsequent generations (Wan et al., 2021), which may mean that heat-treated embryos not only perform better in DNA damage/repair assay, but could also be better protected from subsequent heat events.

Overall, heat rescued embryos from molecular damage in a mutagenic environment, by chaperoning proteins, activating DNA repair, stabilising the genome, and facilitating methylation and epigenetic regulation (**Figure 5.18**). These findings are in line with the concept of hormesis wherein heat protects cells by activating the proteasome, the HSR, and antioxidants (Rattan, 2006; Haarmann-Stemmann et al., 2013). However, only mild heat stress may have hormetic effects, whilst severe heat exacerbates stress-induced damage, following an inverted U-shaped dose-response curve (Haarmann-Stemmann et al., 2013; Matsuda et al., 2013). Therefore, the observed positive outcomes are likely explained by the heat regime used in this experiment, consisting of repeated heat peaks as opposed to prolonged periods of heat.

5.8.3. Heat stress was propagated towards conspecifics through stress metabolites

Stressed aquatic animals communicate with naive neighbours upon biotic predation stress (v. Frisch, 1938; Mathuru, 2016; Crane et al., 2022). Previous chapters (2, 3, and 4) showed that this also happens in response to abiotic stress, mediated by specific classes of stress metabolites. Here, Chapter 5 confirmed that a prior history of

exposure to heat stress-induced metabolites activated immune-, cell structure- and keratin-related genes in receivers following UVR damage/repair assay. Like treatment with direct heat stress, growth in SM was faster at 4 dpf and combined with hypoactivity at 1 and 4 dpf. However, the molecular pathways activated by stress metabolites were markedly different from those activated in the heat stress treatment. All heat stress history conditions, including stress metabolites, but not control embryos, activated a DNA repair response involving *apex2*, which is an important DNA repair gene in embryogenesis (Fortier et al., 2009; Zaksauskaite et al., 2021). Likewise, keratin genes may improve photoprotection against DNA damage in keratinocytes (Wondrak et al., 2006; Wu and Hammer, 2014) and promote repair of DSBs (Nair et al., 2021). However, the response to UVR damage/repair assay in the stress metabolites treatment also downregulated both *brip1* and *rps3*, suggesting DNA damage (Bridge et al., 2005; Elsakrmy et al., 2022) that may have been the cause for the observed malformations. Stress metabolites altered epigenetic and methylation genes, which may mediate downstream transcriptomic changes (Gibney and Nolan, 2010). For instance, SM+UV downregulated *srrt*, which plays a role in DNA repair (Rossman and Wang, 1999; Bui et al., 2019), as well as histone *h1-5* and methyltransferases, suggesting alterations in transcriptional regulation (Albig et al., 1997; Vougiouklakis et al., 2020). One differentially expressed gene was *smyd1b*, playing a key role in skeletal muscles (Tan et al., 2006; Li et al., 2013a), and the downregulation of which may explain how stress metabolites rendered embryos hypoactive. Therefore, while stress metabolites induced markedly more responses to UVR damage/photorepair assay as compared to the UV control, they only allowed embryos to grow faster, but did not limit malformations and failed to protect embryos against UVR damage as efficiently as heat stress (**Figure 5.18B**).

5.8.4. Heat combined with stress metabolites intensified stress and UVR damage

Since direct and indirect heat stress (induced via stress metabolites) influence distinct pathways in UVR damage/repair assay, the combined treatment exposed embryos to both direct and indirect stressors simultaneously, which amplified transcriptomic alterations, both before (Chapter 4) and after UVR damage/repair assay (Chapter 5, here). These embryos had increased stress levels as evidenced by more stress-related functions and further damage to messenger RNA, and inhibition of translation by downregulating ribosomal RNAs. The combined treatment elevated HSPs levels before UVR (Chapter 4). Such elevated basal HSP mRNAs may attenuate the

HSR to subsequent acute stressors (Whitehouse et al., 2017; Sessions et al., 2021). Supporting this idea, the combined treatment drastically limited the upregulation of key HSPs in response to UVR, likely lowering protection against protein damage. Moreover, the combined treatment upregulated both *cdc7*, which may inhibit homologous recombination repair (Wienert et al., 2020), and *rad9*, which promotes apoptosis and tumorigenesis (Broustas and Lieberman, 2012). The interacting effects of heat and stress metabolites in amplifying transcriptome changes also likely costed more energy, as suggested by more pronounced lowered behavioural activities. Overall, the experimental data suggests that the combination of direct heat and indirect heat-induced stress metabolites formed a stronger stressor, which prevented embryos from activating the heat hormetic effect, and shifted the dose-response towards negative outcomes (**Figure 5.18B**).

5.8.5. Perspectives: heat stress history alters fitness in mutagenic environments

In conclusion, this chapter showed that the response to a mutagenic environment depended on the type and intensity of heat stress experienced during early development (**Figure 5.18**). The nonlinear stress-fitness relationship was characterised by positive (growth) and negative (defects) outcomes in chemically-communicated indirect heat stress, by a protective hormetic effect activated by direct heat stress, and by negative fitness outcomes in embryos experiencing combined stress. The findings that heat stress history can alter the response to UVR exposure is relevant for natural populations, which must navigate mutagenic environments that may be exacerbated by climate change (Ficke et al., 2007; Bais et al., 2018).

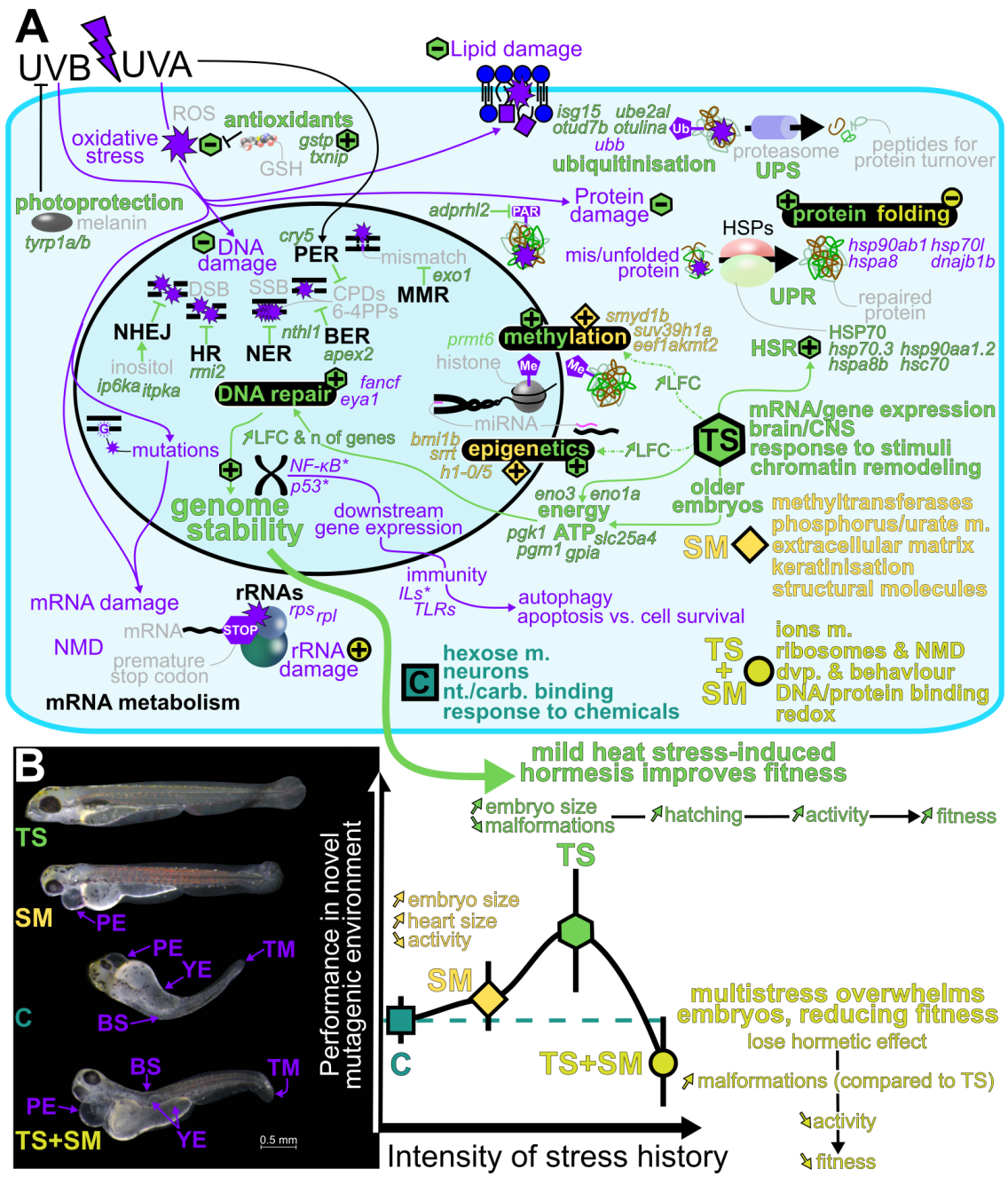

Figure 5.18. Heat stress history alters the response to UVR. A) Mild heat stress-induced hormetic effect protected cells from damage to cellular components (lipids, proteins, ribosomes, RNA, and DNA). All treatments induced a common response to UVR (violet arrows/symbols/font) but also had unique signatures (font/symbols coloured per treatment). Genes are shown in italics (with * denoting inferred genes from enriched functional terms but genes not significant at time of sampling). Function and genes were altered before and/or after UVR. Dashed arrows indicate trends. B) UVR altered fitness outcomes depending on stress intensity which may change evolutionary rates. Compared to C, embryos have fewer defects and grow faster in TS but show larger pericardial-to-embryo length ratios with stress metabolites SM and TS+SM. Trends represent smoothed *loess* lines of PC1 scores (± confidence intervals) averaged between 1 and 4 dpf. Defects include bent spine (BS), pericardial edema (PE), tail malformation (TM), and yolk extension disruption (YE). BER: base excision repair, dvp.: development, LFC: log-fold change, m.: metabolism, MMR: mismatch repair, NER: nucleotide excision repair. NHEJ: non-homologous end joining repair. nt.: nucleotide, PER: photoenzymatic repair. Treatments included C: control, SM: stress metabolites, TS: thermal stress. Image modification: embryos were detoured, lighting was adjusted, and images put on a black background.

Chapter 6. General Discussion

Chemical communication received the most attention in a context of biotic stress such as predation. In contrast, the question of whether aquatic animals can chemically stress each other in abiotic stress conditions has been largely overlooked to date, despite the implications for amplified stress responses in populations in a changing climate. Therefore, this Ph.D. thesis aimed to explore the "language of stress" by determining whether abiotic stressors can induce the propagation of stress responses between aquatic animals. The main findings were that (i) abiotic factors stressed donors by shifting their molecular and physiological responses, (ii) causing the release into their environment of stress-specific metabolites, (iii) that propagated stress responses to receivers.

It was first necessary to confirm that donors were stressed to identify candidate pathways for the release of stress metabolites, and to compare the responses between donors and receivers. In four experiments, embryonic and adult stages of several fish and invertebrate species from marine and freshwater environments were exposed to climate change-related abiotic stressors: repeated heat stress associated with heat events, and pH drop mimicking ocean acidification. Chapter 2 outlined the concept of abiotic stress propagation by showing that wild-caught marine invertebrates reacted to stress metabolites released by conspecifics and/or fish stressed by an acidic pH. Next, this concept was brought into the laboratory to uncover the mechanistic basis of stress propagation. Chapter 3 showed that heat stress induced stress propagation in a freshwater model, zebrafish embryos. These released putative stress metabolites into their medium that influenced the phenotype of conspecific receivers and evidenced a role for immune and antioxidant pathways in stress propagation. Chapter 4 further unravelled the molecular basis of stress propagation using multi-omics, which revealed candidate sulphur- and lipid-containing stress metabolites different from control cues, and fine-tuned transcriptomic changes in receivers. Chapter 5 explored the biological significance of abiotic stress and stress propagation in zebrafish embryos having experienced direct heat stress and indirect heat stress through stress metabolites prior to ultraviolet radiations, which evidenced nonlinear relationships between fitness-relevant outcomes and intensity of stress. The following sections will summarise (i) the main effects of abiotic stressors on aquatic animals, (ii) some major properties of stress metabolites, (iii) their influence on receivers, and (iv) their pH- and temperature-dependent effects. Directions for future studies will then be proposed, before concluding with the ecological relevance of stress propagation.

6.1. Direct exposure to heat and acidification induces stress

Experiments from Chapter 3 and Chapter 4 showed that repeated sublethal heat was a stressor to zebrafish embryos. Heat induced molecular and cellular stress responses in zebrafish embryos and larvae, characterised by the upregulation of known stress biomarkers such as cortisol (Alsop and Vijayan, 2009b; Sadoul and Geffroy, 2019) and heat shock proteins (Pirkkala et al., 2001; Iwama et al., 2004; Logan and Buckley, 2015). Zebrafish embryos mounted the expected heat shock response after 1 day of stress (Chapter 3), but this response disappeared at the protein level after 4 days of heat peaks (Chapter 4). In 1-dpf embryos, the response to oxidative stress was either weak – involving only few antioxidant genes such as Glutathione-s-transferases whilst failing to activate other antioxidant hallmarks such as Catalase – or possibly repressed by repeated heating, as evidenced by a significant downregulation of Superoxide Dismutase (Chapters 3 and 4). Similarly, lake whitefish embryos (*Coronegus clupeaformis*) showed reduced heat shock responses after repeated thermal stress (Whitehouse et al., 2017). This is consistent with the maladaptive effect of repeated exposure to stress due to increased energetic costs (Schreck and Tort, 2016). This suggests that embryonic stages experiencing repeated stress may suffer from cellular exhaustion and may no longer be able to adequately protect cells from protein misfolding and oxidative species during future stress events.

Repeated sublethal heat stress accelerated development in zebrafish embryos, which reached the pharyngula stage earlier through a faster somitogenesis as supported by the downregulation of somite-related transcription repressors (Chapters 3-4). These results are in line with higher temperatures accelerating embryonic development (Jungwirth and Winkler, 1984; Hallare et al., 2005; Schröter et al., 2008). Embryos also grew longer at high temperatures, compared to control embryos that had not completed the segmentation stage. The earlier onset of hatching with thermal stress (Chapter 4) suggests that heated larvae hatched prematurely (Kamler et al., 1998) and/or reached an older developmental age after 4 days. However, once segmentation was completed, high temperatures lowered larval growth rates (Chapter 4). Supporting this, the temperature size rule states that fish in warmer environments are smaller as they invest energy in maturation over growth (Wootton et al., 2022). Heat stress also altered the behaviour of developing zebrafish, which were less mobile as embryos when facing an acute light stimulus (Chapters 3-4) and slower as larvae when physically startled by touch (Chapter 4). Likewise, Chapter 2 showed that short-term acidic pH exposure lowered the time-to-

success in finding a feeding cue in hermit crabs *Diogenes pugilator* and in burrowing in ragworms *Hediste diversicolor*. An acidic pH increased the potency of odour from unstressed predators *Sparus aurata*, triggering more avoidance in shore crab *Carcinus maenas*. Altogether, there was experimental evidence that climate change-induced abiotic stressors may impair locomotory capacities as well as brain and sensory functions. These abiotic stress-induced behavioural and cognitive alterations may in turn modify predator-prey interactions and community structures in the natural environment (Allan et al., 2015; Warren et al., 2017; Domenici et al., 2019). In contrast, fitness outcome data from Chapter 5 showed that, unexpectedly, heat-stressed embryos recovered from ultraviolet radiations better than unstressed conspecifics, likely due to an improved DNA repair efficiency, quicker development, and antioxidants limiting cellular damage.

The experimental data gathered in this Ph.D. thesis indicate that short but repeated heat peaks altered molecular and phenotypic responses, but that experiencing sublethal heat stress alone had an unexpected positive effect in a mutagenic environment. Similarly, short-term acidic pH impaired decision-making strategies in marine invertebrates. Such findings suggest that both repeated temperature anomalies and short-term pH drops may impose further risks to aquatic animal populations in addition to overall higher mean temperatures and more acidic conditions. All experiments evidenced that donors were stressed, which confirmed the first step of stress propagation (**Figure 1.2**). The next knowledge gap to address was to explore the synthesis of stress-induced metabolites that propagate stress to receivers.

6.2. Stressed aquatic animals released stress metabolites which altered molecular profiles in receivers: evidence from multi-omic data

6.2.1. Synthesis of stress cues in donors

The prominent role of chemical communication in aquatic environmments (Lunsford et al., 2019) including in alarm (Ferrari et al., 2010) and disturbance signalling (Crane et al., 2022) points to chemical cues as evident candidates to transmit abiotic stress information between individuals. However, the nature of chemicals involved in disturbance and alarm cues remains largely uncharacterised (Crane et al., 2022). In this thesis, multi-omic experiments in zebrafish embryos helped to explore (i) the transcriptomic response to heat stress leading to the synthesis of stress metabolites,

(ii) the molecular characterisation such stress metabolites, and (iii) the transcriptomic responses they elicit in receivers.

The signalling pathways leading to volatile organic compounds synthesis in donors and the consequences in receivers are well established in plants (Dudareva et al., 2006, 2013; Yoneya and Takabayashi, 2014). For instance, volatile compound secretion likely results from salinity stress damage in plants (Lee and Seo, 2014). Similarly, physically restrained stressed mice released twenty volatile organic compounds, many of which could be traced to known metabolic routes (Schaefer et al., 2010). This led several authors to suggest that stress cues result from stress-induced metabolism shifts rather than the production of new metabolites (Sakuma et al., 2013; Bombail et al., 2018; Bombail, 2019). Likewise, heat and pH stress-induced shifts in cellular and metabolic pathways and their resulting metabolic by-products could be the source of stress metabolites, similar to disturbance cues (Vavrek et al., 2008).

Although there may be differences compared to the animal kingdom, it is possible that some pathways reported in plants are also involved in synthesising animal stress cues. One such example are the glycolysis and pyruvate pathways, upstream of volatile cue synthesis in plants (Dudareva et al., 2006), which were also significantly enriched in the transcriptome of heat-stressed zebrafish embryos (Chapter 4). Whittaker and Feeny (1971) proposed that plant secondary compounds involved in allelochemic interactions originate from sugar and amino acid metabolism. In line with this, transcripts of heat-stressed zebrafish embryos were ascribed to sugar and amino acid metabolism, from which stress metabolites may be synthesised. This suggests that the production of stress cues may be evolutionary conserved across different taxa. After proposing candidate pathways for the synthesis of stress metabolites, their chemical characterisation was explored using metabolomics.

6.2.1. Stress metabolites were lipids, sulphur, peptides, and organic compounds

Stress odours in rodents (Sakuma et al., 2013; Inagaki et al., 2014), stress volatiles in plants (Dicke and Bruin, 2001), and alarm odours in aquatic animals (Parra et al., 2009; Mathuru et al., 2012; Stensmyr and Maderspacher, 2012) likely exist as a bouquet of compounds. Supporting this, stress metabolites in zebrafish embryos contained over twenty compounds unique to heat-stressed individuals, in addition to chemicals more concentrated than in control conditions (Chapter 4). Several compounds have been proposed as stress and alarm cues, such as ammonia and urea in urine (Brown et al.,

2012; Bairos-Novak et al., 2017), cortisol (Barcellos et al., 2011; Bett et al., 2016), or *Schreckstoff* components including hypoxanthine-3-N-oxide (Parra et al., 2009). However, ammonia, cortisol, and known alarm cues were not found in heat-induced stress metabolites in zebrafish embryos (Chapter 4). In contrast, the metabolomics from Chapter 4 indicated that stress metabolites may involve sulphur-containing compounds, such as 3-mercaptolactate. Likewise, mouse alarm pheromones are sulphur-containing volatiles released by predators (Brechbühl et al., 2013) and plant volatiles contain sulfur-containing chemicals (Dicke and Bruin, 2001). Sulphur- and nitrogen-containing compounds may therefore function as general danger messages (Brechbühl et al., 2013), lending support for their role as stress cues. Chapter 4 also identified several peptides and proteins that matched with stress metabolites. Peptides can act as signalling cues since aquatic animals already have the entire cellular machinery to release such water-soluble cues (Decho et al., 1998). Moreover, stress metabolites in zebrafish involved several amino acids and lipids (Chapter 4), in line with the role of derivatives of fatty acids and amino acids in plant stress cues (Dudareva et al., 2006). Plant stress cues may directly originate from stress-induced cellular damage (Lee and Seo, 2014). Similarly, heat-induced alterations of lipid profiles in cell membranes (Hazel, 1995; Crockett, 2008), tissues (Kim et al., 2019), and plasma (Sun et al., 2018) may lead to the release of two glycerophospholipids (phosphocholine and glycerophosphocholine) in the stress-conditioned medium. This is in agreement with a general role for lipids in chemical communication (Watson et al., 2009; Hay, 2010). For instance, sea lampreys *Petromyzon marinus* rely on fatty-acid derivatives as migratory pheromones (Li et al., 2018). To summarise, the multi-omic analyses highlighted lipids, peptides, and sulfur-containing compounds – but not cortisol nor ammonia – as candidate chemicals that signal abiotic stress between aquatic animals.

6.2.1. Stress cues are released by stressed, but not by undisturbed, animals

One could argue that stress metabolites are just upconcentrated compounds from the regular metabolism. To address this hypothesis, embryo medium conditioned by control animals was used in addition to fresh medium. In Chapter 2, the response to pH-induced stress cues differed from that to diluted and tenfold concentrated control odours. In Chapter 3, zebrafish embryos reacted differently when incubated in medium containing control metabolites, stress metabolites, and no metabolites. Metabolomics from Chapter 4 confirmed that these three media (stress and control media after accounting for fresh medium blank correction) contained distinct chemicals and/or the

same metabolites in different concentrations. All chapters consistently showed differences in behavioural and molecular responses to control vs. stress vs. fresh media. Altogether, the data from this Ph.D. thesis suggests that stress metabolites are released *specifically* upon abiotic stress and are distinct from the compounds excreted by unstressed animals. Similarly, the chemical profiles of rat faeces (Bombail et al., 2018), mouse urine (Schaefer et al., 2010), and fly volatiles (Yost et al., 2021) differed between stressed and unstressed individuals. Another possibility is that an altered water chemistry, such as self-acidification and deoxygenation due to stress-induced higher metabolism in donors, is responsible for the observed response of receivers. However, the water pH and oxygen levels were not different between control and stress conditions (Chapters 3-4) which likely excludes their role in stress propagation. Altogether, the multi-omic data confirmed that abiotic stress induced the release of stress metabolites into the environment, which were different from control metabolites: this finding fills the second main knowledge gap of the thesis (**Figure 1.2**). Next, the third main objective was to test the effects of such stress metabolites on the molecular and phenotypic biology of receivers.

6.3. Heat and acidification stress was propagated to neighbours: evidence for extending stress propagation to abiotic stress

6.3.1. Stress metabolites activated different pathways than stress itself

Only few studies investigated the molecular basis of stress signalling in receivers. For instance, stress-induced plant volatiles may activate calcium influx into cells as well as protein phosporylation and dephosphorylation (Yoneya and Takabayashi, 2014) and cause genomic instability in receiver plants (Yao et al., 2011). In contrast, the transcriptomic data (without UV in Chapter 4; and with UV in Chapter 5) showed that stress metabolites induced fine-tuned transcriptome changes involved in lipid/ion transport (*xkr8.2*, *anxa1a*, *best1*), keratinisation (involving several keratins *krt5/17/92/97/222* and cytokeratins *cyt1/cyt1l*), glycosaminoglycans including keratan sulfate (chitin synthase *chs1*, carbohydrate sulfotransferase *chst2b*, and proteoglycan *prg4a*), immune (e.g. toll-like receptor *tlr18*, interleukin *il-1β*, complement factor protein *cfp*), antioxidant (sulfide:quinone oxidoreductase *sqor* and *sod1*), signal transduction (NOD2 ortholog), and cholinergic (*chrng* and *gngt1)* pathways. The molecular data evidenced that stress metabolites induced an immune and antioxidant stress response in receivers but that they did not activate the classical cellular stress response pathways – involving cortisol, metabolism, and heat shock proteins – that was

activated by direct abiotic stressors in donors (Chapter 4). This contrasts with increased cortisol levels in adult zebrafish exposed to alarm cues (Barkhymer et al., 2019) and disturbance cues (Barcellos et al., 2011).

The role of the olfactory system in mediating responses to chemicals including alarm cues (Kermen et al., 2013, 2021), makes it a good candidate system to detect stress metabolites. However, the gene expression data of olfactory receptors from Chapter 4 was conflicting. Isolated inbred AB strain zebrafish embryos did not activate their olfactory system when exposed to stress metabolites alone, whilst group-raised outcrossing PET strain embryos completely inactivated the transcription of the V1R-like vomeronasal chemoreceptor *ora3*. The latter is a chemosensory receptor that may be involved in pheromone and bile detection pheromones (Ota et al., 2012; Saraiva et al., 2015; Cong et al., 2019), suggesting the role of *ora3* in early detection of stress metabolites before its depletion after 24 hours in stress media. Olfactory receptor genes may only be detected around 30-38 hpf (Barth et al., 1996; Byrd et al., 1996). Zebrafish embryos exposed to stress metabolites were 25-hpf old at the time of transcriptome sampling and only very few reads were counted (highest *baseMean* value of 18.4), which may explain why stress propagation could not be ascribed to olfactory receptors in zebrafish embryos exposed to SM only. In contrast, embryos exposed to the combined treatment TS+SM accelerated their development to 31 hpf due to heat stress, and may have utilised olfactory receptors, as supported by the significant elevenfold gene expression increase of the V1R-like vomeronasal chemoreceptor *ora3* as well as the alteration of the V2R-like vomeronasal chemoreceptor *olfcb1*. The gene *olfcb1* is involved in amino acid detection (Zhang et al., 2022) and fright reaction in fish (Yang et al., 2019). This suggests that chemoreceptors were active in the combined treatment TS+SM. Likewise, olfactory receptors may have been involved in mediating stress propagation in 4-dpf larvae.

Other than the classical olfactory system, solitary chemosensory cells (SCCs) and lateral line cells may help detecting stress cues. Fish use SCCs on the epithelia of their skin, gut, and gills to detect chemical cues from the water (Whitear, 1971; Sbarbati and Osculati, 2003; Aurangzeb et al., 2021). These SCCs react to amino acids, bile taurocholic acid, and fish odours (Daghfous et al., 2020). SCCs are involved in recognition of heterospecific fish skin mucous odours (Peters et al., 1991) and conspecific bile (Kotrschal, 1996). However, SCCs only appear with hatching around 3 dpf (Kotrschal, 1996) excluding their involvment in stress cue-detection in 1-dpf

embryos but not in 4-dpf larvae. Taste buds only appear with the onset of exogeneous feeding in 5-dpf zebrafish larvae (Kotrschal et al., 1997; Hansen et al., 2002), also likely limiting their involvment in stress propagation in my experiments. Another set of candidate cue-responsive cells are sensory hair cells within neuromasts of the lateral line system (Mojib et al., 2017; Desban et al., 2022). In zebrafish embryos, neuromasts are deposited in the posterior lateral line primordium starting at 2 dpf, itself appearing at 20 hpf (David et al., 2002; Dow et al., 2018). Lateral line hair cells express over 45 novel chemoreceptors that can detect amino acids, pheromones, hormones, serotonin, and immune-related compounds (Desban et al., 2022). Prior research showed that stressors induce the release of serotonin into the environment, which activates receptors in lateral line hair cells of larval zebrafish conspecific receivers, in turn altering their locomotory behaviour (Desban et al., 2022). Stressors also cause the release of trypsin, which is detected by epidermal receptors in epithelial and keratinocyte cells, and induces aversion in larval zebrafish (Kim et al., 2009; Alsrhani et al., 2021). Likewise, stress metabolites altered many genes (i) involved in keratinocytes and epidermal cells (ii) and also expressed in hair cells of the lateral line in 5-dpf zebrafish larvae (Elkon et al., 2015). In effect, the transcriptomic data from Chapters 4-5 highlighted several structural molecule-coding genes and transcripts associated with skin in general (epidermis, keratinocytes and/or keratinisation) involving many keratins (*krt5/17/92/97/222*) (Wang et al., 2016), and cytokeratin (*cyt1/cyt1l*), epidermis growth factor *eps8l1a* (Edqvist et al., 2015), sciellin (Kvedar et al., 1992; Champliaud et al., 2000), and a transglutaminase *tgm1l4* (Eckert et al., 2005). Interestingly, keratin proteins from fish mucus may also signal infection danger to others (Pawluk et al., 2019). Given that olfactory receptors stimulate keratinocyte proliferation in the skin (Chéret et al., 2018), that odorants induce keratinocyte proliferation (Nakanishi et al., 2021), and the recently uncovered role of skin and keratinocytes in capturing chemical information from the environment (Sondersorg et al., 2014; Denda and Nakanishi, 2022), the role of cells on the body surface in the chemical ecology of stress propagation in zebrafish embryos warrants further investigation. Altogether, the transcriptomic analysis suggests that there may exist a possible role of keratinocyte, epidermal, and hair cells in detecting stress metabolites.

In three experiments (Chapters 3, 4, and 5), stress metabolites activated an immune response in zebrafish embryos, involving interleukins, toll-like receptors, and the complement system. This agrees with the increase of interleukin-4 in receivers of

alarm cues from physically-harmed mice (Moynihan et al., 2000). Based on the common signalling molecules used by the immune and nervous systems for intra- and intersystem communication, the immune system has been described as an extra-sense (Blalock, 2005; Kipnis, 2018) that detects infochemicals not sensed by chemoreceptors (Sbarbati and Osculati, 2006). Lipids can activate the immune response (Hubler and Kennedy, 2016). For instance, lipid A is the major component of bacterial lipopolysaccharides, and activates immune responses, particularly toll-like receptors (Farhana and Khan, 2022). Furthermore, stress metabolites downregulated an NOD2 ortholog (*si:ch211-214b16.2*), which is an intracellular receptor for bacterial peptidoglycans involved in immunity (Strober and Watanabe, 2011). Since stress propagation may involve lipidic compounds, the immune system is also a good candidate to detect stress metabolites.

Stress metabolites altered two antioxidant-related genes, sulfide:quinone oxidoreductase (Kleiner et al., 2018) and superoxide dismutase (Younus, 2018). A similar mechanism was shown in single-cell green algae *Chlamydomonas reinhardtii* cells which, under salt stress, signalled through volatile compounds other cells to prepare for oxidative stress by increasing antioxidant activities (Zuo et al., 2012). This suggests that stress cues increase antioxidant and immune responses so that receivers are prepared to cope with the upcoming abiotic stress. Since a stress response was observed both in donors and in receivers, this is considered stress transmission by Brandl et al. (2022), and is defined as stress propagation in this Ph.D. thesis.

Eventually, the signalling of stress metabolites is integrated into neuronal pathways. In both independent experiments, stress metabolites – alone (Chapters 4) and combined with UV exposure (Chapter 5) – activated their receivers' cholinergic and neurotransmission pathways, involving *chrng* (cholinergic receptor, nicotinic, gamma) and *gngt1* (G Protein Subunit Gamma Transducin 1). Alarm substances also activate the cholinergic pathways in zebrafish, which may then modulate defensive behaviours (Canzian et al., 2017). Since the cholinergic pathway controls behaviour (Ackerman et al., 2009; Chand D and Rajarami G, 2015), there may exist a common pathway that stress cues activate in receivers to alter their behaviour. As a result, stress metabolites elicited behavioural responses in their receivers in all four experiments, with donor-, species-, and stage-specific differences. Stress metabolites from *Sparus aurata* fish induced avoidance behaviours in two crustacean species, shore crabs *Carcinus maenas* and hermit crabs *Diogenes pugilator*, as well as in ragworms *Hediste diversicolor* – in

which it also delayed burrowing time. Stress metabolites from conspecifics delayed time-to-success in ragworm and lowered behavioural activities in zebrafish. Control odours from sea bream, ragworm, and zebrafish, induced behavioural responses distinct to stress metabolites. Combined with the metabolomic data, this confirms the hypothesis that stressed and unstressed animals release different compounds that elicit distinct behaviours in their receivers (**Figure 1.2**).

6.3.2. Significance, role, and characterisation of stress propagation

Experiments from this Ph.D. thesis evidence that stress propagation exists in fish and invertebrate species, in marine and freshwater environments, and as early as during embryogenesis. This suggests that stress propagation is an innate and conserved, cross-taxa mechanism. Supporting the innate nature of stress communication, zebrafish embryos produce and react to biotic stress-induced alarm substances, even as early as 12 hpf (Cao and Li, 2020; Lucon-Xiccato et al., 2020). Cross-taxa stress communication was also shown in another stressed perciform fish, the rock bass *Ambloplites rupestris*, which chemically induced stress in the crustacean crayfish *Orconectes virilis* (Hazlett, 1990b). Although in Chapter 2 crustacean species (hermit and shore crabs) reacted to sea bream stress cues, they did not themselves produce stress metabolites. This may be because (i) stress propagation depends on stress intensity in donors (Bombail et al., 2018), and (ii) crabs were not stressed by a low pH as they inhabit pH-variable intertidal habitats (Fehsenfeld et al., 2011; Appelhans et al., 2012). Still, hermit crabs lowered their feeding rates, indicating that they were stressed, but failed to produce stress metabolites. Since stress cues exist in crustaceans – for instance upon heat stress in crayfish (Hazlett, 1985) – it may be that the release or the detection of stress metabolites is context-dependent in hermit crabs. Likewise, crayfish *Orconectes propinquus* and *O. rusticus* failed to transmit stress information to conspecifics whilst *O. virilis* showed stress propagation (Hazlett, 1990b). Supporting context-dependent effects, many factors may influence chemical communication: season (Jacobsen and Stabell, 1999), hunger in donors (McCormick and Larson, 2008), interindividual variation (Brandl et al., 2022), as well as group size and familiarity (Bairos-Novak et al., 2019). Furthermore, stress cues may elicit a “complex contagion” (Brandl et al., 2022), where receivers integrate stress information based on the concentration of stress cues available to them before mounting a stress response, to avoid a costly maladaptive response.

The fact that stress metabolites alone influenced the behaviour of receiver animals not experiencing the original stressor is a double-edged sword since it would benefit the

receivers in being ready once stress arrives but it may also waste valuable energy if the source of the stress does not reach the receivers. Donors are "carriers of natural information" and stress chemicals correlate with a type of event (Scarantino, 2010). For instance, disturbance cues are reliable "honest" information about a threat (Bairos-Novak et al., 2017). By analogy, stress metabolites may be interpreted by receivers as indicative of an abiotic stress threat. This may be because the production and transmission of chemical signals is costly hence signalling only occurs upon specific contexts (Steiger et al., 2012), such as stress. In addition, selection should favour animals that utilise information available to them from others as "early warning signals" to avoid the costly stress response they would endure if experiencing stress first hand because they ignored stress risk cues (Wisenden et al., 1995; Kiesecker et al., 1999; Vavrek et al., 2008; Brown et al., 2012; Crane et al., 2022).

Stress propagation may induce similar outcomes both in stressed donors and receivers (Brandl et al., 2022). This is in line with similar aversion to pH stress in donors and to pH-induced stress metabolites in invertebrate receivers (Chapter 2), and with similar hypoactivity and a growth catch-up in zebrafish receivers relative to heat-stressed conspecifics (Chapters 3-4). Infochemicals are categorised as aversive (negative valence) or attractants (positive valence) (Nielsen et al., 2015). Despite strain, species, and stage-dependant differences, stress metabolites had a common effect in receivers: they induced anxiety-like behaviours, indicative of a negative valence. Alarm odours are avoided by recipients which suggests that conspecifics are able to interpret alarm cues as danger signals and flee them to avoid encountering a danger (Kikusui et al., 2001). Zebrafish embryos within their chorion could not move away, but their hypoactivity at 1 dpf may lower predation risks by lessening their bioelectric field (Mezrai et al., 2020). Once adult, zebrafish avoid disturbance cues from chemically and physically stressed conspecifics (Abreu et al., 2016). Stress metabolites also induced an acceleration in growth in both zebrafish strains (Chapters 3-4). Alarm cues, too, accelerated development in zebrafish *Danio rerio* and pearl danio *D. albolineatus* (Mourabit et al., 2010). The fact that stress metabolites seemingly act similar to alarm cues in altering behaviour and development may indicate an overlap in the cocktail of cues. If stress metabolites resemble alarm cues, they could activate a common strategy to lower stress risk through synchronous growth and hatching (Colbert et al., 2010; McGlashan et al., 2012).

Altogether, the experiments showed that stress propagation exists in several species of marine (Chapter 2) and freshwater (Chapters 3-4) aquatic animals. The ecological relevance of disturbance cues is to increase vigilance in receiver animals (Jordão, 2004; Ferrari et al., 2010) and to provide others with risk assessment information in the wild (Goldman et al., 2020a). Overall, the response to stress metabolites was weaker than that of stress itself aligning with an increased alertness hypothesis. I propose that receivers use chemical information, in the form of stress metabolites released by stressed donors, to adjust their biology in anticipation of the abiotic stress. In turn, the propagation of stress may benefit the group since it does not require all individuals to sense the threat to induce a collective response (Brandl et al., 2022).

6.4. Stress propagation in multistress: stress metabolites combined with abiotic stressors exerted different responses

Hormesis refers to protective effects of low-dose stress (Costantini et al., 2010), which enhance the resistance to subsequent stress exposures (Calabrese et al., 2007; Berry and López-Martínez, 2020). The concept of xenohormesis has been defined as the benefits such as stress tolerance that chemicals induce in a "stranger" organism (Hooper et al., 2010). Similar to alarm cues and disturbance cues which are thought to improve the fitness of receivers (Jordão, 2004; Ferrari et al., 2010), receivers of stress metabolites showed similar outcomes compared to directly stressed individuals as though they were anticipating adverse conditions. This hypothesis may fit for receivers exposed to stress metabolites only, but the real environment would impose the abiotic stressor additional to stress cues. Experiments where stress metabolites were combined with abiotic stressors (ocean acidification in Chapter 2 or heat stress in Chapters 3-4) or followed by mutagenic ultraviolet stress (Chapter 5) showed that stress propagation has negative consequences on the fitness of receivers.

Heat can degrade compounds faster and shorten their signalling life (Alberts, 1992). For instance, warming annihilated antipredatory responses to alarm cues in the fish Qinling lenok *Brachymystax lenok tsinlingensis* (Xia et al., 2021). In contrast, adding heat stress to stress metabolites (TS+SM) amplified the effect of stress metabolites by altering another 47% of genes not found in single factor treatments TS and SM (Chapter 4). These may impose a greater energetic cost to receivers as more pathways were activated. One such pathway was that of apelin signalling, which protects against oxidative stress (Şişli et al., 2022), and is involved in the response to

acute stress (O'Carroll et al., 2003). This is testimony that the stress load was greater in embryos exposed to both heat and stress metabolites. The amplified transcriptomic effects scaled up to whole-body levels by inducing stronger behavioural impairments in response to novel stimuli. Several mechanisms may explain this stronger response in TS+SM, including that embryos were older with heat, which increases reactivity to cues (Lucon-Xiccato et al., 2020), possibly because they express more olfactory receptors after 30 hpf (Barth et al., 1996; Byrd et al., 1996); because higher metabolic activities associated with elevated temperatures enhance receptivity to infochemicals (Yuan et al., 2009); or because embryos are reciprocally influenced by their own stress chemicals (autoinduction) (Landi, 2020). These findings are in line with additive phenotypic effects of alarm cues and predator presence (Di Rocco et al., 2016; Stephenson, 2016) and may indicate that receivers rely on their own stress perception and others' perception of stress (Giacomini et al., 2015). If stress responses are amplified within a group through stress propagation, the changes in group performance can then feedback to the individuals (Brandl et al., 2022). This lends support for a "positive feedback loop" which was defined as (i) a similar response in the donors and the receivers and (ii) an amplified response in individuals exposed to both the stress and the stress metabolites.

In contrast, a pH drop tended to disrupt the response of receiver shore crabs and ragworms to stress metabolites from sea bream, as in acidic pH conditions they failed to react to stress metabolites that induce avoidance responses in normal pH conditions. This is in agreement with low pH impairing alarm reactions in several species of fish in work by Leduc and colleagues (2003, 2004, 2006, 2007). A decreased pH can cause infodisruption of chemical signalling which results in behavioural changes (Schirrmacher et al., 2021; Roggatz et al., 2022).

Chapter 5 explored whether stress metabolites alone and combined with heat can alter the response to UV radations. Surprisingly, whilst heat alone protected embryos from UV-induced defects, stress metabolites alone did not rescue embryos from damage; and stress cues combined with heat overwhelmed embryos resulting in the loss of protective hormetic effects. These experiments suggested that the fitness effects of stress propagation were worsened in multistress environments, which warrants consideration for stress communication in a changing climate.

6.5. Future studies

The concept of stress propagation has been extensively studied in the context of biotic stress in terrestrial and aquatic systems, in many taxa, from unicellular organisms (Zuo et al., 2012) to plants (Landi et al., 2020) to aquatic animals (Crane et al., 2022) to mammals (Bombail et al., 2018). However, there was a knowledge gap in understanding whether abiotic stress can cause such stress propagation in aquatic animals. In this Ph.D. thesis, four experimental approaches evidenced that two abiotic stressors arising from climate change, namely heat events and ocean acidification, cause directly-stressed aquatic animals to propagate stress responses to naïve receivers. This confirms that abiotic stress induces stress propagation in aquatic animals. I propose here several directions for future studies.

The metabolome and transcriptome were sampled 24 hours after first initiating stress in donors and stress propagation in receivers. The transcriptome of receivers may therefore only capture residual pathways that persist for several hours, or pathways downstream of stress metabolite detection. Likewise, compounds are degraded over time (Chivers et al., 2013). This warrants the need for studies sampling the metabolome of donors shortly after stress exposure. One experiment that would help identifying chemicals involved in stress propagation would be to combine metabolomics with isotope labelling in zebrafish (Naser et al., 2021) to trace the transmission of cues from donors to receivers.

Another major drawback of the experimental designs is the use of negligible volumes (200 µL to 20-L closed systems). One can argue that the observed behavioural responses to stress metabolites are artefacts of enclosed environments in the laboratory (Magurran et al., 1996). However, antipredatory responses to alarm cues (Wisenden et al., 2004; Wisenden, 2008) and disturbance cues (Goldman et al., 2020a) were confirmed in the wild – albeit effects may be weaker than in the laboratory – reinforcing the relevance of laboratory stress propagation studies. Nonetheless, future studies should assess the existence and magnitude of responses to stress metabolites in different concentrations in abiotically stressed wild populations. While this is possible for predation threats (Wisenden et al., 2004; Wisenden, 2008; Goldman et al., 2020a), it would be difficult to manipulate abiotic factors in the wild, and stress propagation studies would likely be confined within the laboratory. One solution suggested by Baldwin et al (2006) is to use mutants unable to release specific compounds (“mute” donors) or detect stress metabolites (“deaf” receivers). Treating zebrafish embryos with

neomycin and zinc sulfate could help determining the role of neuromasts and olfactory cells (Alsrhani et al., 2021) in the response to stress metabolites.

Zebrafish embryos were exposed during ontogeny and over several days. This mimics realistic scenarios within an embryo clutch but induces development as a cofounding factor. One solution would be to monitor behavioural responses of receivers directly after the introduction of stress cues using stage- and size-matched individuals to fully understand responses to stress metabolites – similar to experimental designs used in disturbance and alarm cue studies. Importantly, the experimental data focused on transcriptomics, metabolomics of the medium, cortisol, HSP70 protein levels, behaviour, and growth. Whilst valuable, this data misses on mechanistic links from genetic data to whole-body outcomes which calls for acquiring data of epigenetics, post-translational modifications, proteomics, as well as within-body and body fluid metabolomics (energy levels incl. glucose, lactate, ATP). Last, living in groups may reduce stress responses compared to individually-raised animals – which is called "social buffering" (Kiyokawa and Hennessy, 2018), and may limit stress propagation. More research is needed to evaluate whether stress is amplified (by positive feedback loops) or attenuated (by social buffering) during stress communication within a group.

6.1. Conclusions: stress metabolites are the language of abiotic stress communication

Prior research focused on stress communication in the context of biotic stress such as predation, whilst there was limited information about the existence of similar mechanisms in aquatic animals experiencing abiotic stress. In this Ph.D. thesis, all four experiments provided evidence for abiotic stress-induced stress propagation. This extends known concepts of stress propagation and broadens the idea that stressed animals can stress each other upon abiotic stress, on top of biotic stressors. In a recent review, Brandl et al. (2022) emphasised that it is not well understood whether – and how – stressed animals can influence stress and collective behaviours in other group members. In this Ph.D. thesis, I clarified these points by uncovering the molecular and behavioural basis of stress propagation in donors and receivers. I confirmed that donors were stressed, and that stress-induced molecular shifts caused the release of stress metabolites, which propagated stress responses to receivers (**Figure 6.1**).

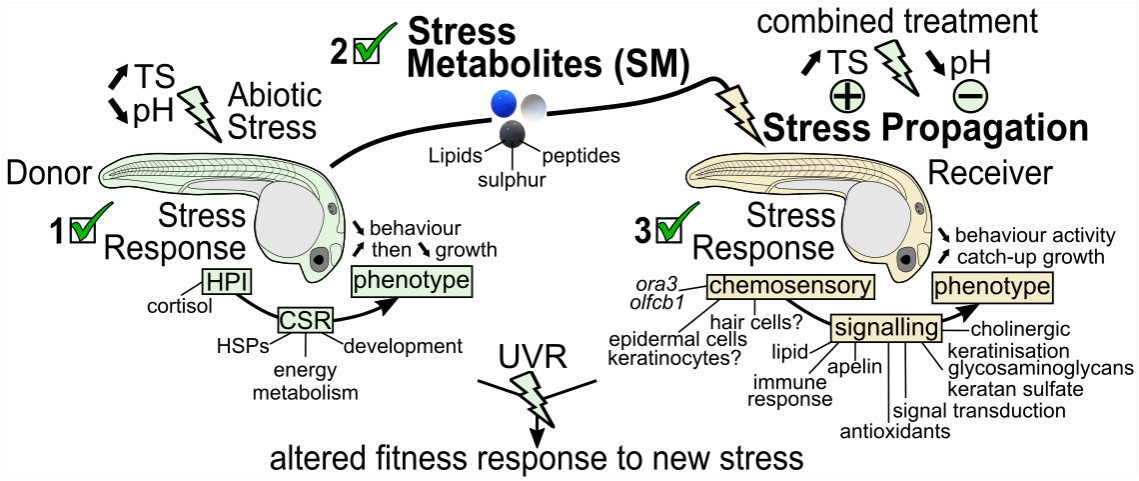

Figure 6.1. Summary of hypotheses and stress propagation mechanisms.
Ticked boxes show the three main hypotheses validated by experimental approaches. Proposed mechanisms for stress propagation are shown below embryos. Abiotic stressors may alter stress propagation by amplifying (+) or disrupting (-) the effects of stress metabolites. Direct (green) or indirect (yellow) abiotic stress can alter the fitness response to new challenges such as ultraviolet radiation (UVR). CSR: cellular stress response. HSP: heat shock proteins. HPI: hypothalamic-pituitary-interrenal axis

The experimental approach supports the main hypotheses of this Ph.D. thesis by showing that (i) donors were stressed by pH and heat, (ii) stressed donors released stress-specific cues in their environment, (iii) and receivers displayed stress responses when facing stress metabolites – this confirms that abiotic stress causes stress propagation to receivers, through activating fine-tuned transcriptomic pathways (**Figure 6.1**).

Research on stress propagation independently focused on alarm cues, disturbance cues, drosophila stress odorants, mammalian stress odours, or phytohormones. Abiotic and biotic stress propagation transmitted by chemical cues has been shown in cells (Pozzer et al., 2022), plants (Falik et al., 2012; Caparrotta et al., 2018; Landi et al., 2020; Jin et al., 2021), platyhelminths (Wisenden and Millard, 2001), polychaetes (Watson et al., 2005), insects (Siepielski et al., 2016; Yost et al., 2021), crustaceans (Hazlett, 1985, 1990b, 1990a), amphibians (Bairos-Novak et al., 2017, 2018, 2020), fish (Abreu et al., 2016; Goldman et al., 2019, 2020a, 2020b, 2021), rodents (Bombail et al., 2018), cattle (Boissy et al., 1998), and humans (Mujica-Parodi et al., 2009; Rubin et al., 2012). In this Ph.D. thesis, stress propagation was observed in marine (Chapter 2) and freshwater (Chapters 3-4) environments; in three donor species, including two fishes with the sea bream *S. aurata* and two strains of zebrafish *D. rerio*, and one polychaete with the ragworm *H. diversicolor*. All tested receiver species reacted to stress metabolites from conspecifics and/or heterospecifics including both strains of fish *D. rerio*, and wild-

caught invertebrates including polychaetes *H. diversicolor,* and two crustaceans with shore crabs *C. maenas* and hermit crabs *D. pugilator*. Stress propagation was shown in early life stages and in mature animals; in experiments utilising very short-term acute stressors (30-min) to longer-term sublethal stress (1 to 4 days); and with two abiotic stressors associated with climate change: heat and pH drop. Consequently, my findings combined with previous research in other species lend support to the idea that stress communication is a widespread, innate, and conserved phenomenon in nature. Since there may be evolutionary and chemical constraints for the synthesis of cues (Wyatt, 2010), stress odours involved in these mechanisms may even share similar chemical characteristics (Bombail et al., 2018). The evolutionary conserved stress axis in fish (Balasch and Tort, 2019) suggests that stress compounds may overlap between species (at least in fish) – albeit the chemical cocktails may vary with each stress condition (Sakuma et al., 2013). The chemical cues found in zebrafish are therefore good candidates as stress signals in chemical communication in other species. It is tentative, from the similarity of these mechanisms, to propose a unified concept by which stressed living organisms transmit public information, in the form of released stress-induced cues, reflective of their physiological distress, which alert others to prepare themselves for the stress by mounting an anticipatory response.

By extending stress propagation to repeated heat peaks and acidified pH in several aquatic species, the significance of this Ph.D. thesis is fivefold. First, predictions of population responses to climate change should consider stress propagation within groups as a positive feedback loop that can drastically amplify negative consequences. Second, stress cues warrant consideration in both in experimental settings and in animal welfare (Bombail et al., 2018) to manage stocks and prevent mass panic and mortalities in aquaculture settings. Third, the evidence that temperature and pH may disrupt stress communication, either by amplifying or impeding the use of stress cues, adds another layer of complexity to chemical stress propagation. Fourth, the nonlinear dose-response relationship between heat stress history and mutagenic stress responses raises concern for populations in multistress environments. Fifth – and most importantly – the evolutionary conserved stress axis across taxa makes findings from the multi-omic experiments in zebrafish embryos relevant for other species, particularly with regards to candidate pathways as priority molecular mechanisms which involvement in stress propagation needs to be confirmed and further investigated.

References

Aanes, H., Collas, P., and Aleström, P. (2014). Transcriptome dynamics and diversity in the early zebrafish embryo. *Brief. Funct. Genomics* 13, 95–105. doi: 10.1093/bfgp/elt049.

Abel, E. L. (1992). Response to alarm substance in different rat strains. *Physiol. Behav.* 51, 345–347. doi: 10.1016/0031-9384(92)90151-q.

Abozaid, H., Wessels, S., and Hörstgen-Schwark, G. (2011). Effect of rearing temperatures during embryonic development on the phenotypic sex in zebrafish (Danio rerio). *Sex Dev.* 5, 259–265. doi: 10.1159/000330120.

Abreu, M. S., Giacomini, A. C. V., Gusso, D., Koakoski, G., Oliveira, T. A., Marqueze, A., et al. (2016). Behavioral responses of zebrafish depend on the type of threatening chemical cues. *J. Comp. Physiol. A Neuroethol. Sens. Neural Behav. Physiol.* 202, 895–901. doi: 10.1007/s00359-016-1129-5.

Ackerman, K. M., Nakkula, R., Zirger, J. M., Beattie, C. E., and Boyd, R. T. (2009). Cloning and spatiotemporal expression of zebrafish neuronal nicotinic acetylcholine receptor alpha 6 and alpha 4 subunit RNAs. *Dev. Dyn.* 238, 980–992. doi: 10.1002/dvdy.21912.

Alberts, A. C. (1992). Constraints on the Design of Chemical Communication Systems in Terrestrial Vertebrates. *Am. Nat.* 139, S62–S89. Available at: http://www.jstor.org/stable/2462428.

Albig, W., Meergans, T., and Doenecke, D. (1997). Characterization of the H1.5 gene completes the set of human H1 subtype genes. *Gene* 184, 141–148. doi: 10.1016/s0378-1119(96)00582-3.

Alderman, S. L., and Bernier, N. J. (2009). Ontogeny of the corticotropin-releasing factor system in zebrafish. *Gen. Comp. Endocrinol.* 164, 61–69. doi: 10.1016/j.ygcen.2009.04.007.

Alexa, A., and Rahnenfuhrer, J. (2020). topGO: Enrichment Analysis for Gene Ontology. Available at: https://rdrr.io/bioc/topGO/ [Accessed March 27, 2021].

Alfonso, S., Gesto, M., and Sadoul, B. (2020). Temperature increase and its effects on fish stress physiology in the context of global warming. *J. Fish Biol.* 98, 1496–1508. doi: 10.1111/jfb.14599.

Allan, B. J. M., Domenici, P., Munday, P. L., and McCormick, M. I. (2015). Feeling the heat: the effect of acute temperature changes on predator-prey interactions in coral reef fish. *Conserv. Physiol.* 3, cov011. doi: 10.1093/conphys/cov011.

Alliance of Genome Resources Consortium (2020). Alliance of Genome Resources Portal: unified model organism research platform. *Nucleic Acids Res.* 48, D650–D658. doi: 10.1093/nar/gkz813.

Allwood, J. W., Williams, A., Uthe, H., van Dam, N. M., Mur, L. A. J., Grant, M. R., et al. (2021). Unravelling plant responses to stress-the importance of targeted and untargeted metabolomics. *Metabolites* 11, 558. doi: 10.3390/metabo11080558.

Almeida, J. R., Gravato, C., and Guilhermino, L. (2015). Effects of Temperature in Juvenile Seabass (Dicentrarchus labrax L.) Biomarker Responses and Behaviour: Implications for Environmental Monitoring. *Estuaries Coasts* 38, 45–55. doi: 10.1007/s12237-014-9792-7.

Alsop, D., and Vijayan, M. (2009a). The zebrafish stress axis: molecular fallout from the teleost-specific genome duplication event. *Gen. Comp. Endocrinol.* 161, 62–66. doi: 10.1016/j.ygcen.2008.09.011.

Alsop, D., and Vijayan, M. M. (2008). Development of the corticosteroid stress axis and receptor expression in zebrafish. *Am. J. Physiol. Regul. Integr. Comp. Physiol.* 294, R711-9. doi: 10.1152/ajpregu.00671.2007.

Alsop, D., and Vijayan, M. M. (2009b). Molecular programming of the corticosteroid stress axis during zebrafish development. *Comp. Biochem. Physiol. A Mol. Integr. Physiol.* 153, 49–54. doi: 10.1016/j.cbpa.2008.12.008.

Alsrhani, A., Raman, R., and Jagadeeswaran, P. (2021). Trypsin induces an aversive response in zebrafish by PAR2 activation in keratinocytes. *PLoS One* 16, e0257774. doi: 10.1371/journal.pone.0257774.

Alton, L. A., and Franklin, C. E. (2012). Do high temperatures enhance the negative effects of ultraviolet-B radiation in embryonic and larval amphibians? *Biol. Open* 1, 897–903. doi: 10.1242/bio.2012950.

Aluru, N., and Vijayan, M. M. (2009). Stress transcriptomics in fish: a role for genomic cortisol signaling. *Gen. Comp. Endocrinol.* 164, 142–150. doi: 10.1016/j.ygcen.2009.03.020.

Alves, R. N., and Agustí, S. (2020). Effect of ultraviolet radiation (UVR) on the life stages of fish. *Rev. Fish Biol. Fish.* 30, 335–372. doi: 10.1007/s11160-020-09603-1.

Andersen, C. L., Jensen, J. L., and Ørntoft, T. F. (2004). Normalization of Real-Time Quantitative Reverse Transcription-PCR Data: A Model-Based Variance Estimation Approach to Identify Genes Suited for Normalization, Applied to Bladder and Colon Cancer Data Sets. *Cancer Research* 64, 5245–5250. doi: 10.1158/0008-5472.can-04-0496.

Andonov, K., Dyugmedzhiev, A., Lukanov, S., Slavchev, M., Vacheva, E., Stanchev, N., et al. (2020). Analyses of Skin Secretions of Vipera ammodytes (Linnaeus, 1758) (Reptilia: Serpentes), with Focus on the Complex Compounds and Their Possible Role in the Chemical Communication. *Molecules* 25. doi: 10.3390/molecules25163622.

Andreeßen, C., Wolf, N., Cramer, B., Humpf, H.-U., and Steinbüchel, A. (2018). In vitro biosynthesis of 3-mercaptolactate by lactate dehydrogenases. *Enzyme Microb. Technol.* 108, 1–10. doi: 10.1016/j.enzmictec.2017.08.005.

Angiulli, E., Pagliara, V., Cioni, C., Frabetti, F., Pizzetti, F., Alleva, E., et al. (2020). Increase in environmental temperature affects exploratory behaviour, anxiety and social preference in Danio rerio. *Sci. Rep.* 10, 5385. doi: 10.1038/s41598-020-62331-1.

Appelhans, Y. S., Thomsen, J., Pansch, C., Melzner, F., and Wahl, M. (2012). Sour times: seawater acidification effects on growth, feeding behaviour and acid–base status of Asterias rubens and Carcinus maenas. *Mar. Ecol. Prog. Ser.* 459, 85–98. doi: 10.3354/meps09697.

Applied Biosystems, A. B. (2006). Application Note TaqMan® Gene Expression Assays. Amplification Efficiency of TaqMan® Gene Expression Assays. Available at: https://assets.thermofisher.com/TFS-Assets/LSG/Application-Notes/cms_040377.pdf.

Araújo, M. B., Ferri-Yáñez, F., Bozinovic, F., Marquet, P. A., Valladares, F., and Chown, S. L. (2013). Heat freezes niche evolution. *Ecol. Lett.* 16, 1206–1219. doi: 10.1111/ele.12155.

Arimura, G., Ozawa, R., Shimoda, T., Nishioka, T., Boland, W., and Takabayashi, J. (2000). Herbivory-induced volatiles elicit defence genes in lima bean leaves. *Nature* 406, 512–515. doi: 10.1038/35020072.

Ashur, M. M., Johnston, N. K., and Dixson, D. L. (2017). Impacts of Ocean Acidification on Sensory Function in Marine Organisms. *Integr. Comp. Biol.* 57, 63–80. doi: 10.1093/icb/icx010.

Atherton, J. A., and McCormick, M. I. (2015). Active in the sac: damselfish embryos use innate recognition of odours to learn predation risk before hatching. *Anim. Behav.* 103, 1–6. doi: 10.1016/j.anbehav.2015.01.033.

Atherton, J. A., and McCormick, M. I. (2017). Kin recognition in embryonic damselfishes. *Oikos* 126, 1062–1069. doi: 10.1111/oik.03597.

Atli, G., Canli, E. G., Eroglu, A., and Canli, M. (2016). Characterization of antioxidant system parameters in four freshwater fish species. *Ecotoxicol. Environ. Saf.* 126, 30–37. doi: 10.1016/j.ecoenv.2015.12.012.

Aubret, F., Blanvillain, G., Bignon, F., and Kok, P. J. R. (2016). Heartbeat, embryo communication and hatching synchrony in snake eggs. *Sci. Rep.* 6, 23519. doi: 10.1038/srep23519.

Augustyn, K. D. C., Jackson, M. R., and Jorns, M. S. (2017). Use of Tissue Metabolite Analysis and Enzyme Kinetics To Discriminate between Alternate Pathways for Hydrogen Sulfide Metabolism. *Biochemistry* 56, 986–996. doi: 10.1021/acs.biochem.6b01093.

Auperin, B., and Geslin, M. (2008). Plasma cortisol response to stress in juvenile rainbow trout is influenced by their life history during early development and by egg cortisol content. *Gen. Comp. Endocrinol.* 158, 234–239. doi: 10.1016/j.ygcen.2008.07.002.

Aurangzeb, Z., Daghfous, G., Innes, L., Dubuc, R., and Zielinski, B. (2021). Current understanding of lamprey chemosensory systems. *J. Great Lakes Res.* 47, S650–S659. doi: 10.1016/j.jglr.2021.04.020.

Bai, Y., Liu, H., Huang, B., Wagle, M., and Guo, S. (2016). Identification of environmental stressors and validation of light preference as a measure of anxiety in larval zebrafish. *BMC Neurosci.* 17, 63. doi: 10.1186/s12868-016-0298-z.

Bairos-Novak, K. R., Crane, A. L., Achtymichuk, G. H., Hsin, J., Rivera-Hernández, I. A. E., Simko, O. M., et al. (2020). Forget the audience: tadpoles release similar disturbance cues regardless of kinship or familiarity. *Behav. Ecol. Sociobiol.* 74, 147. doi: 10.1007/s00265-020-02936-8.

Bairos-Novak, K. R., Crane, A. L., Chivers, D. P., and Ferrari, M. C. O. (2018). Better the devil you know? How familiarity and kinship affect prey responses to disturbance cues. *Behav. Ecol.* 30, 446–454. doi: 10.1093/beheco/ary184.

Bairos-Novak, K. R., Ferrari, M. C. O., and Chivers, D. P. (2019). A novel alarm signal in aquatic prey: Familiar minnows coordinate group defences against predators through chemical disturbance cues. *J. Anim. Ecol.* 88, 1281–1290. doi: 10.1111/1365-2656.12986.

Bairos-Novak, K. R., Mitchell, M. D., Crane, A. L., Chivers, D. P., and Ferrari, M. C. O. (2017). Trust thy neighbour in times of trouble: background risk alters how tadpoles release and respond to disturbance cues. *Proc. Biol. Sci.* 284(1863), 20171465. doi: 10.1098/rspb.2017.1465.

Bais, A. F., Lucas, R. M., Bornman, J. F., Williamson, C. E., Sulzberger, B., Austin, A. T., et al. (2018). Environmental effects of ozone depletion, UV radiation and interactions with climate change: UNEP Environmental Effects Assessment Panel, update 2017. *Photochem. Photobiol. Sci.* 17, 127–179. doi: 10.1039/c7pp90043k.

Baker, M. (2016). 1,500 scientists lift the lid on reproducibility. *Nature* 533, 452–454. doi: 10.1038/533452a.

Balasch, J. C., and Tort, L. (2019). Netting the stress responses in fish. *Front. Endocrinol. (Lausanne)* 10, 62. doi: 10.3389/fendo.2019.00062.

Baldwin, I. T., Halitschke, R., Paschold, A., von Dahl, C. C., and Preston, C. A. (2006). Volatile signaling in plant-plant interactions: "talking trees" in the genomics era. *Science* 311, 812–815. doi: 10.1126/science.1118446.

Balogh, G., Péter, M., Glatz, A., Gombos, I., Török, Z., Horváth, I., et al. (2013). Key role of lipids in heat stress management. *FEBS Lett.* 587, 1970–1980. doi: 10.1016/j.febslet.2013.05.016.

Banaś, A. K., Zgłobicki, P., Kowalska, E., Bażant, A., Dziga, D., and Strzałka, W. (2020). All You Need Is Light. Photorepair of UV-Induced Pyrimidine Dimers. *Genes* 11. doi: 10.3390/genes11111304.

Banerjee, S., and Leptin, M. (2014). Systemic response to ultraviolet radiation involves induction of leukocytic IL-1β and inflammation in zebrafish. *J. Immunol.* 193, 1408–1415. doi: 10.4049/jimmunol.1400232.

Barbosa Júnior, A., Magalhães, E. J., Hoffmann, A., and Ide, L. M. (2010). Conspecific and heterospecific alarm substance induces behavioral responses in piau fish Leporinus piau. *Acta Ethol.* 13, 119–126. doi: 10.1007/s10211-010-0081-6.

Barcellos, L. J. G., Koakoski, G., da Rosa, J. G. S., Ferreira, D., Barreto, R. E., Giaquinto, P. C., et al. (2014). Chemical communication of predation risk in zebrafish does not depend on cortisol increase. *Sci. Rep.* 4, 5076. doi: 10.1038/srep05076.

Barcellos, L. J. G., Volpato, G. L., Barreto, R. E., Coldebella, I., and Ferreira, D. (2011). Chemical communication of handling stress in fish. *Physiol. Behav.* 103, 372–375. doi: 10.1016/j.physbeh.2011.03.009.

Bard, B., and Kieffer, J. D. (2019). The effects of repeat acute thermal stress on the critical thermal maximum (CTmax) and physiology of juvenile shortnose sturgeon (Acipenser brevirostrum). *Can. J. Zool.* 97, 567–572. doi: 10.1139/cjz-2018-0157.

Barkhymer, A. J., Garrett, S. G., and Wisenden, B. D. (2019). Olfactorily-mediated cortisol response to chemical alarm cues in zebrafish Danio rerio. *J. Fish Biol.* 95, 287–292. doi: 10.1111/jfb.13860.

Barreto, R. E., Júnior, A. B., Giassi, A. C. C., and Hoffmann, A. (2010). The 'club' cell and behavioural and physiological responses to chemical alarm cues in the Nile tilapia. *Mar. Freshw. Behav. Physiol.* 43, 75–81. doi: 10.1080/10236241003654139.

Barth, A. L., Justice, N. J., and Ngai, J. (1996). Asynchronous onset of odorant receptor expression in the developing zebrafish olfactory system. *Neuron* 16, 23–34. doi: 10.1016/s0896-6273(00)80020-3.

Barton, B. A. (2002). Stress in fishes: a diversity of responses with particular reference to changes in circulating corticosteroids. *Integr. Comp. Biol.* 42, 517–525. doi: 10.1093/icb/42.3.517.

Barton, B. A., and Iwama, G. K. (1991). Physiological changes in fish from stress in aquaculture with emphasis on the response and effects of corticosteroids. *Annu. Rev. Fish Dis.* 1, 3–26. doi: 10.1016/0959-8030(91)90019-G.

Basu, N., Todgham, A. E., Ackerman, P. A., Bibeau, M. R., Nakano, K., Schulte, P. M., et al. (2002). Heat shock protein genes and their functional significance in fish. *Gene* 295, 173–183. doi: 10.1016/s0378-1119(02)00687-x.

Batten, S. D., and Bamber, R. N. (1996). The effects of acidified seawater on the polychaete Nereis virens Sars, 1835. *Mar. Pollut. Bull.* 32, 283–287. doi: 10.1016/0025-326X(95)00163-H.

Beemelmanns, A., Zanuzzo, F. S., Xue, X., Sandrelli, R. M., Rise, M. L., and Gamperl, A. K. (2021). The transcriptomic responses of Atlantic salmon (Salmo salar) to high temperature stress alone, and in combination with moderate hypoxia. *BMC Genomics* 22, 261. doi: 10.1186/s12864-021-07464-x.

Beitinger, T. L., Bennett, W. A., and McCauley, R. W. (2000). Temperature Tolerances of North American Freshwater Fishes Exposed to Dynamic Changes in Temperature. *Environ. Biol. Fishes* 58, 237–275. doi: 10.1023/A:1007676325825.

Ben-Shachar, M. S., Lüdecke, D., and Makowski, D. (2020). effectsize: Estimation of Effect Size Indices and Standardized Parameters. *Journal of Open Source Software* 5, 2815. doi: 10.21105/joss.02815.

Berger, D., Stångberg, J., Grieshop, K., Martinossi-Allibert, I., and Arnqvist, G. (2017). Temperature effects on life-history trade-offs, germline maintenance and mutation rate under simulated climate warming. *Proc. Biol. Sci.* 284. doi: 10.1098/rspb.2017.1721.

Berry, R., 3rd, and López-Martínez, G. (2020). A dose of experimental hormesis: When mild stress protects and improves animal performance. *Comp. Biochem. Physiol. A Mol. Integr. Physiol.* 242, 110658. doi: 10.1016/j.cbpa.2020.110658.

Best, C., Kurrasch, D. M., and Vijayan, M. M. (2017). Maternal cortisol stimulates neurogenesis and affects larval behaviour in zebrafish. *Sci. Rep.* 7, 40905. doi: 10.1038/srep40905.

Bett, N. N., Hinch, S. G., and Yun, S.-S. (2016). Behavioural responses of Pacific salmon to chemical disturbance cues during the spawning migration. *Behav. Processes* 132, 76–84. doi: 10.1016/j.beproc.2016.10.001.

Bhuiyan, K. A., Rodríguez, B. M., Pires, A., Riba, I., Dellvals, Á., Freitas, R., et al. (2021). Experimental evidence of uncertain future of the keystone ragworm Hediste diversicolor (O.F. Müller, 1776) under climate change conditions. *Sci. Total Environ.* 750, 142031. doi: 10.1016/j.scitotenv.2020.142031.

Bianchi, M., Giacomini, E., Crinelli, R., Radici, L., Carloni, E., and Magnani, M. (2015). Dynamic transcription of ubiquitin genes under basal and stressful conditions and new insights into the multiple UBC transcript variants. *Gene* 573, 100–109. doi: 10.1016/j.gene.2015.07.030.

Blalock, J. E. (2005). The immune system as the sixth sense. *J. Intern. Med.* 257, 126–138. doi: 10.1111/j.1365-2796.2004.01441.x.

Bleckmann, H., and Zelick, R. (2009). Lateral line system of fish. *Integr. Zool.* 4, 13–25. doi: 10.1111/j.1749-4877.2008.00131.x.

Blighe, K., Rana, S., and Lewis, M. (2020). EnhancedVolcano: Publication-ready volcano plots with enhanced colouring and labeling. Available at: https://github.com/kevinblighe/EnhancedVolcano.

Boissy, A., Terlouw, C., and Le Neindre, P. (1998). Presence of cues from stressed conspecifics increases reactivity to aversive events in cattle: evidence for the existence of alarm substances in urine. *Physiol. Behav.* 63, 489–495. doi: 10.1016/s0031-9384(97)00466-6.

Bolger, A. M., Lohse, M., and Usadel, B. (2014). Trimmomatic: a flexible trimmer for Illumina sequence data. *Bioinformatics* 30, 2114–2120. doi: 10.1093/bioinformatics/btu170.

Bombail, V. (2019). Perception and emotions: On the relationships between stress and olfaction. *Appl. Anim. Behav. Sci.* 212, 98–108. doi: 10.1016/j.applanim.2018.12.013.

Bombail, V., Barret, B., Raynaud, A., Jerôme, N., Saint-Albin, A., Ridder, C., et al. (2018). In search of stress odours across species: Behavioural responses of rats to faeces from chickens and rats subjected to various types of stressful events. *Appl. Anim. Behav. Sci.* 205, 216–226. doi: 10.1016/j.applanim.2017.10.013.

Bond, D. (2018). Ocean acidification threat? How pH affects burrowing behaviour of Nereis diversicolor and its bearing on mass extinction scenarios. in (EGU General Assembly Conference Abstracts), 6416. Available at: https://ui.adsabs.harvard.edu/abs/2018EGUGA..20.6416B.

Bowler, K. (2005). Acclimation, heat shock and hardening. *J. Therm. Biol.* 30, 125–130. doi: 10.1016/j.jtherbio.2004.09.001.

Bowman, A. W., and Azzalini, A. (2021). R package sm: nonparametric smoothing methods (version 2.2-5.7).

Braasch, I., Liedtke, D., Volff, J.-N., and Schartl, M. (2009). Pigmentary function and evolution of tyrp1 gene duplicates in fish. *Pigment Cell Melanoma Res.* 22, 839–850. doi: 10.1111/j.1755-148X.2009.00614.x.

Brandl, H. B., Pruessner, J. C., and Farine, D. R. (2022). The social transmission of stress in animal collectives. *Proc. Biol. Sci.* 289, 20212158. doi: 10.1098/rspb.2021.2158.

Brechbühl, J., Moine, F., Klaey, M., Nenniger-Tosato, M., Hurni, N., Sporkert, F., et al. (2013). Mouse alarm pheromone shares structural similarity with predator scents. *Proc. Natl. Acad. Sci. U. S. A.* 110, 4762–4767. doi: 10.1073/pnas.1214249110.

Brenner, M., and Hearing, V. J. (2008). The protective role of melanin against UV damage in human skin. *Photochem. Photobiol.* 84, 539–549. doi: 10.1111/j.1751-1097.2007.00226.x.

Brett, J. R. (1971). Energetic responses of salmon to temperature. A study of some thermal relations in the physiology and freshwater ecology of sockeye salmon (Oncorhynchus nerka). *Am. Zool.* 11, 99–113. doi: 10.1093/icb/11.1.99.

Bridge, W. L., Vandenberg, C. J., Franklin, R. J., and Hiom, K. (2005). The BRIP1 helicase functions independently of BRCA1 in the Fanconi anemia pathway for DNA crosslink repair. *Nat. Genet.* 37, 953–957. doi: 10.1038/ng1627.

Briffa, M., de la Haye, K., and Munday, P. L. (2012). High CO_2 and marine animal behaviour: potential mechanisms and ecological consequences. *Mar. Pollut. Bull.* 64, 1519–1528. doi: 10.1016/j.marpolbul.2012.05.032.

Brinkmann, K., Schell, M., Hoppe, T., and Kashkar, H. (2015). Regulation of the DNA damage response by ubiquitin conjugation. *Front. Genet.* 6, 98. doi: 10.3389/fgene.2015.00098.

Broustas, C. G., and Lieberman, H. B. (2012). Contributions of Rad9 to tumorigenesis. *J. Cell. Biochem.* 113, 742–751. doi: 10.1002/jcb.23424.

Brown, A. R., Owen, S. F., Peters, J., Zhang, Y., Soffker, M., Paull, G. C., et al. (2015). Climate change and pollution speed declines in zebrafish populations. *Proc. Natl. Acad. Sci. U. S. A.* 112, E1237-46. doi: 10.1073/pnas.1416269112.

Brown, G. E., Adrian, J. C., Smyth, E., Leet, H., and Brennan, S. (2000). Ostariophysan Alarm Pheromones: Laboratory and Field Tests of the Functional Significance of Nitrogen Oxides. *J. Chem. Ecol.* 26, 139–154. doi: 10.1023/A:1005445629144.

Brown, G. E., Jackson, C. D., Malka, P. H., Jacques, É., and Couturier, M.-A. (2012). Disturbance cues in freshwater prey fishes: Does urea function as an 'early warning cue' in juvenile convict cichlids and rainbow trout? *Curr. Zool.* 58, 250–259. doi: 10.1093/czoolo/58.2.250.

Buchinger, T. J., Li, W., and Johnson, N. S. (2014). Bile salts as semiochemicals in fish. *Chem. Senses* 39, 647–654. doi: 10.1093/chemse/bju039.

Buck, L., and Axel, R. (1991). A novel multigene family may encode odorant receptors: a molecular basis for odor recognition. *Cell* 65, 175–187. doi: 10.1016/0092-8674(91)90418-x.

Buck, L. B. (2005). Unraveling the sense of smell (Nobel lecture). *Angew. Chem. Int. Ed Engl.* 44, 6128–6140. doi: 10.1002/anie.200501120.

Bucking, C., Lemoine, C. M. R., and Walsh, P. J. (2013). Waste nitrogen metabolism and excretion in zebrafish embryos: effects of light, ammonia, and nicotinamide. *J. Exp. Zool. A Ecol. Genet. Physiol.* 319, 391–403. doi: 10.1002/jez.1802.

Bui, D.-C., Kim, J.-E., Shin, J., Lim, J. Y., Choi, G. J., Lee, Y.-W., et al. (2019). ARS2 Plays Diverse Roles in DNA Damage Response, Fungal Development, and Pathogenesis in the Plant Pathogenic Fungus Fusarium graminearum. *Front. Microbiol.* 10, 2326. doi: 10.3389/fmicb.2019.02326.

Burlinson, F. C., and Lawrence, A. J. (2007). Development and validation of a behavioural assay to measure the tolerance of Hediste diversicolor to copper. *Environ. Pollut.* 145, 274–278. doi: 10.1016/j.envpol.2005.03.014.

Byrd, C. A., Jones, J. T., Quattro, J. M., Rogers, M. E., Brunjes, P. C., and Vogt, R. G. (1996). Ontogeny of odorant receptor gene expression in zebrafish, Danio rerio. *J. Neurobiol.* 29, 445–458. doi: 10.1002/(SICI)1097-4695(199604)29:4<445::AID-NEU3>3.0.CO;2-8.

Cahill, C. M., Waterman, W. R., Xie, Y., Auron, P. E., and Calderwood, S. K. (1996). Transcriptional repression of the prointerleukin 1beta gene by heat shock factor 1. *J. Biol. Chem.* 271, 24874–24879. Available at: https://www.ncbi.nlm.nih.gov/pubmed/8926278.

Calabrese, E. J., Bachmann, K. A., Bailer, A. J., Bolger, P. M., Borak, J., Cai, L., et al. (2007). Biological stress response terminology: Integrating the concepts of adaptive response and preconditioning stress within a hormetic dose-response framework. *Toxicol. Appl. Pharmacol.* 222, 122–128. doi: 10.1016/j.taap.2007.02.015.

Calabrese, E. J., and Baldwin, L. A. (2002). Defining hormesis. *Hum. Exp. Toxicol.* 21, 91–97. doi: 10.1191/0960327102ht217oa.

Caldeira, K., and Wickett, M. E. (2003). Oceanography: anthropogenic carbon and ocean pH. *Nature* 425, 365. doi: 10.1038/425365a.

Calvo-Ochoa, E., and Byrd-Jacobs, C. A. (2019). The olfactory system of zebrafish as a model for the study of neurotoxicity and injury: Implications for neuroplasticity and disease. *Int. J. Mol. Sci.* 20, 1639. doi: 10.3390/ijms20071639.

Canzian, J., Fontana, B. D., Quadros, V. A., and Rosemberg, D. B. (2017). Conspecific alarm substance differently alters group behavior of zebrafish populations: Putative involvement of cholinergic and purinergic signaling in anxiety- and fear-like responses. *Behav. Brain Res.* 320, 255–263. doi: 10.1016/j.bbr.2016.12.018.

Cao, X., and Li, W. (2020). Embryonic substances induce alarm response in adult zebrafish (Danio rerio). *J. Fish Biol.* 97, 225–230. doi: 10.1111/jfb.14354.

Caparrotta, S., Boni, S., Taiti, C., Palm, E., Mancuso, S., and Pandolfi, C. (2018). Induction of priming by salt stress in neighboring plants. *Environ. Exp. Bot.* 147, 261–270. doi: 10.1016/j.envexpbot.2017.12.017.

Carlson, M. (2020). *org.Dr.eg.db: Genome wide annotation for Zebrafish*.

Casati, P., and Walbot, V. (2004). Crosslinking of ribosomal proteins to RNA in maize ribosomes by UV-B and its effects on translation. *Plant Physiol.* 136, 3319–3332. doi: 10.1104/pp.104.047043.

Castillo, J., Teles, M., Mackenzie, S., and Tort, L. (2009). Stress-related hormones modulate cytokine expression in the head kidney of gilthead seabream (Sparus aurata). *Fish Shellfish Immunol.* 27, 493–499. doi: 10.1016/j.fsi.2009.06.021.

Castro, R., Zou, J., Secombes, C. J., and Martin, S. A. M. (2011). Cortisol modulates the induction of inflammatory gene expression in a rainbow trout macrophage cell line. *Fish Shellfish Immunol.* 30, 215–223. doi: 10.1016/j.fsi.2010.10.010.

Ceccato, E., Cramp, R. L., Seebacher, F., and Franklin, C. E. (2016). Early exposure to ultraviolet-B radiation decreases immune function later in life. *Conserv Physiol* 4, cow037. doi: 10.1093/conphys/cow037.

Champliaud, M. F., Baden, H. P., Koch, M., Jin, W., Burgeson, R. E., and Viel, A. (2000). Gene characterization of sciellin (SCEL) and protein localization in vertebrate epithelia displaying barrier properties. *Genomics* 70, 264–268. doi: 10.1006/geno.2000.6390.

Chand D, B., and Rajarami G, R. (2015). Long-term changes in brain cholinergic system and behavior in rats following gestational exposure to lead: protective effect of calcium supplement. *Interdiscip. Toxicol.* 8, 159–168. doi: 10.1515/intox-2015-0025.

Chao, D., He, X., Yang, Y., Balboni, G., Salvadori, S., Kim, D. H., et al. (2012). Hydrogen sulfide induced disruption of Na+ homeostasis in the cortex. *Toxicol. Sci.* 128, 198–208. doi: 10.1093/toxsci/kfs125.

Chapman, N. A., Dupré, D. J., and Rainey, J. K. (2014). The apelin receptor: physiology, pathology, cell signalling, and ligand modulation of a peptide-activated class A GPCR. *Biochem. Cell Biol.* 92, 431–440. doi: 10.1139/bcb-2014-0072.

Charmant, J., and Contributors (2021). Kinovea (0.9.5). Available at: https://www.kinovea.org.

Charron, R. A., Fenwick, J. C., Lean, D. R., and Moon, T. W. (2000). Ultraviolet-B radiation effects on antioxidant status and survival in the zebrafish, Brachydanio rerio. *Photochem. Photobiol.* 72, 327–333. doi: 10.1562/0031-8655(2000)0720327UBREOA2.0.CO2.

Chartier, T. F., Deschamps, J., Dürichen, W., Jékely, G., and Arendt, D. (2018). Whole-head recording of chemosensory activity in the marine annelid Platynereis dumerilii. *Open Biol.* 8, 180139. doi: 10.1098/rsob.180139.

Chatterjee, N., and Walker, G. C. (2017). Mechanisms of DNA damage, repair, and mutagenesis. *Environ. Mol. Mutagen.* 58, 235–263. doi: 10.1002/em.22087.

Chavez, F., MBARI, Pennington, J. T., Michisaki, R., Blum, M., Chavez, G., et al. (2017). Climate variability and change: Response of a coastal ocean ecosystem. *Oceanography* 30, 128–145. doi: 10.5670/oceanog.2017.429.

Chen, S., Zhou, Y., Chen, Y., and Gu, J. (2018). fastp: an ultra-fast all-in-one FASTQ preprocessor. *Bioinformatics* 34, i884–i890. doi: 10.1093/bioinformatics/bty560.

Chen, Y., Ning, J., Cao, W., Wang, S., Du, T., Jiang, J., et al. (2020). Research Progress of TXNIP as a Tumor Suppressor Gene Participating in the Metabolic Reprogramming and Oxidative Stress of Cancer Cells in Various Cancers. *Front. Oncol.* 10, 568574. doi: 10.3389/fonc.2020.568574.

Chen, Z., Gan, J., Wei, Z., Zhang, M., Du, Y., Xu, C., et al. (2022). The Emerging Role of PRMT6 in Cancer. *Front. Oncol.* 12, 841381. doi: 10.3389/fonc.2022.841381.

Chéret, J., Bertolini, M., Ponce, L., Lehmann, J., Tsai, T., Alam, M., et al. (2018). Olfactory receptor OR2AT4 regulates human hair growth. *Nat. Commun.* 9, 3624. doi: 10.1038/s41467-018-05973-0.

Chien, L.-C., Wu, Y.-H., Ho, T.-N., Huang, Y.-Y., and Hsu, T. (2020). Heat stress modulates nucleotide excision repair capacity in zebrafish (Danio rerio) early and mid-early embryos via distinct mechanisms. *Chemosphere* 238, 124653. doi: 10.1016/j.chemosphere.2019.124653.

Chivers, D. P., Dixson, D. L., White, J. R., McCormick, M. I., and Ferrari, M. C. O. (2013). Degradation of chemical alarm cues and assessment of risk throughout the day. *Ecol. Evol.* 3, 3925–3934. doi: 10.1002/ece3.760.

Choi, V. W. Y., Cheng, S. H., and Yu, K. N. (2010). Radioadaptive response induced by alpha-particle-induced stress communicated in vivo between zebrafish embryos. *Environ. Sci. Technol.* 44, 8829–8834. doi: 10.1021/es101535f.

Choi, V. W. Y., Ng, C. Y. P., Kobayashi, A., Konishi, T., Suya, N., Ishikawa, T., et al. (2013). Bystander effect between zebrafish embryos in vivo induced by high-dose X-rays. *Environ. Sci. Technol.* 47, 6368–6376. doi: 10.1021/es401171h.

Chrousos, G. P. (2009). Stress and disorders of the stress system. *Nat. Rev. Endocrinol.* 5, 374–381. doi: 10.1038/nrendo.2009.106.

Cingi, S., Keinänen, M., and Vuorinen, P. J. (2010). Elevated water temperature impairs fertilization and embryonic development of whitefish Coregonus lavaretus. *J. Fish Biol.* 76, 502–521. doi: 10.1111/j.1095-8649.2009.02502.x.

Clark, K. J., Boczek, N. J., and Ekker, S. C. (2011). Stressing zebrafish for behavioral genetics. *Rev. Neurosci.* 22, 49–62. doi: 10.1515/RNS.2011.007.

Clark, T. D., Raby, G. D., Roche, D. G., Binning, S. A., Speers-Roesch, B., Jutfelt, F., et al. (2020a). Ocean acidification does not impair the behaviour of coral reef fishes. *Nature* 577, 370–375. doi: 10.1038/s41586-019-1903-y.

Clark, T. D., Raby, G. D., Roche, D. G., Binning, S. A., Speers-Roesch, B., Jutfelt, F., et al. (2020b). Reply to: Methods matter in repeating ocean acidification studies. *Nature* 586, E25–E27. doi: 10.1038/s41586-020-2804-9.

Clements, J. C., and Darrow, E. S. (2018). Eating in an acidifying ocean: a quantitative review of elevated CO2 effects on the feeding rates of calcifying marine invertebrates. *Hydrobiologia* 820, 1–21. doi: 10.1007/s10750-018-3665-1.

Clements, J. C., and Hunt, H. L. (2015). Marine animal behaviour in a high CO2 ocean. *Mar. Ecol. Prog. Ser.* 536, 259–279. doi: 10.3354/meps11426.

Clements, J. C., Poirier, L. A., Pérez, F. F., Comeau, L. A., and Babarro, J. M. F. (2020). Behavioural responses to predators in Mediterranean mussels (Mytilus galloprovincialis) are unaffected by elevated pCO2. *Mar. Environ. Res.* 161, 105148. doi: 10.1016/j.marenvres.2020.105148.

Clements, J. C., Ramesh, K., Nysveen, J., Dupont, S., and Jutfelt, F. (2021). Animal size and sea water temperature, but not pH, influence a repeatable startle response behaviour in a wide-ranging marine mollusc. *Anim. Behav.* 173, 191–205. doi: 10.1016/j.anbehav.2020.12.008.

Clements, J. C., Sundin, J., Clark, T. D., and Jutfelt, F. (2022). Meta-analysis reveals an extreme "decline effect" in the impacts of ocean acidification on fish behavior. *PLoS Biol.* 20, e3001511. doi: 10.1371/journal.pbio.3001511.

Cockram, M. S. (2002). The biology of animal stress: Basic principles and implications for animal welfare. *Vet. J.* 164, 77. doi: 10.1053/tvjl.2001.0558.

Cohen, J. (1988). *Statistical power analysis for the behavioural sciences (2nd edn.), Hillside, NJ: Erlbaum*. NJ: Erlbaum.

Colbert, P. L., Spencer, R.-J., and Janzen, F. J. (2010). Mechanism and cost of synchronous hatching. *Funct. Ecol.* 24, 112–121. doi: 10.1111/j.1365-2435.2009.01602.x.

Cold Spring Harbor Laboratory Press (2011). E3 medium (for zebrafish embryos). *Cold Spring Harb. Protoc.* 2011, db.rec66449. doi: 10.1101/pdb.rec066449.

Colinet, H., Sinclair, B. J., Vernon, P., and Renault, D. (2015). Insects in fluctuating thermal environments. *Annu. Rev. Entomol.* 60, 123–140. doi: 10.1146/annurev-ento-010814-021017.

Colson, V., Cousture, M., Damasceno, D., Valotaire, C., Nguyen, T., Le Cam, A., et al. (2019). Maternal temperature exposure impairs emotional and cognitive responses and triggers dysregulation of neurodevelopment genes in fish. *PeerJ* 7, e6338. doi: 10.7717/peerj.6338.

Conde-Sieira, M., Chivite, M., Míguez, J. M., and Soengas, J. L. (2018). Stress effects on the mechanisms regulating appetite in teleost fish. *Front. Endocrinol. (Lausanne)* 9. doi: 10.3389/fendo.2018.00631.

Cong, X., Zheng, Q., Ren, W., Chéron, J.-B., Fiorucci, S., Wen, T., et al. (2019). Zebrafish olfactory receptors ORAs differentially detect bile acids and bile salts. *J. Biol. Chem.* 294, 6762–6771. doi: 10.1074/jbc.RA118.006483.

Cook, P. J., Ju, B. G., Telese, F., Wang, X., Glass, C. K., and Rosenfeld, M. G. (2009). Tyrosine dephosphorylation of H2AX modulates apoptosis and survival decisions. *Nature* 458, 591–596. doi: 10.1038/nature07849.

Cortez, V., Verdú, J. R., Ortiz, A. J., and Halffter, G. (2017). Identification and evaluation of semiochemicals for the biological control of the beetle Omorgus suberosus (F.) (Coleoptera: Trogidae), a facultative predator of eggs of the sea turtle Lepidochelys olivacea (Eschscholtz). *PLoS One* 12, e0172015. doi: 10.1371/journal.pone.0172015.

Costantini, D., Metcalfe, N. B., and Monaghan, P. (2010). Ecological processes in a hormetic framework. *Ecol. Lett.* 13, 1435–1447. doi: 10.1111/j.1461-0248.2010.01531.x.

Costantini, D., Monaghan, P., and Metcalfe, N. B. (2012). Early life experience primes resistance to oxidative stress. *J. Exp. Biol.* 215, 2820–2826. doi: 10.1242/jeb.072231.

Cothran, R. D., Monahan, P. J., and Relyea, R. A. (2021). Antipredator behaviour affected by prey condition, food availability and pH-mediated info-disruption. *Anim. Behav.* 171, 111–118. doi: 10.1016/j.anbehav.2020.11.007.

Cramp, R. L., Reid, S., Seebacher, F., and Franklin, C. E. (2014). Synergistic interaction between UVB radiation and temperature increases susceptibility to parasitic infection in a fish. *Biol. Lett.* 10. doi: 10.1098/rsbl.2014.0449.

Crane, A. L., Bairos-Novak, K. R., Goldman, J. A., and Brown, G. E. (2022). Chemical disturbance cues in aquatic systems: a review and prospectus. *Ecol. Monogr.* 92. doi: 10.1002/ecm.1487.

Crockett, E. L. (2008). The cold but not hard fats in ectotherms: consequences of lipid restructuring on susceptibility of biological membranes to peroxidation, a review. *J. Comp. Physiol. B* 178, 795–809. doi: 10.1007/s00360-008-0275-7.

Crossland, M. R., Salim, A. A., Capon, R. J., and Shine, R. (2019). The Effects of Conspecific Alarm Cues on Larval Cane Toads (Rhinella marina). *J. Chem. Ecol.* 45, 838–848. doi: 10.1007/s10886-019-01111-2.

Cukras, S., Morffy, N., Ohn, T., and Kee, Y. (2014). Inactivating UBE2M impacts the DNA damage response and genome integrity involving multiple cullin ligases. *PLoS One* 9, e101844. doi: 10.1371/journal.pone.0101844.

Daghfous, G., Auclair, F., Blumenthal, F., Suntres, T., Lamarre-Bourret, J., Mansouri, M., et al. (2020). Sensory cutaneous papillae in the sea lamprey (Petromyzon marinus L.): I. Neuroanatomy and physiology. *J. Comp. Neurol.* 528, 664–686. doi: 10.1002/cne.24787.

Dahlke, F., Lucassen, M., Bickmeyer, U., Wohlrab, S., Puvanendran, V., Mortensen, A., et al. (2020a). Fish embryo vulnerability to combined acidification and warming coincides with a low capacity for homeostatic regulation. *J. Exp. Biol.* 223. doi: 10.1242/jeb.212589.

Dahlke, F., Wohlrab, S., Butzin, M., and Pörtner, H.-O. (2020b). Thermal bottlenecks in the life cycle define climate vulnerability of fish. *Science* 369, 65–70. doi: 10.1126/science.aaz3658.

Dahms, H.-U., and Lee, J.-S. (2010). UV radiation in marine ectotherms: molecular effects and responses. *Aquat. Toxicol.* 97, 3–14. doi: 10.1016/j.aquatox.2009.12.002.

Das, L., Quintana, V. G., and Sweasy, J. B. (2020). NTHL1 in genomic integrity, aging and cancer. *DNA Repair* 93, 102920. doi: 10.1016/j.dnarep.2020.102920.

David, N. B., Sapède, D., Saint-Etienne, L., Thisse, C., Thisse, B., Dambly-Chaudière, C., et al. (2002). Molecular basis of cell migration in the fish lateral line: role of the chemokine receptor CXCR4 and of its ligand, SDF1. *Proc. Natl. Acad. Sci. U. S. A.* 99, 16297–16302. doi: 10.1073/pnas.252339399.

Davies, G. M., and Gray, A. (2015). Don’t let spurious accusations of pseudoreplication limit our ability to learn from natural experiments (and other messy kinds of ecological monitoring). *Ecol. Evol.* 5, 5295–5304. doi: 10.1002/ece3.1782.

de Barros, F. R. O., and Paula-Lopes, F. F. (2018). Cellular and epigenetic changes induced by heat stress in bovine preimplantation embryos. *Mol. Reprod. Dev.* 85, 810–820. doi: 10.1002/mrd.23040.

de Groot, J. H. B., and Smeets, M. A. M. (2017). Human Fear Chemosignaling: Evidence from a Meta-Analysis. *Chem. Senses* 42, 663–673. doi: 10.1093/chemse/bjx049.

de la Haye, K. L., Spicer, J. I., Widdicombe, S., and Briffa, M. (2011). Reduced sea water pH disrupts resource assessment and decision making in the hermit crab Pagurus bernhardus. *Anim. Behav.* 82, 495–501. doi: 10.1016/j.anbehav.2011.05.030.

de la Haye, K. L., Spicer, J. I., Widdicombe, S., and Briffa, M. (2012). Reduced pH sea water disrupts chemo-responsive behaviour in an intertidal crustacean. *J. Exp. Mar. Bio. Ecol.* 412, 134–140. doi: 10.1016/j.jembe.2011.11.013.

Decho, A. W., Browne, K. A., and Zimmer-Faust, R. K. (1998). Chemical cues: Why basic peptides are signal molecules in marine environments. *Limnol. Oceanogr.* 43, 1410–1417. doi: 10.4319/lo.1998.43.7.1410.

Delignette-Muller, M. L., and Dutang, C. (2015). fitdistrplus: An R Package for Fitting Distributions. *Journal of Statistical Software, Articles* 64, 1–34. doi: 10.18637/jss.v064.i04.

Delomas, T. A., and Dabrowski, K. (2018). Larval rearing of zebrafish at suboptimal temperatures. *J. Therm. Biol.* 74, 170–173. doi: 10.1016/j.jtherbio.2018.03.017.

Denda, M., and Nakanishi, S. (2022). Do epidermal keratinocytes have sensory and information processing systems? *Exp. Dermatol.* 31, 459–474. doi: 10.1111/exd.14494.

Denver, R. J. (2009). Structural and functional evolution of vertebrate neuroendocrine stress systems. *Ann. N. Y. Acad. Sci.* 1163, 1–16. doi: 10.1111/j.1749-6632.2009.04433.x.

Desban, L., Roussel, J., Mirat, O., Lejeune, F.-X., Keiser, L., Michalski, N., et al. (2022). Lateral line hair cells integrate mechanical and chemical cues to orient navigation. *bioRxiv*, 2022.08.31.505989. doi: 10.1101/2022.08.31.505989.

Deshmukh, H. S., Hamburger, J. B., Ahn, S. H., McCafferty, D. G., Yang, S. R., and Fowler, V. G., Jr (2009). Critical role of NOD2 in regulating the immune response to Staphylococcus aureus. *Infect. Immun.* 77, 1376–1382. doi: 10.1128/IAI.00940-08.

D'haene, B., and Hellemans, J. (2010). The importance of quality control during qPCR data analysis. *Int. Drug Discov.* 18, 24. Available at: https://www.qbaseplus.com/sites/default/files/publication/qpcrarticle_roundtable.pdf.

Di Rocco, R. T., Imre, I., Johnson, N. S., and Brown, G. E. (2016). Behavioural response of adult sea lamprey (Petromyzon marinus) to predator and conspecific alarm cues: evidence of additive effects. *Hydrobiologia* 767, 279–287. doi: 10.1007/s10750-015-2508-6.

Dicke, M., and Baldwin, I. T. (2010). The evolutionary context for herbivore-induced plant volatiles: beyond the "cry for help." *Trends Plant Sci.* 15, 167–175. doi: 10.1016/j.tplants.2009.12.002.

Dicke, M., and Bruin, J. (2001). Chemical information transfer between plants: *Biochem. Syst. Ecol.* 29, 981–994. doi: 10.1016/s0305-1978(01)00045-x.

Dicke, M., and Sabelis, M. W. (1988). Infochemical Terminology: Based on Cost-Benefit Analysis Rather than Origin of Compounds? *Funct. Ecol.* 2, 131–139. doi: 10.2307/2389687.

Dimitriadi, A., Beis, D., Arvanitidis, C., Adriaens, D., and Koumoundouros, G. (2018). Developmental temperature has persistent, sexually dimorphic effects on zebrafish cardiac anatomy. *Sci. Rep.* 8, 8125. doi: 10.1038/s41598-018-25991-8.

Djoumbou Feunang, Y., Eisner, R., Knox, C., Chepelev, L., Hastings, J., Owen, G., et al. (2016). ClassyFire: automated chemical classification with a comprehensive, computable taxonomy. *J. Cheminform.* 8, 61. doi: 10.1186/s13321-016-0174-y.

Dobin, A., Davis, C. A., Schlesinger, F., Drenkow, J., Zaleski, C., Jha, S., et al. (2013). STAR: ultrafast universal RNA-seq aligner. *Bioinformatics* 29, 15–21. doi: 10.1093/bioinformatics/bts635.

Domenici, P., Allan, B. J. M., Lefrançois, C., and McCormick, M. I. (2019). The effect of climate change on the escape kinematics and performance of fishes: implications for future predator-prey interactions. *Conserv. Physiol.* 7, coz078. doi: 10.1093/conphys/coz078.

Donaldson, M. R., Cooke, S. J., Patterson, D. A., and Macdonald, J. S. (2008). Cold shock and fish. *Journal of Fish Biology* 73, 1491–1530. doi: 10.1111/j.1095-8649.2008.02061.x.

Doney, S. C., Fabry, V. J., Feely, R. A., and Kleypas, J. A. (2009). Ocean acidification: the other CO2 problem. *Ann. Rev. Mar. Sci.* 1, 169–192. doi: 10.1146/annurev.marine.010908.163834.

Dong, Q., Svoboda, K., Tiersch, T. R., and Monroe, W. T. (2007). Photobiological effects of UVA and UVB light in zebrafish embryos: evidence for a competent photorepair system. *J. Photochem. Photobiol. B* 88, 137–146. doi: 10.1016/j.jphotobiol.2007.07.002.

Dong, Q., Todd Monroe, W., Tiersch, T. R., and Svoboda, K. R. (2008). UVA-induced photo recovery during early zebrafish embryogenesis. *J. Photochem. Photobiol. B* 93, 162–171. doi: 10.1016/j.jphotobiol.2008.07.011.

Døving, K. B., and Lastein, S. (2009). The alarm reaction in fishes--odorants, modulations of responses, neural pathways. *Ann. N. Y. Acad. Sci.* 1170, 413–423. doi: 10.1111/j.1749-6632.2009.04111.x.

Dow, E., Jacobo, A., Hossain, S., Siletti, K., and Hudspeth, A. J. (2018). Connectomics of the zebrafish's lateral-line neuromast reveals wiring and miswiring in a simple microcircuit. *Elife* 7, e33988. doi: 10.7554/elife.33988.

Draper, A. M., and Weissburg, M. J. (2019). Impacts of Global Warming and Elevated CO2 on Sensory Behavior in Predator-Prey Interactions: A Review and Synthesis. *Frontiers in Ecology and Evolution* 7, 72. doi: 10.3389/fevo.2019.00072.

Drougard, A., Duparc, T., Brenachot, X., Carneiro, L., Gouazé, A., Fournel, A., et al. (2014). Hypothalamic apelin/reactive oxygen species signaling controls hepatic glucose metabolism in the onset of diabetes. *Antioxid. Redox Signal.* 20, 557–573. doi: 10.1089/ars.2013.5182.

Dudareva, N., Klempien, A., Muhlemann, J. K., and Kaplan, I. (2013). Biosynthesis, function and metabolic engineering of plant volatile organic compounds. *New Phytol.* 198, 16–32. doi: 10.1111/nph.12145.

Dudareva, N., Negre, F., Nagegowda, D. A., and Orlova, I. (2006). Plant Volatiles: Recent Advances and Future Perspectives. *CRC Crit. Rev. Plant Sci.* 25, 417–440. doi: 10.1080/07352680600899973.

Durinck, S., Moreau, Y., Kasprzyk, A., Davis, S., De Moor, B., Brazma, A., et al. (2005). BioMart and Bioconductor: a powerful link between biological databases and microarray data analysis. *Bioinformatics* 21, 3439–3440. doi: 10.1093/bioinformatics/bti525.

Durinck, S., Spellman, P. T., Birney, E., and Huber, W. (2009). Mapping identifiers for the integration of genomic datasets with the R/Bioconductor package biomaRt. *Nat. Protoc.* 4, 1184–1191. doi: 10.1038/nprot.2009.97.

Dusinska, M., Staruchova, M., Horska, A., Smolkova, B., Collins, A., Bonassi, S., et al. (2012). Are glutathione S transferases involved in DNA damage signalling? Interactions with DNA damage and repair revealed from molecular epidemiology studies. *Mutat. Res.* 736, 130–137. doi: 10.1016/j.mrfmmm.2012.03.003.

Dutta, S. M., Mustafi, S. B., Raha, S., and Chakraborty, S. K. (2018). Biomonitoring role of some cellular markers during heat stress-induced changes in highly representative fresh water mollusc, Bellamya bengalensis: Implication in climate change and biological adaptation. *Ecotoxicol. Environ. Saf.* 157, 482–490. doi: 10.1016/j.ecoenv.2018.04.001.

Eachus, H., Choi, M.-K., and Ryu, S. (2021). The effects of early life stress on the brain and behaviour: Insights from zebrafish models. *Front. Cell Dev. Biol.* 9, 657591. doi: 10.3389/fcell.2021.657591.

Eckert, R. L., Sturniolo, M. T., Broome, A.-M., Ruse, M., and Rorke, E. A. (2005). Transglutaminase function in epidermis. *J. Invest. Dermatol.* 124, 481–492. doi: 10.1111/j.0022-202X.2005.23627.x.

Edqvist, P.-H. D., Fagerberg, L., Hallström, B. M., Danielsson, A., Edlund, K., Uhlén, M., et al. (2015). Expression of human skin-specific genes defined by transcriptomics and antibody-based profiling. *J. Histochem. Cytochem.* 63, 129–141. doi: 10.1369/0022155414562646.

El-Andaloussi, N., Valovka, T., Toueille, M., Steinacher, R., Focke, F., Gehrig, P., et al. (2006). Arginine methylation regulates DNA polymerase beta. *Mol. Cell* 22, 51–62. doi: 10.1016/j.molcel.2006.02.013.

Elkon, R., Milon, B., Morrison, L., Shah, M., Vijayakumar, S., Racherla, M., et al. (2015). RFX transcription factors are essential for hearing in mice. *Nat. Commun.* 6, 8549. doi: 10.1038/ncomms9549.

Elsakrmy, N., Aouida, M., Hindi, N., Moovarkumudalvan, B., Mohanty, A., Ali, R., et al. (2022). C. elegans ribosomal protein S3 protects against H2O2-induced DNA damage and suppresses spontaneous mutations in yeast. *DNA Repair* 117, 103359. doi: 10.1016/j.dnarep.2022.103359.

Ende, S. S. W., Capelle, J., Kals, J., Schrama, J. W., and Verreth, J. A. J. (2017). A matter of perception: The influence of waterborne signals from fish and conspecifics on the feeding related behavior of Alitta virens (Sars). *J. Exp. Mar. Bio. Ecol.* 496, 91–96. doi: 10.1016/j.jembe.2017.08.004.

Engeszer, R. E., Patterson, L. B., Rao, A. A., and Parichy, D. M. (2007). Zebrafish in the wild: a review of natural history and new notes from the field. *Zebrafish* 4, 21–40. doi: 10.1089/zeb.2006.9997.

Eriander, L., Wrange, A.-L., and Havenhand, J. N. (2015). Simulated diurnal pH fluctuations radically increase variance in—but not the mean of—growth in the barnacle Balanus improvisus. *ICES J. Mar. Sci.* 73, 596–603. doi: 10.1093/icesjms/fsv214.

Esbaugh, A. J. (2018). Physiological implications of ocean acidification for marine fish: emerging patterns and new insights. *J. Comp. Physiol. B* 188, 1–13. doi: 10.1007/s00360-017-1105-6.

Essen, L. O., and Klar, T. (2006). Light-driven DNA repair by photolyases. *Cell. Mol. Life Sci.* 63, 1266–1277. doi: 10.1007/s00018-005-5447-y.

Eto, K., Mazilu-Brown, J. K., Henderson-MacLennan, N., Dipple, K. M., and McCabe, E. R. B. (2014). Development of catecholamine and cortisol stress responses in zebrafish. *Mol Genet Metab Rep* 1, 373–377. doi: 10.1016/j.ymgmr.2014.08.003.

Falcon, S., and Gentleman, R. (2007). Using GOstats to test gene lists for GO term association. *Bioinformatics* 23, 257–258. doi: 10.1093/bioinformatics/btl567.

Falik, O., Mordoch, Y., Ben-Natan, D., Vanunu, M., Goldstein, O., and Novoplansky, A. (2012). Plant responsiveness to root-root communication of stress cues. *Ann. Bot.* 110, 271–280. doi: 10.1093/aob/mcs045.

Farhana, A., and Khan, Y. S. (2022). "Biochemistry, Lipopolysaccharide," in *StatPearls [Internet]* (StatPearls Publishing). Available at: https://www.ncbi.nlm.nih.gov/books/NBK554414/ [Accessed September 28, 2022].

Farrell, A. W., Halliday, G. M., and Lyons, J. G. (2011). Chromatin structure following UV-induced DNA damage-repair or death? *Int. J. Mol. Sci.* 12, 8063–8085. doi: 10.3390/ijms12118063.

Feder, M. E., and Hofmann, G. E. (1999). Heat-shock proteins, molecular chaperones, and the stress response: evolutionary and ecological physiology. *Annu. Rev. Physiol.* 61, 243–282. doi: 10.1146/annurev.physiol.61.1.243.

Feely, R. A., Sabine, C. L., Lee, K., Berelson, W., Kleypas, J., Fabry, V. J., et al. (2004). Impact of anthropogenic CO2 on the CaCO3 system in the oceans. *Science* 305, 362–366. doi: 10.1126/science.1097329.

Fehsenfeld, S., Kiko, R., Appelhans, Y., Towle, D. W., Zimmer, M., and Melzner, F. (2011). Effects of elevated seawater pCO(2) on gene expression patterns in the gills of the green crab, Carcinus maenas. *BMC Genomics* 12, 488. doi: 10.1186/1471-2164-12-488.

Fernandes, S., Nogueira, V., Lourenço, J., Mendo, S., and Pereira, R. (2020). Inter-species bystander effect: Eisenia fetida and Enchytraeus albidus exposed to uranium and cadmium. *J. Hazard. Mater.* 399, 122972. doi: 10.1016/j.jhazmat.2020.122972.

Ferrando, S., and Gallus, L. (2013). Is the olfactory system of cartilaginous fishes a vomeronasal system? *Front. Neuroanat.* 7, 37. doi: 10.3389/fnana.2013.00037.

Ferrari, M. C. O., Vavrek, M. A., Elvidge, C. K., Fridman, B., Chivers, D. P., and Brown, G. E. (2008). Sensory complementation and the acquisition of predator recognition by salmonid fishes. *Behav. Ecol. Sociobiol.* 63, 113–121. doi: 10.1007/s00265-008-0641-1.

Ferrari, M. C. O., Wisenden, B. D., and Chivers, D. P. (2010). Chemical ecology of predator–prey interactions in aquatic ecosystems: a review and prospectus. *Can. J. Zool.* 88, 698–724. doi: 10.1139/z10-029.

Ferrier, G. A., Kim, S. J., Kaddis, C. S., Loo, J. A., Ann Zimmer, C., and Zimmer, R. K. (2016). MULTIFUNCin: A Multifunctional Protein Cue Induces Habitat Selection by, and Predation on, Barnacles. *Integr. Comp. Biol.* 56, 901–913. doi: 10.1093/icb/icw076.

Feugere, L., Angell, L., Fagents, J., Nightingale, R., Rowland, K., Skinner, S., et al. (2021a). Behavioural stress propagation in benthic invertebrates caused by acute pH drop-induced metabolites. *Front. Mar. Sci.* 8. doi: 10.3389/fmars.2021.773870.

Feugere, L., Scott, V. F., Rodriguez-Barucg, Q., Beltran-Alvarez, P., and Wollenberg Valero, K. C. (2021b). Thermal stress induces a positive phenotypic and molecular feedback loop in zebrafish embryos. *J. Therm. Biol.* 102, 103114. doi: 10.1016/j.jtherbio.2021.103114.

Ficke, A. D., Myrick, C. A., and Hansen, L. J. (2007). Potential impacts of global climate change on freshwater fisheries. *Rev. Fish Biol. Fish.* 17, 581–613. doi: 10.1007/s11160-007-9059-5.

Fink, P. (2007). Ecological functions of volatile organic compounds in aquatic systems. *Mar. Freshw. Behav. Physiol.* 40, 155–168. doi: 10.1080/10236240701602218.

Fore, S., Acuña-Hinrichsen, F., Mutlu, K. A., Bartoszek, E. M., Serneels, B., Faturos, N. G., et al. (2020). Functional properties of habenular neurons are determined by developmental stage and sequential neurogenesis. *Sci Adv* 6. doi: 10.1126/sciadv.aaz3173.

Fortier, S., Yang, X., Wang, Y., Bennett, R. A. O., and Strauss, P. R. (2009). Base excision repair in early zebrafish development: evidence for DNA polymerase switching and standby AP endonuclease activity. *Biochemistry* 48, 5396–5404. doi: 10.1021/bi900253d.

Freitas, R., Pires, A., Moreira, A., Wrona, F. J., Figueira, E., and Amadeu M V (2016). Biochemical alterations induced in Hediste diversicolor under seawater acidification conditions. *Marine Environmental Research* 117, 75–84. doi: 10.1016/j.marenvres.2016.04.003.

Fridovich, I. (1995). Superoxide radical and superoxide dismutases. *Annu. Rev. Biochem.* 64, 97–112. doi: 10.1146/annurev.bi.64.070195.000525.

Frisch, K. (1938). Zur Psychologie des Fisch-Schwarmes. *Naturwissenschaften* 26, 601–606. doi: 10.1007/BF01590598.

Frost, C. J., Appel, H. M., Carlson, J. E., De Moraes, C. M., Mescher, M. C., and Schultz, J. C. (2007). Within-plant signalling via volatiles overcomes vascular constraints on systemic signalling and primes responses against herbivores. *Ecol. Lett.* 10, 490–498. doi: 10.1111/j.1461-0248.2007.01043.x.

Fuselier, L., Rugg, M., Korpi, N., and Wisenden, B. (2009). Lab and field estimates of active time of chemical alarm cues of a cyprinid fish and an amphipod crustacean. *Behaviour* 146, 1423–1442. doi: 10.1163/156853909X440998.

Gamperl, A. K., Vijayan, M. M., and Boutilier, R. G. (1994a). Experimental control of stress hormone levels in fishes: techniques and applications. *Reviews in Fish Biology and Fisheries* 4, 215–255. doi: 10.1007/bf00044129.

Gamperl, A. K., Vijayan, M. M., and Boutilier, R. G. (1994b). Experimental control of stress hormone levels in fishes: techniques and applications. *Reviews in Fish Biology and Fisheries* 4, 215–255. doi: 10.1007/BF00044129.

Gau, P., Poon, J., Ufret-Vincenty, C., Snelson, C. D., Gordon, S. E., Raible, D. W., et al. (2013). The zebrafish ortholog of TRPV1 is required for heat-induced locomotion. *J. Neurosci.* 33, 5249–5260. doi: 10.1523/JNEUROSCI.5403-12.2013.

Genin, A., Levy, L., Sharon, G., Raitsos, D. E., and Diamant, A. (2020). Rapid onsets of warming events trigger mass mortality of coral reef fish. *Proc. Natl. Acad. Sci. U. S. A.* 117, 25378–25385. doi: 10.1073/pnas.2009748117.

Georgakopoulou, E., Sfakianakis, D. G., Kouttouki, S., Divanach, P., Kentouri, M., and Koumoundouros, G. (2007). The influence of temperature during early life on phenotypic expression at later ontogenetic stages in sea bass. *J. Fish Biol.* 70, 278–291. doi: 10.1111/j.1095-8649.2007.01305.x.

Gerlai, R. (2013). Antipredatory behavior of zebrafish: adaptive function and a tool for translational research. *Evol. Psychol.* 11, 591–605. doi: 10.1177/147470491301100308.

Ghosh, S. G., Becker, K., Huang, H., Dixon-Salazar, T., Chai, G., Salpietro, V., et al. (2018). Biallelic Mutations in ADPRHL2, Encoding ADP-Ribosylhydrolase 3, Lead to a Degenerative Pediatric Stress-Induced Epileptic Ataxia Syndrome. *Am. J. Hum. Genet.* 103, 431–439. doi: 10.1016/j.ajhg.2018.07.010.

Giacomini, A. C. V. V., de Abreu, M. S., Koakoski, G., Idalêncio, R., Kalichak, F., Oliveira, T. A., et al. (2015). My stress, our stress: blunted cortisol response to stress in isolated housed zebrafish. *Physiol. Behav.* 139, 182–187. doi: 10.1016/j.physbeh.2014.11.035.

Giaquinto, P. C., and Hoffmann, A. (2012). The scent of stress: Pintado catfish differentially respond to chemical cues from stressed conspecifics. *Behaviour* 149, 941–951. doi: 10.1163/1568539X-00003022.

Gibney, E. R., and Nolan, C. M. (2010). Epigenetics and gene expression. *Heredity* 105, 4–13. doi: 10.1038/hdy.2010.54.

Giraud-Billoud, M., Rivera-Ingraham, G. A., Moreira, D. C., Burmester, T., Castro-Vazquez, A., Carvajalino-Fernández, J. M., et al. (2019). Twenty years of the 'Preparation for Oxidative Stress' (POS) theory: Ecophysiological advantages and molecular strategies. *Comp. Biochem. Physiol. A Mol. Integr. Physiol.* 234, 36–49. doi: 10.1016/j.cbpa.2019.04.004.

Goellner, E. M., Putnam, C. D., and Kolodner, R. D. (2015). Exonuclease 1-dependent and independent mismatch repair. *DNA Repair* 32, 24–32. doi: 10.1016/j.dnarep.2015.04.010.

Goldberg, J. K., Wallace, A. K., and Weiss, S. L. (2017). Skin lipids of the striped plateau lizard (Sceloporus virgatus) correlate with female receptivity and reproductive quality alongside visual ornaments. *Naturwissenschaften* 104, 81. doi: 10.1007/s00114-017-1503-3.

Goldman, J. A., Crane, A. L., Feyten, L. E. A., Collins, E., and Brown, G. E. (2021). Disturbance cue communication is shaped by emitter diet and receiver background risk in Trinidadian guppies. *Curr. Zool.* doi: 10.1093/cz/zoab025.

Goldman, J. A., Désormeaux, I. S., and Brown, G. E. (2020a). Disturbance cues as a source of risk assessment information under natural conditions. *Freshwater Biology* 65, 981–986. doi: 10.1111/fwb.13484.

Goldman, J. A., Feyten, L. E. A., Ramnarine, I. W., and Brown, G. E. (2020b). Sender and receiver experience alters the response of fish to disturbance cues. *Curr. Zool.* 66, 255–261. doi: 10.1093/cz/zoz050.

Goldman, J. A., Singh, A., Demers, E. E. M., Feyten, L. E. A., and Brown, G. E. (2019). Does donor group size matter? The response of guppies (Poecilia reticulata) and convict cichlids (Amatitlania nigrofasciata) to disturbance cues from conspecific and heterospecific donors. doi: 10.1139/cjz-2018-0170.

Gonzalo, A., López, P., and Martín, J. (2010). Risk level of chemical cues determines retention of recognition of new predators in Iberian green frog tadpoles. *Behav. Ecol. Sociobiol.* 64, 1117–1123. doi: 10.1007/s00265-010-0927-y.

Goshen, I., and Yirmiya, R. (2009). Interleukin-1 (IL-1): a central regulator of stress responses. *Front. Neuroendocrinol.* 30, 30–45. doi: 10.1016/j.yfrne.2008.10.001.

Gregório, S. F., Ruiz-Jarabo, I., Carvalho, E. M., and Fuentes, J. (2019). Increased intestinal carbonate precipitate abundance in the sea bream (Sparus aurata L.) in response to ocean acidification. *PLoS One* 14, e0218473. doi: 10.1371/journal.pone.0218473.

Griffiths, H. R., Mistry, P., Herbert, K. E., and Lunec, J. (1998). Molecular and cellular effects of ultraviolet light-induced genotoxicity. *Crit. Rev. Clin. Lab. Sci.* 35, 189–237. doi: 10.1080/10408369891234192.

Grompe, M., and D'Andrea, A. (2001). Fanconi anemia and DNA repair. *Hum. Mol. Genet.* 10, 2253–2259. doi: 10.1093/hmg/10.20.2253.

Groothuizen, F. S., and Sixma, T. K. (2016). The conserved molecular machinery in DNA mismatch repair enzyme structures. *DNA Repair* 38, 14–23. doi: 10.1016/j.dnarep.2015.11.012.

Guha, R. (2007). Chemical Informatics Functionality in R. *Journal of Statistical Software* 18.

Guo, L., Wang, Y., Liang, S., Lin, G., Chen, S., and Yang, G. (2016). Tissue-overlapping response of half-smooth tongue sole (Cynoglossus semilaevis) to thermostressing based on transcriptome profiles. *Gene* 586, 97–104. doi: 10.1016/j.gene.2016.04.020.

Gutha, R., Yarrappagaari, S., Thopireddy, L., Reddy, K. S., and Saddala, R. R. (2018). Effect of abiotic and biotic stress factors analysis using machine learning methods in zebrafish. *Comp. Biochem. Physiol. Part D Genomics Proteomics* 25, 62–72. doi: 10.1016/j.cbd.2017.10.005.

Haarmann-Stemmann, T., Boege, F., and Krutmann, J. (2013). Adaptive and maladaptive responses in skin: mild heat exposure protects against UVB-induced photoaging in mice. *J. Invest. Dermatol.* 133, 868–871. doi: 10.1038/jid.2012.435.

Hadacek, F. (2015). Low-molecular-weight metabolite systems chemistry. *Front. Environ. Sci.* 3. doi: 10.3389/fenvs.2015.00012.

Hall, J. M., and Warner, D. A. (2021). Thermal sensitivity of lizard embryos indicates a mismatch between oxygen supply and demand at near-lethal temperatures. *J Exp Zool A Ecol Integr Physiol* 335, 72–85. doi: 10.1002/jez.2359.

Hallare, A. V., Schirling, M., Luckenbach, T., Köhler, H.-R., and Triebskorn, R. (2005). Combined effects of temperature and cadmium on developmental parameters and biomarker responses in zebrafish (Danio rerio) embryos. *J. Therm. Biol.* 30, 7–17. doi: 10.1016/j.jtherbio.2004.06.002.

Hallberg, E., and Skog, M. (2010). "Chemosensory Sensilla in Crustaceans," in *Chemical Communication in Crustaceans* (New York, NY: Springer New York), 103–121. doi: 10.1007/978-0-387-77101-4_6.

Hamdani, E. H., and Døving, K. B. (2007). The functional organization of the fish olfactory system. *Prog. Neurobiol.* 82, 80–86. doi: 10.1016/j.pneurobio.2007.02.007.

Hanakahi, L. A., Bartlet-Jones, M., Chappell, C., Pappin, D., and West, S. C. (2000). Binding of inositol phosphate to DNA-PK and stimulation of double-strand break repair. *Cell* 102, 721–729. doi: 10.1016/s0092-8674(00)00061-1.

Hansen, A., Reutter, K., and Zeiske, E. (2002). Taste bud development in the zebrafish, Danio rerio. *Dev. Dyn.* 223, 483–496. doi: 10.1002/dvdy.10074.

Hardege, J. D. (1999). Nereidid polychaetes as model organisms for marine chemical ecology. *Hydrobiologia* 402, 145–161. doi: 10.1023/A:1003740509104.

Hardege, J. D., Bentley, M. G., Beckmann, M., and Müller, C. (1996). Sex pheromones in marine polychaetes: volatile organic substances (VOS) isolated from Arenicola marina. *Mar. Ecol. Prog. Ser.* 139, 157–166. doi: https://www.jstor.org/stable/24857102.

Hashim Abdalla, M. S., Taylor-Robinson, S. D., Sharif, A. W., Williams, H. R. T., Crossey, M. M. E., Badra, G. A., et al. (2011). Differences in phosphatidylcholine and bile acids in bile from Egyptian and UK patients with and without cholangiocarcinoma. *HPB* 13, 385–390. doi: 10.1111/j.1477-2574.2011.00296.x.

Hay, M. E. (2010). "Crustaceans as powerful models in aquatic chemical ecology," in *Chemical Communication in Crustaceans* (New York, NY: Springer New York), 41–62. doi: 10.1007/978-0-387-77101-4_3.

Hayes, J. D., Flanagan, J. U., and Jowsey, I. R. (2005). Glutathione transferases. *Annu. Rev. Pharmacol. Toxicol.* 45, 51–88. doi: 10.1146/annurev.pharmtox.45.120403.095857.

Hayes, J. D., and McLellan, L. I. (1999). Glutathione and glutathione-dependent enzymes represent a co-ordinately regulated defence against oxidative stress. *Free Radic. Res.* 31, 273–300. doi: 10.1080/10715769900300851.

Hazel, J. R. (1995). Thermal adaptation in biological membranes: is homeoviscous adaptation the explanation? *Annu. Rev. Physiol.* 57, 19–42. doi: 10.1146/annurev.ph.57.030195.000315.

Hazlett, B. A. (1985). Disturbance pheromones in the crayfish Orconectes virilis. *J. Chem. Ecol.* 11, 1695–1711. doi: 10.1007/BF01012121.

Hazlett, B. A. (1990a). Disturbance pheromone in the hermit crab Calcinus laevimanus (Randall, 1840). *Crustaceana* 58, 314–316. doi: 10.1163/156854090x00219.

Hazlett, B. A. (1990b). Source and nature of disturbance-chemical system in crayfish. *J. Chem. Ecol.* 16, 2263–2275. doi: 10.1007/bf01026936.

Hellemans, J., Mortier, G., De Paepe, A., Speleman, F., and Vandesompele, J. (2007). qBase relative quantification framework and software for management and automated analysis of real-time quantitative PCR data. *Genome Biol.* 8, R19. doi: 10.1186/gb-2007-8-2-r19.

Henderson, L. J., Ryan, M. R., and Rowland, H. M. (2017). Perch, Perca fluviatilis show a directional preference for, but do not increase attacks toward, prey in response to water-borne cortisol. *PeerJ* 5, e3883. doi: 10.7717/peerj.3883.

Heuer, R. M., and Grosell, M. (2014). Physiological impacts of elevated carbon dioxide and ocean acidification on fish. *Am. J. Physiol. Regul. Integr. Comp. Physiol.* 307, R1061-84. doi: 10.1152/ajpregu.00064.2014.

Hirayama, J., Miyamura, N., Uchida, Y., Asaoka, Y., Honda, R., Sawanobori, K., et al. (2009). Common light signaling pathways controlling DNA repair and circadian clock entrainment in zebrafish. *Cell Cycle* 8, 2794–2801. doi: 10.4161/cc.8.17.9447.

Hofmann, G. E., Smith, J. E., Johnson, K. S., Send, U., Levin, L. A., Micheli, F., et al. (2011). High-frequency dynamics of ocean pH: a multi-ecosystem comparison. *PLoS One* 6, e28983. doi: 10.1371/journal.pone.0028983.

Holopainen, J. K., and Gershenzon, J. (2010). Multiple stress factors and the emission of plant VOCs. *Trends Plant Sci.* 15, 176–184. doi: 10.1016/j.tplants.2010.01.006.

Hooper, P. L., Hooper, P. L., Tytell, M., and Vígh, L. (2010). Xenohormesis: health benefits from an eon of plant stress response evolution. *Cell Stress Chaperones* 15, 761–770. doi: 10.1007/s12192-010-0206-x.

Horsman, J. W., and Miller, D. L. (2016). Mitochondrial Sulfide Quinone Oxidoreductase Prevents Activation of the Unfolded Protein Response in Hydrogen Sulfide. *J. Biol. Chem.* 291, 5320–5325. doi: 10.1074/jbc.M115.697102.

Hosseini, S., Brenig, B., Tetens, J., and Sharifi, A. R. (2019). Phenotypic plasticity induced using high ambient temperature during embryogenesis in domesticated zebrafish, Danio rerio. *Reprod. Domest. Anim.* 54, 435–444. doi: 10.1111/rda.13382.

Howitz, K. T., and Sinclair, D. A. (2008). Xenohormesis: sensing the chemical cues of other species. *Cell* 133, 387–391. doi: 10.1016/j.cell.2008.04.019.

Hubbard, P. C., Barata, E. N., and Canário, A. V. M. (2003). Olfactory sensitivity to catecholamines and their metabolites in the goldfish. *Chem. Senses* 28, 207–218. doi: 10.1093/chemse/28.3.207.

Hubler, M. J., and Kennedy, A. J. (2016). Role of lipids in the metabolism and activation of immune cells. *J. Nutr. Biochem.* 34, 1–7. doi: 10.1016/j.jnutbio.2015.11.002.

Hudson, D. F., Amor, D. J., Boys, A., Butler, K., Williams, L., Zhang, T., et al. (2016). Loss of RMI2 Increases Genome Instability and Causes a Bloom-Like Syndrome. *PLoS Genet.* 12, e1006483. doi: 10.1371/journal.pgen.1006483.

Hurem, S., Fraser, T. W. K., Gomes, T., Mayer, I., and Christensen, T. (2018). Sub-lethal UV radiation during early life stages alters the behaviour, heart rate and oxidative stress parameters in zebrafish (Danio rerio). *Ecotoxicol. Environ. Saf.* 166, 359–365. doi: 10.1016/j.ecoenv.2018.09.082.

Hussain, A. (2011). The Olfactory Nervous System Of Terrestrial And Aquatic Vertebrates. *Nature Precedings*, 1–1. doi: 10.1038/npre.2011.6642.1.

Hussain, A., Saraiva, L. R., Ferrero, D. M., Ahuja, G., Krishna, V. S., Liberles, S. D., et al. (2013). High-affinity olfactory receptor for the death-associated odor cadaverine. *Proc. Natl. Acad. Sci. U. S. A.* 110, 19579–19584. doi: 10.1073/pnas.1318596110.

Icoglu Aksakal, F., and Ciltas, A. (2018). The impact of ultraviolet B (UV-B) radiation in combination with different temperatures in the early life stage of zebrafish (Danio rerio). *Photochem. Photobiol. Sci.* 17, 35–41. doi: 10.1039/c7pp00236j.

Ihaka, R., and Gentleman, R. (1996). R: A Language for Data Analysis and Graphics. *J. Comput. Graph. Stat.* 5, 299–314. doi: 10.1080/10618600.1996.10474713.

Inagaki, H., Kiyokawa, Y., Tamogami, S., Watanabe, H., Takeuchi, Y., and Mori, Y. (2014). Identification of a pheromone that increases anxiety in rats. *Proc. Natl. Acad. Sci. U. S. A.* 111, 18751–18756. doi: 10.1073/pnas.1414710112.

Ingvarsdóttir, A., Birkett, M. A., Duce, I., Genna, R. L., Mordue, W., Pickett, J. A., et al. (2002). Semiochemical strategies for sea louse control: host location cues. *Pest Manag. Sci.* 58, 537–545. doi: 10.1002/ps.510.

Iordanov, M. S., Pribnow, D., Magun, J. L., Dinh, T. H., Pearson, J. A., and Magun, B. E. (1998). Ultraviolet radiation triggers the ribotoxic stress response in mammalian cells. *J. Biol. Chem.* 273, 15794–15803. doi: 10.1074/jbc.273.25.15794.

IPCC (2014). "Summary for Policymakers," in *Climate Change 2013 – The Physical Science Basis: Working Group I Contribution to the Fifth Assessment Report of the Intergovernmental Panel on Climate Change* (Cambridge University Press), 1–30. doi: 10.1017/CBO9781107415324.004.

IPCC (2019). IPCC Special Report on the Ocean and Cryosphere in a Changing Climate. , ed. H.-O. Pörtner, D.C. Roberts, V. Masson-Delmotte, P. Zhai, M. Tignor, E. Poloczanska, K. Mintenbeck, A. Alegría, M. Nicolai, A. Okem, J. Petzold, B. Rama, N.M. Weyer (eds.) Intergovernmental Panel on Climate Change.

IPCC (2022). "Summary for Policymakers," in *Global Warming of 1.5°C: IPCC Special Report on Impacts of Global Warming of 1.5°C above Pre-industrial Levels in Context of Strengthening Response to Climate Change, Sustainable Development, and Efforts to Eradicate Poverty* (Cambridge University Press), 1–24. doi: 10.1017/9781009157940.001.

Irie, N., and Kuratani, S. (2014). The developmental hourglass model: a predictor of the basic body plan? *Development* 141, 4649–4655. doi: 10.1242/dev.107318.

Irmler, I., Schmidt, K., and Starck, J. M. (2004). Developmental variability during early embryonic development of zebra fish, Danio rerio. *J. Exp. Zool. B Mol. Dev. Evol.* 302, 446–457. doi: 10.1002/jez.b.21010.

Ito, Y., Suzuki, T., Shirai, T., and Hirano, T. (1994). Presence of cyclic betaines in fish. *Comparative Biochemistry and Physiology Part B: Comparative Biochemistry* 109, 115–124. doi: 10.1016/0305-0491(94)90148-1.

Iwama, G. K. (1998). Stress in fish. in *Annals of the New York Academy of Sciences* (John Wiley & Sons, Ltd (10.1111)), 304–310. doi: 10.1111/j.1749-6632.1998.tb09005.x.

Iwama, G. K., Afonso, L. O. B., Todgham, A., Ackerman, P., and Nakano, K. (2004). Are hsps suitable for indicating stressed states in fish? *J. Exp. Biol.* 207, 15–19. doi: 10.1242/jeb.00707.

Jackson, M. R., Melideo, S. L., and Jorns, M. S. (2012). Human sulfide:quinone oxidoreductase catalyzes the first step in hydrogen sulfide metabolism and produces a sulfane sulfur metabolite. *Biochemistry* 51, 6804–6815. doi: 10.1021/bi300778t.

Jacobsen, H. P., and Stabell, O. B. (1999). Predator-induced alarm responses in the common periwinkle, Littorina littorea : dependence on season, light conditions, and chemical labelling of predators. *Mar. Biol.* 134, 551–557. doi: 10.1007/s002270050570.

Jantschitsch, C., and Trautinger, F. (2003). Heat shock and UV-B-induced DNA damage and mutagenesis in skin. *Photochem. Photobiol. Sci.* 2, 899–903. doi: 10.1039/b301253k.

Jesus, T. F., Grosso, A. R., Almeida-Val, V. M. F., and Coelho, M. M. (2016). Transcriptome profiling of two Iberian freshwater fish exposed to thermal stress. *J. Therm. Biol.* 55, 54–61. doi: 10.1016/j.jtherbio.2015.11.009.

Jesuthasan, S., Krishnan, S., Cheng, R.-K., and Mathuru, A. (2021). Neural correlates of state transitions elicited by a chemosensory danger cue. *Prog. Neuropsychopharmacol. Biol. Psychiatry* 111, 110110. doi: 10.1016/j.pnpbp.2020.110110.

Jin, J., Zhao, M., Gao, T., Jing, T., Zhang, N., Wang, J., et al. (2021). Amplification of early drought responses caused by volatile cues emitted from neighboring plants. *Hortic Res* 8, 243. doi: 10.1038/s41438-021-00704-x.

Jiricny, J. (2013). Postreplicative mismatch repair. *Cold Spring Harb. Perspect. Biol.* 5, a012633. doi: 10.1101/cshperspect.a012633.

Johansson, M. L., and Banks, M. A. (2011). Olfactory receptor related to class A, type 2 (V1r-like Ora2) genes are conserved between distantly related rockfishes (genus Sebastes). *J. Hered.* 102, 113–117. doi: 10.1093/jhered/esq102.

Jordão, L. C. (2004). Disturbance chemical cues determine changes in spatial occupation by the convict cichlid Archocentrus nigrofasciatus. *Behav. Processes* 67, 453–459. doi: 10.1016/j.beproc.2004.07.006.

Jordão, L. C., and Volpato, G. L. (2000). Chemical Transfer of Warning Information in Non-Injured Fish. *Behaviour* 137, 681–690. doi: 10.1163/156853900502286.

Jørgensen, L. B., Ørsted, M., Malte, H., Wang, T., and Overgaard, J. (2022). Extreme escalation of heat failure rates in ectotherms with global warming. *Nature* 611, 93–98. doi: 10.1038/s41586-022-05334-4.

Jungwirth, M., and Winkler, H. (1984). The temperature dependence of embryonic development of grayling (Thymallus thymallus), Danube salmon (Hucho hucho), Arctic char (Salvelinus alpinus) and brown trout (Salmo trutta fario). *Aquaculture* 38, 315–327. doi: 10.1016/0044-8486(84)90336-3.

Júnior, A. B., Magalhães, E. J., Hoffmann, A., and Ide, L. M. (2010). Conspecific and heterospecific alarm substance induces behavioral responses in piau fish Leporinus piau. *Acta Ethol.* 13, 119–126. doi: 10.1007/s10211-010-0081-6.

Jutfelt, F., Bresolin de Souza, K., Vuylsteke, A., and Sturve, J. (2013). Behavioural disturbances in a temperate fish exposed to sustained high-CO2 levels. *PLoS One* 8, e65825. doi: 10.1371/journal.pone.0065825.

Kalamarz-Kubiak, H. (2018). “Cortisol in correlation to other indicators of fish welfare,” in *Corticosteroids*, ed. A. G. Al-kaf (London, England: InTech). doi: 10.5772/intechopen.72392.

Kamler, E., Keckei, H., and Bauer-Nemeschkal, E. (1998). Temperature-induced changes of survival, development and yolk partitioning in Chondrostoma nasus. *J. Fish Biol.* 53, 658–682. doi: 10.1111/j.1095-8649.1998.tb01009.x.

Kanehisa, M., and Goto, S. (2000). KEGG: kyoto encyclopedia of genes and genomes. *Nucleic Acids Res.* 28, 27–30. doi: 10.1093/nar/28.1.27.

Karakach, T. K., Huenupi, E. C., Soo, E. C., Walter, J. A., and Afonso, L. O. B. (2009). 1H-NMR and mass spectrometric characterization of the metabolic response of juvenile Atlantic salmon (Salmo salar) to long-term handling stress. *Metabolomics* 5, 123–137. doi: 10.1007/s11306-008-0144-0.

Karlson, P., and Lüscher, M. (1959a). Pheromone. *Naturwissenschaften* 46, 63–64. doi: 10.1007/BF00599084.

Karlson, P., and Lüscher, M. (1959b). The proposed biological term 'pheromone.' *Nature* 183, 1835–1835. doi: 10.1038/1831835b0.

Kassahn, K. S., Crozier, R. H., Pörtner, H. O., and Caley, M. J. (2009). Animal performance and stress: responses and tolerance limits at different levels of biological organisation. *Biol. Rev. Camb. Philos. Soc.* 84, 277–292. doi: 10.1111/j.1469-185X.2008.00073.x.

Kassahn, K. S., Crozier, R. H., Ward, A. C., Stone, G., and Caley, M. J. (2007). From transcriptome to biological function: environmental stress in an ectothermic vertebrate, the coral reef fish Pomacentrus moluccensis. *BMC Genomics* 8, 358. doi: 10.1186/1471-2164-8-358.

Kassambara, A. (2020). ggpubr: "ggplot2" Based Publication Ready Plots. Available at: https://CRAN.R-project.org/package=ggpubr.

Kassambara, A. (2021). rstatix: Pipe-Friendly Framework for Basic Statistical Tests. Available at: https://CRAN.R-project.org/package=rstatix.

Kassambara, A., Kosinski, M., and Biecek, P. (2020). Drawing Survival Curves using "ggplot2" [R package survminer version 0.4.8]. Available at: https://CRAN.R-project.org/package=survminer [Accessed February 17, 2021].

Katz, J. N., and Rittschof, D. (1993). Alarm/investigation responses of hermit crabs as related to shell fit and crab size. *Mar. Behav. Physiol.* 22, 171–182. doi: 10.1080/10236249309378845.

Kermen, F., Darnet, L., Wiest, C., Palumbo, F., Bechert, J., Uslu, O., et al. (2020). Stimulus-specific behavioral responses of zebrafish to a large range of odors exhibit individual variability. *BMC Biol.* 18, 66. doi: 10.1186/s12915-020-00801-8.

Kermen, F., Franco, L. M., Wyatt, C., and Yaksi, E. (2013). Neural circuits mediating olfactory-driven behavior in fish. *Front. Neural Circuits* 7, 62. doi: 10.3389/fncir.2013.00062.

Kermen, F., Mandairon, N., and Chalençon, L. (2021). Odor hedonics coding in the vertebrate olfactory bulb. *Cell Tissue Res.* 383, 485–493. doi: 10.1007/s00441-020-03372-w.

Kiesecker, J. M., Chivers, D. P., Marco, A., Quilchano, C., Anderson, M. T., and Blaustein, A. R. (1999). Identification of a disturbance signal in larval red-legged frogs, Rana aurora. *Anim. Behav.* 57, 1295–1300. doi: 10.1006/anbe.1999.1094.

Kikusui, T., Takigami, S., Takeuchi, Y., and Mori, Y. (2001). Alarm pheromone enhances stress-induced hyperthermia in rats. *Physiol. Behav.* 72, 45–50. doi: 10.1016/s0031-9384(00)00370-x.

Killen, S. S. (2020). Behaviour and Learning. *The Physiology of Fishes*, 225–235.

Kim, S., Carrillo, M., Kulkarni, V., and Jagadeeswaran, P. (2009). Evolution of primary hemostasis in early vertebrates. *PLoS One* 4, e8403. doi: 10.1371/journal.pone.0008403.

Kim, S., Kim, A., Ma, S., Lee, W., Lee, S., Yoon, D., et al. (2019). Glutathione Injection Alleviates the Fluctuation of Metabolic Response under Thermal Stress in Olive Flounder, Paralichthys olivaceus. *Metabolites* 10. doi: 10.3390/metabo10010003.

Kim, T. W., Taylor, J., Lovera, C., and Barry, J. P. (2015). CO2-driven decrease in pH disrupts olfactory behaviour and increases individual variation in deep-sea hermit crabs. *ICES J. Mar. Sci.* 73, 613–619. doi: 10.1093/icesjms/fsv019.

Kim, W.-J., Lee, K., Lee, D., Kim, H.-C., Nam, B.-H., Jung, H., et al. (2021). Transcriptome profiling of olive flounder responses under acute and chronic heat stress. *Genes Genomics* 43, 151–159. doi: 10.1007/s13258-021-01053-8.

Kimmel, C. B., Ballard, W. W., Kimmel, S. R., Ullmann, B., and Schilling, T. F. (1995). Stages of embryonic development of the zebrafish. *Dev. Dyn.* 203, 253–310. doi: 10.1002/aja.1002030302.

Kimura, Y., Goto, Y.-I., and Kimura, H. (2010). Hydrogen sulfide increases glutathione production and suppresses oxidative stress in mitochondria. *Antioxid. Redox Signal.* 12, 1–13. doi: 10.1089/ars.2008.2282.

Kind, T., Liu, K.-H., Lee, D. Y., DeFelice, B., Meissen, J. K., and Fiehn, O. (2013). LipidBlast in silico tandem mass spectrometry database for lipid identification. *Nat. Methods* 10, 755–758. doi: 10.1038/nmeth.2551.

Kipnis, J. (2018). Immune system: The “seventh sense.” *J. Exp. Med.* 215, 397–398. doi: 10.1084/jem.20172295.

Kirsten, K., Fior, D., Kreutz, L. C., and Barcellos, L. J. G. (2018). First description of behavior and immune system relationship in fish. *Sci. Rep.* 8, 846. doi: 10.1038/s41598-018-19276-3.

Kiyokawa, Y., and Hennessy, M. B. (2018). Comparative studies of social buffering: A consideration of approaches, terminology, and pitfalls. *Neurosci. Biobehav. Rev.* 86, 131–141. doi: 10.1016/j.neubiorev.2017.12.005.

Kleiner, G., Barca, E., Ziosi, M., Emmanuele, V., Xu, Y., Hidalgo-Gutierrez, A., et al. (2018). CoQ10 supplementation rescues nephrotic syndrome through normalization of H2S oxidation pathway. *Biochim. Biophys. Acta Mol. Basis Dis.* 1864, 3708–3722. doi: 10.1016/j.bbadis.2018.09.002.

Komsta, L. (2011). outliers: Tests for outliers. Available at: https://CRAN.R-project.org/package=outliers.

Korsching, S. (2008). "The molecular evolution of teleost olfactory receptor gene families," in *Results and Problems in Cell Differentiation* Results and problems in cell differentiation. (Berlin, Heidelberg: Springer Berlin Heidelberg), 221–238. doi: 10.1007/400_2008_11.

Kotrschal, K. (1996). Solitary chemosensory cells: why do primary aquatic vertebrates need another taste system? *Trends Ecol. Evol.* 11, 110–114. doi: 10.1016/0169-5347(96)81088-3.

Kotrschal, K., Krautgartner, W. D., and Hansen, A. (1997). Ontogeny of the solitary chemosensory cells in the zebrafish, Danio rerio. *Chem. Senses* 22, 111–118. doi: 10.1093/chemse/22.2.111.

Kowal, P., Gurtan, A. M., Stuckert, P., D'Andrea, A. D., and Ellenberger, T. (2007). Structural determinants of human FANCF protein that function in the assembly of a DNA damage signaling complex. *J. Biol. Chem.* 282, 2047–2055. doi: 10.1074/jbc.M608356200.

Kowatschew, D., Bozorg Nia, S., Hassan, S., Ustinova, J., Weth, F., and Korsching, S. I. (2022). Spatial organization of olfactory receptor gene choice in the complete V1R-related ORA family of zebrafish. *Sci. Rep.* 12, 14816. doi: 10.1038/s41598-022-17900-x.

Krauss, J., Geiger-Rudolph, S., Koch, I., Nüsslein-Volhard, C., and Irion, U. (2014). A dominant mutation in tyrp1A leads to melanophore death in zebrafish. *Pigment Cell Melanoma Res.* 27, 827–830. doi: 10.1111/pcmr.12272.

Kriventseva, E. V., Kuznetsov, D., Tegenfeldt, F., Manni, M., Dias, R., Simão, F. A., et al. (2019). OrthoDB v10: sampling the diversity of animal, plant, fungal, protist, bacterial and viral genomes for evolutionary and functional annotations of orthologs. *Nucleic Acids Res.* 47, D807–D811. doi: 10.1093/nar/gky1053.

Krone, P. H., Lele, Z., and Sass, J. B. (1997). Heat shock genes and the heat shock response in zebrafish embryos. *Biochem. Cell Biol.* 75, 487–497. doi: 10.1139/o97-083.

Kuhl, C., Tautenhahn, R., Böttcher, C., Larson, T. R., and Neumann, S. (2012). CAMERA: an integrated strategy for compound spectra extraction and annotation of liquid chromatography/mass spectrometry data sets. *Anal. Chem.* 84, 283–289. doi: 10.1021/ac202450g.

Kuss-Duerkop, S. K., and Keestra-Gounder, A. M. (2020). NOD1 and NOD2 Activation by Diverse Stimuli: a Possible Role for Sensing Pathogen-Induced Endoplasmic Reticulum Stress. *Infect. Immun.* 88. doi: 10.1128/IAI.00898-19.

Kvedar, J. C., Manabe, M., Phillips, S. B., Ross, B. S., and Baden, H. P. (1992). Characterization of sciellin, a precursor to the cornified envelope of human keratinocytes. *Differentiation* 49, 195–204. doi: 10.1111/j.1432-0436.1992.tb00667.x.

Landi, M. (2020). Airborne signals and abiotic factors: the neglected side of the plant communication. *Commun. Integr. Biol.* 13, 67–73. doi: 10.1080/19420889.2020.1767482.

Landi, M., Araniti, F., Flamini, G., Piccolo, E. L., Trivellini, A., Abenavoli, M. R., et al. (2020). "Help is in the air": volatiles from salt-stressed plants increase the reproductive success of receivers under salinity. *Planta* 251, 48. doi: 10.1007/s00425-020-03344-y.

Landschützer, P., Gruber, N., Bakker, D. C. E., Stemmler, I., and Six, K. D. (2018). Strengthening seasonal marine CO2 variations due to increasing atmospheric CO2. *Nature Climate Change* 8, 146–150. doi: 10.1038/s41558-017-0057-x.

Lawrence, C. (2007). The husbandry of zebrafish (Danio rerio): A review. *Aquaculture* 269, 1–20. doi: 10.1016/j.aquaculture.2007.04.077.

Leduc, A. O. H. C., Ferrari, M. C. O., Kelly, J. M., and Brown, G. E. (2004). Learning to recognize novel predators under weakly acidic conditions: the effects of reduced pH on acquired predator recognition by juvenile rainbow trout. *Chemoecology* 14, 107–112. doi: 10.1007/s00049-003-0268-7.

Leduc, A. O. H. C., Noseworthy, M. K., Adrian, J. C., Jr, and Brown, G. E. (2003). Detection of conspecific and heterospecific alarm signals by juvenile pumpkinseed under weak acidic conditions. *J. Fish Biol.* 63, 1331–1336. doi: 10.1046/j.1095-8649.2003.00230.x.

Leduc, A. O. H. C., Roh, E., Breau, C., and Brown, G. E. (2007). Effects of ambient acidity on chemosensory learning: an example of an environmental constraint on acquired predator recognition in wild juvenile Atlantic salmon (Salmo salar). *Ecol. Freshw. Fish* 16, 385–394. doi: 10.1111/j.1600-0633.2007.00233.x.

Leduc, A. O. H. C., Roh, E., Harvey, M. C., and Brown, G. E. (2006). Impaired detection of chemical alarm cues by juvenile wild Atlantic salmon (Salmo salar) in a weakly acidic environment. *Can. J. Fish. Aquat. Sci.* 63, 2356–2363. doi: 10.1139/f06-128.

Lee, K., and Seo, P. J. (2014). Airborne signals from salt-stressed Arabidopsis plants trigger salinity tolerance in neighboring plants. *Plant Signal. Behav.* 9, e28392. doi: 10.4161/psb.28392.

Lenhard, W., and Lenhard, A. (2016). Computation of effect sizes. *https://www.psychometrica.de/effect_size.html*. doi: 10.13140/RG.2.2.17823.92329.

Lenth, R. (2021). emmeans: estimated marginal means, aka least-squares means. R package version 1.5.5-1. Available at: https://cran.r-project.org/web/packages/emmeans.

Lenth, R. V. (2022). emmeans: Estimated Marginal Means, aka Least-Squares Means. Available at: https://CRAN.R-project.org/package=emmeans.

Li, H., Zhong, Y., Wang, Z., Gao, J., Xu, J., Chu, W., et al. (2013a). Smyd1b is required for skeletal and cardiac muscle function in zebrafish. *Mol. Biol. Cell* 24, 3511–3521. doi: 10.1091/mbc.E13-06-0352.

Li, K., Brant, C. O., Huertas, M., Hessler, E. J., Mezei, G., Scott, A. M., et al. (2018). Fatty-acid derivative acts as a sea lamprey migratory pheromone. *Proc. Natl. Acad. Sci. U. S. A.* 115, 8603–8608. doi: 10.1073/pnas.1803169115.

Li, K., Brant, C. O., Siefkes, M. J., Kruckman, H. G., and Li, W. (2013b). Characterization of a novel bile alcohol sulfate released by sexually mature male sea lamprey (Petromyzon marinus). *PLoS One* 8, e68157. doi: 10.1371/journal.pone.0068157.

Li, S., Pozhitkov, A., Ryan, R. A., Manning, C. S., Brown-Peterson, N., and Brouwer, M. (2010). Constructing a fish metabolic network model. *Genome Biol.* 11, R115. doi: 10.1186/gb-2010-11-11-r115.

Lienart, G. D. H., Ferrari, M. C. O., and McCormick, M. I. (2016). Thermal environment and nutritional condition affect the efficacy of chemical alarm cues produced by prey fish. *Environ. Biol. Fishes* 99, 729–739. doi: 10.1007/s10641-016-0516-7.

Liu, Z.-P., Gu, W.-B., Tu, D.-D., Zhu, Q.-H., Zhou, Y.-L., Wang, C., et al. (2018). Effects of both cold and heat stress on the liver of the giant spiny frog (Quasipaa spinosa): stress response and histological changes. *J. Exp. Biol.* 221. doi: 10.1242/jeb.186379.

Livak, K. J., and Schmittgen, T. D. (2001). Analysis of relative gene expression data using real-time quantitative PCR and the 2- ΔΔCT method. *Methods* 25, 402–408.

Logan, C. A., and Buckley, B. A. (2015). Transcriptomic responses to environmental temperature in eurythermal and stenothermal fishes. *J. Exp. Biol.* 218, 1915–1924. doi: 10.1242/jeb.114397.

Long, Y., Li, L., Li, Q., He, X., and Cui, Z. (2012). Transcriptomic characterization of temperature stress responses in larval zebrafish. *PLoS One* 7, e37209. doi: 10.1371/journal.pone.0037209.

Long, Y., Yan, J., Song, G., Li, X., Li, X., Li, Q., et al. (2015). Transcriptional events co-regulated by hypoxia and cold stresses in Zebrafish larvae. *BMC Genomics* 16, 385. doi: 10.1186/s12864-015-1560-y.

López-Olmeda, J. F., and Sánchez-Vázquez, F. J. (2011). Thermal biology of zebrafish (Danio rerio). *J. Therm. Biol.* 36, 91–104. doi: 10.1016/j.jtherbio.2010.12.005.

Loreto, F., Barta, C., Brilli, F., and Nogues, I. (2006). On the induction of volatile organic compound emissions by plants as consequence of wounding or fluctuations of light and temperature. *Plant Cell Environ.* 29, 1820–1828. doi: 10.1111/j.1365-3040.2006.01561.x.

Love, M. I., Huber, W., and Anders, S. (2014). Moderated estimation of fold change and dispersion for RNA-seq data with DESeq2. *Genome Biol.* 15, 550. doi: 10.1186/s13059-014-0550-8.

Lucon-Xiccato, T., Di Mauro, G., Bisazza, A., and Bertolucci, C. (2020). Alarm cue-mediated response and learning in zebrafish larvae. *Behav. Brain Res.* 380, 112446. doi: 10.1016/j.bbr.2019.112446.

Lüdecke, D. (2021). Data Visualization for Statistics in Social Science. R package sjPlot version 2.8.7. Available at: https://CRAN.R-project.org/package=sjPlot.

Luna-Sánchez, M., Hidalgo-Gutiérrez, A., Hildebrandt, T. M., Chaves-Serrano, J., Barriocanal-Casado, E., Santos-Fandila, Á., et al. (2017). CoQ deficiency causes disruption of mitochondrial sulfide oxidation, a new pathomechanism associated with this syndrome. *EMBO Mol. Med.* 9, 78–95. doi: 10.15252/emmm.201606345.

Lundsgaard, N. U., Cramp, R. L., and Franklin, C. E. (2022). Early exposure to UV radiation causes telomere shortening and poorer condition later in life. *J. Exp. Biol.* 225. doi: 10.1242/jeb.243924.

Lunsford, E. T., Jenkins, K., and Ferrer, R. P. (2019). Chemical signaling in aquatic ecosystems. *Encyclopedia of Water*, 1–17. doi: 10.1002/9781119300762.wsts0188.

Lupu, A., Pechkovskaya, A., Rashkovetsky, E., Nevo, E., and Korol, A. (2004). DNA repair efficiency and thermotolerance in Drosophila melanogaster from 'Evolution Canyon.' *Mutagenesis* 19, 383–390. doi: 10.1093/mutage/geh045.

Lürling, M., and Scheffer, M. (2007). Info-disruption: pollution and the transfer of chemical information between organisms. *Trends Ecol. Evol.* 22, 374–379. doi: 10.1016/j.tree.2007.04.002.

Lushchak, V. I. (2011). Environmentally induced oxidative stress in aquatic animals. *Aquat. Toxicol.* 101, 13–30. doi: 10.1016/j.aquatox.2010.10.006.

Luu, I., Ikert, H., and Craig, P. M. (2021). Chronic exposure to anthropogenic and climate related stressors alters transcriptional responses in the liver of zebrafish (Danio rerio) across multiple generations. *Comp. Biochem. Physiol. C. Toxicol. Pharmacol.* 240, 108918. doi: 10.1016/j.cbpc.2020.108918.

Lyu, L., Wen, H., Li, Y., Li, J., Zhao, J., Zhang, S., et al. (2018). Deep Transcriptomic Analysis of Black Rockfish (Sebastes schlegelii) Provides New Insights on Responses to Acute Temperature Stress. *Sci. Rep.* 8, 9113. doi: 10.1038/s41598-018-27013-z.

MacFadyen, E. J., Williamson, C. E., Grad, G., Lowery, M., Jeffrey, W. H., and Mitchell, D. L. (2004). Molecular response to climate change: temperature dependence of UV-induced DNA damage and repair in the freshwater crustaceanDaphnia pulicaria. *Glob. Chang. Biol.* 10, 408–416. doi: 10.1111/j.1529-8817.2003.00750.x.

Madeira, D., Araújo, J. E., Vitorino, R., Capelo, J. L., Vinagre, C., and Diniz, M. S. (2016a). Ocean warming alters cellular metabolism and induces mortality in fish early life stages: A proteomic approach. *Environ. Res.* 148, 164–176. doi: 10.1016/j.envres.2016.03.030.

Madeira, D., Costa, P. M., Vinagre, C., and Diniz, M. S. (2016b). When warming hits harder: survival, cellular stress and thermal limits of Sparus aurata larvae under global change. *Mar. Biol.* 163, 91. doi: 10.1007/s00227-016-2856-4.

Madeira, D., Vinagre, C., and Diniz, M. S. (2016c). Are fish in hot water? Effects of warming on oxidative stress metabolism in the commercial species Sparus aurata. *Ecol. Indic.* 63, 324–331. doi: 10.1016/j.ecolind.2015.12.008.

Magellan, K., Booth, A. J., and Weyl, O. L. F. (2020). Innate responses to conspecific and heterospecific alarm cues in the endangered eastern cape redfin Pseudobarbus afer. *J. Fish Biol.* 96, 1284–1290. doi: 10.1111/jfb.14197.

Magurran, A. E., Irving, P. W., and Henderson, P. A. (1996). Is there a fish alarm pheromone? A wild study and critique. *Proc. Biol. Sci.* 263, 1551–1556. doi: 10.1098/rspb.1996.0227.

Mahanty, A., Purohit, G. K., Banerjee, S., Karunakaran, D., Mohanty, S., and Mohanty, B. P. (2016). Proteomic changes in the liver of Channa striatus in response to high temperature stress. *Electrophoresis* 37, 1704–1717. doi: 10.1002/elps.201500393.

Mangiafico, S. (2021). rcompanion: Functions to Support Extension Education Program Evaluation. *R package version* 1. Available at: https://CRAN.R-project.org/package=rcompanion.

Manzon, L. A., Zak, M. A., Agee, M., Boreham, D. R., Wilson, J. Y., Somers, C. M., et al. (2022). Thermal acclimation alters both basal heat shock protein gene expression and the heat shock response in juvenile lake whitefish (Coregonus clupeaformis). *J. Therm. Biol.* 104, 103185. doi: 10.1016/j.jtherbio.2021.103185.

Mariana, S., and Badr, G. (2019). Impact of heat stress on the immune response of fishes. *Surv. Fish. Sci.* 5, 149–159. doi: 10.18331/sfs2019.5.2.14.

Martin, B. T., Dudley, P. N., Kashef, N. S., Stafford, D. M., Reeder, W. J., Tonina, D., et al. (2020). The biophysical basis of thermal tolerance in fish eggs. *Proc. Biol. Sci.* 287, 20201550. doi: 10.1098/rspb.2020.1550.

Martinez Arbizu, P. (2017). pairwiseAdonis: Pairwise Multilevel Comparison using Adonis.

Martínez-Álvarez, R. M., Morales, A. E., and Sanz, A. (2005). Antioxidant defenses in fish: Biotic and abiotic factors. *Rev. Fish Biol. Fish.* 15, 75–88. doi: 10.1007/s11160-005-7846-4.

Mathavan, S., Lee, S. G. P., Mak, A., Miller, L. D., Murthy, K. R. K., Govindarajan, K. R., et al. (2005). Transcriptome analysis of zebrafish embryogenesis using microarrays. *PLoS Genet.* 1, 260–276. doi: 10.1371/journal.pgen.0010029.

Mathuru, A. S. (2016). Conspecific injury raises an alarm in medaka. *Sci. Rep.* 6, 36615. doi: 10.1038/srep36615.

Mathuru, A. S., Kibat, C., Cheong, W. F., Shui, G., Wenk, M. R., Friedrich, R. W., et al. (2012). Chondroitin fragments are odorants that trigger fear behavior in fish. *Curr. Biol.* 22, 538–544. doi: 10.1016/j.cub.2012.01.061.

Matsuda, M., Hoshino, T., Yamakawa, N., Tahara, K., Adachi, H., Sobue, G., et al. (2013). Suppression of UV-induced wrinkle formation by induction of HSP70 expression in mice. *J. Invest. Dermatol.* 133, 919–928. doi: 10.1038/jid.2012.383.

Matsumura, K., Matsunaga, S., and Fusetani, N. (2007). Phosphatidylcholine profile-mediated group recognition in catfish. *J. Exp. Biol.* 210, 1992–1999. doi: 10.1242/jeb.02777.

Mazerolle, M. J. (2020a). AICcmodavg: Model selection and multimodel inference based on (Q)AIC(c). Available at: https://cran.r-project.org/package=AICcmodavg.

Mazerolle, M. J. (2020b). Model selection and multimodel inference using the AICcmodavg package. Available at: https://mirror.marwan.ma/cran/web/packages/AICcmodavg/vignettes/AICcmodavg.pdf [Accessed October 4, 2021].

McBriarty, G. J., Kidd, K. A., and Burridge, L. E. (2018). Short-Term Effects of the Anti-sea Lice Therapeutant Emamectin Benzoate on Clam Worms (Nereis virens). *Arch. Environ. Contam. Toxicol.* 74, 539–545. doi: 10.1007/s00244-017-0461-2.

McCormick, M. I., and Larson, J. K. (2008). Effect of hunger on the response to, and the production of, chemical alarm cues in a coral reef fish. *Anim. Behav.* 75, 1973–1980. doi: 10.1016/j.anbehav.2007.12.007.

McEwen, B. S., and Wingfield, J. C. (2003). The concept of allostasis in biology and biomedicine. *Horm. Behav.* 43, 2–15. doi: 10.1016/s0018-506x(02)00024-7.

McGlashan, J. K., Spencer, R.-J., and Old, J. M. (2012). Embryonic communication in the nest: metabolic responses of reptilian embryos to developmental rates of siblings. *Proc. Biol. Sci.* 279, 1709–1715. doi: 10.1098/rspb.2011.2074.

McLean, S., Nichols, D. S., and Davies, N. W. (2021). Volatile scent chemicals in the urine of the red fox, Vulpes vulpes. *PLoS One* 16, e0248961. doi: 10.1371/journal.pone.0248961.

Meents, A. K., and Mithöfer, A. (2020). Plant-plant communication: Is there a role for volatile damage-associated molecular patterns? *Front. Plant Sci.* 11, 583275. doi: 10.3389/fpls.2020.583275.

Metz, J. R., Huising, M. O., Leon, K., Verburg-van Kemenade, B. M. L., and Flik, G. (2006). Central and peripheral interleukin-1beta and interleukin-1 receptor I expression and their role in the acute stress response of common carp, Cyprinus carpio L. *J. Endocrinol.* 191, 25–35. doi: 10.1677/joe.1.06640.

Mezrai, N., Arduini, L., Dickel, L., Chiao, C.-C., and Darmaillacq, A.-S. (2020). Awareness of danger inside the egg: Evidence of innate and learned predator recognition in cuttlefish embryos. *Learn. Behav.* 48, 401–410. doi: 10.3758/s13420-020-00424-7.

Minten, E. V., and Yu, D. S. (2019). DNA Repair: Translation to the Clinic. *Clin. Oncol.* 31, 303–310. doi: 10.1016/j.clon.2019.02.007.

Miyazaki, M., Yamashita, T., Suzuki, Y., Saito, Y., Soeta, S., Taira, H., et al. (2006). A major urinary protein of the domestic cat regulates the production of felinine, a putative pheromone precursor. *Chem. Biol.* 13, 1071–1079. doi: 10.1016/j.chembiol.2006.08.013.

Moberg, G. P. (2000). Biological response to stress: implications for animal welfare. *basic principles and implications for animal welfare*, 1–21. Available at: 10.1079/9780851993591.0001.

Mogdans, J. (2019). Sensory ecology of the fish lateral-line system: Morphological and physiological adaptations for the perception of hydrodynamic stimuli. *J. Fish Biol.* 95, 53–72. doi: 10.1111/jfb.13966.

Mojib, N., Xu, J., Bartolek, Z., Imhoff, B., McCarty, N. A., Shin, C. H., et al. (2017). Zebrafish aversive taste co-receptor is expressed in both chemo- and mechanosensory cells and plays a role in lateral line development. *Sci. Rep.* 7, 1–11. doi: 10.1038/s41598-017-14042-3.

Morgan, I. J., McDonald, D. G., and Wood, C. M. (2001). The cost of living for freshwater fish in a warmer, more polluted world. *Glob. Chang. Biol.* 7, 345–355. doi: 10.1046/j.1365-2486.2001.00424.x.

Morgan, M. (2021). BiocManager: Access the Bioconductor Project Package Repository. Available at: https://CRAN.R-project.org/package=BiocManager.

Morgan, R., Andreassen, A. H., Åsheim, E. R., Finnøen, M. H., Dresler, G., Brembu, T., et al. (2022). Reduced physiological plasticity in a fish adapted to stable temperatures. *Proc. Natl. Acad. Sci. U. S. A.* 119, e2201919119. doi: 10.1073/pnas.2201919119.

Morgan, R., Sundin, J., Finnøen, M. H., Dresler, G., Vendrell, M. M., Dey, A., et al. (2019). Are model organisms representative for climate change research? Testing thermal tolerance in wild and laboratory zebrafish populations. *Conserv Physiol* 7, coz036. doi: 10.1093/conphys/coz036.

Morimoto, R. I. (1998). Regulation of the heat shock transcriptional response: Cross talk between a family of heat shock factors, molecular chaperones, and negative regulators. *Genes and Development* 12, 3788–3796. doi: 10.1101/gad.12.24.3788.

Morishita, V. R., and Barreto, R. E. (2011). Black sea urchins evaluate predation risk using chemical signals from a predator and injured con- and heterospecific prey. *Mar. Ecol. Prog. Ser.* 435, 173–181. doi: 10.3354/meps09253.

Morison, S. A., Cramp, R. L., Alton, L. A., and Franklin, C. E. (2020). Cooler temperatures slow the repair of DNA damage in tadpoles exposed to ultraviolet radiation: Implications for amphibian declines at high altitude. *Glob. Chang. Biol.* 26, 1225–1234. doi: 10.1111/gcb.14837.

Mothersill, C., Smith, R. W., Agnihotri, N., and Seymour, C. B. (2007). Characterization of a radiation-induced stress response communicated in vivo between zebrafish. *Environ. Sci. Technol.* 41, 3382–3387. doi: 10.1021/es062978n.

Mothersill, C., Smith, R., Wang, J., Rusin, A., Fernandez-Palomo, C., Fazzari, J., et al. (2018). Biological Entanglement-Like Effect After Communication of Fish Prior to X-Ray Exposure. *Dose Response* 16, 1559325817750067. doi: 10.1177/1559325817750067.

Mouneyrac, C., Mastain, O., Amiard, J. C., Amiard-Triquet, C., Beaunier, P., Jeantet, A.-Y., et al. (2003). Trace-metal detoxification and tolerance of the estuarine worm Hediste diversicolor chronically exposed in their environment. *Mar. Biol.* 143, 731–744. doi: 10.1007/s00227-003-1124-6.

Mourabit, S., Rundle, S. D., Spicer, J. I., and Sloman, K. A. (2010). Alarm substance from adult zebrafish alters early embryonic development in offspring. *Biol. Lett.* 6, 525–528. doi: 10.1098/rsbl.2009.0944.

Moynihan, J. A., Karp, J. D., Cohen, N., and Ader, R. (2000). Immune deviation following stress odor exposure: role of endogenous opioids. *J. Neuroimmunol.* 102, 145–153. doi: 10.1016/s0165-5728(99)00173-3.

Mujica-Parodi, L. R., Strey, H. H., Frederick, B., Savoy, R., Cox, D., Botanov, Y., et al. (2009). Chemosensory cues to conspecific emotional stress activate amygdala in humans. *PLoS One* 4, e6415. doi: 10.1371/journal.pone.0006415.

Munday, P. L., Dixson, D. L., Donelson, J. M., Jones, G. P., Pratchett, M. S., Devitsina, G. V., et al. (2009). Ocean acidification impairs olfactory discrimination and homing ability of a marine fish. *Proc. Natl. Acad. Sci. U. S. A.* 106, 1848–1852. doi: 10.1073/pnas.0809996106.

Munday, P. L., Dixson, D. L., Welch, M. J., Chivers, D. P., Domenici, P., Grosell, M., et al. (2020). Methods matter in repeating ocean acidification studies. *Nature* 586, E20–E24. doi: 10.1038/s41586-020-2803-x.

Nair, R. R., Hsu, J., Jacob, J. T., Pineda, C. M., Hobbs, R. P., and Coulombe, P. A. (2021). A role for keratin 17 during DNA damage response and tumor initiation. *Proc. Natl. Acad. Sci. U. S. A.* 118. doi: 10.1073/pnas.2020150118.

Nakagawa, Y., and Sonobe, H. (2016). "Subchapter 98A - 20-Hydroxyecdysone," in *Handbook of Hormones*, eds. Y. Takei, H. Ando, and K. Tsutsui (San Diego: Academic Press), 560-e98A-2. doi: 10.1016/B978-0-12-801028-0.00238-5.

Nakanishi, S., Makita, M., and Denda, M. (2021). Effects of trans-2-nonenal and olfactory masking odorants on proliferation of human keratinocytes. *Biochem. Biophys. Res. Commun.* 548, 1–6. doi: 10.1016/j.bbrc.2021.02.050.

Naser, F. J., Jackstadt, M. M., Fowle-Grider, R., Spalding, J. L., Cho, K., Stancliffe, E., et al. (2021). Isotope tracing in adult zebrafish reveals alanine cycling between melanoma and liver. *Cell Metab.* 33, 1493-1504.e5. doi: 10.1016/j.cmet.2021.04.014.

Nasiadka, A., and Clark, M. D. (2012). Zebrafish breeding in the laboratory environment. *ILAR J.* 53, 161–168. doi: 10.1093/ilar.53.2.161.

Nati, J. J. H., Svendsen, M. B. S., Marras, S., Killen, S. S., Steffensen, J. F., McKenzie, D. J., et al. (2021). Intraspecific variation in thermal tolerance differs between tropical and temperate fishes. *Sci. Rep.* 11, 21272. doi: 10.1038/s41598-021-00695-8.

Nelson, A. B., Alemadi, S. D., and Wisenden, B. D. (2013). Learned recognition of novel predator odour by convict cichlid embryos. *Behav. Ecol. Sociobiol.* 67, 1269–1273. doi: 10.1007/s00265-013-1554-1.

Nie, L., Cai, S.-Y., Shao, J.-Z., and Chen, J. (2018). Toll-Like Receptors, Associated Biological Roles, and Signaling Networks in Non-Mammals. *Frontiers in Immunology* 9. doi: 10.3389/fimmu.2018.01523.

Nielsen, B. L., Rampin, O., Meunier, N., and Bombail, V. (2015). Behavioral responses to odors from other species: introducing a complementary model of allelochemics involving vertebrates. *Front. Neurosci.* 9, 226. doi: 10.3389/fnins.2015.00226.

Nishizaki, M. T., and Ackerman, J. D. (2005). A secondary chemical cue facilitates juvenile-adult postsettlement associations in red sea urchins. *Limnol. Oceanogr.* 50, 354–362. doi: 10.4319/lo.2005.50.1.0354.

Nonnis, S., Angiulli, E., Maffioli, E., Frabetti, F., Negri, A., Cioni, C., et al. (2021). Acute environmental temperature variation affects brain protein expression, anxiety and explorative behaviour in adult zebrafish. *Sci. Rep.* 11, 2521. doi: 10.1038/s41598-021-81804-5.

O'Carroll, A.-M., Don, A. L. J., and Lolait, S. J. (2003). APJ receptor mRNA expression in the rat hypothalamic paraventricular nucleus: regulation by stress and glucocorticoids. *J. Neuroendocrinol.* 15, 1095–1101. doi: 10.1046/j.1365-2826.2003.01102.x.

Ogata, F. T., Batista, W. L., Sartori, A., Gesteira, T. F., Masutani, H., Arai, R. J., et al. (2013). Nitrosative/oxidative stress conditions regulate thioredoxin-interacting protein (TXNIP) expression and thioredoxin-1 (TRX-1) nuclear localization. *PLoS One* 8, e84588. doi: 10.1371/journal.pone.0084588.

Oksanen, J., Blanchet, F. G., Friendly, M., Kindt, R., Legendre, P., McGlinn, D., et al. (2020). vegan: Community Ecology Package. Available at: https://CRAN.R-project.org/package=vegan.

Oliveira, M. F., Geihs, M. A., França, T. F. A., Moreira, D. C., and Hermes-Lima, M. (2018). Is "Preparation for Oxidative Stress" a Case of Physiological Conditioning Hormesis? *Front. Physiol.* 9, 945. doi: 10.3389/fphys.2018.00945.

Oliveira, T. A., Koakoski, G., Kreutz, L. C., Ferreira, D., da Rosa, J. G. S., de Abreu, M. S., et al. (2013). Alcohol impairs predation risk response and communication in zebrafish. *PLoS One* 8, e75780. doi: 10.1371/journal.pone.0075780.

Oliver, A., Cavalheri, H. B., Lima, T. G., Jones, N. T., Podell, S., Zarate, D., et al. (2022). Phenotypic and transcriptional response of Daphnia pulicaria to the combined effects of temperature and predation. *PLoS One* 17, e0265103. doi: 10.1371/journal.pone.0265103.

O'Shea, K., Kattupalli, D., Mur, L. A. J., Hardy, N. W., Misra, B. B., and Lu, C. (2018). DIMEdb: an integrated database and web service for metabolite identification in direct infusion mass spectrometery. *bioRxiv*, 291799. doi: 10.1101/291799.

Ota, T., Nikaido, M., Suzuki, H., Hagino-Yamagishi, K., and Okada, N. (2012). Characterization of V1R receptor (ora) genes in Lake Victoria cichlids. *Gene* 499, 273–279. doi: 10.1016/j.gene.2012.03.002.

Otsuka, A., Shimomura, Y., Sakikubo, H., Miura, K., and Kagawa, N. (2022). Effects of single and repeated heat stress on anxiety-like behavior and locomotor activity in medaka fish. *Fish. Sci.* 88, 45–54. doi: 10.1007/s12562-021-01561-2.

Ouchi, Y., Tanizawa, H., Shiraishi, J.-I., Cockrem, J. F., Chowdhury, V. S., and Bungo, T. (2020). Repeated thermal conditioning during the neonatal period affects behavioral and physiological responses to acute heat stress in chicks. *J. Therm. Biol.* 94, 102759. doi: 10.1016/j.jtherbio.2020.102759.

Oulton, L. J., Haviland, V., and Brown, C. (2013). Predator recognition in rainbowfish, Melanotaenia duboulayi, embryos. *PLoS One* 8, e76061. doi: 10.1371/journal.pone.0076061.

Paaijmans, K. P., Heinig, R. L., Seliga, R. A., Blanford, J. I., Blanford, S., Murdock, C. C., et al. (2013). Temperature variation makes ectotherms more sensitive to climate change. *Glob. Chang. Biol.* 19, 2373–2380. doi: 10.1111/gcb.12240.

Pang, Z., Chong, J., Li, S., and Xia, J. (2020). MetaboAnalystR 3.0: Toward an Optimized Workflow for Global Metabolomics. *Metabolites* 10. doi: 10.3390/metabo10050186.

Pang, Z., Chong, J., Zhou, G., de Lima Morais, D. A., Chang, L., Barrette, M., et al. (2021). MetaboAnalyst 5.0: narrowing the gap between raw spectra and functional insights. *Nucleic Acids Res.* doi: 10.1093/nar/gkab382.

Parra, K. V., Adrian, J. C., Jr, and Gerlai, R. (2009). The synthetic substance hypoxanthine 3-N-oxide elicits alarm reactions in zebrafish (Danio rerio). *Behav. Brain Res.* 205, 336–341. doi: 10.1016/j.bbr.2009.06.037.

Patel, D. S., Misenko, S. M., Her, J., and Bunting, S. F. (2017). BLM helicase regulates DNA repair by counteracting RAD51 loading at DNA double-strand break sites. *J. Cell Biol.* 216, 3521–3534. doi: 10.1083/jcb.201703144.

Pawluk, R. J., Stuart, R., Garcia de Leaniz, C., Cable, J., Morphew, R. M., Brophy, P. M., et al. (2019). Smell of Infection: A Novel, Noninvasive Method for Detection of Fish Excretory-Secretory Proteins. *J. Proteome Res.* 18, 1371–1379. doi: 10.1021/acs.jproteome.8b00953.

Pei, D.-S., and Strauss, P. R. (2013). Zebrafish as a model system to study DNA damage and repair. *Mutat. Res.* 743–744, 151–159. doi: 10.1016/j.mrfmmm.2012.10.003.

Perrot-Minnot, M.-J., Banchetry, L., and Cézilly, F. (2017). Anxiety-like behaviour increases safety from fish predation in an amphipod crustacea. *R Soc Open Sci* 4, 171558. doi: 10.1098/rsos.171558.

Peters, R. C., Kotrschal, K., and Krautgartner, W.-D. (1991). Solitary chemoreceptor cells of Ciliata mustela (Gadidae, Teleostei) are tuned to mucoid stimuli. *Chem. Senses* 16, 31–42. doi: 10.1093/chemse/16.1.31.

Peterson, R. (2021). Finding optimal normalizing transformations via bestNormalize. *R J.* 13, 310. doi: 10.32614/rj-2021-041.

Peterson, R. A., and Cavanaugh, J. E. (2020). Ordered quantile normalization: a semiparametric transformation built for the cross-validation era. *J. Appl. Stat.* 47, 2312–2327. doi: 10.1080/02664763.2019.1630372.

Pfaffl, M. W., Tichopad, A., Prgomet, C., and Neuvians, T. P. (2004). Determination of stable housekeeping genes, differentially regulated target genes and sample integrity: BestKeeper--Excel-based tool using pair-wise correlations. *Biotechnol. Lett.* 26, 509–515. doi: 10.1023/b:bile.0000019559.84305.47.

Pirkkala, L., Nykänen, P., and Sistonen, L. (2001). Roles of the heat shock transcription factors in regulation of the heat shock response and beyond. *FASEB J.* 15, 1118–1131. doi: 10.1096/fj00-0294rev.

Poisson, A., Valotaire, C., Borel, F., Bertin, A., Darmaillacq, A.-S., Dickel, L., et al. (2017). Embryonic exposure to a conspecific alarm cue triggers behavioural plasticity in juvenile rainbow trout. *Anim. Behav.* 133, 35–45. doi: 10.1016/j.anbehav.2017.09.013.

Porteus, C. S., Hubbard, P. C., Uren Webster, T. M., van Aerle, R., Canário, A. V. M., Santos, E. M., et al. (2018). Near-future CO 2 levels impair the olfactory system of a marine fish. *Nat. Clim. Chang.* 8, 737–743. doi: 10.1038/s41558-018-0224-8.

Porteus, C. S., Roggatz, C. C., Velez, Z., Hardege, J. D., and Hubbard, P. C. (2021). Acidification can directly affect olfaction in marine organisms. *J. Exp. Biol.* 224. doi: 10.1242/jeb.237941.

Pörtner, H. (2008). Ecosystem effects of ocean acidification in times of ocean warming: a physiologist's view. *Mar. Ecol. Prog. Ser.* 373, 203–217. doi: 10.3354/meps07768.

Pörtner, H. O., and Farrell, A. P. (2008). Ecology. Physiology and climate change. *Science* 322, 690–692. doi: 10.1126/science.1163156.

Pörtner, H. O., and Peck, M. A. (2010). Climate change effects on fishes and fisheries: towards a cause-and-effect understanding. *J. Fish Biol.* 77, 1745–1779. doi: 10.1111/j.1095-8649.2010.02783.x.

Pörtner, H. O., Roberts, D. C., Masson-Delmotte, V., Zhai, P., Tignor, M., Poloczanska, E., et al. (2019). IPCC, 2019: Summary for Policymakers. *IPCC Special Report on the Ocean and Cryosphere in a Changing Climate*.

Poulin, R. X., Lavoie, S., Siegel, K., Gaul, D. A., Weissburg, M. J., and Kubanek, J. (2018). Chemical encoding of risk perception and predator detection among estuarine invertebrates. *Proceedings of the National Academy of Sciences* 115, 662–667. doi: 10.1073/pnas.1713901115.

Pourzand, C., and Tyrrell, R. M. (1999). Apoptosis, the role of oxidative stress and the example of solar UV radiation. *Photochem. Photobiol.* 70, 380–390. doi: 10.1111/j.1751-1097.1999.tb08239.x.

Power, M. (1997). Assessing the effects of environmental stressors on fish populations. *Aquat. Toxicol.* 39, 151–169. doi: 10.1016/S0166-445X(97)00020-9.

Pozzer, A. C., Gómez, P. A., and Weiss, J. (2022). Volatile organic compounds in aquatic ecosystems - Detection, origin, significance and applications. *Sci. Total Environ.* 838, 156155. doi: 10.1016/j.scitotenv.2022.156155.

Pype, C., Verbueken, E., Saad, M. A., Casteleyn, C. R., Van Ginneken, C. J., Knapen, D., et al. (2015). Incubation at 32.5°C and above causes malformations in the zebrafish embryo. *Reprod. Toxicol.* 56, 56–63. doi: 10.1016/j.reprotox.2015.05.006.

Quadros, V. A., Costa, F. V., Canzian, J., Nogueira, C. W., and Rosemberg, D. B. (2018). Modulatory role of conspecific alarm substance on aggression and brain monoamine oxidase activity in two zebrafish populations. *Prog. Neuropsychopharmacol. Biol. Psychiatry* 86, 322–330. doi: 10.1016/j.pnpbp.2018.03.018.

Quadros, V. A., Silveira, A., Giuliani, G. S., Didonet, F., Silveira, A. S., Nunes, M. E., et al. (2016). Strain- and context-dependent behavioural responses of acute alarm substance exposure in zebrafish. *Behav. Processes* 122, 1–11. doi: 10.1016/j.beproc.2015.10.014.

Quiniou, S. M. A., Boudinot, P., and Bengtén, E. (2013). Comprehensive survey and genomic characterization of Toll-like receptors (TLRs) in channel catfish, Ictalurus punctatus: identification of novel fish TLRs. *Immunogenetics* 65, 511–530. doi: 10.1007/s00251-013-0694-9.

Quinzii, C. M., Luna-Sanchez, M., Ziosi, M., Hidalgo-Gutierrez, A., Kleiner, G., and Lopez, L. C. (2017). The Role of Sulfide Oxidation Impairment in the Pathogenesis of Primary CoQ Deficiency. *Front. Physiol.* 8, 525. doi: 10.3389/fphys.2017.00525.

R Core Team (2020). R: A Language and Environment for Statistical Computing. Available at: https://www.R-project.org/.

Ramsay, J. M., Feist, G. W., Varga, Z. M., Westerfield, M., Kent, M. L., and Schreck, C. B. (2009). Whole-body cortisol response of zebrafish to acute net handling stress. *Aquaculture* 297, 157–162. doi: 10.1016/j.aquaculture.2009.08.035.

Rastogi, R. P., Richa, Kumar, A., Tyagi, M. B., and Sinha, R. P. (2010). Molecular mechanisms of ultraviolet radiation-induced DNA damage and repair. *J. Nucleic Acids* 2010, 592980. doi: 10.4061/2010/592980.

Rattan, S. I. S. (2006). Hormetic modulation of aging and longevity by mild heat stress. *Dose Response* 3, 533–546. doi: 10.2203/dose-response.003.04.008.

Rauwerda, H., Pagano, J. F. B., de Leeuw, W. C., Ensink, W., Nehrdich, U., de Jong, M., et al. (2017). Transcriptome dynamics in early zebrafish embryogenesis determined by high-resolution time course analysis of 180 successive, individual zebrafish embryos. *BMC Genomics* 18, 287. doi: 10.1186/s12864-017-3672-z.

Reardon, R. M., Walsh, A. K., Larsen, C. I., Schmidberger, L. H., Morrow, L. A., Thompson, A. E., et al. (2022). An epigenetically inherited UV hyper-resistance phenotype in Saccharomyces cerevisiae. *Epigenetics Chromatin* 15, 31. doi: 10.1186/s13072-022-00464-5.

Reef, R., Dunn, S., Levy, O., Dove, S., Shemesh, E., Brickner, I., et al. (2009). Photoreactivation is the main repair pathway for UV-induced DNA damage in coral planulae. *J. Exp. Biol.* 212, 2760–2766. doi: 10.1242/jeb.031286.

Regnier, F. E. (1971). Semiochemical--structure and function. *Biol Reprod* 4, 309–326. doi: 10.1093/biolreprod/4.3.309.

Reshetnyak, V. I. (2013). Physiological and molecular biochemical mechanisms of bile formation. *World J. Gastroenterol.* 19, 7341–7360. doi: 10.3748/wjg.v19.i42.7341.

Ribas, L., Liew, W. C., Díaz, N., Sreenivasan, R., Orbán, L., and Piferrer, F. (2017). Heat-induced masculinization in domesticated zebrafish is family-specific and yields a set of different gonadal transcriptomes. *Proc. Natl. Acad. Sci. U. S. A.* 114, E941–E950. doi: 10.1073/pnas.1609411114.

Ritchie, M. E., Phipson, B., Wu, D., Hu, Y., Law, C. W., Shi, W., et al. (2015). limma powers differential expression analyses for RNA-sequencing and microarray studies. *Nucleic Acids Res.* 43, e47. doi: 10.1093/nar/gkv007.

Robbins, L., Hansen, M. E., Kleypas, J. A., and Meylan, S. C. (2010). *CO2calc: A user-friendly seawater carbon calculator for Windows, Mac OS X, and iOS (iPhone)*. US Department of the Interior, US Geological Survey.

Rodnick, K. J., and Planas, J. V. (2016). "The stress and stress mitigation effects of exercise: Cardiovascular, metabolic, and skeletal muscle adjustments," in *Fish Physiology* Fish physiology. (Elsevier), 251–294. doi: 10.1016/b978-0-12-802728-8.00007-2.

Roggatz, C. C., Fletcher, N., Benoit, D. M., Algar, A. C., Doroff, A., Wright, B., et al. (2019). Saxitoxin and tetrodotoxin bioavailability increases in future oceans. *Nat. Clim. Chang.* 9, 840–844. doi: 10.1038/s41558-019-0589-3.

Roggatz, C. C., Lorch, M., Hardege, J. D., and Benoit, D. M. (2016). Ocean acidification affects marine chemical communication by changing structure and function of peptide signalling molecules. *Glob. Chang. Biol.* 22, 3914–3926. doi: 10.1111/gcb.13354.

Roggatz, C. C., Saha, M., Blanchard, S., Schirrmacher, P., Fink, P., Verheggen, F., et al. (2022). Becoming nose-blind-Climate change impacts on chemical communication. *Glob. Chang. Biol.* 28, 4495–4505. doi: 10.1111/gcb.16209.

Romero, L. M., Dickens, M. J., and Cyr, N. E. (2009). The Reactive Scope Model - a new model integrating homeostasis, allostasis, and stress. *Horm. Behav.* 55, 375–389. doi: 10.1016/j.yhbeh.2008.12.009.

Rosdy, M. S., Rofiee, M. S., Samsulrizal, N., Salleh, M. Z., and Teh, L. K. (2021). Understanding the effects of Moringa oleifera in chronic unpredictable stressed zebrafish using metabolomics analysis. *J. Ethnopharmacol.* 278, 114290. doi: 10.1016/j.jep.2021.114290.

Rose, P., Moore, P. K., and Zhu, Y. Z. (2017). H2S biosynthesis and catabolism: new insights from molecular studies. *Cellular and Molecular Life Sciences* 74, 1391–1412. doi: 10.1007/s00018-016-2406-8.

Rossman, T. G., and Wang, Z. (1999). Expression cloning for arsenite-resistance resulted in isolation of tumor-suppressor fau cDNA: possible involvement of the ubiquitin system in arsenic carcinogenesis. *Carcinogenesis* 20, 311–316. doi: 10.1093/carcin/20.2.311.

RStudio Team (2020). RStudio: Integrated Development Environment for R. Available at: http://www.rstudio.com/.

Rubin, D., Botanov, Y., Hajcak, G., and Mujica-Parodi, L. R. (2012). Second-hand stress: inhalation of stress sweat enhances neural response to neutral faces. *Soc. Cogn. Affect. Neurosci.* 7, 208–212. doi: 10.1093/scan/nsq097.

Ruzicka, L., Howe, D. G., Ramachandran, S., Toro, S., Van Slyke, C. E., Bradford, Y. M., et al. (2019). The Zebrafish Information Network: new support for non-coding genes, richer Gene Ontology annotations and the Alliance of Genome Resources. *Nucleic Acids Res.* 47, D867–D873. doi: 10.1093/nar/gky1090.

Sabine, C. L., Feely, R. A., Gruber, N., Key, R. M., Lee, K., Bullister, J. L., et al. (2004). The oceanic sink for anthropogenic CO2. *Science* 305, 367–371. doi: 10.1126/science.1097403.

Sadoul, B., and Geffroy, B. (2019). Measuring cortisol, the major stress hormone in fishes. *Journal of Fish Biology* 94, 540–555. doi: 10.1111/jfb.13904.

Sadoul, B., and Vijayan, M. M. (2016). "5 - Stress and Growth," in *Fish Physiology*, eds. C. B. Schreck, L. Tort, A. P. Farrell, and C. J. Brauner (Academic Press), 167–205. doi: 10.1016/B978-0-12-802728-8.00005-9.

Saha, M., Berdalet, E., Carotenuto, Y., Fink, P., Harder, T., John, U., et al. (2019). Using chemical language to shape future marine health. *Front. Ecol. Environ.* 17, 530–537. doi: 10.1002/fee.2113.

Sakai, W., Yuasa-Sunagawa, M., Kusakabe, M., Kishimoto, A., Matsui, T., Kaneko, Y., et al. (2020). Functional impacts of the ubiquitin-proteasome system on DNA damage recognition in global genome nucleotide excision repair. *Sci. Rep.* 10, 19704. doi: 10.1038/s41598-020-76898-2.

Sakuma, K., Hayashi, S., Yasaka, Y., Nishijima, H., Funabashi, H., Hayashi, M., et al. (2013). Analysis of odor compounds in feces of mice that were exposed to various stresses during breeding. *Exp. Anim.* 62, 101–107. doi: 10.1538/expanim.62.101.

Sakuragi, T., Kanai, R., Tsutsumi, A., Narita, H., Onishi, E., Nishino, K., et al. (2021). The tertiary structure of the human Xkr8-Basigin complex that scrambles phospholipids at plasma membranes. *Nat. Struct. Mol. Biol.* 28, 825–834. doi: 10.1038/s41594-021-00665-8.

Salo, H. M., Jokinen, E. I., Markkula, S. E., Aaltonen, T. M., and Penttilä, H. T. (2000). Comparative effects of UVA and UVB irradiation on the immune system of fish. *J. Photochem. Photobiol. B* 56, 154–162. doi: 10.1016/s1011-1344(00)00072-5.

Sample, A., and He, Y.-Y. (2017). Autophagy in UV Damage Response. *Photochem. Photobiol.* 93, 943–955. doi: 10.1111/php.12691.

Samuelsson, L. M., and Larsson, D. G. J. (2008). Contributions from metabolomics to fish research. *Mol. Biosyst.* 4, 974–979. doi: 10.1039/b804196b.

Sanogo, Y. O., Hankison, S., Band, M., Obregon, A., and Bell, A. M. (2011). Brain transcriptomic response of threespine sticklebacks to cues of a predator. *Brain Behav. Evol.* 77, 270–285. doi: 10.1159/000328221.

Sant, K. E., and Timme-Laragy, A. R. (2018). Zebrafish as a Model for Toxicological Perturbation of Yolk and Nutrition in the Early Embryo. *Curr Environ Health Rep* 5, 125–133. doi: 10.1007/s40572-018-0183-2.

Saraiva, L. R., Ahuja, G., Ivandic, I., Syed, A. S., Marioni, J. C., Korsching, S. I., et al. (2015). Molecular and neuronal homology between the olfactory systems of zebrafish and mouse. *Sci. Rep.* 5, 11487. doi: 10.1038/srep11487.

Saraiva, L. R., and Korsching, S. I. (2007). A novel olfactory receptor gene family in teleost fish. *Genome Res.* 17, 1448–1457. doi: 10.1101/gr.6553207.

Sarker, N., Fabijan, J., Emes, R. D., Hemmatzadeh, F., Meers, J., Moreton, J., et al. (2018). Identification of stable reference genes for quantitative PCR in koalas. *Sci. Rep.* 8, 3364. doi: 10.1038/s41598-018-21723-0.

Saroya, R., Smith, R., Seymour, C., and Mothersill, C. (2009). Injection of resperpine into zebrafish, prevents fish to fish communication of radiation-induced bystander signals: confirmation in vivo of a role for serotonin in the mechanism. *Dose Response* 8, 317–330. doi: 10.2203/dose-response.09-043.Saroya.

Sawilowsky, S. S. (2009). New Effect Size Rules of Thumb. *J. Mod. Appl. Stat. Methods* 8, 26. doi: 10.22237/jmasm/1257035100.

Sayols, S., Scherzinger, D., and Klein, H. (2016). dupRadar: a Bioconductor package for the assessment of PCR artifacts in RNA-Seq data. *BMC Bioinformatics* 17, 428. doi: 10.1186/s12859-016-1276-2.

Sbarbati, A., and Osculati, F. (2003). Solitary chemosensory cells in mammals? *Cells Tissues Organs* 175, 51–55. doi: 10.1159/000073437.

Sbarbati, A., and Osculati, F. (2006). Allelochemical communication in vertebrates: kairomones, allomones and synomones. *Cells Tissues Organs* 183, 206–219. doi: 10.1159/000096511.

Scarantino, A. (2010). Animal communication between information and influence. *Anim. Behav.* 79, e1–e5. doi: 10.1016/j.anbehav.2010.03.005.

Schaefer, J., and Ryan, A. (2006). Developmental plasticity in the thermal tolerance of zebrafish Danio rerio. *J. Fish Biol.* 69, 722–734. doi: 10.1111/j.1095-8649.2006.01145.x.

Schaefer, M. L., Wongravee, K., Holmboe, M. E., Heinrich, N. M., Dixon, S. J., Zeskind, J. E., et al. (2010). Mouse urinary biomarkers provide signatures of maturation, diet, stress level, and diurnal rhythm. *Chem. Senses* 35, 459–471. doi: 10.1093/chemse/bjq032.

Schaum, C. E., Batty, R., and Last, K. S. (2013). Smelling danger - alarm cue responses in the polychaete Nereis (Hediste) diversicolor (Müller, 1776) to potential fish predation. *PLoS One* 8, e77431. doi: 10.1371/journal.pone.0077431.

Schirone, R. C., and Gross, L. (1968). Effect of temperature on early embryological development of the zebra fish,Brachydanio rerio. *J. Exp. Zool.* 169, 43–52. doi: 10.1002/jez.1401690106.

Schirrmacher, P., Roggatz, C. C., Benoit, D. M., and Hardege, J. D. (2021). Ocean Acidification Amplifies the Olfactory Response to 2-Phenylethylamine: Altered Cue Reception as a Mechanistic Pathway? *J. Chem. Ecol.* 47, 859–876. doi: 10.1007/s10886-021-01276-9.

Schlötterer, C., Tobler, R., Kofler, R., and Nolte, V. (2014). Sequencing pools of individuals - mining genome-wide polymorphism data without big funding. *Nat. Rev. Genet.* 15, 749–763. doi: 10.1038/nrg3803.

Schmidt, K., and Starck, J. M. (2010). Developmental plasticity, modularity, and heterochrony during the phylotypic stage of the zebra fish, Danio rerio. *J. Exp. Zool. B Mol. Dev. Evol.* 314, 166–178. doi: 10.1002/jez.b.21320.

Schneider, C. A., Rasband, W. S., and Eliceiri, K. W. (2012). NIH Image to ImageJ: 25 years of image analysis. *Nat. Methods* 9, 671–675. doi: 10.1038/nmeth.2089.

Schnurr, M. E., Yin, Y., and Scott, G. R. (2014). Temperature during embryonic development has persistent effects on metabolic enzymes in the muscle of zebrafish. *J. Exp. Biol.* 217, 1370–1380. doi: 10.1242/jeb.094037.

Scholz, S., Fischer, S., Gündel, U., Küster, E., Luckenbach, T., and Voelker, D. (2008). The zebrafish embryo model in environmental risk assessment--applications beyond acute toxicity testing. *Environ. Sci. Pollut. Res. Int.* 15, 394–404. doi: 10.1007/s11356-008-0018-z.

Schreck, C. B., and Tort, L. (2016). "The concept of stress in fish," in *Fish Physiology* Fish physiology. (Elsevier), 1–34. doi: 10.1016/b978-0-12-802728-8.00001-1.

Schröter, C., Herrgen, L., Cardona, A., Brouhard, G. J., Feldman, B., and Oates, A. C. (2008). Dynamics of zebrafish somitogenesis. *Dev. Dyn.* 237, 545–553. doi: 10.1002/dvdy.21458.

Schulte, P. M. (2007). Responses to environmental stressors in an estuarine fish: Interacting stressors and the impacts of local adaptation. *J. Therm. Biol.* 32, 152–161. doi: 10.1016/j.jtherbio.2007.01.012.

Scott, G. R., and Johnston, I. A. (2012). Temperature during embryonic development has persistent effects on thermal acclimation capacity in zebrafish. *Proc. Natl. Acad. Sci. U. S. A.* 109, 14247–14252. doi: 10.1073/pnas.1205012109.

Sessions, K. J., Whitehouse, L. M., Manzon, L. A., Boreham, D. R., Somers, C. M., Wilson, J. Y., et al. (2021). The heat shock response shows plasticity in embryonic lake whitefish (Coregonus clupeaformis) exposed to repeated thermal stress. *J. Therm. Biol.* 100, 103036. doi: 10.1016/j.jtherbio.2021.103036.

Shan, S., Liu, D., Liu, R., Zhu, Y., Li, T., Zhang, F., et al. (2018). Non-mammalian Toll-like receptor 18 (Tlr18) recognizes bacterial pathogens in common carp (Cyprinus carpio L.): Indications for a role of participation in the NF-κB signaling pathway. *Fish Shellfish Immunol.* 72, 187–198. doi: 10.1016/j.fsi.2017.09.081.

Shannon, P., Markiel, A., Ozier, O., Baliga, N. S., Wang, J. T., Ramage, D., et al. (2003). Cytoscape: a software environment for integrated models of biomolecular interaction networks. *Genome Res.* 13, 2498–2504. doi: 10.1101/gr.1239303.

Shen, Y., Stanislauskas, M., Li, G., Zheng, D., and Liu, L. (2017). Epigenetic and genetic dissections of UV-induced global gene dysregulation in skin cells through multi-omics analyses. *Sci. Rep.* 7, 42646. doi: 10.1038/srep42646.

Shi, Q., Xiong, X., Wen, Z., Qin, C., Li, R., Zhang, Z., et al. (2022). Cu/Zn superoxide dismutase and catalase of Yangtze sturgeon, Acipenser dabryanus: Molecular cloning, tissue distribution and response to fasting and refeeding. *G.* 7, 35. doi: 10.3390/fishes7010035.

Shimomura, Y., Inahata, M., Komori, M., and Kagawa, N. (2019). Reduction of Tryptophan Hydroxylase Expression in the Brain of Medaka Fish After Repeated Heat Stress. *Zoolog. Sci.* 36, 223–230. doi: 10.2108/zs180135.

Shinohara, Y., and Kobayashi, M. (2020). Sexual bipotentiality of the olfactory pathway for sexual behavior in goldfish. *Fish. Sci.* 86, 819–827. doi: 10.1007/s12562-020-01454-w.

Shrivastava, J., Ndugwa, M., Caneos, W., and De Boeck, G. (2019). Physiological trade-offs, acid-base balance and ion-osmoregulatory plasticity in European sea bass (Dicentrarchus labrax) juveniles under complex scenarios of salinity variation, ocean acidification and high ammonia challenge. *Aquat. Toxicol.* 212, 54–69. doi: 10.1016/j.aquatox.2019.04.024.

Shulaev, V., Silverman, P., and Raskin, I. (1997). Airborne signalling by methyl salicylate in plant pathogen resistance. *Nature* 385, 718–721. doi: 10.1038/385718a0.

Siepielski, A. M., Fallon, E., and Boersma, K. (2016). Predator olfactory cues generate a foraging-predation trade-off through prey apprehension. *R. Soc. Open Sci.* 3, 150537. doi: 10.1098/rsos.150537.

Simčič, T., Jesenšek, D., and Brancelj, A. (2015). Effects of increased temperature on metabolic activity and oxidative stress in the first life stages of marble trout (Salmo marmoratus). *Fish Physiol. Biochem.* 41, 1005–1014. doi: 10.1007/s10695-015-0065-6.

Simon, M. M., Reikerstorfer, A., Schwarz, A., Krone, C., Luger, T. A., Jäättelä, M., et al. (1995). Heat shock protein 70 overexpression affects the response to ultraviolet light in murine fibroblasts. Evidence for increased cell viability and suppression of cytokine release. *J. Clin. Invest.* 95, 926–933. doi: 10.1172/JCI117800.

Singer, A. G. (1991). A chemistry of mammalian pheromones. *J. Steroid Biochem. Mol. Biol.* 39, 627–632. doi: 10.1016/0960-0760(91)90261-3.

Sinha, R. P., and Häder, D. P. (2002). UV-induced DNA damage and repair: a review. *Photochem. Photobiol. Sci.* 1, 225–236. doi: 10.1039/b201230h.

Şişli, H. B., Hayal, T. B., Şenkal, S., Kıratlı, B., Sağraç, D., Seçkin, S., et al. (2022). Apelin receptor signaling protects GT1-7 GnRH neurons against oxidative stress in vitro. *Cell. Mol. Neurobiol.* 42, 753–775. doi: 10.1007/s10571-020-00968-2.

Skjærven, K. H., Hamre, K., Penglase, S., Finn, R. N., and Olsvik, P. A. (2014). Thermal stress alters expression of genes involved in one carbon and DNA methylation pathways in Atlantic cod embryos. *Comp. Biochem. Physiol. A Mol. Integr. Physiol.* 173C, 17–27. doi: 10.1016/j.cbpa.2014.03.003.

Skomal, G. B., and Mandelman, J. W. (2012). The physiological response to anthropogenic stressors in marine elasmobranch fishes: a review with a focus on the secondary response. *Comp. Biochem. Physiol. A Mol. Integr. Physiol.* 162, 146–155. doi: 10.1016/j.cbpa.2011.10.002.

Smith, C. A., Want, E. J., O'Maille, G., Abagyan, R., and Siuzdak, G. (2006). XCMS: processing mass spectrometry data for metabolite profiling using nonlinear peak alignment, matching, and identification. *Anal. Chem.* 78, 779–787. doi: 10.1021/ac051437y.

Smith, R. J. F. (1992). Alarm signals in fishes. *Rev. Fish Biol. Fish.* 2, 33–63. doi: 10.1007/BF00042916.

Sokolova, I. (2018). Mitochondrial Adaptations to Variable Environments and Their Role in Animals' Stress Tolerance. *Integr. Comp. Biol.* 58, 519–531. doi: 10.1093/icb/icy017.

Somero, G. N. (2010). The physiology of climate change: how potentials for acclimatization and genetic adaptation will determine "winners" and "losers." *J. Exp. Biol.* 213, 912–920. doi: 10.1242/jeb.037473.

Sondersorg, A. C., Busse, D., Kyereme, J., Rothermel, M., Neufang, G., Gisselmann, G., et al. (2014). Chemosensory information processing between keratinocytes and trigeminal neurons. *J. Biol. Chem.* 289, 17529–17540. doi: 10.1074/jbc.M113.499699.

Song, M., Zhao, J., Wen, H.-S., Li, Y., Li, J.-F., Li, L.-M., et al. (2019). The impact of acute thermal stress on the metabolome of the black rockfish (Sebastes schlegelii). *PLoS One* 14, e0217133. doi: 10.1371/journal.pone.0217133.

Sörbo, B. (1987). "3-Mercaptopyruvate, 3-mercaptolactate and mercaptoacetate," in *Methods in Enzymology* (Academic Press), 178–182. doi: 10.1016/0076-6879(87)43033-4.

Sordo, L., Santos, R., Barrote, I., and Silva, J. (2018). High CO2 decreases the long-term resilience of the free-living coralline algae Phymatolithon lusitanicum. *Ecol. Evol.* 8, 4781–4792. doi: 10.1002/ece3.4020.

Sordo, L., Santos, R., Reis, J., Shulika, A., and Silva, J. (2016). A direct CO2 control system for ocean acidification experiments: testing effects on the coralline red algae Phymatolithon lusitanicum. *PeerJ* 4, e2503. doi: 10.7717/peerj.2503.

Sottile, M. L., and Nadin, S. B. (2018). Heat shock proteins and DNA repair mechanisms: an updated overview. *Cell Stress Chaperones* 23, 303–315. doi: 10.1007/s12192-017-0843-4.

Souza, A. R. C., Kozlowski, E. O., Cerqueira, V. R., Castelo-Branco, M. T. L., Costa, M. L., and Pavão, M. S. G. (2007). Chondroitin sulfate and keratan sulfate are the major glycosaminoglycans present in the adult zebrafish Danio rerio (Chordata-Cyprinidae). *Glycoconj. J.* 24, 521–530. doi: 10.1007/s10719-007-9046-z.

Souza, C. de F., Baldissera, M. D., Baldisserotto, B., Heinzmann, B. M., Martos-Sitcha, J. A., and Mancera, J. M. (2019). Essential oils as stress-reducing agents for fish aquaculture: A review. *Front. Physiol.* 10, 785. doi: 10.3389/fphys.2019.00785.

Spence, R., Gerlach, G., Lawrence, C., and Smith, C. (2008). The behaviour and ecology of the zebrafish, Danio rerio. *Biol. Rev. Camb. Philos. Soc.* 83, 13–34. doi: 10.1111/j.1469-185X.2007.00030.x.

Steenbergen, P. J., Metz, J. R., Flik, G., Richardson, M. K., and Champagne, D. L. (2012). "Methods to Quantify Basal and Stress-Induced Cortisol Response in Larval Zebrafish," in *Zebrafish Protocols for Neurobehavioral Research*, eds. A. V. Kalueff and A. M. Stewart (Totowa, NJ: Humana Press), 121–141. doi: 10.1007/978-1-61779-597-8_9.

Steiger, S., Meier, T., and Müller, J. K. (2012). Fitness costs associated with chemical signaling. *Commun. Integr. Biol.* 5, 57–60. doi: 10.4161/cib.17988.

Stensmyr, M. C., and Maderspacher, F. (2012). Pheromones: fish fear factor. *Curr. Biol.* 22, R183-6. doi: 10.1016/j.cub.2012.02.025.

Stephenson, J. F. (2016). Keeping eyes peeled: guppies exposed to chemical alarm cue are more responsive to ambiguous visual cues. *Behav. Ecol. Sociobiol.* 70, 575–584. doi: 10.1007/s00265-016-2076-4.

Stewart, M. D., Ritterhoff, T., Klevit, R. E., and Brzovic, P. S. (2016). E2 enzymes: more than just middle men. *Cell Res.* 26, 423–440. doi: 10.1038/cr.2016.35.

Stincone, A., Prigione, A., Cramer, T., Wamelink, M. M. C., Campbell, K., Cheung, E., et al. (2015). The return of metabolism: biochemistry and physiology of the pentose phosphate pathway. *Biol. Rev. Camb. Philos. Soc.* 90, 927–963. doi: 10.1111/brv.12140.

Storey, K. B., and Storey, J. M. (2011). Heat shock proteins and hypometabolism: adaptive strategy for proteome preservation. *RRB* 2, 57–68. doi: 10.2147/RRB.S13351.

Strecker, R., Seiler, T.-B., Hollert, H., and Braunbeck, T. (2011). Oxygen requirements of zebrafish (Danio rerio) embryos in embryo toxicity tests with environmental samples. *Comp. Biochem. Physiol. C. Toxicol. Pharmacol.* 153, 318–327. doi: 10.1016/j.cbpc.2010.12.002.

Strober, W., and Watanabe, T. (2011). NOD2, an intracellular innate immune sensor involved in host defense and Crohn's disease. *Mucosal Immunol.* 4, 484–495. doi: 10.1038/mi.2011.29.

Sua-Cespedes, C. D., David, D. D., Souto-Neto, J. A., Lima, O. G., Moraes, M. N., de Assis, L. V. M., et al. (2021). Low temperature effect on the endocrine and circadian systems of adult Danio rerio. *Front. Physiol.* 12, 707067. doi: 10.3389/fphys.2021.707067.

Subramanian, D., Rosenstein, B. S., and Muller, M. T. (1998). Ultraviolet-induced DNA damage stimulates topoisomerase I-DNA complex formation in vivo: possible relationship with DNA repair. *Cancer Res.* 58, 976–984. Available at: https://www.ncbi.nlm.nih.gov/pubmed/9500459.

Sun, Y.-C., Wu, S., Du, N.-N., Song, Y., and Xu, W. (2018). High-throughput metabolomics enables metabolite biomarkers and metabolic mechanism discovery of fish in response to alkalinity stress. *RSC Adv.* 8, 14983–14990. doi: 10.1039/C8RA01317A.

Sussman, R. (2007). DNA repair capacity of zebrafish. *Proc. Natl. Acad. Sci. U. S. A.* 104, 13379–13383. doi: 10.1073/pnas.0706157104.

Takele Assefa, A., Vandesompele, J., and Thas, O. (2020). On the utility of RNA sample pooling to optimize cost and statistical power in RNA sequencing experiments. *BMC Genomics* 21, 312. doi: 10.1186/s12864-020-6721-y.

Tamai, T. K., Vardhanabhuti, V., Foulkes, N. S., and Whitmore, D. (2004). Early embryonic light detection improves survival. *Curr. Biol.* 14, R104-5. doi: 10.1016/j.cub.2004.01.014.

Tan, X., Rotllant, J., Li, H., De Deyne, P., and Du, S. J. (2006). SmyD1, a histone methyltransferase, is required for myofibril organization and muscle contraction in zebrafish embryos. *Proc. Natl. Acad. Sci. U. S. A.* 103, 2713–2718. doi: 10.1073/pnas.0509503103.

Tegelenbosch, R. A. J., Lucas P J, Richardson, M. K., and Ahmad, F. (2012). Zebrafish embryos and larvae in behavioural assays. *Behaviour* 149, 1241–1281. doi: 10.1163/1568539X-00003020.

Therneau, T. M. (2021). Survival Analysis [R package survival version 3.2-10]. Available at: https://CRAN.R-project.org/package=survival [Accessed March 27, 2021].

Therneau, T. M., and Grambsch, P. M. (2000). Modeling Survival Data: Extending the Cox Model. *Statistics for Biology and Health*. doi: 10.1007/978-1-4757-3294-8.

Timme-Laragy, A. R., Goldstone, J. V., Imhoff, B. R., Stegeman, J. J., Hahn, M. E., and Hansen, J. M. (2013). Glutathione redox dynamics and expression of glutathione-related genes in the developing embryo. *Free Radic. Biol. Med.* 65, 89–101. doi: 10.1016/j.freeradbiomed.2013.06.011.

Toa, D. G., Afonso, L. O. B., and Iwama, G. K. (2004). Stress response of juvenile rainbow trout (Oncorhynchus mykiss)to chemical cues released from stressed conspecifics. *Fish Physiol. Biochem.* 30, 103–108. doi: 10.1007/s10695-005-0266-5.

Tokarz, J., Norton, W., Möller, G., Hrabé de Angelis, M., and Adamski, J. (2013). Zebrafish 20β-hydroxysteroid dehydrogenase type 2 is important for glucocorticoid catabolism in stress response. *PLoS One* 8, e54851. doi: 10.1371/journal.pone.0054851.

Tomsic, D., Sztarker, J., Berón de Astrada, M., Oliva, D., and Lanza, E. (2017). The predator and prey behaviors of crabs: from ecology to neural adaptations. *J. Exp. Biol.* 220, 2318–2327. doi: 10.1242/jeb.143222.

Torchiano, M. (2016). effsize: efficient effect size computation. *R package*.

Török, Z., Crul, T., Maresca, B., Schütz, G. J., Viana, F., Dindia, L., et al. (2014). Plasma membranes as heat stress sensors: from lipid-controlled molecular switches to therapeutic applications. *Biochim. Biophys. Acta* 1838, 1594–1618. doi: 10.1016/j.bbamem.2013.12.015.

Tresguerres, M., and Hamilton, T. J. (2017). Acid-base physiology, neurobiology and behaviour in relation to CO2-induced ocean acidification. *J. Exp. Biol.* 220, 2136–2148. doi: 10.1242/jeb.144113.

Truchot, J. P., and Duhamel-Jouve, A. (1980). Oxygen and carbon dioxide in the marine intertidal environment: diurnal and tidal changes in rockpools. *Respir. Physiol.* 39, 241–254. doi: 10.1016/0034-5687(80)90056-0.

Trung, N. B., Nan, F.-H., Lee, M.-C., Loh, J.-Y., Gong, H.-Y., Lu, M.-W., et al. (2021). Fish-specific TLR18 in Nile tilapia (Oreochromis niloticus) recruits MyD88 and TRIF to induce expression of effectors in NF-κB and IFN pathways in melanomacrophages. *Fish Shellfish Immunol.* 119, 587–601. doi: 10.1016/j.fsi.2021.11.001.

Tsai, M.-L., Chang, K.-Y., Chiang, C.-S., Shu, W.-Y., Weng, T.-C., Chen, C. R., et al. (2009). UVB radiation induces persistent activation of ribosome and oxidative phosphorylation pathways. *Radiat. Res.* 171, 716–724. doi: 10.1667/RR1625.1.

Tukey, J. W. (1977). *Exploratory data analysis*.

UniProt Consortium (2019). UniProt: a worldwide hub of protein knowledge. *Nucleic Acids Res.* 47, D506–D515. doi: 10.1093/nar/gky1049.

v. Frisch, K. (1938). Zur Psychologie des Fisch-Schwarmes. *Naturwissenschaften* 26, 601–606. doi: 10.1007/BF01590598.

v. Frisch, K. (1942). Über einen Schreckstoff der Fischhaut und seine biologische Bedeutung. *Z. Vgl. Physiol.* 29, 46–145. doi: 10.1007/BF00304445.

van der Veen, J. N., Kennelly, J. P., Wan, S., Vance, J. E., Vance, D. E., and Jacobs, R. L. (2017). The critical role of phosphatidylcholine and phosphatidylethanolamine metabolism in health and disease. *Biochim. Biophys. Acta Biomembr.* 1859, 1558–1572. doi: 10.1016/j.bbamem.2017.04.006.

Vandesompele, J., De Preter, K., Pattyn, F., Poppe, B., Van Roy, N., De Paepe, A., et al. (2002). Accurate normalization of real-time quantitative RT-PCR data by geometric averaging of multiple internal control genes. *Genome Biol.* 3, RESEARCH0034. doi: 10.1186/gb-2002-3-7-research0034.

Vashist, S. K., and Marion Schneider, E. (2014). Editorial: Depression: An Insight and Need for Personalized Psychological Stress Monitoring and Management. *J. Basic Appl. Sci.* 10, 177–182. doi: 10.6000/1927-5129.2014.10.25.

Vasseur, D. A., DeLong, J. P., Gilbert, B., Greig, H. S., Harley, C. D. G., McCann, K. S., et al. (2014). Increased temperature variation poses a greater risk to species than climate warming. *Proc. Biol. Sci.* 281, 20132612. doi: 10.1098/rspb.2013.2612.

Vavrek, M. A., Elvidge, C. K., DeCaire, R., Belland, B., Jackson, C. D., and Brown, G. E. (2008). Disturbance cues in freshwater prey fishes: do juvenile convict cichlids and rainbow trout respond to ammonium as an 'early warning' signal? *Chemoecology* 18, 255–261. doi: 10.1007/s00049-008-0412-5.

Velez, Z., Costa, R. A., Wang, W., and Hubbard, P. C. (2021). Independent effects of seawater pH and high P CO2 on olfactory sensitivity in fish: possible role of carbonic anhydrase. *J. Exp. Biol.* 224. doi: 10.1242/jeb.238485.

Velez, Z., Hubbard, P. C., Welham, K., Hardege, J. D., Barata, E. N., and Canário, A. V. M. (2009). Identification, release and olfactory detection of bile salts in the intestinal fluid of the Senegalese sole (Solea senegalensis). *J. Comp. Physiol. A Neuroethol. Sens. Neural Behav. Physiol.* 195, 691–698. doi: 10.1007/s00359-009-0444-5.

Venables, W. N., and Ripley, B. D. (2002). Modern Applied Statistics with S. Available at: http://www.stats.ox.ac.uk/pub/MASS4.

Venuleo, M., Raven, J. A., and Giordano, M. (2017). Intraspecific chemical communication in microalgae. *New Phytol.* 215, 516–530. doi: 10.1111/nph.14524.

Vermeulen, J., Pattyn, F., De Preter, K., Vercruysse, L., Derveaux, S., Mestdagh, P., et al. (2009). External oligonucleotide standards enable cross laboratory comparison and exchange of real-time quantitative PCR data. *Nucleic Acids Res.* 37, e138. doi: 10.1093/nar/gkp721.

Villamizar, N., Vera, L. M., Foulkes, N. S., and Sánchez-Vázquez, F. J. (2014). Effect of lighting conditions on zebrafish growth and development. *Zebrafish* 11, 173–181. doi: 10.1089/zeb.2013.0926.

Vinagre, C., Madeira, D., Narciso, L., Cabral, H. N., and Diniz, M. (2012). Effect of temperature on oxidative stress in fish: Lipid peroxidation and catalase activity in the muscle of juvenile seabass, Dicentrarchus labrax. *Ecol. Indic.* 23, 274–279. doi: 10.1016/j.ecolind.2012.04.009.

Vitkovic, L., Bockaert, J., and Jacque, C. (2000). "Inflammatory" cytokines: neuromodulators in normal brain? *J. Neurochem.* 74, 457–471. doi: 10.1046/j.1471-4159.2000.740457.x.

Voicu, A., Duteanu, N., Voicu, M., Vlad, D., and Dumitrascu, V. (2020). The rcdk and cluster R packages applied to drug candidate selection. *J. Cheminform.* 12, 3. doi: 10.1186/s13321-019-0405-0.

Vougiouklakis, T., Bernard, B. J., Nigam, N., Burkitt, K., Nakamura, Y., and Saloura, V. (2020). Clinicopathologic significance of protein lysine methyltransferases in cancer. *Clin. Epigenetics* 12, 146. doi: 10.1186/s13148-020-00897-3.

Vu, V. Q. (2011). ggbiplot: A ggplot2 based biplot. Available at: http://github.com/vqv/ggbiplot.

Wage, J., Rohr, S., Hardege, J. D., and Rotchell, J. M. (2016). Short-term effects of CO2-induced low pH exposure on target gene expression in Platynereis dumerilii. *Journal of Marine Biology & Oceanography* 5, 2. doi: 10.4172/2324-8661.1000155.

Walker, S. E., and Lorsch, J. (2013). "Chapter Nineteen - RNA Purification – Precipitation Methods," in *Methods in Enzymology*, ed. J. Lorsch (Academic Press), 337–343. doi: 10.1016/B978-0-12-420037-1.00019-1.

Wan, Q.-L., Meng, X., Dai, W., Luo, Z., Wang, C., Fu, X., et al. (2021). N^6-methyldeoxyadenine and histone methylation mediate transgenerational survival advantages induced by hormetic heat stress. *Sci Adv* 7. doi: 10.1126/sciadv.abc3026.

Wang, F., Zieman, A., and Coulombe, P. A. (2016). Skin keratins. *Methods Enzymol.* 568, 303–350. doi: 10.1016/bs.mie.2015.09.032.

Wang, J. Y. (2001). DNA damage and apoptosis. *Cell Death Differ.* 8, 1047–1048. doi: 10.1038/sj.cdd.4400938.

Wang, Y., Hu, M., Wu, F., Storch, D., and Pörtner, H.-O. (2018). Elevated pCO2 affects feeding behavior and acute physiological response of the brown crab Cancer pagurus. *Front. Physiol.* 9, 1164. doi: 10.3389/fphys.2018.01164.

Wargelius, A., Fjelldal, P. G., and Hansen, T. (2005). Heat shock during early somitogenesis induces caudal vertebral column defects in Atlantic salmon (Salmo salar). *Dev. Genes Evol.* 215, 350–357. doi: 10.1007/s00427-005-0482-0.

Warren, D. T., Donelson, J. M., and McCormick, M. I. (2017). Extended exposure to elevated temperature affects escape response behaviour in coral reef fishes. *PeerJ* 5, e3652. doi: 10.7717/peerj.3652.

Watson, G. J., Hamilton, K. M., and Tuffnail, W. E. (2005). Chemical alarm signalling in the polychaete Nereis (Neanthes) virens (Sars) (Annelida: Polychaeta). *Anim. Behav.* 70, 1125–1132. doi: 10.1016/j.anbehav.2005.03.011.

Watson, S. B., Caldwell, G., and Pohnert, G. (2009). "Fatty acids and oxylipins as semiochemicals," in *Lipids in Aquatic Ecosystems*, eds. M. Kainz, M. T. Brett, and M. T. Arts (New York, NY: Springer New York), 65–92. doi: 10.1007/978-0-387-89366-2_4.

Weger, B. D., Sahinbas, M., Otto, G. W., Mracek, P., Armant, O., Dolle, D., et al. (2011). The light responsive transcriptome of the zebrafish: function and regulation. *PLoS One* 6, e17080. doi: 10.1371/journal.pone.0017080.

Wei, T., and Simko, V. (2021). R package "corrplot": Visualization of a Correlation Matrix. Available at: https://github.com/taiyun/corrplot.

Weiss, L. C., Albada, B., Becker, S. M., Meckelmann, S. W., Klein, J., Meyer, M., et al. (2018). Identification of Chaoborus kairomone chemicals that induce defences in Daphnia. *Nat. Chem. Biol.* 14, 1133–1139. doi: 10.1038/s41589-018-0164-7.

Westerfield, M. (2000). *The zebrafish book. A guide for the laboratory use of zebrafish (Danio rerio)*. http://zfin. org/zf_info/zfbook/zfbk.html.

Whitear, M. (1971). Cell specialization and sensory function in fish epidermis. *J. Zool.* 163, 237–264. doi: 10.1111/j.1469-7998.1971.tb04533.x.

Whitehouse, L. M., McDougall, C. S., Stefanovic, D. I., Boreham, D. R., Somers, C. M., Wilson, J. Y., et al. (2017). Development of the embryonic heat shock response and the impact of repeated thermal stress in early stage lake whitefish (Coregonus clupeaformis) embryos. *J. Therm. Biol.* 69, 294–301. doi: 10.1016/j.jtherbio.2017.08.013.

Whittaker, R. H., and Feeny, P. P. (1971). Allelochemics: chemical interactions between species. *Science* 171, 757–770. doi: 10.1126/science.171.3973.757.

Wickham, H. (2016). ggplot2: Elegant Graphics for Data Analysis. Available at: https://ggplot2.tidyverse.org.

Wienert, B., Nguyen, D. N., Guenther, A., Feng, S. J., Locke, M. N., Wyman, S. K., et al. (2020). Timed inhibition of CDC7 increases CRISPR-Cas9 mediated templated repair. *Nat. Commun.* 11, 2109. doi: 10.1038/s41467-020-15845-1.

Williams, A. B., and Schumacher, B. (2016). p53 in the DNA-Damage-Repair Process. *Cold Spring Harb. Perspect. Med.* 6. doi: 10.1101/cshperspect.a026070.

Williamson, P., Pörtner, H.-O., Widdicombe, S., and Gattuso, J.-P. (2021). Ideas and perspectives: When ocean acidification experiments are not the same, repeatability is not tested. *Biogeosciences* 18, 1787–1792. doi: 10.5194/bg-18-1787-2021.

Wilson, K. S., Matrone, G., Livingstone, D. E. W., Al-Dujaili, E. A. S., Mullins, J. J., Tucker, C. S., et al. (2013). Physiological roles of glucocorticoids during early embryonic development of the zebrafish (Danio rerio). *J. Physiol.* 591, 6209–6220. doi: 10.1113/jphysiol.2013.256826.

Wilson, K. S., Tucker, C. S., Al-Dujaili, E. A. S., Holmes, M. C., Hadoke, P. W. F., Kenyon, C. J., et al. (2016). Early-life glucocorticoids programme behaviour and metabolism in adulthood in zebrafish. *J. Endocrinol.* 230, 125–142. doi: 10.1530/JOE-15-0376.

Wisenden, B. (2008). Active space of chemical alarm cue in natural fish populations. *Behaviour* 145, 391–407. doi: 10.1163/156853908783402920.

Wisenden, B. D. (2019). Evidence for incipient alarm signalling in fish. *J. Anim. Ecol.* 88, 1278–1280. doi: 10.1111/1365-2656.13062.

Wisenden, B. D., Chivers, D. P., and Smith, R. J. (1995). Early warning in the predation sequence: A disturbance pheromone in Iowa darters (Etheostoma exile). *J. Chem. Ecol.* 21, 1469–1480. doi: 10.1007/BF02035146.

Wisenden, B. D., and Millard, M. C. (2001). Aquatic flatworms use chemical cues from injured conspecifics to assess predation risk and to associate risk with novel cues. *Anim. Behav.* 62, 761–766. doi: 10.1006/anbe.2001.1797.

Wisenden, B. D., Vollbrecht, K. A., and Brown, J. L. (2004). Is there a fish alarm cue? Affirming evidence from a wild study. *Anim. Behav.* 67, 59–67. doi: 10.1016/j.anbehav.2003.02.010.

Wolfe, K., Nguyen, H. D., Davey, M., and Byrne, M. (2020). Characterizing biogeochemical fluctuations in a world of extremes: A synthesis for temperate intertidal habitats in the face of global change. *Glob. Chang. Biol.* 26, 3858–3879. doi: 10.1111/gcb.15103.

Wollenberg Valero, K. C., Garcia-Porta, J., Irisarri, I., Feugere, L., Bates, A., Kirchhof, S., et al. (2021). Functional genomics of abiotic environmental adaptation in lacertid lizards and other vertebrates. *J. Anim. Ecol.* doi: 10.1111/1365-2656.13617.

Wondrak, G. T., Jacobson, M. K., and Jacobson, E. L. (2006). Endogenous UVA-photosensitizers: mediators of skin photodamage and novel targets for skin photoprotection. *Photochem. Photobiol. Sci.* 5, 215–237. doi: 10.1039/b504573h.

Wootton, H. F., Morrongiello, J. R., Schmitt, T., and Audzijonyte, A. (2022). Smaller adult fish size in warmer water is not explained by elevated metabolism. *Ecol. Lett.* doi: 10.1111/ele.13989.

Wu, X., and Hammer, J. A. (2014). Melanosome transfer: it is best to give and receive. *Curr. Opin. Cell Biol.* 29, 1–7. doi: 10.1016/j.ceb.2014.02.003.

Wyatt, T. D. (2010). Pheromones and signature mixtures: defining species-wide signals and variable cues for identity in both invertebrates and vertebrates. *J. Comp. Physiol. A Neuroethol. Sens. Neural Behav. Physiol.* 196, 685–700. doi: 10.1007/s00359-010-0564-y.

Wyatt, T. D. (2014). Proteins and peptides as pheromone signals and chemical signatures. *Anim. Behav.* 97, 273–280. doi: 10.1016/j.anbehav.2014.07.025.

Wyatt, T. D., Hardege, J. D., and Terschak, J. (2014). Ocean acidification foils chemical signals. *Science* 346, 176. doi: 10.1126/science.346.6206.176-a.

Xia, J. H., Li, H. L., Li, B. J., Gu, X. H., and Lin, H. R. (2018). Acute hypoxia stress induced abundant differential expression genes and alternative splicing events in heart of tilapia. *Gene* 639, 52–61. doi: 10.1016/j.gene.2017.10.002.

Xia, J., Peng, M., Huang, Y., and Elvidge, C. K. (2021). Acute warming in winter eliminates chemical alarm responses in threatened Qinling lenok Brachymystax lenok tsinlingensis. *Sci. Total Environ.* 764, 142807. doi: 10.1016/j.scitotenv.2020.142807.

Xie, F., Xiao, P., Chen, D., Xu, L., and Zhang, B. (2012). miRDeepFinder: a miRNA analysis tool for deep sequencing of plant small RNAs. *Plant Mol. Biol.*, 80(1), 75–84. doi: 10.1007/s11103-012-9885-2.

Xu, D., Guo, R., Sobeck, A., Bachrati, C. Z., Yang, J., Enomoto, T., et al. (2008). RMI, a new OB-fold complex essential for Bloom syndrome protein to maintain genome stability. *Genes Dev.* 22, 2843–2855. doi: 10.1101/gad.1708608.

Yang, L., Jiang, H., Wang, Y., Lei, Y., Chen, J., Sun, N., et al. (2019). Expansion of vomeronasal receptor genes (OlfC) in the evolution of fright reaction in Ostariophysan fishes. *Commun. Biol.* 2, 235. doi: 10.1038/s42003-019-0479-2.

Yao, C., Du, W., Chen, H., Xiao, S., Huang, L., and Chen, F.-P. (2015). Involvement of Fanconi anemia genes FANCD2 and FANCF in the molecular basis of drug resistance in leukemia. *Mol. Med. Rep.* 11, 4605–4610. doi: 10.3892/mmr.2015.3288.

Yao, Y., Danna, C. H., Zemp, F. J., Titov, V., Ciftci, O. N., Przybylski, R., et al. (2011). UV-C-irradiated Arabidopsis and tobacco emit volatiles that trigger genomic instability in neighboring plants. *Plant Cell* 23, 3842–3852. doi: 10.1105/tpc.111.089003.

Yokogawa, T., Iadarola, M., and Burgess, H. (2014). Thermal response behaviors in larval zebrafish: startle escape, thermotaxis and thermal arousal. *Measuring Behavior 2014*.

Yoneya, K., and Takabayashi, J. (2014). Plant–plant communication mediated by airborne signals: ecological and plant physiological perspectives. *Plant Biotechnol.* 31, 409–416. doi: 10.5511/plantbiotechnology.14.0827a.

Yonezawa, D., Sekiguchi, F., Miyamoto, M., Taniguchi, E., Honjo, M., Masuko, T., et al. (2007). A protective role of hydrogen sulfide against oxidative stress in rat gastric mucosal epithelium. *Toxicology* 241, 11–18. doi: 10.1016/j.tox.2007.07.020.

Yost, R. T., Liang, E., Stewart, M. P., Chui, S., Greco, A. F., Long, S. Q., et al. (2021). Drosophila melanogaster Stress Odorant (dSO) Displays the Characteristics of an Interspecific Alarm Cue. *J. Chem. Ecol.* doi: 10.1007/s10886-021-01300-y.

Younus, H. (2018). Therapeutic potentials of superoxide dismutase. *Int. J. Health Sci. (Qassim)* 12, 88–93. Available at: https://www.ncbi.nlm.nih.gov/pubmed/29896077.

Yu, G., and He, Q.-Y. (2016). ReactomePA: an R/Bioconductor package for reactome pathway analysis and visualization. *Molecular BioSystems* 12, 477–479. doi: 10.1039/C5MB00663E.

Yu, G., Wang, L.-G., Han, Y., and He, Q.-Y. (2012). clusterProfiler: an R package for comparing biological themes among gene clusters. *OMICS: A Journal of Integrative Biology* 16, 284–287. doi: 10.1089/omi.2011.0118.

Yuan, J. S., Himanen, S. J., Holopainen, J. K., Chen, F., and Stewart, C. N., Jr (2009). Smelling global climate change: mitigation of function for plant volatile organic compounds. *Trends Ecol. Evol.* 24, 323–331. doi: 10.1016/j.tree.2009.01.012.

Zagarese, H. E., and Williamson, C. E. (2001). The implications of solar UV radiation exposure for fish and fisheries. *Fish Fish* 2, 250–260. doi: 10.1046/j.1467-2960.2001.00048.x.

Zahangir, M. M., Haque, F., Mustakim, G. M., Khatun, H., and Islam, M. S. (2015). Effect of water pH on the early developmental responses in zebrafish (Danio rerio). doi: 10.3329/pa.v26i1.24521.

Zaksauskaite, R., Thomas, R. C., van Eeden, F., and El-Khamisy, S. F. (2021). Tdp1 protects from topoisomerase 1-mediated chromosomal breaks in adult zebrafish but is dispensable during larval development. *Sci Adv* 7. doi: 10.1126/sciadv.abc4165.

Zdobnov, E. M., Kuznetsov, D., Tegenfeldt, F., Manni, M., Berkeley, M., and Kriventseva, E. V. (2021). OrthoDB in 2020: evolutionary and functional annotations of orthologs. *Nucleic Acids Res.* 49, D389–D393. doi: 10.1093/nar/gkaa1009.

Zeebe, R. E. (2012). History of seawater carbonate chemistry, atmospheric CO2, and ocean acidification. *Annu. Rev. Earth Planet. Sci.* 40, 141–165. doi: 10.1146/annurev-earth-042711-105521.

Zeeck, E., Hardege, J., Bartels-Hardege, H., and Wesselmann, G. (1988). Sex pheromone in a marine polychaete: Determination of the chemical structure. *J. Exp. Zool.* 246, 285–292. doi: 10.1002/jez.1402460308.

Zeileis, A., and Hothorn, T. (2002). Diagnostic Checking in Regression Relationships. Available at: https://CRAN.R-project.org/doc/Rnews/ [Accessed October 19, 2021].

Zhang, Q., Kopp, M., Babiak, I., and Fernandes, J. M. O. (2018). Low incubation temperature during early development negatively affects survival and related innate immune processes in zebrafish larvae exposed to lipopolysaccharide. *Sci. Rep.* 8, 4142. doi: 10.1038/s41598-018-22288-8.

Zhang, Z., Sakuma, A., Kuraku, S., and Nikaido, M. (2022). Remarkable diversity of vomeronasal type 2 receptor (OlfC) genes of basal ray-finned fish and its evolutionary trajectory in jawed vertebrates. *Sci. Rep.* 12, 6455. doi: 10.1038/s41598-022-10428-0.

Zhang, Z., Zhang, Q., Dexheimer, T. S., Ren, J., Neubig, R. R., and Li, W. (2020). Two highly related odorant receptors specifically detect α-bile acid pheromones in sea lamprey (Petromyzon marinus). *J. Biol. Chem.* 295, 12153–12166. doi: 10.1074/jbc.RA119.011532.

Zhao, X.-X., Zhang, Y.-B., Ni, P.-L., Wu, Z.-L., Yan, Y.-C., and Li, Y.-P. (2016). Protein Arginine Methyltransferase 6 (Prmt6) Is Essential for Early Zebrafish Development through the Direct Suppression of gadd45αa Stress Sensor Gene. *J. Biol. Chem.* 291, 402–412. doi: 10.1074/jbc.M115.666347.

Zhou, J. J., Huang, Y., Zhang, X., Cheng, Y., Tang, L., and Ma, X. (2017). Eyes absent gene (EYA1) is a pathogenic driver and a therapeutic target for melanoma. *Oncotarget* 8, 105081–105092. doi: 10.18632/oncotarget.21352.

Zhuang, Z., Xu, L., Yang, J., Gao, H., Zhang, L., Gao, X., et al. (2020). Weighted Single-Step Genome-Wide Association Study for Growth Traits in Chinese Simmental Beef Cattle. *Genes* 11. doi: 10.3390/genes11020189.

Zimme-Faust, R. K., and Tamburri, M. N. (1994). Chemical identity and ecological implications of a waterborne, larval settlement cue. *Limnol. Oceanogr.* 39, 1075–1087. doi: 10.4319/lo.1994.39.5.1075.

Ziosi, M., Di Meo, I., Kleiner, G., Gao, X.-H., Barca, E., Sanchez-Quintero, M. J., et al. (2017). Coenzyme Q deficiency causes impairment of the sulfide oxidation pathway. *EMBO Mol. Med.* 9, 96–111. doi: 10.15252/emmm.201606356.

Zuo, Z.-J., Zhu, Y.-R., Bai, Y.-L., and Wang, Y. (2012). Volatile communication between Chlamydomonas reinhardtii cells under salt stress. *Biochem. Syst. Ecol.* 40, 19–24. doi: 10.1016/j.bse.2011.09.007.

Appendix 1 Supplementary Information to Chapter 2

Table Appendix 1 S1. Summary of conditions for behavioural assays. Tested species included small hermit crab *Diogenes pugilator*, green shore crab *Carcinus maenas*, harbour ragworm *Hediste diversicolor*, and gilt-head sea bream *Sparus aurata*. Factors were: pH drop (0 for control pH, pH = 8.1 *vs.* 1 for pH drop, pH = 7.6), stress metabolites (0 for control metabolites putatively released at pH = 8.1 *vs.* 1 for stress metabolites putatively released at pH = 7.6), and donor (conspecific, or heterospecific i.e., *S. aurata*. Conditioned water from *S. aurata* (except stated otherwise) and *H. diversicolor* was tenfold diluted in the system water at the desired pH. *n* represents the sample size. *pCO_2 (in µatm) as calculated using the CO2calc software and based on dilutions in system water. pH is given in the NBS scale.

Treatment	Donor	Recipient	Donor factor	pH drop	SM	pH adjustment	Dilution	pCO2*	n
Factorial design									
CM	*D. pugilator*	*D. pugilator*	Conspecific	0	0	-	-	537	40
pH drop	*D. pugilator*	*D. pugilator*	Conspecific	1	0	HCl addition to CM conditioned water	-	537	40
SM	*D. pugilator*	*D. pugilator*	Conspecific	0	1	Reef buffer addition to SM conditioned water	-	1922	40
pH drop+SM	*D. pugilator*	*D. pugilator*	Conspecific	1	1	-	-	1922	40
CM	*S. aurata*	*D. pugilator*	Heterospecific	0	0	CM conditioned water diluted in pH = 8.1 system water	10-fold	537	40
pH drop	*S. aurata*	*D. pugilator*	Heterospecific	1	0	CM conditioned water diluted in pH = 7.6 system water	10-fold	1783.5	40
SM	*S. aurata*	*D. pugilator*	Heterospecific	0	1	SM conditioned water diluted in pH = 8.1 system water	10-fold	675.5	40
pH drop+SM	*S. aurata*	*D. pugilator*	Heterospecific	1	1	SM conditioned water diluted in pH = 7.6 system water	10-fold	1922	40
CM	*C. maenas*	*C. maenas*	Conspecific	0	0	-	-	537	29
pH drop	*C. maenas*	*C. maenas*	Conspecific	1	0	HCl addition to CM conditioned water	-	537	20
SM	*C. maenas*	*C. maenas*	Conspecific	0	1	Reef buffer addition to SM conditioned water	-	1922	35
pH drop+SM	*C. maenas*	*C. maenas*	Conspecific	1	1	-	-	1922	35
CM	*S. aurata*	*C. maenas*	Heterospecific	0	0	CM conditioned water diluted in pH = 8.1 system water	10-fold	537	16
pH drop	*S. aurata*	*C. maenas*	Heterospecific	1	0	CM conditioned water diluted in pH = 7.6 system water	10-fold	1783.5	17
SM	*S. aurata*	*C. maenas*	Heterospecific	0	1	SM conditioned water diluted in pH = 8.1 system water	10-fold	675.5	20
pH drop+SM	*S. aurata*	*C. maenas*	Heterospecific	1	1	SM conditioned water diluted in pH = 7.6 system water	10-fold	1922	18

Table Appendix 1 S1. Continued.

Treatment	Donor	Recipient	Donor factor	pH drop	SM	pH adjustment	Dilution	pCO2*	n
CM	*H. diversicolor*	*H. diversicolor*	Conspecific	0	0	CM conditioned water diluted in pH = 8.1 system water	10-fold	537	45
pH drop	*H. diversicolor*	*H. diversicolor*	Conspecific	1	0	CM conditioned water diluted in pH = 7.6 system water	10-fold	1783.5	27
SM	*H. diversicolor*	*H. diversicolor*	Conspecific	0	1	SM conditioned water diluted in pH = 8.1 system water	10-fold	675.5	27
pH drop+SM	*H. diversicolor*	*H. diversicolor*	Conspecific	1	1	SM conditioned water diluted in pH = 7.6 system water	10-fold	1922	45
CM	*S. aurata*	*H. diversicolor*	Heterospecific	0	0	CM conditioned water diluted in pH = 8.1 system water	10-fold	537	45
pH drop	*S. aurata*	*H. diversicolor*	Heterospecific	1	0	CM conditioned water diluted in pH = 7.6 system water	10-fold	1783.5	45
SM	*S. aurata*	*H. diversicolor*	Heterospecific	0	1	SM conditioned water diluted in pH = 8.1 system water	10-fold	675.5	46
pH drop+SM	*S. aurata*	*H. diversicolor*	Heterospecific	1	1	SM conditioned water diluted in pH = 7.6 system water	10-fold	1922	45
Additional treatments									
CM100%	*S. aurata*	*H. diversicolor*	Heterospecific	0	0	-	-	537	45
CM100%	*S. aurata*	*D. pugilator*	Heterospecific	0	0	-	-	537	40

Table Appendix 1 S2. Model selection for time-to-success analysis. Covariates were dropped from Cox proportional hazard models when two analyses of the three model selection analyses showed evidence for their negligible effect compared to the model only including the main terms (pH drop × SM × Donor). [1]Crab size not recorded in 2018 data. Ranks show the best fitting models when considering all three model selection methods. P means P (> |Chisq|). AIC and BIC are Akaike and Bayesian Information criterion, respectively. ΔA/BICc: Delta compared to first-ranked model. LL: log-likelihood.

Terms	Rank	χ^2	p	AICc	ΔAICc	BIC	ΔBICc	LL
D. pugilator								
pH × SM × Donor	1	13.32	0.0646	1333.9	0.36	1359.9	0.00	-659.8
pH × SM × Donor + Water	2	2.47	0.1163	1333.5	0.00	1363.2	3.30	-658.5
pH × SM × Donor + Water + Size	3	0.23	0.6318	1335.4	1.89	1368.7	8.84	-658.4
C. maenas								
pH × SM × Donor	1	18.85	0.0087	1170.8	0.00	1192.8	0.00	-578.1
pH × SM × Donor + Water	2	0.26	0.6104	1172.7	1.92	1197.8	4.98	-577.9
pH × SM × Donor + Water + Year	3	0.93	0.3348	1173.9	3.20	1202.1	9.29	-577.5
pH × SM × Donor (2019)[1]	-	15.66	0.0284	821.9	0.00	842.1	0.00	-403.6
pH × SM × Donor + Size (2019)[1]	-	0.00	0.9995	824.1	2.23	847.1	5.00	-403.6
H. diversicolor								
pH × SM × Donor	1	34.62	< 0.0001	2451.5	0.00	2477.7	0.00	-1218.6
pH × SM × Donor + Water	2	1.24	0.2649	2452.4	0.86	2482.2	4.54	-1217.9

Table Appendix 1 S3. Model selection for avoidance analysis (GLM). Covariates were dropped from models when two analyses of the three model selection analyses showed evidence for their negligible effect compared to the model only including the main terms (pH drop × SM × Donor). [1]Missing condition forced to create two sub-models for *H. diversicolor*. Ranks show the best fitting models when considering all three model selection methods. P means P (> $|\chi^2|$). AIC and BIC are Akaike and Bayesian Information criterion, respectively. ΔA/BICc: Delta compared to first-ranked model. LL: log-likelihood.

Terms	Rank	Deviance	p	AICc	ΔAICc	BIC	ΔBICc	LL
D. pugilator								
pH × SM × Donor	1	65.4	< 0.0001	393.9	0.00	423.6	0.00	-188.7
pH × SM × Donor + Water	2	0.28	0.5963	395.8	1.84	429.1	5.49	-188.6
pH × SM × Donor + Water + Size	3	0.01	0.9158	397.9	3.96	434.9	11.24	-188.6
C. maenas								
pH × SM × Donor	2	141.5	< 0.0001	158.6	1.84	181.7	0.00	-70.8
pH × SM × Donor + Water	1	137.4	0.0429	156.7	0.00	182.6	0.92	-68.7
pH × SM × Donor + Water + Size	3	136.2	0.2710	157.8	1.08	186.4	4.72	-68.1
H. diversicolor[1]								
Donor	2	19.2	< 0.0001	316.5	34.81	323.5	31.32	-156.2
Donor + Water	1	36.9	< 0.0001	281.7	0.00	292.2	0.00	-137.8
H. diversicolor/*H. diversicolor*								
Treatment	1	28.8	< 0.0001	77.1	0.00	84.7	0.00	-35.4
Treatment + Water	2	0.12	0.7291	79.2	2.05	83.1	4.48	-35.4

Table Appendix 1 S4. Post-hoc tests of survival analysis in *D. pugilator*. Results of post-hoc pairwise comparisons of interest from the interaction term between the three main predictors (pH drop, stress metabolites, donor) of the Cox proportional hazard model on the time-to-success analysis in small hermit crab (*Diogenes pugilator*) receiving metabolites from conspecifics (*D. pugilator*) or heterospecific gilt-head sea bream (*Sparus aurata*). Post-hoc tests are split into two terms expressed as '(pH drop:stress metabolites)|donor' and 'donor|(pH drop:stress metabolites)', respectively comparing the four treatments (CM, pH drop, SM, and pH drop+SM) within each donor group and comparing the donor effect within each treatment (CM, pH drop, SM, or pH drop+SM). Events are the success to find a feeding cue in 300 seconds. Unsuccessful animals are censored. Significance ($p \leq 0.05$) is shown in bold. Results are expressed on the log (not the response) scale. SE: standard error of estimate. P-values are adjusted using false discovery rate adjustment for the number of comparisons within each post-hoc term. CM: control metabolites tested in control pH (pH = 8.1), pH drop: control metabolites tested in pH drop (pH = 7.6), SM: stress metabolites tested in control pH (pH = 8.1), pH drop+SM: stress metabolites tested in pH drop (pH = 7.6).

Post-hoc Term	Group	Comparison	Estimate	SE	Z	p-adj
(pH drop:SM)|donor	*D. pugilator*	CM - pH drop	0.7546	0.3530	2.1378	0.1952
(pH drop:SM)|donor	*D. pugilator*	CM - SM	0.2100	0.3167	0.6631	0.6030
(pH drop:SM)|donor	*D. pugilator*	CM - pH drop+SM	0.3836	0.3263	1.1756	0.4710
(pH drop:SM)|donor	*D. pugilator*	pH drop - SM	-0.5447	0.3601	-1.5127	0.3911
(pH drop:SM)|donor	*D. pugilator*	pH drop - pH drop+SM	-0.3710	0.3685	-1.0068	0.4710
(pH drop:SM)|donor	*D. pugilator*	SM - pH drop+SM	0.1736	0.3339	0.5201	0.6030
(pH drop:SM)|donor	*S. aurata*	CM - pH drop	-0.4345	0.4141	-1.0493	0.7898
(pH drop:SM)|donor	*S. aurata*	CM - SM	-0.1934	0.4282	-0.4518	0.7898
(pH drop:SM)|donor	*S. aurata*	CM - pH drop+SM	-0.3338	0.4141	-0.8060	0.7898
(pH drop:SM)|donor	*S. aurata*	pH drop - SM	0.2411	0.3934	0.6127	0.7898
(pH drop:SM)|donor	*S. aurata*	pH drop - pH drop+SM	0.1007	0.3780	0.2665	0.7898
(pH drop:SM)|donor	*S. aurata*	SM - pH drop+SM	-0.1403	0.3934	-0.3566	0.7898
donor|(pH drop:SM)	CM	***S. aurata* - *D. pugilator***	**1.0613**	0.3843	2.7613	**0.0230**
donor|(pH drop:SM)	pH drop	*S. aurata* - *D. pugilator*	-0.1279	0.3852	-0.3320	0.7399
donor|(pH drop:SM)	SM	*S. aurata* - *D. pugilator*	0.6578	0.3689	1.7833	0.1491
donor|(pH drop:SM)	pH drop+SM	*S. aurata* - *D. pugilator*	0.3439	0.3610	0.9527	0.4544

Table Appendix 1 S5. Post-hoc tests of avoidance behaviour in *D. pugilator*. Results of post-hoc pairwise comparisons of interest from the interaction term between the three main predictors (pH drop, stress metabolites, donor) of the binomial generalised linear model on the avoidance behaviour (including freezing and escaping) in small hermit crab (*Diogenes pugilator*) receiving metabolites from conspecifics (*D. pugilator*) or heterospecific gilt-head sea bream (*Sparus aurata*). Post-hoc tests are split into two terms expressed as '(pH drop:stress metabolites)|donor' and 'donor|(pH drop:stress metabolites)', respectively comparing the four treatments (CM, pH drop, SM, and pH drop+SM) within each donor group and comparing the donor effect within each treatment (CM, pH drop, SM, or pH drop+SM). Significance ($P \leq 0.05$) is shown in bold. Results are expressed on the log (not the response) scale. SE: standard error of estimate. P-values are adjusted using false discovery rate adjustment for the number of comparisons within each post-hoc term. CM: control metabolites tested in control pH (pH = 8.1), pH drop: control metabolites tested in pH drop (pH = 7.6), SM: stress metabolites tested in control pH (pH = 8.1), pH drop+SM: stress metabolites tested in pH drop (pH = 7.6).

Post-hoc Term	Group	Comparison	Estimate	SE	Z	p-adj
(pH drop:SM)|donor	*D. pugilator*	CM - pH drop	-0.1221	0.4944	-0.2470	0.8049
(pH drop:SM)|donor	*D. pugilator*	CM - SM	0.1292	0.5086	0.2540	0.8049
(pH drop:SM)|donor	*D. pugilator*	CM - pH drop+SM	0.2674	0.5184	0.5157	0.8049
(pH drop:SM)|donor	*D. pugilator*	pH drop - SM	0.2513	0.5024	0.5003	0.8049
(pH drop:SM)|donor	*D. pugilator*	pH drop - pH drop+SM	0.3895	0.5123	0.7603	0.8049
(pH drop:SM)|donor	*D. pugilator*	SM - pH drop+SM	0.1382	0.5260	0.2626	0.8049
(pH drop:SM)|donor	*S. aurata*	CM - pH drop	-0.8979	0.4841	-1.8549	0.1908
(pH drop:SM)|donor	*S. aurata*	CM - SM	-0.89879	0.4841	-1.8549	0.1908
(pH drop:SM)|donor	*S. aurata*	CM - pH drop+SM	-0.6466	0.4691	-1.3784	0.3361
(pH drop:SM)|donor	*S. aurata*	pH drop - SM	0.0000	0.5164	0.0000	1.0000
(pH drop:SM)|donor	*S. aurata*	pH drop - pH drop+SM	0.2513	0.5024	0.5003	0.7403
(pH drop:SM)|donor	*S. aurata*	SM - pH drop+SM	0.2513	0.5024	0.5003	0.7403
donor|(pH drop:SM)	CM	***S. aurata* - *D. pugilator***	**-1.1701**	0.4758	-2.4591	**0.0139**
donor|(pH drop:SM)	pH drop	***S. aurata* - *D. pugilator***	**-1.9459**	0.5024	-3.8734	**0.0001**
donor|(pH drop:SM)	SM	***S. aurata* - *D. pugilator***	**-2.1972**	0.5164	-4.2549	**0.0001**
donor|(pH drop:SM)	pH drop+SM	***S. aurata* - *D. pugilator***	**-2.0841**	0.5123	-4.0683	**0.0001**

Table Appendix 1 S6. Summary of GLM of freezing behaviour in *D. pugilator*. Results of binomial generalised linear model for the main effects of predictors (pH drop, stress metabolites, donor) on the freezing behaviour in small hermit crab (*Diogenes pugilator*). Significance ($p \leq 0.05$) of predictors is shown in bold. Sample size: 320 observations. Overall significance of models from Chi-squared analyses of deviance when including only predictors was $p < 0.0001$. Covariates were dropped from the model after an analysis of deviance showed that they passed the Chi-squared test (number of water uses: $p = 0.4922$, crab size: $p = 0.4224$). SE is the standard error of estimate.

Predictor	Estimate	SE	Z	p
(Intercept)	-0.9694	0.3541	-2.7376	0.0062
pH drop	0.0000	0.5008	0.0000	1.0000
stress metabolites	-0.2674	0.5184	-0.5157	0.6060
donor	**1.1701**	0.4758	2.4591	**0.0139**
pH drop:stress metabolites	-0.3138	0.7532	-0.4167	0.6769
pH:donor	-0.5030	0.6739	-0.7464	0.4554
stress metabolites:donor	0.2674	0.6861	0.3897	0.6968
pH:stress metabolites:donor	1.0216	0.9878	1.0342	0.3011

Table Appendix 1 S7. Post-hoc tests of freezing behaviour in *D. pugilator*. Results of post-hoc pairwise comparisons of interest from the interaction term between the three main predictors (pH drop, stress metabolites, donor) of the binomial generalised linear model on the freezing behaviour in small hermit crab (*Diogenes pugilator*) receiving metabolites from conspecifics (*D. pugilator*) or heterospecific gilt-head sea bream (*Sparus aurata*). Post-hoc tests are split into two terms expressed as '(pH drop:stress metabolites)|donor' and 'donor|(pH drop:stress metabolites)', respectively comparing the four treatments (CM, pH drop, SM, and pH drop+SM) within each donor group and comparing the donor effect within each treatment (CM, pH drop, SM, or pH drop+SM). Significance ($p \leq 0.05$) is shown in bold. Results are expressed on the log (not the response) scale. SE: standard error of estimate. P-values are adjusted using false discovery rate adjustment for the number of comparisons within each post-hoc term. CM: control metabolites tested in control pH (pH = 8.1), pH drop: control metabolites tested in pH drop (pH = 7.6), SM: stress metabolites tested in control pH (pH = 8.1), pH drop+SM: stress metabolites tested in pH drop (pH = 7.6).

Post-hoc Term	Group	Comparison	Estimate	SE	Z	p-adj
(pH drop:SM)|donor	*D. pugilator*	CM - pH drop	0.0000	0.5008	0.0000	1.0000
(pH drop:SM)|donor	*D. pugilator*	CM - SM	0.2674	0.5184	0.5157	0.7273
(pH drop:SM)|donor	*D. pugilator*	CM - pH drop+SM	0.5812	0.5464	1.0637	0.7273
(pH drop:SM)|donor	*D. pugilator*	pH drop - SM	0.2674	0.5184	0.5157	0.7273
(pH drop:SM)|donor	*D. pugilator*	pH drop - pH drop+SM	0.5812	0.5464	1.0637	0.7273
(pH drop:SM)|donor	*D. pugilator*	SM - pH drop+SM	0.3138	0.5626	0.5578	0.7273
(pH drop:SM)|donor	*S. aurata*	CM - pH drop	0.5030	0.4509	1.1154	0.5293
(pH drop:SM)|donor	*S. aurata*	CM - SM	0.0000	0.4495	0.0000	1.0000
(pH drop:SM)|donor	*S. aurata*	CM - pH drop+SM	-0.2048	0.4530	-0.4521	0.7814
(pH drop:SM)|donor	*S. aurata*	pH drop - SM	-0.5030	0.4509	-1.1154	0.5293
(pH drop:SM)|donor	*S. aurata*	pH drop - pH drop+SM	-0.7077	0.4544	-1.5576	0.5293
(pH drop:SM)|donor	*S. aurata*	SM - pH drop+SM	-0.2048	0.4530	-0.4521	0.7814
donor|(pH drop:SM)	CM	***S. aurata* - *D. pugilator***	**-1.1701**	0.4758	-2.4591	**0.0186**
donor|(pH drop:SM)	pH drop	*S. aurata* - *D. pugilator*	-0.6671	0.4772	-1.3981	0.1621
donor|(pH drop:SM)	SM	***S. aurata* - *D. pugilator***	**-1.4374**	0.4943	-2.9077	**0.0073**
donor|(pH drop:SM)	pH drop+SM	***S. aurata* - *D. pugilator***	**-1.9561**	0.5266	-3.7144	**0.0008**

Table Appendix 1 S8. Summary of GLM of escaping behaviour in *D. pugilator*. Results of binomial generalised linear model for the main effects of predictors (pH drop, stress metabolites, donor) on the escaping behaviour in small hermit crab (*Diogenes pugilator*). Significance ($p \leq 0.05$) is shown in bold. Sample size: 320 observations. Overall significance of models from Chi-squared analyses of deviance when including only predictors was $p < 0.0001$. Covariates were dropped from the model after an analysis of deviance showed that they passed the Chi-squared test (number of water uses: $p = 0.06588$). SE is the standard error of estimate.

Predictor	Estimate	SE	Z	p
(Intercept)	-22.2371	1017.9837	-0.0218	0.9826
pH drop	14.9973	1017.9831	0.0147	0.9882
stress metabolites	14.9756	1017.9831	0.0147	0.9883
donor	15.7622	1017.9828	0.0155	0.9876
crab size	**1.0409**	0.4188	2.4854	**0.0129**
pH drop:stress metabolites	-14.1749	1017.9839	-0.0139	0.9889
pH drop:donor	-12.4512	1017.9834	-0.0122	0.9902
stress metabolites:donor	-13.2210	1017.9834	-0.0130	0.9896
pH drop:stress metabolites:donor	11.4587	1017.9843	0.0113	0.9910

Table Appendix 1 S9. Post-hoc tests of escaping behaviour in *D. pugilator*. Results of post-hoc pairwise comparisons of interest from the interaction term between the three main predictors (pH drop, stress metabolites, donor) of the binomial generalised linear model on the escaping behaviour in small hermit crab (*Diogenes pugilator*) receiving metabolites from conspecifics (*D. pugilator*) or heterospecific gilt-head sea bream (*Sparus aurata*). Post-hoc tests are split into two terms expressed as '(pH drop:stress metabolites)|donor' and 'donor|(pH drop:stress metabolites)', respectively comparing the four treatments (CM, pH drop, SM, and pH drop+SM) within each donor group and comparing the donor effect within each treatment (CM, pH drop, SM, or pH drop+SM). Significance ($p \leq 0.05$) is shown in bold. Results are expressed on the log (not the response) scale. SE: standard error of estimate. P-values are adjusted using false discovery rate adjustment for the number of comparisons within each post-hoc term. CM: control metabolites tested in control pH (pH = 8.1), pH drop: control metabolites tested in pH drop (pH = 7.6), SM: stress metabolites tested in control pH (pH = 8.1), pH drop+SM: stress metabolites tested in pH drop (pH = 7.6).

Post-hoc Term	Subset	Comparison	Estimate	SE	Z	p-adj
(pH drop:SM)|donor	*D. pugilator*	CM - pH drop	-14.9973	1017.98	-0.0147	0.9883
(pH drop:SM)|donor	*D. pugilator*	CM - SM	-14.9756	1017.98	-0.0147	0.9883
(pH drop:SM)|donor	*D. pugilator*	CM - pH drop+SM	-15.7981	1017.98	-0.0155	0.9883
(pH drop:SM)|donor	*D. pugilator*	pH drop - SM	0.0218	1.4376	0.0154	0.9883
(pH drop:SM)|donor	*D. pugilator*	pH drop - pH drop+SM	-0.8007	1.2518	-0.6397	0.9883
(pH drop:SM)|donor	*D. pugilator*	SM - pH drop+SM	-0.8225	1.2535	-0.6561	0.9883
(pH drop:SM)|donor	*S. aurata*	**CM - pH drop**	**-2.5461**	0.8025	-3.1726	**0.0091**
(pH drop:SM)|donor	*S. aurata*	CM - SM	-1.7546	0.8196	-2.1408	0.0969
(pH drop:SM)|donor	*S. aurata*	CM - pH drop+SM	-1.5845	0.8357	-1.8982	0.0982
(pH drop:SM)|donor	*S. aurata*	pH drop - SM	0.7915	0.5003	1.5820	0.1364
(pH drop:SM)|donor	*S. aurata*	pH drop - pH drop+SM	0.9616	0.5220	1.8423	0.0982
(pH drop:SM)|donor	*S. aurata*	SM - pH drop+SM	0.1701	0.5503	0.3091	0.7573
donor|(pH drop:SM)	CM	*S. aurata* - *D. pugilator*	-15.7622	1017.98	-0.0155	0.9876
donor|(pH drop:SM)	pH drop	***S. aurata* - *D. pugilator***	**-3.3110**	1.0701	-3.0940	**0.0079**
donor|(pH drop:SM)	SM	***S. aurata* - *D. pugilator***	**-2.5412**	1.0836	-2.3452	**0.0380**
donor|(pH drop:SM)	pH drop+SM	*S. aurata* - *D. pugilator*	-1.5486	0.8345	-1.8545	0.0849

Table Appendix 1 S10. Post-hoc tests of survival analysis in *C. maenas*. Results of post-hoc pairwise comparisons of interest from the interaction term between the three main predictors (pH drop, stress metabolites, donor) of the Cox proportional hazard model on the time-to-success analysis in green shore crab (*Carcinus maenas*) receiving metabolites from conspecifics (*C. maenas*) or heterospecific gilt-head sea bream (*Sparus aurata*). Post-hoc tests are split into two terms expressed as '(pH drop:stress metabolites)|donor' and 'donor|(pH drop:stress metabolites)', respectively comparing the four treatments (CM, pH drop, SM, and pH drop+SM) within each donor group and comparing the donor effect within each treatment (CM, pH drop, SM, or pH drop+SM). Events are the success to find a feeding cue in 300 seconds. Unsuccessful animals are censored. Significance ($p \leq 0.05$) is shown in bold. Results are expressed on the log (not the response) scale. SE: standard error of estimate. P-values are adjusted using false discovery rate adjustment for the number of comparisons within each post-hoc term. CM: control metabolites tested in control pH (pH = 8.1), pH drop: control metabolites tested in pH drop (pH = 7.6), SM: stress metabolites tested in control pH (pH = 8.1), pH drop+SM: stress metabolites tested in pH drop (pH = 7.6).

Post-hoc Term	Group	Comparison	Estimate	SE	Z	p-adj
(pH drop:SM)|donor	*C. maenas*	CM - pH drop	0.2890	0.3620	0.7982	0.5987
(pH drop:SM)|donor	*C. maenas*	CM - SM	-0.1953	0.2887	-0.6762	0.5987
(pH drop:SM)|donor	*C. maenas*	CM - pH drop+SM	0.2359	0.3089	0.7639	0.5987
(pH drop:SM)|donor	*C. maenas*	pH drop - SM	-0.4842	0.3452	-1.4027	0.4821
(pH drop:SM)|donor	*C. maenas*	pH drop - pH drop+SM	-0.0530	0.3619	-0.1466	0.8835
(pH drop:SM)|donor	*C. maenas*	SM - pH drop+SM	0.4312	0.2890	1.4922	0.4821
(pH drop:SM)|donor	*S. aurata*	**CM - pH drop**	**1.5374**	0.5177	2.9694	**0.0179**
(pH drop:SM)|donor	*S. aurata*	**CM - SM**	**1.0150**	0.4092	2.4804	**0.0394**
(pH drop:SM)|donor	*S. aurata*	CM - pH drop+SM	0.8983	0.4092	2.1950	0.0563
(pH drop:SM)|donor	*S. aurata*	pH drop - SM	-0.5224	0.5478	-0.9536	0.4084
(pH drop:SM)|donor	*S. aurata*	pH drop - pH drop+SM	-0.6391	0.5478	-1.1666	0.3650
(pH drop:SM)|donor	*S. aurata*	SM - pH drop+SM	-0.1167	0.4472	-0.2609	0.7941
donor|(pH drop:SM)	CM	*S. aurata* - *C. maenas*	-0.3678	0.3385	-1.0865	0.3697
donor|(pH drop:SM)	pH drop	*S. aurata* - *C. maenas*	0.8806	0.5326	1.6535	0.1965
donor|(pH drop:SM)	SM	*S. aurata* - *C. maenas*	0.8425	0.3687	2.2850	0.0893
donor|(pH drop:SM)	pH drop+SM	*S. aurata* - *C. maenas*	0.2945	0.3843	0.7665	0.4434

Table Appendix 1 S11. Post-hoc tests of avoidance behaviour in *C. maenas*. Results of post-hoc pairwise comparisons of interest from the interaction term between the three main predictors (pH, metabolites, donor) of the binomial generalised linear model on the avoidance behaviour (including freezing and escaping) in green shore crab (*Carcinus maenas*) receiving metabolites from conspecifics (*C. maenas*) or heterospecific gilt-head sea bream (*Sparus aurata*). Post-hoc tests are split into two terms expressed as '(pH drop:stress metabolites)|donor' and 'donor|(pH drop:stress metabolites)', respectively comparing the four treatments (CM, pH drop, SM, and pH drop+SM) within each donor group and comparing the donor effect within each treatment (CM, pH drop, SM, or pH drop+SM). Significance ($p \leq 0.05$) is shown in bold. Results are expressed on the log (not the response) scale. SE: standard error of estimate. P-values are adjusted using false discovery rate adjustment for the number of comparisons within each post-hoc term. CM: control metabolites tested in control pH (pH = 8.1), pH drop: control metabolites tested in pH drop (pH = 7.6), SM: stress metabolites tested in control pH (pH = 8.1), pH drop+SM: stress metabolites tested in pH drop (pH = 7.6).

Post-hoc Term	Group	Comparison	Estimate	SE	Z	p-adj
(pH drop:SM)|donor	*C. maenas*	CM-pH drop	1.1263	0.9173	1.2279	0.3292
(pH drop:SM)|donor	*C. maenas*	CM-SM	1.1263	0.9173	1.2279	0.3292
(pH drop:SM)|donor	*C. maenas*	CM-pH drop+SM	0.0000	0.7429	0.0000	1.0000
(pH drop:SM)|donor	*C. maenas*	pH drop-SM	0.0000	1.0628	0.0000	1.0000
(pH drop:SM)|donor	*C. maenas*	pH drop-pH drop+SM	1.1263	0.9173	1.2279	0.3292
(pH drop:SM)|donor	*C. maenas*	SM-pH drop+SM	1.1263	0.9173	1.2279	0.3292
(pH drop:SM)|donor	*S. aurata*	**CM-pH drop**	**-4.4288**	1.2325	-3.5933	**0.0020**
(pH drop:SM)|donor	*S. aurata*	**CM-SM**	**-2.7536**	0.8402	-3.2773	**0.0031**
(pH drop:SM)|donor	*S. aurata*	**CM-pH drop+SM**	**-1.8936**	0.8141	-2.3259	**0.0400**
(pH drop:SM)|donor	*S. aurata*	pH drop-SM	1.6752	1.1639	1.4393	0.1801
(pH drop:SM)|donor	*S. aurata*	pH drop-pH drop+SM	**2.5352**	1.1465	2.2112	**0.0405**
(pH drop:SM)|donor	*S. aurata*	SM-pH drop+SM	0.8600	0.7148	1.2031	0.2289
donor|(pH drop:SM)	CM	*S. aurata - C. maenas*	0.4626	0.8326	0.5556	0.5785
donor|(pH drop:SM)	pH drop	***S. aurata - C. maenas***	**-5.0925**	1.2919	-3.9417	**0.0003**
donor|(pH drop:SM)	SM	***S. aurata - C. maenas***	**-3.4173**	0.9249	-3.6949	**0.0004**
donor|(pH drop:SM)	pH drop+SM	*S. aurata - C. maenas*	-1.4310	0.7197	-1.9882	0.0624

Table Appendix 1 S12. Summary of GLM of freezing behaviour in *C. maenas*. Results of binomial generalised linear model for the main effects of predictors (pH drop, stress metabolites, donor) on the freezing behaviour in green shore crab (*Carcinus maenas*). Significance ($p \leq 0.05$) of is shown in bold. Sample size: 320 observations. Overall significance of models from Chi-squared analyses of deviance when including only predictors was p = 0.009. Covariates were dropped from the model after an analysis of deviance showed that they passed the Chi-squared test (number of water uses: p = 0.8469, crab size: p = 0.0798). SE: standard error of estimate.

Predictor	Estimate	SE	Z	p
(Intercept)	-1.3863	0.5590	-2.4799	0.0131
pH drop	-0.8109	0.9317	-0.8704	0.3841
stress metabolites	-1.5581	1.1683	-1.3336	0.1823
donor	-0.6286	0.9376	-0.6704	0.5026
pH drop:stress metabolites	2.6568	1.4789	1.7964	0.0724
pH drop:donor	**2.8258**	1.2980	2.1771	**0.0295**
stress metabolites:donor	2.7257	1.4730	1.8505	0.0642
pH drop:stress metabolites:donor	**-4.0475**	1.8620	-2.1738	**0.0297**

Table Appendix 1 S13. Post-hoc tests of freezing behaviour in *C. maenas*. Results of post-hoc pairwise comparisons of interest from the interaction term between the three main predictors (pH drop, stress metabolites, donor) of the binomial generalised linear model on the freezing behaviour in green shore crab (*Carcinus maenas*) receiving metabolites from conspecifics (*C. maenas*) or heterospecific gilt-head sea bream (*Sparus aurata*). Post-hoc tests are split into two terms expressed as '(pH drop:stress metabolites)|donor' and 'donor|(pH drop:stress metabolites)', respectively comparing the four treatments (CM, pH drop, SM, and pH drop+SM) within each donor group and comparing the donor effect within each treatment (CM, pH drop, SM, or pH drop+SM). Significance ($p \leq 0.05$) is shown in bold. Results are expressed on the log (not the response) scale. SE: standard error of estimate. P-values are adjusted using false discovery rate adjustment for the number of comparisons within each post-hoc term. CM: control metabolites tested in control pH (pH = 8.1), pH drop: control metabolites tested in pH drop (pH = 7.6), SM: stress metabolites tested in control pH (pH = 8.1), pH drop+SM: stress metabolites tested in pH drop (pH = 7.6).

Post-hoc Term	Group	Comparison	Estimate	SE	Z	p-adj
(pH drop:SM)|donor	*C. maenas*	CM-pH drop	0.8109	0.9317	0.8704	0.5761
(pH drop:SM)|donor	*C. maenas*	CM-SM	1.5581	1.1683	1.3336	0.4514
(pH drop:SM)|donor	*C. maenas*	CM-pH drop+SM	-0.2877	0.7610	-0.3780	0.7054
(pH drop:SM)|donor	*C. maenas*	pH drop-SM	0.7472	1.2681	0.5892	0.6668
(pH drop:SM)|donor	*C. maenas*	pH drop-pH drop+SM	-1.0986	0.9068	-1.2116	0.4514
(pH drop:SM)|donor	*C. maenas*	SM-pH drop+SM	-1.8458	1.1486	-1.6074	0.4514
(pH drop:SM)|donor	*S. aurata*	CM-pH drop	-2.0149	0.9037	-2.2396	0.1321
(pH drop:SM)|donor	*S. aurata*	CM-SM	-1.1676	0.8974	-1.3016	0.3378
(pH drop:SM)|donor	*S. aurata*	CM-pH drop+SM	-1.7918	0.8898	-2.0138	0.1331
(pH drop:SM)|donor	*S. aurata*	pH drop-SM	0.8573	0.6986	1.2128	0.3378
(pH drop:SM)|donor	*S. aurata*	pH drop-pH drop+SM	0.2231	0.6892	0.3238	0.7461
(pH drop:SM)|donor	*S. aurata*	SM-pH drop+SM	-0.6242	0.6805	-0.9182	0.4309
donor|(pH drop:SM)	CM	*S. aurata* - *C. maenas*	0.6286	0.9376	0.6704	0.5026
donor|(pH drop:SM)	pH drop	*S. aurata* - *C. maenas*	-2.1972	0.8975	-2.4481	0.0574
donor|(pH drop:SM)	SM	*S. aurata* - *C. maenas*	-2.0971	1.1361	-1.8460	0.1298
donor|(pH drop:SM)	pH drop+SM	*S. aurata* - *C. maenas*	-0.8755	0.7012	-1.2485	0.2824

Table Appendix 1 S14. Summary of GLM of escaping behaviour in *C. maenas*. Results of binomial generalised linear model for the main effects of predictors (pH drop, stress metabolites, donor) on the escaping behaviour in green shore crab (*Carcinus maenas*). Significance ($p \leq 0.05$) is shown in bold. Sample size: 151 observations. Overall significance of models from Chi-squared analyses of deviance when including only predictors was $p < 0.0001$. Covariates were dropped from the model after an analysis of deviance showed that they passed the Chi-squared test (number of water uses: $p = 0.2393$, crab size: $p = 0.3273$). SE is the standard error of estimate.

Predictor	Estimate	SE	Z	p
(Intercept)	-2.1972	0.7454	-2.9479	0.0032
pH drop	-17.3688	2404.6705	-0.0072	0.9942
stress metabolites	0.0000	1.0541	0.0000	1.0000
donor	-0.5754	1.2720	-0.4523	0.6510
pH drop:stress metabolites	0.0000	3400.7177	0.0000	1.0000
pH drop:donor	21.6078	2404.6708	0.0090	0.9928
stress metabolites:donor	**3.1781**	1.5434	2.0592	**0.0395**
pH drop:stress metabolites:donor	-5.5999	3400.7179	-0.0016	0.9987

Table Appendix 1 S15. Post-hoc tests of escaping behaviour in *C. maenas*. Results of post-hoc pairwise comparisons of interest from the interaction term between the three main predictors (pH drop, stress metabolites, donor) of the binomial generalised linear model on the escaping behaviour in green shore crab (*Carcinus maenas*) receiving metabolites from conspecifics (*C. maenas*) or heterospecific gilt-head sea bream (*Sparus aurata*). Post-hoc tests are split into two terms expressed as '(pH drop:stress metabolites)|donor' and 'donor|(pH drop:stress metabolites)', respectively comparing the four treatments (CM, pH drop, SM, and pH drop+SM) within each donor group and comparing the donor effect within each treatment (CM, pH drop, SM, or pH drop+SM). Significance ($p \leq 0.05$) is shown in bold. Results are expressed on the log (not the response) scale. SE: standard error of estimate. P-values are adjusted using false discovery rate adjustment for the number of comparisons within each post-hoc term. Comparisons were calculated using the *emmeans* R package (Lenth, 2021) on the generalised linear model computed via the *stats* R package (R Core Team, 2020). CM: control metabolites tested in control pH (pH = 8.1), pH drop: control metabolites tested in pH drop (pH = 7.6), SM: stress metabolites tested in control pH (pH = 8.1), pH drop+SM: stress metabolites tested in pH drop (pH = 7.6).

Post-hoc Term	Subset	Comparison	Estimate	SE	Z	p-adj
(pH drop:SM)|donor	*C. maenas*	CM - pH drop	17.3688	2404.67	0.0072	1.0000
(pH drop:SM)|donor	*C. maenas*	CM - SM	0.0000	1.0541	0.0000	1.0000
(pH drop:SM)|donor	*C. maenas*	CM - pH drop+SM	17.3688	2404.67	0.0072	1.0000
(pH drop:SM)|donor	*C. maenas*	pH drop - SM	-17.3688	2404.67	-0.0072	1.0000
(pH drop:SM)|donor	*C. maenas*	pH drop - pH drop+SM	0.0000	3400.718	0.0000	1.0000
(pH drop:SM)|donor	*C. maenas*	SM - pH drop+SM	17.3688	2404.67	0.0072	1.0000
(pH drop:SM)|donor	*S. aurata*	**CM - pH drop**	**-4.2389**	1.2136	-3.4929	**0.0029**
(pH drop:SM)|donor	*S. aurata*	**CM - SM**	**-3.1781**	1.1273	-2.8191	**0.0096**
(pH drop:SM)|donor	*S. aurata*	CM - pH drop+SM	-1.8171	1.1573	-1.5701	0.1397
(pH drop:SM)|donor	*S. aurata*	pH drop - SM	1.0609	0.7865	1.3488	0.1774
(pH drop:SM)|donor	*S. aurata*	**pH drop - pH drop+SM**	**2.4218**	0.8290	2.9215	**0.0096**
(pH drop:SM)|donor	*S. aurata*	SM - pH drop+SM	1.3610	0.6966	1.9537	0.0761
donor|(pH drop:SM)	CM	*S. aurata* - *C. maenas*	0.5754	1.2720	0.4523	0.9938
donor|(pH drop:SM)	pH drop	*S. aurata* - *C. maenas*	-21.0324	2404.67	-0.0087	0.9938
donor|(pH drop:SM)	SM	***S. aurata* - *C. maenas***	**-2.6027**	0.8740	-2.9779	**0.0116**
donor|(pH drop:SM)	pH drop+SM	*S. aurata* - *C. maenas*	-18.6106	2404.67	-0.0077	0.9938

Table Appendix 1 S16. Post-hoc tests of survival analysis in *H. diversicolor*. Results of post-hoc pairwise comparisons of interest from the interaction term between the three main predictors (pH, metabolites, donor) of the Cox proportional hazard model on the time-to-success analysis in harbour ragworm (*Hediste diversicolor*) receiving metabolites from conspecifics (*H. diversicolor*) or heterospecific gilt-head sea bream (*Sparus aurata*). Post-hoc tests are split into two terms expressed as '(pH drop:stress metabolites)|donor' and 'donor|(pH drop:stress metabolites)', respectively comparing the four treatments (CM, pH drop, SM, and pH drop+SM) within each donor group and comparing the donor effect within each treatment (CM, pH drop, SM, or pH drop+SM). Events are the success to completely burrow the head in the sand in 300 seconds. Significance ($p \leq 0.05$) is shown in bold. Results are expressed on the log (not the response) scale. SE: standard error of estimate. P-values are adjusted using false discovery rate adjustment for the number of comparisons within each post-hoc term. CM: control metabolites tested in control pH (pH = 8.1), pH drop: control metabolites tested in pH drop (pH = 7.6), SM: stress metabolites tested in control pH (pH = 8.1), pH drop+SM: stress metabolites tested in pH drop (pH = 7.6).

Post-hoc Term	Group	Comparison	Estimate	SE	Z	p-adj
(pH drop:SM)|donor	*H. diversicolor*	**CM - pH drop**	**1.1899**	0.3045	3.9075	**0.0006**
(pH drop:SM)|donor	*H. diversicolor*	**CM - SM**	**1.0442**	0.3049	3.4251	**0.0012**
(pH drop:SM)|donor	*H. diversicolor*	**CM - pH drop+SM**	**0.8500**	0.2453	3.4652	**0.0012**
(pH drop:SM)|donor	*H. diversicolor*	pH drop - SM	-0.1456	0.3652	-0.3988	0.6900
(pH drop:SM)|donor	*H. diversicolor*	pH drop - pH drop+SM	-0.3399	0.3181	-1.0684	0.4280
(pH drop:SM)|donor	*H. diversicolor*	SM - pH drop+SM	-0.1943	0.3182	-0.6104	0.6499
(pH drop:SM)|donor	*S. aurata*	CM - pH drop	0.2869	0.2315	1.2392	0.2583
(pH drop:SM)|donor	*S. aurata*	CM - SM	0.4951	0.2317	2.1365	0.0653
(pH drop:SM)|donor	*S. aurata*	**CM - pH drop+SM**	**0.8714**	0.2605	3.3452	**0.0049**
(pH drop:SM)|donor	*S. aurata*	pH drop - SM	0.2082	0.2358	0.8828	0.3773
(pH drop:SM)|donor	*S. aurata*	pH drop - pH drop+SM	0.5845	0.2639	2.2151	0.0653
(pH drop:SM)|donor	*S. aurata*	SM - pH drop+SM	0.3763	0.2639	1.4261	0.2308
donor|(pH drop:SM)	CM	*S. aurata* - *H. diversicolor*	0.3616	0.2258	1.6013	0.2186
donor|(pH drop:SM)	pH drop	*S. aurata* - *H. diversicolor*	-0.5413	0.3076	-1.7598	0.2186
donor|(pH drop:SM)	SM	*S. aurata* - *H. diversicolor*	-0.1875	0.3079	-0.6090	0.5425
donor|(pH drop:SM)	pH drop+SM	*S. aurata* - *H. diversicolor*	0.3831	0.2761	1.3876	0.2204

Table Appendix 1 S17. Post-hoc tests of avoidance behaviours in *H. diversicolor*. Results of post-hoc pairwise comparisons of interest from the interaction term between the main predictors (pH drop, stress metabolites) of the binomial generalised linear model on the avoidance behaviour (including freezing, curling, flipping, and slime secretion) in harbour ragworm (*Hediste diversicolor*) receiving metabolites from conspecifics (*H. diversicolor*) or heterospecific gilt-head sea bream (*Sparus aurata*). Due to missing observations in conspecific control metabolites at control pH (CM) treatment, the model was built only for treatments SM, pH drop, and pH drop+SM allowing for post-hoc comparisons between those three treatments. In the *S. aurata* group, the model included the interactive effects of pH drop and stress metabolites allowing for post-hoc comparisons between the four treatments (CM, SM, pH drop, pH drop+SM). Significance ($p \leq 0.05$) is shown in bold. Results are expressed on the log (not the response) scale. SE: standard error of estimate. P-values are adjusted using false discovery rate adjustment for the number of comparisons within each post-hoc term. CM: control metabolites tested in control pH (pH = 8.1), pH drop: control metabolites tested in pH drop (pH = 7.6), SM: stress metabolites tested in control pH (pH = 8.1), pH drop+SM: stress metabolites tested in pH drop (pH = 7.6).

Post-hoc Term	Group	Comparison	Estimate	SE	Z	p-adj
Treatment	*H. diversicolor*	pH drop - pH drop+SM	18.8729	1603.1137	0.0118	0.9906
Treatment	*H. diversicolor*	pH drop - SM	-0.3185	0.5658	-0.5629	0.9906
Treatment	*H. diversicolor*	pH drop+SM - SM	-19.1914	1603.1137	-0.0120	0.9906
pH drop:SM	*S. aurata*	CM - pH drop	18.8729	1603.1137	0.0120	0.9906
pH drop:SM	*S. aurata*	**CM - SM**	**-3.3557**	0.7788	-4.3086	**0.0001**
pH drop:SM	*S. aurata*	CM - pH drop+SM	-0.7376	0.5822	-1.2670	0.4103
pH drop:SM	*S. aurata*	pH drop - SM	-22.2287	1603.1137	-0.0139	0.9906
pH drop:SM	*S. aurata*	pH drop - pH drop+SM	-19.6105	1603.1136	-0.0122	0.9906
pH drop:SM	*S. aurata*	**SM - pH drop+SM**	**2.6181**	0.6675	3.9225	**0.0003**

Table Appendix 1 S18. Summary of survival analysis compared to CM100%. Results of post-hoc pairwise comparisons from Cox proportional hazard models on the time-to-success analysis in small hermit crab (*Diogenes pugilator*) (model 1) and harbour ragworm (*Hediste diversicolor*) (model 2) receiving metabolites from heterospecific gilt-head sea bream (*Sparus aurata*). Events are the success to find a feeding cue in *D. pugilator* or to burrow the head in *H. diversicolor* in 300 seconds. Unsuccessful animals are censored. Significance ($p \leq 0.05$) is shown in bold. Overall significance of models from Chi-squared analyses of deviance were: *D. pugilator*: p = 0.8503; *H. diversicolor*: p = 0.0137. Covariates were dropped from the model after an analysis of deviance showed that they passed the Chi-squared test both in model 1 (number of water uses: p = 0.4551, crab size: p = 0.7333) and model 2 (number of water uses: p = 0.7566). Results are expressed on the log (not the response) scale. SE: standard error of estimate. P-values are adjusted using false discovery rate adjustment for the number of pairwise comparisons in each species. Comparisons were calculated using the *emmeans* R package (Lenth, 2021) on the Cox proportional hazard model computed via the *survival* R package (Therneau and Grambsch, 2000; Therneau, 2021). CM100%: undiluted control metabolites tested in control pH (pH = 8.1), CM: tenfold diluted control metabolites tested in control pH (pH = 8.1), SM: tenfold diluted stress metabolites tested in control pH (pH = 8.1).

Species	Comparison	Success ratio	Estimate	SE	Z	p-adj
D. pugilator	CM-CM100%	0.97	0.0285	0.4472	0.0638	0.9492
	CM-SM	0.97	-0.1943	0.4282	-0.4538	0.9492
	CM100%-SM	1.21	-0.2228	0.4282	-0.5203	0.9492
H. diversicolor	CM-CM100%	1.04	-0.0407	0.2244	-0.1812	0.8562
	CM-SM	**1.04**	0.5511	0.2314	2.3714	**0.0266**
	CM100%-SM	**0.58**	0.5917	0.2291	2.5828	**0.0266**

Table Appendix 1 S19. Summary of avoidance behaviours compared to CM100%. Results of post-hoc pairwise comparisons from binomial generalised linear models on the escaping behaviour (model 1) in small hermit crab (*Diogenes pugilator*) and the avoidance behaviour (including freezing, curling, flipping, and slime secretion) (model 2) in harbour ragworm (*Hediste diversicolor*) receiving metabolites from heterospecific gilt-head sea bream (*Sparus aurata*). Significance ($p \leq 0.05$) is shown in bold. Overall significance of models from Chi-squared analyses of deviance were: *D. pugilator*: $p = 0.0078$; *H. diversicolor*: $p < 0.0001$. Covariates were dropped from the model after an analysis of deviance showed that they passed the Chi-squared test both in model 1 (number of water uses: $p = 0.5274$, crab size: $p = 0.0983$) and model 2 (number of water uses: $p = 0.4201$). Results are expressed on the log (not the response) scale. SE: standard error of estimate. P-values are adjusted using false discovery rate adjustment for the number of pairwise comparisons in each species. CM100%: undiluted control metabolites tested in control pH (pH = 8.1), CM: tenfold diluted control metabolites tested in control pH (pH = 8.1), SM: tenfold diluted stress metabolites tested in control pH (pH = 8.1).

Species	Comparison	Estimate	SE	Z	p-adj
D. pugilator	CM-CM100%	0.0000	1.0260	0.0000	1.0000
	CM-SM	**-1.8458**	0.8122	-2.2728	**0.0346**
	CM100%-SM	**-1.8458**	0.8122	-2.2728	**0.0346**
H. diversicolor	CM-CM100%	0.8383	0.6341	1.3222	0.1861
	CM-SM	**-3.3557**	0.7787	-4.3087	< **0.0001**
	CM100%-SM	**-4.1941**	0.7132	-5.8809	< **0.0001**

Table Appendix 1 S20. Validation of estimates through bootstrapping on subsets. One-sample z-tests comparing the term estimate for the Cox proportional hazard model for the entire statistical population versus 100 random subsets of 50% of the data. For both the full dataset and each individual subset, the formula of the Cox proportional hazard model was pH drop × SM × Donor. Only the three main terms are represented: pH drop, SM, and donor. The analysis was done for each tested species: small hermit crab *Diogenes pugilator,* green shore crab *Carcinus maenas,* and harbour ragworm *Hediste diversicolor.* SM: Stress Metabolites.

Species	z (pH drop)	p (pH drop)	z (SM)	p (SM)	z (Donor)	p (Donor)
D. pugilator	0.1453	0.8844	1.3974	0.1623	-1.7732	0.0762
C. maenas	-0.9165	0.3594	-0.2577	0.7966	-0.0190	0.9848
H. diversicolor	-1.6457	0.0998	0.3297	0.7416	-0.3167	0.7515

Appendix 2 Supplementary Information to Chapter 3

Table Appendix 2 S1. Treatments for Chapter 3 Zebrafish embryos (*Danio rerio*) in treatments for 24 hours starting approx. 2.75 hrs post fertilisation**.** The design aimed to investigate the effects of fluctuating thermal stress and stress medium excreted by stressed embryos. In addition, control embryos were incubated at 27°C for different incubation times starting approx. 2.75 hrs post fertilisation. Hpf: hours post fertilisation. The final behavioural dataset contained 405 observations (C: n = 57; CM: n = 67; TS: n = 90; SM: n = 34; TS+SM: n = 56; C31: n = 32; C37: n = 32; C46: n = 37). Gene expression analysis was conducted on CM, C, SM, TS, TS+SM with 3 samples containing 60 embryos per treatment.

Treatments	Detail
Control (C)	Incubation at 27°C starting 3.3 hpf for 24 hrs (from 11 am at day 1 to 11 am at day 2) in the dark. Incubation in fresh 1X E3 medium. Endpoints: qPCR, behaviour, growth, and cortisol.
Control Medium (CM)	Incubation at 27°C starting 3.3 hpf for 24 hrs (from 11 am at day 1 to 11 am at day 2) in the dark. Incubation in reused 1X E3 medium, in which an embryo from the C treatment was exposed beforehand and containing putative control metabolites. Endpoints: qPCR, behaviour, and growth.
Thermal Stress (TS)	Incubation in thermal stress treatment starting 3.3 hpf for 24 hrs (from 11 am at day 1 to 11 am at day 2) in the dark. Thermal stress spanned 16.25 hrs, divided into thirteen 75-min series of temperature fluctuations between 27, 29, 32, 29, and 27°C, with each temperature step being maintained for 15 min. Incubation in fresh 1X E3 medium. Endpoints: qPCR, behaviour, growth, and cortisol.
Stress Medium (SM)	Incubation at 27°C starting 3.3 hpf for 24 hrs (from 11 am at day 1 to 11 am at day 2) in the dark. Incubation in reused 1X E3 medium, in which an embryo from the TS treatment was exposed beforehand and containing putative stress medium. Endpoints: qPCR, behaviour, growth, and cortisol.
Thermal Stress + Stress Medium (TS+SM)	Incubation in thermal stress treatment starting 3.3 hpf for 24 hrs (from 11 am at day 1 to 11 am at day 2) in the dark. Incubation in reused 1X E3 medium, in which an embryo from the TS treatment was exposed beforehand and containing putative stress medium. Endpoints: qPCR, behaviour, growth, and cortisol.
C31, C37, and C46	Incubation at 27°C from 3.3 hpf to 25 hpf (reached after approx. 31 hrs, prim-6), 31 hpf (reached after approx. 37 hrs, prim-16), or 35-42 hpf (reached after approx. 46 hrs, late pharyngula) in the dark. Exposure in fresh 1X E3 medium. Endpoints: behaviour and growth.

Table Appendix 2 S2. Thermal stress and stress medium accelerate the growth index of zebrafish embryos. A two-way ANOVA was used to test the effects of the predictors (thermal stress and stress medium) on changes in growth index. Pairwise Student's tests with Bonferroni adjustments compare all treatments to C and SM to CM. Effect size (Cohen's |d|) is interpreted following Sawilowsky (2009). C: control (n = 57), SM: stress medium (n = 34), TS: thermal stress (n = 90), TS+SM: thermal stress + stress medium (*n* = 56), CM: control medium (n = 67). Significant terms ($p < 0.05$) are shown in bold.

Terms	Statistic	p	Effect size |d|	interpretation
Stress Medium	F = 6.291	**0.0128**	0.29	**small**
Thermal Stress	F = 75.502	**0.0001**	1.14	**large**
Thermal Stress × Stress Medium	F = 7.498	**0.0067**	1.27	**very large**
Pairwise comparisons				
C-SM	T = -3.6784	**0.0012**	0.75	**medium**
C-TS	T = -7.9874	**0.0001**	1.42	**very large**
C-TS+SM	T = -7.2413	**0.0001**	1.36	**very large**
C-CM	T = 2.3472	**0.0418**	0.43	**small**
SM-CM	T = -6.7215	**0.0001**	1.45	**very large**

Table Appendix 2 S3. Thermal stress and stress medium advance the final stage (hours post fertilisation) of 1-dpf zebrafish embryos. A two-way Scheirer-Ray-Hare test was used to test the effects of predictors (thermal stress and stress medium) across C, SM, TS, and TS+SM. Pairwise Wilcoxon-Mann-Whitney's tests with Bonferroni adjustments compared all treatments to C and SM to CM. Effects of clutch median initial stages across all treatments were analysed with a Kruskal-Wallis' test whereas correlation with final stage was estimated with a Spearman's test. Effect size (Cohen's |d|) is interpreted following Sawilowsky (2009). Significant terms ($p < 0.05$) are shown in bold. C: control (n = 57), SM: stress medium (n = 34), TS: thermal stress (n = 90), TS+SM: thermal stress + stress medium (n = 56), CM: control medium (n = 67).

Terms	Statistic	p	Effect size |d|	Interpretation
Stress Medium	H = 1.221	0.2693	0.10	very small
Thermal Stress	H = 71.096	**0.0001**	1.23	**very large**
Thermal Stress × Stress Medium	H = 6.074	**0.0137**	1.25	**very large**
Pairwise comparisons	Statistic	p	Effect size |d|	Interpretation
C-SM	W = 611.5	**0.0056**	0.56	**medium**
C-TS	W = 766.5	**0.0001**	1.42	**very large**
C-TS+SM	W = 526.5	**0.0001**	1.34	**very large**
C-CM	W = 1893	1.000	0.07	very small
SM-CM	W = 699	**0.0015**	0.75	**medium**
Covariate	Kruskal-Wallis' test terms		Spearman's test terms	
Initial stage	$\chi^2 = 104.59$, **$p < 0.0001$**		$\rho = 0.25$, **$p < 0.0001$**	

Table Appendix 2 S4. Effects of thermal stress and stress medium shift the final stage period of 1-dpf zebrafish embryos. Final stages were expressed as binary embryonic periods (segmentation or pharyngula). A generalised linear model for logistic regression was tested the effects of (i) thermal stress and medium predictors across C, SM, TS, and TS+SM, and (ii) embryo clutch median initial stages across all treatments. Pairwise tests with Bonferroni adjustments compared all treatments to C and SM to CM. Effect size (Cohen's |d|) is interpreted following Sawilowsky (2009). Significant terms ($p < 0.05$) are shown in bold. CM: control medium (n = 67), C: control (n = 57), SM: stress medium (n = 34), TS: thermal stress (n = 90), TS+SM: thermal stress + stress medium (n = 56).

Terms	Estimates	SE	Z statistic	p
Stress Medium	-1.5092	0.4637	-3.255	**0.0011**
Thermal Stress	-3.3569	0.4771	-7.035	**0.0001**
Thermal Stress × Stress Medium	2.0447	0.7057	2.897	**0.0038**
Pairwise comparisons				
C-SM	-1.51	0.464	-3.255	**0.0034**
C-TS	-3.36	0.477	-7.035	**0.0001**
C-TS+SM	-2.82	0.486	-5.804	**0.0001**
C-CM	-0.05	0.411	-0.120	1.000
SM-CM	1.56	0.451	3.456	**0.001**
Covariate				
Initial stage	-0.4056	0.1609	-2.5211	**0.0117**

Table Appendix 2 S5. Thermal stress and stress medium lower burst activity % of 1-dpf zebrafish embryos. A two-way Scheirer-Ray-Hare test was used to test the effects of the predictors (thermal stress and stress medium) on burst activity % across treatments. Pairwise Wilcoxon-Mann-Whitney's tests with Bonferroni adjustments compared all treatments to C and SM to CM. Spearman's correlation tests tested the confounding effects of covariates (clutch median initial stage, individual final stage expressed as hours post fertilisation, hpf, or growth index) on burst activity %. Effect size (Cohen's |d|) is interpreted following Sawilowsky (2009). Significant terms ($p < 0.05$) are shown in bold. CM: control medium (n = 67), C: control (n = 57), SM: stress medium (n = 34), TS: thermal stress (n = 90), TS+SM: thermal stress + stress medium (n = 56).

Terms	Statistic	p	Effect size |d|	Interpretation
Stress Medium	H = 9.3222	**0.0023**	0.49	**small**
Thermal Stress	H = 17.0080	**0.0001**	0.55	**medium**
Thermal Stress × Stress Medium	H = 1.8193	0.1774	0.99	large
Pairwise comparisons				
C-SM	W = 1387	**0.0018**	0.81	**large**
C-TS	W = 3548	**0.0003**	0.68	**medium**
C-TS+SM	W = 2455	**0.0001**	1.04	**large**
C-CM	W = 3287	**0.0001**	1.64	**very large**
SM-CM	W = 1745	**0.0001**	1.05	**large**
Covariates				
Initial stage	$\rho = -0.33$	**0.0001**	-	-
Final stage (in hpf)	$\rho = -0.08$	0.1627	-	-
Growth index	$\rho = 0.04$	0.5027	-	-

Table Appendix 2 S6. Burst activity % lowers with time in control zebrafish embryos. Embryos were raised at a control temperature of 27°C starting approx. 2.75 hrs post fertilisation for 24 hrs (C, n = 57), 31 hrs (C31, n = 32), 37 hrs (C37, n = 32), and 46 hrs (C46, n = 37). A Kruskal-Wallis test evaluated the effects of incubation times in control embryos. Pairwise Wilcoxon-Mann-Whitney's tests with Bonferroni adjustments were used to compare C31, C37, and C46 to C; and stressed embryos (SM, TS, TS+SM) to stage-matched controls (C31). Effect size (Cohen's |d|) is interpreted following Sawilowsky (2009). Significant terms ($p < 0.05$) are shown in bold. SM: stress medium (n = 34), TS: thermal stress (n = 90), TS+SM: thermal stress + stress medium (n = 56).

Term	Statistic	p	Effect size |d|	Interpretation
Incubation time	$\chi^2 = 99.639$	**0.0001**	-	-
	$\rho = -0.70$	**0.0001**	-	-
Pairwise comparisons				
C-C31	W = 1762	**0.0001**	2.37	**huge**
C-C37	W = 1775	**0.0001**	2.41	**huge**
C-C46	W = 2065	**0.0001**	2.59	**huge**
Stressed vs stage-matched control				
C31-SM	W = 37	**0.0001**	2.63	**huge**
C31-TS	W = 146	**0.0001**	1.64	**very large**
C31-TS+SM	W = 96	**0.0001**	1.75	**very large**

Table Appendix 2 S7. Thermal stress increases protein level of heat shock protein 70 (HSP70) in 1-dpf zebrafish embryos. A two-way Scheirer-Ray-Hare test was used to compute the effect of predictors on HSP70 levels across all treatments. Sample size was n = 3 biological replicates (each containing 20 embryos) per treatment, except in C (n = 2) where one significant table-wide outlier was detected by a Grubbs' test. Effect size (Cohen's |d|) is interpreted following Sawilowsky (2009). Significant terms ($p < 0.05$) are shown in bold. C: control, SM: stress medium, TS: thermal stress, TS+SM: thermal stress + stress medium, C31: control at 31 hours reaching the stage of prim-6 reached by stressed embryos. Embryos in C, TS, SM, and TS+SM were exposed to treatments for 24 hours.

Model terms	H statistic	p	Effect size |d|	Interpretation
Stress Medium	0.8595	0.3539	0.21	small
Thermal Stress	4.8167	**0.0282**	1.33	**very large**
Thermal Stress × Stress Medium	0.2305	0.6312	1.54	very large

Table Appendix 2 S8. Neither thermal stress nor stress medium alter cortisol levels in 1-dpf zebrafish embryos. A two-way Scheirer-Ray-Hare model tested the effects of predictors on cortisol levels across all treatments (n = 3 biological replicates, each containing 20 embryos, per treatment). Effect size (Cohen's |d|) is interpreted following Sawilowsky (2009). Significant terms ($p < 0.05$) are shown in bold. C: control, SM: stress medium, TS: thermal stress, TS+SM: thermal stress + stress medium.

Model terms	H statistic	P	|d|	Effect size
Stress Medium	0.0066	0.9350	0.42	small
Thermal Stress	0.0266	0.8705	0.18	very small
Thermal Stress × Stress Medium	0.5380	0.4632	0.65	medium

Table Appendix 2 S9. Effect of thermal stress and stress medium on the gene expression of 1-dpf zebrafish embryos. CM: control medium, C: control, SM: stress medium, TS: thermal stress, TS+SM: thermal stress + stress medium. Pairwise tests of treatments were computed via moderated t-tests (t-statistic), corrected for multiple using the *limma* R package. Treatments (SM, TS, TS+SM) were compared to control C. Additionally, CM was compared to C and SM. Sample size was n = 3 biological replicates (each containing 60 embryos) per treatment. Effect size (Cohen's |d|) is interpreted following Sawilowsky (2009). Significant terms ($p < 0.05$) are shown in bold.

Pairwise comparisons	t	B	p	Effect size |d|	Interpretation
il-1β					
C-SM	1.60	-4.50	0.393	1.24	very large
C-TS	0.75	-5.63	1.00	0.82	large
C-TS+SM	2.37	-3.48	0.097	1.51	very large
C-CM	1.02	-5.77	0.639	0.89	large
SM-CM	2.62	-3.068	**0.034**	1.82	**very large**
sod1					
C-SM	1.59	-4.51	0.401	1.03	large
C-TS	2.76	-2.93	**0.045**	1.78	**very large**
C-TS+SM	1.69	-4.45	0.336	1.03	large
C-CM	-3.78	-0.992	**0.003**	2.20	**huge**
SM-CM	-2.64	-3.05	**0.034**	1.94	**very large**
sqor					
C-SM	-2.22	-3.67	0.13	2.09	huge
C-TS	-0.19	-5.89	1.00	0.19	very small
C-TS+SM	-2.36	-3.49	0.098	3.22	huge
CM-C	-0.62	-6.09	1.00	0.77	medium
CM-SM	-2.20	-3.80	0.08	2.34	huge

Appendix 3 Supplementary Information to Chapter 4

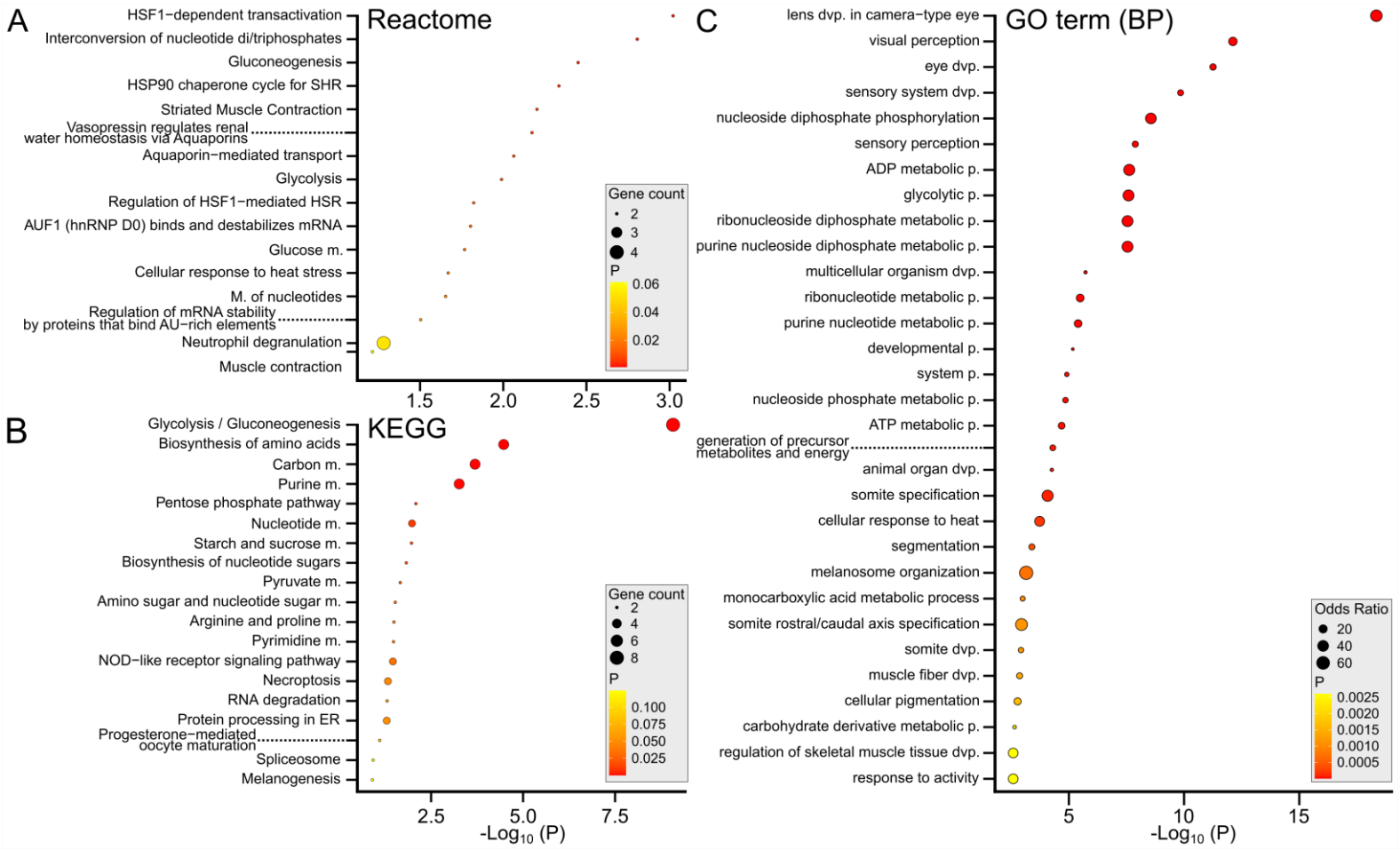

Figure Appendix 3 S1. Heat stress alters important transcriptome pathways in zebrafish embryos. Functional enrichment of (A) KEGG pathways, (B) Reactome pathways, and (C) Biological Processes (BP) gene ontology (GO) terms of differentially expressed genes in thermal stress (TS) compared to C. All represented terms have ≥ 2 gene counts and are ranked by decreasing significance. Abbreviations: m: metabolism, dvp: development, ER: endoplasmic reticulum, HSR: heat shock response, p: process, SHR: steroid hormone receptor.

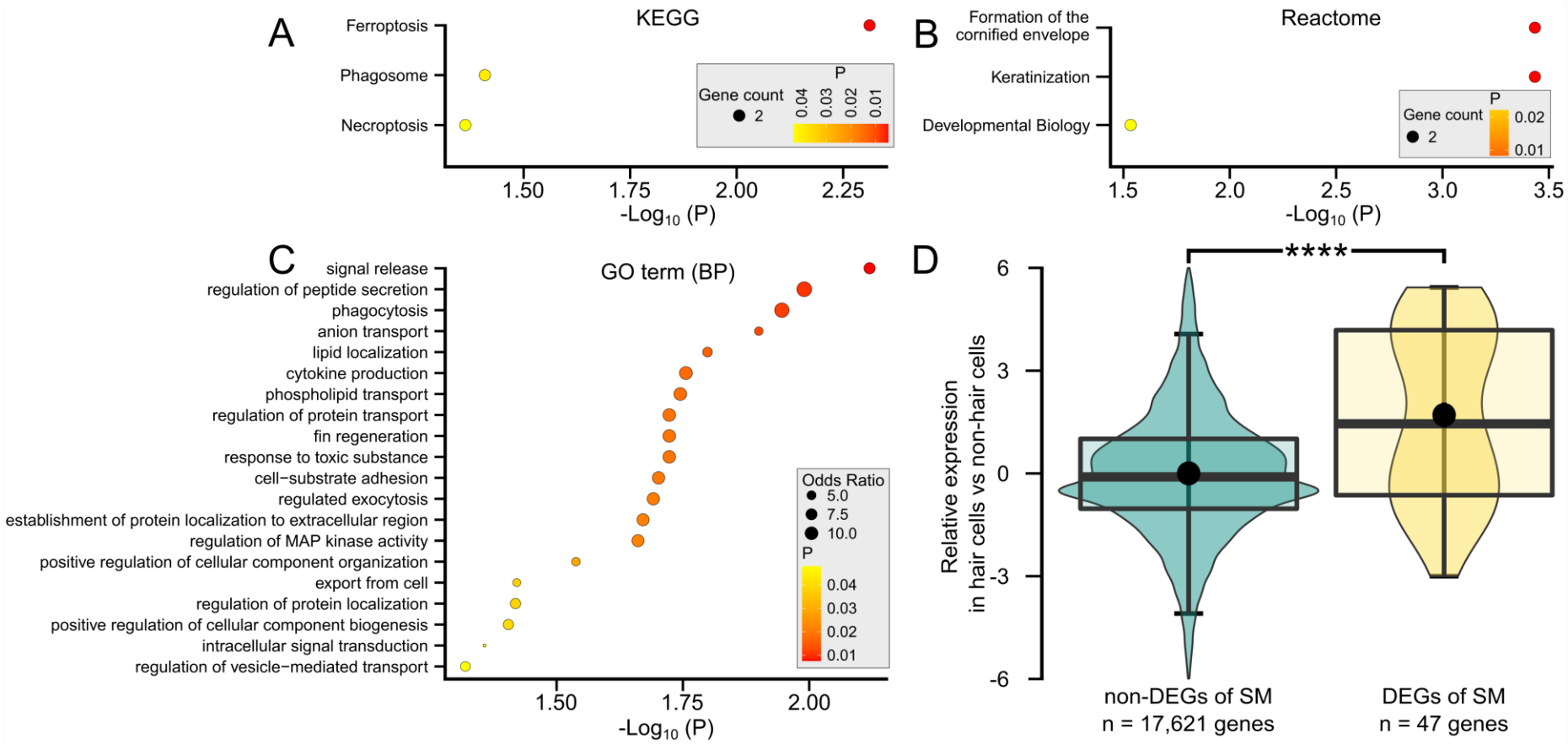

Figure Appendix 3 S2. Stress metabolites alter signalling, immunity, and keratan pathways in zebrafish embryos. Functional enrichment of (A) KEGG pathways, (B) Reactome pathways, and (C) Biological Processes (BP) gene ontology (GO) terms of differentially expressed genes in stress metabolites (SM) compared to C. All represented terms have ≥ 2 gene counts and are ranked by decreasing significance. D) **Genes of SM are also expressed in sensory hair cells of the lateral line.** Relative expression of hair cells compared to non-hair cells of larval zebrafish lateral line were retrieved from Elkon et al. (2015).

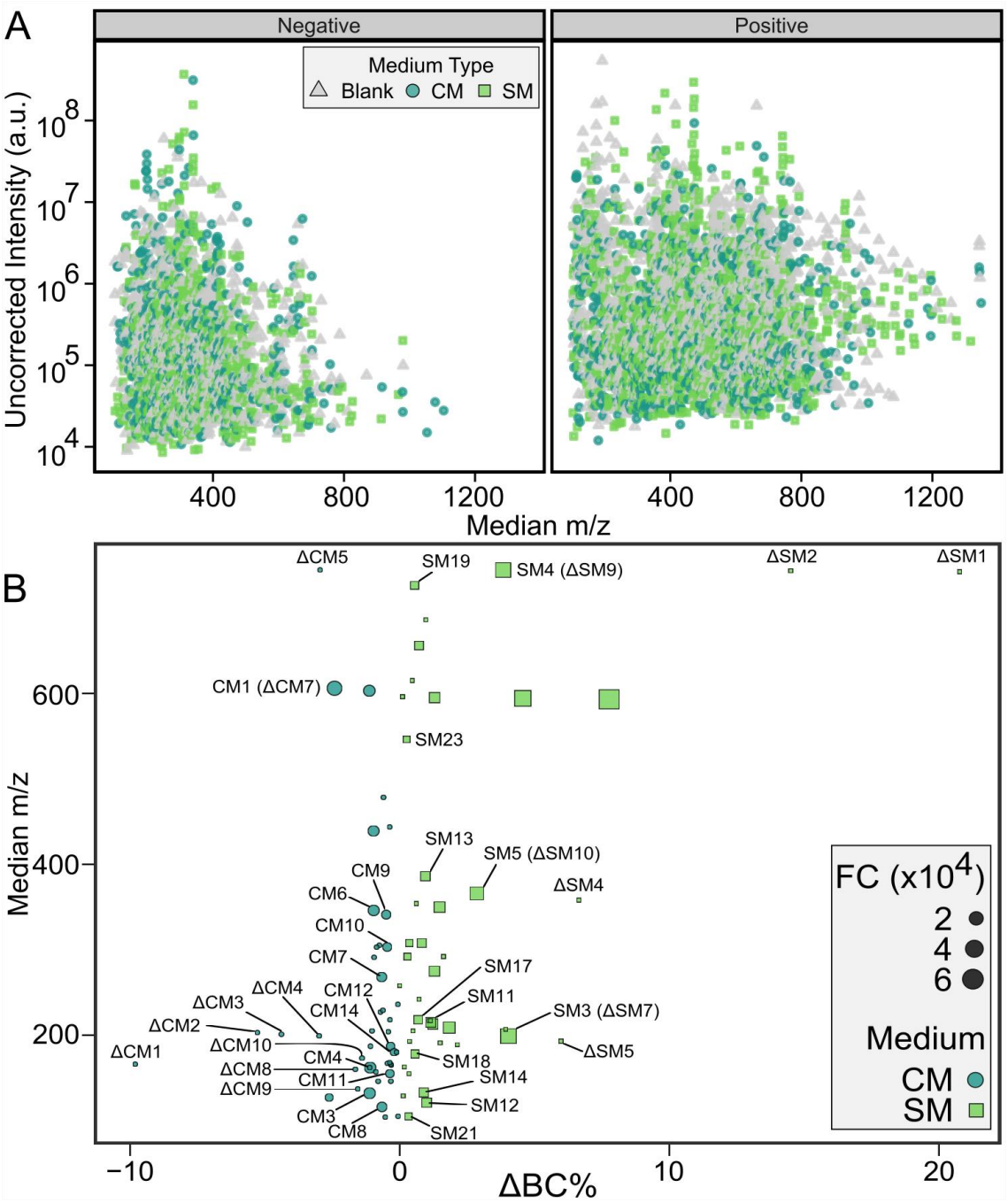

Figure Appendix 3 S3. Manhattan and volcano plots of the metabolomic data. A) Raw MS data was pre-processed to yield 5,583 unique masstags in negative (n = 2,238, left) and positive (n = 3,345, right) ion modes. Uncorrected raw intensity areas are displayed in arbitrary units (a.u.). Masstags were assigned to medium types (blank, CM, SM) based on which medium had the highest average intensity. CM: control metabolites, SM: stress metabolites. B) Volcano plot is showing filtered (n = 89) masstags that are possible biomarkers of control metabolites (CM) and stress metabolites (SM) groups (and not present predominantly in the blank) in both negative and positive modes along with their masses (m/z). Data is blank corrected and is presented as the absolute distance of blank corrected total percent intensity between CM and SM. Far-left dots represent CM-specific compounds, and far-right dots represent SM-specific compounds. Labels show the top masstags biomarkers of each group that have possible hits.

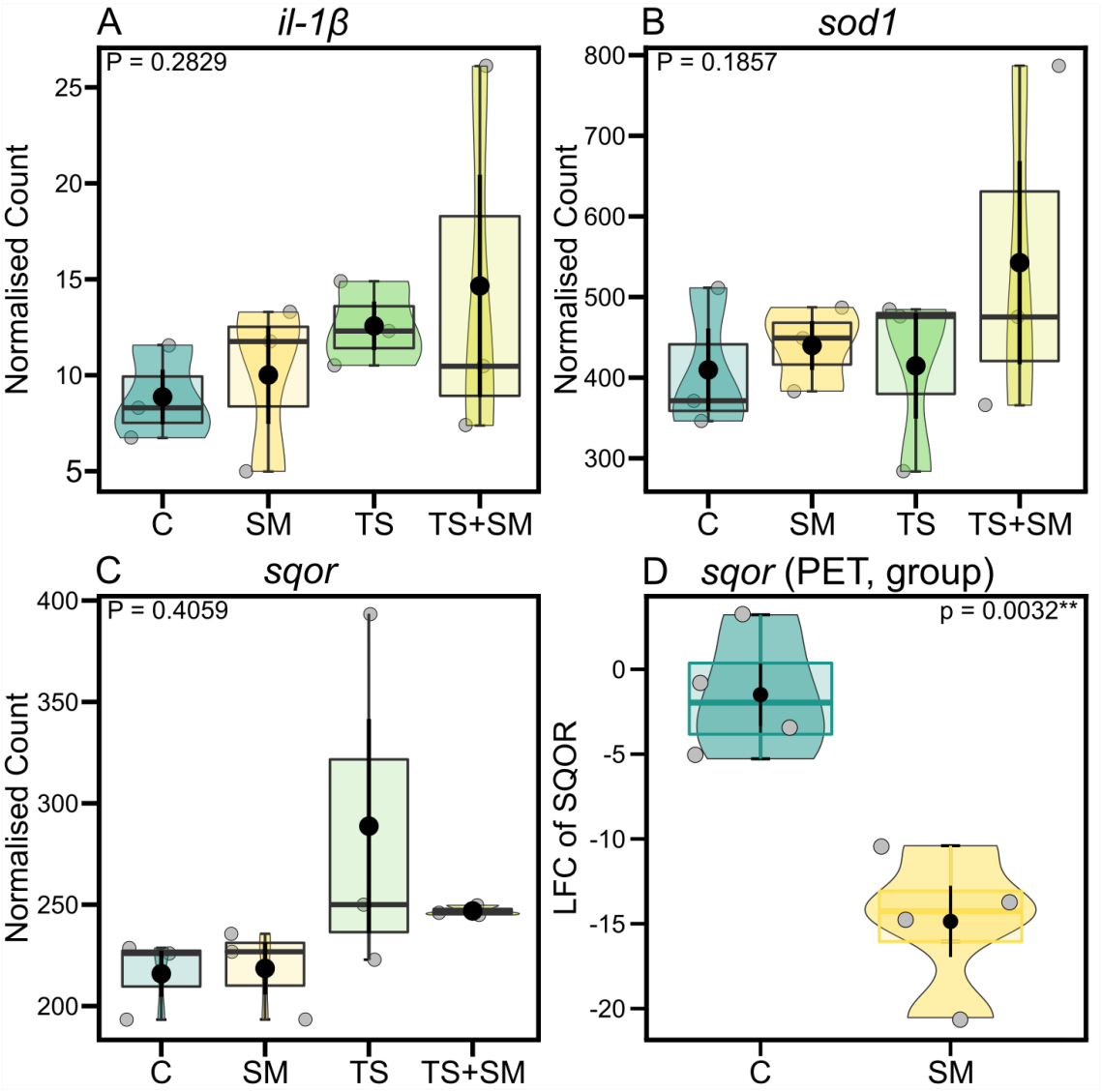

Figure Appendix 3 S4. Stress metabolites downregulate *sqor* in group-raised embryos. Normalised counts of reads from RNA-seq data in isolated inbred AB embryos for A) *il-1β* (interleukin-1β), B) *sod1* (superoxide dismutase 1), and C) *sqor* (sulfide:quinone oxidoreductase). Boxes show median and 25%-75% quartiles, and whiskers are min/max values within 1.5 IQR. Jittered raw data given as grey circles. Black dots show mean ± SE values of each treatment. P-values in upper corners represent treatment effects (DESeq2 model in A-C, and Student's t-test in D). Sample sizes are n = 3 (A-C) or n = 4 (D) biological replicate pools for each treatment each representing the average gene expression of 20 (A-C) or 60 (D) embryos per replicate. Treatments were C: control in fresh medium at 27°C, SM: stress metabolites at 27°C, TS: fresh medium in thermal stress, TS+SM: stress metabolites in thermal stress.

Table Appendix 3 S1. List of potential stress metabolite candidate chemicals. Candidates were used for automatic annotation of references from the spectral database. Only candidate chemicals having a registered CID were kept. Candidate stress metabolites (SM) were retrieved from literature focusing on stress and animal communication incl. alarm substances (AS), kairomones (K), decay cues (D), and social cues (S).

Chemical	Reference	Function	PubChem	Structure
Hydrocortisone	Barcellos et al. (2011)	SM	5754	C21H30O5
Cortisone	Tokarz et al. (2013)	SM	222786	C21H28O5
Corticotropin	Tokarz et al. (2013)	SM	16132265	C207H308N56O58S
20β-hydroxycortisone	Tokarz et al. (2013)	SM	13367714	C21H30O5
L-Arg	Crossland et al. (2019)	AS	6322	C6H14N4O2
L-Leu-L-Leu-OH	Crossland et al. (2019)	AS	76807	C12H24N2O3
Suberic acid	Crossland et al. (2019)	AS	10457	C8H14O4
N-palmitoleyl glutamine	Weiss et al. (2018)	K	100937253	C21H38N2O4
N-linoleoyl glutamine	Weiss et al. (2018)	K	76970188	C23H40N2O4
N-linolenoyl-glutamine	Weiss et al. (2018)	K	5470079	C23H38N2O4
N-olenoyl-glutamine	Weiss et al. (2018)	K	52922072	C23H42N2O4
Serotonin	Saroya et al. (2009)	SM	5202	C10H12N2O
Glutathione	-	SM	124886	C10H17N3O6S
Hypoxanthine-3 N-oxide	Parra et al. (2009)	AS	192963	C5H4N4O2
Chondroitin sulfate	Mathuru et al. (2012)	AS	24766	C13H21NO15S
Ichthyopterin	-	AS	135449065	C9H11N5O4
7-hydroxybiopterin	Døving and Lastein (2009)	AS	50883477	C9H11O4N5
Histamine	-	SM	774	C5H9N3
Pyridine-N-oxide	Døving and Lastein (2009)	AS	12753	C5H5NO
Taurocholic acid	Kermen et al. (2020)	S	6675	C26H45NO7S
Prostaglandin 2 alpha	Kermen et al. (2020)	S	448457	C20H32O5
Cadaverine	Kermen et al. (2020)	D	273	C5H14N2
L-Cysteine	Kermen et al. (2020)	D	5862	C3H7NO2S
Spermine	Kermen et al. (2020)	D	1103	C10H26N4
Putrescine	Kermen et al. (2020)	AS	1045	C4H12N2
Acetylcholine	Canzian et al. (2017)	AS	187	C7H16NO2+
Pyrimidine	Brown et al. (2000)	AS	9260	C4H4N2
Trigonelline	Ito et al. (1994)	SM	5570	C7H7NO2
Homarine	Ito et al. (1994)	SM	3620	C7H7NO2
20-hydroxyecdysone	Nakagawa and Sonobe (2016)	SM	5459840	C27H44O7

Table Appendix 3 S2. Post-hoc pairwise comparisons of cortisol levels of 4-dpf zebrafish larvae. Sample size was n = 3 pooled sample of 60 embryos per treatment. P-values are corrected for false discovery rate for multiple comparisons. Significant terms are shown in with p-values in bold. CM: control metabolites at 27°C, C: control in fresh medium at 27°C, SM: stress metabolites at 27°C, TS: fresh medium in thermal stress.

Contrast	Estimate	SE	T ratio	P	Cohen's |d|	Effect size
C-CM	-0.5615	0.379	-1.4816	0.4895	6.04	Huge
C-TS	-1.8408	0.379	-4.8574	**0.0055**	6.17	**Huge**
C-SM	0.5219	0.379	1.3771	0.5453	0.88	Large
CM-SM	1.0834	0.379	2.8587	0.0812	1.85	Very large

Table Appendix 3 S3. Possible hits for the top 14 biomarkers of CM cloud and top 23 biomarkers of SM cloud. The order of identifier numbers for CM and SM are based on decreasing CM-to-SM and SM-to-CM fold-change values, respectively. "Unidentified metabolite: found in previous studies but with no annotation. "Unknown masstag": no record in available online databases. Lipid abbreviations indicate the constituent + C-atom:double bond. CE: cholesterol ester, DG: diacylglycerol, DGGA: diacylglyceryl glucuronides, FA: fatty acid, MG: monoradyglycerols, PI: phosphatidylinositols, PG: phosphatidylglycerols, PE: phosphatidylethanolamines, PC: phosphatidylcholine, PS: phosphatidylserine, TG: triglycerol, WE: wax monoester. *Candidates of stress metabolites found in control metabolites. In bold: chemical classification. Note: masses may include adducts, see methods for details.

Masstag	ID	Possible hits
CM compounds		
M606.0748T37	CM1	**Nucleosides, nucleotides, and analogues:** UDP-N-Acetyl-D-Galactosamine; UDP-N-Acetylglucosamine; UDP-N-Acetyl-D-Mannosamine; **Others:** Unidentified Metabolite
M603.1316T36	CM2	Unidentified Metabolite
M132.0769T32	CM3	Amino acids, peptides, and analogues: Creatine; Creatinine
M162.1125T28	CM4	Amino acids, peptides, and analogues: L-Carnitine; Lipids*:* FA 7:1;O; WE 7:1;O
M439.0533T39	CM5	Unknown masstag
M346.0558T84	CM6	**Nucleosides, nucleotides, and analogues:** 2'-Deoxyguanosine 3'-Monophosphate; dGMP; 2-Hydroxy-dAMP; 3'-AMP; 7-(5-Phospho-α-D-Ribosyl) Adenine; 9-(2-Deoxy-5-O-Phosphono-β-L-Ribofuranosyl) Guanine; 8-Hydroxy-dAMP; **Monosaccharides:** Adenosine 2'-Phosphate; Adenosine 5'-Monophosphate; **Others:** Unidentified Metabolite
M268.1040T90	CM7	Nucleosides, nucleotides, and analogues: Adenosine; Deoxyguanosine
M116.0708T90	CM8	Amino acids, peptides, and analogues: L-Proline; D-Proline; Lipid: FA 5:2
M341.1089T38	CM9	**Lipids and lipid-like molecules (fatty acyl glycosides):** 3-B-Galactopyranosyl Glucose; α-D-Glucosyl-(1->4)-Aldehydo-D-Mannose; β-D-Glucosyl-(1->4)-Aldehydo-D-Mannose; D-Glucopyranosyl-(1->4)-Aldehydo-D-Mannose; Kojibiose; Turanose; Maltulose; **Carbohydrates and carbohydrate conjugates:** Sucrose; Lactose; Galactinol; Isomaltose; Epimelibiose; 6-O-α-D-Glucopyranosyl-α-D-Fructofuranose; 6-O-α-D-Glucopyranosyl-β-D-Fructofuranose; α,β-Trehalose; α-D-Aldosyl β-D-Fructoside; Galabiose; α-D-Galactosyl-(1->2)-α-D-Galactose; α-D-Galactosyl-(1->2)-β-D-Galactose; α-D-Galactosyl-(1->2)-D-Galactose; α-D-Galactosyl-(1->3)-α-D-Galactose; α-D-Galactosyl-(1->3)-β-D-Mannose; α-D-Galactosyl-(1->3)-D-Galactose; α-D-Galp-(1->3)-β-D-Galp; α-D-Galp-(1->4)-β-D-Galp; α-D-Galp-(1->6)-D-Galp; α-D-Glcp-(1->2)-β-D-Galp; α-D-Glcp-(1->3)-β-D-Glcp; α-D-Glcp-(1->6)-D-Manp; α-D-Glucosyl-(1->2)-D-Mannose; α-D-Glucosyl-(1,3)-D-Mannose; α-D-Glucosyl-(1->3)-D-Mannopyranose; α-D-Glucosyl-(1->4)-β-D-Mannose; α-D-Glucosyl-(1->4)-D-Mannopyranose; α-D-Manp-(1->2)-α-D-Manp; α-D-Manp-(1->2)-D-Manp;3-O-α-D-Mannopyranosyl-α-D-Mannopyranose; Mannobiose; α-D-Manp-(1->6)-β-D-Manp; Neoglyco Interleukin-1a; β-(1->3)-Galactobiose; β-(1->6)-Galactobiose; β,β-Trehalose;Mannosylfructose; β-D-Gal-(1->4)-D-Man;β-D-Galactopyranosyl-(1->4)-α-D-Galactopyranose; β-D-Galactopyranosyl-(1->4)-D-Galactopyranose; β-D-Galactopyranosyl-(1->6)-β-D-Mannopyranose; β-D-Galactosyl-(1->3)-α-D-Mannose;β-D-Galf-(1->2)-D-Manp; β-D-Galf-(1->3)-α-D-Manp; β-D-Galp-(1->2)-β-D-Galp; β-D-Galp-(1->6)-D-Galp;

Table Appendix 3 S3. Continued.

Masstag	ID	Possible hits
M341.1089T38	CM9	**Carbohydrates and carbohydrate conjugates** (continued): β-D-Glcp-(1->2)-α-D-Manp; β-D-Glcp-(1->2)-β-D-Galp; β-D-Glucosyl-(1->4)-α-D-Mannose; β-D-Glucosyl-(1->4)-β-D-Mannose; β-D-Glucosyl-(1->4)-D-Mannopyranose; β-D-Manp-(1->2)-α-D-Manp; β-1,2-Mannobiose; D-Fructosyl-D-Fructofuranose; D-Galactosyl-(1->4)-β-D-Glucose; D-Glucopyranosyl-(1->3)-D-Mannopyranose; D-Glucopyranosyl-(1->4)-D-Mannopyranose; Laminarabiose; Nigerose; Palatinose; Trehalose; α-Maltose; β-Cellobiose; β-Maltose; Maltose; Melibiose; Sophorose; Neotrehalose; β-Lactose; Arabinofuranobiose; Galactose; **Others**: C12H22O11-Disaccharide-(6C/6C; Glc-Glc/Glc-Frc/Gal-Glc); Sucrose And Disaccharides-13C0[-H+]-; Unidentified Metabolite
M341.1089T38	CM9	**Others**: C12H22O11-Disaccharide-(6C/6C; Glc-Glc/Glc-Frc/Gal-Glc); Sucrose and Disaccharides-13C0[-H+]-; Unidentified Metabolite
M303.2175T212	CM10	**Lipids and lipid-like molecules:** Ustilic Acid B; 11,12,15-Trihydroxy Palmitic Acid; 2,15,16-Trihydroxy Palmitic Acid; 8,9,16-Trihydroxy Palmitic Acid; Aleuritic Acid; 2-Hydroxymyristic Acid; 9-Hydroxymyristic Acid; 10-Hydroxytetradecanoic Acid; 11-Hydroxytetradecanoic Acid; 11S-Hydroxytetradecanoic Acid; 3-Hydroxytetradecanoic Acid; 5-Hydroxytetradecanoic Acid; 6-Hydroxytetradecanoic Acid; 6R-Hydroxytetradecanoic Acid; 2S-Hydroxytetradecanoic Acid; Omega-Hydroxy Myristic Acid; (R)-3-Hydroxytetradecanoic Acid; 2-Methoxytetradecanoic Acid; 3R-Hydroxymyristic Acid Methyl Ester; 9-Hydroxy-Pentadecanoic Acid; 15-Hydroxypentadecanoic Acid; 2-Hydroxypentadecanoic Acid; 2R-Hydroxypentadecanoic Acid; 3-Hydroxypentadecanoic Acid; 3R-Hydroxypentadecanoic Acid; 3S-Hydroxypentadecanoic Acid; 4-Hydroxypentadecanoic Acid; Ethyl 3-Hydroxydodecanoate; FA 16:0;O3; MG 13:0;O; FA 15:0;O; MG O-12:1; FA 14:0;O; MG O-11:1; **Others:** Unidentified Metabolite;
M155.0816T28	CM11	Alkaloids and derivatives: Trigonelline*; Amino acids, peptides, and analogues: Glycyl-Tyrosine; Tyrosyl-Glycine; Benzenoids: Anthranilate; Pyridines and derivatives: Homarine*
M187.1077T30	CM12	**Amino acids, peptides, and analogues:** Pro-Ala; N(5)-(L-1-Carboxyethyl)-L-Ornithine; N(6)-Carboxymethyl-L-Lysine;Ser-Val; Val-Ser; (Ac)2-L-Lysyl-D-Alanyl-D-Alanine; Glu-Pro-Lys; Pro-Glu-Lys; 2-Amino-5-Oxohexanoic Acid; 4-Acetamidobutanoic Acid; Isobutyrylglycine; L-Allysine; 5-Hydroxypipecolic Acid; N-Butyrylglycine; Gly-Pro; Pro-Gly; Prolyl-Alanine; Alanyl-Proline; **Keto acids and derivatives**: 2-Keto-6-Aminocaproate; (5S)-5-Amino-3-Oxohexanoic Acid; Glu-Lys-Pro; Lys-Glu-Pro; Lys-Pro-Glu; Pro-Lys-Glu; (4R)-5-Oxo-L-Leucine; **Carbonyl compounds**: 1-Ethyl-1H-Pyrrole-2-Carboxaldehyde; **Benzenediols**: 5-Hydroxydopamine; Norepinephrine; **Pyridines and derivatives**: 6-Acetyl-2,3-Dihydro-2-(Hydroxymethyl)-4(1H)-Pyridinone; Ala-Pro; Pyridoxine
M127.0728T33	CM13	Unknown masstag
M180.0667T83	CM14	Amino acids, peptides, and analogues: L-Tyrosine

Table Appendix 3 S3. Continued.

Masstag	ID	Possible hits
SM compounds		
M593.1612T383	SM1	Unknown masstag
M594.1646T383	SM2	Unidentified Metabolite
M199.0047T124	SM3	**Lipids and lipid-like molecules**: Dihydroxyacetone Phosphate Acyl Ester; Others: Unidentified Metabolite
M744.5022T467	SM4	**Lipids and lipid-like molecules**: DGGA 31:1;O; PI(O-14:0/13:0); PI(O-16:0/11:0); PG(25:0/4:0); PG(27:0/2:0); PG(12:0/17:0); PG(13:0/16:0); PG(14:0/15:0); PG(15:0/14:0); PG(16:0/13:0); PG(17:0/12:0); **Others**: Unidentified Metabolite; **UniProt proteins**: Spondin-2 A0A1Y8Ely7 of *Homo sapiens* (A0A1Y8Ely7_Human); Bbrv_Locus22923 Of *Bracon brevicornis* A0A6V7Ii27 (A0A6V7Ii27_9Hyme); Bzw1 Of Prickly gecko *Heteronotia binoei* A0A0U3Jgs3 (A0A0U3Jgs3_9Saur).
M365.9712T82	SM5	**Lipids**: TG 69:8;O and TG O-69:9;O2
M208.9947T164	SM6	Unidentified Metabolite
M349.9763T124	SM7	Unknown masstag
M595.1675T383	SM8	Unidentified Metabolite
M274.9905T124	SM9	Unidentified Metabolite
M213.0121T189	SM10	Unidentified Metabolite
M214.9994T82	SM11	**Lipids and lipid-like molecules**: 2-Oxo-4-Methylthiobutanoic Acid; **Other**: Unidentified Metabolite
M120.9964T82	SM12	Organic acids and derivatives: Thioacetate; Organic oxygen compounds: 3-Mercaptolactate
M386.1569T153	SM13	**Tripeptides**: Met-Pro-Thr; Met-Thr-Pro; Pro-Met-Thr; Pro-Thr-Met; Thr-Met-Pro; Thr-Pro-Met; Asp-Pro-Pro; Pro-Asp-Pro; Pro-Pro-Asp; Glu-Pro-Pro; Pro-Glu-Pro; Pro-Pro-Glu
M133.0507T72	SM14	**Lipids and lipid-like molecules**: 2,3-Dihydroxy-2-Methylbutanoic Acid;(R)-2,3-Dihydroxy-Isovalerate;2,3-Dihydroxyisovaleric Acid;2,3-Dihydroxy-Valeric Acid; (R)-Glycerol 1-Acetate; **Organic oxygen compounds**: 1-Deoxy-D-Xylulose;Deoxyribose;5-Deoxy-D-Ribose; Xylitol; Deoxyribose; **Organoheterocyclic compounds:** 2-Deoxy-α-D-Ribopyranose;2-Deoxy-L-Arabinose; **Lipids**: FA 5:0;O2;FA 4:0;WE 4:0;FA 3:0

Table Appendix 3 S3. Continued.

Masstag	ID	Possible hits
M307.9657T124	SM15	Unknown masstag
M656.1570T383	SM16	Unidentified Metabolite
M218.0356T27	SM17	**Organic nitrogen compounds**: Phosphocholine; **Other**: Unidentified Metabolite
M178.0262T124	SM18	**Organic oxygen compounds**: α-D-Kdo-4P-Oall; α-D-Kdo-5P-Oall; **Other**: Unidentified Metabolite
M726.6238T461	SM19	**Lipids and lipid-like molecules**: GalCer(D14:0/23:0); GalCer(D17:0/20:0); GlcCer(D14:0/23:0); GlcCer(D17:0/20:0); DG(17:0/22:2(13Z,16Z)/0:0); DG(17:1(9Z)/22:1(13Z)/0:0); DG(17:2(9Z,12Z)/22:0/0:0); DG(18:2(9Z,12Z)/21:0/0:0); DG(19:0/20:2(11Z,14Z)/0:0); DG(19:1(9Z)/20:1(11Z)/0:0); DGTS(16:0/16:0); GalCer(D19:0/18:0);GlcCer(D19:0/18:0); N-Glycoloylganglioside Gm2; Cholest-5-En-3Beta-Yl (7Z,10Z,13Z,16Z,19Z-Docosapentaenoate); CE(22:5(4Z,7Z,10Z,13Z,16Z)); CE(22:5(7Z,10Z,13Z,16Z,19Z)); CE(22:3); GalCer(D15:0/22:0); GalCer(D16:0/21:0); GalCer(D18:0/19:0); GalCer(D20:0/17:0); GalCer(D21:0/16:0); GalCer(D22:0/15:0); GlcCer(D15:0/22:0); GlcCer(D16:0/21:0); GlcCer(D18:0/19:0); GlcCer(D20:0/17:0); GlcCer(D21:0/16:0); GlcCer(D22:0/15:0); **UniProt Protein**: Uncharacterized Protein From Gobi Fish, Protein Contains Lim Domain, Blast Hit Zebrafish Gene Ldb1A
M307.9647T82	SM20	Unidentified Metabolite
M105.0007T82	SM21	**Organic oxygen compounds**: 3-Mercaptolactate
M291.9702T124	SM22	Unknown masstag
M546.1609T495	SM23	**UniProt Protein**: Fungal Cutinase 2; Scorpion Toxin Tetrapandin-2; **Others**: Unidentified Metabolite

Table Appendix 3 S4. Permutational multivariate analysis of variance of morphological data of 1-dpf zebrafish embryos. Two-way PERMANOVA representing the effects of thermal stress (TS) and stress metabolites (SM). Effect size interpretation according to Sawilowsky (2009). Only complete cases for all the response variables are analysed. n = 999 permutations. Response variables: otic vesicle length (OVL), eye length (EL), shortest embryo length (SEL), longest embryo length (LEL), dorsoventral length (DVL), yolk extension length (YEL), yolk ball length (YBL), tail width (TW), yolk extension-to-yolk ball ratio (YE/YB), head-trunk angle (HTA), eye area (EA), whole-body area (WBA), yolk extension area (YEA), yolk ball area (YBA), Final stage (hours post fertilisation), defects %, final stage period (segmentation or pharyngula). Adjusted p-values are given for post-hoc comparisons. Significance ($p < 0.05$) is shown in bold.

Term	Sum sq.	Mean sq.	F	R2	P
2-way PERMANOVA					
TS	2432.2669	2432.2669	**30.1022**	0.2475	**0.0010**
SM	13.0015	13.0015	0.1609	0.0013	0.7610
TS:SM	189.0455	189.0455	2.3397	0.0192	0.1320
Residuals	7191.2206	80.80002	-	0.7319	-
Total	9825.5346	-	-	1.0000	-
Post-hoc comparisons					
TS-C	0.0395	-	**23.2814**	0.3360	**0.0015**
SM-C	0.0019	-	1.1101	0.0316	0.3050
(TS+SM)-C	0.0295	-	**17.9542**	0.2852	**0.0015**
CM-C	-4E-4	-	-0.2211	-0.0059	0.9960
CM-SM	-5E-4	-	0.3231	0.0089	0.9960

Table Appendix 3 S5. Analysis of variance of burst count per minute of 1-dpf zebrafish embryos. Two-way ANOVA representing the effects of thermal stress (TS) and stress metabolites (SM). Only active embryos (burst count per min > 0) are analysed. Significance ($p < 0.05$) is shown in bold.

Term	Sum sq.	Mean sq.	Statistic	P	Cohen's |d|	Effect size
TS	44.0656	44.0656	18.1540	**0.0001**	0.91	**Large**
SM	0.7134	0.7134	0.2939	0.5891	0.11	Very small
TS:SM	0.1780	0.1780	0.0733	0.7872	0.05	Tiny
Residuals	211.1766	2.4273	-	-	-	-

Table Appendix 3 S6. Post-hoc comparison of burst count per minute of 1-dpf zebrafish embryos. CM: control metabolites at 27°C (n = 28), C: control in fresh medium at 27°C (n = 20), SM: stress metabolites at 27°C (n = 17), TS: fresh medium in thermal stress (n = 26), TS+SM: stress metabolites in thermal stress (n = 28). P-values are corrected by false discovery rate for multiple comparisons. Only active embryos (burst count per min > 0) are analysed. Significance ($p < 0.05$) is shown in bold.

Contrast	Estimate	SE	T ratio	P	Cohen's |d|	Effect size
SM-C	-0.0701	0.5140	-0.1363	0.8919	0.03	Tiny
TS-C	-1.3190	0.4634	-2.8464	**0.0083**	0.91	**Large**
(TS+SM)-C	-1.5695	0.4561	-3.4409	**0.0027**	1.19	**Large**
C-CM	1.141	0.577	1.9776	0.0821	0.64	Medium
SM-CM	1.071	0.606	1.7674	0.0821	0.51	Medium

Table Appendix 3 S7. Analysis of variance of increment in embryo size (ΔSEL) between 1 and 4 dpf. Two-way ANOVA representing the effects of thermal stress (TS) and stress metabolites (SM). P-values are corrected for false discovery rate for multiple comparisons. Significance ($p < 0.05$) is shown in bold.

Term	Sum Sq.	Mean Sq.	Statistic	P	Cohen's |d|	Effect size
TS	1.2520	1.2520	20.9948	**0.0000**	0.81	**Large**
SM	0.3969	0.3969	6.6546	**0.0112**	0.43	**Small**
Batch	0.3997	0.3997	6.7027	**0.0109**	0.44	**Small**
TS:SM	0.0021	0.0021	0.0355	0.8509	0.03	Tiny
Residuals	6.7985	0.0596	-	-	-	-

Table Appendix 3 S8. Stress Metabolites alter the expression of *chs1* and *prg4a* group-raised outcrossing 1-dpf zebrafish embryos. C: control in fresh medium at 27°C, SM: stress metabolites at 27°C. Sample size was n = 4 pooled samples of 20 embryos per treatment. Computed using Student's t-tests with effect size interpretation according to Sawilowsky (2009). Data collected at 1 day post fertilisation using Loop-Mediated Isothermal Amplification (LAMP). Significance ($p < 0.05$) is shown in bold. c*hs1*: chitin synthase 1, *ldha*: lactate dehydrogenase A4, *ora3*: olfactory receptor class A related 3* (undetected in SM), *otofa*: otoferlin a, *prg4a*: proteoglycan 4a, *tlr18*: toll-like receptor 18.

Contrast	Gene	T ratio	P	Cohen's |d|	Effect size
C-SM	***chs1***	3.08	**0.0487**	2.18	**Huge**
C-SM	*ldha*	-0.14	0.8960	-0.10	Tiny
C-SM	***ora3****	-	-	-	-
C-SM	*otofa*	-1.67	0.1760	-1.18	Large
C-SM	***prg4a***	-8.01	**0.0026**	-6.52	**Huge**
C-SM	*tlr18*	-1.32	0.2410	-0.93	Large

Appendix 4 Supplementary Information to Chapter 5

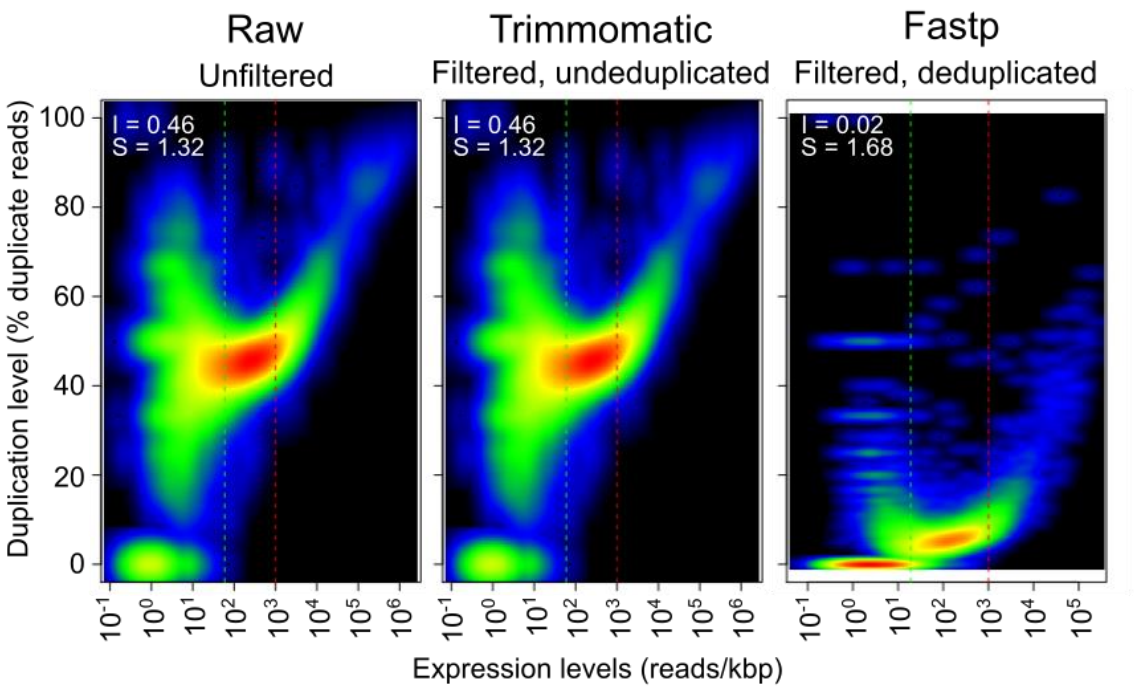

Figure Appendix 4 S1. Duplication level in function of read expression levels. Example data from one control UV-treated embryos (C+UV). Smooth colour density plot of duplication rates in unfiltered (left), filtered but not deduplicated (middle), and filtered and deduplicated (right) reads. Red spots indicate high duplication levels which are expected to naturally raise with expression level but to be low in lowly expressed reads. The *dupRadar* R package (Sayols et al., 2016) found technical duplication bias if reads were not deduplicated as indicated by red spots at around 46% of duplication intercept. Using *fastp* for deduplication lowered the rate of duplication in lowly expressed reads. Intercepts (I) and slopes (S) are shown in top-left corners.

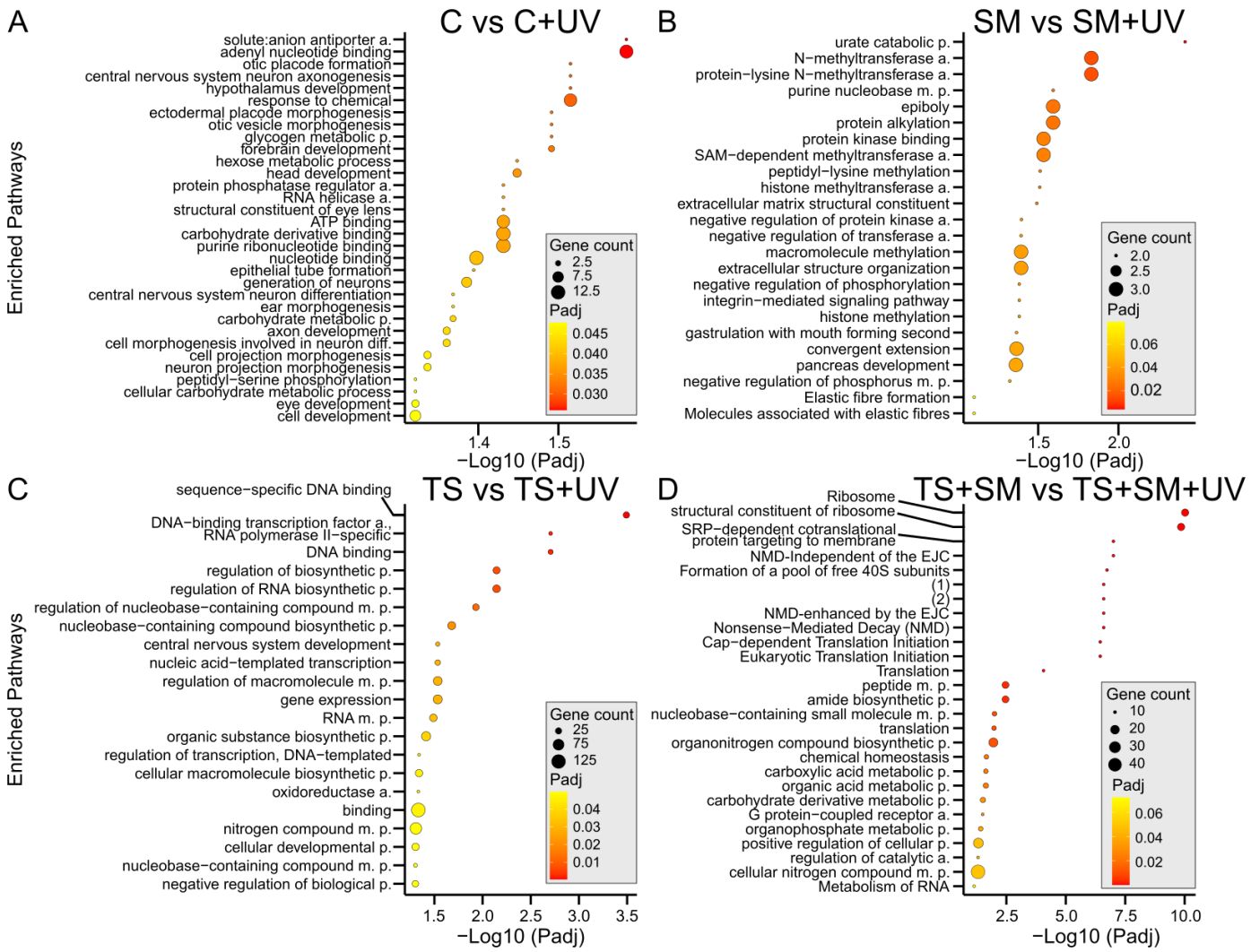

Figure Appendix 4 S2. Heat stress history altered the transcriptomic response to UV. Top functionally enriched terms (based on highest gene count/term with n ≥ 2 genes/term) of the differentially expressed genes unique to each UV treatments compared to their non-UV pairs. A) C vs C+UV, B). SM vs SM+UV, C) TS vs TS+UV, and D) TS+SM vs TS+SM+UV. Treatments were C: control in fresh medium at 27°C, SM: stress metabolites at 27°C, TS: fresh medium in thermal stress, TS+SM: stress metabolites in thermal stress, all compared to their non-UV pairs. (1) "*GTP hydrolysis and joining of the 60S ribosomal subunit*". (2) "*L13a−mediated translational silencing of Ceruloplasmin expression*". a.: activity, diff. differentiation, m.: metabolic, NMD: nonsense-mediated decay, p.: process, SAM: S−adenosylmethionine.

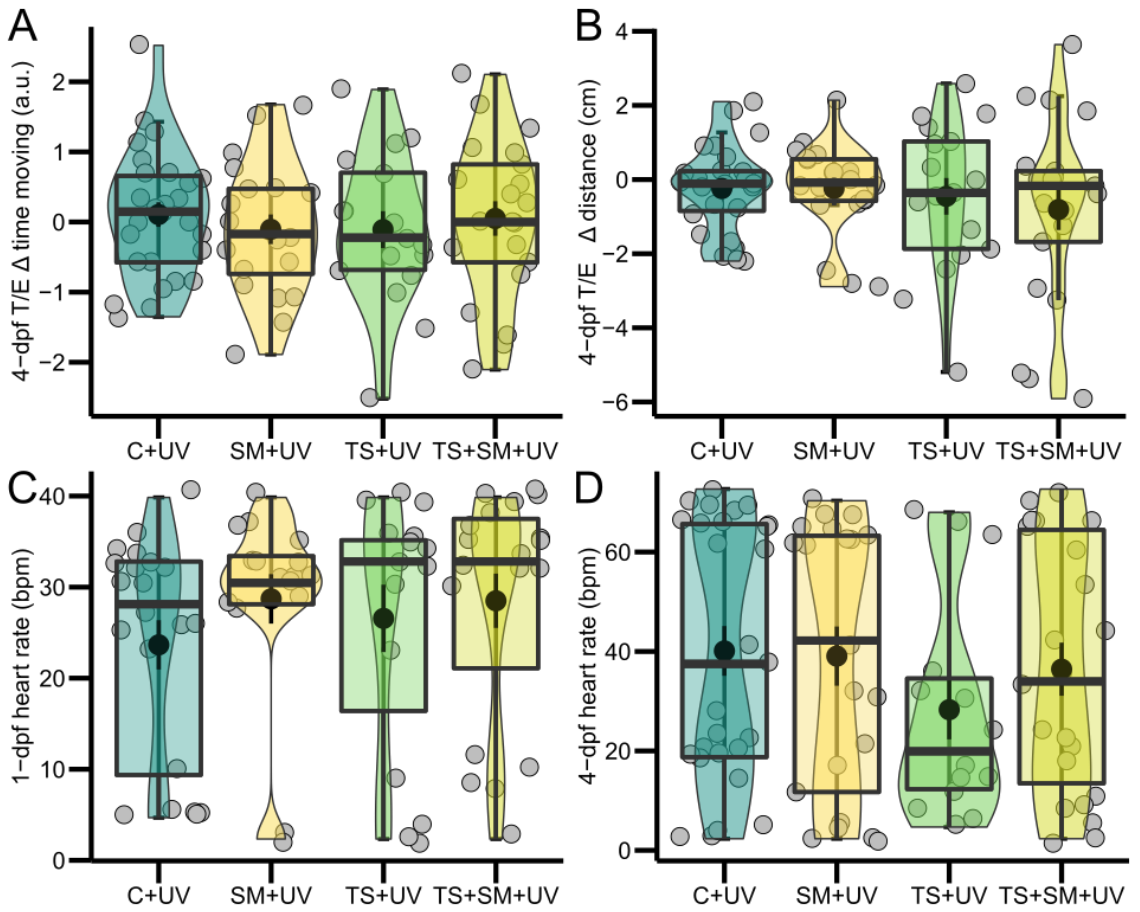

Figure Appendix 4 S3. Neither stress metabolites nor heat altered swimming fatigability and heart rates. Delta time (A) and delta distance (B) swam after the 3rd and 1st touch stimuli in the touch-evoked (T/E) swimming assay 4 days post fertilisation (dpf). Beat per min in the startle response to acute light change at (C) 1 and (D) 4 dpf. Model terms (heat × medium) are not significant according to analyses of variance (A, C-D) and a Scheirer-Ray-Hare test (B). Treatments were C+UV: control in fresh medium at 27°C, SM+UV: stress metabolites at 27°C, TS+UV: fresh medium in thermal stress, TS+SM+UV: stress metabolites in thermal stress.

Table Appendix 4 S1. Optimisation of UV treatments. UVA: 28 min of bottom-up exposure, UVB, 6 minutes of bottom-up exposure. Survival and defect percentages in UVA, UVB, and UVB+A treatments were observed at 2, 3, 4 days post fertilisation (dpf). *At 3 dpf, n = 4 embryos from the UVA treatment were treated with 6 min of UVB exposure to see how late developmental deformities can be induced (UVA+B treatment). Data shows observed event/total sample size (percentages). UV treatments were applied on 24 hours old embryos and defects were observed in the subsequent days.

Treatment	2 dpf	3 dpf	4 dpf
Survival			
UVA	9/9 (100%)	9/9 (100%)	5/5 (100%)*
UVB	9/10 (90%)	6/10 (60%)	5/10 (50%)
UVB+A	10/10 (100%)	10/10 (60%)	10/10 (100%)
UVA+B	-	-	3/4 (75%)
Defects			
UVA	0/9 (0%)	0/9 (0%)	0/5 (0%)
UVB	10/10 (100%)	6/6 (100%)	4/5 (80%)
UVB+A	2/10 (20%)	3/10 (30%)	6/10 (60%)
UVA+B	-	2/4 (50%)	-

Table Appendix 4 S2. Method development of UVA exposure time. This aimed to assess whether 15 min of UVA induces enough repair whilst staying in the range of time at which RNA-seq sampling will capture DNA repair genes. Successful recovery of lethal effects of UVB (6 min) by UVA (15 min with double source) in zebrafish embryos. C: control embryos without UV treatment.

Treatment	n	Death	Survival	Hatching
C	26	0 (0%)	26 (100%)	11 (42%)
UVB	29	23 (80%)	6 (20%)	0 (0%)
UVB+UVA	28	4 (15%)	24 (85%)	2 (9%)

Table Appendix 4 S3. UVA induced successful recovery of lethal effects of UVB at 4 dpf. Zebrafish embryos were dechorionated at 4 dpf to score defects under the stereomicroscope. Treatments were: Control C, UVB (6 min, 306 nm, bottom-up exposure) alone, and UVB followed by UVA (15 min, 365 nm, top-bottom + bottom-up exposure).

Treatment	n	Healthy	Defect	Dead
C	21	19 (90%)	2 (10%)	0 (0%)
UVB	24	0 (0%)	10 (42%)	14 (58%)
UVB+UVA	23	14 (61%)	9 (39%)	0 (0%)

Table Appendix 4 S4. Heat stress increased DNA repair efficiency and tended to potentiate epigenetic and methylation-related genes. Statistics are from two-way Scheirer-Ray-Hare tests (H statistic) or ANOVAs (F statistic) comparing absolute log-fold change of transcripts associated with DNA repair (n = 288 genes), protein folding (n = 125 genes), methylation (n = 131 genes), and epigenetics (n = 84 genes) between treatments in response to UV. The "heat" term compares TS vs TS+UV and TS+SM vs TS+SM+UV to C vs C+UV and SM vs SM+UV. The "medium" term compares SM vs SM+UV and TS+SM vs TS+SM+UV to C vs C+UV and TS vs TS+UV. Effect size classification from Sawilowsky (2009). Significance ($p < 0.05$) is shown in bold.

Term	Sum square	Statistic	p	Cohen's |d|
Shared response				
Medium	0.3207	F = 0.3197	0.5720	0.05 (tiny)
Heat	0.9653	F = 0.9624	0.3271	0.09 (tiny)
Heat:medium	0.1889	F = 0.1883	0.6645	0.04 (tiny)
DNA repair				
Medium	53997.2	H = 0.4878	0.4849	0.01 (tiny)
Heat	468108.8	H = 4.2291	**0.0397**	**0.05 (very small)**
Heat:medium	142867.4	H = 1.2907	0.2559	0.03 (tiny)
Protein folding				
Medium	0.0003	F = 0.0003	0.9862	0.00 (tiny)
Heat	0.1786	F = 0.1777	0.6736	0.04 (tiny)
Heat:medium	0.0024	F = 0.0024	0.9612	0.00 (tiny)
Methylation				
Medium	0.3111	F = 0.3112	0.5772	0.05 (tiny)
Heat	2.7447	F = 2.7461	0.0981 (**trend**)	0.15 (very small)
Heat:medium	0.1988	F = 0.1988	0.6558	0.04 (tiny)
Epigenetics				
Medium	571	H = 0.0605	0.8057	0.01 (tiny)
Heat	26857	H = 2.8463	0.0916 (**trend**)	0.19 (very small)
Heat:medium	2273	H = 0.2409	0.6235	0.05 (tiny)

Table Appendix 4 S5. UVR decreased RNA integrity number (RIN). Statistics are from an ANOVA. Effect size classification from Sawilowsky (2009). Significance ($p < 0.05$) is shown in bold.

Term	Sum square	F	p	Cohen's |d|
UV	12.4704	6.4449	**0.0195**	**1.13 (large)**
heat	0.0204	0.0106	0.9192	0.04 (tiny)
medium	0.3504	0.1811	0.6750	0.17 (very small)

Table Appendix 4 S6. Heat stress history altered the percentage of hatching and pericardial edema at 4 dpf. Statistics are from two-way generalised linear models for binomial distribution data. The "heat" term compares TS+UV and TS+SM+UV vs C+UV and SM+UV. The "medium" term compares SM+UV and TS+SM+UV to C+UV and TS+UV. Effect size classification from Sawilowsky (2009). Pairwise tests are corrected for multiple testing. Significance ($p < 0.05$) is shown in bold.

Term	Estimate	CI	Z	p
Survival %				
Heat	0.3514	1.4456	0.243	0.8079
Medium	0.2513	1.4438	0.174	0.8618
Heat:medium	-0.4849	2.0442	-0.237	0.8125
Hatching %				
Heat	2.1203	0.7572	**2.800**	**0.0051**
Medium	0.2744	0.8714	0.315	0.7528
Heat:medium	-1.0282	1.0692	-0.962	0.3362
(C+UV) - (SM+UV)	-0.2744	0.8714	-0.315	0.7528
(C+UV) - (TS+UV)	-2.1203	0.7572	**-2.8003**	**0.0306**
(C+UV) - (TS+SM+UV)	-1.3665	0.7464	-1.8308	0.1343
(SM+UV) - (TS+UV)	-1.8458	0.7655	-2.4113	**0.0477**
(SM+UV) - (TS+SM+UV)	-1.0921	0.7548	-1.4467	0.2222
(TS+UV) - (TS+SM+UV)	0.7538	0.6195	1.2167	0.2685
Pericardial edema %				
Heat	-2.2992	0.6979	**-3.2945**	**0.0010**
Medium	-1.0405	0.6674	-1.5591	0.1190
Heat:medium	2.4423	0.9384	**2.6026**	**0.0093**
(C+UV) - (SM+UV)	1.0405	0.6674	1.5591	0.1784
(C+UV) - (TS+UV)	2.2992	0.6979	**3.2945**	**0.0059**
(C+UV) - (TS+SM+UV)	0.8974	0.6597	1.3605	0.2084
(SM+UV) - (TS+UV)	1.2587	0.6675	1.8858	0.1186
(SM+UV) - (TS+SM+UV)	-0.1431	0.6274	-0.2281	0.8196
(TS+UV) - (TS+SM+UV)	-1.4018	0.6597	-2.1248	0.1008

Table Appendix 4 S7. Heat stress history altered the morphology of larvae after UV exposure. Statistics are from two-way Scheirer-Ray-Hare tests (H statistic) or ANOVAs (F statistic). The "heat" term compares TS+UV and TS+SM+UV vs C+UV and SM+UV. The "medium" term compares SM+UV and TS+SM+UV to C+UV and TS+UV. Pairwise tests are computed with Wilcoxon-Mann-Whitney (W statistic) tests or *emmeans* (T statistic) with correction for multiple testing. Effect size classification from Sawilowsky (2009). Significance ($p < 0.05$) is shown in bold.

Term	Sum square	Statistic	p	Cohen's |d|
4-dpf embryo size				
Heat	0.0965	F = 1.7518	0.1891	0.26 (small)
Medium	0.0206	F = 0.3741	0.5424	0.12 (very small)
Heat:medium	0.8880	F = 16.1140	**0.0001**	**0.85 (large)**
(C+UV) - (SM+UV)	-	T = -2.2879	**0.0491**	**0.70 (medium)**
(C+UV) - (TS+UV)	-	T = -3.8048	**0.0016**	**1.02 (large)**
(C+UV) - (TS+SM+UV)	-	T = -0.3231	0.7474	0.1 (tiny)
(SM+UV) - (TS+UV)	-	T = -1.4858	0.1692	0.44 (small)
(SM+UV) - (TS+SM+UV)	-	T = 1.8871	0.0937 (**trend**)	0.66 (medium)
(TS+UV) - (TS+SM+UV)	-	T = 3.3546	**0.0035**	**0.97 (large)**
4-dpf embryo size-normalised pericardial width				
Heat	2.5836	F = 2.8584	0.0945 (**trend**)	0.34 (small)
Medium	4.4717	F = 4.9472	**0.0287**	**0.46 (small)**
Heat:medium	4.3078	F = 4.7660	**0.0317**	**0.45 (small)**
(C+UV) - (SM+UV)	-	T = -0.1401	0.8889	0.05 (tiny)
(C+UV) - (TS+UV)	-	T = 2.9161	**0.0104**	**1.14 (large)**
(C+UV) - (TS+SM+UV)	-	T = -0.3499	0.8889	0.09 (tiny)
(SM+UV) - (TS+UV)	-	T = 2.8652	**0.0104**	**1.02 (large)**
(SM+UV) - (TS+SM+UV)	-	T = -0.1922	0.8889	0.05 (tiny)
(TS+UV) - (TS+SM+UV)	-	T = -3.1134	**0.0104**	**0.88 (large)**
4-dpf embryo size-normalised eye length				
Heat	0.0002	F = 8.2667	**0.0051**	**0.61 (medium)**
Medium	0.0000	F = 0.0137	0.9071	0.02 (tiny)
Heat:medium	0.0000	F = 0.9404	0.3349	0.2 (very small)
(C+UV) - (SM+UV)	-	T = 0.5752	0.5667	0.17 (very small)
(C+UV) - (TS+UV)	-	T = -1.3438	0.2738	0.37 (small)
(C+UV) - (TS+SM+UV)	-	T = -2.2890	0.0735 (**trend**)	0.61 (medium)
(SM+UV) - (TS+UV)	-	T = -1.7858	0.1552	0.61 (medium)
(SM+UV) - (TS+SM+UV)	-	T = -2.6843	**0.0522**	**0.89 (large)**
(TS+UV) - (TS+SM+UV)	-	T = -0.7895	0.5184	0.24 (small)
4-dpf defect score				
Heat	201	H = 0.3023	0.5824	0.14 (very small)
Medium	1407	H = 2.1110	0.1463	0.29 (small)
Heat:medium	3800	H = 5.7016	**0.0170**	**0.54 (medium)**
(C+UV) - (SM+UV)	-	W = 320	0.8520	0.19 (very small)
(C+UV) - (TS+UV)	-	W = 371	0.1030	0.69 (medium)
(C+UV) - (TS+SM+UV)	-	W = 280	0.8520	0.17 (very small)
(SM+UV) - (TS+UV)	-	W = 251	0.6080	0.50 (medium)
(SM+UV) - (TS+SM+UV)	-	W = 194	0.7650	0.38 (small)
(TS+UV) - (TS+SM+UV)	-	W = 116	**0.0490**	**0.93 (large)**

Table Appendix 4 S8. Heat stress history altered the 1-dpf light-induced startle response after UV exposure. Statistics are from two-way Scheirer-Ray-Hare tests (H statistic). The "heat" term compares TS+UV and TS+SM+UV vs C+UV and SM+UV. The "medium" term compares SM+UV and TS+SM+UV to C+UV and TS+UV. Pairwise tests are computed with Wilcoxon-Mann-Whitney (W statistic) tests with correction for multiple testing. Effect size classification from Sawilowsky (2009). Significance ($p < 0.05$) is shown in bold.

Term	Sum square	Statistic	p	Cohen's |d|
1-dpf burst %				
Heat	28633	H = 38.0544	**< 0.0001**	**1.67 (very large)**
Medium	2982	H = 3.9634	**0.0465**	**0.36 (small)**
Heat:medium	866	H = 1.1516	0.2832	0.27 (small)
(C+UV) - (SM+UV)	-	W = 349	0.4280	0.11 (very small)
(C+UV) - (TS+UV)	-	W = 457	**0.0009**	**1.20 (very large)**
(C+UV) - (TS+SM+UV)	-	W = 661	**< 0.0001**	**2.37 (huge)**
(SM+UV) - (TS+UV)	-	W = 345.5	**0.0050**	**1.04 (large)**
(SM+UV) - (TS+SM+UV)	-	W = 485	**< 0.0001**	**2.18 (huge)**
(TS+UV) - (TS+SM+UV)	-	W = 383	**0.0050**	**1.04 (large)**
1-dpf burst count/min				
Heat	4924	H = 6.5512	**0.0105**	**0.34 (small)**
Medium	5875	H = 7.817	**0.0052**	**0.48 (small)**
Heat:medium	1655	H = 2.2019	0.1378	0.47 (small)
(C+UV) - (SM+UV)	-	W = 358	0.9930	0.03 (tiny)
(C+UV) - (TS+UV)	-	W = 305	1.0000	0.19 (very small)
(C+UV) - (TS+SM+UV)	-	W = 563	**0.0008**	**0.99 (large)**
(SM+UV) - (TS+UV)	-	W = 198	1.0000	0.18 (very small)
(SM+UV) - (TS+SM+UV)	-	W = 400	**0.0260**	**0.78 (medium)**
(TS+UV) - (TS+SM+UV)	-	W = 376	**0.0160**	**0.88 (large)**

Table Appendix 4 S9. Stress metabolites lowered the 4-dpf dark/light-induced swimming after UV exposure. Statistics are from two-way Scheirer-Ray-Hare tests (H statistic). The "heat" term compares TS+UV and TS+SM+UV vs C+UV and SM+UV. The "medium" term compares SM+UV and TS+SM+UV to C+UV and TS+UV. Effect size classification from Sawilowsky (2009). Significance ($p < 0.05$) is shown in bold.

Term	Sum square	Statistic	p	Cohen's |d|
4-dpf dark-light total distance swam				
Heat	836	H = 1.351	0.2451	0.22 (small)
Medium	1669	H = 2.697	0.1005	0.24 (small)
Heat:medium	770	H = 1.244	0.2647	0.22 (small)
4-dpf dark-light mean swimming speed				
Heat	226	H = 0.3653	0.5456	0.11 (very small)
Medium	1290	H = 2.0847	0.1488	0.10 (very small)
Heat:medium	1318	H = 2.1298	0.1445	0.33 (small)
4-dpf dark-light number of swimming bursts				
Heat	1062	H = 1.7213	0.1895	0.29 (small)
Medium	2081	H = 3.3727	0.0662 (**trend**)	0.37 (small)
Heat:medium	616	H = 0.9982	0.3178	0.27 (small)
4-dpf dark-light activity percentage				
Heat	982	H = 1.5863	0.2079	0.15 (very small)
Medium	2387	H = 3.8566	**0.0496**	**0.38 (small)**
Heat:medium	537	H = 0.8679	0.3515	0.12 (small)

Table Appendix 4 S10. Stress metabolites lowered the 4-dpf touch-evoked swimming after UV exposure. Statistics are from two-way Scheirer-Ray-Hare tests (H statistic) or ANOVAs (F statistic). The "heat" term compares TS+UV and TS+SM+UV vs C+UV and SM+UV. The "medium" term compares SM+UV and TS+SM+UV to C+UV and TS+UV. Pairwise tests are computed with *emmeans* (T statistic) with correction for multiple testing. Effect size classification from Sawilowsky (2009). Significance is ($p < 0.05$) shown in bold.

Term	Sum square	Statistic	p	Cohen's |d|
4-dpf touch-evoked mean swimming speed				
Heat	0.1246	F = 0.1379	0.7114	0.08 (tiny)
Medium	3.2914	F = 3.6417	0.0599 (**trend**)	0.42 (small)
Heat:medium	2.9215	F = 3.2435	0.0754 (**trend**)	0.39 (small)
(C+UV) - (SM+UV)	-	T = 0.2075	0.8361	0.07 (very small)
(C+UV) - (TS+UV)	-	T = -1.7007	0.1857	0.55 (medium)
(C+UV) - (TS+SM+UV)	-	T = 1.1233	0.3969	0.31 (small)
(SM+UV) - (TS+UV)	-	T = -1.7818	0.1857	0.62 (medium)
(SM+UV) - (TS+SM+UV)	-	T = 0.8501	0.4773	0.25 (small)
(TS+UV) - (TS+SM+UV)	-	T = 2.6157	0.0637 (**trend**)	0.79 (medium)
4-dpf touch-evoked total distance swam				
Heat	1.2498	F = 1.2830	0.2607	0.25 (small)
Medium	0.0060	F = 0.0061	0.9377	0.02 (tiny)
Heat:medium	3.8373	F = 3.9391	**0.0506**	**0.44 (small)**
4-dpf touch-evoked delta time moving				
Heat	0.0298	F = 0.0291	0.8650	0.04 (tiny)
Medium	0.0410	F = 0.0401	0.8419	0.04 (tiny)
Heat:medium	0.7041	F = 0.6882	0.4092	0.18 (small)
4-dpf touch-evoked delta distance swam				
Heat	160	H = 0.2629	0.6082	0.23 (small)
Medium	8	H = 0.1355	0.9073	0.09 (tiny)
Heat:medium	112	H = 0.1836	0.6683	0.1 (tiny)

Table Appendix 4 S11. Heat stress history did not alter heart rates at 1 and 4 dpf. Statistics are from ANOVAs (F statistic). The "heat" term compares TS+UV and TS+SM+UV vs C+UV and SM+UV. The "medium" term compares SM+UV and TS+SM+UV to C+UV and TS+UV. Effect size classification from Sawilowsky (2009). Significance ($p < 0.05$) is shown in bold.

Term	Sum square	Statistic	p	Cohen's |d|
1-dpf heart rate				
Heat	2.6177	F = 2.9775	0.0890 (trend)	0.42 (small)
Medium	0.9284	F = 1.0560	0.3078	0.54 (small)
Heat:medium	0.0032	F = 0.0037	0.9519	0.01 (tiny)
4-dpf heart rate				
Heat	0.7329	F = 0.7687	0.3833	0.2 (very small)
Medium	0.0377	F = 0.0395	0.8430	0.04 (tiny)
Heat:medium	0.8149	F = 0.8546	0.3581	0.21 (small)

Table Appendix 4 S12. Heat alone increased 4-dpf fitness score whilst heat combined with stress metabolites lowered overall fitness. Statistics are from PERMANOVAs, and ANOVAs (F statistics) followed by post-hoc tests, using respectively pairwise PERMANOVAs and *emmeans*, with correction for multiple testing. The "heat" term compares TS+UV and TS+SM+UV vs C+UV and SM+UV. The "medium" term compares SM+UV and TS+SM+UV to C+UV and TS+UV. Effect size classification from Sawilowsky (2009). Significance ($p < 0.05$) is shown in bold.

Term	Sum square	Statistic	p	Effect size
PERMANOVA of 1-dpf startle response				
Heat	3.8381	F = 28.0361	**0.001**	R2 = 0.2132
Medium	1.2517	F = 9.1434	**0.001**	R2 = 0.0695
Heat:medium	0.4555	F = 3.3271	**0.046**	R2 = 0.0253
(C+UV) - (SM+UV)	0.1637	F = 1.7735	1.000	R2 = 0.0356
(C+UV) - (TS+UV)	0.8155	F = 7.7777	**0.006**	R2 = 0.1446
(C+UV) - (TS+SM+UV)	4.4882	F = 34.7394	**0.006**	R2 = 0.4052
(SM+UV) - (TS+UV)	0.6828	F = 4.6535	0.120	R2 = 0.1042
(SM+UV) - (TS+SM+UV)	3.0525	F = 17.9925	**0.006**	R2 = 0.2856
(TS+UV) - (TS+SM+UV)	1.5435	F = 8.2675	**0.024**	R2 = 0.1613
PERMANOVA of 4-dpf fitness outcome				
Heat	0.1022	F = 2.3901	0.071 (**trend**)	R2 = 0.0266
Medium	0.1261	F = 2.950	0.058 (**trend**)	R2 = 0.0328
Heat:medium	0.1495	F = 3.4975	**0.025**	R2 = 0.0389
(C+UV) - (SM+UV)	0.0475	F = 0.7833	1.000	R2 = 0.0171
(C+UV) - (TS+UV)	0.3643	F = 5.6159	**0.030**	R2 = 0.1179
(C+UV) - (TS+SM+UV)	0.0617	F = 0.8799	1.000	R2 = 0.0188
(SM+UV) - (TS+UV)	0.3098	F = 4.7158	0.078 (**trend**)	R2 = 0.1187
(SM+UV) - (TS+SM+UV)	0.0287	F = 0.3995	1.000	R2 = 0.0101
(TS+UV) - (TS+SM+UV)	0.3645	F = 4.6901	0.066 (**trend**)	R2 = 0.1153
ANOVA of 1-dpf fitness score (PC1 of 1-dpf PERMANOVA)				
Heat	23.9789	F = 27.0076	**< 0.0001**	**|d| = 1.05 (large)**
Medium	6.3001	F = 7.0958	**0.0093**	**|d| = 0.49 (small)**
Heat:medium	9.5661	F = 10.7743	**0.0015**	**|d| = 0.61 (medium)**
(C+UV) - (SM+UV)	-	t = -0.2258	0.8220	|d| = 0.07 (tiny)
(C+UV) - (TS+UV)	-	t = 1.1120	0.3233	|d| = 0.36 (small)
(C+UV) - (TS+SM+UV)	-	t = 5.9167	**< 0.0001**	**|d| = 2.04 (huge)**
(SM+UV) - (TS+UV)	-	t = 1.2456	0.3233	|d| = 0.35 (small)
(SM+UV) - (TS+SM+UV)	-	t = 5.7231	**< 0.0001**	**|d| = 1.70 (very large)**
(TS+UV) - (TS+SM+UV)	-	t = 4.2213	**0.0001**	**|d| = 1.22 (very large)**
ANOVA of 4-dpf fitness score (PC1 of 4-dpf PERMANOVA)				
Heat	3.3771	F = 3.8087	**0.0544**	**|d| = 0.41 (small)**
Medium	1.8604	F = 2.0981	0.1513	|d| = 0.30 (small)
Heat:medium	6.9412	F = 7.8283	**0.0064**	**|d| = 0.60 (medium)**
(C+UV) - (SM+UV)	-	t = -0.8022	0.6372	|d| = 0.26 (small)
(C+UV) - (TS+UV)	-	t = -3.4746	**0.0049**	**|d| = 1.14 (large)**
(C+UV) - (TS+SM+UV)	-	t = -0.2810	0.7794	|d| = 0.08 (tiny)
(SM+UV) - (TS+UV)	-	t = -2.5437	**0.0257**	**|d| = 0.87 (large)**
(SM+UV) - (TS+SM+UV)	-	t = 0.4958	0.7457	|d| = 0.15 (very small)
(TS+UV) - (TS+SM+UV)	-	t = 3.0468	**0.0094**	**|d| = 0.89 (large)**
ANOVA of average fitness score (average of PC1s)				
Heat	0.0046	F = 0.0053	0.9421	|d| = 0.01 (tiny)
Medium	4.1007	F = 4.7374	**0.0324**	**|d| = 0.45 (small)**
Heat:medium	9.7805	F = 11.2991	**0.0012**	**|d| = 0.73 (medium)**
(C+UV) - (SM+UV)	-	t = -0.6401	0.5239	|d| = 0.23 (small)
(C+UV) - (TS+UV)	-	t = -2.5102	**0.0422**	**|d| = 0.79 (medium)**
(C+UV) - (TS+SM+UV)	-	t = 1.7614	0.0983 (**trend**)	|d| = 0.84 (medium)
(SM+UV) - (TS+UV)	-	t = -1.7835	0.0983 (**trend**)	|d| = 0.55 (medium)
(SM+UV) - (TS+SM+UV)	-	t = 2.2448	0.0550 (**trend**)	|d| = 0.69 (medium)
(TS+UV) - (TS+SM+UV)	-	t = 3.9531	**0.0010**	**|d| = 1.10 (large)**

This page is intentionally left blank.